Pedro Miguel Araújo Campos de Castro

HEMODINÂMICA E DOENÇA VASCULAR CEREBRAL

Evolução e fator prognóstico da autorregulação dinâmica do fluxo sanguíneo cerebral no Acidente vascular cerebral agudo

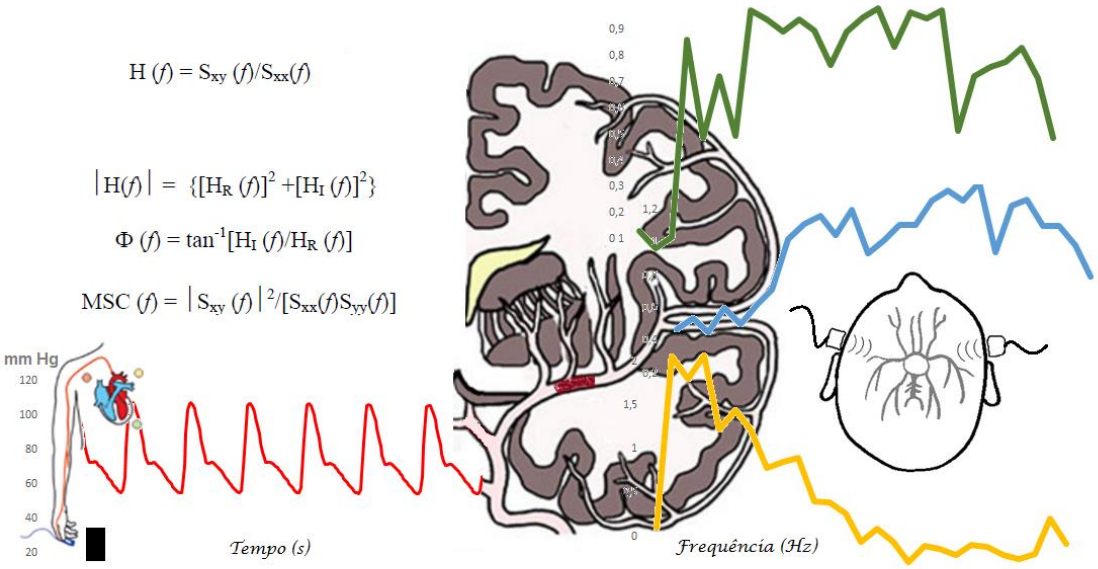

Dissertação de candidatura ao grau de Doutor

Apresentada à Faculdade de Medicina da Universidade do Porto

Orientadora: Doutora Elsa Azevedo
Departamento de Neurociências Clínicas e Saúde Mental

U.PORTO
FMUP FACULDADE DE MEDICINA UNIVERSIDADE DO PORTO

Porto • 2017

Artigo 48, parágrafo 3º

"A Faculdade não responde pelas doutrinas expedidas na dissertação"

Regulamento da Faculdade de Medicina da Universidade do Porto

Decreto-lei nº 19337, de 29 de janeiro de 1931

Título *Hemodinâmica e Doença vascular cerebral: evolução e fator prognóstico da autorregulação dinâmica do fluxo sanguíneo cerebral no Acidente vascular cerebral*

Autor *Pedro Miguel Araújo Campos de Castro*

Edição *do autor*

ISBN

Ano 2017

CORPO CATEDRÁTICO DA FACULDADE DE MEDICINA DA UNIVERSIDADE DO PORTO

PROFESSORES EFECTIVOS

Alberto Manuel Barros da Silva
Altamiro Manuel Rodrigues Costa Pereira
António Albino Coelho M. Abrantes Teixeira
Deolinda Maria Valente Alves Lima Teixeira
Francisco Fernando Rocha Gonçalves
Isabel Maria Amorim Pereira Ramos
João Francisco Montenegro A. L. Bernardes
Joaquim Adelino Correia F. Leite Moreira
José Agostinho Marques Lopes
José Carlos Neves da Cunha Areias
José Eduardo Torres Eckenroth Guimarães
José Henrique Dias Pinto de Barros
José Manuel Lopes Teixeira Amarante
José Manuel Pereira Dias de Castro Lopes
Manuel Alberto Coimbra Sobrinho Simões
Manuel Jesus Falcão Pestana Vasconcelos
Maria Amélia Duarte Ferreira
Maria Dulce Cordeiro Madeira
Maria Fátima Machado Henriques Carneiro
Maria Leonor Martins Soares David
Patrício Manuel Vieira Araújo Soares Silva
Raquel Ângela Silva Soares Lino
Rui Manuel Lopes Nunes

PROFESSORES JUBILADOS/APOSENTADOS

Alexandre Alberto Guerra Sousa Pinto
Álvaro Jerónimo L. Machado de Aguiar
António Augusto Lopes Vaz
António Carlos de Freitas Ribeiro Saraiva
António Carvalho Almeida Coimbra
António Fernandes O. B. Ribeiro Braga
António José Pacheco Palha
António Manuel Sampaio de A. Teixeira
Belmiro dos Santos Patrício
Cândido Alves Hipólito Reis
Carlos Rodrigo Magalhães Ramalhão
Cassiano Pena de Abreu e Lima
Daniel Filipe de Lima Moura
Eduardo Jorge Cunha Rodrigues Pereira
Fernando Tavarela Veloso
Henrique José F. G. Lecour de Menezes
Jorge Manuel Mergulhão Castro Tavares
José Carvalho de Oliveira
José Fernando Barros Castro Correia
José Luís Medina Vieira
José Manuel Costa Mesquita Guimarães
Levi Eugénio Ribeiro Guerra
Luís Alberto Martins Gomes de Almeida
Manuel António Caldeira Pais Clemente
Manuel Augusto Cardoso de Oliveira
Manuel Machado Rodrigues Gomes
Manuel Maria Paula Barbosa
Maria da Conceição F. Marques Magalhães
Maria Isabel Amorim de Azevedo
Rui Manuel Almeida Mota Cardoso
Serafim Correia Pinto Guimarães
Valdemar Miguel B. dos Santos Cardoso
Walter Friedrich Alfred Osswald

CONSTITUIÇÃO DO JÚRI

PRESIDENTE

Doutor José Agostinho Marques Lopes

Professor catedrático da Faculdade de Medicina da Universidade do Porto

VOGAIS

Doutor José Manuel Morão Cabral Ferro

Professor catedrático da Faculdade de Medicina de Lisboa

Doutor Luís Augusto Salgueiro Cunha

Professor catedrático da Faculdade de Medicina de Coimbra

Doutor Joaquim Adelino Correia Ferreira Leite Moreira

Professor catedrático da Faculdade de Medicina da Universidade do Porto

Doutora Maria Carolina Lobo Almeida Garrett

Professora associada da Faculdade de Medicina da Universidade do Porto

Doutor Rui Manuel Bento de Almeida Coelho

Professor associado da Faculdade de Medicina da Universidade do Porto

Doutora Elsa Irene Peixoto Azevedo Silva

Professora auxiliar da Faculdade de Medicina da Universidade do Porto

À Catarina

Aos meus Pais e Irmão

À minha família

“Não existem métodos fáceis para resolver problemas difíceis.”

René Descartes

AGRADECIMENTOS

Um projeto de investigação em doutoramento é uma longa caminhada, feita de sucessos, ora revezes, que se torna decisivamente mais fácil com apoio inestimável de vários intervenientes. Tenho a certeza de que tal empreitada apenas chegou a bom porto pelo suporte que recebi de todos incluindo família, colegas e outros profissionais de saúde, e dos doentes e suas famílias.

Gostaria de realçar a motivação que recebi da minha orientadora, Doutora Elsa Azevedo, assim como as suas opiniões críticas e discussões científicas, essenciais para a condução dos trabalhos. A ela lhe devo, também, o despertar da curiosidade e introdução no mundo da neurossonologia.

Devo também um agradecimento particular a todos os co-investigadores e coautores das publicações, pois sem este trabalho de grupo e multidisciplinar não se atingiriam conhecimentos com tal alcance clínico, fisiológico e patológico.

Agradeço aos Professores Jorge Serrador (*Rutgers Biomedical Health Sciences, New jersey*, Estados Unidos), Farzaneh Sorond (*Northwestern University Feinberg School of Medicine, Boston*, Estados Unidos), Ronney Panerai (*University of Leicester,* Reino Unido) e Isabel Rocha (Instituto de Fisiologia da Faculdade de Medicina da Universidade do Porto) com os quais pude partilhar o esforço deste projeto e deles recebi conhecimentos e experiência úteis para atingir as metas a que me propus. Também tiveram a gentileza de ceder as ferramentas analíticas por eles desenvolvidas, contribuição fundamental para finalizar o projeto. Deixo uma palavra de agradecimento particular às Dras. Rosa Santos e Cármen Ferreira que, pelo espírito crítico e dedicação à neurossonologia, sempre se prontificaram para qualquer ajuda técnica ou laboratorial necessária. Alguns trabalhos prévios contaram com a colaboração do Centro de Estudos da Função Autonómica. Agradeço ao seu coordenador, Doutor João Freitas, que em colaboração com a Doutora Elsa Azevedo, minha orientadora, tive o prazer de ter acompanhado e participado na análise dos dados relativos ao estudo da hemodinâmica cerebral na síncope e que constam das respetivas teses de doutoramento, cuja conclusão e defesa assisti nesta mesma casa.

Ao Pessoal do Serviço de Neurologia, Unidade de AVC e a todo Grupo de Doença Vascular Cerebral do Centro Hospitalar de São João, agradeço, além do apoio humano e material, a colaboração prestada.

Por último, um agradecimento àqueles que sempre foram os mais importantes, à minha esposa Catarina Rodrigues, Pais e irmão na ajuda e incentivo neste projeto.

ÍNDICE

ÍNDICE DE ILUSTRAÇÕES

CONTRIBUIÇÕES DO AUTOR

Artigos científicos resultantes da investigação específica de autorregulação cerebral no AVC isquémico, reproduzidos integralmente na secção dos "Capítulos"

Madureira, J.*, **Castro, P.*,** & Azevedo, E. (2017). Demographic and Systemic Hemodynamic Influences in Mechanisms of Cerebrovascular Regulation in Healthy Adults. *J Stroke Cerebrovasc Dis, 26*(3), 500-508. doi: 10.1016/j.jstrokecerebrovasdis.2016.12.003

* Os autores contribuíram igualmente para o artigo

Castro, P., Serrador, J., Rocha, I., Sorond, F., & Azevedo, E. (2017). Efficacy of Cerebral Autoregulation in Early Ischemic Stroke Predicts Smaller Infarcts and Better Outcomes. *Frontiers in Neurology, 8*(113). doi: 10.3389/fneur.2017.00113

Castro, P., Azevedo, E., Serrador, J., Rocha, I., & Sorond, F. (2017). Hemorrhagic transformation and cerebral edema in acute ischemic stroke: Link to cerebral autoregulation. *Journal of the neurological sciences, 372*, 256-261. doi: 10.1016/j.jns.2016.11.065

Castro, P., E. Azevedo, I. Rocha, F. Sorond, J. Serrador (2017). Chronic Kidney Disease and Poor Outcomes in Ischemic Stroke: is Impaired Cerebral Autoregulation the Missing Link?. *Clin J am Soc Nephrol* (em revisão)

Castro, P., E. Azevedo, J. Serrador, Chaves, P., I. Rocha, F. Sorond (2017). Heart Failure Patients with Severe Aortic Stenosis Have Enhanced Cerebral Autoregulation Response in Acute Ischemic Stroke. *Int J Cardiol* (em revisão).

Artigos científicos iniciais sobre hemodinâmica que contribuíram para o desenvolvimento do projeto da dissertação, compilados na íntegra na secção "Anexos":

Castro, P., Freitas, J., Santos, R., Panerai, R. B., & Azevedo, E. (2017). Indexes of cerebral autoregulation do not reflect impairment in syncope: insights from head-up tilt test of vasovagal and autonomic failure subjects. *Eur J Appl Physiol, 117(9),* 1817-1831. doi: 10.1007/s00421-017-3674-1

Castro, P., Santos, R., Freitas, J., Rosengarten, B., Panerai, R., & Azevedo, E. (2012). Adaptation of cerebral pressure-velocity hemodynamic changes of neurovascular coupling to orthostatic challenge. *Perspectives in Medicine, 1*(1–12), 290-296. doi: http://dx.doi.org/10.1016/j.permed.2012.02.052

Castro, P., Santos, R., Freitas, J., Panerai, R. B., & Azevedo, E. (2014). Autonomic dysfunction affects dynamic cerebral autoregulation during Valsalva maneuver: comparison between healthy and autonomic dysfunction subjects. *J Appl Physiol (1985), 117*(3), 205-213. doi: 10.1152/japplphysiol.00893.2013

Azevedo, E., **Castro, P.**, Santos, R., Freitas, J., Coelho, T., Rosengarten, B., & Panerai, R. (2011). Autonomic dysfunction affects cerebral neurovascular coupling. *Clin Auton Res, 21*(6), 395-403. doi: 10.1007/s10286-011-0129-3

Azevedo, E., Mendes, A., Seixas, D., Santos, R., **Castro, P.**, Ayres-Basto, M.,... Oliveira, J. P. (2012). Functional transcranial Doppler: presymptomatic changes in Fabry disease. *Eur Neurol, 67*(6), 331-337. doi: 10.1159/000337906

Videira, G., **Castro, P.**, Vieira, B., Filipe, J. P., Santos, R., Azevedo, E., Sá, M.J., Abreu, P. (2016). Autonomic dysfunction in multiple sclerosis is better detected by heart rate variability and is not correlated with central autonomic network damage. *J Neurol Sci, 367*, 133-137. doi: 10.1016/j.jns.2016.05.049

Capítulos de livro no âmbito do sistema nervoso autónomo, neurossonologia e autorregulação cerebral que se enquadram neste projeto da dissertação

Azevedo, E., & **Castro, P.** (2016). Cerebral autoregulation. In L. Csiba & C. Baracchini (Eds.), *Manual of neurosonology* (pp. ix, 322 pages). Cambridge: Cambridge University Press.

Azevedo, E., & **Castro, P.** (2013). Novel Applications of Ultrasound Vascular Imaging. In J. N. Ramalho, M. Castillo & R. C. Semelka (Eds.), *Vascular imaging of the central nervous system : physical principles, clinical applications and emerging techniques* (pp. 1 online resource (427 pages)). Hoboken, New Jersey: Wiley-Blackwell.

Carvalho, T., & **Castro, P.** (2013). Disfunções do Sistema Nervoso Autónomo. In M. J. Sá (Ed.), *Manual de Neurologia Clínica: Compreender as Doenças Neurológicas* (2nd ed.). Porto: Edições Universidade Fernando Pessoa

LISTA DE ABREVIATURAS

ACA	Artéria cerebral anterior
ACI	Artéria carótida interna
ACM	Artéria cerebral média
ACoA	Artéria comunicante anterior
ACoP	Artéria comunicante posterior
ACP	Artéria cerebral posterior
AFT	Análise da Função de transferência
ANV	Acoplamento neurovascular
ARC	Autorregulação cerebral
ATP	Adenosina trifosfato
AVC	Acidente Vascular Cerebral
BHE	Barreira hematoencefálica
BR	Barorreflexo
cGMP	Guanil monofosfato cíclico
CO_2	Dióxido de carbono
CO_2TE	CO_2 tele-expiratório
DTC	Doppler transcraniano
ECG	Eletrocardiograma
FC	Frequência cardíaca
FSC	Fluxo sanguíneo cerebral
iRVC	Índice de resistência vascular cerebral
IC	Insuficiência cardíaca
K+	Potássio
NO	Monóxido de azoto ou óxido nítrico
NOS	Sintetase de NO
PA	Pressão arterial
$PaCO_2$	Pressão parcial de CO_2
PAF	Polineuropatia amiloidótica familiar
PAM	Pressão arterial média
PaO_2	Pressão parcial de oxigénio
PCrE	Pressão crítica de encerramento
PRA	Produto resistência-área
RAC	Rede autonómica central
SNA	Sistema nervoso autónomo
VFM	Velocidade de fluxo (sanguíneo cerebral) média
VFSC	Velocidade de fluxo sanguíneo cerebral
VR	Vasorreatividade cerebral

I. RESUMO

Os mecanismos que governam a homeostasia do fluxo sanguíneo cerebral são desafiados de modo crítico no acidente vascular cerebral (AVC) isquémico agudo. A autorregulação cerebral (ARC) é um dos principais operadores desse controlo vascular cerebral, assegurando um fluxo sanguíneo constante em resposta às variações de pressão arterial. Mantendo-se efetiva, pode proteger a penumbra isquémica de níveis de pressão arterial deletérios e minimizar a lesão neurológica. A ARC dinâmica pode ser avaliada de modo não invasivo através da função de transferência entre as oscilações espontâneas da pressão arterial e da velocidade de fluxo sanguíneo cerebral obtidas, respetivamente, por pletismografia digital e por Doppler transcraniano. O principal objetivo deste projeto de investigação foi avaliar o papel da ARC dinâmica no contexto de isquemia cerebral aguda, incluindo a capacidade de predizer complicações neurológicas graves, assim como o prognóstico funcional a longo prazo.

Antes de iniciar o estudo dos doentes com AVC, investigou-se o efeito dos fatores demográficos e hemodinâmicos sistémicos nos principais mecanismos de regulação cerebrovascular. A partir de uma população saudável distribuída equitativamente por sexo e por décadas de idade, dos 20 aos 80 anos, medimos a ARC, o acoplamento neurovascular e a vasorreatividade ao dióxido de carbono com métodos baseados no Doppler transcraniano. Verificámos que os diversos mecanismos de controlo cerebrovascular não foram significativamente influenciados pelo sexo ou idade. Podemos explicar os resultados pela existência de uma reserva cerebral vascular funcional que colmata as alterações morfológicas da vasculatura associadas ao envelhecimento. Um dos aspetos inovadores deste trabalho foi juntar num só estudo os vários parâmetros de controlo cerebrovascular, que verificámos não se correlacionarem entre si. Dado não haver relação entre os diversos mecanismos, devemos ter cuidado na comparação entre estudos que avaliaram a "reatividade" cerebral partindo de metodologias distintas. No que concerne à aplicação para o estudo da ARC no AVC, foi relevante demonstrar que os parâmetros da função de transferência da ARC não eram influenciados significativamente pelo sexo e idade, retirando-se este efeito confundidor.

A segunda etapa dos trabalhos refere-se à avaliação da ARC em doentes com AVC isquémico agudo. Foram introduzidos alguns aspetos inovadores na abordagem, sendo o mais significativo o facto de se avaliar a ARC dentro das primeiras 6 horas de início de sintomas do AVC, período em que a decisão médica tem mais impacto na morbilidade do doente a longo prazo. Avaliou-se o impacto da ARC no estado funcional dos doentes aos 3 meses pela escala de Rankin

modificada, no volume de enfarte, e na ocorrência de transformação hemorrágica ou edema cerebral. Obtivemos novos dados a respeito da fisiopatologia do AVC isquémico agudo e demonstrou-se o valor prognóstico da ARC medida em fase aguda.

Uma ARC precoce mais efetiva, traduzida por uma fase maior e um ganho reduzido, associou-se a um melhor resultado neurológico nos doentes com AVC isquémico. Um ponto de corte no valor de fase pelos 37 graus mostrou ter boa acuidade para determinar o estado funcional aos 3 meses. Mais precisamente, verificámos que a probabilidade de estar independente aos 3 meses aumentava 14 vezes nos doentes com AVC isquémico se fosse detetada uma melhor ARC (fase > 37 graus) no território da artéria cerebral média. Adicionalmente, um melhor nível de ARC determinou enfartes com menor volume às 24 horas. Verificámos a existência de uma correlação entre baixa pressão arterial e maior área isquémica, mas, curiosamente, tal só ocorreu no subgrupo de doentes com ARC menos eficaz (fase <37 graus). Também se verificou que níveis de ARC menos eficazes nas primeiras horas após isquemia cerebral estavam associados a um risco aumentado de transformação hemorrágica e edema cerebral às 24 horas, resultados nunca descritos previamente. Os doentes que vieram a desenvolver edema cerebral também revelaram baixa resistência vascular cerebral, o que demonstra uma desregulação vasomotora dos pequenos vasos de resistência. No seu conjunto, as alterações registadas nos parâmetros hemodinâmicos cerebrais estão de acordo com fenómenos de hiperperfusão deletéria e lesão microvascular. Também se procurou obter algum esclarecimento sobre os fatores que possam modelar a ARC na fase aguda do AVC isquémico, particularmente, no que concerne os binómios cérebro-coração e cérebro-rim. Pela primeira vez, descreveu-se a existência de uma relação entre a função renal e a ARC no AVC isquémico agudo. Os valores estimados para a taxa de depuração da creatinina apresentaram uma correlação positiva com os valores de ganho, ou seja, quanto pior a função renal, tanto menor a capacidade autorregulatória a nível vascular cerebral. Para além da ARC, também uma função renal diminuída se associou a pior prognóstico. A disfunção da ARC poderá ser parte de uma desregulação microvascular mais sistémica. Por último, foi possível demonstrar uma resposta autorreguladora cerebral aumentada nos doentes com disfunção cardíaca. Perceber os mecanismos fisiológicos que governam esta relação poderá conduzir a novos alvos terapêuticos que melhorem o prognóstico do doente com AVC isquémico.

Em resumo, este projeto de investigação apresentou novos achados acerca da fisiopatologia do AVC isquémico agudo, introduzindo a ARC como um marcador com importância prognóstica e de risco para complicações neurológicas. A ARC tem potencial para ser explorada no futuro, com vista a melhorar a orientação terapêutica dos doentes com AVC isquémico.

II. ABSTRACT

The mechanisms that govern the homeostasis of cerebral blood flow are vigorously challenged in the acute ischemic stroke (AIS). Cerebral autoregulation (CA) is one of the main operators of cerebrovascular control that keep cerebral blood flow constant in response to blood pressure changes. An effective CA may protect the vulnerable ischemic penumbra from deleterious blood pressure levels and minimize neurological injury. Dynamic CA can be assessed non-invasively with a transfer function analysis of spontaneous oscillations of blood pressure and cerebral blood flow velocity, recorded with finger plethysmography and transcranial Doppler, respectively. The main objective of this project of investigation was to examine the role of dynamic CA in the setting of acute brain ischemia, including its capability to predict serious neurological complications and its prognostic value for a long-term functional outcome.

Before assessing patients with AIS, we investigated the effect of demographic and systemic hemodynamic parameters in main cerebral regulatory mechanisms based on functional tests using transcranial Doppler. For this goal, we selected a healthy population equally distributed sex groups and by decades of age from 20 to 80 years. We found that cerebral autoregulatory transfer function parameters, neurovascular coupling and vasoreactivity to carbon dioxide challenge were not significantly affected by age and gender, despite the decrease in basal cerebral blood flow velocity and the increased cerebrovascular resistance with age. This finding means that the brain seems to have some functional vascular reserve to deal with the morphological vasculature changes that occur with ageing. One of the innovative aspects of this investigation was to join in the same study a correlation analysis of several outputs of distinct aspects of cerebrovascular control. Having found no relationship between them, we conclude that one should be careful in comparing studies that have used different methodologies to assess the “reactivity” of cerebral microvasculature, since they measure distinct aspects of cerebrovascular control. In what concerns to stroke pathophysiologic study, it was relevant to demonstrate that transfer function parameters of cerebral autoregulation were not influenced by age and gender, both of which can interact with several aspects in stroke patients.

The second part of this thesis concerned the evaluation of AIS patients. For the first time, dynamic cerebral autoregulation was assessed strictly within 6 hours from ischemic stroke symptoms onset, when medical actions can decisively change the patient’s disability in the long term. The main outcome measures were functional status at 3 months based on the modified

Rankin scale, infarct volume, and the presence of hemorrhagic transformation and edema. We obtained new findings related to AIS pathophysiology and found that CA measurement carries relevant prognostic information.

An early and more effective dynamic CA, which has a higher phase and reduced gain, was associated with better neurological outcome in patients with AIS. We found that a cut-off of phase at 37 degrees provides good accuracy to predict the functional outcome. Based on this cut-off value, we found that the odds of being independent at 3 months increases 14-fold when a higher phase (better CA) is detected in the middle cerebral artery territory. Also, at 24 hours, infarct volumes were significantly smaller with intact cerebral autoregulation. We also found a correlation between low blood-pressure levels and increased ischemic area, but, curiously, only in the subgroup of patients with worse CA at presentation (phase <37 degrees). Moreover, a less effective CA in the early hours after AIS is associated with an increased risk of hemorrhagic transformation and cerebral edema, which had not been described before. We also found that cerebrovascular resistance was very low at presentation in these patients, which demonstrates a deregulation of small vessels in the affected parenchyma. Taken together, these abnormalities possibly reflect breakthrough hyperperfusion and microvascular injury.

Exploring the factors that influence CA in AIS, we also looked at the role of CA within the binomial relationships of kidney-brain and heart-brain. We found that a poor renal function correlates with a less-effective dynamic CA in acute ischemic stroke, both predicting a bad outcome. Therefore, the dysfunctional CA may be a part of a more widespread microvascular deregulation. Lastly, an enhanced dynamic CA response was detected in heart-failure patients. Understanding the physiological mechanisms that govern this complex interplay can be useful to find novel therapeutic targets that could improve outcome in ischemic stroke.

Overall, this investigation project led to new findings about the pathophysiology of acute ischemic stroke and gave a role for CA in what concerns the functional prognosis and the risk of complications presented by these patients. CA has the potential to be used in future research in acute ischemic stroke.

III. INTRODUÇÃO

CIRCULAÇÃO CEREBRAL

Durante 1500 anos, a Medicina permaneceu letárgica sob o conceito de "rede maravilhosa" (do latim, *rete mirabile)* apregoada por Galeno (Pérgamo, atual Turquia, 129 – 199) (Galen, 1531). Inexplicavelmente, apesar de três centúrias de dissecções humanas, só em 1522 Jacopo Berengaro (Carpi, Itália, 1460-1530) nega formalmente a sua existência (Berengarus, 1552), identificando as artérias carótidas. Na sequência, em 1561, Gabriel Falópio (Modena, 1523 - 1562) faz a primeira descrição, não ilustrada, do circuito arterial na base do crânio (Fallopius, 1561). Contudo, seria Thomas Willis (*Great Bedwyn*, Inglaterra; 1621 - 1675) quem, pela primeira vez, contando com a descrição mais detalhada da vascularização cerebral por Johann Jakob Wepfer em 1568 (*Schaffhausen*, Suíça; 1620 - 1625) (Wepfer, 1658) e as pistas hemodinâmicas de William Harvey (*Folkestone*, Inglaterra 578 - 1657) (Harvey, 1628), iria reconhecer a função da rede anastomótica das artérias da base do crânio, que tão eloquentemente descreveu em *Cerebri anatome* no ano de 1664 (Willis, 1664).

Nas secções seguintes serão descritos os conceitos elementares sobre circulação cerebral humana e os mecanismos que a regulam, dando especial enfoque à autorregulação cerebral (ARC). Será ainda feita uma breve referência à fisiopatologia do acidente vascular cerebral (AVC) isquémico, a entidade nosológica sobre a qual se debruçam os trabalhos desta tese. Em suma, deseja-se que o texto introdutório crie um enquadramento clínico e fisiopatológico que seja suficientemente claro para que se compreenda a relevância do estudo da hemodinâmica cerebral no prognóstico dos doentes com AVC.

Anatomia da circulação cerebral

A irrigação cerebral conta com quatro troncos arteriais ascendentes (Figura 1A), duas artérias carótidas internas (ACI) e duas vertebrais. Estas formam duas redes complementares designadas por circulação anterior ou carotídea e posterior ou vertebrobasilar, respetivamente (Nolte & Sundsten, 2009). A ACI origina-se na bifurcação da carótida comum. Descreve um trajeto

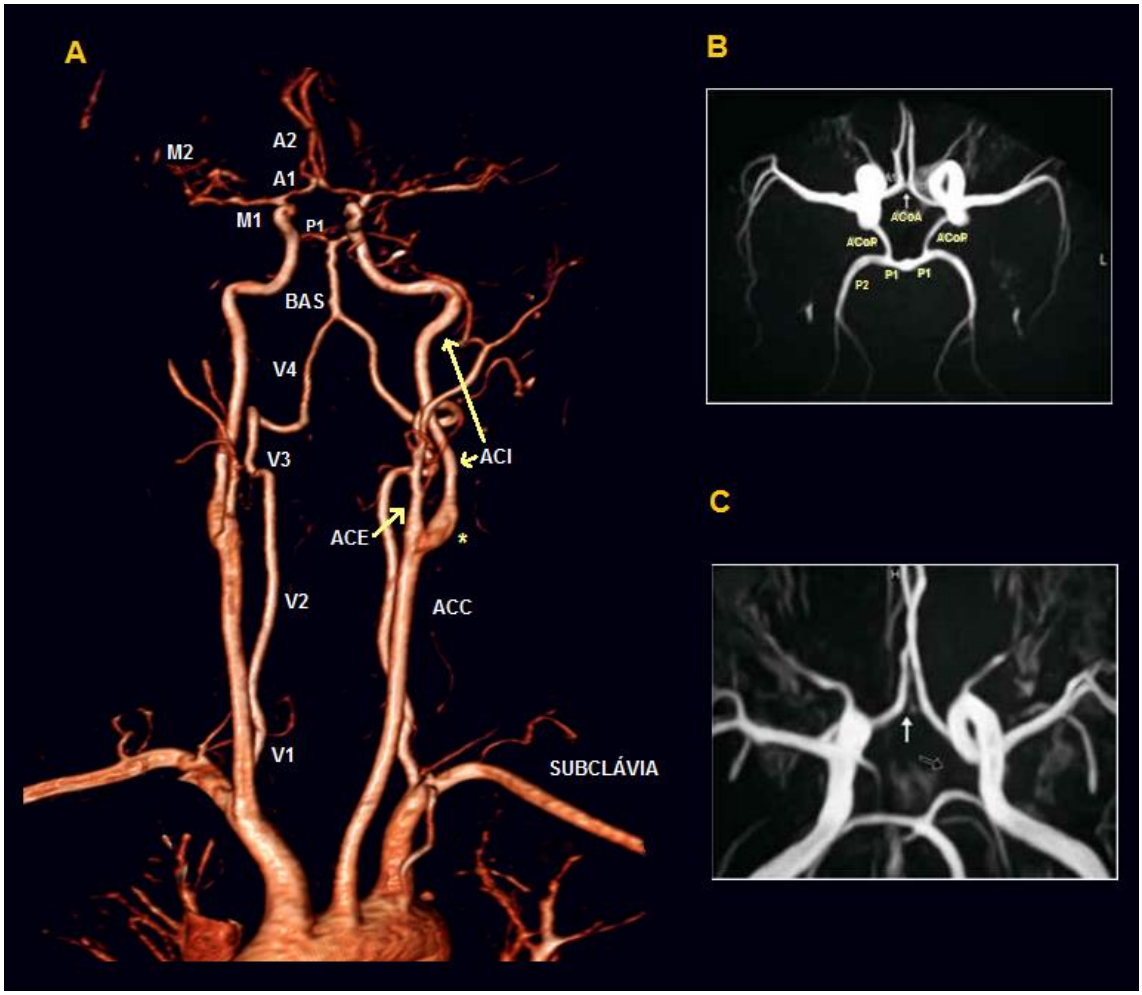

Figura 1 – Vascularização Cerebral
Angiografia por Tomografia computorizada (**A**) evidenciando as várias artérias da circulação cerebral. Da circulação anterior identificámos as artérias carótida comum (ACC), externa (ACE) e interna (ACI), incluindo o seu seio carotídeo (*), os segmentos M1 e M2 da cerebral média e os segmentos A1 e A2 da cerebral anterior. Na circulação posterior, estão apontados os sucessivos segmentos da artéria vertebral (V1, V2, V3, V4), a artéria basilar (BAS) e o segmento P1 da cerebral posterior. O segmento P2 da cerebral posterior pode ser visualizado numa angiografia por Ressonância Magnética em **B.** Aqui também observamos os constituintes do círculo arterial da base do cérebro – artéria comunicante anterior (ACoA) e posterior (ACoP). Em **C**, usando o mesmo tipo de imagem, demonstra-se um círculo arterial incompleto com hipoplasia de ACoA e agenesia da ACoP esquerda.

ascendente, retromandibular, acompanhada da veia jugular interna e do nervo vago, conjunto esse designado por feixe vasculonervoso do pescoço. O primeiro centímetro proximal é ligeiramente dilatado, onde se forma o seio carotídeo (Figura 1A), um importante barorrecetor (BR) arterial (Nolte & Sundsten, 2009). Após percorrer o canal carotídeo dentro do osso temporal, segue anterior e superiormente formando o sifão carotídeo, onde, então, inflete o seu trajeto posteriormente, perfurando a dura-máter do teto do seio cavernoso. Agora, em pleno espaço subaracnoideu, a porção supraclinoidea origina, entre outras, a artéria comunicante posterior (ACoP), antes de se dividir nos seus dois ramos terminais – artéria

cerebral média (ACM) e anterior (ACA) (Figura 1A e 1B). A ACA junta-se na linha média à sua homóloga via artéria comunicante anterior (ACoA), sendo os segmentos pré e pós-anastomóticos designados de A1 e A2. Irriga a tira medial de cada hemisfério. A ACM possui uma primeira porção horizontal (M1) que percorre o tronco do sulco lateral, vindo-se a bifurcar em dois ramos (M2) ao mesmo tempo que se arqueia em ângulo reto sob o córtex insular. A ACM irriga os dois terços laterais de cada hemisfério cerebral (Nolte & Sundsten, 2009).

A artéria vertebral tem uma origem na 1ª porção da artéria subclávia (V0), dirige-se para o 6º buraco transversário (V1) e percorre sucessivamente os restantes (V2) até alcançar o bordo superior do arco posterior do atlas (V3), onde perfura a membrana atlanto-occipital posterior e dura para alcançar o espaço subaracnoideu (V4) (Figura 1A). Na face anterior do tronco cerebral, une-se à contralateral formando a artéria basilar. Esta ascende até se bifurcar em duas artérias cerebrais posteriores (ACP) que irrigam *grosso modo* os lobos occipitais. A ACoP junta-se à ACP dividindo-a em dois segmentos, pré e pós-anastomótico, P1 e P2 (Nolte & Sundsten, 2009) (Figura 1B).

Completa-se então o círculo anastomótico que une as duas ACI intracranianas e o topo da basilar (ACoA, 2×A1, 2×AcoP, 2×P1), constituindo uma via de colateralização importante no caso de obstrução hemodinâmica de um dos troncos a montante. Estima-se, contudo, que apenas 25% da população tenha um círculo completo e de calibres simétricos (Nolte & Sundsten, 2009). Na Figura 1C mostra-se um exemplo de um círculo incompleto.

O parênquima cerebral propriamente dito é nutrido por um sistema dual de pequenos vasos. A porção basal ou rostral do encéfalo é da responsabilidade das artérias perfurantes que nascem diretamente dos troncos arteriais proximais do círculo anastomótico da base. Dirigem-se sobretudo para os núcleos da base, diencéfalo e cápsula interna. Por seu turno, o córtex cerebral é irrigado a partir de uma rede anastomótica pial formada pela bifurcação e redução progressiva do calibre e dos ramos cerebrais da ACM, ACA e ACP. Das pequenas artérias piais surgem arteríolas em ângulo reto, que penetram a superfície cortical e se dispõem radialmente até alcançarem o ventrículo lateral e centro semioval. São estas arteríolas penetrantes que originam a malha de capilares que nutre o tecido cerebral, percorrendo os hemisféricos paralelamente à superfície cortical (Duvernoy et al., 1981).

Sistemas de colateralização

Existe uma rede arterial subsidiária pronta a ser ativada quando o vaso principal falha. Podemos considerar dois sistemas de colateralização cerebral – intra e extracraniano (Liebeskind, 2003). O sistema extracraniano diz respeito a anastomoses entre ramos da artéria carótida externa

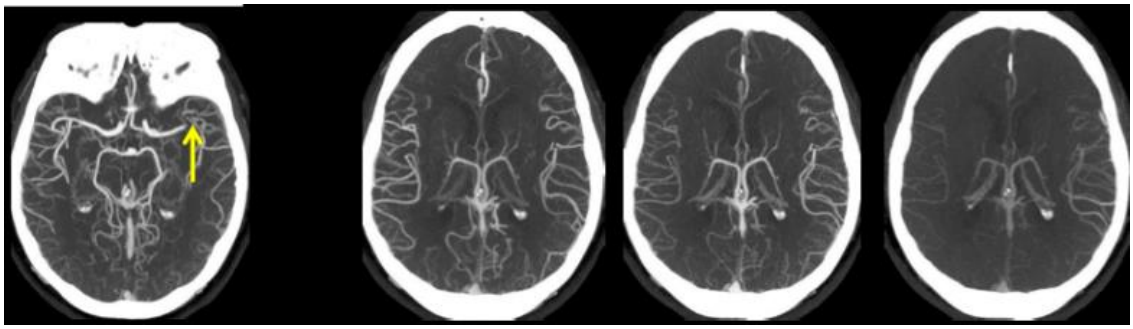

Figura 2 – Exemplo de colateralização cerebral intrínseca
Acidente vascular cerebral isquémico agudo por oclusão do segmento M1 da ACM esquerda (seta amarela). Observa-se extensa rede de vasos piais nesse hemisférico, sendo sinal de boa ativação da colateralização intrínseca. Em *http://www.aspectsinstroke.com/collateral-scoring*.

com a ACI intracraniana, e de ramos da externa e da subclávia com a artéria vertebral. Por exemplo, no caso de uma ACI gravemente obstruída a nível proximal cervical, a artéria oftálmica pode passar a irrigar a ACI terminal com fluxo invertido, vindo da artéria angular do nariz, ramo da artéria facial que, por sua vez, provém da carótida externa.

A nível intracraniano, para além do circuito anastomótico basal (*"polígono de Willis"*), podemos considerar uma rede pial superficial formada pelos ramos da ACA, ACP e ACM e outra desenvolvida entre as artérias cerebelosas. A Figura 2 coloca em evidência esta ativação colateral num caso de oclusão de M1, que é o panorama mais frequente de AVC isquémico agudo. Neste cenário, a colateralização primária intracraniana (ACoA e ACoP) não é ativada. Podemos, contudo, detetar fluxo globalmente aumentado na ACA e ACP ipsilaterais, sendo sinal de colateralização via leptomeníngea. O segmento A1 contralateral também tem fluxo aumentado, que diverge, via ACoA, para o A2 ipsilateral à oclusão e, assim, fortalece a irrigação leptomeníngea anterior.

Microcirculação cerebral e unidade neurovascular

À medida que as arteríolas penetram o parênquima, vão perdendo a inervação perivascular e as camadas adventícia e muscular, ficando seladas e separadas das estruturas nervosas pelos pés astrocitários (Girouard & Iadecola, 2006, Iadecola & Nedergaard, 2007, Hamel, 2006). Destas arteríolas, desenvolvem-se ramificações capilares que vão nutrir o tecido cerebral (Figura 3). A densidade capilar está estimada em 400 capilares/mm^{-2} (Williams & Leggett, 1989), pelo que o cérebro se torna, curiosamente, num órgão relativamente pouco vascularizado quando comparado, por exemplo, com o músculo esquelético. A microcirculação cerebral apresenta a particularidade de as suas células endoteliais estarem criticamente justapostas por junções

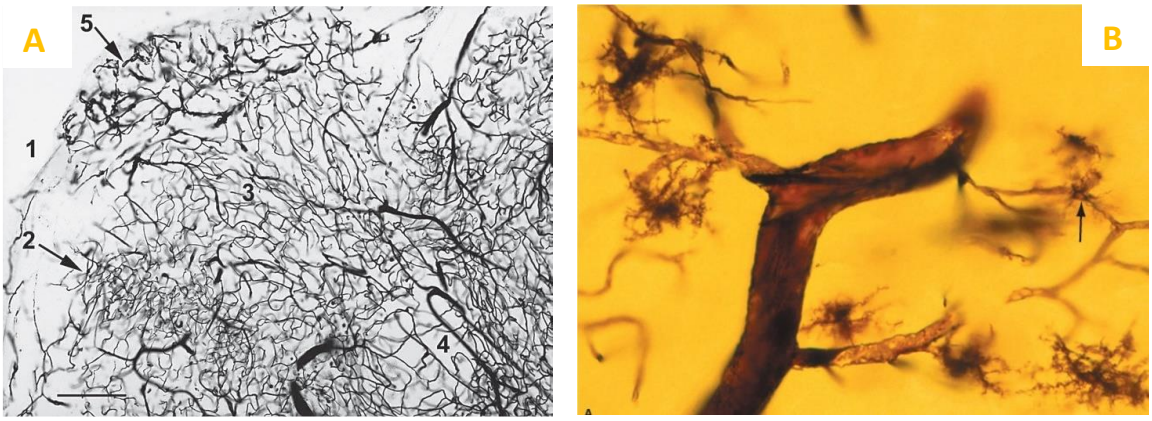

Figura 3 – Microcirculação cerebral
À direita (**A**), observam-se a fina rede capilar do 4º ventrículo. A figura **B** mostra uma ampliação de um capilar que é envolvido por vários pés astrocitários ao longo do seu trajeto. *Fontes: A – Duvernoy et al., 1981; B – Nolte & Sundsten, 2009.*

apertadas (Nolte & Sundsten, 2009). Este fator permite criar uma barreira hematoencefálica (BHE), que faz com que pouco mais do que água, gases arteriais e algumas substâncias lipossolúveis não sejam por ela barrados (Nolte & Sundsten, 2009). A disfunção da BHE pode dar origem ao extravasamento de conteúdo sanguíneo para o parênquima, o que causa edema vasogénico ou até transformação hemorrágica da área de enfarte cerebral (Simard et al., 2007). O fluxo cerebral tem de estar intimamente acoplado à atividade neuronal. A vasodilatação que ocorre com o incremento da atividade sináptica pode ser explicada em parte pela libertação de moléculas vasoativas, tais como a adenosina, monóxido de azoto (NO), prostaglandinas, potássio (K+) sobre os pericitos que rodeiam os capilares cerebrais. Para orquestrar este conjunto, o modelo mais consensual dá um papel de destaque ao astrócito e seus prolongamentos (Girouard & Iadecola, 2006, Iadecola & Nedergaard, 2007). Para além de coadjuvar na criação da BHE, os pés astrocitários (Figura 3) têm recetores excitatórios para o glutamato que extravasa da fenda sináptica, levando à entrada de cálcio (Ca^{2+}) na célula. Este condiciona um aumento de produção astrocitária de NO e prostaciclinas pela ativação da sintetase do NO (NOS) e da ciclo-oxigenase tipo 1 (COX-1) astrocitárias, respetivamente. Estas moléculas exercem então os seus efeitos vasomoduladores por ação sobre as células musculares lisas das arteríolas e pericitos dos capilares. Parecem ser particularmente fulcrais os capilares de 1ª e 2ª ordem na ignição vasodilatadora (Hall et al., 2014). Na Figura 4 podemos ver estes mecanismos em detalhe.

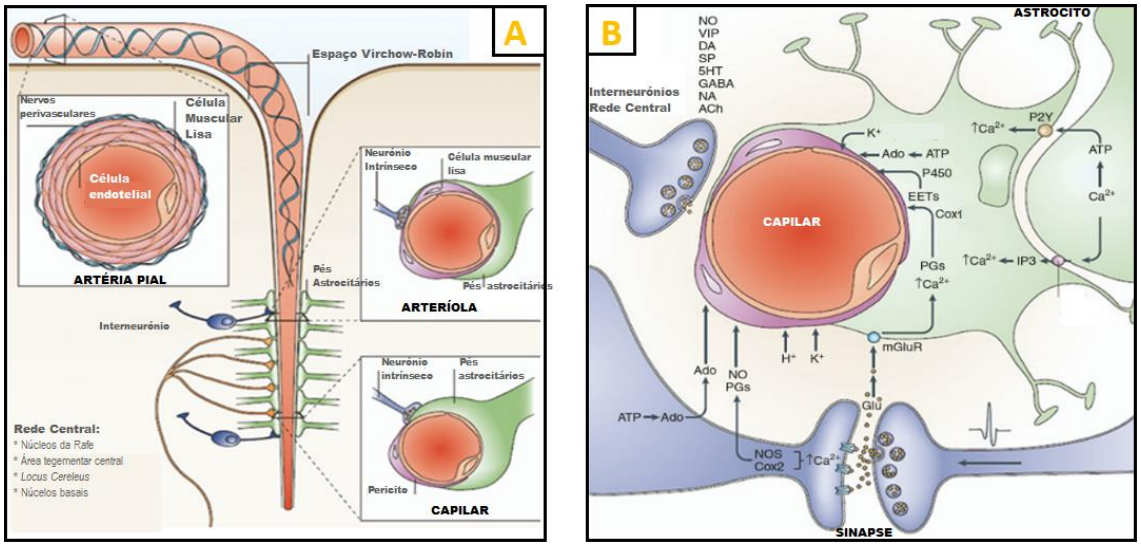

Figura 4 – Unidade e Acoplamento Neurovascular
As arteríolas perdem a sua inervação e camada muscular ao penetrar no córtex cerebral (**A**). A nível arteriolar e capilar, os pés astrocitários rodeiam os pericitos e células musculares lisas. O astrócito e o pericitos são, assim, os protagonistas da regulação vasomotora, sendo que alguns interneurónios GABAérgicos e núcleos centrais contribuem para o modular. À esquerda (**B**), observa-se os detalhes bioquímicos que governam este controlo. Os produtos que escoam da fenda sináptica, tais como o glutamato (Glu), adenosina (Ado), monóxido de azoto (NO) e prostanoides derivados da atividade da cicloxigenase tipo 2 (COX-2), exercem efeitos sobre os pericitos ou sobre os pés astrocitários, com especial relevo para a ativação de recetores metabotrópicos do Glu (mGluR). Aumenta, então, o cálcio (Ca2+) intracelular que despoleta a ativação da produção astrocitária de NO (via COX-1), prostaglandinas e ácidos epoxi-eicosatrienóicos (EET) que levem à vasodilatação. *Adaptado de Iadecola & Nedergaard, 2007.*

Inervação perivascular cerebral

Os vasos cerebrais são densamente inervados com fibras de duas redes distintas (Figura 4A): uma extrínseca, até nível pial, constituída por fibras do nervo trigémio e do sistema nervoso autónomo (SNA), tanto simpático como parassimpático; e outra intrínseca, com origem em núcleos subcorticais e interneurónios (Hamel, 2006).

A inervação parassimpática provém dos núcleos salivatórios superior e inferior do tronco cerebral, donde partem fibras pré-sinápticas destinadas aos gânglios ótico e pterigopalatino, respetivamente (Nolte & Sundsten, 2009, Hamel, 2006). Daqui, as fibras pós-sinápticas são retransmitidas aos vasos cerebrais (Shimizu, 1994, Edvinsson et al., 1989, Hara et al., 1989, Hara et al., 1993). As fibras parassimpáticas causam vasodilatação ao ativarem os recetores muscarínicos M5 das células endoteliais, o que leva ao aumento do Ca^{2+} intracelular, e consequente aumento da produção de NO, um relaxante muscular da parede vascular (Elhusseiny & Hamel, 2000, Yamada et al., 2001).

A inervação simpática tem origem pré-sináptica no primeiro segmento medular torácico (Carvalho & Castro, 2013). As fibras sinaptizam no gânglio da cadeia do simpático ao mesmo nível, e daqui ascendem ao longo da cadeia simpática cervical. Nos gânglios desta, têm origem as fibras que formam os plexos arteriais carotídeo e vertebral (Carvalho & Castro, 2013). Os terminais nervosos simpáticos libertam noradrenalina, que causa vasoconstrição por ação sobre os adrenorrecetores α_1 das células musculares lisas (Edvinsson, 1975, Nelson & Rennels, 1970).
O sistema trigeminovascular consiste em fibras nervosas com corpo celular no gânglio trigémio, prolongamento periférico nas estruturas durais e vasculares e uma ramificação central que sinaptiza no núcleo espinhal do trigémio (Arbab et al., 1986). Apesar de a informação ser aferente, certas respostas despolarizadoras junto dos terminais podem causar a libertação local dos seus neurotransmissores, tais como a substância P e o péptido relacionado com o gene da calcitonina, promovendo a vasodilatação (Saito et al., 1988, Visocchi et al., 1996). Este reflexo tem sido implicado na fisiopatologia da enxaqueca (Saito et al., 1988).
Os vasos cerebrais também estão providos de uma inervação intrínseca. Esta é composta quer por interneurónios GABAérgicos locais, quer por axónios vindos de núcleos subcorticais detentores de uma plêiade de neurotransmissores (e.g., serotonina, catecolaminas, acetilcolina, substância P) (Iadecola, 2004, Iadecola & Nedergaard, 2007, Hamel, 2006). Para tornar a situação ainda mais complexa, alguns destes núcleos estão intimamente interligados a estruturas constituintes da rede autonómica central (RAC) (Benarroch, 1993) que modela o SNA periférico.

Rede autonómica central

A nível do SNC, a RAC inclui a ínsula, os córtices do cíngulo anterior e pré-frontal ventromedial, os núcleos central da amígdala, paraventricular e outros do hipotálamo, a substância cinzenta periaquedutal, o núcleo parabraquial, o núcleo do trato solitário, os bolbos ventrolateral e ventromedial e o tegmento bulbar lateral (Benarroch, 1993). Esta rede está envolvida na regulação vascular via SNA e controlo de barorrecetor periférico (Benarroch, 1993). Contudo, num estudo realizado em doentes com esclerose múltipla, um maior atingimento nas proximidades da RAC e suas ligações não se correlacionou com a disautonomia apresentada por estes doentes (Videira et al., 2016). Isto sugere haver redes redundantes e compensadoras na regulação central do SNA.

HEMODINÂMICA CEREBRAL E SUA REGULAÇÃO

O cérebro é um órgão peculiarmente exigente do ponto de vista metabólico. Apesar de representar apenas 2% do peso corporal, consume 20% do total de oxigénio corporal e reclama 15% do débito cardíaco (Williams & Leggett, 1989), de modo a manter um elevado nível de atividade metabólica na ordem dos 3,5 ml/min/100 g de parênquima cerebral (Lassen, 1959). A interrupção generalizada do fluxo sanguíneo cerebral (FSC) global por escassos segundos provoca perda de consciência (síncope). Se persistente, culmina na anoxia cerebral e finalmente morte cerebral (Azevedo et al., 2000). No caso de uma redução focal do FSC, tal como sucede no AVC isquémico, o estado de viabilidade do tecido nervoso exibe um padrão heterogéneo, com áreas periféricas de oligoemia que evoluem para lesão celular irreversível se não houver desobstrução do vaso (Hossmann, 1994, Hossmann, 2006). O cérebro é, pois, um órgão pouco tolerante à isquemia (Dirnagl et al., 1999), tema a desenvolver posteriormente na secção *"Fisiopatologia da isquemia cerebral"*.

Princípios hemodinâmicos básicos

O fluxo sanguíneo não segue as leis simples dos fluidos newtonianos, sendo melhor estudado pelos princípios reológicos (Segal, 2005). Contudo, numa perspetiva mais simplista, podemos descrever o fluxo sanguíneo pela lei de Ohm segundo a fórmula $\dot{Q} = \frac{\Delta P}{R}$, na qual $\dot{Q}$ representa o fluxo em ml.min^{-1}, ΔP o gradiente de pressão arterial (PA) e R a resistência vascular. No caso do cérebro (Panerai, 2009, Panerai, 2003), ΔP é a pressão de perfusão cerebral (PPC), a diferença entre a PA média (PAM) e a pressão transmural de oposição ao fluxo. Na circulação sistémica, o único fator contributivo e relevante para esta é a pressão venosa (2-5 mm Hg) (Segal, 2005). Tendo em conta os valores normais de PAM periférica (≈80 mm Hg), podemos aproximar a fórmula de tal modo que $\dot{Q} \cong \frac{PAM}{R}$ para a circulação periférica geral (Klabunde, 2011).

Por seu turno, os determinantes da R são explicados pela lei Hagen-Poiseuille, $R = \frac{8 \times L\eta}{\pi \times r^4}$, onde L é o comprimento do vaso, η a viscosidade do sangue e r o raio da seção transversal do vaso. Daqui se percebe a importância fulcral dos vasos de resistência, nos quais pequenas variações do seu diâmetro modificam exponencialmente o fluxo sanguíneo no órgão que nutrem.

Não obstante ao que já foi dito, são necessárias algumas precauções no estudo do FSC ($\dot{Q}\ cerebral$). Em primeiro lugar, a PAM geralmente é medida com o referencial ao nível do coração (aurícula direita). Se o indivíduo estiver em posição supina, esta também será próxima do valor do cérebro. Contudo, à medida que nos levantamos, vai aumentando a distância entre cérebro e coração e o gradiente de pressão ortostática na mesma proporção. Chegando à posição ortostática, há uma diferença, em média, de 15-20 mm Hg, mas que varia de indivíduo para indivíduo, entre a PAM a nível craniano e a PAM medida ao nível do coração (Figura 5). Em segundo lugar, a circulação intracraniana tem um carácter especial, em que o órgão perfundido está dentro de um crânio rígido banhado no líquido cefalorraquidiano (LCR). Assim, a pressão do LCR, i.e., a pressão intracraniana (PIC), que normalmente se situa entre 0 e 15 mm Hg, pode dominar e substituir a pressão venosa em ΔP. Em condições não invasivas, não temos acesso a este valor, pelo que é ignorado na fórmula de cálculo do FSC. Mas, em certas situações fisiológicas ou patológicas, a PIC poderá atingir valores superiores a 30-40 mm Hg e alterar significativamente os parâmetros a ter em conta na fórmula. Exemplo disso é o que sucede na manobra de Valsalva, que exige um aumento transitório de PIC ≈20 mm Hg em relação à normalidade. A omissão deste valor poderá dar valores de R erróneos e até contraditórios do que se esperaria em termos fisiológicos, tal como demonstrado na Figura 6. Assim, na circulação cerebral geralmente devemos, sempre que possível, considerar a $PPC = PAM - PIC$, pelo que $FSC = \frac{PPC}{R}$. Geralmente, o valor de PIC apenas está disponível em regime de cuidados intensivos (Dias, 2014) não havendo método válido para o calcular de modo não invasivo.

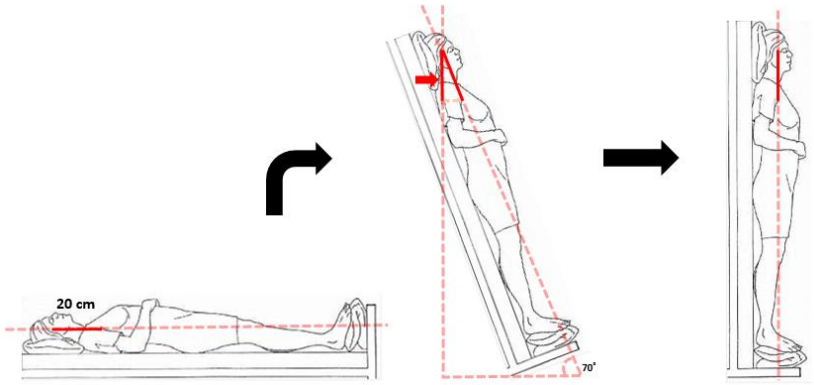

Figura 5 – Estimativa da pressão arterial a nível craniano
Exemplificação do cálculo da pressão arterial média (PAM) a nível da artéria cerebral média (ACM) a partir da PAM medida ao nível do coração (e.g., Finometer® com corretor de altitude ou braço colocado ao nível do coração). Assumamos $PAM = 100\ mm\ Hg$. A distância entre a ACM e o 2º espaço intercostal (aurícula direita) é de cerca de 20 cm. Em decúbito dorsal, a ACM está ao nível do coração, ou seja, a PAM é semelhante. Após levantar a 70˚ numa mesa basculante, a altura da coluna de pressão hidrostática (seta vermelha, cm H_2O) entre a ACM e o coração pode ser estimada pela fórmula. $cos\ 70^{\circ} \times 20\ cm$. Convertendo cm H_2O em mm Hg ($\times 0{,}735$), obtemos o valor a subtrair à PAM (coração) para estimar o seu valor a nível da ACM (66 mm Hg). Em posição ortostática, este diferencial é $20\ cm \times 0{,}735 = 14{,}7\ mm\ Hg$ e, por isso, a PAM ao nível da ACM é de 65 mm Hg.

Modelos de resistência vascular cerebral

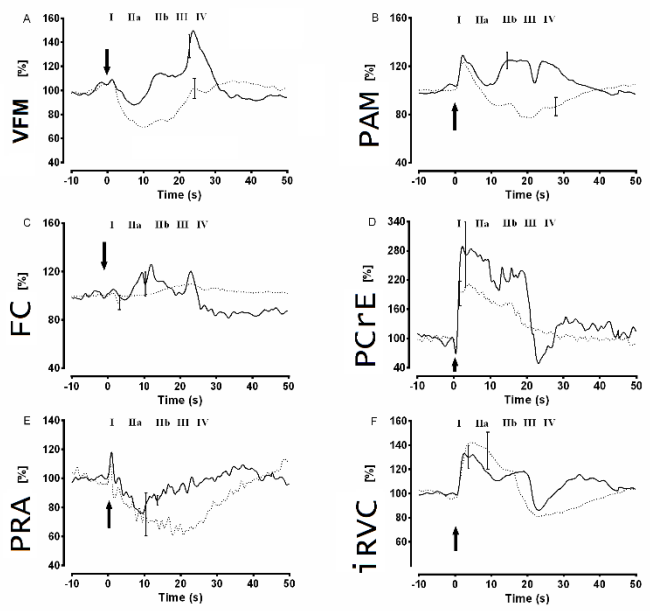

Figura 6 – Modelos de resistência vascular cerebral durante a manobra de Valsalva Durante a manobra, há diminuição da pressão de perfusão e vasodilatação cerebral compensatória. Na figura 8F podemos verificar que o índice de resistência cerebral (iRVC = PAM/VFM) aumenta durante a prova, sugerindo, paradoxalmente, vasoconstrição cerebral. No entanto, quando utilizamos o modelo dual, verificamos que a pressão crítica de encerramento (PCrE) aumenta em função da pressão intracraniana. Retirado este efeito, o valor de produto resistência-área (PRA) mostra uma redução durante a prova, de acordo com vasodilatação fisiológica. VFM, Velocidade de fluxo (sanguíneo cerebral) médio; PAM, pressão arterial média. *Adaptado de Castro et al., 2014.*

Na Figura 6 podemos apreciar vários modelos de cálculo de resistência vascular. Antes de prosseguir, é necessário esclarecer que o FSC geralmente é aproximado pela velocidade de FSC (VFSC), já que o método mais comum para o determinar é o Doppler transcraniano (DTC). Os princípios e limitações do DTC serão explicados nas secções subsequentes (*"Doppler transcraniano"*). Neste caso, calculámos o valor de resistência cerebral como um índice, usando os valores da PA média (PAM), em mm Hg, e de VFSC média (VFM), em cm.s^{-1}: $iRVC = \frac{PAM}{VFM}$. Um aumento do iRVC, expresso em *mm Hg.cm^{-1}.s^{-2}*, traduzirá vasoconstrição cerebral e a sua diminuição, uma vasodilatação. Mas, tal como podemos ver na Figura 6, nem sempre o iRVC é o esperado do ponto de vista fisiológico. Nesse sentido, Panerai (Panerai, 2003) desenvolveu um modelo de vasomotricidade assente em dois parâmetros, introduzindo o conceito de pressão crítica de encerramento cerebral (PCrE) e de produto resistência-área (PRA) da circulação cerebral. A PCrE é o valor de PA para a qual a VFSC atinge 0 cm.s^{-1} e aproxima-se de≈30 mm Hg (Panerai, 2003). O método de cálculo da PCrE está evidenciado na Figura 7 tendo sido introduzidas algumas modificações posteriormente para cálculos mais precisos (Panerai et al., 2011). A partir da PCrE podemos estimar o PRA: $PRA = \frac{PAM-PCrE}{VFM}$. Retirando o fator da PCrE da fórmula geral de resistência, o PRA poderá traduzir com maior aproximação o valor do estado vasomotor dos vasos de resistência (Carey et al., 2001, Castro et al., 2014). A PCrE é mais sensível aos fatores metabólicos e pressão intracraniana (Panerai, 2003, Panerai et al., 1995), sendo que

o PRA varia mais consistentemente em função de respostas de índole miogénica (Maggio et al., 2013, Azevedo et al., 2011, Carey et al., 2001, Panerai, 2003, Panerai et al., 2012).

Quais são os vasos de resistência cerebral?

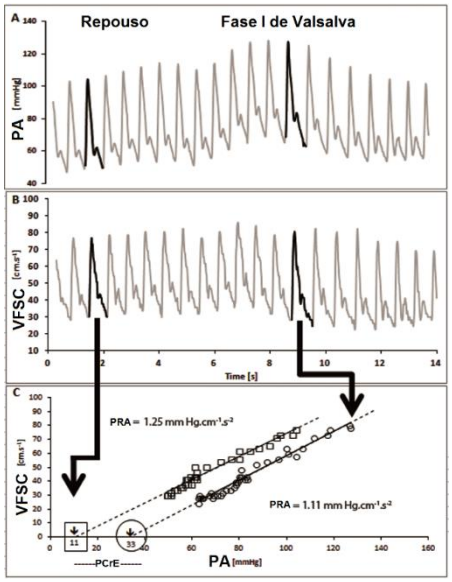

Figura 7 – Cálculo de pressão crítica de encerramento e produto resistência-área Na passagem da posição de repouso para o início (fase I) da manobra de Valsalva, verificamos aumento da pressão crítica de encerramento (PCrE). Para cada ciclo cardíaco, representamos graficamente a relação entre pontos amostrais da velocidade de fluxo sanguíneo cerebral (VFSC) e da pressão arterial (PA). O ponto onde a reta de regressão linear intercepta o eixo das abcissas representa o valor teórico de PA para o qual a VFSC cessa (colapso vascular). Este valor corresponde a PCrE. O inverso da inclinação da reta permite estimar o valor de PRA. *Adaptado de Castro et al., 2014.*

Os vasos de resistência são geralmente as pequenas artérias e arteríolas com diâmetro <100 µm que nutrem um determinado órgão (Segal, 2005, Johnson, 1981). Tal como evidenciado na Figura 4, estas apresentam uma parede constituída por 3 camadas concêntricas: a túnica íntima, constituída por uma camada simples de células endoteliais e uma lâmina elástica interna; a túnica média, constituída por células muscular lisas, algumas fibras de colagénio e elastina; e a túnica adventícia, mais exterior, constituída por fibras de tecido colagénio e fibroblastos (Segal, 2005). A nível cerebral, a observação da vasodilatação ou vasoconstrição sobre a superfície cortical em resposta a estímulos pressóricos fez perdurar o dogma, por mais de 70 anos, de serem as artérias piais os únicos efetores da regulação do fluxo cerebral (Fog, 1937, Fog, 1938, Forbes, 1928). Esta visão, que continua a ser aceite pela maioria dos autores atuais (Panerai, 2003, Serrador et al., 2000, Claassen et al., 2016, Segal, 2008), começa a ser posta em causa por outros (Hall et al., 2014, Willie et al., 2012).

Na circulação cerebral, as artérias de maior calibre, extra e intracranianas, poderão contribuir de modo não desprezível para a resistência vascular cerebral. Willie et al. (Willie et al., 2012) mostraram que a ACI e a artéria vertebral em humanos podem variar o seu fluxo ≈25% durante a hipercapnia e hipoxia extremas (Willie et al., 2012). Este papel vasomotor dos grandes vasos cerebrais já tinha sido avançado por McHedlishvili 60 anos antes, embora somente reconhecido

mais tarde (McHedlishvili et al., 1973, McHedlishvili, 1980). McHedlishvili mediu diretamente o gradiente de pressão ao longo da vasculatura cerebral de animais, sugerindo que as artérias de grande calibre, inclusive as ACI e vertebrais cervicais, poderão contribuir para cerca de um 1/3 da resistência vascular cerebral total em igual medida que os vasos piais (Heistad et al., 1978, Faraci & Heistad, 1990). Somos levados a pensar que toda a árvore vascular cerebral poderá contribuir para um sistema de resistência "protetor" pré-cerebral, que se torna ativo face a mudanças extremas de parâmetros fisiológicos e que as artérias maiores não serão apenas condutos rígidos. No entanto, durante variações de dióxido de carbono (CO_2) próximas de variações fisiológicas ou das usadas em teste de inalação do carbogénio, não parece haver uma variação de diâmetro significativa (Serrador et al., 2006).

Outra corrente atual centra-se na rede capilar (Hall et al., 2014). A constatação de que os pericitos são células musculares lisas despertou a curiosidade e construção de um modelo alternativo de resistência vascular da responsabilidade dos capilares cerebrais de primeira e segunda ordem (Hall et al., 2014). No entanto, esta modulação refere-se sobretudo ao aumento de FSC causado pela atividade neuronal, não contradizendo o facto das pequenas arteríolas controlarem o FSC global.

Reiterando, quais os vasos e em que proporção estes contribuem para a resistência vascular cerebral ainda não é um assunto encerrado. Mas qualquer que seja a visão adotada, não podemos ignorar que o cérebro goza de alguma excentricidade no controlo vascular: alguma resistência pode ser efetuada a nível de grandes vasos e capilares e, mesmo os vasos piais e arteríolas, classicamente tidos como os principais agentes vasomotores, encontram-se no exterior do parênquima do órgão que nutrem, o que não se verifica nos demais órgãos do corpo humano nos quais a vasculatura de resistência jaz junto dos mesmos.

Mecanismos de regulação vascular cerebral

A característica fundamental dos vasos de resistência e que determina a sua função, são as células musculares lisas. Prova disso é que, mesmo que sejam removidos o endotélio e a adventícia, os vasos mantêm um estado de contração constante que designamos por tónus vascular (Busija & Heistad, 1984). Acredita-se que seja o resultado da resistência ativa das células musculares lisas ao estiramento provocado pela PA contínua, embora possam contribuir fatores vasomotores de origem endotelial (Segal, 2005).

É sobre este tónus basal que vários fatores externos exercem os seus efeitos, balanceando entre um estado de vasoconstrição ou de vasodilatação, de modo a permitir que cada órgão possa

suprimir as suas necessidades metabólicas correntes e, ao mesmo tempo, consiga reagir a estímulos exteriores que perturbam a homeostasia cerebral. Estas influências poderão ser separadas em 4 categorias básicas: metabólicas, endoteliais, miogénicas e neurogénicas.

Metabólicas

As células musculares lisas que formam a parede das arteríolas perfurantes e pericitos dos capilares ficam expostas à composição química do fluído intersticial cerebral. A sua composição resulta do balanço entre a atividade metabólica neuronal e o suprimento sanguíneo (Segal, 2005). A atividade neuronal leva a uma degradação de adenosina trifosfato (ATP) e à produção e libertação local de adenosina, um potente vasodilatador (Brundege & Dunwiddie, 1997). Adicionalmente, também baixa a pressão parcial de oxigénio tecidular e arterial (PaO_2), ao mesmo tempo que aumenta a pressão parcial de CO_2 ($PaCO_2$) e diminui o pH (Segal, 2005). Todos estes produtos metabólicos causam vasodilatação ativa, que se traduz por um aumento compensatório do FSC local (Segal, 2005), até que se atinja novo ponto equilíbrio (Figura 8).

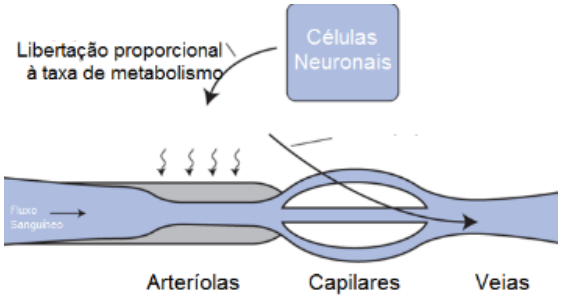

Figura 8 – Teoria metabólica geral da regulação do fluxo sanguíneo
Sempre que o metabolismo aumenta numa proporção superior à do suprimento sanguíneo, os metabolitos vasodilatadores acumulam e promovem a vasodilatação arteriolar. Consequentemente, haverá um aumento de fluxo, que escoará mais rapidamente esses metabolitos. Este sistema de retroatividade mantém-se até que sejam completadas as necessidades metabólicas do órgão.

Em contexto experimental, podemos aumentar artificialmente o $PaCO_2$, pela inalação de CO_2, que, lembremo-nos, atravessa livremente a BHE. Os vasos cerebrais são extremamente sensíveis ao $PaCO_2$, podendo aumentar o seu fluxo em 40% por inalação de gás com CO_2 a 5% (Castro et al., 2014). Por outro lado, a descida de $PaCO_2$ (i.e., induzida pela hiperventilação), pode reduzir em igual grandeza e em segundos o FSC (Castro et al., 2014). Esta última, ao produzir vasoconstrição cerebral intensa, pode levar à diminuição do fluxo ao ponto de causar sintomas pré-sincopais (Carey et al., 2001, Van Lieshout et al., 2003). O facto de as artérias vertebrais serem mais sensíveis à hipocapnia (Willie et al., 2012), conjugado com o menor calibre das ACP, pode explicar a predominância de sintomas de índole vertebrobasilar com redução momentânea do FSC global (Freitas, 2010).

A descida de PaO_2 também é um estímulo vasodilatador, mas apenas demonstrável em condições experimentais altamente controladas e para valores de PaO_2 inferiores a 40-45 mmHg (Ainslie & Ogoh, 2010). Os seus efeitos vasodilatadores podem ser diretos ou mediados pela

libertação de adenosina, K+, ou NO (Segal 2008). Na prática, é difícil avaliar a resposta à hipoxia, já que, para atingir um limiar de PaO_2 que provoque vasodilatação, surge em igual medida uma vasoconstrição cerebral causada pela hiperventilação compensatória (Ainslie & Ogoh, 2010). Para tal, são necessários aparelhos de controlo ventilatório e de gases mais dispendiosos e complexos tal como o Respiract® (Robbins et al., 1982, Slessarev et al., 2007). Ainda assim, a resposta do FSC à hipoxia pode ser relevante fisiológica e clinicamente em atletas de alta competição, efeitos da altitude elevada, doenças crónicas pulmonares e disfunção cardíaca (Galvin et al., 2010, Ainslie & Duffin, 2009, Ainslie & Ogoh, 2010). De seguida descrevem-se aspetos especiais da resposta metabólica local que ocorre em órgãos com taxas metabólicas elevadas.

Hiperémia ativa ou funcional

Este conceito refere-se ao fenómeno de aumento do fluxo sanguíneo regional em determinado órgão em virtude de este estar metabolicamente mais ativo. Um exemplo simples pode verificar-se durante o exercício dinâmico do músculo esquelético (Figura 9). O acoplamento temporal entre irrigação arterial e trabalho muscular é extraordinário: alguns segundos após o início do exercício, o fluxo sanguíneo aumenta rapidamente, retornando a valores basais pouco tempo depois de a atividade cessar. Para além dos fatores metabólicos locais, também participam o endotélio e o músculo liso ao propagarem o estímulo vasodilatador às artérias a montante (Segal, 2005, Shoemaker et al., 1996).

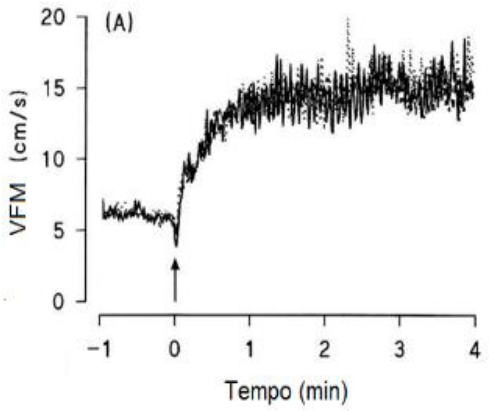

Figura 9 – Hiperémia ativa
Exercício manual durante 4 minutos que consistia em levantar um peso correspondente a 8-12% da capacidade de força muscular máxima. Medição da velocidade de fluxo média (VFM) da artéria braquial com eco-Doppler. *Adaptado de Shoemaker et al., 1996.*

No caso do cérebro, a hiperémia ativa reveste-se de especial complexidade dadas as particularidades de funcionamento e especialização territorial do tecido cerebral. A unidade neurovascular (ver secção *"Microcirculação cerebral e unidade neurovascular"*) assegura o FSC local, e este acoplamento adapta o fluxo regional às necessidades metabólicas e atividade de determinada área cortical (Iadecola, 1993). Tal como descrito previamente, nesta participam neurónios, astrócitos e vasos sanguíneos cerebrais, configurando uma unidade integrada de distribuição do FSC local. O modo como se processa essa ativação está descrito na Figura 4. Na

secção "*Acoplamento neurovascular*", vamos encontrar vários aspetos demonstrativos de como o podemos avaliar e que tipo de curva de FSC é gerada.

Endoteliais

As células endoteliais exercem uma ação contínua sobre o tónus vascular (Ozkor & Quyyumi, 2011). A sua importância pode ser facilmente entendida ao remover o endotélio em contexto experimental (Andresen et al., 2006). Vejamos aqui o exemplo da ação da acetilcolina: com endotélio intacto provoca vasodilatação, mas na sua ausência provocará vasoconstrição marcada (Edvinsson et al., 1977). Esta resposta paradoxal resulta do facto de a acetilcolina poder atuar diretamente nos recetores muscarínicos M3 do músculo liso vascular (Harvey, 2012), causando aumento do Ca^{2+} intracelular e contração do mesmo. No entanto, num vaso completo e em condições fisiológicas, a acetilcolina ativa avidamente os recetores muscarínicos endoteliais, levando à produção de NO que difunde para o músculo liso subjacente, iniciando o seu relaxamento (Furchgott & Zawadzki, 1980). Os vasos cerebrais parecem mediar a resposta especificamente pelos subtipos M5 (Yamada et al., 2001) ao contrário dos M3 vasculares periféricos (Beny et al., 2008). Outros exemplos de mecanismos vasodilatadores com origem endotelial são explorados no esquema da Figura 10.

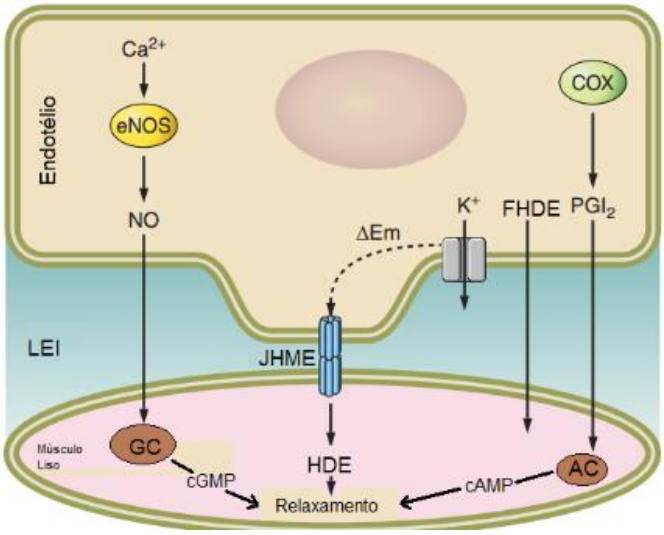

Figura 10 – Vasodilatação dependente do endotélio
Nas células endoteliais, o influxo de cálcio (Ca^{2+}) estimula a atividade da sintetase (eNOS do monóxido de azoto [NO]). O NO produzido difunde-se livremente pela lâmina elástica interna (LEI), onde atua no músculo liso, potenciando a atividade da guanil ciclase (GC) e aumentando o guanil monofosfato cíclico (cGMP). Também o aumento da atividade da cicloxigenase (COX) promove o relaxamento via adenil ciclase (AC) e a produção de adenosina monofosfato cíclica (cAMP). Um conjunto de substâncias solúveis, coletivamente reconhecidas como *fator de hiperpolarização derivado do endotélio* (FHDE), promove o relaxamento muscular, em parte, pelo efluxo de potássio (K+) do endotélio e diminuição do potencial de membrana (ΔEm). Por fim, o alastramento deste potencial pelas junções de hiato mioendoteliais (JHME) incrementa o relaxamento do músculo liso, fenómeno não humoral apelidado de *hiperpolarização derivada do endotélio* (HDE), para de diferenciar do FHDE. *Adaptado de Earley & Brayden, 2015.*

O NO, produzido a partir de L-arginina, difunde-se livremente para o músculo liso, onde promove o relaxamento ao aumentar a guanil monofosfato cíclica (cGMP) (Faraci & Brian, 1994). Esta é a via comum onde converge a ação de vários agentes vasodilatadores, tais como ATP, adenosina, peptídeo intestinal vasoativo e substância P (Edvinsson et al., 1985, Andresen et al., 2006).

Outros mecanismos de vasodilatação são as prostaglandinas e um coletivo de agentes ainda mal esclarecidos designados por fator de hiperpolarização dependente do endotélio (Andresen et al., 2006, Ozkor & Quyyumi, 2011). Mais ainda, existe uma produção basal de NO que contribui continuadamente para o estado do tónus vascular basal, fenómeno dependente do aumento de Ca^{2+} no endotélio causado pelas forças de cisalhamento (Faraci & Brian, 1994).

O endotélio também produz potentes agentes vasoconstritores como a entotelina-1 (Andresen et al., 2006). A nível cerebral, tal é a potência da sua ação, que esta é usada em modelos de isquemia cerebral em laboratório (Roulston et al., 2008). Curiosamente, também parece estar aumentada no AVC isquémico (Ziv et al., 1992). A ação do endotélio pode ser testada e demonstrada no teste de hiperémia reativa.

Hiperémia reativa

A hiperémia reativa é o termo usado para descrever o aumento temporário do fluxo sanguíneo, para além do valor basal, que surge após um período de oclusão arterial (Brier, 1897). É um fenómeno indubitavelmente dependente da ação vasodilatadora do endotélio (Pohl et al., 1986, Olesen et al., 1988, Sun et al., 1999). Por conseguinte, foram desenvolvidos métodos para avaliar o estado da função endotelial baseada na resposta à oclusão arterial temporária, que doravante se designou por *"dilatação mediada pelo fluxo"*. O método mais comum, e não invasivo, tem sido através da ultrassonografia da artéria braquial tal como demonstrado na Figura 11. Uma resposta inadequada do tipo da dilatação mediada pelo fluxo poderá estar subjacente à lesão de reperfusão que surge após a recanalização da oclusão arterial aguda sobre o tecido cerebral enfartado, tornando-se deletéria ao induzir excitotoxicidade e edema cerebral (Nour et al., 2013). É, por isso, apropriadamente designada de perfusão luxuriante (Kunz & Iadecola, 2009).

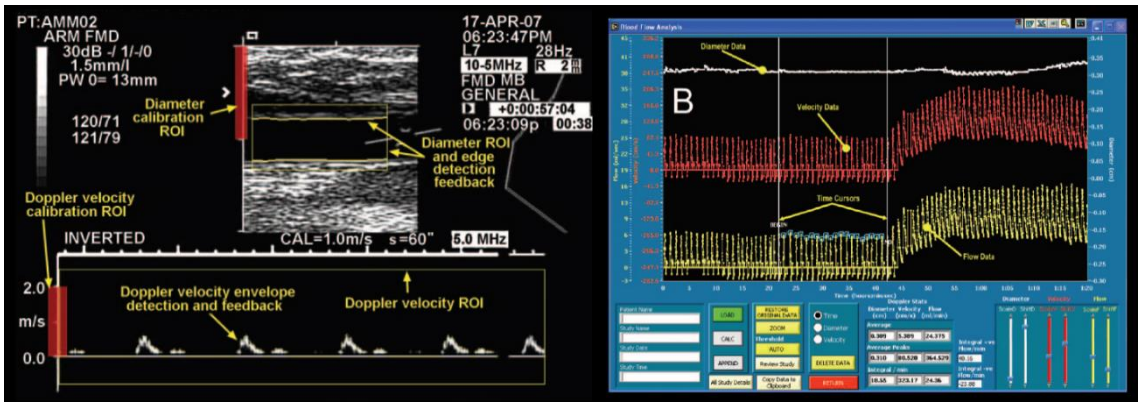

Figura 11 – Teste de hiperémia reativa
A artéria braquial é avaliada continuamente quanto ao seu calibre e velocidade de fluxo por eco-Doppler. Cerca de 60s após a oclusão do braço, atinge-se o pico de aumento do fluxo conforme se observa em **B**. A dilatação mediada pelo fluxo corresponde à variação percentual do calibre em relação ao valor basal e é tida como índice de função endotelial. *Adaptado de Black et al., 2008.*

Miogénicas

A adaptação do calibre arterial em reação a variações de pressão transmural foi descrita pela primeira vez em 1902 por Bayliss (Bayliss, 1902). Esta resposta miogénica (Figura 12) está presente em vários leitos vasculares (Davis, 2012) e explica o facto de o aumento da PA provocar vasoconstrição e da sua redução despertar uma resposta vasodilatadora. É da responsabilidade dos vasos de resistência e de efeito extraordinariamente potente a nível das artérias piais cerebrais (Osol et al., 1991, Osol et al., 2002) quando comparado com outros sistemas periféricos (Schubert & Mulvany, 1999).

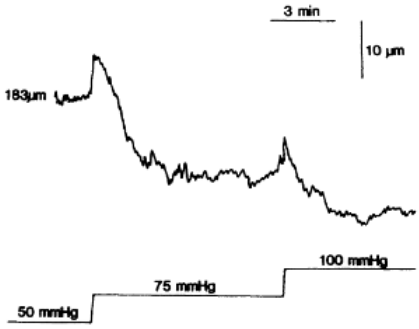

Figura 12 – Resposta miogénica vascular cerebral
Um degrau de aumento da pressão intraluminal provoca, após uma dilatação transitória, uma redução persistente do calibre do vaso pial cerebral em relação ao basal. Um maior aumento da pressão provoca um novo ajuste inferior do calibre. *Adaptado de Osol et al., 1991.*

É uma reação intrínseca do músculo liso vascular, ocorrendo mesmo que o endotélio ou inervação perivascular sejam removidos (Busija & Heistad, 1984). Para o sucesso da resposta miogénica é crucial a mobilização intracelular de Ca^{2+} provocada pela ativação dos recetores do músculo liso mecano-responsivos em resposta ao estiramento vascular (Knot & Nelson, 1998, Schubert et al., 2008, Hill et al., 2001). Os mecanismos moleculares envolvidos estão detalhados na Figura 13. Na Figura 14 podemos verificar que a resposta miogénica adapta o calibre vascular e, inerentemente o fluxo sanguíneo, mas apenas dentro de certos limites de PA.

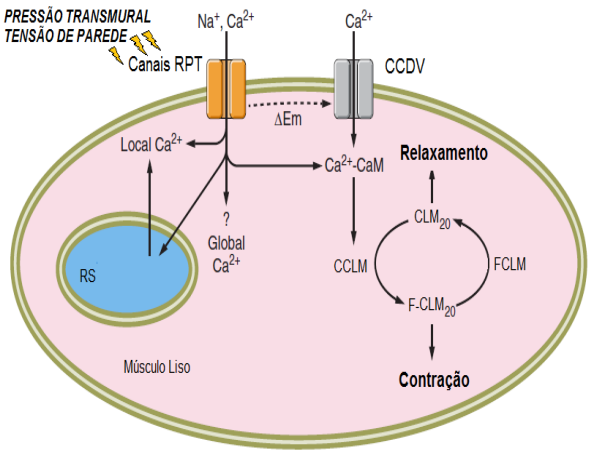

Figura 13 – Mecanismos celulares envolvidos na resposta miogénica
Os canais iónicos do tipo Recetores de potencial transitório (RPT) atuam como mecanotransdutores, respondendo ao estiramento da parede do vaso e despolarizando a membrana (ΔEm). Os próprios RPT e os Canais de Cálcio dependentes da Voltagem (CCDV), entretanto ativados, promovem o influxo de Ca^{2+} e a sua mobilização intracelular a partir do Reticulo sarcoplasmático (RS). O aumento de Ca^{2+} e do complexo Ca^{2+}-calmodulina (CaM), assim como a produção de metabolitos do ácido araquidónico (e.g., 20-HETEs) pela fosfolipase A2, levam a ativação da cínase (CCLM) da cadeia leve da miosina (CLM_{20}), que no estado de fosforilação ($F\text{-}CLM_{20}$) resulta em encurtamento da fibra muscular lisa e vasoconstrição. *Adaptado de Earley & Brayden, 2015.*

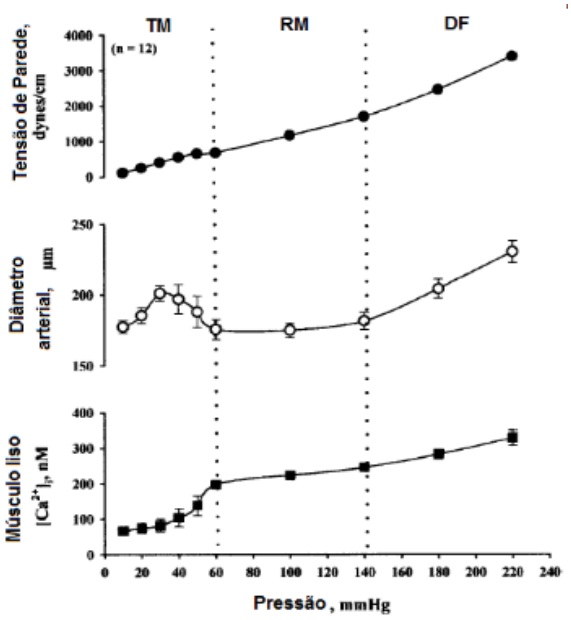

Figura 14 – Tensão de parede e calibre arterial em função da pressão endoluminal Gráfico que sumariza três estádios diferentes de regulação miogénica em ramos da artéria cerebral posterior. Na fase de tónus miogénico (TM), à medida que a pressão arterial desce a partir do 60 mm Hg, ocorre diminuição do cálcio (Ca^{2+}) intracelular e vasodilatação até ao colapso vascular. Entre valores de pressão de 60 a 140 mm Hg, ocorre regulação miogénica (RM) com ajuste do calibre arterial e regulação do Ca^{2+} apesar da tensão arterial crescente. Na subida extrema da pressão intraluminal ocorre falha da resposta miogénica e surge uma (vaso)dilatação forçada (DF). *Adaptado de Osol et al., 2002.*

Esta questão da manutenção homeostática do fluxo sanguíneo face a variações de PA, dentro de certos limites, introduz-nos o conceito de autorregulação. Descrito em vários leitos vasculares (Aaslid et al., 1989, Carlstrom et al., 2015, Davis, 2012, Johnson, 1986, Lassen, 1959), a autorregulação assegura pois um fluxo sanguíneo constante e independente das variações de PA.

Autorregulação cerebral

A hipótese de existir ARC em humanos foi avançada, pela primeira vez, por Niels Lassen em 1959 (Lassen, 1959) (Figura 15). Dentro de uma gama relativamente ampla da PA, entre 50 a 150 mm Hg de PAM, a alteração do fluxo cerebral será insignificante se a ARC estiver preservada (Strandgaard & Paulson, 1984, Paulson et al., 1990). A Figura 16 pretende mostrar de forma esquematizada essa adaptação. O principal mecanismo ativo neste processo é a resposta miogénica. Ainda assim, fenómenos metabólicos locais poderão contribuir para a resposta vasoconstritora, dado que o aumento instantâneo de fluxo promove uma lavagem dos metabolitos

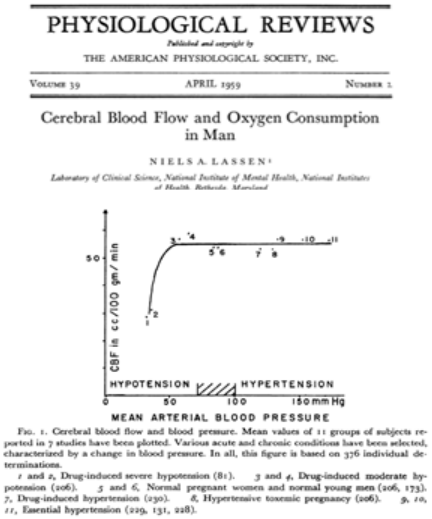
PHYSIOLOGICAL REVIEWS

THE AMERICAN PHYSIOLOGICAL SOCIETY, INC.

Cerebral Blood Flow and Oxygen Consumption in Man

NIELS A. LASSEN

CBF in cc/100 gm/min

HYPOTENSION HYPERTENSION

MEAN ARTERIAL BLOOD PRESSURE

Figura 15 – Artigo seminal de Lassen. Publicação de Niels Lassen onde se comparam os diferentes estudos de manipulação de pressão arterial com as medições do fluxo sanguíneo cerebral em humanos. Esta relação ficou conhecida como *"Curva de Lassen"*. *Em Lassen, 1959.*

vasodilatadores (K+, CO_2, ATP) e consequente redução do calibre arterial (Czosnyka et al., 1999). Na Figura 14 é bem evidente este controlo ativo miogénico. A ARC é um processo adaptativo relativamente rápido, visível em cerca de 3-10 segundos em relação à variação de PA (Aaslid et al., 1989).

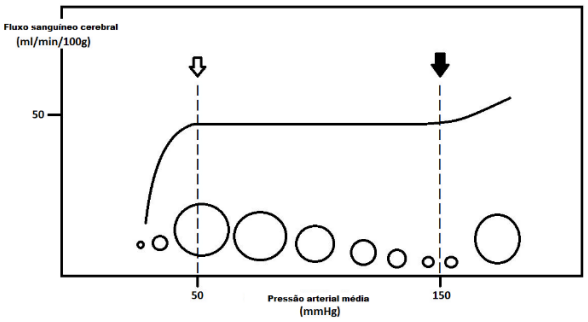

Figura 16 – Modelo teórico de autorregulação cerebral
Baseado em Azevedo e Castro, 2016.

Neurogénicas

Na secção *"Inervação perivascular cerebral",* ficou claro que os vasos cerebrais são densamente inervados por fibras autonómicas e trigeminais, assim como por axónios prevenientes de um conjunto vasto de neurónios intracerebrais. Nos próximos parágrafos descrevem-se sucintamente esses efeitos.

Apesar de alguma controvérsia (van Lieshout & Secher, 2008), os estudos efetuados por bloqueio ganglionar parecem corroborar a tese de que o SNA tem alguma importância na regulação do FSC face a variações hemodinâmicas intensas (Zhang et al., 2002, Willie et al., 2014). O SNA poderá ser igualmente importante para o controlo de fenómenos mais subtis como a hiperémia funcional (Azevedo et al., 2011) e na resposta à hipertensão intracraniana (Castro et al., 2014).

Em investigação animal, a excisão do gânglio pterigopalatino provocou uma redução da perfusão cerebral, sem influência na pressão PA (Boysen et al., 2009), facto que realça a influência vasodilatadora parassimpática nos vasos cerebrais. Hoje em dia, levanta-se a hipótese de se estimular o gânglio pterigopalatino como proteção contra a isquemia no AVC (Oluigbo et al., 2011). No caso da enxaqueca, parece haver um reflexo trigémino-autonómico que promove a vasodilatação cerebral pelo parassimpático (Amin et al., 2013).

A relação entre ARC e SNA simpático tem resultados muito díspares na literatura (van Lieshout & Secher, 2008, Ogoh, 2008). Uma revisão dos estudos mostra grande heterogeneidade e dificuldade de discernir os efeitos do simpático das variações de PA ou de CO_2 (Willie et al., 2014). Os estudos com bloqueio da cadeia do simpático cervical (Jeng et al., 1999, Umeyama et al., 1995, Nitahara & Dan, 1998, Shenkin et al., 1951) sugerem a existência de uma ação do simpático sobre o tónus vascular cerebral, já que parece haver um aumento do FSC após a intervenção. O bloqueio ganglionar com trimetofano parece conferir uma menor capacidade de ARC (Zhang et al., 2002) e incapacidade de controlo da hiperémia cerebral que sucede à manobra de Valsalva (Zhang et al., 2004a). O SNA simpático parece também ser relevante para

controlar a vasodilatação cerebral durante a hipercapnia (Jordan et al., 2000). Contudo, a relevância do simpático dentro de condições fisiológicas é questionável. Por exemplo, o bloqueio simpático com beta-agonista ou a sua ativação pelo exercício (Ogoh et al., 2007) parece não afetar a controlo do FSC. Mais ainda, o SNA simpático parece não ser o responsável por manter a vasoconstrição cerebral associada ao ortostatismo (Zhang & Levine, 2007), que sabemos ser um potente ativador do simpático (Freitas et al., 2007). Ainda assim, a modulação da ARC é feita de modo diferente entre indivíduos saudáveis e outros com disautonomia (Castro et al., 2014). Há também evidência de que os núcleos subcorticais interferem no tónus vasomotor. Assim, a estimulação do núcleo basal promove vasodilatação via acetilcolina/NO (Yamada et al., 2001, Elhusseiny & Hamel, 2000), o núcleo *locus coeruleus* vasoconstrição via noradrenalina (Mulligan & MacVicar, 2004) e os núcleos da rafe (serotonina) promovem vasodilatação ou vasoconstrição conforme a zona do tronco cerebral ativa (Cohen et al., 1996). Por fim, ressalva-se o papel relevante dos interneurónios corticais GABAérgicos no controlo dinâmico vasomotor durante o processo de hiperémia funcional (Cauli et al., 2004).

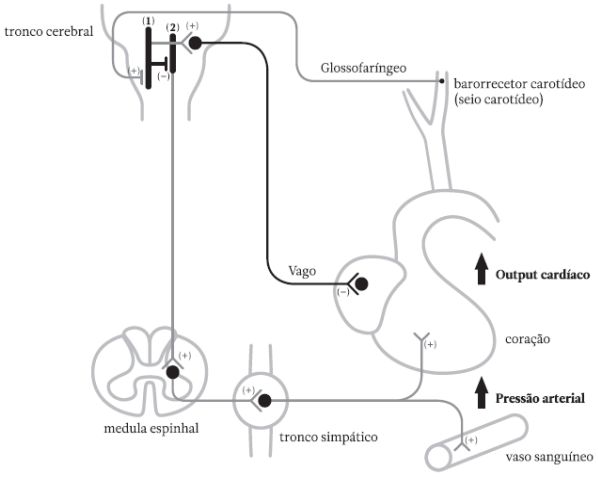

Figura 17 – Reflexo de barorrecetor arterial
O aumento de pressão arterial provoca uma resposta a nível dos barorrecetores arteriais (seio carotídeo, arco aorta), cuja informação é levada ao núcleo do feixe solitário (1). Este promove uma resposta dual: estimulação do centro cardioinibitório do núcleo ambíguo (2), que atua pelo nervo vago; e inibição da porção caudal da VLM. Esta mantém, normalmente, uma excitação tónica sobre a parte rostral da mesma, que, por sua vez, excita os neurónios da coluna intermediolateral do simpático medular. No seu conjunto, surge uma resposta de diminuição do crono e ionotropismo cardíaco e da pressão arterial. *Adaptado de Carvalho & Castro, 2013.*

Barorreflexo

O controlo neurogénico vascular sistémico tem a particularidade de recorrer a um conjunto de barorrecetores arteriais. O seio carotídeo e o arco aórtico apresentam terminais nervosos na sua parede provenientes dos nervos vago e glossofaríngeo e participam num arco barorreflexo (BR) relevante para o controlo da PA (Di Rienzo et al., 2001, Smyth et al., 1969). O circuito está detalhado na Figura 17, onde se percebe que um aumento da PA ativa o BR com consequente inibição do simpático e facilitação da atividade vagal, resultando em redução da resistência periférica e da PA (Carvalho & Castro, 2013).

MÉTODOS DE AVALIAÇÃO DO FLUXO CEREBRAL

Kety e Schmidt foram os primeiros a descrever um método de quantificação do FSC usando um gás inerte, neste caso o óxido nitroso (N_2O) (Kety & Schmidt, 1945). Este método baseia-se no princípio de Fick, no qual a diferença arteriovenosa de um gás inerte circulante é proporcional ao volume de fluxo sanguíneo que perfunde um órgão (Figura 18). O marcador difunde-se livremente no cérebro até atingir um ponto de saturação (equilíbrio) ao final de 10 minutos de infusão. A partir deste ponto, a concentração do marcador decresce exponencialmente até ao valor de zero (fase de dessaturação). Com amostras simultâneas, da artéria carotídea e da veia jugular interna, é possível calcular o FSC pela fórmula apresentada na Figura 18. Este princípio foi aplicado a outros marcadores como o ^{133}Xenon, o hidrogénio e a iodoantipirina (Edvinsson & Krause, 2002). A introdução de gases radioativos como o ^{133}Xénon permitiu alguma diferenciação regional a nível cerebral quando em co-registo com tomografia computadorizada (Edvinsson & Krause, 2002). Acrescenta-se a desvantagem do uso de radiação. Como se depreende do exposto, tratam-se de métodos morosos, com necessidade de cateterização invasiva e necessidade de compostos radioativos no caso do FSC regional. Além do mais, são estudos de FSC estáticos, não permitindo a avaliação da dinâmica temporal do FSC.

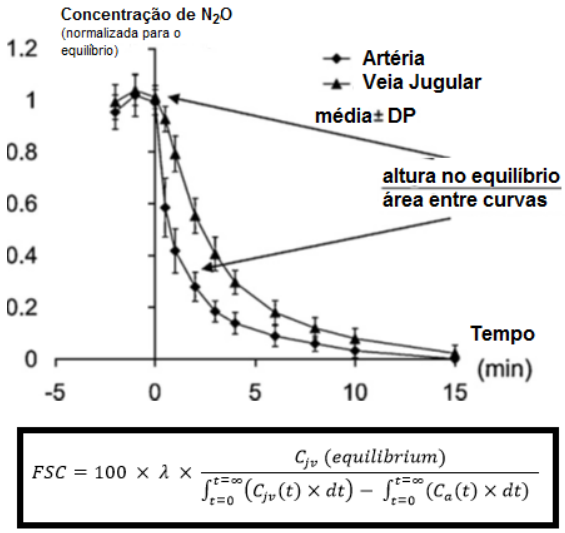

Figura 18 – Método de Kety-Schmidt
A $C_{jv}(t)$ e $C_a(t)$ são as concentrações do marcador na veia jugular e na artéria carótida interna, respetivamente, no tempo t (minutos), e λ é o coeficiente de partilha cérebro-sanguíneo (ml.g^{-1}). *Adaptado de Kety & Schmidt, 1945.*

A ultrassonografia havia então iniciado um processo revolucionário de translação dos laboratórios industriais para os corredores médicos, atribuindo-se esse feito ao génio do japonês Shigeo Satomura, em 1958 (Satomura, 1958). O seu co-investigador, Ziro Kaneko sugere, entusiasticamente, o seu uso para distinguir, entre os doentes demenciados, aqueles com patologia de Alzheimer dos que teriam alguma causa vascular (Kaneko, 1986). Contudo, as sondas de 3 MHz não podiam atravessar a barreia do osso craniano, que atenuava os ultrassons.

A orientalidade também barrara a difusão destes métodos à Europa e aos Estados Unidos da América (Coman & Popescu, 2015), onde as primeiras publicações para o estudo da doença vascular cerebral (Barber et al., 1974, Spencer et al., 1974, Reutern et al., 1976, Spencer, 1977) se registaram na década de 1970. Já a barreira física craniana, foi ultrapassada por Aaslid em 1982 (Aaslid et al., 1982). Para tal, Aaslid reduziu as frequências das sondas para cerca de 1-2 MHz e escolheu para locais de sondagem, ou janelas acústicas, as zonas menos espessas da calote craniana. Pela primeira vez, a VFSC pôde ser determinada continuamente, com uma resolução temporal de ≈5 milissegundos que ainda hoje é indestronável. Um ponto relevante para os trabalhos desta tese foi o facto de os testes de ARC baseados no DTC se mostrarem comparáveis aos das técnicas prévias de medição de FSC (Tiecks et al., 1995a). Atualmente, é possível estimar, de modo não invasivo, o FSC por ressonância magnética com maior detalhe espacial (Malojcic et al., 2017, Willie et al., 2011), nomeadamente através da técnica *arterial spin labeling* (Rocha et al., 2014). A ressonância magnética também pode ser utilizada para estimar a ARC, embora requeira manobras provocatórias (Saeed et al., 2011). No entanto, são técnicas dispendiosas, associadas a um rácio sinal-ruído reduzido e também limitadas ao material heterólogo paramagnético e à claustrofobia.

Doppler transcraniano

Princípios da ultrassonografia

O som é uma onda mecânica de pressão longitudinal que se caracteriza pela sua amplitude, frequência e comprimento de onda. O ouvido humano não é capaz de detetar as ondas com frequência superior a 20 KHz, motivo pelo qual as chamamos de ultrassons (Oláh, 2016). A possibilidade de podermos utilizar ultrassons deve-se à descoberta do efeito piezoelétrico de alguns cristais de quartzo pelos irmãos Curie, em 1880 (Curie & Curie, 1880). As sondas de ultrassonografia não são mais do que transdutores de energia elétrica em vibratória e vice-versa (Oláh, 2016). O uso dos ultrassons para medir a velocidade de fluxo baseia-se na aplicação do efeito de Doppler, inicialmente descrito em relação à luz emitida pelos corpos celestes em movimento por Christian Andreas Doppler, em 1843 (Doppler, 1843). Corresponde ao fenómeno de aumento ou diminuição das frequências emitidas ou refletidas por um objeto em movimento, quando este se aproxima ou afasta, respetivamente, de um recetor fixo (Figura 19). No caso da ultrassonografia, a sonda é, simultaneamente, o emissor e o recetor. Pode emitir ultrassons de forma contínua, mas o mais habitual é fazê-lo de modo intermitente (Doppler pulsado). No caso

da corrente sanguínea, este efeito permite estimar a velocidade de fluxo dos eritrócitos em movimento, pela fórmula $v = df \times \frac{c}{2} \times f(t) \times \cos\theta$, tal como explicado na Figura 19. Como se depreende da equação, é muito importante o controlo do ângulo de incidência do feixe de ultrassons sobre o vaso. Por exemplo, se o ângulo for de 90˚, não se consegue medir a velocidade, pois $\cos(90^{\circ}) = 0$. Assim, recomenda-se que o ângulo não exceda os 60˚ (Oláh, 2016). Para além de medir a velocidade de fluxo sanguíneo, a ultrassonografia também pode produzir imagens das estruturas anatómicas (ecografia), assim como codificar espacialmente a direção do fluxo (eco-Doppler codificado a cor).

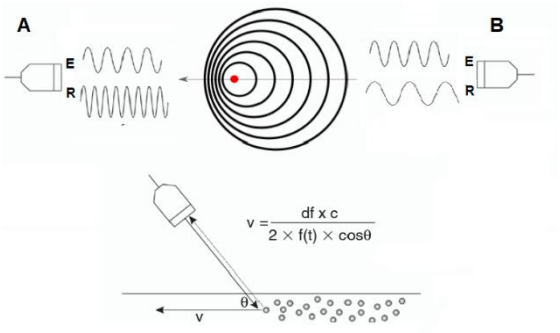

Figura 19 – Efeito de Doppler
A diferença entre a frequência emitida (**E**) por um transdutor e a refletida (**R**) pelo objeto em movimento corresponde a uma mudança de frequência (do termo inglês *Doppler shift*) que será proporcional à velocidade de movimento do mesmo. No caso do sangue, a velocidade dos eritrócitos pode ser estimada pela fórmula descrita onde v é a velocidade de fluxo sanguíneo, df é o desvio de frequência, c é a velocidade de propagação dos ultrassons no meio, $f(t)$ é a frequência transmitida pela sonda e θ é o ângulo de sondagem. No caso **A**, o objeto aproxima-se da sonda e a frequência de R > E, logo, o df é superior à da situação **B**, onde E > R, dado o afastamento do objeto. *Adaptado de Ólah, 2016.* .

Técnica de exame

Apesar de a ultrassonografia permitir a combinação da imagem anatómica em modo B e a velocidade de fluxo codificado a cor para orientação espacial, o DTC apenas produz os espectros de velocidade de fluxo que variam de acordo com o binómio direção da sonda/profundidade de sondagem. Um avanço subsequente foi a introdução de sondas compostas por vários canais de amostragem em paralelo e dirigidos a várias profundidades, permitindo a obtenção simultânea de múltiplos sinais de Doppler direcional ao longo de um tecido. Este modo, designado por *power-motion* ou *power-M*, na nomina inglesa, permite melhorar a acuidade e rapidez de localização dos vários segmentos arteriais e maior sensibilidade na deteção de microêmbolos (Moehring & Spencer, 2002).

A realização do DTC com sucesso depende da destreza técnica do operador, além do seu conhecimento da anatomia, fisiologia e patologia vascular cerebral. Os segmentos arteriais são identificados (1) pela orientação da sonda (2) pela profundidade selecionada e (3) pelo sentido de fluxo detetado (Arnolds & von Reutern, 1986, Bartels et al., 1995, DeWitt & Wechsler, 1988, Hennerici et al., 1987, Ringelstein et al., 1990). As principais janelas acústicas são a (1) temporal,

(2) a orbitária e (3) a suboccipital, cada uma acedendo a segmentos arteriais distintos (Titianova & Vastagh, 2016).

Janela temporal

Ao longo do osso temporal, podemos encontrar uma zona de sondagem mais anterior ou posterior, variável de pessoa para pessoa (Ringelstein et al., 1990b) (Figura 20). O local mais habitual, sobretudo nos mais idosos, é a janela posterior (Ringelstein et al., 1990b). Aqui a sonda é colocada sob a apófise zigomática e imediatamente anterior ao pavilhão auricular. Uma ligeira angulação antero-superior da mesma é necessária para registar o primeiro segmento arterial de referência que é o tronco (M1) da ACM a 50 mm de profundidade (Figura 21). Trata-se de um fluxo positivo, i.e., em direção à sonda, e com uma VFM de cerca de 60 cm.s^{-1}. Percorremos a ACM até aos 45-45 mm de profundidade, onde um fluxo bifásico marcará a sua bifurcação (M2). De seguida, voltamos até profundidades de 55-60 mm, até encontrar um fluxo bifásico da bifurcação de ACI com registo simultâneo da origem da ACM e da ACA. Esta última deve ser registada com sonda

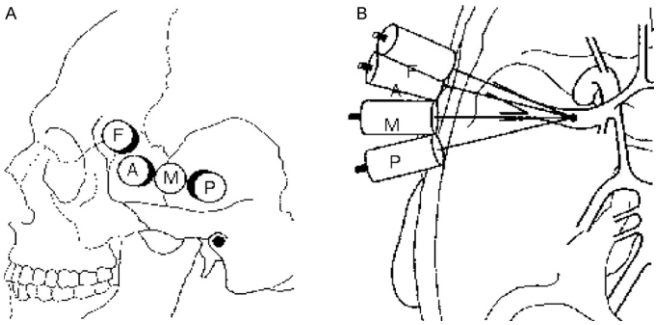

Figura 20 – Janela temporal
Posição esquemática das variantes da janela temporal em relação à posição média (M). Nos idosos, geralmente é mais posterior (P) e nos mais jovens a (F) e (A) podem ser mais acessíveis e com menor ângulo de erro em relação à artéria cerebral média. *Em Newell & Aaslid, 1992.*

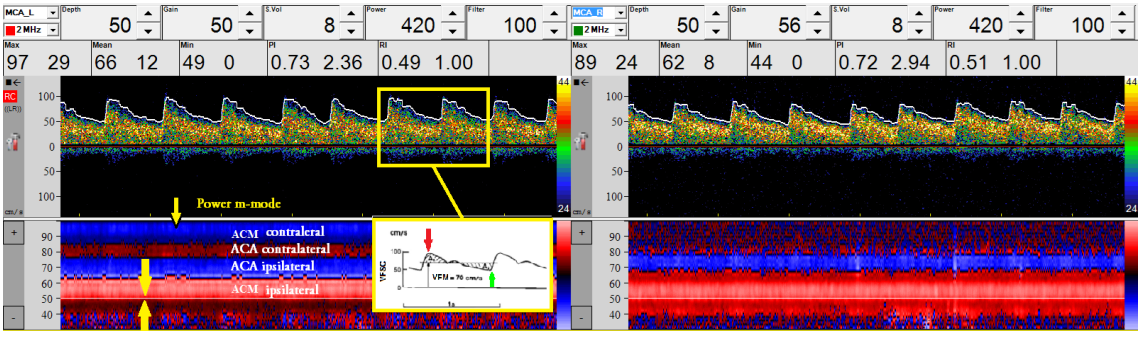

Figura 21 – Painel de monitorização do aparelho de Doppler transcraniano BoxX®
Nos painéis superiores observamos dois espectros (direito e esquerdo) de sinal do Doppler de uma monitorização bilateral das artérias cerebrais médias. Sob o espectro surge o invólucro (linha branca), a partir do qual podemos calcular os valores das velocidades de fluxo sanguíneo cerebral sistólico (seta vermelha), diastólica (seta verde) e média por cada ciclo cardíaco. A miniatura delimitada a amarelo, representa esquematicamente as várias velocidades a calcular. Nos painéis de baixo podemos visualizar o aspeto conferido pelo modo de *Power M-Mode*. Aqui, a escala refere-se à profundidade (*mm*) e mostra o fluxo direcional (por convenção o *vermelho* é em direção à sonda e o *azul* em direção oposta à da sonda). Entre as setas amarelas, a linha branca corresponde à profundidade de amostragem do espectro de fluxo do painel superior. *Dados pessoais não publicados.*

orientada para um plano ligeiramente superior e a 60-70 mm de profundidade, apresentando um fluxo negativo, i.e., com direção oposta à sonda, e VFM de cerca de 50 $cm.s^{-1}$. Por último, angulamos a sonda posteriormente para encontrarmos a ACP a uma profundidade de cerca de 60 mm. Trata-se de um fluxo negativo com VFM de cerca de 40 $cm.s^{-1}$ (segmento P2), sendo útil e característico reconhecer um fluxo contínuo basal e negativo com VFSC máxima de ≈10 $cm.s^{-1}$ e sem pulsatilidade, que corresponde à veia basal (Valdueza et al., 1996). Se angularmos mais anteriormente, podemos registar o seu segmento P1, com fluxo dirigido à sonda. Este pode distinguir-se do M1 pela prospeção do vaso até ao nível superficial, onde se espera encontrar apenas ramos da ACM. É expectável que o gradiente de VFM seja ACM > ACA > ACP.

Outras janelas

Na janela orbitária, a sonda é colocada sob a palpebral encerrada, com a potência da sonda reduzida a 10%. Permite a visualização da artéria oftálmica a 40-50 mm e, mais profundamente, da porção cavernosa da ACI. Na abordagem suboccipital, através do buraco magno, a sonda é colocada na região suboccipital em posição paramediana e orientada cranial e medialmente, com a cabeça do examinando fletida. Podemos identificar, a 50-70 mm, a artéria vertebral (segmento V4) ipsilateral com um fluxo negativo. Embora seja variável, a cerca de 75-80 mm geralmente ocorre a junção dos dois segmentos V4 numa artéria basilar, que podemos tentar percorrer desde a sua origem até a sua porção distal (cerca de 12 mm).
Adicionalmente, a janela submandibular permite alcançar a ACI cervical distal, sendo útil para a determinação de índices de vasospasmo cerebral (Lindegaard et al., 1989).

Parâmetros hemodinâmicos básicos

O sinal de Doppler corresponde a um conjunto de velocidades de várias partículas em movimento (Aaslid et al., 1982). Considerando o fluxo como laminar ou parabólico, a velocidade do centro do vaso será a velocidade máxima que os eritrócitos conseguem atingir. Assim, usamos o invólucro do espectro (máxima velocidade) para derivar os parâmetros hemodinâmicos fundamentais (Figura 21) – velocidades (de pico) sistólica, diastólica e média. A VFM é calculada pela integração temporal no ciclo cardíaco (Newell & Aaslid, 1992), preferível à estimativa feita por $VFM = (sistólica + 2 \times diastólica)/3$. Também podemos caracterizar o fluxo pelos seus índices de pulsatilidade ou de Gosling - $(sistólica - diastólica)/VFM$ - e de resistência ou de Pourcelot - $(sistólica - diastólica)/sistólica$. No entanto, estas medidas são aproximações grosseiras do estado de resistência vascular, quando comparadas com

aquelas que incorporam os valores de PA, tais como iRVC, PRA ou PCrE (ver *"Modelos de resistência vascular cerebral"*).

Instrumentos adicionais

A avaliação funcional dos mecanismos reguladores do FSC, como a ARC, requer o registo síncrono de outros parâmetros sistémicos. Para a ARC, torna-se óbvia a avaliação da PA, a qual é realizada de modo contínuo, batimento a batimento. Para além disso, devem ser sempre monitorizados os valores de $PaCO_2$, um importante fator vasomodulador do FSC. Assim, os testes de avaliação cerebrovascular funcional requerem aparelhagem adicional; estes serão referidos sucintamente nos parágrafos subsequentes.

Pressão arterial não invasiva

A PA contínua pode ser obtida através de canulação arterial ou de modo não invasivo com o recurso ao Finometer® (usado nesta tese), Finapres® ou Portapres®. Estes aparelhos usam uma dedeira pletismográfica que é colocada à volta da falange média do 3º dedo (Figura 22). Desta maneira, as variações da pressão da dedeira acompanham as variações da PA do dedo com excelente correlação com a PA intra-arterial (Imholz et al., 1998, Omboni et al., 1993).

Figura 22 – Medição de pressão arterial contínua por pletismografia
Aparelho Finometer ® (FMS, Amesterdão, Holanda) onde se pode observar a curva de pressão arterial, batimento a batimento. À direita, mostra-se o aspeto gráfico do *software* BeatScope1.1® que acompanha o aparelho. *Dados pessoais não publicados.*

Capnografia não invasiva

Este método é indispensável nos testes de vasorreatividade ao CO_2 e também deve ser medido como parâmetro de controlo na avaliação da ARC. Através de um capnógrafo medimos os níveis de CO_2 expirado de modo contínuo (Figura 23). A partir da curva de capnografia gerada, podemos estimar o $PaCO_2$ arterial em cada ciclo respiratório, dado este ser próximo do valor tele-expiratório (CO_2TE; termo inglês: *end-tidal* CO_2, $ETCO_2$) (Raemer & Calalang, 1991).

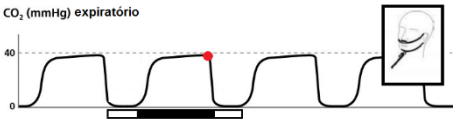

Figura 23 – Curva de capnografia normal
Capnografia normal. Após a fase inspiratória (barra branca), em que não se deteta fluxo na cânula, o aparelho regista um aumento súbito de dióxido de carbono (CO_2) durante a expiração, logo atingindo uma fase estacionária, de equilíbrio alveolar de $PaCO_2$. Assim, o valor tele-expiratório de CO_2 (CO_2TE) aproxima-se do valor de real $PaCO_2$.

Integração multimodal

Todos os sinais analógicos obtidos – o invólucro da VFSC do DTC, a curva de PA, o eletrocardiograma (ECG) e o CO_2, são registados síncrona e continuadamente num aparelho de conversão analógico-digital e armazenados em formato digital num computador para posterior análise. Abaixo está o exemplo do Power LAB 8/35® (AD instruments, Reino Unido), usado nos trabalhos desta tese (Figura 24).

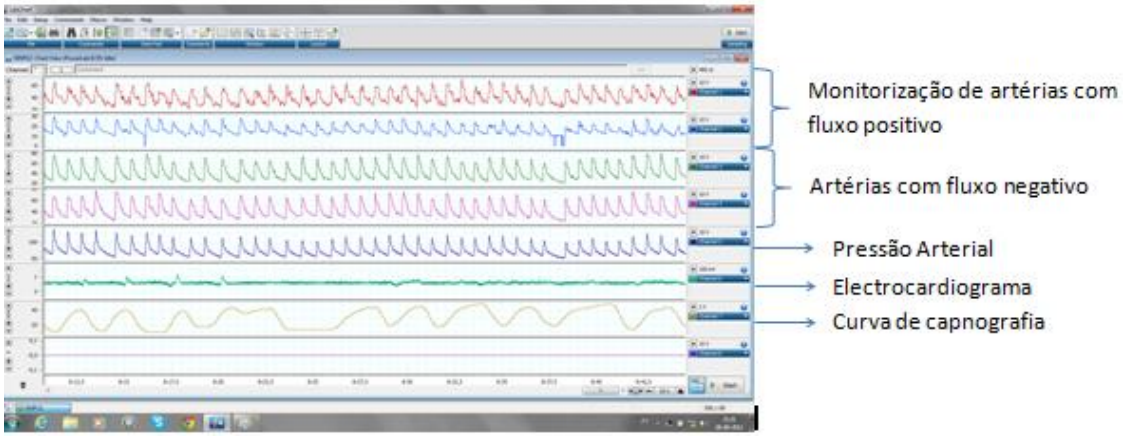

Figura 24 – Integração multimodal
Aspeto gráfico do painel do *software* LabChart 7.3.1® evidenciando os vários sinais de velocidade de fluxo cerebral (Doppler transcraniano), pressão arterial (Finometer®), eletrocardiograma e curva de capnografia provenientes da conversão analógica-digital realizada pelo aparelho PowerLab 8.35®. *Dados pessoais não publicados.*

Limitações do Doppler transcraniano

O DTC apresenta algumas limitações. Em primeiro lugar, cerca de 10-20% da população submetida a exame não tem janela acústica temporal adequada (Postert et al., 1997), sobretudo indivíduos do sexo feminino e idosos. Os agentes de contraste ultrassónico para exames de rotina (Postert et al., 1997, Eyding et al., 2006, Nabavi et al., 1998, Baumgartner et al., 1997), que aumentam o sinal em indivíduos com más janelas, têm efeito fugaz, sendo inadequados para o tempo de monitorização durante as provas funcionais. O DTC também não permite a medição do calibre vascular intracraniano. Deste modo, apenas podemos medir a velocidade como índice do FSC. Vários trabalhos já demonstraram que o calibre da ACM se mantem constante durante as provas dinâmicas de variação de PA e CO_2 (Serrador et al., 2006, Serrador et al., 2000). Para outros autores, a VFSC pode subestimar a capacidade total de vasorreatividade, sobretudo em condições extremas (Willie et al., 2012). O DTC também mede o fluxo global da artéria sondada e não regional, i.e., carece de resolução espacial. Isto poderá ser relevante quando sabemos que existem diferenças regionais de fluxo cerebral (Piechnik et al., 2008, Noth et al., 2008).

Neste momento, convém elucidar que é possível estudar os pequenos vasos de resistência pela sondagem de um vaso como a ACM, ACA ou ACP. Caso não haja patologia do mesmo (i.e. estenose intracraniana), os parâmetros hemodinâmicos medidos (sobretudo VFM e velocidade diastólica) dependem mais do estado de resistência do leito vascular distal (Newell & Aaslid, 1992, Aaslid et al., 2003). Tal como referido anteriormente, o vaso sondado não varia de calibre significativamente. Deste modo, quando medimos com DTC o aumento de VFSC a um estímulo, seja ele a PA, CO_2 ou cognitivo, estamos maioritariamente a avaliar os pequenos vasos cerebrais e não o vaso intracraniano sondado propriamente dito. Estudos com angiografia por ressonância magnética vêm confirmar que a maior parte da variação do calibre arterial se verifica a nível dos pequenos vasos (Bizeau et al., 2017). Ainda assim, existe alguma controvérsia acerca do papel dos grandes vasos como agentes de resistência pré-cerebral, dilema discutido na secção *"Quais são os vasos de resistência cerebral"*.

Aplicações do Doppler transcraniano

De forma resumida e geral, são enumeradas as potencialidades do DTC:

- Diagnóstico de estenoses e oclusões intracranianas (Alexandrov et al., 2012, Feldmann et al., 2007, Sloan et al., 2004);
- Determinação da gravidade de oclusão vascular intracraniana no contexto de AVC isquémico agudo pela escala de *TIBI* (acrónimo inglês de *Thrombolysis in Brain Ischemia*) (Azevedo & P., 2013);
- Avaliação do risco de AVC na drepanocitose (Adams et al., 1997, Adams et al., 1998);
- Avaliação da repercussão hemodinâmica e colateralização associadas às lesões arteriais extracranianas (von Reutern et al., 2012);
- Avaliação da vasorreatividade arterial intracraniana como preditor de AVC em lesões arteriais extracranianas (Silvestrini et al., 2009, Silvestrini et al., 1999, Vernieri et al., 2001);
- Avaliação da eficácia terapêutica em ensaios clínicos de medicação antitrombótica (Lau et al., 2014, Wang et al., 2013, Wong et al., 2010, Markus et al., 2005);
- Deteção de sinais microembólicos no estudo de embolia criptogénica e caracterização da instabilidade das placas ateroscleróticas (King & Markus, 2009, Ritter et al., 2009);
- Demonstração de *shunt* direito-esquerdo, geralmente por *foramen ovale* patente, mas vindo de qualquer outro *shunt* sistémico (Jauss & Zanette, 2000);
- Monitorização de vasospasmo cerebral na hemorragia subaracnoideia (Lindegaard et al., 1989, Sloan et al., 2004) ou síndrome de vasoconstrição cerebral/encefalopatia posterior reversíveis (Costa et al., 2015);

- Monitorização da resposta cerebrovascular em resposta a fármacos, i.e., manitol, trombolítico (Azevedo & P., 2013);
- Monitorização do VFSC e embolia, durante intervenções cirúrgicas cardíacas ou de endarterectomia carotídea (Edmonds et al., 1996);
- Determinação de paragem circulatória cerebral como auxiliar de diagnóstico de morte cerebral (Azevedo et al., 2000);
- Estabelecimento da dominância cerebral da área da linguagem (Deppe et al., 2004), o poderá ser útil na neurocirurgia de resseção tumoral ou de foco epilético;
- Outras potencialidades em estudo:
  - Potenciação da ação do trombolítico no AVC isquémico agudo ou sonotrombólise (Molina et al., 2009, Amaral-Silva et al., 2011);
  - Administração seletiva de medicamentos ou marcadores veiculados em microbolhas (Stride et al., 2009);
  - Estudos funcionais no esclarecimento fisiopatológico e como predição de complicações e risco de várias doenças, como as doenças vasculares cerebrais (Azevedo & Castro, 2016, Claassen et al., 2016), as doenças metabólicas com atingimento vascular (Azevedo et al 2012), a demência (Malojcic et al., 2017), as doenças pulmonares (Tsivgoulis & Alexandrov, 2009), a apneia do sono (Cassaglia et al., 2009), a encefalopatia hepática (Aggarwal et al., 2008) e o traumatismo crânio-encefálico (Dias et al., 2015)

MÉTODOS DE AVALIAÇÃO DA FUNÇÃO CEREBROVASCULAR

Vasorreatividade cerebral

A vasorreatividade cerebral (VR) corresponde a um índice de variação de VFSC ou FSC após a administração de um estímulo vasomodulador, seja ele um fármaco (e.g., acetazolamida endovenosa), gases (e.g., carbogénio) ou uma manobra que provoque alterações do $PaCO_2$ (e.g., apneia) (Malojcic et al., 2017). Geralmente, provoca-se vasodilatação. O intuito da avaliação da VR é medir a capacidade e amplitude de variação de calibre dos vasos de resistência, o que para alguns autores pode ser entendido como "reserva cerebrovascular" (Malojcic et al., 2017, Silvestrini et al., 1999). Geralmente, ambas as ACM são monitorizadas por representarem uma maior área cerebral e terem valores de referência na literatura (Malojcic et al., 2017). O teste

de VR ao CO_2 é o mais utilizado em investigação, enquanto o teste de apneia (Markus & Harrison, 1992), mais simples, poderá ser mais prático no meio clínico.

São três os métodos principais para determinar a VR ao CO_2:

1. <u>Teste de Apneia</u> (Markus & Harrison, 1992): após um período de repouso e uma inspiração normal, o indivíduo é instruído para permanecer em apneia de cerca de 30 segundos com consequente aumento de $PaCO_2$. Calcula-se um índice de VR à apneia (iVRA) pela fórmula $iVRA = \frac{(VFMmax - VFMbase)/VFMbase}{tempo\ de\ apneia\ (segundos)} \times 100$, onde $VFMmax$ corresponde à VFM nos últimos 4 segundos de apneia e $VFMbase$ à média dos valores de VFM no minuto precedente à apneia.

2. <u>Teste de VR ao CO_2</u>: aqui as alterações de VFM são monitorizadas continuamente com as do CO_2TE por capnografia (Figura 25). Podemos utilizar uma máscara com circuito não-recirculante acoplada a um reservatório ou uma válvula de não-retorno. A hipercapnia é conseguida pela inalação de uma mistura de 2-8% de CO_2 (carbogénio), provocando um aumento de CO_2TE ≥7 mm Hg. Adicionalmente, podemos testar resposta à hipocapnia através da hiperventilação para reduzir o CO_2TE em cerca de 10 mm Hg. Para obter a VR global (% ou $cm.s^{-1}$ por mm Hg de CO_2), calculamos a inclinação da reta de regressão linear entre os valores médios de CO_2TE, no eixo das abcissas, e os respetivos valores médios de VFM nas fases de hiperventilação, repouso e sob carbogénio. Também podemos calcular separadamente os valores de VR para as fases de hipercapnia e hipocapnia (Madureira et al., 2017). Outro parâmetro passível de ser calculado é a capacidade vasodilatadora total dada pela fórmula $\frac{VFMhipercapnia - VFMhipocapnia}{VFMbase} \times 100\%$.

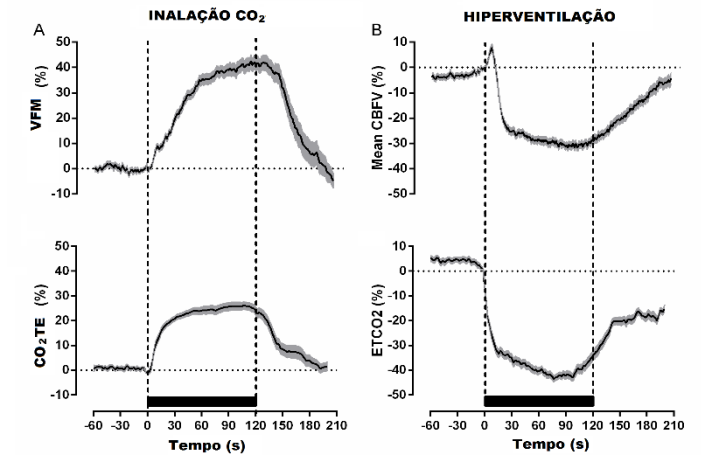

Figura 25 – Prova de vasorreatividade cerebral
Variação normalizada de velocidade de fluxo média (VFM) e de CO_2 tele-expiratório (CO_2TE) durante as provas inalatória e de hiperventilação para determinar o grau de vasorreatividade cerebral ao CO_2. *Adaptado de Madureira, Castro et al, 2016.*

3. <u>Farmacológico</u>: são perfundidas substâncias vasodilatadoras como a L-arginina (500 mg/Kg durante 30 minutos) ou acetazolamida (15mg/Kg durante 5 minutos; efeito máximo em 10-12 minutos), que promovem a vasodilatação cerebral por aumento da produção

de NO (Zimmermann et al., 2004) ou do pH tecidual cerebral (Vorstrup et al., 1984), respetivamente.

Acoplamento neurovascular

Uma década antes de Roy e Sherrington (Roy & Sherrington, 1890) apresentarem as suas conclusões à comunidade científica, já Angelo Mosso (1846 – 1910) tinha dado provas da existência de uma íntima relação entre FSC e atividade mental. Baseava-se no estudo de doentes com defeitos ósseos cranianos, tendo, posteriormente, inventado um método não invasivo curioso através de uma mesa pletismográfica por ele desenvolvida (Mosso, 1880). Este acoplamento entre atividade neuronal e FSC regional, de modo a suprir as suas necessidades metabólicas, é atualmente um dogma (Girouard & Iadecola, 2006). Os mecanismos que governam este acoplamento neurovascular (ANV) estão descritos na secção *"Microcirculação cerebral e unidade neurovascular"*.

Os esquemas mais comuns de monitorização são ambas as ACP ou a ACP esquerda mais a ACM direita (de controlo) durante as provas de estímulo visual (Azevedo et al., 2007), ou ambas as ACM para testes de estimulação motora/sensitiva (Silvestrini et al., 1995, Salinet et al., 2013), cognitiva (Sorond et al., 2011) e linguística (Deppe et al., 2004). Alguns autores estudaram a ACA (Boban et al., 2014) para provas de atividade frontal, embora as ACM também sejam ativadas durante o processo. É fulcral o registo automático do início do estímulo, já que 66-90% da resposta máxima pode ser atingida dentro de um segundo (klingelhöfer, 2016, Rosengarten et al., 2001b), no caso do ANV visual. Sempre que possível, dever-se-á utilizar a média ponderada de vários ciclos de estimulação-repouso para eliminar as variações de VFSC espontâneas, visto que a VFM tem uma variância de ≈10% em repouso (Panerai, 2009). Procede-se à normalização das velocidades de fluxo, de forma a tornarem-se independentes do ângulo de sondagem. A análise dos resultados depende de cada paradigma. Geralmente, considera-se as variações da VFM. O aparelho de DTC poderá ter *software* de análise próprio, mas existem alternativas comerciais ou de uso livre disponíveis, tais como o *dopOSCCI* (Badcock et al., 2012) ou o *AVERAGE* (Knecht et al., 1998). Descreve-se de seguida os paradigmas de estímulo mais comuns.

Visual

O estímulo pode ser a leitura de um texto ou um padrão xadrez alternante, e monitorizamos o segmento P2 da ACP (Figura 26). O paradigma habitual corresponde a 5-10 blocos de 1 minuto, cada um alternando entre estimulação (40 segundos) e repouso de olhos fechados (20 segundos); calcula-se então o valor da resposta de fluxo evocada (RFE) pela fórmula $RFE = \frac{VFMmaxima - VFMbase}{VFMbase} \times 100\%$ (Malojcic et al., 2017, klingelhöfer, 2016). Em termos matemáticos, corresponde ao valor de excursão máxima de VFM ($VFMmaxima$), normalizada pelo valor inicial ($VFMbase$) (Sturzenegger et al., 1996). Na literatura utiliza-se com frequência a designação de "*overshoot*" ou sobre-elevação que, do ponto de vista puramente matemático de análise de sistemas de controlo, deveria ser o valor percentual em relação ao valor final. Assim, é preferível o termo RFE. Rosengarten et al. propuseram ainda uma análise de sistema de controlo de 2ª ordem com vários parâmetros (ganho ou valor final, tempo de subida, fator de amortecimento e frequência natural) que traduzissem toda a dinâmica da curva de fluxo evocada (Rosengarten et al., 2001a). Nesta última abordagem é considerada a velocidade de pico sistólico, parecendo ser sensível a várias patologias com desnervação autonómica (Azevedo et al., 2011), diabetes *mellitus* (Rosengarten et al., 2002) ou com disfunção endotelial (Azevedo et al., 2012). Outros métodos de análise multidimensional foram propostos (Castro et al., 2012).

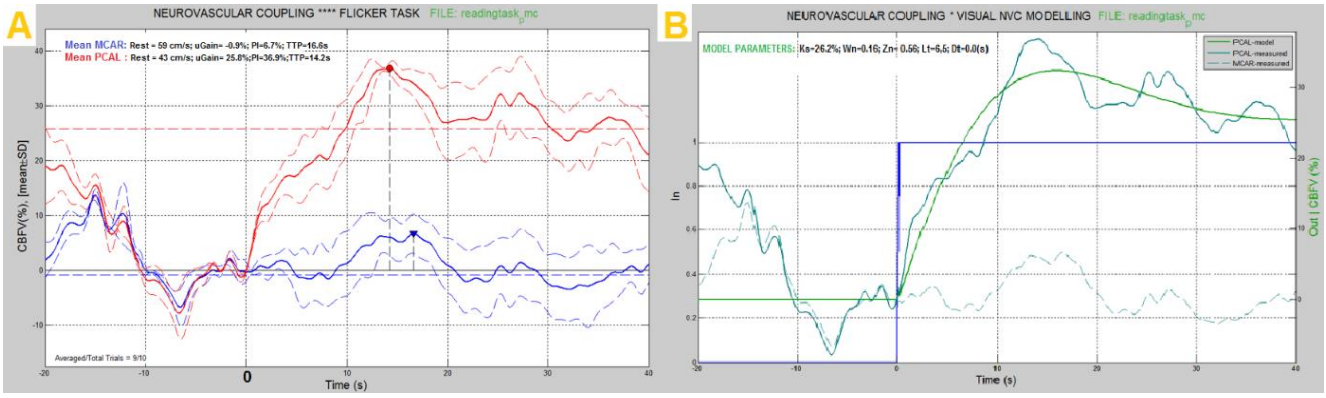

Figura 26 – Avaliação do acoplamento neurovascular pelo paradigma visual
Em **A** são mostradas as curvas de VFSC média da ACP esquerda (vermelho) e da ACM direita (azul; controlo). A VFSC da ACP aumenta rapidamente após o estímulo visual, apresentando uma RFE (ver texto) de cerca de 37%, enquanto a ACM direita tem apenas valor máximo de aumento de 7%. O paradigma compreende 10 ciclos de estimulação visual com olhos abertos (xadrez alternante) durante 40s seguidos de 20s de fase de repouso com olhos fechados. As linhas contínuas representam a média sincronizada dos 10 ciclos e as linhas a tracejado o desvio padrão. A curva da ACP foi modelada em **B** segundo a proposta de Rosengarten (Rosengarten et al., 2001b), de onde se extraíram vários parâmetros (canto superior direito). *Dados pessoais não publicados obtidos em software particular baseado em Matlab®.*

Prova cognitiva executiva: teste "N-back"

Na posição de decúbito, é projetada no teto uma sequência de letras, cada uma durante 2 segundos e intercaladas (2 segundos) por uma fundo preto com a mesma duração (Sorond et al., 2011); pede-se ao sujeito que identifique as letras e que as repita (prova de "*1-back*"), ou que as repita a cada duas ("*2-back*"). Antes de cada uma destas provas, pedimos ao sujeito para identificar a letra "X", o que servirá de controlo. Monitorizamos as ACM, e a VFM extraída é normalizada para o valor basal (2 minutos repouso). O grau de ativação calcula-se por $RFEnbt = \frac{VFMnbt - VFMx}{VFMx} \times 100\,\%$, onde $VFMnbt$ e $VFMx$ correspondem à média da VFM durante as provas de *"N-back"* e de identificação das letras "X" precedente, respetivamente.

Prova cognitiva linguística

São projetadas 15-20 letras aleatórias, uma de cada vez, sinalizando-se por um tom de alarme (t=0). Durante 15 segundos, o sujeito pensa no máximo de palavras iniciadas por essa letra. Segue-se uma fase de repouso (Deppe et al., 2004, Knecht et al., 1998). Cada ciclo contem uma letra e dura 50 segundos. As VFM são normalizadas para o valor em t=0 e é calculada a diferença entre o lado esquerdo e o direito; a diferença inter-hemisférica corresponde um índice de lateralidade (IL). Um IL positivo significa que há dominância esquerda e um LI negativo dominância direita, sendo que um teste próximo de zero é inconclusivo ou corresponderá a um caso de localização bi-hemisférica (Figura 27).

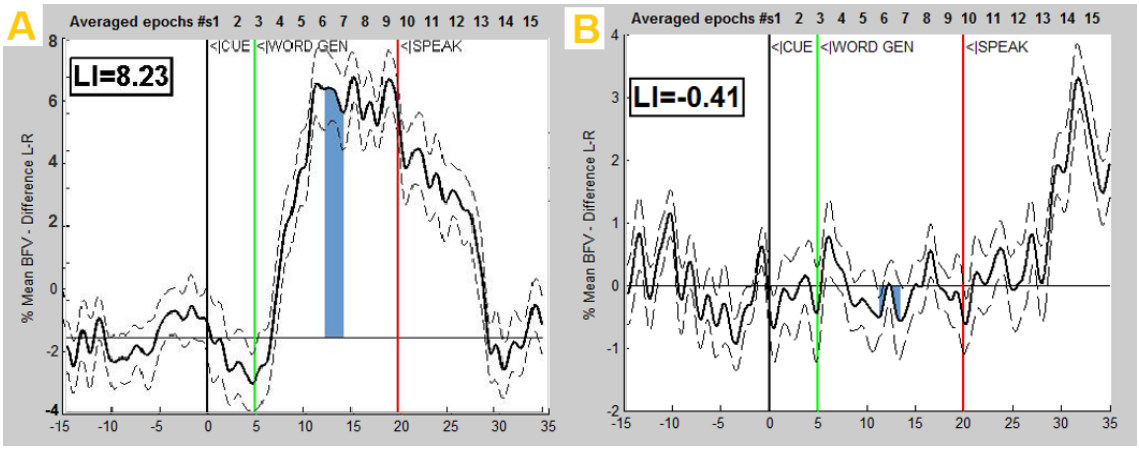

Figura 27 – Exemplos de resultados da prova linguística
Nesta prova pretende-se encontrar a dominância hemisférica da área da linguagem. Monitorizam-se as duas ACM e calcula-se a diferença inter-hemisférica "esquerda – direita". Em **A**, vemos um caso de um indivíduo com dominância esquerda (aumento positivo da diferença). Em **B**, trata-se de um doente esquerdino ao qual foi indicada cirurgia de epilepsia e foi necessário determinar a área da linguagem para prever a gravidade das sequelas cognitivas após a hipocampectomia. Neste caso, o resultado mostrou não haver assimetria hemisférica, tendo sido concordante com os resultados da ressonância magnética funcional. *Dados pessoais não publicados obtidos em software particular baseado em Matlab®*

Autorregulação cerebral

A ARC é tradicionalmente vista como a capacidade de manter o FSC constante dentro de valores de PA entre os 60 – 150 mm Hg, pelo menos em situações não patológicas (Lassen, 1959). A partir desta visão estática (Figura 16), o estudo da ARC moveu-se em direção à avaliação das flutuações mais rápidas da PA, que designamos por ARC dinâmica. Por outras palavras, mudou-se a questão "Para este novo patamar de pressão arterial alterou-se significativamente o nível fluxo sanguíneo cerebral?" para "Como reage o fluxo sanguíneo cerebral e quão eficiente foi essa resposta perante esta variação de pressão arterial?". Como depreendemos, não são conceitos necessariamente antagónicos. De qualquer das formas, para medir a ARC, o ponto essencial é haver variações da PA. Estas podem ser obtidas por manobras provocatórias ou utilizando as próprias oscilações espontâneas (Azevedo & Castro, 2016). Nos próximos parágrafos serão detalhados os métodos conhecidos para a medição da ARC.

Autorregulação estática

Antes do advento de tecnologias com boa resolução temporal, como o DTC, a ARC era analisada em condições de estado de equilíbrio, nas quais se manipulava a PA para diferentes níveis e, nessas novas condições, se observava a variação do valor de FSC (Paulson et al., 1990). Estes métodos caíram largamente em desuso, já que são morosos e de difícil aplicação clínica.

Um dos métodos possíveis, a técnica modificada de Oxford, consiste na infusão lenta de fenilefrina ou nitroprussiato de sódio para aumentar ou diminuir a PA, respetivamente. Utilizando apenas o braço hipertensivo, Tiecks et al. (Tiecks et al., 1995a) calcularam a ARC estática pela seguinte fórmula: $ARCestática = \frac{(iRVCfenilefrina - iRVCbasal)/iRVCbasal}{(PAMfenilefrina - PAMbasasl)/PAMbasal} \times 100\ (\%)$. Uma resposta de iRVC que compensasse totalmente a variação de PAM corresponderia a um valor de ARC de 100%, enquanto uma ausência de resposta (igual a 0%) significaria uma falha total da ARC. Este método é criticável em vários aspetos. Em primeiro lugar, não permite controlar a influência do BR a nível da ARC (Ebert, 1990), os quais parecem suprimir-se mutuamente (Tzeng et al., 2010). Em segundo lugar, é difícil atingir valores de PA junto do limite superior, dado que o uso de fenilefrina em altas doses produz efeitos cardiotóxicos (Azevedo & Castro, 2016). Por último, o uso de fármacos vasoativos também modifica a ventilação e valores de $PaCO_2$ que, como vimos, é um potente modulador da FSC, o que poderá confundir os resultados obtidos.

Autorregulação dinâmica

O tema da autorregulação dinâmica surge com o trabalho seminal de Aaslid em 1989 (Aaslid et al., 1989), que utilizou a desinsuflação rápida de braçadeiras dos membros inferiores, de modo a compreender o modo como a VFSC respondia perante uma variação abrupta da PA. Desde então, foram introduzidas uma miríade de técnicas provocatórias da PA para avaliar a ARC dinâmica. Contudo, para aplicação no contexto clínico, prevalecem os índices que relacionam o FSC e a PA a partir das suas oscilações espontâneas, facilmente reconhecidas na Figura 28. Assim, evita-se a necessidade de colaboração do doente, que será impossível em diversas situações clínicas tais como o traumatismo crânio-encefálico ou o AVC.

Técnica de braçadeiras dos membros inferiores

Introduzida por Aaslid et al. (Aaslid et al., 1989), o equipamento consiste em duas braçadeiras largas para aplicar em torno de ambas as coxas, conectadas com tubos largos a uma peça-em-forma de "Y". Após dois minutos em estabilização num nível de PA suprassistólico (período basal), as braçadeiras são subitamente desinsufladas, provocando uma queda abrupta da PA em cerca de $\approx$ 200 milissegundos (Figura 29). Em condições normais, a VFSC acompanha imediatamente esta descida, mas retorna a níveis próximos do basal antes da PA recuperar, o que reflete um mecanismo de ARC ativa (Figura 29). Podemos então calcular essa taxa de recuperação, TdR, como um marcador de uma ARC mais ou menos eficiente, a partir da taxa de variação do iRVC ($\Delta iRVC$) por unidade de queda de PAM (ΔPAM) durante o intervalo de tempo

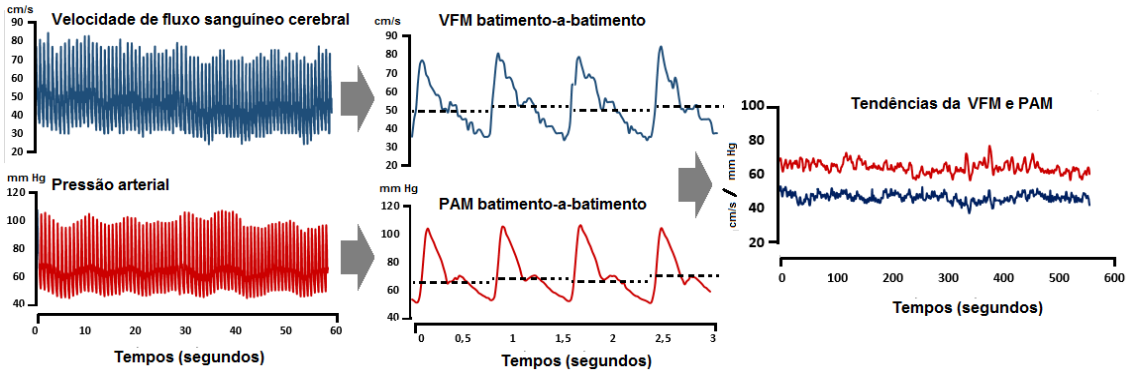

Figura 28 – Oscilação espontânea dos sinais hemodinâmicos sistémico e cerebral
Representação gráfica da pressão arterial obtida por Finometer® e do fluxo sanguíneo cerebral por Doppler transcraniano. À esquerda, note-se a oscilação espontânea ao longo de 1 minuto de monitorização. No centro, observa-se uma inspeção de 4 ciclos cardíacos com cálculo das médias de ambos os sinais (PAM e VFM, respetivamente), batimento a batimento. Mais à direita, observa-se a variação da VFM e PAM ao longo de quase 10 minutos de monitorização. Estas oscilações permitem o cálculo da autorregulação cerebral, por exemplo, pela análise de função de transferência. *Dados pessoais não publicados.*

entre 1 a 3,5 segundos após o estímulo (ΔT): $TdR = \frac{\Delta iRVC/\Delta T}{\Delta MBP}$ (s^{-1}). Todos os valores são normalizados em relação aos valores basais, que correspondem aos valores médios dos 4 segundos prévios à desinsuflação.

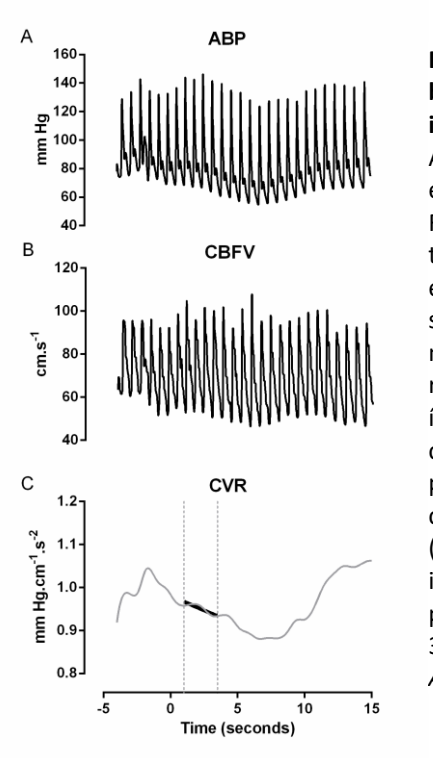

Figura 29 – Técnica de braçadeiras dos membros inferiores
As curvas de pressão arterial (**A**) e de VFSC (**B**) medidas pelo Finometer® e Doppler transcraniano, respetivamente, em resposta à desinsuflação súbita das braçadeiras dos membros inferiores. Em **C**, está representada a variação do índice de resistência vascular cerebral (iRVC) normalizado pelo valor basal. Daqui, pode-se calcular a taxa de recuperação (TdR). Esta corresponde à inclinação (linha negra) obtida por regressão linear entre 1 e 3,5 segundos. *Adaptado de Azevedo e Castro, 2016.*

A partir das respostas TdR da mesma manobra, Tiecks et al. desenvolveram o cálculo de um índice de autorregulação (IARC) (Tiecks et al., 1995a). Estes autores notaram que as respostas de VFM durante a queda de PAM podiam ser previstas a partir do valor de VFM basal ($VFMbase$), por uma equação linear de 2ª ordem:

$$VFM(prevista) = VFMbase \times (1 + dPn - K \times x2n)$$

Aqui, dPn corresponde aos valores de PAM normalizada como $dPn = \frac{PAM - PAMbase}{PAMbase - PCrE}$ e as variáveis de estado $x1$ e $x2$ (equivalentes a zero no nível basal) são modeladas por três parâmetros de ganho (K), constante de tempo (T) e fatores de amortecimento (D), de modo que, para tal frequência de amostragem f e número de amostras n:

$$(1)\ x2n = x2n - 1 - \frac{x1 - 2D.x2n - 1}{f.T};\ (2)\ x1n = x1n - 1 + \frac{dPn - x2n - 1}{f.T}$$

Para obter o valor de IARC para determinada prova, compararam a variação real da VFM com dez respostas-padrão hipotéticas (Figura 30A), que são geradas pela resolução da equação diferencial acima descrita, com combinações predefinidas dos seus três parâmetros modeladores (T, D, K) e que estão tabeladas na Figura 30B. Um IARC = 0 representa um fenómeno passivo da VFSC pela PA. Já um IARC = 9 representa uma ARC rápida e eficaz, em que as variações de pressão de perfusão são imediatamente contrabalançadas a nível cerebral, e a VFM retorna a valores de base de modo praticamente instantâneo. O modelo que melhor se aproxima da variação da VFM real durante determinada prova corresponderá então ao IARC desse indivíduo nessa prova (Panerai et al., 1998a, Panerai et al., 1998b).

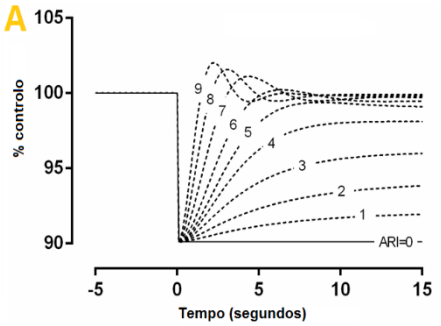

B

T	D	K	IARC	TdR	Interpretação
2.00	0.00	0	**0**	0	ARC ausente
2.00	1.60	0.20	**1**	2.5	
2.00	1.50	0.40	**2**	5.0	
2.00	1.15	0.60	**3**	10.0	
2.00	0.90	0.80	**4**	15.0	
1.90	0.75	0.90	**5**	20.0	ARC normal
1.60	0.65	0.94	**6**	30.0	
1.20	0.55	0.96	**7**	40.0	
0.87	0.52	0.97	**8**	60.0	
0.65	0.50	0.98	**9**	80.0	ARC máxima

Figura 30 – Respostas-padrão do modelo de Tiecks
Respostas hipotéticas de VFM face a queda em escalão de 10% de PAM (A). Tabeladas em **B** estão as dez combinações de parâmetros *T* (constante de tempo), *D* (fator de amortecimento) e *K* (ganho) a partir das quais se obtêm as resposta-padrão hipotéticas de índice de autorregulação cerebral (IARC) (Tiecks et al., 1995a). O IARC varia de 0 a 9 e tem correspondência a valores hipotéticos de taxa de recuperação (TdR) obtidos pela técnica de braçadeiras dos membros inferiores. *Adaptado de Azevedo e Castro, 2016.*

Manobra de Valsalva

A manobra de Valsalva é geralmente usada para estudar a função autonómica cardiovascular (Videira et al., 2016, Carvalho & Castro, 2013), foi proposta para estudar a ARC (Tiecks et al., 1996, Tiecks et al., 1995b). A manobra deve ser feita na posição supina, em que o examinando sopra contra um bucal adaptado a uma manga de manometria, mantendo um nível de pressão de 40 mm Hg, durante 15 – 20 segundos (Carvalho & Castro, 2013). As variações de PA típicas são evidenciadas na Figura 31. Numa fase inicial de aumento da pressão intratorácica (fase I), a PA diminui (fase IIa) até se verificar uma vasoconstrição periférica, causada pelo simpático, o que restitui os valores de PA até praticamente aos valores de base (fase IIb). Cessando o esforço expiratório subitamente, a PA cai abruptamente por diminuição abrupta da pressão intratorácica, sendo imediatamente seguida

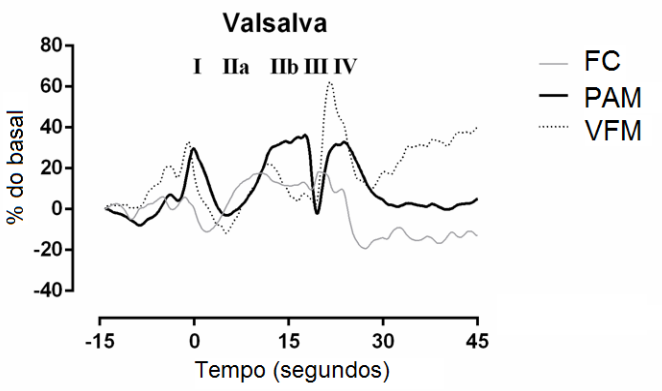

Figura 31 – Manobra de Valsalva
As suas fases estão identificadas com números romanos. Os valores são normalizados e expressos em variação percentual em relação ao valor de base. A frequência cardíaca (FC) representa a taquicardia esperada pela queda de PA e ativação simpática. O valor da velocidade de fluxo cerebral média (VFM) não segue exatamente o percurso da pressão arterial média (PAM) indicando potencialmente fenómenos de regulação ativos. Os índices de ARC podem ser calculados então pelas fórmulas descritas no texto. Os valores são de IARC-II e de IARC-IV são de 1.23 e 1.21 o que significa que a ARC está preservada (> 1). *Adaptado de Castro, 2016*.

por um pico de PA devido ao facto de o leito vascular periférico estar ainda sob vasoconstrição intensa (fase IV). Ao inspecionar as curvas de VFM e PAM, Tiecks et al. (Tiecks et al., 1996, Tiecks et al., 1995b) concluíram que a manobra apresentava indícios da ação de ARC, já que a queda de VFM não era semelhante ao verificado na PAM, e parecia recuperar em adianto dos valores da mesma. Estes autores calcularam os índices de ARC com $AII = \frac{(VFMIIb - VFMIIa)/\,VFMIIa}{(\mathrm{PAM}IIb - \mathrm{PAM}IIa)/\,\mathrm{PAM}IIa} \times 100\ (\%)$ e $AIV = \frac{(VFMIV - VFMVI)/\,VFMVI}{(PAMIV - PAMI)/\,RAMI} \times 100\ (\%)$. Para ambas as equações, valores > 1 significam que a VFM recupera antes da PAM, logo, a ARC estará preservada (Tiecks et al., 1996, Tiecks et al., 1995b). Dada a complexidade fisiológica da manobra de Valsalva, esta não teve grande acolhimento na literatura. Mais ainda, num estudo com um novo modelo de prospeção contínua da IARC (Castro et al., 2014), verificou-se que a própria ARC não é estacionária durante a manobra, pelo que o uso deste teste é desaconselhado.

Teste de resposta de hiperémia transitória

Este método foi introduzido por Giller (Giller, 1991) e, mais tarde, estandardizado por Smielewski et al. (Smielewski et al., 1996). O teste de resposta de hiperémia transitória (TRHT) compreende uma curta compressão carotídea (< 5 segundos) enquanto monitorizamos a VFSC. O cálculo é simples e utiliza a velocidade de pico sistólico: $TRHT = \mathrm{VFS}\ hiperémia\ /\ VFSbasal\ (a.u.)$. Um TRHT > 1,09 é sinal de uma ARC intacta, isto é, espera-se pelo menos um aumento de 10% da velocidade de fluxo com esta manobra (Figura 32). Dada a baixa reprodutibilidade e fatores inerentes à compressão carotídea, este teste raramente é utilizado (Azevedo & Castro, 2016).

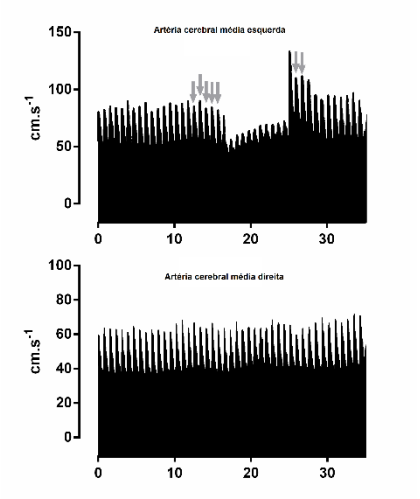

Figura 32 – Teste da compressão carotídea esquerda
Registos simultâneos das curvas de VFSC da artéria cerebral média esquerda (acima) e da direita (abaixo) durante o teste de resposta hiperémica transitória (TRHT) com compressão da carotídea comum esquerda. As setas cinzentas mostram os valores de pico sistólico que serão utilizados para o cálculo final. O valor basal corresponde à média dos picos sistólicos dos 5 batimentos cardíacos prévios à manobra e a fase de hiperémia corresponde à média dos 2º e 3º ciclos após a libertação da compressão. *Adaptado de Azevedo e Castro, 2016.*

Respiração sincronizada

Esta prova pretende determinar a influência das oscilações cíclicas da PA provocadas pela respiração sincronizada a 6 ciclos por minuto (0,1 Hz). Diehl et al. (Diehl et al., 1995)

usaram um método no domínio da frequência para calcular o desfasamento oscilatório da VFM e da PAM. Quanto maior este desfasamento, maior a independência da VFM em relação à PAM e, logo, maior grau de ARC. Este é o mesmo teste que se utiliza para obter uma medida de atividade parassimpática pela análise concomitante da frequência cardíaca (FC), já que esta manobra exacerba a variação sinusal de causa vagal em resposta às oscilações mecânicas da PA (Carvalho & Castro, 2013). Isso é uma vantagem em relação às manobras que envolvem a ação do simpático, tais como a ativação postural, a Valsalva e o TRHT. O processo de análise matemática é descrito e explicado em pormenor na secção *"Função de transferência – autorregulação cerebral espontânea"*. A grande diferença é que apenas se utiliza o valor de desvio de fase na frequência provocada (0,1 Hz), que se torna redutor face a toda a informação espectral. Para além disso, não se consegue evitar a vasoconstrição cerebral inicial, como é evidente na redução da VFSC nos primeiros 10 segundos da Figura 33. Foi proposto que valores de fase < 30° refletissem uma ARC deficiente, baseada nos resultados obtidos de doentes com malformações arteriovenosas cerebrais ou lesões obstrutivas carotídeas (Diehl et al., 1998, Diehl, 2002). Esta prova foi largamente abandonada pelas razões referidas, mas o método analítico perdurou.

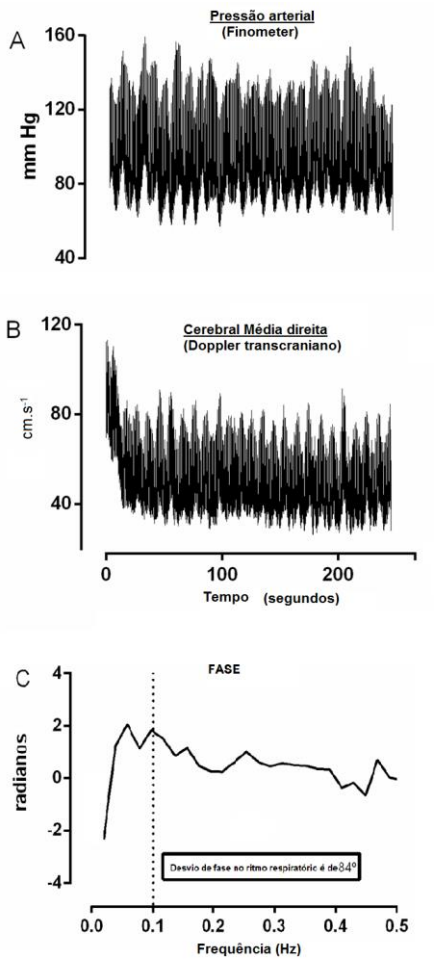

Figura 33 – Respiração sincronizada
O sujeito é ajudado com metrómetro a inspirar e expirar a cada 5 segundos (6 cpm). Podemos ver as oscilações de PA produzidas (**A**) e também na VFSC (**B**). A análise de função de transferência mostra que existe um desvio positivo de fase de 84°, sendo considerada uma ARC normal. Adaptado de Azevedo e Castro, 2016.

Ativação postural

Durante a passagem da posição sentada para a ortostática, ocorre uma queda inicial de PAM de cerca de 25 mm Hg (Van Lieshout et al., 2003). Esta oscilação de PA é acompanhada por uma resposta de VFSC à qual se pode aplicar o cálculo do IARC segundo o modelo de Tiecks (Serrador et al., 2005). Este teste tem a vantagem de não causar dor como a despertada pela insuflação das braçadeiras dos membros inferiores. Mais interessantes são as manobras posturais cíclicas (e.g., a cada 10 segundos sentado/em pé ou agachado/em pé) que possam provocar oscilações

da PA a uma frequência predefinida (neste exemplo, 0,05 Hz), onde se possa aplicar um método analítico espetral para verificar a resposta da VFSC nessa frequência em particular. Uma das formas de o fazer, tal como na respiração cíclica, é utilizar a análise detalhada na secção "Análise da função de transferência". Este teste não tem a desvantagem de induzir hipocapnia, o que acontece nas manobras respiratórias (Claassen et al., 2009). Contudo, como se pode imaginar, também não é útil para doentes não colaborantes ou para aqueles em que não sejam adequadas as mudanças posturais (e.g., AVC agudo).

Neste capítulo também será de referir o teste de Tilt ou de mesa basculante (Hetzel et al., 2003, Lagi et al., 2001, Ocon et al., 2009, Schondorf et al., 2001, Serrador et al., 2006, Zhang et al., 2004b). Este teste é geralmente utilizado para estudar síndromes de intolerância ortostática, como síncope neurocardiogénica, hipotensão postural, hipersensibilidade do seio carotídeo e síndrome da taquicardia postural, entre outras (Freitas, 2010, Freitas et al., 1998, Freitas et al., 2015, Freitas et al., 1999, Freitas et al., 1994, Freitas et al., 2007, Freitas et al., 2000). No teste de Tilt, o *stress* ortostático provoca uma grande transferência gravitacional do volume sanguíneo para o sistema venoso de capacitância, altamente distensível, abaixo do diafragma (Freitas, 2010). Este facto provoca uma redução superior a 700 ml de volume plasmático nos primeiros minutos de ortostatismo passivo em humanos (Van Lieshout et al., 2003) e ativação significativa do simpático e das resistências arteriais periféricas (Freitas et al., 2007). Dada a mistura de influências autonómica, débito cardíaco e volume plasmático, não tem sido utilizado para o estudo da ARC (Carey et al., 2003).

Função de transferência – autorregulação cerebral espontânea

Os métodos até agora descritos requerem algum tipo de manobra ou fármaco para obter uma variação da PA para se calcular um índice de ARC. Isso, por si só, torna a interpretação dos resultados difícil de destrinçar de variações sistémicas concomitantes, tais como efeitos do SNA e da $PaCO_2$. Mais relevante é o facto de, nas mais variadas situações clínicas onde a medição da ARC poderia ser útil, as manobras provocativas não serem adequadas ou os doentes não se encontrarem colaborantes (e.g., cuidados intensivos, AVC agudo).

Um dos avanços na avaliação da ARC foi a possibilidade de aproveitar as variações espontâneas de PA, desobrigando o doente do esforço de colaboração. Tal é possível porque a PA, assim como a VFSC, tem flutuações espontâneas (Figura 28). Partindo destas, e graças à análise de função de transferência (AFT), podemos obter vários parâmetros que traduzam essa relação. A AFT é uma representação matemática, no domínio da frequência, que explica a relação linear entre dois sinais, um de entrada e outro de saída. Se substituirmos os vetores de entrada e de

saída pelas séries temporais de PAM e VFM, respetivamente, podemos então estudar o efeito das oscilações da PA espontâneas sobre a vasculatura cerebral num leque variado de frequências. A AFT começa por transportar para o domínio da frequência as séries temporais da VFM e da PAM, obtendo os respetivos auto-espectros, S_{yy} e S_{xx}, assim como o espectro-cruzado, S_{xy} pelo método de Welch (Claassen et al., 2016). Podemos então deduzir a influência oscilatória da PAM sobre a VFM a determinada frequência f pela função de transferência H:

$$H(f) = \frac{S_{xy}(f)}{S_{xx}(f)}$$

A partir das partes real H_R e imaginária H_I podemos calcular;

(1) ganho ou amplitude, $|H(f)| = \sqrt{(|H_R(f)|^2 + |H_I(f)|^2)}$;

(2) fase, $\varphi = \tan^{-1}\left(\frac{H_I(f)}{H_R(f)}\right)$;

De modo a assegurar o prossuposto da linearidade entre PAM e VFM, calculamos também a coerência (γ^2) entre os dois sinais pela fórmula:

$$\gamma^2 = \frac{|S_{xy}(f)|^2}{|S_{xy}(f) \cdot S_{yy}(f)|}$$

A coerência é simplesmente um coeficiente de correlação entre VFM e PAM e aproxima-se de zero à medida que as oscilações entre os sinais são mais dissimilares. O ganho traduz a amplitude ou magnitude de transferência entre as oscilações da PA e da VFM, sendo que, quanto menor o seu valor, maior o amortecimento da PAM, ou seja, uma ARC mais eficaz. Quanto maior o valor de fase, menos síncronas são as oscilações entre a PA e VFSC, pelo que mais ativa será a ARC. Neste caso será um desfasamento positivo. À primeira vista, poderá causar alguma perplexidade um desvio positivo, i.e., pelo facto de as oscilações da VFM precederem as da PAM, sabendo que ARC consiste numa reação da VFSC às variações da PA. Contudo, dado este ser um processo dinâmico, um desvio positivo traduz o atraso de resposta miogénica ao longo do tempo. Um desvio de fase menor a baixas frequências traduz uma ARC diminuída. A Figura 34 representa esquematicamente o modo como o ganho e fase da AFT operam no controlo cerebrovascular.

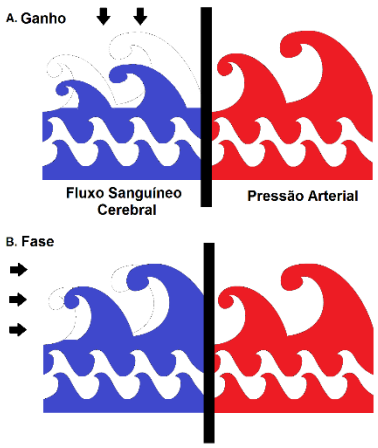

Figura 34 - Representação esquemática do efeito do ganho e fase

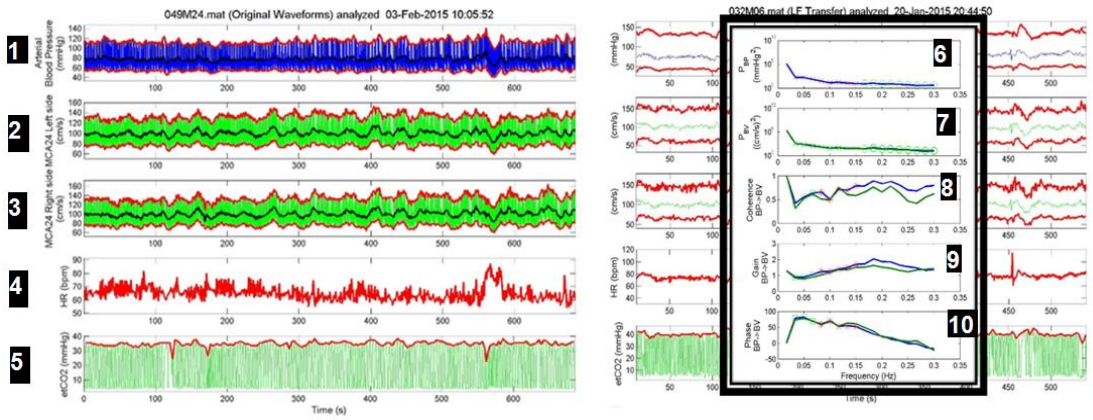

Figura 35 – Análise da Função de transferência
A partir das séries temporais da monitorização contínua da pressão arterial **(1)** e velocidade de fluxo sanguíneo cerebral **(2,3)**, derivamos os seus valores de média (VFM e PAM, respetivamente). Notar a oscilação espontânea destas variáveis fisiológicas. A análise de função de transferência (AFT) verifica a influência da PAM (*input*) sobre a VFM (*output*) no domínio da frequência a partir dos seus espectros (**6 e 7**, respetivamente). A AFT produz 3 parâmetros: coerência (**8**), ganho (**9**) e desvio de fase (**10**). Neste caso, denotamos que a autorregulação funciona como um filtro passa-alto, havendo uma filtragem das oscilações de PAM mais lentas (< 0,2 Hz), que se manifesta por um maior amortecimento (descida do ganho **(9)**) e um maior afastamento (aumento da fase **(10)**). *Dados pessoais, não publicados, calculados com software privado com base em Matlab®.*

Após o primeiro trabalho de Diehl et al. (Diehl et al., 1995), Zhang et al. (Zhang et al., 1998) e Panerai (Panerai et al., 1998b) descreveram em maior detalhe o comportamento destes sistemas. A Figura 35 demonstra um exemplo de aplicação da AFT. Pela AFT, a ARC é tida como um filtro passa-alto, ou seja, oscilações rápidas da PAM (acima de 0,2 Hz) são transmitidas na sua globalidade para a VFSC, mas em frequências mais baixas estas são filtradas com base nos parâmetros de H. Assim, na Figura 35 podemos verificar que, para oscilações com frequência < 0,2 Hz, o ganho diminui (amortecimento) e o desvio de fase aumenta (dessincronização das oscilações).

A AFT requer um registo síncrono de pelo menos 5 minutos das séries temporais de VFSC e de PA (Claassen et al., 2016). Os parâmetros mais utilizados na interpretação da ARC são a fase e o ganho. A coerência, por seu turno, é encarada como um fator de controlo da linearidade e validade da AFT calculada. Medindo os graus de liberdade da nossa função (Claassen et al., 2016), podemos encontrar um limite mínimo de coerência que permita aceitar os valores de H.

Índice de autorregulação espontâneo

Panerai et al. (Panerai et al., 1998a) mostraram ser possível calcular um IARC semelhante ao que se obtém na manobra de desinsuflação das braçadeiras dos membros inferiores, mas a partir das oscilações espontâneas de PA. Para tal, calcularam a função de impulso, que não é mais do

que a transformada de Fourier inversa da função de transferência H previamente obtida por AFT. À função de impulso corresponde uma resposta de escalão no domínio do tempo, tal como descrita na Figura 36. Este método tem a vantagem de simplificar o número de variáveis a analisar (em vez de ganho e fase e várias bandas de frequência temos apenas um valor de IARC), mas é mais sensível às não linearidades e artefactos (Panerai et al., 2016).

Existe alguma discordância acerca de qual o verdadeiro intervalo de frequências em que a ARC opera, mas este poderá variar consoante a patologia e condições hemodinâmicas periféricas.

Existe ainda alguma discordância acerca dos melhores parâmetros da AFT. Muitos autores preferem a fase ao ganho como fator mais estável e não influenciável da PA (Tzeng et al., 2012).

Uma das falhas deste método é que, para ser válido, terá de assumir-se condições estacionárias, que não são necessariamente cumpridas em várias condições clínicas, fora do ambiente altamente controlado do laboratório onde existem múltiplas fontes de não linearidades (ativação cognitiva, nível de consciência, respiração, variações de $PaCO_2$) (Czosnyka et al., 2009, Castro et al., 2014).

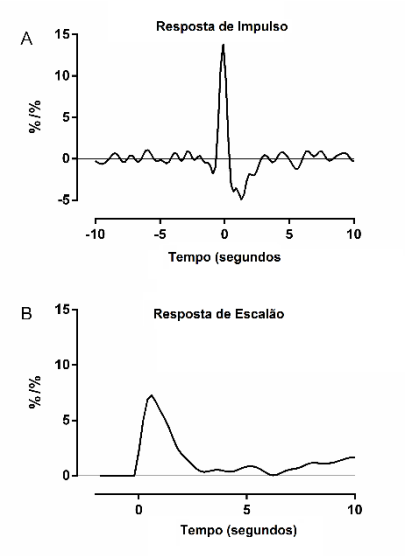

Figura 36 – Índice de autorregulação espontâneo
A partir de séries temporais das médias de pressão arterial (PAM) e velocidade de fluxo (VFM), foi calculada a função de transferência. Para obter o índice de autorregulação cerebral espontâneo (IARC), aplicamos uma transformada de Fourier rápida inversa da mesma função de transferência. O valor real desta inversão constitui uma função de impulso que estima a resposta de VFC (**A**) perante um nível de PAM. A resposta de escalão (**B**) pode então ser obtida pela integração (convolução) da resposta de impulso com uma unidade de escalão. Repare que, agora, a resposta de escalão se exprime em função do tempo. Comparando esta unidade de resposta com os modelos de IARC de Tiecks (Figura 30) invertidos, podemos verificar que são semelhantes. A diferença é que o último autor calculou a resposta a uma queda de PAM, embora a resposta de impulso corresponda a um nível de aumento da mesma. *Adaptado de Azevedo & Castro, 2016.*

Medição contínua na autorregulação cerebral

IARC contínuo

Apesar de ainda ser necessário bastante trabalho de validação, podemos obter uma estimativa contínua do valor de IARC – o $IARC_{(t)}$. Os valores de $IARC_{(t)}$ são baseados nos mesmos valores de IARC produzido por Tiecks et al. (Tiecks et al., 1995a). O mesmo modelo foi implementado numa

estrutura ARMA (do termo inglês a*uto-regressive moving average*) (Panerai et al., 1998b) e usou-se uma decomposição ortogonal para estimar os parâmetros do modelo de Tiecks ao longo de uma série temporal de PAM e VFM (Panerai et al., 2008). Usando este método, foi possível evidenciar as variações fisiológicas esperadas da IARC durante o teste de apneia e hiperventilação (Dineen et al., 2010). Também foi utilizado para estudar a variação temporal da ARC durante a manobra de Valsalva (Castro et al., 2014) e a desinsuflação das braçadeiras nos membros inferiores (Panerai et al., 2015), demonstrando que a ARC não é um fenómeno estacionário e que ela própria oscila com o tempo e em resposta a novas condições fisiológicas.

Mx e PRx

Czosnyka et al. (Czosnyka et al., 1996) desenvolveram um método diferente de cálculo da ARC no domínio do tempo votado, sobretudo a doentes em regime de cuidados intensivos. Neste contexto, é importante recordar a importância do valor de PIC, que poderá estar significativamente elevado (e.g., traumatismo crânio-encefálico), para estimar a PPC (ver secção *"Hemodinâmica cerebral e sua regulação"*). Estes índices de ARC baseiam-se no cálculo do coeficiente de correlação de Pearson entre PAM e VFM. Para diminuir o ruído, é calculada a média dos valores a cada 5-10s; depois, os segmentos de 30-60 pontos são usados para o cálculo da correlação. Este valor foi designado por índice de velocidade média (Mx) (Czosnyka et al., 1996, Steiner et al., 2002). A interpretação é simples – quanto maior e mais positivo o valor de Mx, menor será a capacidade de ARC (a VFM é proporcionalmente dependente do valor de PAM)

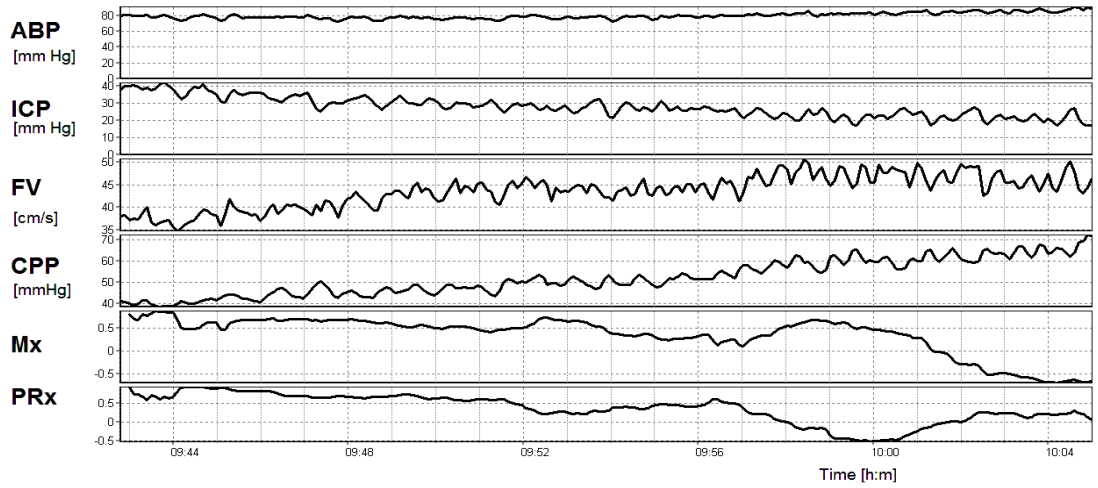

Figura 37 – Índices de Autorregulação por pressão (PRx) e velocidade de fluxo cerebral (Mx)
Monitorização com Mx e PRx com o *software* ICM+®. Caso de um doente com 24 anos, com traumatismo crânio-encefálico, com pontuação de 6 na Escala de Coma de Glasgow. A PIC cai progressivamente de 40 para 30 mm Hg em 25 minutos, melhorando os níveis de autorregulação com diminuição do valor de Mx e PRx. *Cortesia of Professor Marek Czosnyka, Department of Clinical Neurosciences, Neurosurgical Unit, University of Cambridge, Cambridge, Reino Unido.*

e, quanto mais próximo de zero ou mais negativo, maior a reserva de ARC. Também podemos obter um índice de ARC baseado na relação PPC-PIC. Assim, o Mx vê-se substituído pelo índice de reatividade à pressão (do termo inglês *pressure-reactivity index*, PRx), em que a única diferença de análise se prende com o facto de se usarem 3-6 minutos para fazer a média deslizante (Czosnyka et al., 1997). A Figura 37 mostra o exemplo de uma monitorização multimodal de um doente com traumatismo crânio-encefálico, mostrando os valores de Mx e PRx. Outros métodos de medir o FSC são através da espectroscopia de infravermelho-próximo (do termo inglês *near-infrared spectrocopy*, NIRS) e da pressão tecidual de oxigénio ($PtiO_2$). Apesar de ter sido demonstrada uma correlação razoável entre a NIRS e o valor de Mx (Czosnyka et al., 2009), estes métodos continuam a ser pouco utilizados.

Importância clínica dos índices de autorregulação cerebral

Doença vascular cerebral crónica

Foi demonstrado que, no caso de uma estenose carotídea grave, se a ARC está gravemente alterada, o doente encontra-se em maior risco de eventos vasculares (Reinhard et al., 2001, Hu et al., 1999, Panerai et al., 1998b). O mesmo foi evidenciado para as estenoses intracranianas, onde o valor de fase se pode aproximar do valor de 0°, que teoricamente pode revelar total falha de capacidade regulatória (Haubrich et al., 2003). Esta desregulação vasomotora poderá ser um fator de risco relevante para um futuro evento vascular, embora ainda não haja muitos estudos a demonstrá-lo. Por seu turno, as provas de VR já têm sido empregues como auxiliar na decisão de indicação para endarterectomia em doentes com estenose carotídea grave (Silvestrini et al., 1999, Soinne et al., 2003, Alexandrov, 2003). As técnicas de ANV também têm sido usadas para estudar fases pré-sintomáticas de problemas vasculares em doentes com diabetes mellitus (Rosengarten et al., 2002) e na doença de Fabry (Azevedo et al., 2012).

Doença vascular cerebral aguda

A ARC parece estar alterada precocemente nos doentes com hemorragia subaracnoidea (Santos et al., 2016, Fontana et al., 2015, Otite et al., 2014, Soehle et al., 2004). A avaliação da ARC pode ter importância prognóstica no desenvolvimento do vasospasmo ou isquemia cerebral tardia (Otite et al., 2014, Lang et al., 2001, Santos et al., 2016, Fontana et al., 2015, Calviere et al., 2015, Budohoski et al., 2015). No caso da hemorragia intracerebral primária, sinais de uma ARC menos eficaz, ou seja, um ganho elevado e um desvio de fase reduzido, foram registados nos primeiros

dias e associaram-se a um maior volume de hematoma, a gravidade clínica e a um pior resultado funcional aos 3 meses (Nakagawa et al., 2011, Ma et al., 2016). Não obstante, outros autores sugerem que não há um distúrbio primário da ARC, mas antes uma deterioração com o tempo nos hematomas de maior volume (Reinhard et al., 2010).

Demência vascular

Têm sido avançados dados interessantes sobre outras manifestações da doença microvascular cerebral que não o AVC, através de testes funcionais por DTC. Uma ARC, VR ou ANV menos eficazes associaram-se a alterações significativas cognitivas e do equilíbrio e velocidade de marcha, que se traduzem de outro modo em risco maior de quedas (Purkayastha et al., 2014, Purkayastha & Sorond, 2014, Sorond et al., 2013, Sorond et al., 2011, Sorond et al., 2010). Num estudo conjunto de investigações inovadoras, mostrou-se que o cacau puro (Sorond et al., 2013) e a desferroxamina (Sorond et al., 2015) melhoravam a ANV e a ARC, respetivamente, o que abre caminho à modulação terapêutica da função neurovascular, por exemplo, no AVC isquémico agudo. A avaliação e monitorização dos mecanismos de regulação vascular cerebral poderá, por isso, ajudar a compreender e tratar as doenças cerebrovasculares relacionadas com o envelhecimento.

Traumatismo crânio-encefálico: o conceito de PPC ótima

No que toca aos cuidados intensivos neurocríticos, o Mx ou o PRx são adequados para estudar prospectivamente a ARC (Dias, 2014). O PRx está associado de modo independente ao prognóstico do doente neurocrítico (Dias et al., 2015, Czosnyka et al., 2009, Steiner et al., 2002, Czosnyka et al., 1997). Quando o PRx está acima de 0,3, a mortalidade aumenta abruptamente de 20% para 70% (Balestreri et al., 2006). A relação entre PRx e CPP segue uma curva em U (Steiner et al., 2002) de tal modo que há um intervalo de PPC em que a PRx é mais eficaz. Fora destes limites, é pior o desfecho clínico (Steiner et al., 2002). Este intervalo de PPC ideal pode ser estimado por interpolação parabólica entre os valores de PRx e PPC numa janela > 3 horas (Steiner et al., 2002). Estão em curso ensaios para determinar se esta abordagem baseada da "PPC ótima" pode contribuir para melhorar o ajuste hemodinâmico e, deste modo, o prognóstico de doente com traumatismo crânio-encefálico (Dias et al., 2015).

ACIDENTE VASCULAR CEREBRAL: NOÇÕES ESSENCIAIS

O AVC é um sério problema de saúde pública nos países industrializados e em vias de desenvolvimento (Feigin et al., 2016). Os custos diretos para a sociedade e serviços de saúde estão avaliados em 7,6 mil milhões de libras no Reino Unido e em 40,9 mil milhões de dólares nos Estados Unidos da América (AHA, 1997). A incidência é variável, quer a nível mundial quer a nível regional, sendo que em Portugal (norte) está estimada em 1,73 por 1000 habitantes (Correia et al., 2017). Portugal, juntamente com os Países de Leste, ocupa os lugares cimeiros no contexto europeu (Feigin et al., 2016). O AVC causa 9% das mortes em todo o mundo, sendo apenas ultrapassado pelo enfarte do miocárdio (Murray & Lopez, 1997). Em Portugal, ocupa o primeiro lugar no *ranking* de mortalidade, representando uma fatia de 30% (DGS, 2016). Para além disso, é de realçar a morbilidade de que se faz acompanhar (DGS, 2015), sendo também a primeira causa de epilepsia no idoso (Rothwell et al., 2005) e causa frequente de depressão (O'Brien et al., 2003) e demência (Mijajlović et al., 2017).

Por AVC, entende-se a ocorrência de uma disfunção neurológica que surge de modo súbito e explicado por uma disrupção do fluxo sanguíneo focal a nível cerebral, quer por oclusão de um vaso cerebral – AVC isquémico – quer por rutura dos mesmos – AVC hemorrágico. O AVC isquémico ou enfarte cerebral é a patologia mais comum, correspondendo a 80% dos casos (Caplan, 2006). É sobre este último que os trabalhos desta tese se irão debruçar. É subclassificado em termos de território afetado pela classificação OSCP (do projeto Oxfordshire Stroke Community Project)(Bamford et al., 1991), sendo o mais frequente o que ocorre por oclusão de artéria cerebral da circulação anterior ou carotídea. Em termos etiológicos, diferencia-se pela classificação de TOAST (Trial of ORG 10172 in Acute Stroke Treatment) (Adams et al., 1993), sendo as causas mais comuns o cardioembolismo (e.g., fibrilhação auricular), a aterosclerose de grandes vasos, que origina fenómenos de tromboembolismo ou de oclusão arterial local (e.g., estenose da artéria carotídea interna), e a patologia dos pequenos vasos cerebrais, embora existam causas mais raras (Castro et al., 2016).

Fisiopatologia da isquemia cerebral

A fisiopatologia do enfarte cerebral é tudo menos um processo estático. Compreende um desenrolar de eventos em cascata, que se inicia com a depleção da energia celular e acumulação de radicais livres, seguida de inflamação, até culminar na morte celular (Dirnagl et al., 1999).

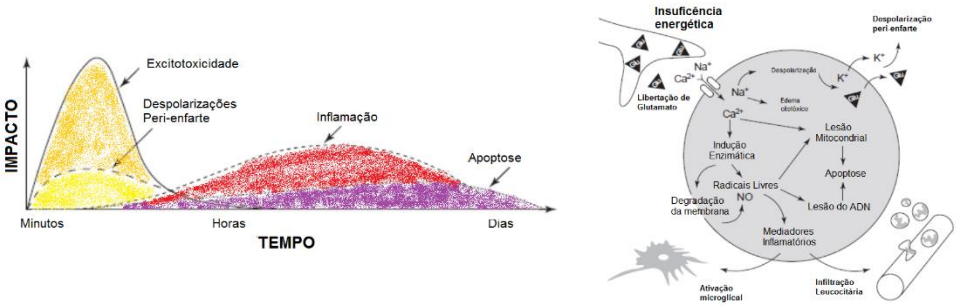

Figura 38 – Mecanismos fisiopatológicos da isquemia cerebral
Cascata de eventos que concorrem para a lesão cerebral no AVC isquémico agudo. A despolarização dos neurónios hipoperfundidos leva à libertação de glutamato excitatório, que, por sua vez, aumenta o cálcio (Ca^{2+}), o sódio (Na^{+}) e o cloro (Cl^{-}) intracelular. Este influxo promove o extravasamento de K^{+} para o meio extracelular. O glutamato e o Ca^{2+} provocam ondas de despolarização nas zonas peri-enfarte. O gradiente osmótico criado leva ao desvio de H_2O para o nível intracelular (edema citotóxico). Entretanto, o Ca^{2+} ativa uma cascata de mediadores inflamatórios e apoptóticos que culmina na inflamação local por quimiotaxia leucocitária extracerebral e da micróglia residente. *Adaptado de Dirnagl et al., 1999.*

Numa fase precoce, ocorre excitotoxicidade com despolarização e morte de neurónios e células gliais. Esta excitotoxicidade pode propagar-se à zona peri-enfarte, contribuindo para uma maior zona disfuncional e sintomática, para além do foco isquémico inicial (Dirnagl et al., 1999) (Figura 38).

Para além das vias isquémicas, inflamatória e da morte celular, também temos de contar com outros fatores que poderão contribuir para a lesão cerebral, por vezes de modo catastrófico. A lesão dos capilares do parênquima isquémico envolvido leva à perda de função da BHE com extravasamento de conteúdo para o meio extracelular (edema vasogénico), culminando em edema cerebral e transformação hemorrágica (Simard et al., 2007). Também poderá ocorrer micro-embolização e micro-obstrução da rede capilar (Figura 39), o que poderá impedir a recuperação do território afetado, apesar da recanalização do vaso major (Balami et al., 2011). Neste cenário, Ames et al. (Ames et al., 1968) descrevem aquilo a que se chama de fenómeno de não-recirculação (Figura 40), para o qual podem contribuir a disfunção dos pequenos vasos de resistência vascular cerebral. Atualmente, pensa-se que um dos principais responsáveis por este

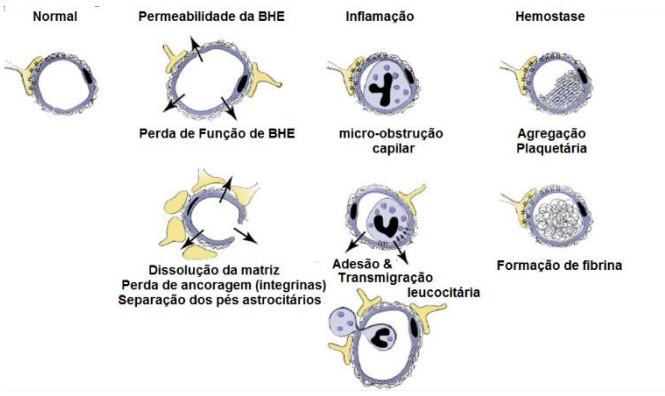

Figura 39 – Patologia microvascular na Isquemia Cerebral
Adaptado de Dirnagl et al., 1999.

fenómeno são os pericitos dos capilares cerebrais que desenvolvem uma contração prolongada e desadaptada em virtude do aumento do Ca^{2+} intracelular (Hall et al., 2014). No entanto, na prática clínica, ainda não existem métodos, sejam eles imagiológicos ou bioquímicos, que possam determinar com acuidade suficientemente a gravidade da disrupção da BHE. As escalas de classificação com base em itens clínico-demográficos estão muito aquém de serem capazes de prever satisfatoriamente quais os doentes que terão esse risco aumentado (Whiteley et al., 2012).

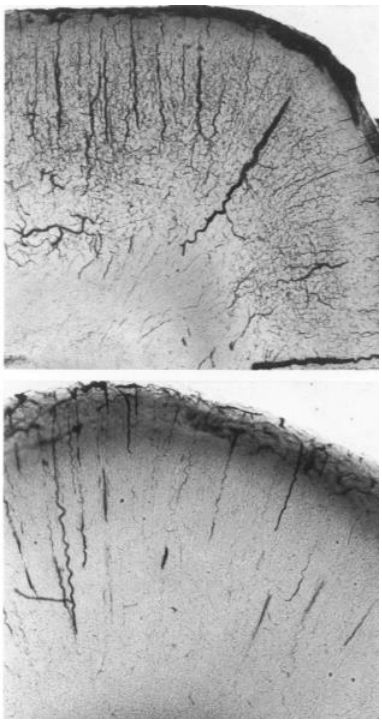

Figura 40 – Fenómeno de não-recirculação
Após 15 minutos de isquemia cerebral por ligação carotídea em ratos, restabelece-se a circulação. No slide acima, assiste-se ao preenchimento vascular, desde que o cérebro fosse pré-lavado com solução de Ringer. Caso contrário, como mostra a figura abaixo, não há preenchimento microvascular. Portanto, fatores presentes no tecido cerebral enfartado promovem este fenómeno, hoje atribuído maioritariamente à contração dos pericitos. *Adaptado de Ames et al, 1968.*

O conceito de penumbra isquémica

A área cerebral imediatamente a jusante da artéria ocluída, sendo desprovida de compensação de fluxo, fica irremediavelmente isquemiada em pouco tempo, com morte celular pela despolarização terminal da membrana destas células (Hossmann, 2006). Contudo, os sistemas de colateralização permitem alguma compensação da perfusão na região mais periférica do território sob insulto isquémico (Liebeskind, 2003), definindo-se uma zona de isquemia latente, eletricamente disfuncional mas que ainda será viável se o FSC local for restituído (Figura 41). Tal facto implica que, nas primeiras horas do evento, para além da área de enfarte estabelecida, designada por isquémica central (Tikhonoff et al., 2009), haja uma área de penumbra isquémica, na qual a perfusão cerebral está comprometida mas não de modo irremediável. Tanto a zona de isquemia central e como a de penumbra isquémica são clinicamente sintomáticas.

Devido à existência desta penumbra isquémica e da possibilidade do seu resgate, surgiram os tratamentos de recanalização no AVC isquémico agudo. Assim, a revascularização química (Jauch et al., 2013a, European Stroke Organisation Executive & Committee, 2008) ou mecânica (Molina & Saver, 2005, Wahlgren et al., 2016) batem-se pelo restabelecimento do fluxo na área de penumbra, permitindo "salvar" uma área de tecido cerebral da isquemia definitiva, com limitação dos défices neurológicos e maior grau de funcionalidade do doente a longo prazo.

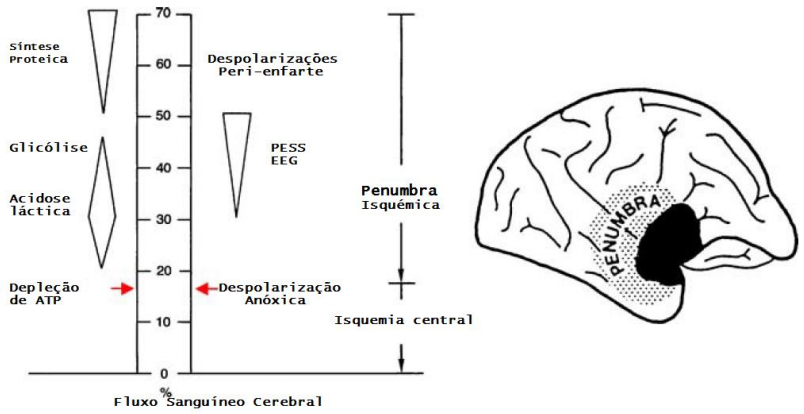

Figura 41 – Penumbra isquémica
Limiares metabólico (esquerda) e eletrofisiológico (direita) durante a redução gradual focal do fluxo sanguíneo cerebral. A região de isquemia central ocorre quando a diminuição do fluxo tem lugar abaixo do limiar da falha energética, enquanto a penumbra ocorre quando há falha de irrigação, mas com estado metabólico preservado. Potencial evocado somato-sensitivo (PESS); eletroencefalograma (EEG). *Adaptado de Hossmann, 1994.*

ESTUDOS INICIAIS SOBRE REGULAÇÃO VASCULAR CEREBRAL

Antes de me envolver nos trabalhos da tese propriamente ditos, iniciei a minha atividade científica com outros estudos funcionais com DTC e noutras perspetivas. Pude então familiarizar-me com os métodos de avaliação da função cerebrovascular e produzir novos conhecimentos sobre os aspetos do controlo cerebrovascular tanto em indivíduos normais como em situações patológicas de disautonomia e Doença de Fabry. Estes trabalhos prévios, que podem ser consultados em texto completo em "Anexos", referem-se à influência do ortostatismo, do SNA e da disfunção endotelial nos mecanismos que governam a regulação vascular cerebral, que podem também estar envolvidos na desregulação cerebrovascular do AVC isquémico agudo. De seguida descrevo sucintamente cada um dos trabalhos em particular.

Síncope e síndromes de intolerância ortostática

A síncope corresponde a uma perda de consciência devida à diminuição global da perfusão sanguínea cerebral (Freitas, 2010). Existem muitas influências hemodinâmicas e neuro-hormonais (Freitas et al., 2007) que podem comprometer a circulação sistémica, mas pouco se sabe sobre as consequências hemodinâmicas cerebrais neste contexto. As síndromes de

intolerância ortostática incluem a síncope neurocardiogénica, a síndrome da taquicardia postural com o ortostatismo, a hipersensibilidade do seio carotídeo e a hipotensão ortostática. Assim, fruto da colaboração entre os de Serviços de Neurologia e Cardiologia, nasceu um projeto de colaboração devoto ao estudo hemodinâmico cerebral em doentes com intolerância ortostática, realizado no Centro de Estudos de Função Autonómica do Hospital de São João e com especial enfoque no papel do SNA. Os estudos efetuados pela equipa de investigação referida têm revelado aspetos fisiopatológicos importantes (Freitas, 2010, Freitas et al., 1998, Freitas et al., 2007).

A monitorização das velocidades de fluxo cerebral com DTC permitiu estudar melhor as características hemodinâmicas particulares das várias síndromes de intolerância ortostática (Freitas, 2010). No caso da síncope neurocardiogénica, o estudo hemodinâmico cerebral mostrou que estes doentes apresentam um fenómeno de aumento do tónus vascular cerebral marcado, que se já se verifica pelo menos 5 minutos antes da queda abruta da PA no momento da síncope (ver "Anexos - *Indexes of cerebral autoregulation do not reflect impairment in syncope: insights from head-up tilt test of vasovagal and autonomic failure*"). Esta vasoconstrição cerebral poderá ser fruto da hiperventilação e hipocapnia, podendo predispor estes indivíduos à ocorrência do reflexo neurocardiogénico e, consequentemente, à síncope. Neste estudo adotou-se uma estratégia de análise da ARC inovadora com medição contínua do índice de autorregulação ($IARC_t$). Assim, foi possível comprovar que a ARC permanece intacta até ao momento em que ocorre a síncope. Não parece, pois, que estes doentes tenham *a priori* uma disfunção regulatória do fluxo cerebral perante as variações de PA que os predispõem à ocorrência de síncope.

No caso de doentes com polineuropatia amiloidótica familiar (PAF), observaram-se dois aspetos relevantes. O primeiro prende-se com o facto de haver uma dificuldade particular de avaliação da ARC nos doentes com disautonomia, o que pode ser extrapolado nas futuras investigações em que possa haver essa interferência (e.g., diabetes *mellitus*, AVC isquémico agudo). De facto, a coerência entre PAM e VFM foi muito baixa, certamente devido à baixa variabilidade da PA, uma característica da falência do SNA. Isso tornou a interpretação dos parâmetros da AFT pouco válida do ponto de vista matemático. Não deixa de ser interessante notar que a variabilidade da VFM não fica afetada, contrariamente a outros sinais biológicos como a FC e a PA, sendo muito semelhante à dos indivíduos normais em todas as bandas de frequência. Estes resultados sugerem a existência de múltiplas influências que sobressaem na flutuação do FSC (cognitivas, hormonais, etc.). Estes achados apenas haviam sido relatados num estudo experimental, numa população saudável submetida a bloqueio ganglionar farmacológico (Zhang et al., 2002). Pela

primeira vez, são confirmadas estas alterações num grupo de doentes com disautonomia. O segundo resultado relevante foi mostrar que a ARC permanece em níveis elevados durante a prova de *Tilt*, tendo-se estudado, pela primeira vez, as respostas ao ortostatismo com medição contínua da ARC ($IARC_t$). Observou-se pois uma resposta vasodilatadora cerebral compensatória e esperada perante a descida marcada da PA e da VFSC. Esta resposta vasodilatadora parece ser melhor explicada por um decréscimo do PRA ao invés do clássico iRVC, que permaneceu constante durante a prova, não refletindo a resposta fisiológica esperada. Pelo contrário, verifica-se um aumento da PCrE semelhante ao que foi registado nos indivíduos normais. Deste modo, a diminuição excessiva de valores de PRA para além da PCrE poderá levar rapidamente ao colapso vascular e, consequentemente, à ocorrência de síncope.

No seu conjunto, os resultados deste trabalho mostram que a ARC não parece estar envolvida primariamente na fisiopatologia da síncope, quer em condições hiperadrenérgicas típicas da síncope neurocardiogénica, quer na disautonomia. Neste último caso, também se dá enfoque ao facto de o modelo dual PRA+PCrE parecer ser vantajoso em relação à análise do estado vasomotor baseada apenas num só parâmetro, o iRVC.

Adaptação hemodinâmica cerebral a duplo estímulo: ortostático e visual

Um trabalho prévio de Azevedo *et al* mostrou que o ANV se mantinha constante ao longo das várias condições de ortostatismo progressivo: desde a posição supina, passando para sentado até terminar na prova de Tilt a 70° (Azevedo et al., 2007). Contudo, não foi investigado o modo como a hemodinâmica cerebral reage ou interage com os mecanismos reguladores cerebrais, de modo a manter o ANV intacto. Assim, comparam-se os valores de resistência vascular cerebral nas diferentes posições durante a fase de repouso e a sua variação com o estímulo visual.

Neste estudo evidenciou-se que, apesar de a variação da VFM durante o ANV ser semelhante nas três posições, este foi fisiologicamente diferente. Todos estes parâmetros de resistência, PCrE, PRA e iRVC, diminuíram durante a estimulação visual, mas a magnitude dessa variação não foi equivalente. Na posição de máximo stresse ortostático, ou seja, durante o tilt, a variação da PCrE contribui pouco para o aumento do VFSC em relação ao que sucede em supino ou na posição de sentado, enquanto o PRA se mostrou semelhante nas três posições. Este facto poderá estar relacionado com o facto de a PCrE aumentar em valor absoluto, em fase pré-estimulação, com o ortostatismo e, deste modo, não reduzir tanto durante o ANV. Estes resultados mostram uma adaptação complexa da hemodinâmica cerebral ao ortostatismo, de modo a preservar o acoplamento vascular e, por isso mesmo, as necessidades metabólicas

necessárias para a manutenção da atividade mental. Este trabalho foi importante porque evidenciou que os vasos de resistência se adaptam de modo a manter a pressão de perfusão aceitável, impedindo o comprometimento nutritivo dos microvasos parenquimatosos.

Influência do sistema nervoso central na regulação hemodinâmica sistémica

Um dos mecanismos reguladores hemodinâmicos sistémicos que podem ter influência cerebral é o sistema de BR (ver sessão "Barorreflexo"). Sabe-se que este controlo do sistema nervoso central se faz por várias estruturas que designamos por RAC (ver secção "Neurogénicas "). No AVC isquémico ocorre lesão do sistema nervoso central, o que pode danificar a RAC. Como vimos anteriormente (ver secção *"Síncope e síndromes de intolerância ortostática"*), a disautonomia, e consequentemente perda de BR, pode alterar a dinâmica da regulação cerebral e até inviabilizar a interpretação dos dados da mediação de ARC, particularmente da AFT. Neste estudo determinou-se até que ponto lesões mais conspícuas sobre a RAC podiam afetar os mecanismos gerais de regulação de BR. Selecionou-se um modelo de esclerose múltipla, dado que estes doentes podem apresentar lesões na vizinhança e conexões da RAC sem, contudo, afetar uma grande área contígua. Para o efeito, criou-se uma pontuação de lesão da RAC, em que a existência de uma lesão justaposta a uma das áreas deste sistema contribuía com um ponto para essa escala.

Verificaram-se dois resultados importantes. Em primeiro lugar, os doentes com esclerose múltipla, mesmo que em fases iniciais, apresentam uma disfunção autonómica melhor demonstrada pela análise de variabilidade da FC do que por testes clássicos da bateria de Ewing. Em segundo lugar, esta disfunção não mostrou qualquer correlação com o atingimento central. A exceção foi o facto de lesões peri-insulares condicionarem um aumento do tónus simpático (mediana ou amplitude interquartil LF/HF: 1,1 (0,6–2,1) vs. 0,9 (0,4–1,3), p = 0,035). Este envolvimento insular como modificador do tónus simpático-parassimpático tem sido descrito no AVC, embora não tenha sido descrito em nenhuma outra patologia do sistema nervoso central. A disautonomia destes doentes foi, em parte, explicada por lesões espinhais que podem facilmente atingir a coluna intermediolateral do SNA simpático, cujos segmentos torácicos altos controlam a FC via plexo cardíaco. Assim, podemos esperar que o atingimento do RAC no AVC não seja um fator primordial na interferência dos mecanismos de regulação da hemodinâmica periférica e que possa interferir nos resultados da ARC.

Autorregulação cerebral e efeito da disautonomia durante a manobra de Valsalva

Tal como vimos na introdução, a manobra de Valsalva é geralmente usada para testar o SNA e também a ARC, já que apresenta variações previsíveis da PA ao longo das suas fases. Para além das variações de PA, também existe um aumento da pressão intratorácica que se transmite a nível intracraniano durante o esforço respiratório. O interesse desta prova é que, ao manipular o valor de PIC, podemos testar o modo como os índices de autorregulação se comportam durante a prova e, daqui, retirar consequências para o uso destes em situações em que a PIC tem oscilações ou em que haja mudanças do SNA, como é frequente no AVC isquémico (De Raedt et al., 2015).

Usámos uma estratégia nova (ver secção *"IARC contínuo"*) para calcular o valor de IAR ao longo do tempo de forma contínua ($IARC_t$). Podemos, pois, comprovar que o valor de IARC não se mantém estável durante a manobra, como se pode evidenciar na Figura 31. Nos indivíduos saudáveis, a ARC aumenta face ao estímulo de descida da PA e parece "desligar" após um período de bradicardia final sob o risco de provocar uma queda de FSC excessivo nesta fase final. Outro aspeto relevante foi o de demonstrar, mais uma vez, que o modelo PCrE + PRA é superior ao simples iRVC para demostrar aspetos fisiológicos. Assim, verificamos claramente que a PIC tem uma influência direta nos valores de PCrE, mesmo nos doentes com disautonomia. Contudo, como a PA cai progressivamente devido à ausência de ativação do simpático, ocorre uma vasodilatação cerebral demonstrada pela redução do PRA. Se tivéssemos apenas em conta o iRVC, chegaríamos à conclusão de que os doentes com disautonomia apresentavam vasoconstrição cerebral durante a prova, o que seria "paradoxal" de acordo com o esperado fisiologicamente.

Ao contrário de Zhang et al. (Zhang et al., 2004a), não se verificou uma hiperémia final no grupo de disautonomia. O nosso grupo de doentes com PAF representa um modelo de desnervação autonómica persistente que poderá levar a fenómenos adaptativos a longo prazo, o que poderá explicar as diferenças com os seus resultados. Assim, este estudo mostra as diferenças entre um modelo de disautonomia crónica e outros em que se provoca uma disautonomia aguda (e.g., bloqueio ganglionar com trimetafano). Os resultados deste estudo, juntamente com outros (Panerai, 2003, Panerai et al., 2005, Maggio et al., 2013, Salinet et al., 2013), demonstram que o PRA parece ser um fator de resposta miogénica mais fidedigno do que o iRVC e que não é tão influenciado por variáveis metabólicas, cognitivas ou de PIC como a PCrE.

Influência do sistema nervoso autónomo no acoplamento neurovascular

Neste estudo procurou-se perceber de que modo a disautonomia poderia comprometer os mecanismos que regulam a hiperémia funcional regional durante a atividade cognitiva. Assim, comparou-se a resposta de ANV, através de um paradigma visual e monitorizando a ACP com DTC, entre dois grupos: um composto por indivíduos saudáveis e outro por indivíduos com disautonomia causada por PAF. Esta avaliação ocorreu em dois graus de stresse hemodinâmico: supino e sentado. Utilizou-se a parametrização de Rosengarten (ver secção *"Visual"*). Descobriu-se que, no grupo com disautonomia, o ANV se encontrava afetado já na posição de supino e que agravava com a posição sentado, ao contrário dos indivíduos saudáveis. De notar que nos doentes com PAF, apesar da disautonomia marcada (com hipotensão ortostática em tilt), não havia ainda uma variação significativa da PA na posição de sentado. Na posição de sentado, foi notória a diminuição da aceleração inicial e de valor final (ganho) de VFSC durante a estimulação visual no grupo de doentes com disautonomia.

Além disso, pode verificar-se alguma alteração da regulação dos vasos de resistência cerebrais. Para tal, comparam-se o iRVC, o PRA e a PCrE. Embora não se tenha verificado nenhuma diferença significativa entre os grupos em cada posição, houve diferenças no comportamento dos vários índices, com a mudança de posição e na estimulação visual. Realça-se a diminuição significativa de PRA nos dois grupos de doentes com PAF, ao contrário dos controlos, da posição supina para sentada. Uma vez que este marcador de resistência vascular cerebral se relaciona mais com o mecanismo miogénico, sugere uma vasodilatação predominantemente miogénica na adaptação ao estímulo ortostático. Este facto está de acordo com o que foi verificado durante a prova de tilt do estudo prévio (ver sessão *" Síncope e síndromes de intolerância ortostática"*).

Com a estimulação visual e na posição sentada, verificou-se que, nos doentes com disautonomia, a variação do PRA e da PCrE reforçou os achados obtidos pelo sistema de controlo, podendo sugerir, num contexto de perturbação autonómica, maior envolvimento local dos mecanismos miogénico e metabólico. Até então, não haviam sido descritas alterações destes parâmetros, nem com alterações posturais, nem com estimulação metabólica regional.

Nos doentes com menor grau de disfunção autonómica, que estavam ainda assintomáticos, é curioso verificar que se encontrou uma perturbação ligeira da VR. Estes achados poderão reforçar a ideia de haver já um atingimento pré-sintomático da regulação hemodinâmica, o que está de acordo com os trabalhos preliminares da hemodinâmica sistémica já referidos, relativos ao registo da variabilidade de PA e FC nas 24 horas (Carvalho et al., 2000).

Os resultados obtidos no estudo da adaptação postural e do ANV favorecem então a ideia da importância do mecanismo neurogénico na regulação hemodinâmica cerebral no que concerne

ao ANV. Assim, nas situações de disfunção autonómica, em que pelo menos a inervação extrínseca dos vasos corticais estará afetada, verifica-se perturbação da hiperémia funcional e maior relevância dos mecanismos miogénico e metabólico na regulação da VR, comparativamente com os controlos.

A discussão acerca do papel do SNA, e nomeadamente do sistema nervoso simpático, foi introduzida previamente na secção *"Neurogénicas"*. Apesar da evidência de uma boa inervação por fibras simpáticas do leito vascular cerebral (Sercombe et al., 1975, Edvinsson, 1975), o seu papel na regulação vasomotora é ainda pouco conhecido e mesmo controverso (van Lieshout & Secher, 2008). Como o SN simpático é, em geral, mais ativado com o ortostatismo, o facto de as alterações do ANV nos doentes com PAF se manifestarem predominantemente na posição sentada, em relação à supina, levará a pensar que seja o compromisso simpático mais responsável pelas alterações encontradas. Como se sabe, a ação vascular do simpático é geralmente de vasoconstrição, e poderá levantar-se a hipótese de a sua ação ser importante na contração de leitos vasculares não ativos, "focando" a zona estimulada. Contudo, não se pode afastar a hipótese de a ausência de vasodilatação por um parassimpático comprometido ter um papel nas alterações regionais do ANV. Porque o simpático e o parassimpático podem ser importantes para regular a nível extraparenquimatoso (pial) o fluxo sanguíneo dos vasos intracerebrais onde se dá o ANV, poderá haver dificuldade em preservar a perfusão correta focal que é despertada pelas arteríolas corticais que promovem o ANV.

O papel do endotélio na regulação vascular cerebral

Uma vez que na doença de Fabry existe um atingimento precoce de doença vascular cerebral, com AVC ou acidentes isquémicos transitórios (Fellgiebel et al., 2005, Sims et al., 2009, Rolfs et al., 2005), (Rolfs et al., 2005, Fellgiebel et al., 2005, Sims et al., 2009) tentou-se estudar uma população de doentes ainda assintomáticos para doença vascular cerebral, procurando achados pré-clínicos. Tratam-se de pacientes adultos portadores de mutação do gene GLA, resultando na ausência ou diminuição de atividade da enzima α-galactosidase A, com fenótipo clássico da doença (Desnick et al., 2003). Para além da avaliação do ANV, procuraram-se marcadores imagiológicos de doença vascular cerebral. O estudo concluiu haver evidência hemodinâmica e imagiológica de envolvimento assintomático do SNC na doença de Fabry, incluindo aumento da espessura íntima-média na carótida comum na ausência de placas ateroscleróticas focais, diminuição da velocidade em repouso do fluxo sanguíneo na ACP, perturbação do ANV no córtex occipital, lesões de substância branca, diminuição da razão entre os volumes da substância

branca e cinzenta, alongamento e tortuosidade das grandes artérias intracranianas e aumento do diâmetro da artéria basilar. Não há marcadores hemodinâmicos estabelecidos para o atingimento cerebral da Doença de Fabry. Apenas se encontram na literatura dois estudos com resultados contraditórios com recurso a DTC (Moore et al., 2002, Hilz et al., 2004). O nosso estudo revelou uma perturbação funcional do ANV que poderá ser útil como marcador da doença ainda em fase assintomática, permitindo eventual modulação do tratamento, embora não haja evidência robusta de ação da terapêutica enzimática de substituição na vasculatura cerebral. Este estudo mostra como a parede vascular e o endotélio poderão também afetar a normal regulação vascular, pelo que estes mecanismos deverão ser tidos em conta no estudo da hemodinâmica do AVC isquémico cerebral.

JUSTIFICAÇÃO DAS BASES QUE CONDUZIRAM AOS OBJETIVOS DO PROJETO

Apesar dos avanços no tratamento de fase aguda do AVC isquémico, muitos doentes com AVC isquémico não são submetidos a tratamento de revascularização aguda, nalguns casos ficando-se apenas pelos 1-3% to total de AVC isquémicos (Molina & Saver, 2005). Além disso, numa metanálise do conjunto dos ensaios clínicos mais recentes sobre trombectomia (o tratamento mais eficaz), a independência funcional aos três meses não ultrapassou os 50% (Goyal et al., 2016). Num estudo menos controlado e mais próximo da vida real, esta ficou-se pelos 33% (Berkhemer et al., 2015). Assim sendo, apesar de haver recanalização numa curta janela terapêutica de 6 horas (Powers et al., 2015), um grupo considerável de doentes não melhora, pelo que necessitamos de entender melhor que fatores limitam a viabilidade da penumbra isquémica.

Dois dos aspetos que afetam o prognóstico do doente após revascularização cerebral são o edema cerebral e a transformação hemorrágica do tecido enfartado (Balami et al., 2011). As características clínicas e laboratoriais analíticas de rotina não permitem predizer estas complicações com acuidade suficiente (Whiteley et al., 2012) para a tomada de decisões perante o doente individual. Há evidência de que uma microvasculatura cerebral cronicamente danificada poderá estar envolvida na fisiopatologia das complicações neurológicas referidas, já que os sinais imagiológicos que com ela se relacionam (e.g., grau de leucoencefalopatia) aumentam significativamente o risco de hemorragia (Curtze et al., 2015) e edema (Strbian et al., 2013) do tecido cerebral isquemiado após trombólise endovenosa. Serão os pequenos vasos de resistência um dos participantes nestas complicações?

Sabemos que existe grande variabilidade na resposta à isquemia cerebral (Giffard et al., 2004, Gonzalez et al., 2010). Se, por um lado, existem doentes que progridem rapidamente para a isquemia cerebral, incluindo a zona de penumbra isquémica, também se verificam alguns casos de dissociação entre a clínica e os achados imagiológicos de gravidade (e.g., défices neurológicos ligeiros e oclusão de M1) (d'Esterre et al., 2015). Alguns autores focam a sua interpretação no grau de colateralização (Liebeskind, 2003) que um doente consegue atingir de modo a proteger a penumbra isquémica. Contudo, o que determina a disparidade observada na ativação das colaterais arteriais no AVC isquémico agudo? Tal não explica as complicações da lesão de reperfusão, o edema cerebral ou a hemorragia secundária. Isto leva-nos à questão: não será o estado funcional dos vasos de resistência e a sua incapacidade regulatória na zona sob isquemia o que poderá contribuir, em parte, para a progressão isquémica ou complicações do enfarte cerebral?

Um dos fatores que podem influenciar o destino das células da penumbra isquémica são os níveis de PA na fase aguda (Tikhonoff et al., 2009). A relação da PA com o prognóstico do AVC isquémico agudo descreve uma curva em U, i.e., valores extremos de PA podem conduzir a um pior prognóstico (Figura 42) (Leonardi-Bee et al., 2002, Geeganage & Bath, 2009). Isso conduziu à elaboração de vários estudos de manipulação da PA, que acabaram por ter sempre resultados neutros (Tikhonoff et al., 2009). A negatividade destes estudos poderá estar relacionada com o facto de terem ignorado o estado hemodinâmico da circulação cerebral. O simples facto de sabermos se o vaso foi ou não recanalizado afeta decisivamente essa relação (Martins et al., 2016). Assim, no que ao manuseamento e objetivos de PA na fase aguda do AVC isquémico diz respeito, as linhas de orientação permanecem desoladoramente evasivas (European Stroke Organisation Executive & Committee, 2008, Jauch et al., 2013a). É interessante notar que os valores de PA também têm uma relação através de uma curva de aspeto em "U" com o prognóstico de outras patologias cerebrais agudas como o traumatismo craniano (Butcher et al., 2007) e a hemorragia intracerebral (Vemmos et al., 2004). Neste contexto, essa relação já se mostrou intimamente ligada ao estado da ARC (Czosnyka et al., 1997, Steiner et al., 2002, Dias et al., 2015), tal como detalhado na secção "*Importância clínica dos índices de autorregulação cerebral*".

Neste contexto, e relativamente a estas questões hemodinâmicas, o ponto essencial poderá não ser qual o melhor nível de PA que devemos manter, mas o facto de percebermos se a vasculatura

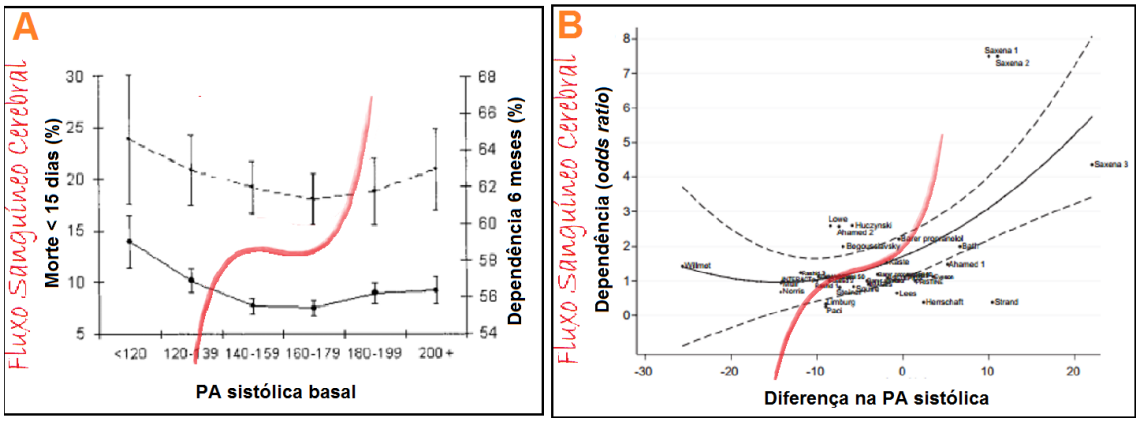

Figura 42 – Pressão arterial e AVC isquémico agudo
Interpretação do autor acerca da relação da pressão arterial (PA) e prognóstico no AVC isquémico agudo. O texto e linhas escuras dizem respeito a resultados de dois estudos em que se mostra que (**A**) (Leonardi-Bee et al., 2002) os doentes que se apresentam nos extremos de PA se associação a pior prognóstico em termos de mortalidade e estado funcional a longo prazo e que a manipulação excessiva da PA na fase aguda do AVC isquémico (**B**) (Geeganage & Bath, 2009) parece contribuir para um prognóstico funcional pior. O autor da tese reinterpreta os resultados numa perspetiva de autorregulação cerebral. Os níveis de PA elevados ou baixos poderão associar-se a pior prognóstico dado terem sido cruzados os limites da autorregulação (linhas a vermelho) e o fluxo cerebral (texto a vermelho) diminuiu (e.g., progressão da isquemia) e ou aumenta (e.g., risco de transformação hemorrágica) proporcionalmente com a PA.

cerebral tem capacidade ou não de manter um FSC constante independente das variações da PA, ou seja, se a ARC estará ou não preservada. Se esta estiver intacta, então as alterações da PA, dentro de certos limites, não irão afetar a perfusão do território arterial cerebral afetado, já que uma eficiente constrição ou dilação vascular permitirá manter o FSC. No entanto, no caso de haver disfunção deste mecanismo, um episódio hipotensivo poderá levar à hipoperfusão cerebral e extensão da área de enfarte à zona de penumbra; pelo contrário, se houver níveis elevados de PA, poderá resultar em hiperperfusão de um leito vascular fragilizado e consequente transformação hemorrágica e edema cerebral. Seguindo este raciocínio, poderemos concluir que o conhecimento da capacidade de ARC no AVC isquémico agudo poderá ajudar a delinear melhores estratégias terapêuticas e predizer complicações neurológicas.

Apesar de a ARC poder ser relevante para o sucesso da recuperação da penumbra isquémica e para a predição de complicações neurológicas, tem sido estudada no AVC isquémico (Aries et al., 2010) fora da janela terapêutica mais relevante, ou seja, até às 6 horas de início de sintomas (Powers et al., 2015). Uma das limitações dos estudos da ARC na fase aguda do AVC refere-se ao tempo de avaliação, que variou entre 20 – 96 horas após o início de sintomas (Reinhard et al., 2005, Immink et al., 2005, Dohmen et al., 2007, Reinhard et al., 2008, Eames et al., 2002, Dawson et al., 2003, Dawson et al., 2000b). Além disso, os estudos existentes são marcados

também pela heterogeneidade em termos de população; no entanto, os resultados, globalmente, mostram uma disfunção da ARC (Aries et al., 2010).

A ARC também não tem sido estudada como binómio cérebro-rim e cérebro-coração.
A doença renal crónica aumenta o risco de AVC isquémico, aumenta a sua gravidade e piora o prognóstico (Kumai et al., 2012, Toyoda & Ninomiya, 2014, Naganuma et al., 2011). O mecanismo exato que governa esta relação está pouco esclarecido (Toyoda & Ninomiya, 2014). Uma explicação possível pode ser o facto de terem árvores microvasculares semelhantes. Em ambos os órgãos, a vasculatura tem um fluxo de baixa resistência e precisa de manter o fluxo sanguíneo constante regulado por mecanismos miogénicos bem afinados, para o proteger das variações de PA, i.e., de ARC {(Panerai, 1998, Lassen, 1959, Carlstrom et al., 2015, Aaslid et al., 2003, Davis, 2012, Loutzenhiser et al., 2006). A ARC é, pois, vista como um mecanismo geral que protege os órgãos contra os insultos (e.g. hipertensão arterial não controlada e diabetes *mellitus*) (Wardlaw et al., 2009, O'Rourke & Safar, 2005) (Purkayastha et al., 2014). De facto, a esclerose glomerular da doença renal crónica (Bidani & Griffin, 2004), os enfartes lacunares e as lesões de substância branca são caracterizados por condições patológicas semelhantes: disfunção endotelial, arteriolosclerose isquémica, perfusão reduzida e extravasamento vascular (Fazekas et al., 1993, Wardlaw, 2010. A lesão renal está associada a lesões microvasculares cerebrais {Yang, 2017 #818). No estudo do estado funcional da microvasculatura, a ARC pode ser um fator que explique o pior desfecho clínico dos doentes com doença renal crónica.

A relação entre coração e cérebro tem sido cada vez mais salientada. A Insuficiência cardíaca (IC) crónica tem sido associada ao mau prognóstico no AVC, sendo que tal é devido em grande medida à sua associação a fibrilhação auricular e a AVC mais graves (Haeusler et al., 2011).
Por outro lado, podemos pensar na IC como uma situação de hipoperfusão cerebral crónica, o que pode induzir alterações morfofuncionais nos vasos de resistência cerebral de modo a ter maior capacidade de resposta ao insulto isquémico, aquilo que designamos por pré-condicionamento isquémico (Koch et al., 2014). Um trabalho prévio mostrou que existe desoxigenação cerebral em postura ortostática nos doentes com IC com disfunção ventricular (Cornwell & Levine, 2015), possivelmente como resultado da vasoconstrição cerebral provocada por um aumento do simpático (van Lieshout & Secher, 2008), embora tal se possa dever simplesmente à diminuição do débito cardíaco. São poucos os estudos que se debruçam sobre a regulação cerebrovascular nos doentes com IC. Um estudo prévio mostrou que poderá existir algum défice de VR ao CO_2, embora tal não seja ARC (Georgiadis et al., 2000). Um único estudo

recente mostrou que existe alguma limitação de ARC em doentes com disfunção sistólica e em repouso, numa fase sem descompensação ou doença aguda (Caldas et al., 2017). Não há estudos de ARC na IC na fase de isquemia cerebral aguda. Um melhor conhecimento dos mecanismos da hipoperfusão pode levar ao melhor tratamento das complicações neurológicas na IC crónica, assim como originar novos dados sobre o modo como o cérebro responde à hipoxia global.

Em suma, há importantes lacunas no conhecimento científico que justificam o estudo da ARC na fase aguda do AVC isquémico e do seu papel no prognóstico e risco de complicações cerebrais.

IV. OBJETIVOS

Objetivo geral

O objetivo geral deste projeto foi investigar o papel que a ARC dinâmica tem no AVC isquémico agudo, avaliado por DTC e medição não invasiva contínua da PA, para aumentar o conhecimento fisiopatológico da doença, assim como determinar o seu valor prognóstico.

Objetivos específicos

O projeto de investigação dividiu-se em duas fases: num primeiro momento (Parte **A**), avaliou-se a ARC numa população normal sem fatores de risco vascular; e num segundo momento (Parte **B**), avaliaram-se doentes com AVC isquémico agudo. Os objetivos mais específicos são:

Parte A

- Determinar entre que valores opera a ARC dinâmica, avaliada pela AFT, numa população saudável sem fatores de risco vascular;
- Compreender melhor a influência de parâmetros demográficos, como idade e sexo, e de parâmetros hemodinâmicos sistémicos básicos, nos valores da ARC dinâmica;
- Determinar qual a correlação entre os parâmetros que avaliam os vários mecanismos de regulação vascular cerebral – ARC, VR e ANV.

Parte B

- Avaliar a possibilidade de medição da ARC dinâmica dentro das primeiras 6 horas de sintomas de AVC isquémico agudo;
- Determinar a sua relação com o volume de enfarte às 24 horas e prognóstico funcional, avaliada pela escala modificada de Rankin aos 3 meses;
- Determinar a sua relação com o risco de complicações neurológicas mais comuns – transformação hemorrágica e edema cerebral às 24 horas;
- Avaliar a relação entre a ARC e a função renal, estimada pela taxa de depuração da creatinina basal nos doentes com AVC isquémico agudo;
- Avaliar a influência que a hipoperfusão crónica causada pela IC tem na resposta da ARC na fase aguda e crónica do AVC isquémico.

V. CAPÍTULOS

PARTE A: ESTUDO DA AUTORREGULAÇÃO CEREBRAL NUMA POPULAÇÃO NORMAL

Capítulo 1: Influência dos fatores demográficos e hemodinâmicos sistémicos nos mecanismos de regulação vascular cerebral

---

Madureira, J., Castro, P., & Azevedo, E. (2016). Demographic and Systemic Hemodynamic Influences in Mechanisms of Cerebrovascular Regulation in Healthy Adults. *J Stroke Cerebrovasc Dis*. doi: 10.1016/j.jstrokecerebrovasdis.2016.12.003

Demographic and Systemic Hemodynamic Influences in Mechanisms of Cerebrovascular Regulation in Healthy Adults

João Madureira, MSc, MD,* Pedro Castro, MD,*,† and Elsa Azevedo, PhD, MD*,†

Objectives: A competent cerebrovascular regulation maintains an adequate cerebral blood flow by 3 major mechanisms: cerebral autoregulation (CA), vasomotor reactivity (VMR), namely to CO_2, and neurovascular coupling (NVC). However, most studies generalize their results based on a response to a single parameter. Using a full battery of neurovascular stress tests, our study aims to evaluate the relationships among grades of CA, VMR, and NVC, and how their interplay is influenced by demographic and systemic hemodynamic factors. *Methods:* Fifty-eight healthy adults were recruited to fit each decade age stratum from 20 to 80 years old with similar sex ratio. Arterial blood pressure (Finometer), cerebral blood flow velocity in the middle cerebral arteries (transcranial Doppler), electrocardiogram, and end-tidal CO_2 were monitored. We assessed CA by transfer function analysis, VMR at hypocapnia and hypercapnia (carbogen 5%), and NVC response during the N-Back Task. The Montreal Cognitive Assessment scores were recorded. *Results:* Neurovascular stress tests were not affected by age or gender, and no correlation was found between their outputs ($P > .05$). Systemic hemodynamic parameters during tasks as well as cognitive scores had no correlation with cerebrovascular measurements ($P > .05$). *Conclusions:* Age and gender do not have major influence on the 3 major cerebrovascular regulation mechanisms. Our results also pinpoint the fact that neurovascular stress tests measure different aspects of cerebrovascular control, and that their outputs are uncorrelated and cannot be used interchangeability. Being independent of age and cognitive status, neurovascular stress tests seem adequate for studying several cerebrovascular conditions affecting the aging brain. **Key Words:** Cerebrovascular reactivity—cerebral blood flow—cerebral autoregulation—vasomotor reactivity—neurovascular coupling—transcranial Doppler.

Introduction

Harmonious control of the cerebrovascular bed is crucial for maintaining an adequate cerebral blood perfusion in response to a myriad of vasoactive stimuli.[1] In order to compensate the high metabolic rate and limited energy stores of brain tissue, a complex interplay among metabolic,[2] neuronal,[3-5] and pressure- and shear-dependent[2,3,6] myogenic mechanisms modulates cerebral resistance, allowing the cerebral vasculature to constrict or dilate in response to hemodynamic and neurophysiological stimuli.[1]

Transcranial Doppler is a powerful and versatile tool for noninvasive assessment of intracranial vessels. It allows easy access to the health of the cerebral microvascular bed using neurovascular tests.[2,7,8] These procedures allow the evaluation of 3 major physiological processes

From the *Department of Clinical Neurosciences and Mental Health, Faculty of Medicine, University of Porto, Porto, Portugal; and †Department of Neurology, Hospital Center São João, Porto, Portugal.
Received July 29, 2016; revision received August 24, 2016; accepted December 5, 2016.
João Madureira and Pedro Castro contributed equally to the article.
Address correspondence to Pedro Castro, MD, Department of Clinical Neurosciences and Mental Health, Faculty of Medicine, University of Porto, Alameda Professor Hernâni Monteiro, 4200-319 Porto, Portugal. E-mail: pedromacc@gmail.com.
1052-3057/$ - see front matter

http://dx.doi.org/10.1016/j.jstrokecerebrovasdis.2016.12.003

that underlie cerebral blood flow preservation: (1) cerebral autoregulation (CA), which is the capacity of the cerebral blood vessels to maintain constant cerebral blood flow regardless of the fluctuation in arterial blood pressure (ABP)[7]; (2) vasomotor reactivity (VMR), the response blood vasoactive substances like carbon dioxide (CO_2)[2]; and (3) neurovascular coupling (NVC), or functional hyperemia, which adapts local flow in response to neuronal activity.[1,2,9,10]

Impairment of cerebrovascular regulation has been linked to several disorders, such as Alzheimer[11,12] and Parkinson[13] diseases, trauma,[14] subarachnoid hemorrhage,[15] carotid artery disease,[16] stroke,[17] metabolic diseases,[18] and autonomic failure.[3,19] However, in most reports, considerations about global cerebrovascular regulation status are supported by only one of these components. Therefore, there is a lack of evidence on the interplay among CA, VMR, and NVC in both healthy and pathologic states, and how age, gender, and other demographic factors influence them per se, regardless of disease.

Using a comprehensive neurovascular stress tests battery, this study seeks to determine how different mechanisms of cerebrovascular control (CA, VMR, and NVC) relate to each other in healthy adults and how they might be influenced by age, gender, and systemic hemodynamic factors.

Materials and Methods

This study was conducted in São João Hospital Center, a university hospital in Porto, Portugal. It was approved by the appropriate local institutional ethical committee and performed in accordance with the Declaration of Helsinki ethical standards. All participants gave written and signed informed consent.

Population Studied

Subjects were selected by advertising within university facilities. We predefined to include 10 Caucasian participants, with a sex ratio of 1:1 in each decade of age strata, ranging from 20 to 80 years old. All participants fulfilled a comprehensive questionnaire to exclude common vascular risk factors (hypertension, diabetes, and smoking), history of vascular disease (e.g., heart failure, atrial fibrillation, etc.), or any neuropsychiatric disease affecting central or autonomic nervous system. Systolic and diastolic blood pressures were averaged from 3 measurements in the sitting position with an oscillometric cuff (Omron M6, Kyoto, Japan). Body mass index was calculated. Participants above 35 years old underwent cervical and transcranial ultrasound examinations (Vivid e, GE, Little Chalfont, UK) to exclude hemodynamically significant carotid stenosis. The Montreal Cognitive Assessment (MoCA) test, which is sensitive to vascular cognitive impairment and has been validated in the Portuguese population, was applied to all participants.[20]

Monitoring Protocol

Evaluations were carried out in a dim-lighted room, with a temperature of around 20°C, in supine position, and with bed head at 0°. Subjects were refrained from taking caffeine, alcohol, exercise, or vasoactive drugs for at least 12 hours before monitorization. Cerebral blood flow velocity (CBFV) was recorded bilaterally from the M1 segment of the middle cerebral artery (MCA), at a depth of 50-55 mm, with 2-MHz monitoring probes secured with a headband (Doppler-Box X, DWL, Singen, Germany). Continuous ABP was recorded with Finometer MIDI (FMS, Amsterdam, Netherlands) on the nondominant side. Heart rate (HR) was assessed from lead II of a standard 3-lead electrocardiogram. End-tidal carbon dioxide ($EtCO_2$) was recorded by nasal cannula with capnograph (RespSense, Nonin, Amsterdam, Netherlands). All data were synchronized and digitized at 400 Hz with PowerLab (AD Instruments, Oxford, UK) and stored for offline analysis. After resting for 20 minutes, a 10-minute period of resting data was stored for CA calculations. Afterwards, VMR and NVC protocols were performed.

Vasomotor Reactivity Protocol

After resting, subjects inspired a gas mixture of 5% CO_2, 21% O_2, and balance nitrogen for 2 minutes. After stabilization of hemodynamic parameters back to baseline, they hyperventilated to an $EtCO_2$ ~20 mm Hg for another 2 minutes. VMR is calculated as the slope of the relationship between $EtCO_2$ plotted against relative mean CBFV at the last 30 seconds of hypocapnia or hypercapnia and expressed as change % of the mean CBFV/mm Hg CO_2. VMR was also calculated separately for hypercapnia and hypocapnia.

Neurovascular Coupling Protocol

N-Back Task was performed and analyzed as by Sorond et al.[10] While in supine position, a sequence of single letters was displayed onto the ceiling. Subjects were instructed to press the mouse button each time a letter was repeated (1-Back) or each time a letter was repeated every other letter (2-Back). A control task was performed before each task—"Identify the letter X"; NVC was calculated as the ratio of the relative CBFV increase during the N-Back (CBFVNB) compared with the control task of "Identify the letter X" (CBFVIDX) using the following formula: $[(CBFVNB - CBFVIDX) / (CBFVIDX)] \times 100$.

Data Analysis and CA Calculations

For each heartbeat, the systolic, mean, and diastolic values of ABP and CBFV were calculated. Cerebrovascular resistance index (CVRi) was computed as the mean ABP / mean CBFV. Dynamic CA was assessed by transfer function analysis (TFA), which was done by calculating the coherence, gain, and phase parameters from beat-to-beat

spontaneous oscillations in CBFV and ABP.[21,22] TFA parameter settings were in compliance with standard recommendations[22]: 10 minutes of data interpolated at 10 Hz with a third-order polynomial spline; window length of 102 seconds; Hanning anti-leakage window; and 50% superposition window, triangular smooth filtering. Lower coherence (correlation coefficient), lower gain (damping of ABP oscillations), and higher phase (speed of the autoregulatory response) between oscillations of ABP and CBFV indicate more effective CA. Values were reported in 3 bands: very low frequencies (VLF: .02-0.07 Hz), low frequencies (LF: .07-0.20 Hz), and high frequencies (HF: .20-0.50 Hz). CA is believed to operate at slower VLF and LF bands.[21,23,24]

Statistics

Normality of the variables was determined by Shapiro–Wilk test. No statistically significant differences were detected between the right and left MCA hemodynamic measurements (Table S1). Thus, both MCA values were averaged and used in subsequent analysis. Differences in baseline characteristics among age strata or genders were determined by one-way analysis of variance/Kruskal–Wallis or Student's *t*-test/Mann–Whitney tests, respectively. Multiple linear regression analysis was then used to study the influence of demographic and systemic hemodynamic factors on cerebrovascular outputs. Age, as a continuous variable, and sex were inserted as explicative variables in a straight line model to predict each cerebrovascular measurement (CBFV, CVRi, CA, VMR, and NVC). Estimation method was chosen after visual inspection of scatterplots. As CBFV and CVRi showed significant association with gender, we also presented data stratified by this variable. Nevertheless, we also tested other curve estimation functions to find significant effects but did find relevant results. Besides R^2 and F test results, goodness of fit was also assumed from the visual inspection of plots of residuals checking for normality and presence of heteroscedasticity (formally tested with Kolmogorov–Smirnov test and Levene's test, respectively). Multicollinearity and autocorrelation between sex and age were controlled by variance inflation factor <10 and Durbin–Watson around 2, respectively. Paired *t*-tests and Wilcoxon signed-rank tests were used to assess the significance of the variation of ABP, HR, and $EtCO_2$ between the rest and activation phases of VMR and NVC protocols. The relationships among CA, VMR, and NVC were evaluated by Pearson or Spearman's correlations.

Results

Age and Gender Effects

Table 1 and Table S2 describe the demographic and systemic hemodynamic characteristics of all subjects (N = 58). Older participants had higher mean ABP ($P < .001$) and MoCA scores ($P < .001$), but other characteristics were similar (Table S2). Table 2 regards the effects of age and gender on cerebrovascular measurements evaluated with multiple linear regression analysis. The mean CBFV decreased significantly with age ($\beta = -.343$, $P < .001$) in both genders. On the other hand, CVRi showed opposite trend increasing toward older subjects ($\beta = .008$, $P = .002$), but only significantly in females ($P = .002$). Females have mean CBFV 7.5 $cm.s^{-1}$ higher than males ($\beta = 7.529$, $P = .013$). Nevertheless, we found age and gender to have no significant effects on the cerebrovascular regulatory mechanisms of CA, VMR, and NVC tests.

Table 1. *Baseline characteristics of all participants (N = 58)*

Demographics	
Males, n (%)	28 (48)
Age, years	48 ± 18
BMI, $kg.m^{-2}$	24.6 ± 3.6
MoCA score	
Total [median (P25-75)]	26.5 (24.5-29)
Visuo/Exec	5 (4-5)
Naming	3 (3-3)
Attention	5 (4-6)
Language	2 (1-3)
Abstraction	2 (2-2)
Delayed recall	4 (4-5)
Orientation	6 (6-6)
Hemodynamics	
Systolic BP, mm Hg	126 ± 16
Diastolic BP, mm Hg	77 ± 9
Mean BP, mm Hg	93.4 ± 11
HR, bpm	69 ± 10
PP, mm Hg	62 ± 15
$EtCO_2$, mm Hg	38 ± 3

Abbreviations: BMI, body mass index; BP, blood pressure; $EtCO_2$, end-tidal CO_2; HR, heart rate; MoCA, Montreal Cognitive Assessment; PP, pulse pressure; SD, standard deviation.

Gender is expressed as count and percentage; other values are given in mean ± SD, except for the MoCA test results which are given in median (percentile: 25-75).

Interplay of VMR, CA, and NVC

The cerebrovascular measurements are presented in Table 2 and their correlations in Table 3. Generally, CA, VMR, and NVC did not correlate significantly with each other. The global VMR was weakly correlated with TFA gain both at the CA operative range (LF band: r = .326, $P = .014$) and outside of it (HF band: r = .324, $P = .015$) and showed no relationship with VMR in hypercapnia or hypocapnia separately ($P > .05$). Curiously, hypercapnic and hypocapnic responses were not correlated (r = .214, $P = .113$).

Influences of Systemic Hemodynamics

The baseline mean ABP, HR, and $EtCO_2$ did not correlate the CA, NVC, and VMR results (Table 4). The same

Table 2. *Multiple linear regression analysis: age and gender effects in cerebrovascular measurements*

								Model	Age		Gender	
	Total	21-30	31-40	41-50	51-60	61-70	70-80	R^2	β (95% CI)	*P*	β (95% CI)	*P*
Number (M:F)	58 (28:30)	10 (5:5)	10 (5:5)	12 (6:6)	10 (5:5)	7 (3:4)	9 (4:5)					
Mean CBFV, cm.sec^{-1}	65.7 ± 12.5	73.7 ± 14.8	67.7 ± 8.7	68.9 ± 10.5	63.1 ± 12.2	62.9 ± 11.9	55.8 ± 11.6	.302	−.343 (−.521, −.171)	<.001	7.53 (1.36, 13.4)	.013
Male	62.0 ± 13.6	70.6 ± 19.1	63.3 ± 7.1	62.4 ± 11.4	60.7 ± 11.7	66.6 ± 18.5	45.8 ± 10.6	.186	−.352 (−.670, −.034)	.031	—	—
Female	68.9 ± 10.7	76.1 ± 12.3	75.0 ± 5.9	74.4 ± 6.2	65.6 ± 13.4	60.1 ± 5.7	61.8 ± 7.7	.330	−.336 (−.529, −.143)	.001	—	—
CVRi, mm Hg · cm^{-1}.s^{-2}	1.3 ± .3	1.1 ± .3	1.1 ± .3	1.3 ± .3	1.30 ± .4	1.4 ± .3	1.5 ± .3	.183	.008 (−.003, −.013)	.002	−.069 (−2.44, .11)	.434
Male	1.3 ± .4	1.1 ± .5	1.2 ± .3	1.3 ± .4	1.32 ± .6	1.2 ± .3	1.6 ± .3	.107	.008 (−.003, .018)	.120	—	—
Female	1.2 ± .3	1.1 ± .2	1.0 ± .2	1.3 ± .3	1.29 ± .4	1.5 ± .3	1.4 ± .2	.295	.008 (−.003, −.014)	.002	—	—
Autoregulation												
Coherence, a.u.												
VLF	.5 ± .2	.5 ± .2	.5 ± .2	.4 ± .2	.5 ± .1	.5 ± .2	.5 ± .2	.010	.001 (−.001, .002)	.510	−.015 (−.11, .02)	.726
LF	.6 ± .2	.6 ± .1	.7 ± .1	.6 ± .2	.7 ± .1	.6 ± .1	.6 ± .2	.035	−.001 (−.002, .001)	.406	.047 (−.11, .02)	.254
HF	.7 ± .1	.7 ± .1	.8 ± .1	.7 ± .2	.7 ± .1	.7 ± .2	.8 ± .1	.019	−.001 (−.002, .002)	.524	−.029 (−.11, .02)	.439
Gain, cm.sec^{-1}.mm Hg^{-1}												
VLF	.7 ± .3	.7 ± .23	.7 ± .4	.7 ± .4	.6 ± .18	.6 ± .2	.7 ± .3	.001	<.001 (.000, .000)	.913	.013 (−.11, .02)	.863
LF	1.0 ± .3	1.0 ± .45	1.1 ± .3	1.1 ± .3	1.0 ± .20	.9 ± .2	.9 ± .3	.055	−.004 (−.008, .004)	.105	.057(−.11, .02)	.460
HF	1.3 ± .4	1.4 ± .55	1.5 ± .5	1.3 ± .3	1.3 ± .29	1.2 ± .1	1.2 ± .4	.071	−.006 (−.009, .002)	.052	.056 (−.11, .02)	.591
Phase, radius												
VLF	1.0 ± .4	1.0 ± .4	.8 ± .5	1.3 ± .3	1.2 ± .3	.9 ± .5	.8 ± .5	.025	−.002 (−.012, .010)	.483	.115 (−.11, .02)	.340
LF	.6 ± .2	.7 ± .2	.6 ± .3	.6 ± .2	.7 ± .2	.5 ± .2	.6 ± .2	.014	−.001 (−.014, .012)	.403	−.014 (−.11, .02)	.820
HF	.2 ± .2	.2 ± .2	.1 ± .2	.1 ± .2	.2 ± .2	.2 ± .3	.2 ± .2	.006	.001 (−.005, .008)	.788	−.029 (−.11, .02)	.609
Vasoreactivity												
Hypercapnia, %.mm Hg^{-1}	4.9 ± 1.7	5.2 ± 2.7	4.8 ± 2.5	4.3 ± 1.1	5.6 ± 1.8	4.9 ± 1.0	4.6 ± .7	.015	−.004 (−.010, .002)	.793	−.396 (−1.35, .54)	.402
Hypocapnia, %.mm Hg^{-1}	1.7 ± .5	1.6 ± .6	1.8 ± .6	1.8 ± .3	1.7 ± .4	1.8 ± .4	1.7 ± .5	.041	<.001 (.000, .000)	.924	−.182 (−1.10, .25)	.140
Global, %.mm Hg^{-1}	4.2 ± 1.8	4.3 ± 1.3	5.2 ± 3.5	4.0 ± 1.3	4.4 ± 1.1	3.5 ± .5	3.6 ± 1.2	.047	−.022 (−.041, .013)	.114	−.015 (−.18, .12)	.974
Neurovascular coupling												
1-Back gain, %$^{-1}$	.2 ± 7.3	5.0 ± 17	−.8±2.4	−1.5±2.2	.2 ± 3.5	−1.5±2.0	.1 ± 3.4	.067	−.058 (−.127, .024)	.298	−3.088 (−5.27, 2.49)	.115
2-Back gain, % $^{-1}$	6.3 ± 4.6	5.6 ± 4.9	6.1 ± 6.5	7.1 ± 4.8	7.1 ± 3.9	3.4 ± 2.2	7.3 ± 4.0	.014	−.001 (−.004, .003)	.983	1.103 (−1.41, 3.62)	.384

Abbreviations: a.u., arbitrary units; CBFV, cerebral blood flow velocity; CI, confidence interval; CVRi, cerebrovascular resistance index; HF, high frequencies (.20-0.50 Hz); LF, low frequencies (.07-0.20 Hz); SD, standard deviation; VLF, very low frequencies (.02-0.07 Hz).

All values are given as mean ± SD.

Table 3. *Correlations among distinct mechanisms of cerebrovascular control—cerebral autoregulation, vasomotor reactivity, and neurovascular coupling*

				1	2	3	4	5	6	7	8	9	10	11	12
1	Autoregulation	Coherence, a.u.	VLF												
2			LF	.11											
3			HF	−.02	.25										
4		Gain, cm.sec^{-1}	VLF	.52**	−.13	−.06									
5			LF	−.23	.57**	.16	−.17								
6			HF	−.20	.30*	.10	−.34**	.65**							
7		Phase, radius	VLF	−.04	.09	.15	−.09	−.02	.05						
8			LF	−.14	.01	−.03	−.24	.14	.27*	.17					
9			HF	.18	−.03	−.22	−.11	−.21	.10	−.04	.37**				
10	Vasoreactivity	Hypercapnia, %.mm Hg^{-1}		.24	.05	−.17	.16	.05	.01	−.07	.07	.04			
11		Hypocapnia, %.mm Hg^{-1}		−.22	−.16	−.04	−.02	.04	−.02	.05	.04	.04	.21		
12		Global, %.mm Hg^{-1}		−.01	.14	−.06	.10	.33*	.32*	.02	.06	−.08	.41**	.22	
13	Neurovascular coupling	1-Back gain, %		.16	−.02	−.08	−.04	.13	.19	−.04	.11	.19	.20	.13	.07
14		2-Back gain, %		−.02	.13	−.01	.04	.05	−.02	−.18	−.18	−.08	.05	−.03	−.01

Abbreviations: a.u., arbitrary units; HF, high frequencies (.2-0. 5); LF, low frequencies (.07-0.2 Hz); VLF, very low frequencies (.02-0.07 Hz).
*$P < .05$ and ** $P < .001$ significance of Spearman's correlation coefficient.

was true for systemic hemodynamic variations in the active phases of VMR or NVC (Table 4). Additionally, the time course of hemodynamic changes during VMR and NVC can be visually inspected in Figure 1 and Figure 2, respectively. Hemodynamic changes during hypercapnia and hypocapnia VMR testing were very different: whereas the mean ABP increased modestly during hypercapnia, HR was the main systemic hemodynamic parameter that changed during hyperventilation (Fig 1).

The average CBFV increase during the 2-Back task was 6.3 ± 4.6 % (Fig 2). There was a statistical significance but mild change in the mean ABP, HR, and $EtCO_2$ ($P < .001$) during the NVC, but again these did not influence the relative CBFV increase ($P > .05$).

Cerebrovascular tests were not correlated with MoCA global and subtotal scores ($P > .05$).

Discussion

The main conclusion of this study is that age, gender, and systemic hemodynamics do not have significant influence on the distinct aspects of cerebrovascular control of healthy adults, namely CA, VMR, or NVC. Moreover, our results emphasize the fact that the estimation of only one of these regulatory mechanisms cannot be used as indicative of the status of the others as they are not correlated.

Aging is associated with a decrease of CBFV and an increase of cerebrovascular resistance,[25,26] which agrees with our results. However, we show that cerebrovascular functional control is preserved with increasing age. A literature review[27] depicts conflicting results in favor[9,28,29] or against[26,30-32] this perspective. Although we present a small sample, this is the first study to report such an extensive work-up and combined data of NVC, CA, and VMR. Most studies rely on the evaluation of a single regulatory parameter. Our data suggest that cerebrovascular adaptive mechanisms have a functional reserve, compensating for the age-related deterioration of the cerebrovascular bed as proposed by others.[28,33] For example, in patients with higher burden of cerebral white matter lesions, a preserved NVC and CA prevent them of having a slower gait[10] and high risk of falls.[10] Also, studies show higher brain activation with successful aging, compensating for age-related neural changes and achieving an accuracy that equals young subjects.[9,10] Nevertheless, we cannot exclude that transcranial Doppler-based methods may be too coarse and may miss subtle microvascular changes. On this account, advanced brain imaging could reveal new insights into the effects of aging.

The lack of gender effect on cerebrovascular regulation was unexpected as there are some studies demonstrating hormonal influences on vasomotor control, perhaps through modulation of nitric oxide pathway.[1,2] As we have not controlled for menstrual cycle or hormonal therapy, this could explain our different results.

Table 4. *Variation of systemic hemodynamic parameters—ABP, HR, and $EtCO_2$—during neurovascular stress tests and their effects on cerebrovascular measurements*

	Resting phase			Activation phase			Difference		
	MAP mm Hg	HR bpm	$EtCO_2$ mm Hg	MAP mm Hg	HR bpm	$EtCO_2$ mm Hg	MAP mm Hg	HR bmp	$EtCO_2$ mm Hg
Autoregulation TFA parameters	80 ± 13	69 ± 9	38 ± 3	—	—	—	—	—	—
Vasoreactivity									
Hypercapnia, %.mm Hg^{-1}	80 ± 15	68 ± 9	37 ± 4	91 ± 17†	68 ± 10	46 ± 4†	11 ± 8	1 ± 7	9 ± 3
Hypocapnia, %.mm Hg^{-1}	81 ± 15	69 ± 10	36 ± 4	83 ± 17	88 ± 15†	19 ± 3†	2 ± 8	20 ± 13*	−17±3
Neurovascular coupling									
1-Back gain, %	88 ± 18	70 ± 12	37 ± 4	88 ± 18	72 ± 12†	38 ± 6†	0 ± 3	1 ± 2	1 ± 4
2-Back gain, %	87 ± 18	71 ± 12	38 ± 4	90 ± 18†	76 ± 14†	37 ± 5†	3 ± 5	5 ± 6	0 ± 2

Abbreviations: $EtCO_2$, end-tidal CO_2; HR, heart rate; MAP, mean arterial pressure; SD, standard deviation; TFA, transfer function analysis. All values are given as mean ± SD.
*$P < .05$, Spearman's correlation of cerebrovascular measurements with systemic hemodynamic parameters.
†$P < .01$, *t*-test value comparing the variations of systemic hemodynamic parameters from resting to activation phases.

Curiously, we found that the grade of hypercapnia CBFV response was unrelated to the hypocapnia one. This is an unexpected yet novel finding of the study. Although systemic hemodynamic parameters were not enough to explain this finding, HR and ABP have very distinct time course patterns in hypercapnia and hypocapnia (Fig 1). This suggests a different autonomic[3,19] or cardiac output[3] modulation during these tasks that needs further investigation. A better understanding of these changes could help in the standardization of the techniques.

The results of NVC task show similar patterns, as published by Sorond et al.[10] Intuitively, we would expect that a better cognitive performance, as measured by MoCA score, would be correlated with higher CBFV response during NVC task. Yet, in our study, there was a lack of correlation between these two measurements. This could be explained though by the fact that NVC protocol measures more subtle cerebrovascular activations than MoCA score. For example, in the same study, the 2-Back task NVC was nicely correlated with Trail B time performance but not with global cognitive score.

The lack of correlation between cerebrovascular functional measurements can have some impact on how we study cerebrovascular regulation. Not so infrequently, we find comparison between studies concerning cerebrovascular regulation that have evaluated distinct mechanisms. Our work also supports the notion that these procedures could be simplified because ABP, HR, or $EtCO_2$ do not present major effects on cerebrovascular measurements.

The limitations of this study concern, in the first place, the limitations of Doppler studies and the assumptions that CBFV could be used as a surrogate of CBF.[21] On the other hand, we did not assess cerebral white matter pathology, which may have limited our capability to compare functional CBFV measurements with microvascular pathologic findings. Some participants had mild dyslipidemia and were on pharmacologic control with statins. However, carotid atherosclerosis was excluded by cervical ultrasound studies. The intentional absence of common vascular risk factors in our study could have diminished the applicability of our results to general population. However, this was done to control cofounders of the main variables in question—gender and age. We already mentioned that small sample may account for the lower statistical power of this study, but similar cerebral hemodynamic profiles (CBFV and CVRi changes with age and gender) compared with larger cohorts give us some support to the representability of our sample. Low-adjusted R^2 values (Table 2) suggest that a higher number could increase confidence in our findings. Nevertheless, the estimated coefficients were within confidence intervals. The lack of hormonal information already mentioned has a possible bias in studying gender effects.

There are also some concerns about the lower cognitive performance of older decades included in this study. The results of MoCA test (<26) in this group indicate cognitive decline, which was related to impaired cerebrovascular reactivity in many studies so far, causing uncertainty about our results and if these subjects could be considered to be healthy. Nevertheless, the scores remain within the normal range proposed by previous extensive validation study in the Portuguese population.[20]

Overall, our data suggest that in healthy subjects, despite age- and gender-related changes in cerebral blow flow velocity and resistance, they do not present major influence on the 3 major cerebrovascular regulation mechanisms. Our results also pinpoint the fact that neurovascular stress tests measure different aspects of cerebrovascular control and cannot be used interchangeably. Thus, a complete full battery might be more useful in future studies on neurovascular control. Being independent of age and cognitive status, cerebrovascular regulation tests seem

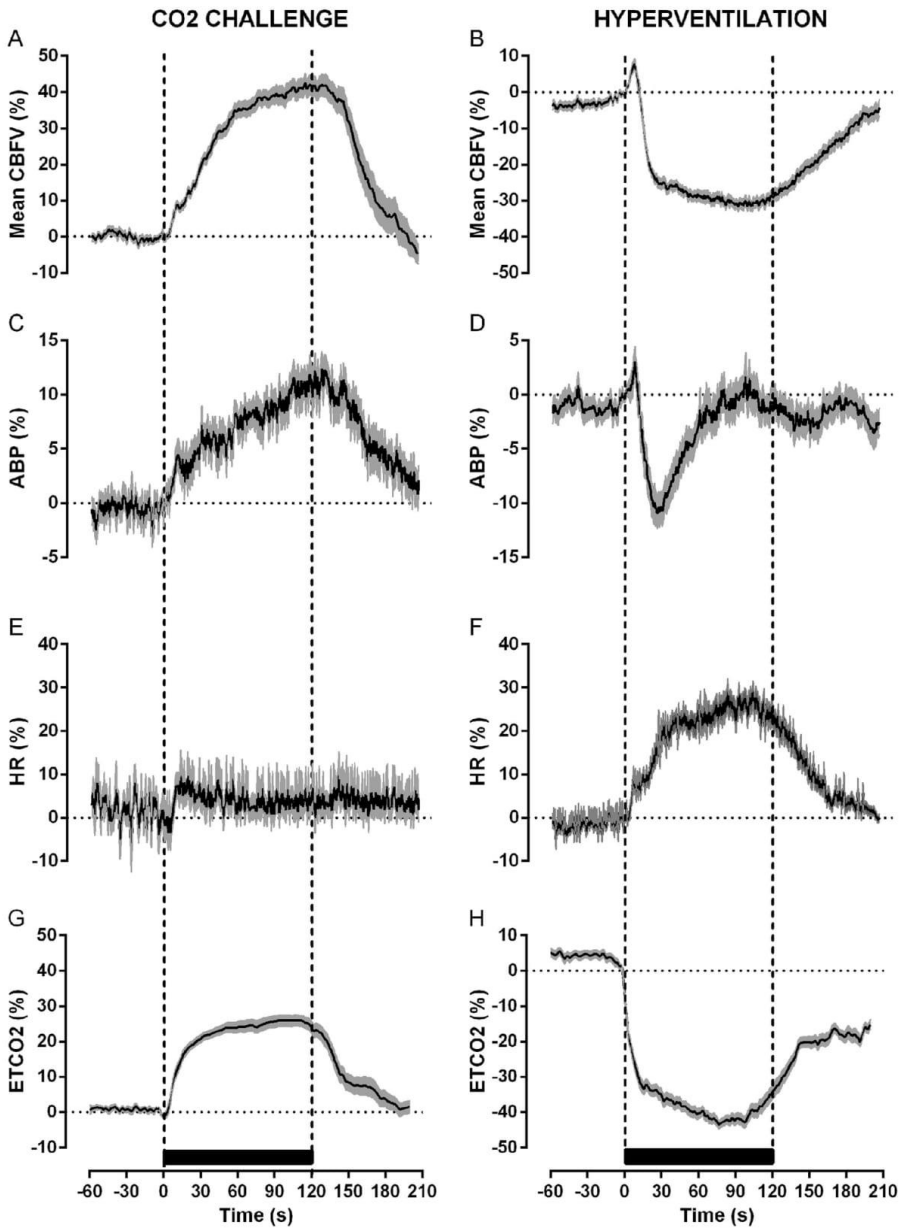

Figure 1. *Group-averaged time course of normalized mean CBFV (A and B), mean ABP (C and D), HR (E and F), and $EtCO_2$ (G and H) during the hypercapnic challenge (left) and hyperventilation-induced hypocapnia (right). Gray-shaded regions represent mean ± SE. The beginning and ending of each task are marked with vertical dashed lines. Abbreviations: ABP, mean arterial pressure; CBFV, cerebral blood flow velocity; $EtCO_2$, end-tidal CO_2; HR, heart rate; SE, standard error.*

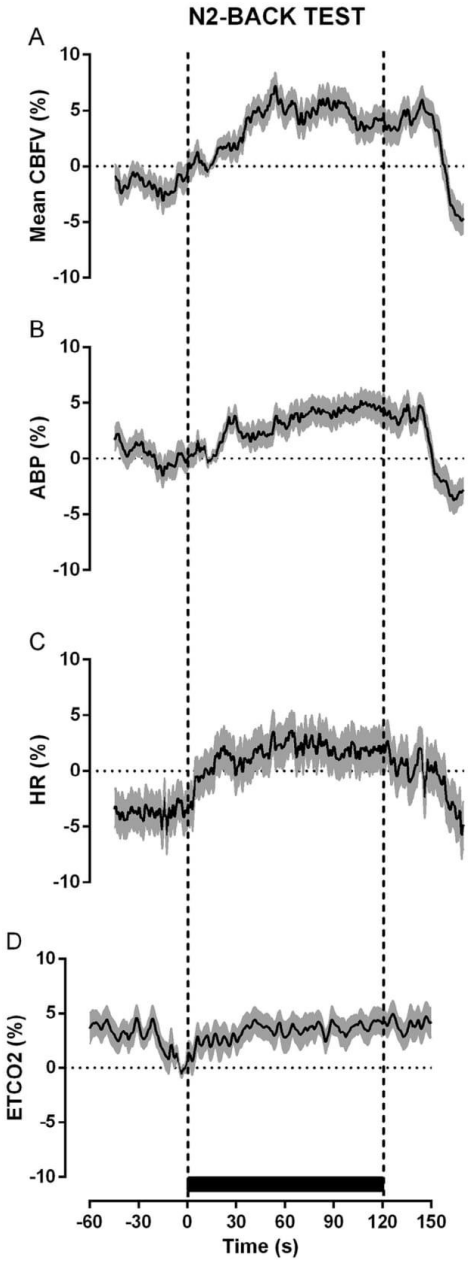

Figure 2. *Group-averaged time course of normalized mean CBFV (A), mean ABP (B), HR (C), and $EtCO_2$ (D) during the N2-Back test task. Gray-shaded regions represent mean ± SE. The beginning and ending of each task are marked with vertical dashed lines. Abbreviations: ABP, mean arterial pressure; CBFV, cerebral blood flow velocity; $EtCO_2$, end-tidal CO_2; HR, heart rate; SE, standard error.*

promising for studying several cerebrovascular conditions affecting the aging brain.

Acknowledgment: This study is part of JM MSc thesis.

Appendix: Supplementary Material

Supplementary data to this article can be found online at doi:10.1016/j.jstrokecerebrovasdis.2016.12.003.

References

1. Willie CK, Tzeng YC, Fisher JA, et al. Integrative regulation of human brain blood flow. J Physiol 2014; 592:841-859.
2. Ainslie PN, Duffin J. Integration of cerebrovascular CO_2 reactivity and chemoreflex control of breathing: mechanisms of regulation, measurement, and interpretation. Am J Physiol Regul Integr Comp Physiol 2009;296:R1473-R1495.
3. Castro PM, Santos R, Freitas J, et al. Autonomic dysfunction affects dynamic cerebral autoregulation during Valsalva maneuver: comparison between healthy and autonomic dysfunction subjects. J Appl Physiol 2014; 117:205-213.
4. Azevedo E, Rosengarten B, Santos R, et al. Interplay of cerebral autoregulation and neurovascular coupling evaluated by functional TCD in different orthostatic conditions. J Neurol 2007;254:236-241.
5. Rosengarten B, Huwendiek O, Kaps M. Neurovascular coupling and cerebral autoregulation can be described in terms of a control system. Ultrasound Med Biol 2001;27:189-193.
6. Castro PM, Santos R, Freitas J, et al. Adaptation of cerebral pressure-velocity hemodynamic changes of neurovascular coupling to orthostatic challenge. Perspect Med 2012; 1:290-296.
7. Aaslid R, Lindegaard KF, Sorteberg W, et al. Cerebral autoregulation dynamics in humans. Stroke 1989;20:45-52.
8. Panerai RB, Rennie JM, Kelsall AW, et al. Frequency-domain analysis of cerebral autoregulation from spontaneous fluctuations in arterial blood pressure. Med Biol Eng Comput 1998;36:315-322.
9. Sorond FA, Schnyer DM, Serrador JM, et al. Cerebral blood flow regulation during cognitive tasks: effects of healthy aging. Cortex 2008;44:179-184.
10. Sorond FA, Kiely DK, Galica A, et al. Neurovascular coupling is impaired in slow walkers: the MOBILIZE Boston Study. Ann Neurol 2011;70:213-220.
11. van Beek AH, Lagro J, Olde-Rikkert MG, et al. Oscillations in cerebral blood flow and cortical oxygenation in Alzheimer's disease. Neurobiol Aging 2012;33:428. e21-31.
12. Stefani A, Sancesario G, Pierantozzi M, et al. CSF biomarkers, impairment of cerebral hemodynamics and degree of cognitive decline in Alzheimer's and mixed dementia. J Neurol Sci 2009;283:109-115.
13. Azevedo E, Santos R, Freitas J, et al. Deep brain stimulation does not change neurovascular coupling in non-motor visual cortex: an autonomic and visual evoked blood flow velocity response study. Parkinsonism Relat Disord 2010;16:600-603.
14. Czosnyka M, Balestreri M, Steiner L, et al. Age, intracranial pressure, autoregulation, and outcome after brain trauma. J Neurosurg 2005;102:450-454.

15. Santos GA, Petersen N, Zamani AA, et al. Pathophysiologic differences in cerebral autoregulation after subarachnoid hemorrhage. Neurology 2016;86:1950-1956.
16. Marshall RS, Rundek T, Sproule DM, et al. Monitoring of cerebral vasodilatory capacity with transcranial Doppler carbon dioxide inhalation in patients with severe carotid artery disease. Stroke 2003;34:945-949.
17. Dawson SL, Blake MJ, Panerai RB, et al. Dynamic but not static cerebral autoregulation is impaired in acute ischaemic stroke. Cerebrovasc Dis 2000;10:126-132.
18. Azevedo E, Mendes A, Seixas D, et al. Functional transcranial Doppler: presymptomatic changes in Fabry disease. Eur Neurol 2012;67:331-337.
19. Azevedo E, Castro P, Santos R, et al. Autonomic dysfunction affects cerebral neurovascular coupling. Clin Auton Res 2011;21:395-403.
20. Freitas S, Simoes MR, Alves L, et al. Montreal Cognitive Assessment (MoCA): normative study for the Portuguese population. J Clin Exp Neuropsychol 2011;33:989-996.
21. Panerai RB. Assessment of cerebral pressure autoregulation in humans–a review of measurement methods. Physiol Meas 1998;19:305-338.
22. Claassen JA, Meel-van den Abeelen AS, Simpson DM, et al. Transfer function analysis of dynamic cerebral autoregulation: a white paper from the International Cerebral Autoregulation Research Network. J Cereb Blood Flow Metab 2016;36:665-680.
23. Zhang R, Zuckerman JH, Giller CA, et al. Transfer function analysis of dynamic cerebral autoregulation in humans. Am J Physiol 1998;274(1 Pt 2):H233-H241.
24. Meel-van den Abeelen AS, van Beek AH, Slump CH, et al. Transfer function analysis for the assessment of cerebral autoregulation using spontaneous oscillations in blood pressure and cerebral blood flow. Med Eng Phys 2014;36:563-575.
25. Krejza J, Mariak Z, Walecki J, et al. Transcranial color Doppler sonography of basal cerebral arteries in 182 healthy subjects: age and sex variability and normal reference values for blood flow parameters. AJR Am J Roentgenol 1999;172:213-218.
26. Bakker SL, de Leeuw FE, den Heijer T, et al. Cerebral haemodynamics in the elderly: the Rotterdam Study. Neuroepidemiology 2004;23:178-184.
27. Purkayastha S, Sorond FA. Cerebral hemodynamics and the aging brain. Int J Clin Neurosci Ment Health 2014;1(Supp1):S07.
28. Carey BJ, Eames PJ, Blake MJ, et al. Dynamic cerebral autoregulation is unaffected by aging. Stroke 2000;31: 2895-2900.
29. Coverdale NS, Badrov MB, Kevin Shoemaker J. Impact of age on cerebrovascular dilation versus reactivity to hypercapnia. J Cereb Blood Flow Metab 2017 Jan;37:344-355. [Epub 2016 Jan 12].
30. Barnes JN, Schmidt JE, Nicholson WT, et al. Cyclooxygenase inhibition abolishes age-related differences in cerebral vasodilator responses to hypercapnia. J Appl Physiol 2012;112:1884-1890.
31. Fluck D, Beaudin AE, Steinback CD, et al. Effects of aging on the association between cerebrovascular responses to visual stimulation, hypercapnia and arterial stiffness. Front Physiol 2014;5:49.
32. Yamamoto M, Meyer JS, Sakai F, et al. Aging and cerebral vasodilator responses to hypercarbia: responses in normal aging and in persons with risk factors for stroke. Arch Neurol 1980;37:489-496.
33. Groschel K, Terborg C, Schnaudigel S, et al. Effects of physiological aging and cerebrovascular risk factors on the hemodynamic response to brain activation: a functional transcranial Doppler study. Eur J Neurol 2007;14:125-131.

PARTE B: ESTUDO DE AUTORREGULAÇÃO CEREBRAL NO AVC ISQUÉMICO AGUDO

Capítulo 2: Uma autorregulação cerebral mais eficaz no AVC isquémico agudo prediz enfartes cerebrais de menor volume e melhor resultado funcional

---

Castro P, Serrador JM, Rocha I, Sorond F and Azevedo E (2017). Efficacy of Cerebral Autoregulation in Early Ischemic Stroke Predicts Smaller Infarcts and Better Outcomes. *Front. Neurol.* 8:113. doi: 10.3389/fneur.2017.00113

frontiers in Neurology

ORIGINAL RESEARCH
published: 24 March 2017
doi: 10.3389/fneur.2017.00113

Efficacy of Cerebral Autoregulation in Early Ischemic Stroke Predicts Smaller Infarcts and Better Outcome

Pedro Castro[1], Jorge Manuel Serrador[2,3,4], Isabel Rocha[5], Farzaneh Sorond[6] and Elsa Azevedo[1]*

[1] Department of Neurology, São João Hospital Center, Faculty of Medicine, University of Porto, Porto, Portugal, [2] Department of Pharmacology, Physiology and Neuroscience, Rutgers Biomedical Health Sciences, Newark, NJ, USA, [3] Department of Veteran Affairs, Veterans Biomedical Institute, War Related Illness and Injury Study Center, East Orange, NJ, USA, [4] Cardiovascular Electronics, National University of Ireland Galway, Galway, Ireland, [5] Faculty of Medicine, Cardiovascular Centre, Institute of Physiology, University of Lisbon, Lisbon, Portugal, [6] Department of Neurology, Division of Stroke and Neurocritical Care, Northwestern University Feinberg School of Medicine, Chicago, IL, USA

Background and purpose: Effective cerebral autoregulation (CA) may protect the vulnerable ischemic penumbra from blood pressure fluctuations and minimize neurological injury. We aimed to measure dynamic CA within 6 h of ischemic stroke (IS) symptoms onset and to evaluate the relationship between CA, stroke volume, and neurological outcome.

Methods: We enrolled 30 patients with acute middle cerebral artery IS. Within 6 h of IS, we measured for 10 min arterial blood pressure (Finometer), cerebral blood flow velocity (transcranial Doppler), and end-tidal-CO_2. Transfer function analysis (coherence, phase, and gain) assessed dynamic CA, and receiver-operating curves calculated relevant cut-off values. National Institute of Health Stroke Scale was measured at baseline. Computed tomography at 24 h evaluated infarct volume. Modified Rankin Scale (MRS) at 3 months evaluated the outcome.

Results: The odds of being independent at 3 months (MRS 0–2) was 14-fold higher when 6 h CA was intact (Phase > 37°) (adjusted OR = 14.0 (IC 95% 1.7–74.0), $p = 0.013$). Similarly, infarct volume was significantly smaller with intact CA [median (range) 1.1 (0.2–7.0) vs 13.1 (1.3–110.5) ml, $p = 0.002$].

Conclusion: In this pilot study, early effective CA was associated with better neurological outcome in patients with IS. Dynamic CA may carry significant prognostic implications.

Keywords: cerebral autoregulation, blood pressure, stroke, ischemic stroke, transcranial Doppler

OPEN ACCESS

Edited by:
Ashfaq Shuaib,
University of Alberta, Canada

Reviewed by:
Vincent Thijs,
Florey Institute of Neuroscience and Mental Health, Australia
Marc Malkoff,
University of Tennessee Health Sciences Center, USA

****Correspondence:***
Pedro Castro
pedromacc@gmail.com

Specialty section:
This article was submitted to Stroke, a section of the journal Frontiers in Neurology

Received: *03 December 2016*
Accepted: *10 March 2017*
Published: *24 March 2017*

Citation:
Castro P, Serrador JM, Rocha I, Sorond F and Azevedo E (2017) Efficacy of Cerebral Autoregulation in Early Ischemic Stroke Predicts Smaller Infarcts and Better Outcome. Front. Neurol. 8:113. doi: 10.3389/fneur.2017.00113

INTRODUCTION

Reperfusion and neuroprotection are the current mainstays of acute ischemic stroke (IS) management. In this regard, arterial blood pressure (ABP) management may play a central role to maintain optimal perfusion within the vulnerable ischemic penumbra (1, 2). Unfortunately, several clinical trials in ABP modulation had no effect on prognosis (2) and, therefore, the corresponding current guidelines remain evasive (3). Perhaps, the crucial factor is not ABP *per se*, but rather how cerebral

blood flow can adapt to pressure changes and/or demand, i.e., cerebral autoregulation (CA) (4).

Dynamic CA (dCA) can be assessed using transfer function analysis (TFA) between spontaneous oscillations of ABP and cerebral blood flow velocity (CBFV) (4). CA has been studied in acute stroke (5) with conflicting results (5–8), but the early hours, where penumbra is more vulnerable, has been largely ignored.

Therefore, we aimed to assess dCA within 6 h of IS symptoms and its relationship with final infarct volume and 90-day functional outcome.

MATERIALS AND METHODS

Study Population

São João Hospital center ethical committee approved the study. Written informed consent was obtained. We included consecutive patients with middle cerebral artery (MCA) territory acute IS, admitted to our stroke unit. Ultrasound studies (Vivid *e*; GE) excluded hemodynamically significant extra- or intracranial stenoses. Patients with MCA proximal occlusion were excluded, as it prevented monitoring.

Monitoring and Data Analysis

Evaluations were carried out at stroke unit in supine position. We monitored for 10 min CBFV with transcranial Doppler M1-MCA (BoxX-DWL, Germany), ABP with Finometer MIDI (FMS, Netherlands), heart-rate and end-tidal carbon dioxide ($EtCO_2$) with capnograph (Respsense/Nonin, Netherlands). Systolic, diastolic, and mean values of ABP (MBP) and of CBFV (MFV) were calculated (4). TFA assessed dCA by calculating coherence, gain, and phase parameters from beat-to-beat MFV and MBP spontaneous oscillations in low frequency range (0.03–0.15 Hz) (4) as previously detailed (9).

Outcomes and Statistics

Baseline National Institutes of Health Stroke Scale (NIHSS) scores were calculated. Independence, modified Rankin Scale (0–2), at 90 days determined the outcome by a stroke physician blinded for the initial assessment. Head CT (Siemens Somaton/Emotion Duo, Germany) at 24 h measured infarct volume with ABC/2 formula.

Shapiro–Wilk test determined normality. Mann–Whitney and χ^2 tests compared hemodynamic measurements between subgroups. ROC analysis found relevant cutoff values. After dichotomization, multivariate logistic regression calculated the odds ratio. Relationship between continuous variables was determined by Spearman's correlation and adjusted with multivariate linear regression models. Level of significance was $p < 0.05$.

RESULTS

We recruited 30 patients characterized in **Table 1**. The relationship between dCA and outcome is presented in **Table 2**. Independence at 3 months was associated with higher phase ($p = 0.024$) and lower gain ($p = 0.045$) in the stroke hemisphere within 6 h of onset. ROC curve analysis found best cutoffs, associated with independency, in phase at 37° (affected side, AUC = 0.713, $p = 0.028$; sensitivity 70%, specificity 79%) but gain underperformed (AUC = 0.654, $p = 0.112$). Based on these cutoffs, independency at 3 months (**Figure 1A**) could be predicted by phase level in the affected side [phase ≥ 37°, adjusted OR = 14.0 (IC 95% 1.7–74.0), $p = 0.013$] when adjusted to baseline NIHSS and age. Additionally, lower infarct volumes at 24 h (**Figure 1C**) were measured in subgroups of higher phase in the affected side [median (range) 1.1 (0.2–7.0) vs 13.1 (1.3–110.5) ml, $p = 0.002$]. Low and high phase subgroups were also not significantly different in baseline NIHSS (**Figure 1B**, $p = 0.062$). When phase was

TABLE 1 | Patients characteristics according to outcome at 3 months.

	Total	Independency	
		Yes	No
	N = 30	*N* = 17	*N* = 13
Gender male, *n* (%)	16 (53)	9 (53)	5 (39)
Age, years (mean ± SD)	69 ± 13	63 ± 13	76 ± 9*
BMI, kg m^{-2} (mean ± SD)	26.9 ± 5.5	26.9 ± 4.0	26.9 ± 7.0
Atrial fibrillation, *n* (%)	11 (37)	4 (23)	7 (55)
Hypertension, *n* (%)	20 (67)	9 (53)	11 (85)
Diabetes mellitus, *n* (%)	12 (40)	4 (25)	8 (60)
Dyslipidemia, *n* (%)	22 (74)	12 (71)	10 (76)
Tobacco, *n* (%)	5 (17)	3 (18)	2 (15)
Large vessel atherosclerosis	4 (13)	2 (10)	2 (20)
Cardioembolic	11 (37)	4 (20)	7 (60)
Small vessel disease, *n* (%)	3 (10)	1 (1)	2 (5)
Undetermined, *n* (%)	8 (27)	2 (10)	6 (55)
Thrombolysis, *n* (%)	20 (67)	11 (55)	9 (53)
Baseline NIHSS, median (IQR)	9 (5–15)	6 (4–13)	12 (8–20)*

BMI, body-mass index; NIHSS, National Institutes of Health Stroke Scale.
**P < 0.05 significance value of Mann–Whitney. Values in mean ± SD.*

TABLE 2 | Cerebral autoregulation and outcome at 3 months.

	Total	Independency	
		Yes	No
	N = 30	*N* = 17	*N* = 13
Heart rate, bpm	70 ± 11	70 ± 10	71 ± 12
Systolic ABP, mmHg	136 ± 23	134 ± 20	138 ± 23
Mean ABP, mmHg	81 ± 14	84 ± 15	77 ± 17
Diastolic ABP, mmHg	54 ± 13	57 ± 13	50 ± 17
$EtCO_2$, mmHg	37 ± 6	36 ± 5	37 ± 5
Cerebral hemodynamics			
Infarct hemisphere			
MFV, cm/s	42 ± 15	46 ± 18	49 ± 13
Coherence, a.u.	0.5 ± 0.2	0.5 ± 0.2	0.5 ± 0.2
Gain,%/mmHg	1.0 ± 0.4	0.8 ± 0.2	*1.1 ± 0.5
Phase, degrees	36 ± 38	50 ± 25	*21 ± 47
Non-infarct hemisphere			
MFV, cm/s	50 ± 16	50 ± 17	46 ± 12
Coherence, a.u.	0.5 ± 0.2	0.5 ± 0.2	0.6 ± 0.2
Gain,%/mmHg	1.1 ± 0.6	0.9 ± 0.2	1.1 ± 0.6
Phase, degrees	43 ± 33	48 ± 21	39 ± 40

Interhemispheric = ipsilateral-minus-contralateral values; MFV, mean flow velocity; ABP, arterial blood pressure; $EtCO_2$, end-tidal carbon dioxide; a.u., arbitrary units.
**P < 0.05 significance value of Mann–Whitney. Values in mean ± SD.*

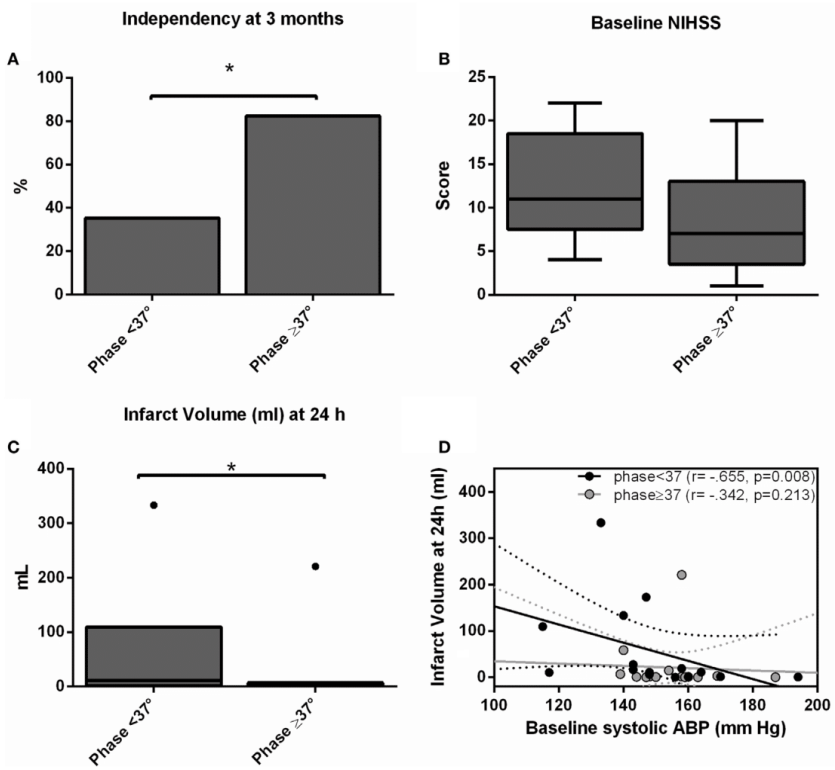

FIGURE 1 | Independency at 3 months (A), baseline National Institutes of Health Stroke Scale score (B) and infarct volume (C) accordingly subgroups of worse (phase < 37°) and better (phase ≥ 37°) dynamic CA (dCA) on the ischemic hemisphere. Bars represent % and box-and-whiskers plots medians/interquartile ranges. Significant results ($p < 0.05$) are topped by asterisks. **(D)** Scatter plot showing infarct volumes at 24 h (ml) plotted against baseline systolic arterial blood pressure level separated by subgroups of worse (phase <37°, black dots) and better (phase ≥37°, gray dots) dCA, and respective linear regression lines and 95% confidence interval.

analyzed as a continuous variable, it correlated with stroke volume in the affected side ($r = -0.444$, $p = 0.020$) but not contralateral ($r = -0.125$, $p = 0.409$). In multivariate linear regression, only NIHSS significantly predicted infarct volume at 24 h ($p = 0.002$) but not phase ($p = 0.457$). Baseline systolic ABP was inversely correlated with infarct volume at 24 h ($r = -0.665$, $p = 0.008$) but only in the subgroup with lower phase in the infarct side (**Figure 1D**).

DISCUSSION

We showed that the efficacy of dCA during the first 6 h after symptom onset is associated with smaller infarct volumes at 24 h and better neurological outcome at 3 months.

Transfer function analysis of the spontaneous ABP and CBFV oscillations is increasingly used to assess dCA in a number of neurovascular disorders (7–10). The phase of this relationship, which represents the time delay between these oscillating waveforms, has emerged as a significant predictor of outcome. Lower phase shift (ineffective CA) has been linked to carotids or MCA stenosis (11) or development of vasospasm after subarachnoid hemorrhage (10). In patients with IS, phase has also been linked to stroke severity (5, 7). The impaired CA can be also related to patient medical conditions not addressed in this study. For example, impaired cerebral autoregulation in patients with sleep apnea has been linked to an increased risk of stroke (12). Our findings, which build on these prior studies, show that effective dCA, as demonstrated by higher phase shift, is linked to smaller stroke volumes and better neurological outcome. Moreover, consistent with prior work where a phase >30 represents effective or intact autoregulation (4, 5, 9), we also found a cutoff value of 37° for phase that was predictive of neurological independence at 3 months and smaller stroke volumes at 24 h.

Interestingly, we also found that a lower systolic ABP is associated with larger infarcts but only if CA is impaired in the infarct side (phase <37°). This observation enhances the biological plausibility of the link between phase (dCA), stroke volume and clinical outcome, since lower ABP would only endanger the ischemic penumbra with further hypoperfusion if CA was impaired. Taken together, CA assessment could, therefore, identify patients who would benefit from BP augmentation in future clinical trials (13) Perfusion imaging, instead of CA assessment, may have been more helpful to explain larger infarcts at 24 h by estimation of initial penumbra area. However, an impaired CA at baseline could itself be responsible for this larger penumbra. The question remains to be answered in future studies with correlative measurements with perfusion scanning.

In line with prior studies (5), gain seems not to be a good marker for stroke outcome. Nevertheless, lower gain values (more effective CA) on the stroke side seemed to be associated with independence at 3 months.

This study has some limitations. As it is a pilot study, we enrolled a small number of subjects. Regarding the TCD method, there are limitations inherent to CA assessment with TCD (4), as some non-stationary conditions (e.g., agitation, mental changes) might turn linear methods like TFA less reliable. Also, M1 occlusions could not be assessed. As CA was assessed after IV thrombolysis within 6 h of symptoms, non-occluded M1 cases in this study include recanalyzed MCA or branch occlusions while those who were excluded due to M1 occlusion are mostly non-recanalized MCA. Having said that, we still can see this as a limitation but occluded M1 after IV thrombolysis is itself a maker for very bad prognosis and we believed that CA assessment would not add any significant contribution in this scenario; we also monitored this excluded cases and only 1/16 (6%) was independent at 3 months and all had total MCA area involvement. So, what our study points out is that even if we recanalyze the MCA artery <6h, those with better CA (phase ≥37°) will have higher chance of being independent at 3 months.

Concerning the infarct volume, we used CT scan, which is not as reliable as MRI. However, most of the stroke patients had easily identifiable partial or total areas of MCA infarct. Although CT scan is a coarse measure, we believe that the overall results were not influenced by this method.

1. In summary, we showed that the efficacy of dCA in the early hours of IS is linked to infarct volume at 24 h and neurological outcome at 3 months. Rapid bedside assessment of CA may help to identify a high risk population with impaired CA who would benefit from different BP management.

ETHICS STATEMENT

This study was carried out in accordance with the recommendations of São João Hospital center ethical committee with written informed consent from all subjects. All subjects gave written informed consent in accordance with the Declaration of Helsinki. The protocol was approved by the São João Hospital center ethical committee.

AUTHOR CONTRIBUTIONS

PC reviewed the literature, designed the study, extracted the data, analyzed the results, and wrote the paper. EA designed the study, analyzed the results, and co-wrote the paper. IR and JS designed the study, analyzed the results, and reviewed the paper. FS reviewed the literature, designed the study, analyzed the results, and co-wrote the paper.

FUNDING

This study was part of Ph.D. thesis of PC and received public national grant from Fundação para a Ciência e a Tecnologia (FCT), Portugal, PTDC/SAU-ORG/113329/2009. FS is supported by R01 NS085002 (NINDS).

REFERENCES

1. Martins AI, Sargento-Freitas J, Silva F, Jesus-Ribeiro J, Correia I, Gomes JP, et al. Recanalization modulates association between blood pressure and functional outcome in acute ischemic stroke. *Stroke* (2016) 47(6):1571–6. doi:10.1161/STROKEAHA.115.012544
2. Tikhonoff V, Zhang H, Richart T, Staessen JA. Blood pressure as a prognostic factor after acute stroke. *Lancet Neurol* (2009) 8(10):938–48. doi:10.1016/S1474-4422(09)70184-X
3. Jauch EC, Saver JL, Adams HP Jr, Bruno A, Connors JJ, Demaerschalk BM, et al. Guidelines for the early management of patients with acute ischemic stroke: a guideline for healthcare professionals from the American Heart Association/American Stroke Association. *Stroke* (2013) 44(3):870–947. doi:10.1161/STR.0b013e318284056a
4. Panerai RB. Assessment of cerebral pressure autoregulation in humans – a review of measurement methods. *Physiol Meas* (1998) 19(3):305–38. doi:10.1088/0967-3334/19/3/001
5. Aries MJ, Elting JW, De Keyser J, Kremer BP, Vroomen PC. Cerebral autoregulation in stroke: a review of transcranial Doppler studies. *Stroke* (2010) 41(11):2697–704. doi:10.1161/STROKEAHA.110.594168
6. Eames PJ, Blake MJ, Dawson SL, Panerai RB, Potter JF. Dynamic cerebral autoregulation and beat to beat blood pressure control are impaired in acute ischaemic stroke. *J Neurol Neurosurg Psychiatry* (2002) 72(4):467–72. doi:10.1136/jnnp.72.4.467
7. Reinhard M, Neunhoeffer F, Gerds TA, Niesen WD, Buttler KJ, Timmer J, et al. Secondary decline of cerebral autoregulation is associated with worse outcome after intracerebral hemorrhage. *Intensive Care Med* (2010) 36(2):264–71. doi:10.1007/s00134-009-1698-7
8. Reinhard M, Wihler C, Roth M, Harloff A, Niesen WD, Timmer J, et al. Cerebral autoregulation dynamics in acute ischemic stroke after rtPA thrombolysis. *Cerebrovasc Dis* (2008) 26(2):147–55. doi:10.1159/000139662
9. Nakagawa K, Serrador JM, LaRose SL, Sorond FA. Dynamic cerebral autoregulation after intracerebral hemorrhage: a case-control study. *BMC Neurol* (2011) 11:108. doi:10.1186/1471-2377-11-108
10. Otite F, Mink S, Tan CO, Puri A, Zamani AA, Mehregan A, et al. Impaired cerebral autoregulation is associated with vasospasm and delayed cerebral ischemia in subarachnoid hemorrhage. *Stroke* (2014) 45(3):677–82. doi:10.1161/STROKEAHA.113.002630
11. Hu HH, Kuo TB, Wong WJ, Luk YO, Chern CM, Hsu LC, et al. Transfer function analysis of cerebral hemodynamics in patients with carotid stenosis. *J Cereb Blood Flow Metab* (1999) 19(4):460–5. doi:10.1097/00004647-199904000-00012
12. Tsivgoulis G, Alexandrov AV. Cerebral autoregulation impairment during wakefulness in obstructive sleep apnea syndrome is a potential mechanism increasing stroke risk. *Eur J Neurol* (2009) 16(3):283–4. doi:10.1111/j.1468-1331.2008.02501.x
13. Sorond FA, Tan CO, LaRose S, Monk AD, Fichorova R, Ryan S, et al. Deferoxamine, cerebrovascular hemodynamics, and vascular aging: potential

role for hypoxia-inducible transcription factor-1-regulated pathways. *Stroke* (2015) 46(9):2576–83. doi:10.1161/STROKEAHA.115.009906

Conflict of Interest Statement: The authors declare that the research was conducted in the absence of any commercial or financial relationships that could be construed as a potential conflict of interest.

Capítulo 3: Transformação hemorrágica e edema cerebral no AVC isquémico agudo: conexão à autorregulação cerebral

Castro, P., Azevedo, E., Serrador, J., Rocha, I., & Sorond, F. (2017). Hemorrhagic transformation and cerebral edema in acute ischemic stroke: Link to cerebral autoregulation. *J Neurol Sci*, *372*, 256–261. http://doi.org/10.1016/j.jns.2016.11.065

Journal of the Neurological Sciences 372 (2017) 256–261

Contents lists available at ScienceDirect

Journal of the Neurological Sciences

journal homepage: www.elsevier.com/locate/jns

Hemorrhagic transformation and cerebral edema in acute ischemic stroke: Link to cerebral autoregulation

Pedro Castro [a,*], Elsa Azevedo [a], Jorge Serrador [b,c], Isabel Rocha [d], Farzaneh Sorond [e]

[a] Department of Neurology, São João Hospital Center, Faculty of Medicine of University of Porto, Portugal
[b] Veterans Biomedical Institute and War Related Illness and Injury Study Center, Department of Veterans Affairs, New Jersey Healthcare System, East Orange, USA
[c] New Jersey Medical School, Newark, NJ, USA
[d] Cardiovascular Autonomic Function Lab, Institute of Physiology, Faculty of Medicine of University of Lisbon, Portugal
[e] Department of Neurology, Division of Stroke and Neurocritical, Northwestern University Feinberg School of Medicine, Chicago, IL, United States

ARTICLE INFO

Article history:
Received 14 September 2016
Received in revised form 1 November 2016
Accepted 28 November 2016
Available online 30 November 2016

Keywords:
Cerebral autoregulation
Cerebral vasoreactivity
Cerebral edema
Cerebral hemorrhage
Ischemic stroke
Transcranial Doppler

ABSTRACT

Background: Hemorrhagic transformation and cerebral edema are feared complications of acute ischemic stroke but mechanisms are poorly understood and reliable early markers are lacking. Early assessment of cerebrovascular hemodynamics may advance our knowledge in both areas. We examined the relationship between dynamic cerebral autoregulation (CA) in the early hours post ischemia, and the risk of developing hemorrhagic transformation and cerebral edema at 24 h post stroke

Methods: We prospectively enrolled 46 patients from our center with acute ischemic stroke in the middle cerebral artery territory. Cerebrovascular resistance index was calculated. Dynamic CA was assessed by transfer function analysis (coherence, phase and gain) of the spontaneous blood flow velocity and blood pressure oscillations. Infarct volume, hemorrhagic transformation, cerebral edema, and white matter changes were collected from computed tomography performed at presentation and 24 h.

Results: At admission, phase was lower (worse CA) in patients with hemorrhagic transformation [6.6 ± 30 versus 45 ± 38°; adjusted odds ratio 0.95 (95% confidence internal 0.94–0.98), $p = 0.023$] and with cerebral edema [6.6 ± 30 versus 45 ± 38°, adjusted odds ratio 0.96 (0.92–0.999), $p = 0.044$]. Progression to edema was associated with lower cerebrovascular resistance (1.4 ± 0.2 versus 2.3 ± 1.5 mm Hg/cm/s, $p = 0.033$) and increased cerebral blood flow velocity (51 ± 25 versus 42 ± 17 cm/s, $p = 0.033$) at presentation. All hemodynamic differences resolved at 3 months

Conclusions: Less effective CA in the early hour post ischemic stroke is associated with increased risk of hemorrhagic transformation and cerebral edema, possibly reflecting breakthrough hyperperfusion and microvascular injury. Early assessment of dynamic CA could be useful in identifying individuals at risk for these complications.

1. Introduction

Hemorrhagic transformation (HT) and cerebral edema (CE) are feared complications of acute ischemic stroke (IS), which are often associated with poor neurological outcome [1]. HT is especially serious when caused by thrombolysis with recombinant tissue plasminogen activator (rtPA) [2] and in severe strokes. Larger infarcts can also develop malignant CE [3]. Predicting CE and HT could prevent further cerebral damage [4]. Yet, we know very little about their underlying mechanisms and early predictors are still inexistent [5].

Microvascular disruption following brain ischemia are key players in causing vasogenic CE and HT in animal models [4,6] as well as in humans [7]. Imaging studies also suggest that cerebral microvascular injury, manifested as white matter changes, increase the risk of HT [8]. Therefore, impaired microvascular function and less effective CA may be one mechanism linking white matter changes to HT.

Dynamic cerebral autoregulation (CA) can be rapidly and noninvasively assessed at the bedside by transfer function analysis (TFA) between spontaneous oscillations in blood pressure and cerebral blood flow velocity [9–14]. There is an overall agreement that dynamic CA is impaired in acute IS [15,16] but its relationship with HT or CE is not known.

We examined the relationship between dynamic CA, measured within 6 h of symptom-onset through the chronic phase of IS, and the risk to development of HT or CE.

2. Methods

2.1. Population studied

All patients, or proxy, gave written and signed consent. Local ethical committee approved the study. We consecutively included patients

* Corresponding author at: Department of Neurology, São João Hospital Center, Alameda Professor Hernani Monteiro, 4200-319 Porto, Portugal.
E-mail addresses: pedromacc@gmail.com (P. Castro), eazevedo@med.up.pt (E. Azevedo), Jorge.Serrador@va.gov (J. Serrador), isabelrocha0@gmail.com (I. Rocha), farzaneh.sorond@nm.org (F. Sorond).

http://dx.doi.org/10.1016/j.jns.2016.11.065
0022-510X/

with acute IS in the middle cerebral artery (MCA) territory admitted to the stroke unit at Hospital São João Centre, Porto. Exclusion criteria included hemodynamic instability requiring vasoactive agents, other central neurological co-morbidities or insufficient temporal acoustic window. We recruited 46 patients. In sixteen patients the symptomatic MCA was occluded. Separate analyses were performed for patients with and without occlusion of symptomatic MCA. In 3 cases we did not have imaging confirmation of the infarcted territory and patients were included based on clinical signs of MCA territory infarction (aphasia). All patients underwent neurological examination at presentation and National Institutes of Health Stroke Scale (NIHSS) scores were recorded from admission to discharge. All participants underwent cervical and transcranial ultrasound studies (Vivid *e*; GE) before evaluation to exclude hemodynamically significant extra- or intracranial stenoses.

2.2. Monitoring protocol

Evaluations were carried out in the stroke unit with head of the bed at 0° during the 10 min of recording. Arterial blood pressure (ABP) was continuously monitored with a finger cuff in the unaffected side using Finometer MIDI (FMS, Amsterdam, Netherlands). Additionally, blood pressure was assessed with oscillometric cuff (Dash 2500, GE, UK). HR was assessed from lead II of a standard 3-lead electrocardiogram (ECG). Cerebral blood flow velocity (CBFV) was recorded bilaterally from M1 segment of MCA (depth of 50–55 mm) with 2-MHz monitoring probes secured with a headband (Doppler BoxX, DWL, Singen, Germany). End-tidal carbon dioxide (CO_2) was evaluated by nasal cannula attached to Respsense capnograph (Nonin, Amsterdam, The Netherlands). All data was synchronized at 400 Hz with Powerlab (AD Instruments, Oxford, UK) and stored for offline analysis. Data collection occurred for 10 min within 6 h and at 24 h from symptoms-onset and also at 3 months in survivors (n = 31).

2.3. Data analysis

All signals were inspected and artifacts removed. Systolic, diastolic and mean values of ABP (MBP) and CBFV (MFV) were calculated. Cerebrovascular resistance index (CVRi) was calculated by MBP/MFV reflecting vasomotor function [17]. Transfer function Analysis (TFA) was used to assess dynamic CA by calculating coherence, gain and phase parameters from beat-to-beat spontaneous oscillations in MFV and MBP as previously reported [13,18]. Ten minutes of normalized data were interpolated at 100 Hz into uniform time basis; averaged periodogram was calculated by Welch method [13] with Hanning window of 30 s, with two-third overlap. The cross spectrum between MBP and MFV signals was calculated and used to determine coherence, phase and gain in the low (autoregulatory) frequency range (0.03–0.15 Hz). Lower coherence (correlation coefficient) and gain (damping mechanism) and higher phase (speed of the autoregulatory response) between oscillations of MBP and MFV indicate more effective CA [13].

2.4. Neuroimaging assessment

Head CT (Siemens Somaton Emotion Duo, Erlangen, Germany), with 3 to 6 mm slices, was performed on admission and repeated at 24 h. Any hemorrhagic transformation (from petechial hyperdensities to parenchymal hematoma, defined by ECASS [2] was considered. Cerebral edema was defined as any focal brain swelling causing midline shift [19]. Subtle edema, such as sulci or ventricular effacement was not included. Infarct volume was measured at 24 h following ABC/2 rule [20]. White matter changes were graded by the van Swieten scale [21,22].

2.5. Statistical analysis

Normality was determined by Shapiro-Wilk test. Groups with and without HT or CE were compared with chi-square/Fisher's exact test for nominal variables and Student *t*-test or Mann-Whitney for continuous variables as appropriate. Repeated measures ANOVA was used to find significant differences in hemodynamic variables along time and between groups with multiple comparisons corrected by Bonferonni's post-hoc test. Spearman's rho correlation analysis was performed to evaluate the relationship between TFA parameters and continuous baseline variables. We estimated the effects of CA parameters in HT or CE by calculating the odds ratios and 95% interval confidence using logistic regression with adjustment to baseline variables by forward conditional method. Statistical significance was set at $p < 0.05$.

Table 1
Demographic, clinical and radiographic characteristics of subjects at baseline.

	Total	Hemorrhage		Cerebral edema	
		Yes	No	Yes	No
	n = 46	n = 10	n = 36	n = 8	n = 38
Demographics					
Male	25 (54)	5 (50)	20 (55)	5 (62)	20 (53)
Age, years (mean ± SD)	73 ± 12	76 ± 15	72 ± 11	77 ± 10	73 ± 13
BMI, $kg \cdot m^{-2}$ (mean ± SD)	27 ± 5	26 ± 5	28 ± 4	26 ± 6	28 ± 5
Previous stroke/TIA, n (%)	7 (15)	1 (10)	6 (17)	3 (38)	5 (62)
Atrial fibrillation, n (%)	20 (43)	6 (60)	14 (39)	3 (34)	17 (45)
Hypertension, n (%)	24 (74)	8 (80)	26 (72)	6 (75)	28 (73)
Diabetes mellitus, n (%)	17 (37)	4 (40)	13 (36)	3 (37)	14 (37)
Dyslipidemia, n (%)	37 (73)	7 (70)	27 (75)	8 (100)	26 (68)
Tobacco, n (%)	6 (13)	0 (0)	6 (17)	0 (0)	6 (16)
Ipsilateral carotid stenosis 50–60%, n (%)	6 (13)	0 (0)	6 (17)	0 (0)	6 (16)
Stroke characteristics					
Occlusion of affected MCA, n (%)	16 (35)	4 (40)	12 (33)	4 (50)	12 (31)
Thrombolysis, n (%)	35 (76)	10 (100)	25 (70)	7 (88)	28 (74)
NIHSS score [median(IQR)]	14 (9–22)	20 (8–22)	13 (9–21)	22 (18–22)	*12 (9–20)
Neuroimaging [median(IQR)]					
Infarct volume, mL	19 (2–9)	99 (23 − 212)	*16 (1–104)	§172 (109–333)	15 (1–62)
Severity of white matter changes	2 (1–3)	3 (2–4)	*2 (1–3)	2 (1–3)	2 (1–4)

Body-Mass Index (BMI), Transient Ischemic Attack (TIA), Modified Rankin Scale (MRS), middle cerebral artery (MCA), National Institutes of Health Stroke Scale (NIHSS).

* $p < 0.05$ for Student's *t*-test/Mann-Whitney or Chi-square/Fisher's exact test *p* value for differences in continuous or categorical variables, respectively, between subgroups with and without hemorrhagic transformation or cerebral edema.

§ $p < 0.001$ for Student's *t*-test/Mann-Whitney or Chi-square/Fisher's exact test *p* value for differences in continuous or categorical variables, respectively, between subgroups with and without hemorrhagic transformation or cerebral edema.

3. Results

Demographic and clinical characteristics were similar between subgroups with and without HT or CE (Table 1). Four patients had both CE and HT. Ten patients developed HT scored H2 in 3, PH1 in 5, and PH2 in 2. Eight patients developed CE with mean midline shift of 5.6 ± 2.2 mm. Patients with HT, had higher stroke volumes ($p = 0.028$) and greater severity of white matter changes ($p = 0.030$). CE was also associated with larger stroke volumes ($p < 0.001$) and higher NIHSS admission scores ($p = 0.023$). MCA occlusion was detected at admission (after thrombolysis if applied) in 16 (35%) of our cohort by transcranial ultrasound allowing only contralateral MCA to be monitored.

Hemodynamic data is presented in Table 2. MBP was elevated during the first 24 h as compared to 3 months ($p = 0.003$) without differences between subgroups. Most patients, showed increased CVRi in the ischemic hemisphere at acute stage (<6 h compared to 24 h $p = 0.033$ and to 3 months $p = 0.039$), but those who developed CE, had opposite profile, with lower CVRi in the infarcted hemisphere (<6 h $p = 0.033$ and 24 h $p = 0.044$). This subgroup also showed increased MFV in ipsilateral hemisphere during the acute period (<6 h $p = 0.033$ and 24 h $p = 0.020$). All hemodynamic differences resolved at 3 months.

We first examined the relationship between dynamic CA measures and baseline clinical and radiographic characteristics in all cohort. Ipsilateral phase was negatively correlated with stroke volume (Spearmean's rho −0.444, $p = 0.020$), and bilateral gain was positively correlated with severity of white matter changes (ipsilateral $r = 0.368$, $p = 0.040$; contralateral $r = 0.402$, $p = 0.006$).

Next, we examined the relationship between dynamic CA measures at admission and development of HT and CE at 24 h. Figs. 1 and 2 compares dynamic CA measures (phase and gain) between those with and without HT or CE, respectively. At admission, phase was significantly lower in ipsilateral hemisphere in those patients who subsequently developed HT (<6 h $p = 0.033$; 24 h $p = 0.047$) or CE (<6 h $p = 0.002$) on their 24 h head CT. These differences resolved at 3 months ($p = 0.094$ and $p = 0.567$, respectively). Gain was not associated with HT or CE (ipsilateral, $p = 0.597$ and 0.247; contralateral side $p = 0.169$ and 643). Coherence was not different between groups and times (data not shown).

Table 2
Temporal changes in systemic and cerebral hemodynamics.

		Total	Hemorrhage		Cerebral edema	
			Yes	No	Yes	No
		n = 46	n = 10	n = 36	n = 8	n = 38
Systemic hemodynamics (mean ± SD)						
Systolic ABP, mm Hg	<6	†144 ± 19	†148 ± 18	†146 ± 19	†154 ± 19	†142 ± 19
	24	†142 ± 19	†141 ± 24	†142 ± 18	†135 ± 19	†143 ± 20
	3 M	124 ± 17	113 ± 21	126 ± 19	120 ± 18	124 ± 17
Mean ABP, mm Hg	<6	†101 ± 14	†97 ± 7	†101 ± 11	†97 ± 12	†101 ± 14
	24	†97 ± 11	†96 ± 11	†97 ± 10	†91 ± 10	†98 ± 11
	3 M	87 ± 11	78 ± 11	90 ± 11	87 ± 16	87 ± 11
Diastolic ABP, mm Hg	<6	†75 ± 11	†72 ± 9	†77 ± 11	†71 ± 12	†76 ± 10
	24	†74 ± 10	†73 ± 9	75 ± 10	†69 ± 10	†75 ± 10
	3 M	69 ± 10	60 ± 7	72 ± 9	70 ± 15	69 ± 10
Heart rate, bpm	<6	67 ± 11	61 ± 10	*71 ± 11	58 ± 8	*70 ± 11
	24	67 ± 11	67 ± 14	68 ± 12	67 ± 17	67 ± 11
	3 M	71 ± 15	83 ± 23	69 ± 13	87 ± 22	70 ± 13
$EtCO_2$, mm Hg	<6	36 ± 7	35 ± 7	36 ± 7	37 ± 6	37 ± 7
	24	36 ± 6	37 ± 7	36 ± 7	38 ± 6	36 ± 7
	3 M	37 ± 7	34 ± 7	35 ± 7	38 ± 6	39 ± 7
Cerebral hemodynamics (mean ± SD)						
Subgroup without MCA occlusion						
		n = 30	n = 6	n = 24	n = 4	n = 26
Infarct hemisphere						
MFV, cm/s	<6	±25	41 ± 25	25 ± 17	*51 ± 25	42 ± 17
	24	51 ± 18	51 ± 18	46 ± 18	*57 ± 16	46 ± 17
	3 M	43 ± 21	43 ± 21	39 ± 16	44 ± 20	43 ± 17
CVRi, mm Hg/cm/s	<6	†2.1 ± 0.9	2.1 ± 1.3	2.2 ± 1.2	*1.4 ± 0.2	2.3 ± 1.5
	24	1.6 ± 0.2	1.6 ± 0.2	1.8 ± 0.8	*1.2 ± 0.3	1.8 ± 0.7
	3 M	1.8 ± 0.8	1.8 ± 0.8	1.8 ± 0.8	1.7 ± 0.8	1.8 ± 0.8
Non-infarct hemisphere						
MFV, cm/s	<6	49 ± 15	50 ± 18	50 ± 16	56 ± 11	48 ± 15
	24	53 ± 16	60 ± 18	51 ± 15	60 ± 10	52 ± 17
	3 M	46 ± 17	45 ± 17	46 ± 17	39 ± 12	48 ± 17
CVRi, mm Hg/cm/s	<6	1.8 ± 1.3	1.4 ± 0.6	1.9 ± 0.6	1.3 ± 0.2	1.8 ± 0.7
	24	1.5 ± 0.2	1.2 ± 0.3	1.6 ± 0.8	1.0 ± 0.4	1.5 ± 0.6
	3 M	2.0 ± 0.8	1.9 ± 0.5	2.0 ± 0.6	2.3 ± 0.6	1.7 ± 1.3
Subgroup with MCA occlusion (only non-infarct hemisphere monitored)						
		n = 16	n = 4	n = 12	n = 4	n = 12
Non-infarct hemisphere						
MFV, cm/s	<6	53 ± 17	47 ± 15	55 ± 18	53 ± 25	53 ± 23
	24	58 ± 26	47 ± 15	62 ± 28	59 ± 11	58 ± 15
	3 M	52 ± 24	39	53 ± 26	27	55 ± 20
CVRi, mm Hg/cm/s	<6	1.7 ± 1.2	1.6 ± 0.6	1.8 ± 0.8	1.4 ± 0.3	1.7 ± 0.6
	24	1.4 ± 0.7	1.4 ± 0.4	1.7 ± 0.6	1.2 ± 0.4	1.5 ± 0.5
	3 M	2.0 ± 0.8	2.2	1.9 ± 1.4	3.2	1.9 ± 1.0

Mean flow velocity (MFV), cerebrovascular resistance index (CVRi), arterial blood pressure (ABP), end-tidal carbon dioxide ($EtCO_2$), within 6 h (<6) and at 24 h from symptom-onset; 3 months (3 M).

* $p < 0.05$ for Repeated-Measures ANOVA p value for differences between subgroups with and without hemorrhagic transformation or cerebral edema.

† $p < 0.05$ for Repeated-Measures ANOVA p value for variations with time (3 months as a reference).

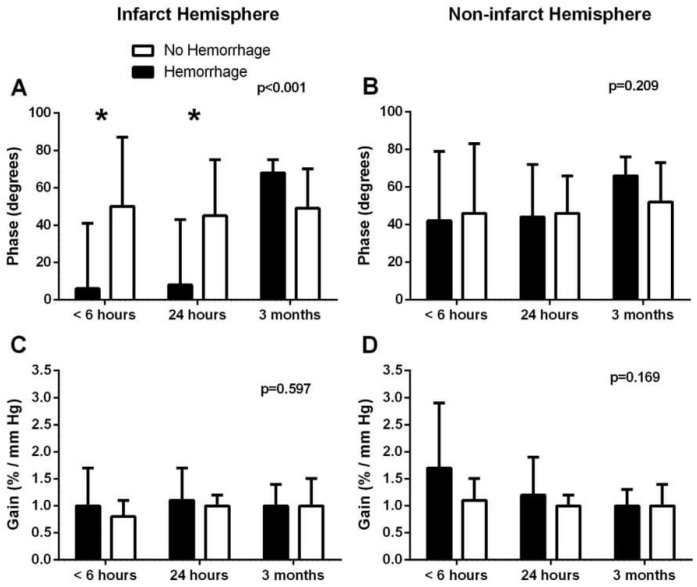

Fig. 1. Variations in phase (degrees) and gain (%/mmHg), in the ischemic and contralateral hemispheres, over time in subgroups with and without hemorrhagic transformation. Bars/whisker represents mean/side deviation. P value obtained with repeated-measures ANOVA. Significant differences are identified by asterisks.

We estimated the effects of ipsilateral phase <6 h and the risk of HT or CE by calculating the odds ratios and 95% interval confidence using logistic regression adjusted to (stroke volume and white matter changes or NIHSS, respectively) by forward conditional method. Phase (< 6 h) was lower (worse CA) in patients with hemorrhagic transformation [6.6 ± 30 versus 45 ± 38°; adjusted odds ratio 0.95 (95% confidence internal 0.94–0.98), $p = 0.023$] and with cerebral edema [9.9 ± 30 versus 41 ± 38°; adjusted odds ratio 0.96 (0.92–0.999), $p = 0.044$].

4. Discussion

Our data show that early impairments in dynamic CA during acute ischemic stroke are associated with development of HT and CE. In these patients, lower phase in the acute (<6 h) period was associated with development of HT and CE on the 24 h CT scan.

Dynamic cerebral autoregulation using transfer function analysis has been widely studied in cerebrovascular disease [9–11,15,16,23–30].

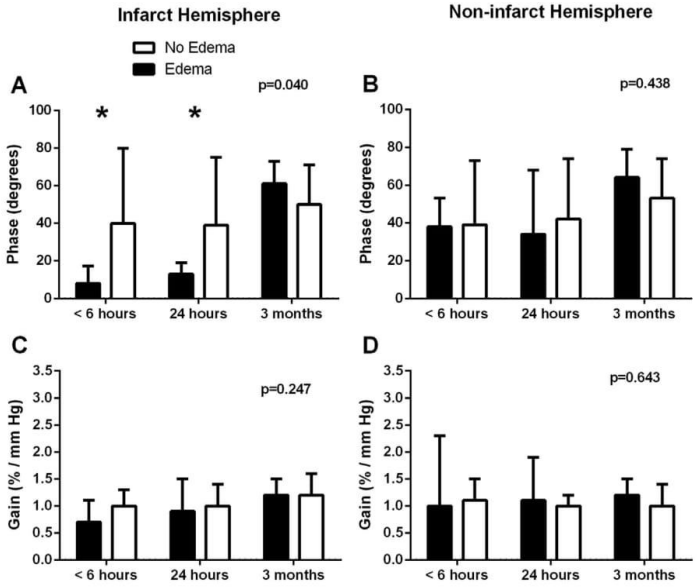

Fig. 2. Variations in phase (degrees) and gain (%/mmHg), in the ischemic and contralateral hemispheres, over time in subgroups with and without cerebral edema. Bars/whisker represents mean/side deviation. P value obtained with repeated-measures ANOVA. Significant differences are identified by asterisks.

Lower phase shift, reflecting less effective autoregulation, has been demonstrated in poorly compensated carotid or MCA stenosis [27,29,30] or vasospasm after subarachnoid hemorrhage [27,28] as well as in ischemic stroke [15,16]. However, most prior studies did not assess phase in the early hyperacute period post ischemia, nor did they relate it to HT or CE. We show that in this hyperacute period (<6 h), impaired cerebral autoregulation, as reflected by lower phase, is associated with development of CE and HT. One mechanistic pathway explaining these observations is that the failure of the autoregulatory capability of cerebral resistance vessels results in disruption of Starling's principle and pathological elevation of the hydrostatic pressure across the capillary bed, which could then aggravate the existing blood-brain barrier leakage and cause CE and HT [12,13]. In favor of this hypothesis, we found abnormally lower CVRi and increased MFV in ischemic hemisphere preceding the development of CE. A less effective CA will also endanger the ischemic penumbra [31], which is acutely perfusion dependent. This may be the mechanisms linking low phase values at presentation to larger infarct area at 24 h in our data. Unlike phase, gain has not been linked to ischemic stroke in prior studies [16,26] which is in line with our findings.

Dohmen et al. [32] reported previously that impaired cerebral autoregulation measured by tissue oxygen pressure correlation seems to play a key role for development of a malignant course and might serve as a predictive marker. We extend their results by showing that this deregulation is already present from in the very early hours of ischemia and also in less severe patients able to be monitored non-invasively with TCD.

Another finding of this study relates to temporal changes in CVRi. Higher CVRi in the early hours post stroke suggests an acute cerebral vasoconstriction response. This may be explained by high endotelin-1 levels [33], a potent cerebral vasoconstrictor, but also by the presence of microthrombosis [6] and/or cytotoxic edema [4]. Curiously, patients who developed CE show a paradoxical response, with lower CVRi at presentation. This maladaptive vasodilatory response could contribute to CE. The molecular mechanisms underlying this observation warrant further investigation and offer a potential target for preventing secondary malignant cerebral edema in large strokes.

Finally, all the acute changes in CA resolved within 3 months. The transient nature of autoregulatory failure is pathophysiologically intuitive and provides biological plausibility for early CA measures as meaningful quantitative markers of disease severity and risk for CE and HT. Early modulation of cerebral autoregulation [4] may therefore, be a potential therapeutic target towards improve outcome in ischemic stroke.

This study has some limitations. We recognize the limitation on the number of subjects enrolled. For instance patients with HT were 4 years older, 60% vs. 39% had AF, 100% vs. 70% performed thrombolysis. However there was no statistical significance, likely related to the small sample size. This might explain the reason why HT and CE were not found to be significantly related to thrombolysis [2].

Regarding the limitations inherent CA assessment to TCD [34], some non-stationary conditions (e.g., agitation, mental changes) might turn linear methods like TFA less reliable. Further development of non-linear techniques to assess CA could clarify this point.

Finally, we did not assess MCA patency before thrombolysis. Therefore, we cannot be ascertained about recanalization or non-recanalization. However, the subgroup of patients with non-occluded MCA at presentation represents mostly recanalyzed (by thrombolysis or spontaneously) cases whereas MCA occlusion subgroup represents mainly non-recanalyzed (all except one had thrombolysis).

5. Conclusions

In conclusion, our findings provide support for early autoregulatory impairment as a possible mechanism leading to development of HT and CE in patients who present with acute ischemic stroke. Assessment of dynamic CA may help to identify high risk individuals and possibly provide a therapeutic target in the future.

Funding

This study was part of PhD thesis of Castro PM and received public national grant from Fundação para a Ciência e a Tecnologia (FCT), Portugal, PTDC/SAU-ORG/113329/2009. FA Sorond is supported by R01 NS085002 (NINDS).

References

[1] J.M. Wardlaw, V. Murray, E. Berge, G. del Zoppo, P. Sandercock, R.L. Lindley, G. Cohen, Recombinant tissue plasminogen activator for acute ischaemic stroke: an updated systematic review and meta-analysis, Lancet 379 (9834) (2012) 2364–2372.
[2] M. Fiorelli, S. Bastianello, R. von Kummer, G.J. del Zoppo, V. Larrue, E. Lesaffre, A.P. Ringleb, S. Lorenzano, C. Manelfe, L. Bozzao, Hemorrhagic transformation within 36 hours of a cerebral infarct: relationships with early clinical deterioration and 3-month outcome in the European Cooperative Acute Stroke Study I (ECASS I) cohort, Stroke 30 (11) (1999) 2280–2284.
[3] T. Steiner, P. Ringleb, W. Hacke, Treatment options for large hemispheric stroke, Neurology 57 (5 Suppl 2) (2001) S61–S68.
[4] J.S. Balami, R.L. Chen, I.Q. Grunwald, A.M. Buchan, Neurological complications of acute ischaemic stroke, Lancet Neurol. 10 (4) (2011) 357–371.
[5] W.N. Whiteley, K.B. Slot, P. Fernandes, P. Sandercock, J. Wardlaw, Risk factors for intracranial hemorrhage in acute ischemic stroke patients treated with recombinant tissue plasminogen activator: a systematic review and meta-analysis of 55 studies, Stroke 43 (11) (2012) 2904–2909.
[6] X. Wang, E.H. Lo, Triggers and mediators of hemorrhagic transformation in cerebral ischemia, Mol. Neurobiol. 28 (3) (2003) 229–244.
[7] O.Y. Bang, B.H. Buck, J.L. Saver, J.R. Alger, S.R. Yoon, S. Starkman, B. Ovbiagele, D. Kim, L.K. Ali, N. Sanossian, R. Jahan, G.R. Duckwiler, F. Vinuela, N. Salamon, J.P. Villablanca, D.S. Liebeskind, Prediction of hemorrhagic transformation after recanalization therapy using $T2^*$-permeability magnetic resonance imaging, Ann. Neurol. 62 (2) (2007) 170–176.
[8] S. Curtze, E. Haapaniemi, S. Melkas, S. Mustanoja, J. Putaala, T. Sairanen, G. Sibolt, M. Tiainen, T. Tatlisumak, D. Strbian, White matter lesions double the risk of post-thrombolytic intracerebral hemorrhage, Stroke (2015).
[9] P.M. Castro, R. Santos, J. Freitas, R.B. Panerai, E. Azevedo, Autonomic dysfunction affects dynamic cerebral autoregulation during Valsalva maneuver: comparison between healthy and autonomic dysfunction subjects, J. Appl. Physiol. 117 (3) (2014) 205–213.
[10] S. Purkayastha, O. Fadar, A. Mehregan, D.H. Salat, N. Moscufo, D.S. Meier, C.R. Guttmann, N.D. Fisher, L.A. Lipsitz, F.A. Sorond, Impaired cerebrovascular hemodynamics are associated with cerebral white matter damage, J. Cereb. Blood Flow Metab. 34 (2) (2014) 228–234.
[11] K. Nakagawa, J.M. Serrador, S.L. LaRose, F.A. Sorond, Dynamic cerebral autoregulation after intracerebral hemorrhage: a case-control study, BMC Neurol. 11 (2011) 108.
[12] R.B. Panerai, Assessment of cerebral pressure autoregulation in humans–a review of measurement methods, Physiol. Meas. 19 (3) (1998) 305–338.
[13] R. Zhang, J.H. Zuckerman, C.A. Giller, B.D. Levine, Transfer function analysis of dynamic cerebral autoregulation in humans, Am. J. Phys. 274 (1 Pt 2) (1998) H233–H241.
[14] A.S. Meel-van den Abeelen, A.H. van Beek, C.H. Slump, R.B. Panerai, J.A. Claassen, Transfer function analysis for the assessment of cerebral autoregulation using spontaneous oscillations in blood pressure and cerebral blood flow, Med. Eng. Phys. 36 (5) (2014) 563–575.
[15] M.J. Aries, J.W. Elting, J. De Keyser, B.P. Kremer, P.C. Vroomen, Cerebral autoregulation in stroke: a review of transcranial Doppler studies, Stroke 41 (11) (2010) 2697–2704.
[16] M. Reinhard, C. Wihler, M. Roth, A. Harloff, W.D. Niesen, J. Timmer, C. Weiller, A. Hetzel, Cerebral autoregulation dynamics in acute ischemic stroke after rtPA thrombolysis, Cerebrovasc. Dis. 26 (2) (2008) 147–155.
[17] R.B. Panerai, The critical closing pressure of the cerebral circulation, Med. Eng. Phys. 25 (8) (2003) 621–632.
[18] R. Aaslid, K.F. Lindegaard, W. Sorteberg, H. Nornes, Cerebral autoregulation dynamics in humans, Stroke 20 (1) (1989) 45–52.
[19] D. Strbian, A. Meretoja, J. Putaala, M. Kaste, T. Tatlisumak, G. Helsinki Stroke Thrombolysis Registry, Cerebral edema in acute ischemic stroke patients treated with intravenous thrombolysis, Int. J. Stroke 8 (7) (2013) 529–534.
[20] J.R. Sims, L.R. Gharai, P.W. Schaefer, M. Vangel, E.S. Rosenthal, M.H. Lev, L.H. Schwamm, ABC/2 for rapid clinical estimate of infarct, perfusion, and mismatch volumes, Neurology 72 (24) (2009) 2104–2110.
[21] J.C. van Swieten, A. Hijdra, P.J. Koudstaal, J. van Gijn, Grading white matter lesions on CT and MRI: a simple scale, J. Neurol. Neurosurg. Psychiatry 53 (12) (1990) 1080–1083.
[22] L. Pantoni, M. Simoni, G. Pracucci, R. Schmidt, F. Barkhof, D. Inzitari, Visual rating scales for age-related white matter changes (leukoaraiosis): can the heterogeneity be reduced? Stroke 33 (12) (2002) 2827–2833.
[23] M. Reinhard, F. Neunhoeffer, T.A. Gerds, W.D. Niesen, K.J. Buttler, J. Timmer, B. Schmidt, M. Czosnyka, C. Weiller, A. Hetzel, Secondary decline of cerebral autoregulation is associated with worse outcome after intracerebral hemorrhage, Intensive Care Med. 36 (2) (2010) 264–271.

[24] E.W. Lang, R.R. Diehl, H.M. Mehdorn, Cerebral autoregulation testing after aneurysmal subarachnoid hemorrhage: the phase relationship between arterial blood pressure and cerebral blood flow velocity, Crit. Care Med. 29 (1) (2001) 158–163.
[25] R.B. Panerai, R.P. White, H.S. Markus, D.H. Evans, Grading of cerebral dynamic autoregulation from spontaneous fluctuations in arterial blood pressure, Stroke 29 (11) (1998) 2341–2346.
[26] M. Reinhard, M. Roth, B. Guschlbauer, A. Harloff, J. Timmer, M. Czosnyka, A. Hetzel, Dynamic cerebral autoregulation in acute ischemic stroke assessed from spontaneous blood pressure fluctuations, Stroke 36 (8) (2005) 1684–1689.
[27] M. Reinhard, A. Hetzel, M. Lauk, C.H. Lucking, Dynamic cerebral autoregulation testing as a diagnostic tool in patients with carotid artery stenosis, Neurol. Res. 23 (1) (2001) 55–63.
[28] F. Otite, S. Mink, C.O. Tan, A. Puri, A.A. Zamani, A. Mehregan, S. Chou, S. Orzell, S. Purkayastha, R. Du, F.A. Sorond, Impaired cerebral autoregulation is associated with vasospasm and delayed cerebral ischemia in subarachnoid hemorrhage, Stroke 45 (3) (2014) 677–682.
[29] H.H. Hu, T.B. Kuo, W.J. Wong, Y.O. Luk, C.M. Chern, L.C. Hsu, W.Y. Sheng, Transfer function analysis of cerebral hemodynamics in patients with carotid stenosis, J. Cereb. Blood Flow Metab. 19 (4) (1999) 460–465.
[30] C. Haubrich, W. Kruska, R.R. Diehl, W. Moller-Hartmann, C. Klotzsch, Dynamic autoregulation testing in patients with middle cerebral artery stenosis, Stroke 34 (8) (2003) 1881–1885.
[31] V. Tikhonoff, H. Zhang, T. Richart, J.A. Staessen, Blood pressure as a prognostic factor after acute stroke, Lancet Neurol. 8 (10) (2009) 938–948.
[32] C. Dohmen, B. Bosche, R. Graf, T. Reithmeier, R.I. Ernestus, G. Brinker, J. Sobesky, W.D. Heiss, Identification and clinical impact of impaired cerebrovascular autoregulation in patients with malignant middle cerebral artery infarction, Stroke 38 (1) (2007) 56–61.
[33] I. Ziv, G. Fleminger, R. Djaldetti, A. Achiron, E. Melamed, M. Sokolovsky, Increased plasma endothelin-1 in acute ischemic stroke, Stroke 23 (7) (1992) 1014–1016.
[34] J.A. Claassen, A.S. Meel-van den Abeelen, D.M. Simpson, R.B. Panerai, N. International Cerebral Autoregulation Research, Transfer function analysis of dynamic cerebral autoregulation: A white paper from the International Cerebral Autoregulation Research Network, J. Cereb. Blood Flow Metab. (2016).

Capítulo 4: Doença renal crónica e resultado funcional desfavorável no AVC isquémico agudo: será a autorregulação cerebral o elo de ligação perdido?

Castro, P., Azevedo, E., Rocha, I., Sorond, F. & Serrador, J. (2017). Chronic Kidney Disease and Poor Outcomes in Ischemic Stroke: is Impaired Cerebral Autoregulation the Missing Link?. *Clin J am Soc Nephrol* (em revisão)

Title:

Chronic Kidney Disease and Poor Outcomes in Ischemic Stroke: is Impaired Cerebral Autoregulation the missing link?

Authors:

Pedro Castro, MD

Dept. Neurology, São João Hospital Center, Faculty of Medicine of University of Porto

pedromacc@gmail.com

Elsa Azevedo, MD, PhD

Dept. Neurology, São João Hospital Center, Faculty of Medicine of University of Porto

eazevedo@med.up.pt

Isabel Rocha, PhD

Cardiovascular Autonomic Function Lab, Institute of Physiology, Faculty of Medicine of University of Lisbon, Potugal; isabelrocha0@gmail.com

Farzaneh Sorond, MD, PhD

Department of Neurology, Division of Stroke and Neurocritical, Northwestern University Feinberg School of Medicine, Chicago, Illinois.farzaneh.sorond@nm.org

Jorge M. Serrador, PhD

Dept of Pharmacology, Physiology and Neuroscience, Rutgers Biomedical Health Sciences, Newark, NJ, USA and Veterans Biomedical Research Institute and War Related Illness and

Injury Study Center, Department of Veterans Affairs, East Orange, USA and Cardiovascular Electronics, National University of Ireland Galway, Galway, Ireland.

Jorge.Serrador@rutgers.edu

Corresponding author:

Pedro Castro, MD

Dept. Neurology, São João Hospital Center, Faculty of Medicine of University of Porto

Alameda Professor Hernani Monteiro, 4200-319 Porto, PORTUGAL

Fax: +351 225 025 766, Telephone: +351 931 725 181, e-mail: pedromacc@gmail.com

Cover title:

Renal function and cerebral autoregulation in stroke

Itemized list:

(1) Table 1: Demographic, clinical and laboratorial characteristics

(2) Table 2: Systemic and cerebral hemodynamic characteristics

(3) Table 3: Relationship between renal function and cerebral autoregulation

(4) Figure 1: Spectra of cerebral autoregulation accordingly to subgroups of eGFR

(5) Figure 2: CCB and association with renal function and cerebral autoregulation

(6) Figure 3: Renal function and stroke outcome and complications risk

(7) Figure 4: CA level and stroke outcome and complications risk

(8) Figure 5: Interaction between eGFR and CA on stroke outcome and complications risk

(9) Supplementary table 4: Univariate linear regression analysis between TFA parameters and baseline independent variables at acute stroke

Keywords: cerebral autoregulation, kidney, glomerular filtration rate, ischemic stroke, transcranial Doppler

Subject Codes: Hemodynamics; Ischemia; Mechanisms; Nephrology and Kidney; Physiology; Pathophysiology; Vascular Biology; Cardiovascular Disease; Blood Pressure; Ultrasound; Ischemic Stroke; Vascular Disease

Text word count: 4453/4500; Abstract 245/250

Abstract

Background and Purpose:

Chronic kidney disease increases stroke incidence and severity but the mechanisms behind this cerebro-renal interaction are mostly unexplored. Since both vascular beds share similar features, microvascular dysfunction could be the possible missing link. Therefore, we examined the relationship between renal function and cerebral autoregulation (CA) in the early hours post ischemia and its impact on outcome.

Methods: We enrolled 46 ischemic strokes (middle cerebral artery). Dynamic CA was assessed by transfer function (coherence, phase and gain) of spontaneous blood pressure oscillations to blood flow velocity within 6 hours from symptom-onset. Estimated glomerular filtration rate (eGFR) was calculated. Hemorrhagic transformation (HT) and white matter lesions (WML) were collected from computed tomography performed at presentation and 24h. Outcome was evaluated with Modified Rankin Scale at 3 months.

Results: High gain (less effective CA) was correlated with lower eGFR irrespective of infarct side ($p<0.05$). Both lower eGFR and higher gain correlated with WML grade ($p<0.05$). Lower eGFR and increased gain, alone and in combination, progressively reduced the odds of a good functional outcome [ipsilateral OR=5.34 (CI95% 1.20 – 32.5), p=0.040; contralateral OR=7.37 (CI95% 2.04 – 26.5), p=0.002] and increased risk of HT [ipsilateral OR=2.50 (CI95% 0.41 – 15.0), p=0.318; contralateral OR=6.00 (CI95% 1.36 – 26.4), p=0.018].

Conclusions: Lower renal function correlates with less effective dynamic CA in acute ischemic stroke, both predicting a bad outcome. The evaluation of serum biomarkers of renal dysfunction could have interest in the future for assessing cerebral microvascular risk and relationship with stroke complications.

Text

Introduction

Chronic kidney disease (CKD) increases the risk of ischemic stroke (IS)[1-3], its severity and the chance of poor outcome[4, 5]. The exact mechanisms that govern this cerebro-renal interaction are scarcely understood[6]. A possible explanation may involve the similar features of kidney and brain microvascular beds. Both vascular beds are low resistance arterial beds that rely on continuous blood flow that is maintained at relatively constant levels by a fine-tuned myogenic regulatory system protecting both the brain and kidney from blood pressure (BP) fluctuations that could cause large swings in blood flow[7-12]. This property, called autoregulation, has been long known to exist in renal [12, 13] and cerebral[8, 10, 14] vasculature. Despite differences between organ systems, it can be viewed as a generalized vascular protective mechanism[11] with failure resulting in microvessel damage (e.g.: from uncontrolled hypertension and diabetes[15-18]). In fact, glomerular sclerosis of chronic kidney failure[19] as well as lacunar infarcts and white matter lesions in the brain[15, 20] are characterized by similar pathological conditions: endothelial dysfunction; ischaemic arteriosclerosis; low perfusion and small vessel leakage.[15, 20] Recent evidence has shown that kidney impairment is associated with a greater severity of cerebral white matter lesions[21].

Therefore microvascular dysfunction that could impair myogenic autoregulation may be the missing link between renal function and stroke morbidity and worthwhile of being explored. Dynamic cerebral autoregulation (CA) can be rapidly and noninvasively assessed at patient bedside by transfer function analysis (TFA) using spontaneous oscillations in blood pressure and cerebral blood flow velocity[22 7, 17, 23-25] which is known to be impaired in acute IS[26, 27].

In this study we examined the relationship between renal function and CA, assessed from TFA measured within 6 hours of symptom-onset and its impact on long-term outcome.

Methods

Population studied

We included patients with acute IS admitted to stroke unit at São João Hospital Centre, Porto, that were able to be monitored within 6 hours of symptoms. Exclusion criteria included hemodynamic instability requiring vasoactive agents, other central neurological co-morbidities (e.g. tumor) or acute renal injury or insufficient temporal acoustic window. We recruited 46 with ischemic stroke of middle cerebral artery (MCA) territory. All participants underwent cervical and transcranial ultrasound studies (Vivid e; GE) before evaluation to exclude hemodynamically significant extra- or intracranial stenoses. Blood samples were collected at admission for C-reactive protein (CRP) and creatinine levels. Estimated glomerular filtration rate (eGFR) was calculated using the Chronic Kidney Disease Epidemiology Collaboration formula[28]. In the first fasting sample, with total, low-density lipoprotein (LDL) and high-density lipoprotein (HDL) cholesterol, glucose, glycated hemoglobin (HgA1C).

Clinical Assessment

All patients underwent neurological examination at presentation and National Institute of Health Stroke Scale (NIHSS) scores were calculated at baseline and on a daily basis until discharge. Outcome, assessed by clinical interview, corresponded to mortality and functional independency [modified Rankin Scale (MRS) 0–2] at 90 days.

Monitoring protocol

Evaluations were carried out in the stroke unit with head of the bed at 0° during the 10min of recording. Arterial blood pressure (ABP) was continuously monitored with a finger cuff in the unaffected side using Finometer MIDI (FMS, Amsterdam, Netherlands). Additionally, blood pressure was assessed with oscillometric cuff (Dash 2500, GE, UK). HR was assessed from lead II of a standard 3-lead electrocardiogram (ECG). Cerebral blood flow velocity (CBFV) was recorded bilaterally from M1 segment of MCA (depth of 50–55 mm) with 2-MHz monitoring probes secured with a headband (Doppler BoxX, DWL, Singen, Germany). End-tidal carbon dioxide (CO2) was evaluated by nasal cannula attached to Respsense capnograph (Nonin, Amsterdam, The Netherlands). All data was synchronized at 400 Hz with Powerlab (AD Instruments, Oxford, UK) and stored for offline analysis. Data collection occurred for 10 min within 6 from symptoms-onset.

Cerebral autoregulation data analysis

All signals were inspected using a custom based Matlab® program and artifacts removed by linear interpolation[29]. Systolic, mean and diastolic values of ABP and CBFV were calculated. For each heart-beat cerebrovascular resistance index (CVRi) was calculated by mean ABP/CBFV, reflecting vasomotor function[30]. Transfer function Analysis (TFA) was used to assess dynamic CA by calculating coherence, gain and phase parameters from beat-to-beat spontaneous oscillations of CBFV and ABP as previously reported[23, 31, 32]. Ten minutes of normalized data were interpolated at 100 Hz into uniform time basis; averaged periodogram was calculated by Welch method[23] with Hanning window of 30 seconds, with two-third overlap. Coherence was calculated between input auto-spectra of ABP over cross-spectra of CBFV/ABP and transfer functions of phase and gain were determined by dividing the cross-spectrum by the input auto-spectrum[24]. Coherence, gain and phase are reported for the low frequency range (0.03-0.15 Hz) which is the autoregulatory frequency[7, 23, 24, 31]. In short,

coherence is the coefficient of correlation between the signals; higher coherence between the oscillations is reflective of less effective CA. Gain quantifies the damping effect of CA on the magnitude of ABP oscillations. Phase shift represents the time delay between ABP and CBFV oscillations. Lower gain and higher phase represent tighter, more effective autoregulatory response[23, 33].

Neuroimaging Assessment

All subjects were assessed with admission CT brain scan (Siemens Somaton Emotion Duo, Erlangen, Germany), with 3 to 6 mm slices, at presentation and repeated at 24 hours. Hemorrhagic transformation was defined as any hemorrhage ranging from petechial hyperdensities to parenchymal hematoma[34]. White matter lesions , a correlate of cerebral microvascular disease[20], were graded by the van Swieten[35] scale based on the first CT scan, a method validated against MRI in IS[36-38].

Statistical analysis

Normality was determined by Shapiro-Wilk test. Baseline data are presented for all subjects. The relationship between baseline characteristics, including eGFR, and CA parameters was determined by multivariate and univariate linear regression analysis adjusting for age, gender and other significantly related variables at previous univariate analysis. To better depict the relationship between renal function and eGFR both were divided into terciles or medians. Any subgroups were compared with Kruskal-Wallis and Mann-Whitney tests. The impact of eGFR on outcome (MRS 0 – 6) and association with white matter lesions grades (0 – 4) was characterized by ordinal regression analysis. Logistic regression analysis was used to access the risk of hemorrhagic transformation. To avoid spurious associations, we considered statistically significant at $P<0.01$ level for univariate regression analysis. Otherwise, $P<0.05$

cut-off was used. All statistics were performed using IBM Statistical Package for Social Sciences (SPSS) Statistics v21™.

Results

Renal function and cerebral autoregulation

Baseline characteristics and hemodynamic data are reported in Tables 1 and 2, respectively. In a multivariate linear regression analysis, greater LF and HF gain values (less effective CA) were significantly associated with lower eGFR irrespective of infarct side ($p<0.05$, Table 3). Phase and coherence were not related to any baseline variable. Complete univariate linear regression analysis are presented in table 4. To better depict this relationship between renal function and dynamic CA, eGFR was divided in terciles subgroups of low (<65 ml/min), medium (65-87 ml/min) and high (>87 ml/min) values. Inspection of figure 1, showing the distribution of CA parameters throughout all spectrum of frequencies shows gain significantly increased in low eGFR subgroup compared to the higher one ($p<0.05$).

Previous use of Calcium Channel Blockers (CCB) was also associated with higher gain values bilaterally ($p<0.05$, Table 3). To explore further the influence of chronic medication of CCB we compared subgroups with (n=10) and without it regarding gain levels (Figure 2A and B) and renal function (Figure 2C). CCB use was associated with lower gain values ($p<0.05$) and also with lower eGFR (57 and 75 ml/min, p=0.022) but not statistically significant if only chronic hypertensive patients were selected (N=37, 57 and 70 ml/min, p=0.082). CCB users an non-users did not show different ABP values at presentation (systolic 137±21 vs 138±20 mm Hg, p=0.901; diastolic 47±12 vs 55±14 mm Hg, p=0.125)

Relationship with cerebral microvascular disease (White Matter Lesions)

White matter lesions grade was correlated in an inverse manner with lower levels of eGFR (rho spearman = - 0.52, p<0.0001) and proportionally to higher levels of LF gain (ipsilateral r= 0.368, p= 0.040; contralateral r= 0.402, p= 0.006). This can be depicted clearly in figures 3C and 4C+F, where we explored the distribution of white matter lesions grades accordingly to terciles of eGFR and LF gain, respectively. In Figure 5C and 5F, we demonstrate the interaction between renal function and dynamic CA, by studying subgroups of eGFR and LF gain split by their medians. The lower the eGFR and the higher the LF gain (worse CA) the more severe were the white matter lesions grade (ordinal shift analysis infract side p=0.09; non-infarct side p=0.05) but not reaching statistical significant at ischemic side.

Renal function, cerebral autoregulation and outcome

As presented in Figure 4A, lower GFR reduces significantly the odds of a good outcome measured by MRS at 3 months [Figure 3A, lower eGFR as reference, ordinal regression odds ratio, OR = 0.36 (confidence interval, CI, 95% 0.18 – 0.73), p=0.005] and higher risk of hemorrhagic transformation [Figure 3B, logistic regression OR 0.97 (CI95% 0.95 – 0.99), p=0.026].

Figure 4 depicts outcome accordingly to CA status. Higher LF gain (worse CA) also increased the odds of a poor outcome [Figure 4A, ipsilateral OR=2.18 (CI95% 1.01 – 5.28), p=0.048; figure 4D, contralateral OR=2.17 (CI95% 1.12 – 4.17), p=0.022], and the risk of developing hemorrhagic transformation [Figure 4B, ipsilateral OR=1.98 (CI95% 1.002 – 8.12), Figure 4E, p=0.042; contralateral OR=2.79 (CI95% 1.03 – 7.56), p=0.043].

A ordinal regression model with interaction between decreasing eGFR and increasing LF gain (Figure 5A and D) found that both factors combine to progressively reducing the odds of a

good functional outcome [ipsilateral OR=5.34 (CI95% 1.20 – 32.5), p=0.040; contralateral OR=7.37 (CI95% 2.04 – 26.47), p=0.002]. Multinomial logistic regression also found the interaction of lower eGFR and higher LF gain for increased risk of hemorrhagic transformation only with statistical significant at contralateral side [Figure 5B and 5E, ipsilateral OR=2.50 (CI95% 0.41 – 15.0), p=0.318; contralateral OR=6.00 (CI95% 1.36 – 26.4), p=0.018].

Discussion

Our data shows significant association between impaired cerebral autoregulation (higher dynamic CA gain values) assessed during acute ischemic stroke (<6 hours) and impaired renal function (lower glomerular filtration rate) independent of age, vascular risk factors and relevant laboratory metabolic control parameters. Moreover, both reduced renal function and high gain values were associated with greater white matter abnormalities and with reduced likelihood of a good functional outcome as assessed by Modified Rankin Scale at 3 months.

To understand why impaired renal function might be linked to impaired cerebral autoregulation, we need to consider the physiology of autoregulation. Renal autoregulation adjusts vascular resistance to stabilize renal blood flow and GFR during changes in renal perfusion pressure.[9, 12] Basically, as pressure changes stretch the smooth muscles of the afferent and cortical arterioles, a myogenic response occurs to adjust vascular resistance to maintain flow. Since blood flow in a vascular bed is determined by perfusion pressure and resistance (Blood flow = perfusion pressure / vascular resistance), if perfusion pressure increases, stretching the smooth muscle surrounding the arterioles, the arterioles will then constrict to increase resistance and maintain the ratio of pressure to resistance and thus maintain blood flow.[9] In fact, renal autoregulation status has been well documented by the same method of

TFA we used to assess dynamic CA. This method quantifies the transfer of blood pressure changes into flow change, thus high gain means pressure changes are causing flow changes, and thus autoregulation is impaired. In the kidney, previous work in hypertensive rats with adenine-induced chronic renal failure has shown that gain is increased in the <0.1 Hz band, indicating that higher gain is an indicator of impaired renal autoregulation[39].

The same characteristics are found in the cerebrovasculature with increased gain in the low frequency range associated with impaired cerebral autoregulation.[14, 23] In fact, myogenic autoregulation is widely distributed over various vascular beds including the brain, coronary, pulmonary, mesenteric, and skeletal muscle.[11]

Considering the similarities in the characteristics of autoregulation in the kidney and brain, one could propose that microvascular damage (e.g. caused by hypertension, diabetes) that causes impairment in kidney function[9, 19] could also affect the brain in a similar fashion. Support for this idea is found in stroke-prone spontaneously-hypertensive rats that have a genetic predisposition to rapid glomerulosclerosis and stroke.[40] In fact in these rats, both renal autoregulation (as assessed by TFA) and cerebral autoregulation are impaired prior to the development of stroke and death.[41, 42] Examination of the histopathology of cerebral arteries in the spontaneously hypertensive rates have also shown medial hypertrophy and remodeling,[43] that are hallmarks of small vessel disease, as in humans.[20] Thus it would appear that the stroke prone spontaneously hypertensive rats show impairments of autoregulation in both the kidney and brain, prior to stroke. These data would suggest, in this animal model, that impairment of autoregulation is occurring in multiple vascular beds.

Taken together, this would suggest that if patients demonstrate less effective autoregulation in cerebral vasculature (high gain) they would likely also have impaired renal myogenic autoregulation, which would cause glomerular dysfunction.

One interesting finding was that previous CCB use was correlated to increased LF gain values in both cerebral hemispheres as well as reduced eGFR. A possible explanation for this finding lies in the effect of CCB on autoregulation. In fact, previous work has demonstrated that CCB impairs the myogenic response in the kidney in animal models[9, 44] and perhaps in humans.[3, 45] CCB block the L-type voltage-gated calcium channels that are activated by stretch of the arterial vessel wall.[9, 12] Thus changes in pressure that result in changes in stretch of the walls will no longer activate the release of calcium and contraction of smooth muscle to modulate vascular resistance to maintain flow, which we would expect to result in increased gain (i.e. worse autoregulation). The finding that CCB are associated with increased gain and poor eGFR may be due to CCB impairing autoregulation in both organs (brain and kidney), consistent with our hypothesis. However, the effect of CCB on cerebral autoregulation in humans is not as clear with studies using measures other than TFA showing impaired autoregulation[3, 45, 46], while another study found no change in TFA derived gain in 8 healthy individuals[47]. Further work is necessary to determine if CCB could be affecting autoregulation in both the kidney and brain in patients.

Our finding that both low eGFR and high gain were significantly associated with severe white matter lesions does suggest that impaired autoregulation in the brain and kidney may be associated. One suggested mechanism for this is that microvascular damage is the basis of this autoregulatory dysfunction. Further prospective studies could untangle what´s cause or consequence.

Another finding in our study was the relationship between high gain, low eGFR and hemorrhagic transformation. Higher gain values reflect less effectiveness in the dampening capability of cerebral resistance vessels in the insonated vascular territory to BP oscillations[7, 23]. These dysfunctional vessels disrupt Starling's principle by increasing the hydrostatic pressure across the capillary bed and contribute to the existing blood-brain barrier leakage[48]. Therefore, this might explain the association of higher gain and the risk of hemorrhagic transformation. Also, high gain values have been implicated in acute intracerebral hemorrhage[24, 49] and hematoma expansion[49].

In the infarct hemisphere, gain had more non-significant relationships with outcome measurements. This can be observed by inspecting figures 4 and 5. One obvious explanation is that some patients had occluded MCA at infarct side and CA cannot be assessed at infarct side in the severe cases. Therefore, gain apparently had weaker associations with outcome measures. A second possibility may be that the gain in the ischemic hemisphere is artificially lowered and cerebral autoregulation falsely normalized due to the increased vascular resistance caused by microthrombosis (6) and/or cytotoxic edema (5) in the infarcted area (34). Clearly, much more work on the physiological determinants influencing each TFA parameter is needed. However, much more work on the clinical and physiological determinants influencing each TFA parameter is needed, namely with biomarkers, to confirm our results.

In conclusion, our findings provide support that early autoregulatory impairment of cerebral small vessels as well as renal vessels may be a possible mechanism linking low renal function with higher severity of ischemic stroke. Rapid assessment of serum markers of renal dysfunction could be used as surrogates of cerebral microvascular function integrity which may

help identify high risk individuals for complications like hemorrhagic transformation and possibly provide a therapeutic target in the future.

Sources of Funding:

This study received public national grant from Fundação para a Ciência e a Tecnologia (FCT), Portugal, PTDC/SAU-ORG/113329/2009

Disclosures: None

References

1. Lee M, Saver JL, Chang KH, Liao HW, Chang SC, Ovbiagele B. Low glomerular filtration rate and risk of stroke: Meta-analysis. *Bmj*. 2010;341:c4249
2. Weiner DE, Tighiouart H, Amin MG, Stark PC, MacLeod B, Griffith JL, et al. Chronic kidney disease as a risk factor for cardiovascular disease and all-cause mortality: A pooled analysis of community-based studies. *Journal of the American Society of Nephrology : JASN*. 2004;15:1307-1315
3. Hamner JW, Tan CO. Relative contributions of sympathetic, cholinergic, and myogenic mechanisms to cerebral autoregulation. *Stroke*. 2014;45:1771-1777
4. Kumai Y, Kamouchi M, Hata J, Ago T, Kitayama J, Nakane H, et al. Proteinuria and clinical outcomes after ischemic stroke. *Neurology*. 2012;78:1909-1915
5. Naganuma M, Koga M, Shiokawa Y, Nakagawara J, Furui E, Kimura K, et al. Reduced estimated glomerular filtration rate is associated with stroke outcome after intravenous rt-pa: The stroke acute management with urgent risk-factor assessment and improvement (samurai) rt-pa registry. *Cerebrovasc Dis*. 2011;31:123-129
6. Toyoda K, Ninomiya T. Stroke and cerebrovascular diseases in patients with chronic kidney disease. *Lancet Neurol*. 2014;13:823-833
7. Panerai RB. Assessment of cerebral pressure autoregulation in humans--a review of measurement methods. *Physiol Meas*. 1998;19:305-338
8. Lassen NA. Cerebral blood flow and oxygen consumption in man. *Physiol Rev*. 1959;39:183-238
9. Carlstrom M, Wilcox CS, Arendshorst WJ. Renal autoregulation in health and disease. *Physiol Rev*. 2015;95:405-511
10. Aaslid R, Lash SR, Bardy GH, Gild WH, Newell DW. Dynamic pressure--flow velocity relationships in the human cerebral circulation. *Stroke*. 2003;34:1645-1649
11. Davis MJ. Perspective: Physiological role(s) of the vascular myogenic response. *Microcirculation*. 2012;19:99-114
12. Loutzenhiser R, Griffin K, Williamson G, Bidani A. Renal autoregulation: New perspectives regarding the protective and regulatory roles of the underlying mechanisms. *Am J Physiol Regul Integr Comp Physiol*. 2006;290:R1153-1167

13. Bayliss WM. On the local reactions of the arterial wall to changes of internal pressure. *J Physiol*. 1902;28:220-231
14. Panerai RB, Rennie JM, Kelsall AW, Evans DH. Frequency-domain analysis of cerebral autoregulation from spontaneous fluctuations in arterial blood pressure. *Med Biol Eng Comput*. 1998;36:315-322
15. Wardlaw JM, Doubal F, Armitage P, Chappell F, Carpenter T, Munoz Maniega S, et al. Lacunar stroke is associated with diffuse blood-brain barrier dysfunction. *Ann Neurol*. 2009;65:194-202
16. O'Rourke MF, Safar ME. Relationship between aortic stiffening and microvascular disease in brain and kidney: Cause and logic of therapy. *Hypertension*. 2005;46:200-204
17. Purkayastha S, Fadar O, Mehregan A, Salat DH, Moscufo N, Meier DS, et al. Impaired cerebrovascular hemodynamics are associated with cerebral white matter damage. *J Cereb Blood Flow Metab*. 2014;34:228-234
18. Sorond FA, Galica A, Serrador JM, Kiely DK, Iloputaife I, Cupples LA, et al. Cerebrovascular hemodynamics, gait, and falls in an elderly population: Mobilize boston study. *Neurology*. 2010;74:1627-1633
19. Bidani AK, Griffin KA. Pathophysiology of hypertensive renal damage: Implications for therapy. *Hypertension*. 2004;44:595-601
20. Fazekas F, Kleinert R, Offenbacher H, Schmidt R, Kleinert G, Payer F, et al. Pathologic correlates of incidental mri white matter signal hyperintensities. *Neurology*. 1993;43:1683-1689
21. Khatri M, Wright CB, Nickolas TL, Yoshita M, Paik MC, Kranwinkel G, et al. Chronic kidney disease is associated with white matter hyperintensity volume: The northern manhattan study (nomas). *Stroke*. 2007;38:3121-3126
22. Meel-van den Abeelen AS, van Beek AH, Slump CH, Panerai RB, Claassen JA. Transfer function analysis for the assessment of cerebral autoregulation using spontaneous oscillations in blood pressure and cerebral blood flow. *Med Eng Phys*. 2014;36:563-575
23. Zhang R, Zuckerman JH, Giller CA, Levine BD. Transfer function analysis of dynamic cerebral autoregulation in humans. *Am J Physiol*. 1998;274:H233-241.
24. Nakagawa K, Serrador JM, LaRose SL, Sorond FA. Dynamic cerebral autoregulation after intracerebral hemorrhage: A case-control study. *BMC Neurol*.11:108
25. Castro P, Santos R, Freitas J, Rosengarten B, Panerai R, Azevedo E. Adaptation of cerebral pressure-velocity hemodynamic changes of neurovascular coupling to orthostatic challenge. *Perspectives in Medicine*. 2012:http://dx.doi.org/10.1016/j.permed.2012.1002.1052 [Available online 1028 March 2012]
26. Aries MJ, Elting JW, De Keyser J, Kremer BP, Vroomen PC. Cerebral autoregulation in stroke: A review of transcranial doppler studies. *Stroke*. 2010;41:2697-2704
27. Reinhard M, Wihler C, Roth M, Harloff A, Niesen WD, Timmer J, et al. Cerebral autoregulation dynamics in acute ischemic stroke after rtpa thrombolysis. *Cerebrovasc Dis*. 2008;26:147-155
28. Levey AS, Stevens LA, Schmid CH, Zhang YL, Castro AF, 3rd, Feldman HI, et al. A new equation to estimate glomerular filtration rate. *Annals of internal medicine*. 2009;150:604-612
29. Deegan BM, Serrador JM, Nakagawa K, Jones E, Sorond FA, Olaighin G. The effect of blood pressure calibrations and transcranial doppler signal loss on transfer function estimates of cerebral autoregulation. *Med Eng Phys*. 2011;33:553-562

30. Panerai RB. The critical closing pressure of the cerebral circulation. *Med Eng Phys*. 2003;25:621-632
31. Aaslid R, Lindegaard KF, Sorteberg W, Nornes H. Cerebral autoregulation dynamics in humans. *Stroke*. 1989;20:45-52
32. Serrador JM, Sorond FA, Vyas M, Gagnon M, Iloputaife ID, Lipsitz LA. Cerebral pressure-flow relations in hypertensive elderly humans: Transfer gain in different frequency domains. *Journal of applied physiology*. 2005;98:151-159
33. Diehl RR, Linden D, Lucke D, Berlit P. Phase relationship between cerebral blood flow velocity and blood pressure. A clinical test of autoregulation. *Stroke*. 1995;26:1801-1804
34. Fiorelli M, Bastianello S, von Kummer R, del Zoppo GJ, Larrue V, Lesaffre E, et al. Hemorrhagic transformation within 36 hours of a cerebral infarct: Relationships with early clinical deterioration and 3-month outcome in the european cooperative acute stroke study i (ecass i) cohort. *Stroke*. 1999;30:2280-2284
35. van Swieten JC, Hijdra A, Koudstaal PJ, van Gijn J. Grading white matter lesions on ct and mri: A simple scale. *J Neurol Neurosurg Psychiatry*. 1990;53:1080-1083
36. Pantoni L, Simoni M, Pracucci G, Schmidt R, Barkhof F, Inzitari D. Visual rating scales for age-related white matter changes (leukoaraiosis): Can the heterogeneity be reduced? *Stroke*. 2002;33:2827-2833
37. Curtze S, Haapaniemi E, Melkas S, Mustanoja S, Putaala J, Sairanen T, et al. White matter lesions double the risk of post-thrombolytic intracerebral hemorrhage. *Stroke*. 2015
38. Curtze S, Melkas S, Sibolt G, Haapaniemi E, Mustanoja S, Putaala J, et al. Cerebral computed tomography-graded white matter lesions are associated with worse outcome after thrombolysis in patients with stroke. *Stroke*. 2015;46:1554-1560
39. Saeed A, DiBona GF, Grimberg E, Nguy L, Mikkelsen ML, Marcussen N, et al. High-nacl diet impairs dynamic renal blood flow autoregulation in rats with adenine-induced chronic renal failure. *Am J Physiol Regul Integr Comp Physiol*. 2014;306:R411-419
40. Churchill PC, Churchill MC, Griffin KA, Picken M, Webb RC, Kurtz TW, et al. Increased genetic susceptibility to renal damage in the stroke-prone spontaneously hypertensive rat. *Kidney international*. 2002;61:1794-1800
41. Abu-Amarah I, Bidani AK, Hacioglu R, Williamson GA, Griffin KA. Differential effects of salt on renal hemodynamics and potential pressure transmission in stroke-prone and stroke-resistant spontaneously hypertensive rats. *American journal of physiology. Renal physiology*. 2005;289:F305-313
42. Smeda JS, VanVliet BN, King SR. Stroke-prone spontaneously hypertensive rats lose their ability to auto-regulate cerebral blood flow prior to stroke. *Journal of hypertension*. 1999;17:1697-1705
43. Izzard AS, Graham D, Burnham MP, Heerkens EH, Dominiczak AF, Heagerty AM. Myogenic and structural properties of cerebral arteries from the stroke-prone spontaneously hypertensive rat. *Am J Physiol Heart Circ Physiol*. 2003;285:H1489-1494
44. Nakamura Y, Ono H, Frohlich ED. Differential effects of t- and l-type calcium antagonists on glomerular dynamics in spontaneously hypertensive rats. *Hypertension*. 1999;34:273-278
45. Endoh H, Honda T, Komura N, Shibue C, Watanabe I, Shimoji K. The effects of nicardipine on dynamic cerebral autoregulation in patients anesthetized with propofol and fentanyl. *Anesth Analg*. 2000;91:642-646
46. Tan CO, Hamner JW, Taylor JA. The role of myogenic mechanisms in human cerebrovascular regulation. *J Physiol*. 2013;591:5095-5105

47. Tzeng YC, Chan GS, Willie CK, Ainslie PN. Determinants of human cerebral pressure-flow velocity relationships: New insights from vascular modelling and ca(2)(+) channel blockade. *J Physiol*. 2011;589:3263-3274
48. Simard JM, Kent TA, Chen M, Tarasov KV, Gerzanich V. Brain oedema in focal ischaemia: Molecular pathophysiology and theoretical implications. *Lancet Neurol*. 2007;6:258-268
49. Reinhard M, Neunhoeffer F, Gerds TA, Niesen WD, Buttler KJ, Timmer J, et al. Secondary decline of cerebral autoregulation is associated with worse outcome after intracerebral hemorrhage. *Intensive Care Med*. 2010;36:264-271

FIGURE LEGENDS

Figure 1 Frequency spectra from 0.03 to 0.5 Hz of Coherence and Transfer Function Gain and Phase measured in acute stroke patients (< 6 hours) accordingly to their estimated glomerular filtration rate (eGFR). Continuous, interrupted and spotted lines within dark grey, light grey and spotted white strips corresponds to means±SE of groups of low (<65 ml/min), medium (65 – 87 ml/min) and high (>87 ml/min) terciles of eGFR, respectively. Groups were compared with ANOVA and P values presented at right superior corner of each plot. Lower GFR shows higher gain values bilaterally which indicate less effective dynamic cerebral autoregulation.

Figure 2 Box plots comparing median and quartiles distribution of cerebral autoregulation Gain, at low (LF: 0.03-0.15 Hz) and high (HF: 0.15-0.5 Hz) frequency bands, and estimated glomerular filtration rate (GFR) by groups with and without chronic use of calcium channel blockers (CCB). Statistical p value of Mann-whitey test (A, B) and T-test (C) is presented.

Figure 3 Relationship between renal function subgroups of low (<65 ml/min), medium (65 – 87 ml/min) and high (>87 ml/min) terciles of estimated glomerular filtration rate (eGFR) and outcome accordingly to modified Rankin scale (A), risk of hemorrhage (B) and the severity of white matter lesions assessed at 24-hour head Computed Tomography, accordingly to vanSwieten scale [35]. Subgroups were compared with ordinal regression or logistic regression as appropriate.

Figure 4 Relationship between cerebral autoregulation subgroups of low, medium and high terciles of LF gain at infarct (≤0.82, 0.83-1.01, >1.01 $\%^2/mmHg^2$, respectively) and non-infarct hemisphere (≤0.89, 0.90-1.23, >1.23 $\%^2/mmHg^2$, respectively) and outcome accordingly to

modified Rankin scale (A), risk of hemorrhage (B) and the severity of white matter lesions assessed at 24-hour head Computed Tomography, accordingly to vanSwieten scale [35]. Subgroups were compared with ordinal regression or logistic regression as appropriate.

Figure 5 Interaction between cerebral autoregulation and renal function on outcome accordingly to modified Rankin scale (A), risk of hemorrhage (B) and on severity of white matter lesions assessed at 24-hour head Computed Tomography, accordingly to vanSwieten scale [35]. Subgroups were created by splitting by median values: renal function into low (≤72 ml/min) and high (>72 ml/min) subgroups of estimated glomerular filtration rate (eGFR); cerebral autoregulation into low (Lo gain) and high (Hi gain) subgroups of LF gain in infract (≤ 0.87 and >0.87 $\%^2/mmHg^2$) and non-infarct hemisphere (≤ 1.02 and >1.02 $\%^2/mmHg^2$). Notice that higher gain values represents worse levels of cerebral autoregulation. The interaction effect in outcome and white matter lesions was tested in multinomial logistic or ordinal regression models as appropriate.

Table 1 Demographics and Baseline characteristics of patients (N=46)

Demographics	
Male	19 (51)
Age, years (mean±SD)	73±12
BMI, $Kg.m^{-2}$ (mean±SD)	27±5
Previous stroke/TIA, n (%)	6 (16)
Hypertension, n (%)	28 (77)
Diabetes Mellitus, n (%)	14 (38)
Dyslipidemia, n (%)	27 (73)
Tobacco, n (%)	4 (11)
Previous MI, n (%)	2 (4)
Atrial Fibrillation, n (%)	20 (43)
Chronic Medication, n (%)	
Antiplatelet	18 (49)
Statin	17 (46)
Beta-Blocker	10 (27)
ACEI/ARiB	15 (41)
CCB	9 (24)
Stroke characteristics	
Etiology (TOAST), n (%)	
Large Vessel	6 (16)
Cardioembolic	18 (49)
Small vessel	2 (5)
Other	1 (3)
Undetermined	12 (27)
Occlusion of affected MCA	16 (35)
NIHSS score *[median(IQR)]*	14 (9-22)
Neuroimaging [median(IQR)]	
Infarct Volume, mL	19 (2-139)
Leucoencephalopathy grade (VanSwieten scale[35])	2 (1-3)
Laboratorial (mean±SD)	
C-reactive protein, mg/L	7.7±14.7
Total cholesterol, mg/dL	174±72
LDL cholesterol, mg/dL	105±42
HDL cholesterol, mg/dL	46±11
Triglycerides, mg/dL	111±68
Glucose, mg/dL	140±81
HbA1C, %	6.4±1.4
Creatinine, mg/dL	1.0±1.0

Renal Function	
eGFR, ml/min/1.73 m^2	80±39
CDK–EPI Stage 0-1, n (%)	10 (20)
CDK–EPI Stage 2, n (%)	23 (46)
CDK–EPI Stage 3, n (%)	13 (25)
CDK–EPI Stage 4, n (%)	1 (2)
CDK–EPI Stage 5, n (%)	1 (2)

Body-Mass Index (BMI), Transitory Ischemic Attack (TIA), Modified Rankin Scale (MRS), angiotensin-conversion-enzyme inhibitor (ACEI), angiotensin receptor blocker (ARB), calcium channel blocker (CCB), Trial of ORG10172 in Acute Stroke Treatment (TOAST), middle cerebral artery (MCA), National Institutes of Health Stroke Scale (NIHSS), Low-density lipoprotein (LDL), High-density lipoprotein (LDL), glycated hemoglobin (HbA1C), eGFR (estimated glomerular filtration rate) by Chronic Kidney Disease Epidemiology Collaboration (CKD-EPI) formula[28].

Table 2 Systemic and cerebral hemodynamic characteristics of patients (N=46)

Systemic hemodynamics (mean±SD)	
Systolic ABP, mm Hg	144±19
Mean ABP, mm Hg	98±11
Diastolic ABP, mm Hg	75±11
Heart rate, bpm	67±11
LF BP variability, $(mm\ Hg)^2$	85±111
HF BP variability, $(mm\ Hg)^2$	13±20
EtCO2, mm Hg	36±7
Cerebral hemodynamics (mean±SD)	
Ipsilateral	
MFV, cm/sec	40±20
CVRi, mm Hg/cm/sec	2.3±0.9
LF BV variability, $(cm/sec)^2$	128±142
HF BV variability, $(cm/sec)^2$	35±49
Contralateral	
MFV, cm/sec	48±17
CVRi, mm Hg/cm/sec	1.7±0.7
LF BV variability, $(cm/sec)^2$	200±250
HF BV variability, $(cm/sec)^2$	47±68
Dynamic cerebral autoregulation	
Ipsilateral	
LF coherence	0.5±0.2
LF gain, %/mm Hg	1.0±0.3
LF phase, degrees	32±23
HF coherence	0.6±0.2
HF gain, %/mm Hg	1.5±0.6
HF phase, degrees	– 0.1±13
Contralateral	
LF coherence	0.5±0.2
LF gain, %/mm Hg	1.2±0.5
LF phase, degrees	44±26
HF coherence	0.7±0.2
HF gain, %/mm Hg	1.5±0.6
HF phase, degrees	– 0.7±13

Arterial blood pressure (ABP), cerebrovascular resistance index (CVRi), end-tidal carbon dioxide (EtCO2), low (LF: 0.3 – 0.15 Hz) and high (HF: 0.15 – 0.5 Hz) frequency spectral bands.

Table 3 Association between estimated glomerular filtration rate and cerebral autoregulation parameters in acute stroke (<6 hours)

	Multiple Linear Regression – Beta coefficients and estimated 95% confidence interval					
	Coherence (a.u.)		Gain ($\%^2$/ $mmHg^2$)		Phase (degrees)	
	LF band	HF band	LF band	HF band	LF band	HF band
Ipsilateral (N=37)						
eGFR, min/min	– 0.03 (0,01, 0.01)	– 0.08 (– 0.23, 0,15)	*– 0.61 (–0.01,–0.004)	*– 0.47 (–0.18,–0.003)	0.10 (– 0.24, 0.43)	– 0.08 (– 0.26, 0.14)
CCB	– 0.32 (– 45.6, 7.5)	– 0.32 (– 45.6, 7.5)	* 0.52 (0.22, 0.71)	* 0.35 (0.06, 1.12)	0.17 (– 0.09, 0.26)	0.17 (– 0.05, 0.12)
MBP, mm Hg	0.01 (– 0.01, 0.01)	0.06 (– 0.27, 0.37)	– 0.39 (– 0.02, 0.001)	– 0.01 (– 0.03, 0.01)	0.28 (– 1.21, 0.60)	0.28 (– 1.21, 0.60)
Heart Rate, bpm	– 0.11 (– 0.01, 0.00)	– 0.02 (– 0.43, 0.37)	– 0.30 (– 0.03, 0.03)	– 0.32 (– 0.01, 0.02)	0.13 (– 0.33, 1.26)	0.24 (– 1.23, 0.23)
EtCO2, mmHg	– 0.13 (– 0.01, 0.01)	– 0.03 (– 0.78, 0.67)	– 0.34 (– 0.08, 0.05)	– 0.23 (– 0.10, 0.02)	0.31 (– 0.10, .34)	0.13 (– 0.13, 2.31)
Contralateral (N=46)						
eGFR, min/min	– 0.19 (–0.01, 0.01)	0.09 (– 0.13, 0.25)	*– 0.45 (–0.01,–0.004)	*– 0.42 (–0.02,–0.004)	0.06 (– 0.23, 0.35)	0.09 (– 0.13, 0.25)
CCB	– 0.15 (– 34.5, 10.2)	– 0.32 (– 45.6, 7.5)	* 0.40 (0.16, 0.81)	0.25 (– 0.04, 0.76)	0.14 (– 0.06, 0.24)	0.17 (– 0.05, 0.12)
MBP, mm Hg	– 0.20 (– 0.01, 0.001)	0.10 (– 0.22, 0.45)	*– 0.49 (–0.03,–0.01)	*– 0.47 (–0.03, –0.01)	0.17 (– 0.26, 0.84)	0.21 (– 1.23, 1.01)
Heart Rate, bpm	– 0.08 (– 0.01, 0.003)	– 0.02 (– 0.45, 0.38)	– 0.15 (– 0.02, 0.01)	– 0.32 (– 0.01, 0.13)	– 0.04 (– 0.58, 1.03)	– 0.10 (– 2.33, 0.12)
EtCO2, mmHg	– 0.03 (– 0.01, 0.01)	– 0.17 (– 1.12, 0.28)	– 0.29 (– 0.04, 0.00)	– 0.24 (– 0.01, 0.12)	0.13 (0.14, 2.56)	– 0.25 (– 0.23, 3.12)

Estimated glomerular filtration rate (eGFR), mean arterial blood pressure (MBP), end-tidal carbon dioxide (EtCO2), low (LF: 0.03 – 0.15 Hz) and high (HF: 0.15 – 0.5 Hz) frequency spectral bands.* P<0.01 for multivariate linear regression analysis adjusting for age, gender and all significantly related variables in univariate analysis

Figure 1

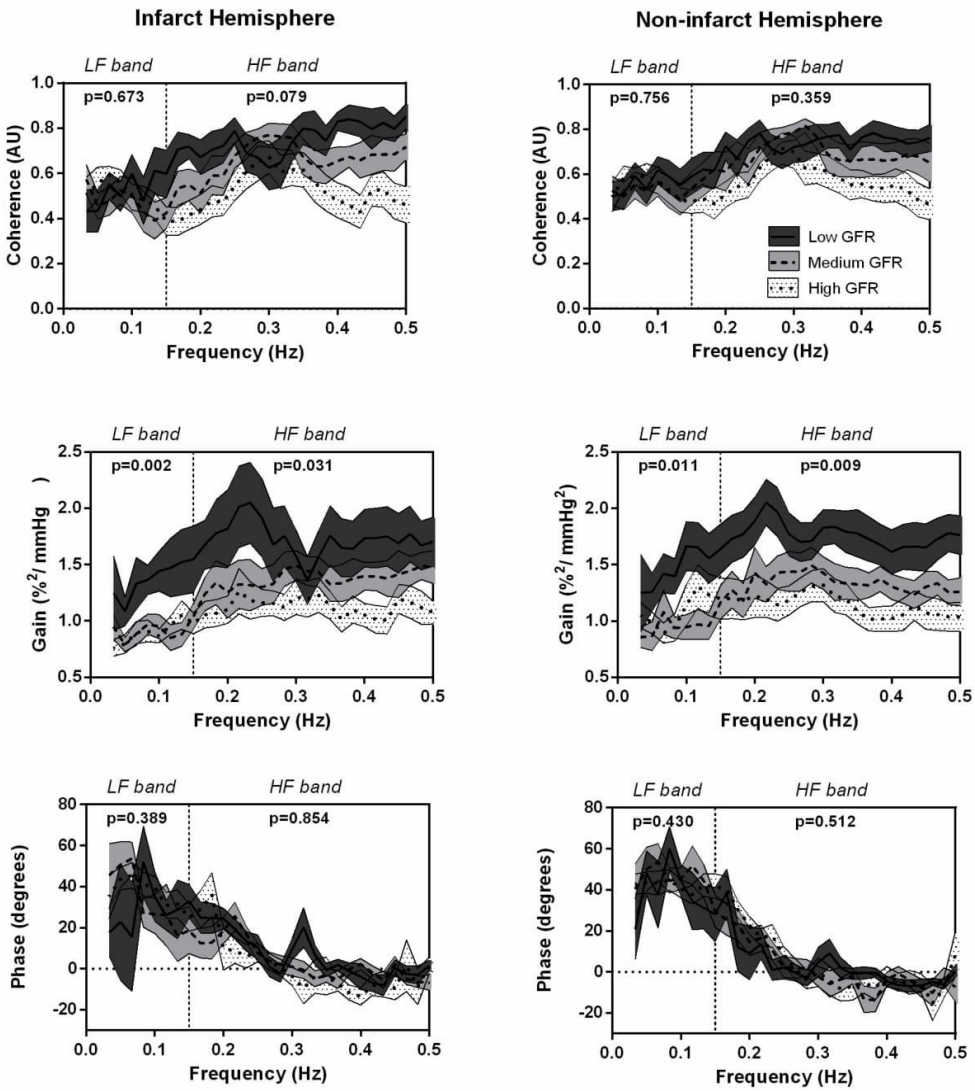
Infarct Hemisphere
Non-infarct Hemisphere
LF band
HF band
p=0.673
p=0.079
p=0.756
p=0.359
Coherence (AU)
Low GFR
Medium GFR
High GFR
Frequency (Hz)
p=0.002
p=0.031
p=0.011
p=0.009
Gain (%²/ mmHg²)
p=0.389
p=0.854
p=0.430
p=0.512
Phase (degrees)

Figure 2

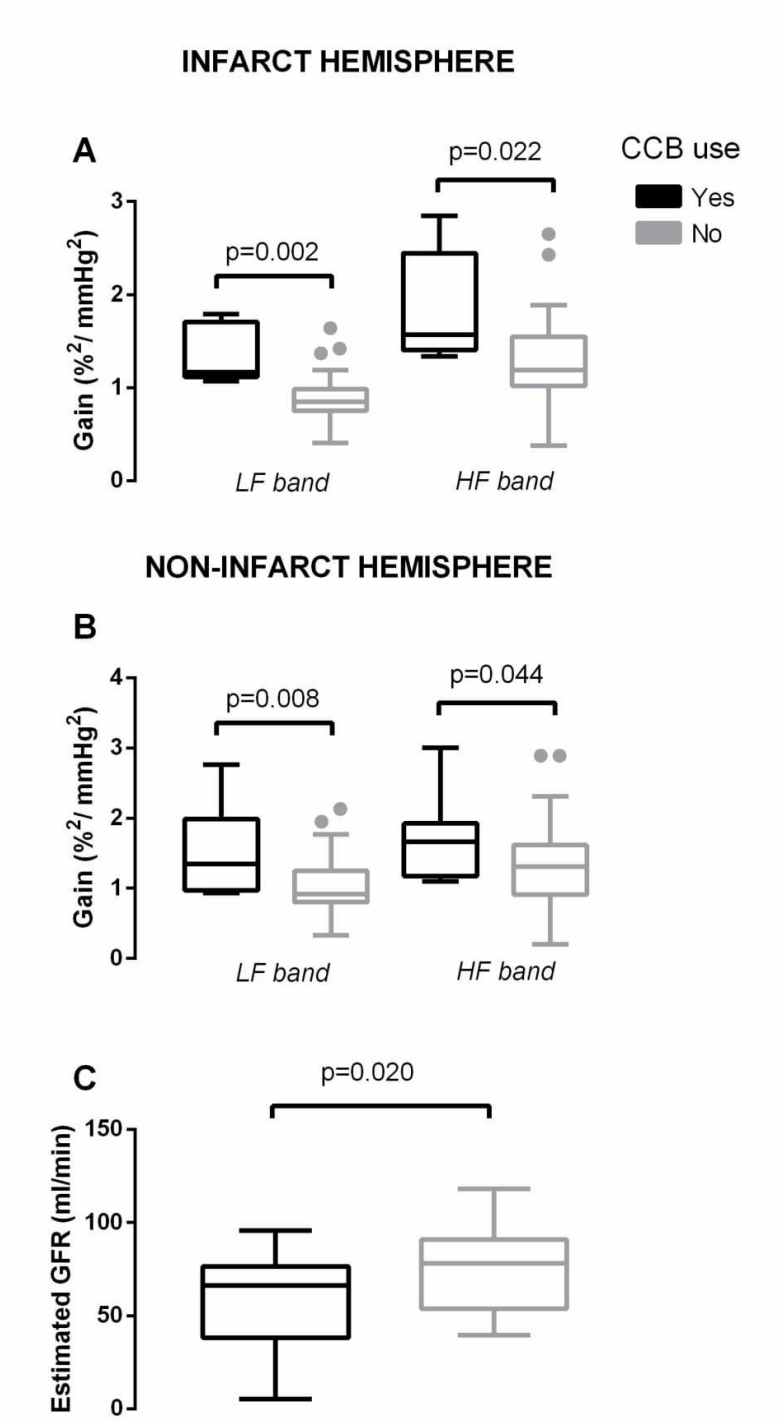
INFARCT HEMISPHERE
A
p=0.022
CCB use
Yes
No
p=0.002
Gain (%²/ mmHg²)
3
2
1
0
LF band
HF band
NON-INFARCT HEMISPHERE
B
p=0.044
p=0.008
Gain (%²/ mmHg²)
4
3
2
1
0
LF band
HF band
C
p=0.020
Estimated GFR (ml/min)
150
100
50
0

Figure 3

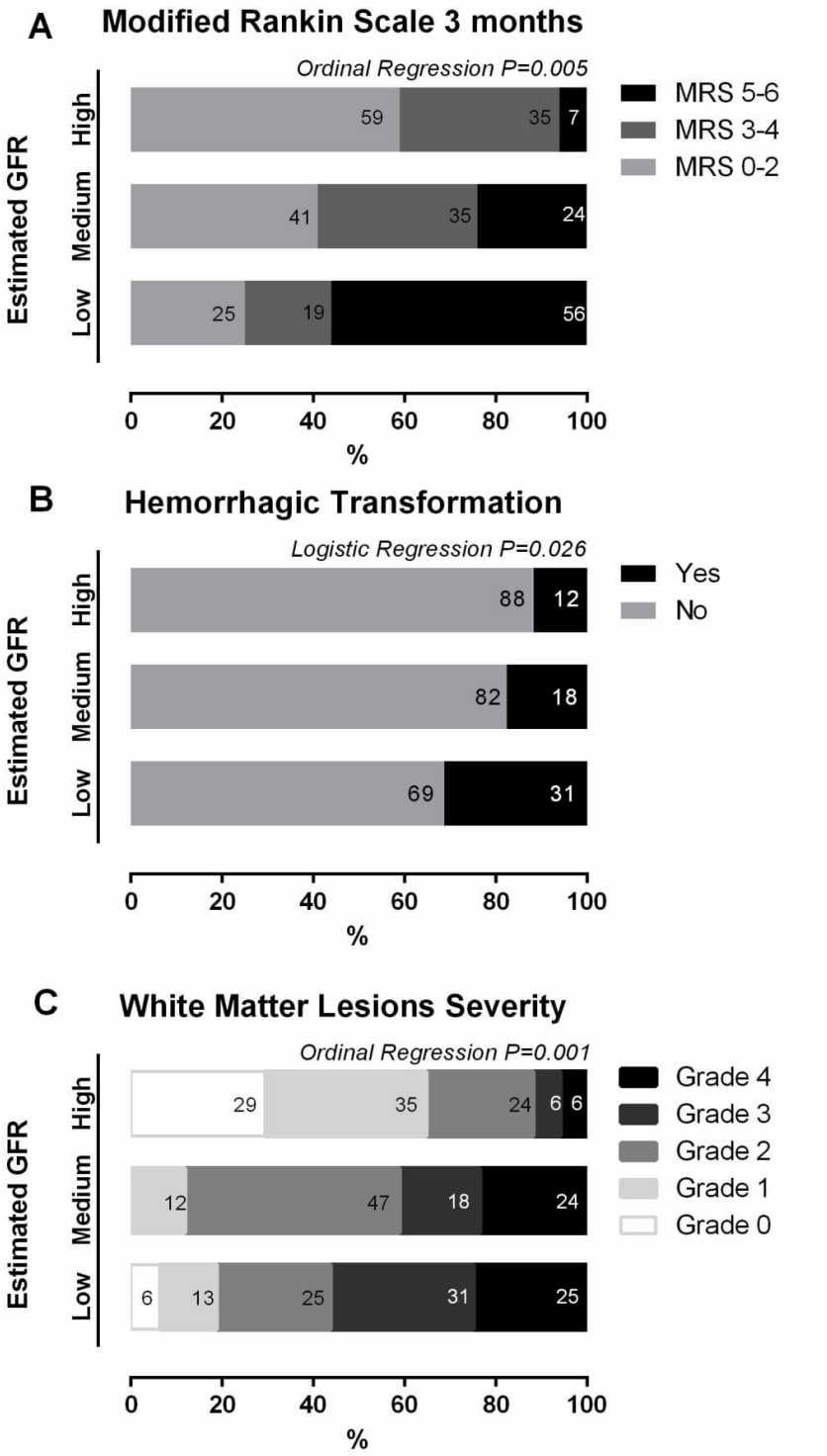
A
Modified Rankin Scale 3 months
Ordinal Regression P=0.005
Estimated GFR
High
Medium
Low
59
35
7
41
35
24
25
19
56
MRS 5-6
MRS 3-4
MRS 0-2
0
20
40
60
80
100
%
B
Hemorrhagic Transformation
Logistic Regression P=0.026
Estimated GFR
High
Medium
Low
88
12
82
18
69
31
Yes
No
0
20
40
60
80
100
%
C
White Matter Lesions Severity
Ordinal Regression P=0.001
Estimated GFR
High
Medium
Low
29
35
24
6
6
12
47
18
24
6
13
25
31
25
Grade 4
Grade 3
Grade 2
Grade 1
Grade 0
0
20
40
60
80
100
%

Figure 4

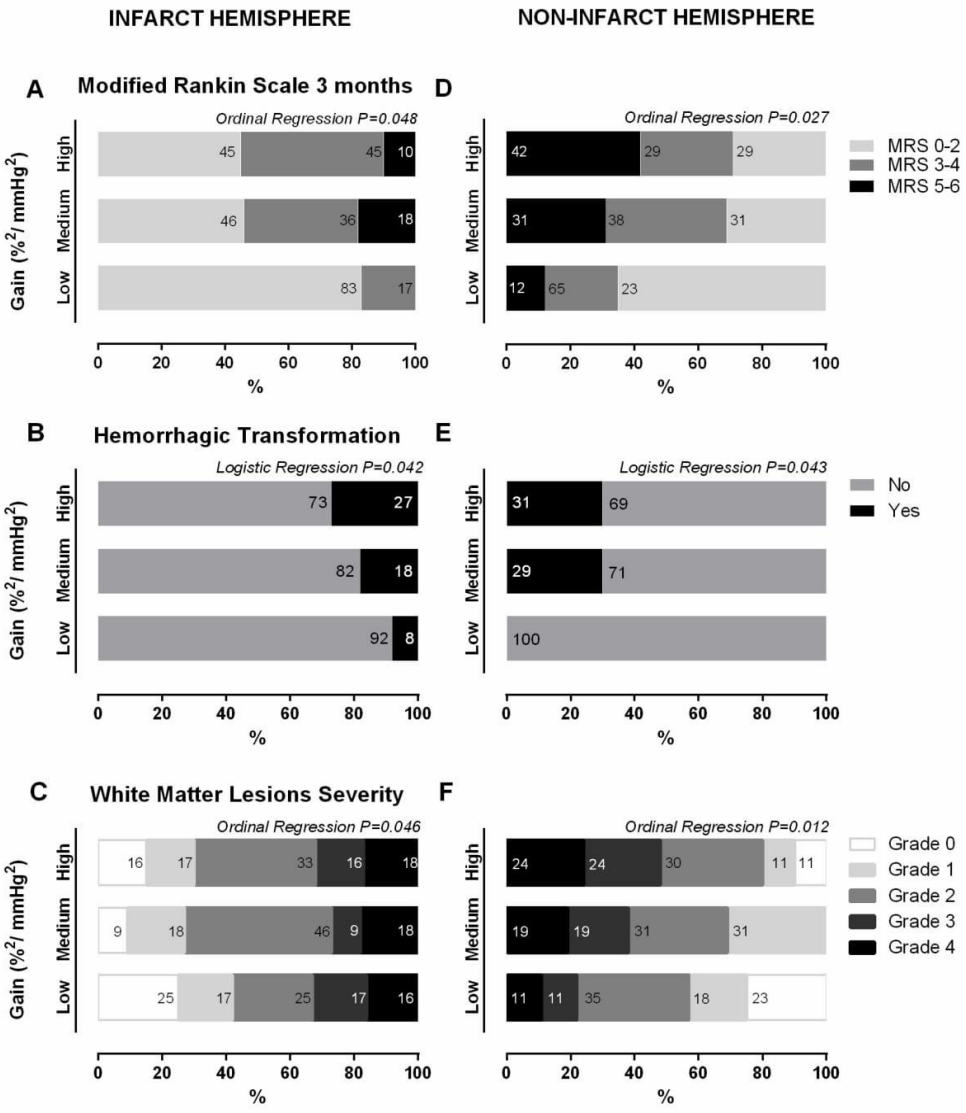
INFARCT HEMISPHERE
NON-INFARCT HEMISPHERE
A
Modified Rankin Scale 3 months
Ordinal Regression P=0.048
D
Ordinal Regression P=0.027
Gain (%²/ mmHg²)
High
Medium
Low
45 45 10
46 36 18
83 17
42 29 29
31 38 31
12 65 23
0 20 40 60 80 100
%
MRS 0-2
MRS 3-4
MRS 5-6
B
Hemorrhagic Transformation
Logistic Regression P=0.042
E
Logistic Regression P=0.043
73 27
82 18
92 8
31 69
29 71
100
No
Yes
C
White Matter Lesions Severity
Ordinal Regression P=0.046
F
Ordinal Regression P=0.012
16 17 33 16 18
9 18 46 9 18
25 17 25 17 16
24 24 30 11 11
19 19 31 31
11 11 35 18 23
Grade 0
Grade 1
Grade 2
Grade 3
Grade 4

Figure 5

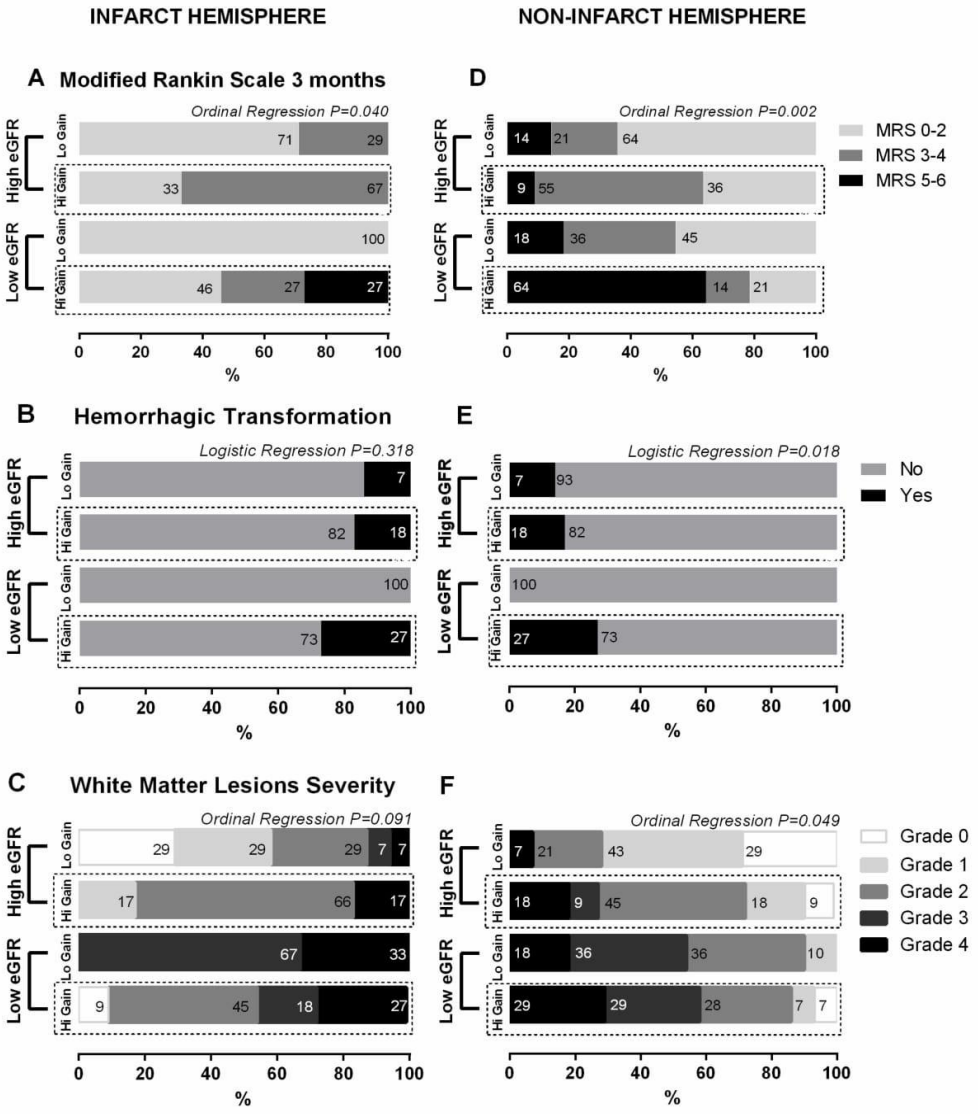
INFARCT HEMISPHERE
NON-INFARCT HEMISPHERE
A Modified Rankin Scale 3 months
Ordinal Regression P=0.040
D
Ordinal Regression P=0.002
MRS 0-2
MRS 3-4
MRS 5-6
B Hemorrhagic Transformation
Logistic Regression P=0.318
E
Logistic Regression P=0.018
No
Yes
C White Matter Lesions Severity
Ordinal Regression P=0.091
F
Ordinal Regression P=0.049
Grade 0
Grade 1
Grade 2
Grade 3
Grade 4
High eGFR
Low eGFR
Lo Gain
Hi Gain
%

Capítulo 5: Doentes com insuficiência cardíaca e com estenose aórtica grave apresentam uma resposta autorreguladora cerebral superior no AVC isquémico agudo

Castro, P., Rocha, I., Serrador, J., Chaves, P., Sorond, F., & Azevedo, E. (2017). Heart Failure Patients with Severe Aortic Stenosis Have Enhanced Cerebral Autoregulation Response in Acute Ischemic Stroke. *Int J Cardiol* (em revisão)

Title:

Heart Failure Patients with Severe Aortic Stenosis Have Enhanced Cerebral Autoregulation Response in Acute Ischemic Stroke

Authors:

Pedro Castro, MD

Dept. Neurology, São João Hospital Center, Faculty of Medicine of University of Porto, Portugal

pedromacc@gmail.com

Isabel Rocha, PhD

Cardiovascular Autonomic Function Lab, Institute of Physiology, Faculty of Medicine of University of Lisbon, Portugal; isabelrocha0@gmail.com

Jorge Serrador, PhD

Veterans Biomedical Institute and War Related Illness and Injury Study Center, Department of Veterans Affairs, New Jersey Healthcare System, East Orange, USA; New Jersey Medical School, Newark, NJ, USA; Harvard Medical School, Boston, MA, USA

Jorge.Serrador@va.gov

Paulo Chaves, PhD

Cardiovascular Research and Development Center, Faculty of Medicine of University of Porto, Portugal

pchaves@med.up.pt

Farzaneh Sorond, MD, PhD

Department of Neurology, Division of Stroke and Neurocritical, Northwestern University Feinberg School of Medicine, Chicago, Illinois.farzaneh.sorond@nm.org

Elsa Azevedo, MD, PhD

Dept. Neurology, São João Hospital Center, Faculty of Medicine of University of Porto, Portugal

eazevedo@med.up.pt

Corresponding author:

Pedro Castro, MD

Dept. Neurology, São João Hospital Center, Faculty of Medicine of University of Porto

Alameda Professor Hernani Monteiro, 4200-319 Porto, PORTUGAL

Fax: +351 225 025 766, Telephone: +351 931 725 181, e-mail: pedromacc@gmail.com

Cover title:

Heart failure and cerebral autoregulation in stroke

Itemized list:

(1) Table 1: Baseline characteristics of CHF and non-HF patients.

(2) Table 2: Relationship between cardiac disease markers and cerebral autoregulation

(3) Figure 1**:** Coherence, phase and gain at <6h, at 24h and 3 months in CHF and non-CHF patients

Keywords: cerebral autoregulation, heart failure, myocardial infarction, ischemic stroke, transcranial Doppler

Subject Codes: Hemodynamics; Ischemia; Mechanisms; Heart Failure; Physiology; Pathophysiology; Vascular Biology; Cardiovascular Disease; Blood Pressure; Ultrasound; Ischemic Stroke; Vascular Disease

Text word count: 4386/4500; Abstract 247/250

Abstract

Background and Purpose:

The cerebrovascular effects of a failing heart-pump, namely its relation to the capability of cerebral autoregulation, are largely unknown. Understanding the influence of chronic heart failure (CHF) in cerebral autoregulation in the setting of acute ischemic stroke can reveal new insights into the vasomotor control and targets that can benefit all stroke patients. In this study we examined the relationship between CHF and dynamic cerebral autoregulation (CA), within 6 hours of symptom-onsetthrough a chronic stage of ischemic stroke.

Methods: We prospectively enrolled 50 patients with acute ischemic stroke. Groups with CHF (N=8) and without CHF were compared. Arterial blood pressure (Finometer), cerebral blood flow velocity (transcranial Doppler), electrocardiogram and end-tidal-CO_2 were recorded over 10 minutes within 6 and at 24 hours from symptom-onset and at 3 months. We assessed CA by transfer function analysis (coherence, phase and gain). Cardiac disease markers were assessed at presentation.

Results: CHF associated with higher phase (better CA) at ischemic hemisphere within 6 ($p=0.042$) and at 24 hours ($p=0.006$) but this effect resolved at 3 months ($p>0.05$). Gain and Coherence trends were similar between groups. We found a positive correlation

between Phase values and troponin I levels at presentation (Spearman's r= 0.348, p=0.044.

Conclusions: Our findings advances the knowledge of how brain and heart interact is acute ischemic stroke by showing an enhanced dynamic cerebral autoregulation response in CHF patients. Understanding the physiological mechanisms that govern this complex interplay can be useful to find novel therapeutic targets which can improve outcome in ischemic stroke.

Text

Introduction

Increasing attention is being given to the complex interplay between heart and brain and in this context chronic heart failure (CHF) is an illustrative challenge. In fact, it is known that CHF increases the risk, severity and poor outcome of ischemic stroke (IS)[1], in part due to frequent concomitant atrial fibrillation (AF). On the other hand, CHF causes chronic brain hypoxia and thereby may induce changes in the capability of small resistance vessels to react to ischemic insult, i.e. may promote ischemic preconditioning[2]. There is some evidence that CHF can have impact in cerebral hemodynamics and reduced oxygenation upon standing[3], possibly caused by augmented vasoconstriction due to overactivity of sympathetic nervous system[4], although the decrease in cerebral perfusion pressure can be caused by the reduced ejection fraction itself. However, despite its clinical and physiological interest, the cerebrovascular control to blood pressure fluctuations, the so called cerebral autoregulation (CA), has never been properly studied before in CHF patients. Exception goes for a recent study on ischemic CHF that found

impaired CA and an previous work reporting impaired cerebrovascular vasodilation to CO_2 challenge[5], which is definitely not a synonym of CA. There are no studies of CA response of patients with CHF under acute stress or acute stroke not to subtypes of heart failure due to valvulopathy. Understanding the effects of chronic low perfusion pressure on brain can lead, not only to better treatment of neurological complications of CHF, but also to unravel the mechanisms of cerebral vascular control to global hypoxia.

Dynamic CA can be rapidly and noninvasively assessed at the bedside by transfer function analysis (TFA) using spontaneous oscillations in blood pressure and cerebral blood flow velocity[7-12] which is known to be impaired in acute IS[13, 14].

In this study we compare the Dynamic CA response measured by TFA between patients with and without CHF, from acute through chronic stage of IS.

Methods

Population studied

We consecutively included patients with acute IS admitted to stroke unit at São João Hospital Centre, Porto, and able to be monitored within 6 hours of symptoms. Exclusion criteria included hemodynamic instability requiring vasoactive agents, other central neurological co-morbidities (e.g. tumor), acute renal injury, myocardial infarction (clinical, electrocardiographic ST-elevation or serial myocardial injury enzymes) or insufficient temporal acoustic window. We recruited 50 patients, 46 with IS of middle (MCA) and 4 of posterior (PCA) cerebral arteries territories. In 3 of these cases we did not have imaging confirmation of the definitive infarcted territory and patients were included based on clinical signs of MCA territory infarction (aphasia). All participants underwent cervical and transcranial duplex scan (Vivid *e*; GE) before evaluation. All

patients underwent neurological examination at presentation and National Institutes of Health Stroke Scale (NIHSS) scores were calculated at baseline and on a daily basis until discharge. IS patients with or without CHF were identified and compared. **CHF was diagnosed** previously on cardiac CHF symptoms with functional class I to III, according to the New York Heart Association (NYHA) classification{Bennett, 2002 #555} irrespective of left ventricle ejection fraction (LVEF).

Monitoring protocol

Evaluations were carried out in the stroke unit with head of the bed at 0º during the 10 min of recording. Arterial blood pressure (ABP) was continuously monitored with a finger cuff in the unaffected side using Finometer MIDI (FMS, Amsterdam, Netherlands). Additionally, blood pressure was assessed using an oscillometric cuff (Dash 2500, GE, UK) hourly in the first 24-hours and at 3 months. HR was assessed from lead II of a standard 3-lead electrocardiogram (ECG). Cerebral blood flow velocity (CBFV) was recorded bilaterally from M1 segment of MCA (depth of 50-55 mm) and P2 segment if PCA (depth 50-60 mm) with 2-MHz monitoring probes secured with a standard headband (Doppler BoxX, DWL, Singen, Germany). End-tidal carbon dioxide (CO_2) was continuously recorded with nasal cannula attached to Respsense capnograph (Nonin, Amsterdam, Netherlands). All data were synchronized and digitized at 400 Hz with Powerlab (AD Instruments, Oxford, UK) and stored for offline analysis. Data collection occurred for 10 minutes within 6 hours and at 24 hours from symptoms-onset and also at 3 months in survivors available for follow-up (n=36).

Heart disease markers

Blood samples were collected immediately at admission for B-type natriuretic peptide (BNP), troponin I (TpI), myoglobin, creatinine kinase–MB, C-reactive protein (CRP) and creatinine levels. Estimated glomerular filtration rate (eGFR) was calculated using the Chronic Kidney Disease Epidemiology Collaboration formula[15]. In the first fasting sample we measured total, low-density lipoprotein (LDL) and high-density lipoprotein (HDL) cholesterol, glucose and glycated hemoglobin (HgA1C).

Transthoracic Echocardiography (Philips, iE33, Amsterdam) was performed during the first 48 hours and validated by experienced cardiologist and let ventricle ejection fraction (LVEF) and mass (LVM) were calculated accordingly to guidelines[16]. CHF patients were reviewed for previous echographic studies to exclude those with acute heart changes.

Data analysis

All signals were inspected and artifacts removed by linear interpolation. Systolic, mean and diastolic values of ABP and CBFV were calculated. For each heart-beat cerebrovascular resistance index (CVRi) was calculated by ABP/CBFV reflecting vasomotor function[17]. Transfer function Analysis (TFA) was used to assess Dynamic CA by calculating coherence, gain and phase parameters from beat-to-beat spontaneous oscillations of CBFV and ABP as previously reported[9, 18]. Ten minutes of normalized data were interpolated at 100 Hz into uniform time basis; averaged periodogram was calculated by Welch method[9] with Hanning window of 30 seconds, with two-third overlap. Coherence was calculated between input auto-spectra of ABP over cross-spectra of CBFV/ABP and transfer functions of phase and gain were determined by dividing the cross-spectrum by the input auto-spectrum[10]. Coherence, gain and phase are reported for the low frequency range (0.03-0.15 Hz) which is the autoregulatory frequency[8-10, 18]. In short, coherence is the coefficient of correlation between the signals; higher coherence

between the oscillations is reflective of less effective Dynamic CA. Gain quantifies the damping effect of Dynamic CA on the magnitude of ABP oscillations. Phase shift represents the time delay between ABP and CBFV oscillations. Lower gain and higher phase represent tighter, more effective autoregulatory response[9, 19].

Neuroimaging Assessment

All subjects were assessed with admission CT brain scan (Siemens Somaton Emotion Duo, Erlangen, Germany), with 3 to 6 mm slices, at presentation and repeated at 24 hours. Infarct volume was measured at 24h following ABC/2 rule[20].

Statistical analysis

Normality was determined by Shapiro-Wilk test. Baseline data are presented for all subjects. Groups with and without CHF were compared with qui-square test for nominal variables and Student t-test or Mann-Whitney for continuous variables as appropriate. Repeated measures ANOVA was used to find significant time changes in hemodynamic variables. Polynomial contrast compared serial time marks; differences between dichotomous groups with and without CHF were achieved by repeating the model with fixed factors. Bonferonni's post-hoc test was used to correct for multiple comparisons. The relationship between continuous variables, such as TFA parameters and cardiac disease markers, were analyzed with Spearman's rho correlation analysis. All effects were considered statistically significant at $P<0.05$ level. All statistics were performed using IBM Statistical Package for Social Sciences (SPSS) Statistics v21™.

Results

We identified 8 patients with CHF: 6/8 had severe aortic stenosis and 6/8 had previous ischemic heart disease. Etiological classification was considered to be primary due to valvulopahty in 6/8 and the remain ischemic. Only 2 patients had preserved CHF with LVEF; 5/8 patients were in NYHA class II, 2 in class III and 1 in class I. Baseline characteristics and hemodynamic data are reported in Tables 1. CHF group was older (p=0.034), had lower BMI (p=0.039) and, as excepted, higher levels of cardiac dysfunction (TpI, BNP, LVEF and LVM p<0.05). Stroke severity (infarct volume or NIHSS score) were not different in CHF compared to the others (p>0.05). As shown in Figure 1, CHF patients had higher VLF Phase (better CA) at ischemic hemisphere within 6 (p=0.042) and at 24 hours (p=0.006) of symptom-onset which resolved at 3 months (p> 0.05). Tlain and Coherence trends were similar between groups. Concerning laboratory and laboratorial markers of cardiac dysfunction, we found a positive correlation between VLF Phase values and TpI levels at presentation (Spearman's r= 0.348, p=0.044). NYHA class, BNP and LVEF were not correlated with TFA parameters (p>0.05). Analysis of the relationship between TFA parameters and baseline characteristics reveled that VLF Phase were inversely correlated with infarct volume (<6 hours, Spearman´s Rho r= – 0.483, p=0.007; at 24 hours r= – 0.456, p=0.007) but not with any other independent variable. The presence of AF did not influence it either (p=0.281).

Discussion

Our data shows that patients with CHF have a significantly higher Dynamic CA (higher VLF Phase) in affected arterial territory of acute IS then those without CHF. Also, a higher Phase was correlated with increased myocardial injury as detected by TpI at presentation.

An increased phase shift at lower frequencies is generally accepted as a marker of more effective Dynamic CA, as continuous counter-regulation of CBFV to oscillations of BP. A lower phase (usually < 20-30 degrees) has been reported in several cerebrovascular diseases such as IS[14, 21], intracerebral hemorrhage[22], MCA stenosis[23-25], carotid stenosis[24] and even predictor of cerebral vasospasm or delayed cerebral ischemia[26-28] supporting its value as a marker of impaired Dynamic CA.

The explanation for our findings it not easily depicted from the exhaustive characterization of the patients. BNP were not correlated with VLF Phase, meaning that CHF severity was not a determining for the higher Dynamic CA. Also, systemic hemodynamic parameters were similar between groups apart from obvious lower cardiac output (lower LVEF) in CHF.

Increased sympathetic autonomic activity, frequently found in CHF[1] or IS[29] could be a possible link since it may interfere with cerebrovascular control[30, 31]. Curiously, higher TpI was also modestly related to higher VLF phase at affected hemisphere. Increased sympathetic activity could be the cause of increased myocyte necrosis which is commonly described in stress myocardiopathy[29]. However, the available evidence points in favor of an impaired cerebral hemodynamics by increased autonomic activity[1, 4], which is not in accordance to our results. Increased sympathetic activity in CHF could cause cerebral vasoconstriction impairing cerebral autoregulation, contrary to what we have found. Unfortunately, the high prevalence of AF in CHF subgroup prevented us to explore HR variability, a surrogate for autonomic activity to clarify this point.

Another possible explanation to our results might derive from the fact that chronic brain hypoperfusion in CHF patients could induce some direct or remote preconditioning effects at cerebral level rendering it more resistant to ischemia[2]. Supporting this hypothesis, we remember that most of our CHF patients had concomitant ischemic heart

disease. Hypoxia-inducible factor-1 (HIF-1) is increased in CHF patients even with preserved LVEF and correlates with the increased TpI levels at admission of decompensated CHF[32]. HIF-1-activation pathway reacts to ischemia by increasing serum vascular endothelial growth factor and erythropoietin concentrations[33, 34]. Also, in animal models, iron chelation and HIF-1 activation have been shown to be neuroprotective in acute ischemic stroke and subarachnoid hemorrhage[35-37]. Recent work elegantly demonstrated that activation of HIF-1-regulated pathway with deferoxamine improved CA[34]. Therefore, higher Dynamic CA response in our study can be an expression of this hypoxic-ischemic preconditioning. Another possibility is that augmented CA is the expression the severe aortic obstruction of many patients with CHF. It should be noticed, however, that this could not be accounted by low peripheral arterial BP levels because MBP was similar between groups.

Future studies should thus measure these biomarkers to assess their relevance in IS. Studies should also be sought to compared CA in patients with severe aortic stenosis or HF and between both acute ischemic settings (eg, controlled forearm ischemia) and chronic stable conditions.

As in previous works[14, 21, 38, 39], gain did not show unequivocal proofs of being altered in acute IS which are in line with our results. Phase may be a much more sensitive measure of Dynamic CA than gain[40].

In conclusion, our findings contribute to the knowledge of how brain and heart interact in acute ischemic stroke by showing an enhanced dynamic cerebral autoregulation response in CHF patients. Understanding the physiological mechanism that govern this complex interplay can be useful to allow searching therapeutic targets that can improve outcome in ischemic stroke.

Sources of Funding:

This study received public national grant from Fundação para a Ciência e a Tecnologia (FCT), Portugal, PTDC/SAU-ORG/113329/2009

Disclosures: None

References

1. Haeusler KG, Laufs U, Endres M. Chronic heart failure and ischemic stroke. *Stroke*. 2011;42:2977-2982
2. Koch S, Della-Morte D, Dave KR, Sacco RL, Perez-Pinzon MA. Biomarkers for ischemic preconditioning: Finding the responders. *J Cereb Blood Flow Metab*. 2014;34:933-941
3. Cornwell WK, 3rd, Levine BD. Patients with heart failure with reduced ejection fraction have exaggerated reductions in cerebral blood flow during upright posture. *JACC. Heart failure*. 2015;3:176-179
4. van Lieshout JJ, Secher NH. Point:Counterpoint: Sympathetic activity does/does not influence cerebral blood flow. Point: Sympathetic activity does influence cerebral blood flow. *J Appl Physiol*. 2008;105:1364-1366
5. Georgiadis D, Sievert M, Cencetti S, Uhlmann F, Krivokuca M, Zierz S, et al. Cerebrovascular reactivity is impaired in patients with cardiac failure. *European heart journal*. 2000;21:407-413
6. Madureira J, Castro P, Azevedo E. Demographic and systemic hemodynamic influences in mechanisms of cerebrovascular regulation in healthy adults. *J Stroke Cerebrovasc Dis*. 2016
7. Meel-van den Abeelen AS, van Beek AH, Slump CH, Panerai RB, Claassen JA. Transfer function analysis for the assessment of cerebral autoregulation using spontaneous oscillations in blood pressure and cerebral blood flow. *Med Eng Phys*. 2014;36:563-575
8. Panerai RB. Assessment of cerebral pressure autoregulation in humans--a review of measurement methods. *Physiol Meas*. 1998;19:305-338
9. Zhang R, Zuckerman JH, Giller CA, Levine BD. Transfer function analysis of dynamic cerebral autoregulation in humans. *Am J Physiol*. 1998;274:H233-241.
10. Nakagawa K, Serrador JM, LaRose SL, Sorond FA. Dynamic cerebral autoregulation after intracerebral hemorrhage: A case-control study. *BMC Neurol*.11:108
11. Purkayastha S, Fadar O, Mehregan A, Salat DH, Moscufo N, Meier DS, et al. Impaired cerebrovascular hemodynamics are associated with cerebral white matter damage. *J Cereb Blood Flow Metab*. 2014;34:228-234
12. Castro P, Santos R, Freitas J, Rosengarten B, Panerai R, Azevedo E. Adaptation of cerebral pressure-velocity hemodynamic changes of neurovascular coupling to orthostatic challenge. *Perspectives in Medicine*. 2012:http://dx.doi.org/10.1016/j.permed.2012.1002.1052 [Available online 1028 March 2012]

13. Aries MJ, Elting JW, De Keyser J, Kremer BP, Vroomen PC. Cerebral autoregulation in stroke: A review of transcranial doppler studies. *Stroke*. 2010;41:2697-2704
14. Reinhard M, Wihler C, Roth M, Harloff A, Niesen WD, Timmer J, et al. Cerebral autoregulation dynamics in acute ischemic stroke after rtpa thrombolysis. *Cerebrovasc Dis*. 2008;26:147-155
15. Levey AS, Stevens LA, Schmid CH, Zhang YL, Castro AF, 3rd, Feldman HI, et al. A new equation to estimate glomerular filtration rate. *Annals of internal medicine*. 2009;150:604-612
16. Pepi M, Evangelista A, Nihoyannopoulos P, Flachskampf FA, Athanassopoulos G, Colonna P, et al. Recommendations for echocardiography use in the diagnosis and management of cardiac sources of embolism: European association of echocardiography (eae) (a registered branch of the esc). *European journal of echocardiography : the journal of the Working Group on Echocardiography of the European Society of Cardiology*. 2010;11:461-476
17. Panerai RB. The critical closing pressure of the cerebral circulation. *Med Eng Phys*. 2003;25:621-632
18. Aaslid R, Lindegaard KF, Sorteberg W, Nornes H. Cerebral autoregulation dynamics in humans. *Stroke*. 1989;20:45-52
19. Diehl RR, Linden D, Lucke D, Berlit P. Phase relationship between cerebral blood flow velocity and blood pressure. A clinical test of autoregulation. *Stroke*. 1995;26:1801-1804
20. Sims JR, Gharai LR, Schaefer PW, Vangel M, Rosenthal ES, Lev MH, et al. Abc/2 for rapid clinical estimate of infarct, perfusion, and mismatch volumes. *Neurology*. 2009;72:2104-2110
21. Reinhard M, Roth M, Guschlbauer B, Harloff A, Timmer J, Czosnyka M, et al. Dynamic cerebral autoregulation in acute ischemic stroke assessed from spontaneous blood pressure fluctuations. *Stroke*. 2005;36:1684-1689
22. Reinhard M, Neunhoeffer F, Gerds TA, Niesen WD, Buttler KJ, Timmer J, et al. Secondary decline of cerebral autoregulation is associated with worse outcome after intracerebral hemorrhage. *Intensive Care Med*. 2010;36:264-271
23. Hu HH, Kuo TB, Wong WJ, Luk YO, Chern CM, Hsu LC, et al. Transfer function analysis of cerebral hemodynamics in patients with carotid stenosis. *J Cereb Blood Flow Metab*. 1999;19:460-465
24. Reinhard M, Hetzel A, Lauk M, Lucking CH. Dynamic cerebral autoregulation testing as a diagnostic tool in patients with carotid artery stenosis. *Neurol Res*. 2001;23:55-63
25. Haubrich C, Kruska W, Diehl RR, Moller-Hartmann W, Klotzsch C. Dynamic autoregulation testing in patients with middle cerebral artery stenosis. *Stroke*. 2003;34:1881-1885
26. Lang EW, Diehl RR, Mehdorn HM. Cerebral autoregulation testing after aneurysmal subarachnoid hemorrhage: The phase relationship between arterial blood pressure and cerebral blood flow velocity. *Critical care medicine*. 2001;29:158-163
27. Soehle M, Czosnyka M, Pickard JD, Kirkpatrick PJ. Continuous assessment of cerebral autoregulation in subarachnoid hemorrhage. *Anesth Analg*. 2004;98:1133-1139, table of contents
28. Otite F, Mink S, Tan CO, Puri A, Zamani AA, Mehregan A, et al. Impaired cerebral autoregulation is associated with vasospasm and delayed cerebral ischemia in subarachnoid hemorrhage. *Stroke*. 2014;45:677-682

29. De Raedt S, De Vos A, De Keyser J. Autonomic dysfunction in acute ischemic stroke: An underexplored therapeutic area? *J Neurol Sci*. 2015;348:24-34
30. Azevedo E, Castro P, Santos R, Freitas J, Coelho T, Rosengarten B, et al. Autonomic dysfunction affects cerebral neurovascular coupling. *Clin Auton Res*. 2011;21:395-403
31. Castro PM, Santos R, Freitas J, Panerai RB, Azevedo E. Autonomic dysfunction affects dynamic cerebral autoregulation during valsalva maneuver: Comparison between healthy and autonomic dysfunction subjects. *Journal of applied physiology*. 2014;117:205-213
32. Li G, Lu WH, Wu XW, Cheng J, Ai R, Zhou ZH, et al. Admission hypoxia-inducible factor 1alpha levels and in-hospital mortality in patients with acute decompensated heart failure. *BMC cardiovascular disorders*. 2015;15:79
33. Fernando MS, Simpson JE, Matthews F, Brayne C, Lewis CE, Barber R, et al. White matter lesions in an unselected cohort of the elderly: Molecular pathology suggests origin from chronic hypoperfusion injury. *Stroke*. 2006;37:1391-1398
34. Sorond FA, Tan CO, LaRose S, Monk AD, Fichorova R, Ryan S, et al. Deferoxamine, cerebrovascular hemodynamics, and vascular aging: Potential role for hypoxia-inducible transcription factor-1-regulated pathways. *Stroke*. 2015;46:2576-2583
35. Prass K, Ruscher K, Karsch M, Isaev N, Megow D, Priller J, et al. Desferrioxamine induces delayed tolerance against cerebral ischemia in vivo and in vitro. *J Cereb Blood Flow Metab*. 2002;22:520-525
36. Bergeron M, Gidday JM, Yu AY, Semenza GL, Ferriero DM, Sharp FR. Role of hypoxia-inducible factor-1 in hypoxia-induced ischemic tolerance in neonatal rat brain. *Ann Neurol*. 2000;48:285-296
37. Hishikawa T, Ono S, Ogawa T, Tokunaga K, Sugiu K, Date I. Effects of deferoxamine-activated hypoxia-inducible factor-1 on the brainstem after subarachnoid hemorrhage in rats. *Neurosurgery*. 2008;62:232-240; discussion 240-231
38. Dawson SL, Blake MJ, Panerai RB, Potter JF. Dynamic but not static cerebral autoregulation is impaired in acute ischaemic stroke. *Cerebrovasc Dis*. 2000;10:126-132.
39. Eames PJ, Blake MJ, Dawson SL, Panerai RB, Potter JF. Dynamic cerebral autoregulation and beat to beat blood pressure control are impaired in acute ischaemic stroke. *J Neurol Neurosurg Psychiatry*. 2002;72:467-472
40. Panerai RB, Deverson ST, Mahony P, Hayes P, Evans DH. Effects of co2 on dynamic cerebral autoregulation measurement. *Physiol Meas*. 1999;20:265-275

FIGURE LEGENDS

Figure 1 Differences in cerebral autoregulation between groups of CHF and without CHF. TFA parameters – Coherence, Gain and Phase – are presented across different spectral bands of Very Low Frequency (VLF, 0.03-0.07 Hz) 0.03-0.07 Hz; HF), low frequency (LF, 0.07-0.15 Hz) to high frequency (HF, 0.015-0.3 Hz) and at successive time marks from stroke symptoms (< 6 hours, 24 hours and 3 months). Significant differences ($P<0.05$) between groups with CHF and without CHF in repeated-measures ANOVA are highlighted with bracket with asterisk (*) on top.

Table 1 Baseline characteristics of patients with and without Heart Failure (N=50)

Demographics	TOTAL (N=50)	HF (N=8)	Non-HF (N=42)	P value
Male, n (%)	23 (46)	3 (11)	24 (57)	0.444
Age, years (mean±SD)	73±12	80±9	69±13	**0.034**
BMI, $Kg.m^{-2}$ (mean±SD)	27±5	24±3	28±5	**0.039**
Previous stroke/TIA, n (%)	7 (14)	1 (13)	6 (14)	1.000
Previous MI, n (%)	2 (4)	0 (0)	2 (5)	1.000
Hypertension, n (%)	37 (74)	6 (75)	31 (74)	0.944
Diabetes Mellitus, n (%)	18 (36)	3 (38)	15 (36)	1.000
Dyslipidemia, n (%)	38 (76)	6 (63)	33 (78)	0.379
Tobacco, n (%)	6 (12)	2 (25)	4 (10)	0.242

Chronic Medication, n (%)				
Antiplatelet	27 (46)	5 (62)	18 (43)	0.444
Statin	17 (46)	5 (62)	16 (38)	0.255
Beta-Blocker	10 (22)	4 (50)	7 (17)	**0.037**
ACEI/ARiB	10 (20)	5 (62)	15 (36)	0.240
CCB	10 (20)	0 (0)	10 (24)	0.184
Stroke characteristics				
Atrial Fibrillation, n (%)	21 (42)	6 (75)	15 (36)	0.039
Large Vessel atherosclerosis, n (%)	6 (12)	1 (12)	5 (12)	1.000
Lacunar infract, n (%)	6 (12)	0 (0)	6 (14)	0.572
Thrombolysis, n (%)	37 (74)	6 (75)	31 (74)	1.000
Occlusion of affected MCA	16 (32)	3 (38)	13 (31)	0.699
NIHSS score *[median(IQR)]*	12 (7-21)	14 (7-20)	11 (5-21)	0.887
Infarct Volume, mL*[median(IQR)]*	15 (1-112)	6 (0.4-53)	16 (1-123)	0.296
Laboratorial (mean±SD)				
C-reactive protein, mg/L	7.7±14.7	4.8±2.7	6.9±14	0.683
Total cholesterol, mg/dL	174±72	151±36	182±48	0.096
LDL cholesterol, mg/dL	105±42	91±39	110±40	0.214
HDL cholesterol, mg/dL	46±11	44±9	45±11	0.659
Triglycerides, mg/dL	111±68	85±28	127±71	0.105

Glucose, mg/dL	140±81	134±51	142±80	0.773
HbA1C, %	6.4±1.4	6.0±0.6	6.5±1.5	0.429
eGFR, ml/min/1.73 m^2	71±24	68±20	72±25	0.692
Cardiac markers (mean±SD)				
Troponin I, ng/ml	0.06±0.28	0.31±0.68	0.02±0.04	**0.0001**
BNP, pg/ml	428±668	1176±1198	267±341	**0.008**
LVEF, %	56±11	45±14	61±8	**0.006**
LV mass, g/1.73 m^2 *(mean±SD)*	136±32	158±36	133±29	**0.046**
Systemic hemodynamics (mean±SD)				
Systolic ABP, mm Hg	144±19	143±29	148±19	0.486
Mean ABP, mm Hg	98±11	102±25	101±11	0.825
Diastolic ABP, mm Hg	75±11	82±23	78±11	0.386
Heart rate, bpm	67±11	75±15	68±11	0.122
LF BP variability, mm Hg^2	85±111	117±170	102±150	0.789
HF BP variability, mm Hg^2	13±20	8±8	15±25	0.442
EtCO2, mm Hg	36±7	36±4	37±7	0.516
Cerebral hemodynamics (mean±SD)				
Ipsilateral				
MFV, cm/sec	40±20	40±18	41±19	0.847
CVRi, mm Hg/cm/sec	2.3±0.9	2.3±0.7	2.3±1.0	0.987

LF variability, $(cm/sec)^2$	128±142	148±230	120±108	0.649
HF variability, $(cm/sec)^2$	35±49	22±23	35±49	0.561
Contralateral				
MFV, cm/sec	48±17	40±9	52±17	0.076
CVRi, mm Hg/cm/sec	1.7±0.7	2.2±0.7	1.8±0.6	0.110
LF BV variability, $(cm/sec)^2$	200±250	212±250	189±229	0.794
HF BV variability, $(cm/sec)^2$	45±68	36±41	45±67	0.733

Body-Mass Index (BMI), Transitory Ischemic Attack (TIA), Modified Rankin Scale (MRS), angiotensin-conversion-enzyme inhibitor (ACEI), angiotensin receptor blocker (ARB), calcium channel blocker (CCB), Trial of ORG10172 in Acute Stroke Treatment (TOAST), middle cerebral artery (MCA), National Institutes of Health Stroke Scale (NIHSS), Low-density lipoprotein (LDL), High-density lipoprotein (LDL), glycated hemoglobin (HbA1C), eGFR (estimated glomerular filtration rate) by Chronic Kidney Disease Epidemiology Collaboration (CKD-EPI) formula[15]. Arterial blood pressure (ABP), cerebrovascular resistance index (CVRi), end-tidal carbon dioxide (EtCO2), low (LF: 0.3 – 0.15 Hz) and high (HF: 0.15 – 0.5 Hz) frequency spectral bands.

Table 2 Association between cardiac disease markers and cerebral autoregulation parameters in acute stroke (<6 hours)

	Spearman´s Correlation Coefficients and P value			
	Tropopin I, ng/ml	BNP, pg/ml	LVEF (%)	LV mass, g/ min/1.73 m^2
Age, years	r= 0.598, p<0.00001	r= 0.695, p<0.00001	r= – 0.503, p=0.001	r= 0.444, p=0.004
eGFR, ml/min/1.73 m^2	r= – 0.424, p<0.004	r= – 0.491, p<0.00002	r= 0.534, p=0.0003	r= – 0.453, p=0.003
Infarct side (N=34)				
VLF (0.03-0-07 Hz)				
Phase, degrees	r= 0.348, **p=0.044**	r= – 0.010, p=0.956	r= – 0.195, p=0.301	r= 0.068, p=0.722
Gain, %/mm Hg	r= – 0.103, p=0.562	r= 0.183, p=0.468	r= – 0.183, p=0.333	r= 0.090, p=0.333
Coherence, a.u.	r= – 0.244, p=0.195	r= – 0.309, p=0.075	r= 0.037, p=0.847	r= – 0.056, p=0.769
LF (0.07-0.15 Hz)				
Phase, degrees	r= 0.123, p=0.489	r= – 0.018, p=0.927	r= 0.021, p=0.921	r= – 0.208, p=0.271
Gain, %/mm Hg	r= 0.018, p=0.920	r= 0.098, p=0.606	r= 0.033, p=0.862	r= – 0.174, p=0.357
Coherence, a.u.	r= 0.016, p=0.928	r= – 0.092, p=0.628	r= 0.174, p=0.359	r= – 0.121, p=0.525
HF (0.15-0.3 Hz)				
Phase, degrees	r= 0.025, p=0.889	r= – 0.175, p=0.356	r= 0.190, p=0.315	r= – 0.219, p=0.246
Gain, %/mm Hg	r= 0.232, p=0.187	r= – 0.301, p=0.105	r= – 0.123, p=0.519	r= 0.047, p=0.806
Coherence, a.u.	r= 0.116, p=0.345	r= 0.179, p=0.513	r= – 0.003, p=0.989	r= 0.072, p=0.706
Non-infarct side (N=50)				
VLF (0.03-0-07 Hz)				
Phase, degrees	r= 0.198, p=0.169	r= – 0.007, p=0.964	r= – 0.015, p=0.924	r= – 0.034, p=0.169
Gain, %/mm Hg	r= 0.024, p=0.868	r= 0.210, p=0.166	r= 0.015, p=0.928	r= 0.125, p=0.435
Coherence, a.u.	r= 0.139, p=0.335	r= – 0.102, p=0.506	r= – 0.093, p=0.565	r= 0.207, p=0.088
LF (0.07-0.15 Hz)				
Phase, degrees	r= – 0.065, p=0.653	r= – 0.174, p=0.254	r= 0.085, p=0.596	r= – 0.192, p=0.229
Gain, %/mm Hg	r= 0.091, p=0.529	r= 0.169, p=0.267	r= 0.041, p=0.801	r= 0.000, p=1.000
Coherence, a.u.	r= 0.153, p=0.289	r= – 0.067, p=0.663	r= 0.107, p=0.507	r= – 0.040, p=0.804
HF (0.15-0.3 Hz)				
Phase, degrees	r= – 0.049, p=0.735	r= – 0.167, p=0.272	r= 0.054, p=0.736	r= – 0.184, p=0.249
Gain, %/mm Hg	r= 0.264, p=0.064	r= 0.285, p=0.058	r= – 0.149, p=0.352	r= 0.103, p=0.521
Coherence, a.u.	r= 0.191, p=0.183	r= – 0.181, p=0.234	r= – 0.142, p=0.374	r= 0.205, p=0.199

Estimated glomerular filtration rate (eGFR), mean arterial blood pressure (MBP), end-tidal carbon dioxide (EtCO2), low (LF: 0.3 – 0.15 Hz) and high (HF: 0.15 – 0.5 Hz) frequency spectral bands.* P<0.01 for multivariate linear regression analysis adjusting for age, gender and all significantly related variables in univariate analysis

Figure 1

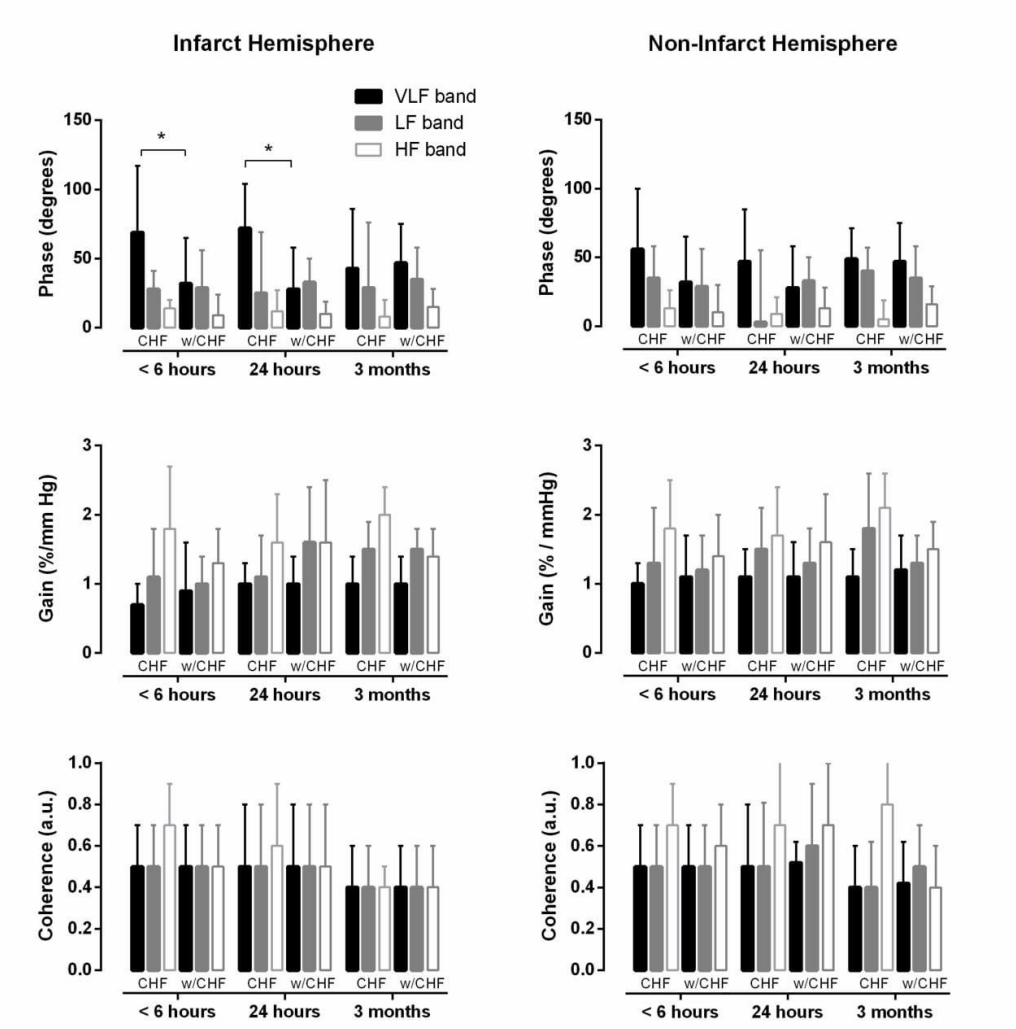
Infarct Hemisphere
Non-Infarct Hemisphere
VLF band
LF band
HF band
Phase (degrees)
Gain (%/mm Hg)
Gain (% / mmHg)
Coherence (a.u.)
CHF
w/CHF
< 6 hours
24 hours
3 months
*

VI. DISCUSSÃO

O presente projeto de investigação baseou-se na exploração das potencialidades da ARC dinâmica no contexto de AVC isquémico agudo, nomeadamente como marcador de prognóstico e preditor de complicações neurológicas.

Numa primeira fase, foi estudada uma população de indivíduos saudáveis, de modo a perceber entre que valores a ARC normalmente opera e a influência de fatores demográficos como sexo e idade nas suas medições. Numa segunda fase, estudou-se a fase aguda do AVC isquémico agudo com monitorização multimodal seriada dentro das primeiras 6 horas de início de sintomas de AVC, e depois às 12, 24 e 48 horas. Os sobreviventes foram ainda analisados aos 3 meses. Excluíram-se doentes com lesão hemodinâmica significativa dos vasos cervicais. Consideraram-se os AVC resultantes do atingimento de qualquer artéria intracraniana (ACM, ACA, ACP). Contudo, após 50 doentes incluídos, apenas um reduzido número de casos apresentava oclusão de outro vaso intracraniano que não a ACM (ACP, n=4/50). A análise de resultados foi então dirigida para o grupo de 46 casos de oclusão da ACM, exceto no capítulo 5. Esta escolha permitiu estudar uma população mais homogénea de doentes e, no final, melhorar o enquadramento no panorama de estudos no AVC isquémico, onde é hábito privilegiar a circulação anterior.

Houve ainda a preocupação de utilizar metodologias sensíveis, atuais e não invasivas no estudo da hemodinâmica cerebral. O DTC parece cumprir esses requisitos, tem uma excelente resolução temporal e apresenta uma grande flexibilidade ao permitir investigações em diferentes condições e locais. As técnicas de medição da ARC pela AFT também são as mais valorizadas pela comunidade científica internacional {Claassen, 2016 #501}. O recurso a flutuações espontâneas dos sinais biológicos tem a vantagem de obviar a colaboração do doente e dos efeitos confundidores ou clinicamente inapropriados das manipulações farmacológicas, no contexto agudo da isquemia cerebral.

Após estas considerações genéricas iniciais, e atendendo aos objetivos do projeto, passa-se a discutir os principais resultados obtidos.

Fatores demográficos, hemodinâmica sistémica e autorregulação cerebral

O primeiro estudo demonstrou que a medição da ARC, da VR e da ANV não é influenciada pela idade ou sexo em indivíduos saudáveis. Também mostrou que os parâmetros que medem os diversos mecanismos de regulação não são correlacionáveis entre si. Se, do ponto de vista teórico, tal seria esperado de distintos fatores de controlo cerebrovascular, este resultado chama a atenção para alguns aspetos práticos relevantes. Na literatura é comum a comparação entre estudos da "reatividade cerebral" através de metodologias distintas. Os nossos resultados sugerem que a ARC, a ANV ou o VR não devem ser usados e interpretados de modo permutável. Por conseguinte, será desejável uma bateria alargada de testes para se obter uma visão completa do estado da função vascular cerebral. A ausência de qualquer efeito da idade sobre os mecanismos de regulação cerebral poderá parecer, à primeira vista, um achado inesperado. Aliás, têm sido descritas alterações hemodinâmicas na árvore vascular cerebral com o avançar da idade (Krejza et al., 1999, Bakker et al., 2004), pelo que podemos ter algumas reservas quanto à sensibilidade dos procedimentos técnicos naquilo que pretendem medir. Não obstante, a amostra selecionada mostrou de forma clara uma diminuição da VFSC e aumento do valor de resistência vascular (Purkayastha & Sorond, 2014), iRVC, com o aumento da idade. Isto revela aspetos já bem documentados quanto ao envelhecimento vascular cerebral (Bakker et al., 1999, Bakker et al., 2004, Krejza et al., 1999), o que deixa alguma segurança acerca da sua representatividade. Já no que concerne à VR, alguns estudos encontram um efeito significativo da idade em resposta ao CO_2 (Sorond et al., 2015, Coverdale et al., 2016), embora vários trabalhos demonstrem o contrário (Bakker et al., 2004, Yamamoto et al., 1980, Fluck et al., 2014, Barnes et al., 2012). Não podemos, contudo, esquecer que esta população é saudável e a ausência de fatores de risco vascular pode contribuir para essa ausência de correlação. Apesar de pequeno, este estudo mostrou que há uma preservação do controlo vascular cerebral a vários níveis, sendo pioneiro no facto de combinar num só estudo medições de vários aspetos da regulação cerebrovascular - ANV, CA e VR. A maior parte dos estudos prévios apenas avaliaram um desses parâmetros.

Assim, poderá haver alguma reserva funcional que compense a deterioração cerebrovascular associada ao envelhecimento. De acordo com esta hipótese, estudos prévios mostraram que indivíduos com lesões marcadas na substância branca apenas se tornariam sintomáticos (alteração da marcha e risco de quedas) se a ANV estivesse alterada (Sorond et al., 2010). Contudo, não podemos excluir o facto de a avaliação por DTC poder não ser suficientemente sensível para detetar alterações mais subtis na regulação microvascular quando comparado com outros métodos com maior resolução especial (e.g., ressonância magnética). A avaliação por

DTC é, pois, uma avaliação global da capacidade funcional cerebrovascular do território sondado. Os resultados obtidos são relevantes para o estudo da ARC no AVC isquémico, já que afeta uma população idosa. O efeito da idade parece não vir a influenciar diretamente os nossos resultados, embora possa haver interação com fatores de risco vascular.

A ausência de um efeito do sexo no controlo vascular foi um tanto inesperada, já que têm sido demonstradas várias alterações hormonais no controlo vasomotor, talvez pela modulação da via do NO (Matteis et al., 1998, Cagnacci et al., 2003) e um risco cardiovascular associado à menopausa (El Khoudary et al., 2015). Dado que não foi controladopara a fase do ciclo ovárico, podemos não ter apreciado corretamente a influência do sexo nos vários mecanismos de regulação vascular.

Este estudo mostrou ainda novos dados no que concerne o estudo da VR, já que se verificou que a amplitude da resposta da VFSC à hipercapnia não se correlaciona com o grau de resposta à hipocapnia. Como monitorizámos concomitantemente outros parâmetros hemodinâmicos (PA e CO_2TE) durante as manobras, podemos avançar com a explicação de que se tratam simplesmente de manobras diferentes do ponto de vista hemodinâmico sistémico. A prova inalatória de CO_2 (carbogénio) promove uma subida lenta da PA e tem pouco efeito sobre a FC. Pelo contrário, a hipocapnia, conseguida à custa de trabalho ventilatório, provoca uma queda transitória inicial de PA, sobressaindo o aumento da FC durante toda a prova. Assim, o efeito da diferente ativação do SNA simpático pode condicionar influências não previstas sobre a árvore vascular cerebral e enviesar os resultados. De outro modo, podem a hipo ou hipercapnia corresponder a diferentes respostas fisiológicas vasculares, o que merece estudo subsequente. Este estudo alerta assim, mais uma vez, para o facto de os resultados dos estudos na literatura poderem não ser comparáveis entre si se usarem diferentes métodos, ainda que se fale do mesmo mecanismo de controlo cerebrovascular.

Este estudo foi importante já que mostrou que:

- A idade e o sexo, não são por si sós fatores determinantes para o estado vascular cerebral funcional, nomeadamente, a ARC, a VR e o ANV, quando avaliado por DTC;
- Devemos ter precaução ao comparar os resultados de estudos que utilizaram diferentes métodos de avaliação da função vascular cerebral para investigar aspetos fisiológicos ou patológicos cerebrovasculares; pelo menos a ARC, a VR e o ANV não são sempre correlacionáveis.

Uma autorregulação cerebral mais eficaz no AVC isquémico agudo prediz enfartes cerebrais de menor volume e melhor resultado funcional

Neste estudo avaliámos a ARC dinâmica por AFT dentro das primeiras 6 horas de sintomas de AVC isquémico em território da ACM, e verificou-se que uma melhor eficácia autorregulatória na fase aguda (maior fase e ganho reduzido) conduziu a um menor volume de enfarte estabelecido em tomografia computadorizada cerebral às 24 horas e a um melhor resultado funcional aos 3 meses.

A AFT é cada vez mais usada para analisar a ARC (Meel-van den Abeelen et al., 2014b, Malojcic et al., 2017) em doenças neurológicas. O desvio de fase, isto é, o atraso temporal da oscilação da VFSC em relação à PA, mostrou ser um preditor significativo em situações como a doença carotídea (Hu et al., 1999, Panerai et al., 1998b) ou estenose intracraniana (Haubrich et al., 2003), ou o desenvolvimento de vasospasmo após hemorragia subaracnoideia (Budohoski et al., 2015, Calviere et al., 2015, Otite et al., 2014, Soehle et al., 2004). Este parâmetro também tem sido avaliado no AVC isquémico (Aries et al., 2010, Dawson et al., 2000a, Dawson et al., 2003, Eames et al., 2002, Reinhard et al., 2005, Reinhard et al., 2008), parecendo estar relacionado com a sua gravidade (Reinhard et al., 2005, Reinhard et al., 2008). No seu conjunto, todos estes estudos mostram que a fase parece ser um parâmetro importante que reflete a capacidade regulatória no território arterial afetado. Os nossos resultados parecem estar de acordo com esta visão, já que mostram que uma fase melhor está relacionada com enfartes mais pequenos e melhor estado funcional a longo prazo. O ponto de corte que estimámos também está perto de um valor de ≈30˚, aproximado do nível que se pensa ser o limite da ARC alterada ou não (Diehl et al., 1995, Aries et al., 2010, Panerai et al., 1998a). Com base num ponto de corte de fase em 37˚, verificou-se que a probabilidade de estar independente funcionalmente aos 3 meses era 14 vezes superior no caso de uma ARC mais eficiente (fase > 37 ˚). Este subgrupo também evidenciou enfartes de menor volume às 24 horas. Estes resultados dizem respeito à ARC medida no hemisfério afetado, o que demonstra alguma plausibilidade fisiopatológica dos achados.

Também foi interessante notar que valores menores de PA sistólica se associaram a enfartes maiores, mas apenas se a ARC estivesse diminuída. Uma PA menor num território de penumbra isquémica que não consegue autorregular poderá significar uma hipoperfusão progressiva (Bang et al., 2008). Este resultado lança o interesse em se modelar a ARC (Sorond et al., 2015) para preservar a penumbra isquémica ou usar a ARC para selecionar melhor os doentes que

beneficiam de terapêutica hipertensiva, de modo a evitar a isquemia definitiva em áreas cerebrais em risco.

Os fatores de risco vascular não se relacionaram com os parâmetros de ARC. Ainda assim, dado o número reduzido de participantes, não podemos excluir de modo perentório o facto de que estas comorbilidades não influenciaram a ARC. Por exemplo, uma ARC alterada foi registada num doente com apneia do sono com risco aumentado de AVC (Tsivgoulis & Alexandrov, 2009). São necessários mais estudos para perceber a relação da ARC com fatores de risco vascular.

Os resultados obtidos poderão explicar os resultados negativos de ensaios clínicos com manipulação da PA na fase aguda do AVC isquémico. Estes não demonstraram qualquer benefício clínico para os doentes, i.e., não alteraram significativamente o prognóstico (Tikhonoff et al., 2009). Isto poderá resultar da possibilidade de nem todos os doentes poderem beneficiar do ajuste hemodinâmico, pois dependeria da preservação da sua ARC, reduzindo o poder estatístico desses trabalhos. Baseando-nos nos resultados deste estudo, poderíamos sugerir que uma avaliação da ARC pode identificar doentes com menor capacidade autorregulatória (fase < 37º), nos quais se poderiam tomar atitudes para manter a PA e o fluxo em níveis mais adequados.
Em linha com estudos prévios, notámos que o ganho não parece ser um marcador tão sensível como a fase para o resultado funcional. De qualquer das formas, um maior ganho (menor amortecimento das oscilações de PA) associou-se a um pior estado funcional aos 3 meses.

Algumas precauções devem ser tidas em conta na interpretação dos resultados. No contexto do AVC isquémico agudo, existiram certamente múltiplos fatores que levaram a variações não lineares na avaliação hemodinâmica (e.g., agitação, alterações cognitivas, alterações autonómicas), que poderão invalidar os resultados da AFT, um método linear. Também convém refletir sobre as oclusões da ACM no seu segmento M1. Neste caso, não temos acesso à VFSC por DTC. A maior parte dos casos em que a M1 não esteve acessível foram casos de revascularização infrutífera de trombólise endovenosa. Esta limitação da aplicabilidade da ARC na fase aguda do AVC pode ser vista como uma falha metodológica importante. Contudo, uma oclusão que persiste nas primeiras horas de AVC, mesmo após trombólise endovenosa, é por si só um fator de muito mau prognóstico (Saqqur et al., 2007). Nesta situação, a avaliação da ARC com certeza não acrescentará nenhuma mais-valia no que toca ao prognóstico, já de si muito reservado. De facto, estes doentes foram acompanhados e apenas 1/16 se encontrava

independente aos 3 meses e todos eles apresentavam enfartes em território total de ACM. O que o estudo vem revelar é que, mesmo que a ACM recanalize, uma ARC mais eficaz (fase > 37˚) traduz-se numa probabilidade aumentada de recuperação funcional aos 3 meses.

Estes novos dados têm importância porque:

- Uma disfunção da ARC parece estar envolvida na fisiopatologia do AVC isquémico agudo;
- Demonstram pela primeira vez que a ARC dinâmica pode ser avaliada dentro de 6 horas de sintomas, janela de tempo durante a qual as decisões médicas são cruciais para o prognóstico (European Stroke Organisation Executive & Committee, 2008, Jauch et al., 2013b);
- Os níveis de ARC modelam a relação da PA com o volume de enfarte estabelecido às 24 horas. Assim, os doentes com uma ARC menos eficaz (fase < 37°) apresentam uma área de enfarte cerebral maior quanto menor a PA;
- Em futuros ensaios clínicos, a ARC poderá ser um bom marcador de seleção dos doentes que mais beneficiarão de terapêutica modificadora da PA na fase aguda.

Transformação hemorrágica e edema cerebral: conexão à autorregulação cerebral

Neste estudo, mostrámos que as alterações precoces da ARC (dentro de 6 horas do início de sintomas) aumentam o risco de complicações futuras, como o edema cerebral e a transformação hemorrágica evidenciados por tomografia computadorizada às 24 horas.

Este estudo mostra, pela primeira vez, que o risco de edema cerebral e de transformação hemorrágica pode ser predito pelo estado da ARC individual numa fase ainda precoce da isquemia cerebral.

Estudos prévios (Reinhard et al., 2005, Reinhard et al., 2008) mostraram uma relação da ARC com o prognóstico, mas não com o risco de complicações. A explicação simples para os resultados é que a falha da capacidade autorreguladora, muito assente em mecanismos miogénicos, pode significar que os vasos de resistência cerebral, ao não conseguirem absorver as oscilações de PA, provoquem uma elevação da pressão hidrostática na rede capilar e um consequente agravamento da lesão de BHE. Esta disrupção dos pequenos vasos cerebrais promove o extravasamento do conteúdo intravascular, ou seja, o edema cerebral e a

transformação hemorrágica (Wang & Lo, 2003, Bang et al., 2007, Balami et al., 2011). A favorecer esta hipótese, encontramos um iRVC diminuído e a VFM aumentada no hemisférico afetado pela isquemia nos doentes que tiverem estas complicações. Podemos considerar então que estes doentes apresentam uma resposta vasodilatadora cerebral inapropriada e sem efeito tampão (menor capacidade de ARC) sobre os estímulos pressóricos.

A variação do iRVC desde uma fase tão precoce de isquemia cerebral não foi descrita anteriormente. Considerando toda a coorte de doentes, um maior iRVC nas primeiras horas sugere uma resposta de vasoconstrição cerebral como resposta aguda. Podemos colocar a hipótese de que tal se deve a agentes vasoconstritores libertados. Por exemplos, sabemos que no AVC agudo são libertadas substâncias como a endotelina-1 em grandes quantidades, um potente vasoconstritor cerebral (Ziv et al., 1992). Também existem modelos experimentais que mostram que uma isquemia transitória de curta duração pode exibir um fenómeno de uma contração prolongada dos pericitos pelo influxo de Ca^{2+}. Assim, mesmo que restituído o fluxo sanguíneo, o tecido cerebral pode permanecer sob isquemia profunda (Hall et al., 2014). Para este aumento do iRVC também poderão contribuir a microtrombose e o edema citotóxico, que se instalam na microcirculação da área de enfarte (Balami et al., 2011). Os resultados deste estudo revelam então indícios de que no AVC isquémico, em geral, há uma vasoconstrição mantida no tecido cerebral, mesmo que restituído o fluxo no tronco principal, neste caso, a ACM. Esta condição está de acordo com o fenómeno de não recirculação avançado por Ames na década de 70 (Ames et al., 1968) em modelo experimental de isquemia cerebral, o que faria deste estudo o primeiro relato em humanos deste fenómeno. Esta condição está bem documentada após revascularização coronária, podendo contribuir para o resultado funcional após o enfarte do miocárdio (Ito, 2001, Harding, 2006).

Por fim, verificámos que estas alterações se resolveram aos 3 meses. A natureza transitória da ARC alterada é fisiopatologicamente intuitiva e oferece mais uma prova biológica plausível para as medidas de ARC como marcadores de risco de AVC grave com risco de edema ou transformação hemorrágica.

Reiterando, percebendo quais as vias moleculares determinantes para esta ARC ineficaz, vasodilatação inapropriada ou vasoconstrição pós-recanalização, podemos oferecer uma oportunidade de melhorar o prognóstico nos doentes com AVC isquémico agudo, preservando uma maior área de penumbra isquémica, perceber melhor os mecanismos e evitar a progressão para edema maligno ou transformação hemorrágica.

Este estudo foi importante porque mostrou que:

- Uma ARC diminuída no AVC isquémico agudo coloca o tecido cerebral em risco de progresso para edema cerebral ou transformação hemorrágica;
- Os doentes com estas complicações parecem ter uma resposta vasodilatadora em fase precoce (< 6 horas de início de sintomas de AVC) que sugere disfunção vasomotora.

Doença renal crónica e resultado funcional desfavorável no AVC isquémico agudo: será a autorregulação cerebral a ligação perdida?

Nos trabalhos prévios (“*Capítulo 2: Uma autorregulação cerebral mais eficaz no AVC isquémico agudo prediz enfartes cerebrais de menor volume e melhor resultado funcional” e “Capítulo 3: Transformação hemorrágica e edema cerebral no AVC isquémico agudo: conexão à autorregulação cerebral”*) demonstrámos que a ARC é importante para o prognóstico e previsão de complicações do AVC isquémico. Procurou-se então saber que fatores poderiam contribuir para uma ARC menos eficaz.

No estudo *“Capítulo 4: Doença renal crónica e resultado funcional desfavorável no AVC isquémico agudo: será a autorregulação cerebral o elo de* ligação perdido?*”* estudou-se a relação entre a ARC na fase aguda do AVC isquémico e a doença renal crónica. Verificou-se que a função renal e a ARC apresentam alterações paralelas, sugerindo a existência de uma disfunção microvascular sistémica subjacente nos doentes que se apresentam com pior ARC.

O estudo mostrou haver uma associação entre uma ARC menos eficaz (níveis elevados de ganho) e uma insuficiência renal traduzida por menor taxa de depuração da creatinina, independentemente da idade, fatores de risco vascular e marcadores séricos de controlo metabólico. Também se verificou que a disfunção renal ou de ARC (ganho elevado) se relacionava com a gravidade de alterações da substância branca cerebral determinada por tomografia computadorizada. Cada um destes fatores relacionaram-se com o pior prognóstico aos 3 meses, com redução da probabilidade de serem independentes (escala de Rankin modificada 0 – 2).

Para percebermos melhor esta cumplicidade cerebrorrenal, temos de nos debruçar, em primeira instância, sobre a fisiologia da autorregulação renal. Com efeito e propósito similar ao da ARC a nível cerebral, esta permite estabilizar o fluxo e a taxa de filtração renal, apesar das variações da pressão de perfusão. Sucintamente, à medida que a PA varia e, consequentemente, se altera o estiramento das células musculares lisas das arteríolas aferentes e corticais renais, ocorre uma

resposta miogénica para ajustar a resistência vascular de modo a manter o fluxo constante (Carlstrom et al., 2015). Não deixa de ser curioso que a autorregulação renal também seja estudada com a mesma técnica de AFT (Abu-Amarah et al., 2005, Loutzenhiser et al., 2006, Saeed et al., 2014). Contudo, dado o carácter invasivo da mediação de fluxo na artéria renal, esta apenas está descrita em animais de laboratório (Abu-Amarah et al., 2005, Saeed et al., 2014, Carlstrom et al., 2015). Modelos de ratos hipertensivos com insuficiência renal induzida pela adenina mostraram um ganho de AFT aumentado na banda < 0,1 Hz, indicando uma falha de autorregulação renal (Saeed et al., 2014). Do mesmo modo, ganhos elevados a nível cerebral em bandas de frequência também baixas refletem autorregulação limitada e incapacidade de amortecimento das oscilações pressóricas a nível cerebral (Zhang et al., 1998, Panerai, 1998, Azevedo & Castro, 2016). Isto faz sentido, já que os mecanismos de regulação miogénica serão, teoricamente, os mesmos em vários leitos vasculares, sejam eles os do cérebro, rim, coronárias, mesentério ou músculo esquelético (Davis, 2012). Considerando estas similitudes, pressupõem-se que a lesão microvascular (e.g., causado pela HTA ou diabetes) que causa a disfunção renal (Bidani & Griffin, 2004) também pode afetar a ARC. Podemos encontrar sustentação para esta premissa em ratos espontaneamente hipertensivos com predisposição genética para glomerulosclerose rápida e AVC (Churchill et al., 2002). De facto, estes ratos apresentaram autorregulações cerebral e renal disfuncionais antes do desenvolvimento de AVC e morte (Abu-Amarah et al., 2005, Smeda et al., 1999). A histopatologia destes animais mostrou artérias cerebrais com hipertrofia da média e sinais de remodelagem (Izzard et al., 2003), as mesmas alterações que caracterizam a doença de pequenos vasos cerebrais (Fazekas et al., 1993). Portanto, somos levados a pensar que a disfunção do mecanismo de autorregulação estará a decorrer em vários territórios. Voltando aos resultados dos doentes com AVC isquémico do Capítulo 4: Doença renal crónica e resultado funcional desfavorável no AVC isquémico agudo: será a autorregulação cerebral o elo de ligação perdido?, é-nos permitido supor que aqueles que se apresentaram com uma ARC menos eficaz (ganho elevado) possam ter também menor capacidade de regulação miogénica renal, um dos fatores associados à insuficiência renal.

Foi interessante notar que o uso corrente de bloqueadores de canais de cálcio se correlacionou com um aumento de ganho (menor ARC) na banda de frequências baixas, o domínio espectral da ARC (Zhang et al., 1998, Panerai, 1998), em ambos os hemisférios cerebrais (Figura 2 do Capítulo 4: Doença renal crónica e resultado funcional desfavorável no AVC isquémico agudo: será a autorregulação cerebral o elo de ligação perdido?). O uso destes fármacos

estava igualmente associado a taxas de depuração de creatinina reduzidas. Em modelos animais, verificou-se que os bloqueadores de canais de cálcio reduziam a resposta miogénica a nível renal (Nakamura et al., 1999, Carlstrom et al., 2015), o que talvez possa acontecer também em humanos (Tan et al., 2013, Hamner & Tan, 2014, Endoh et al., 2000). Os bloqueadores de canais de cálcio bloqueiam os canais de Ca^{2+} tipo L dependentes da voltagem, que são ativados pelo estiramento do músculo liso vascular (Earley & Brayden, 2015). Assim, para além da vasodilatação periférica que os caracteriza como agentes anti-hipertensores, também bloqueiam o mecanismo de resposta vasoconstritora provocado pelo aumento da PA (Nakamura et al., 1999). Pela sua ação, a pressão transmural não provocará a entrada de cálcio e consequente contração da célula muscular lisa de modo a aumentar a resistência vascular e conservar um fluxo sanguíneo constante. Isto reflete-se numa maior transmissão da amplitude de oscilação pressórica para o fluxo, i.e., maior ganho e menor capacidade autorreguladora. O facto de termos encontrado uma associação entre ganho elevado a nível cerebral e função renal diminuída pode estar relacionado com o efeito dos bloqueadores de canais de cálcio nos dois órgãos. Contudo, o efeito de bloqueadores de canais de cálcio a nível da ARC humana não é totalmente claro nalguns estudos (Endoh et al., 2000, Tan et al., 2013, Hamner & Tan, 2014). Alguns autores não encontraram alterações do ganho da AFT em indivíduos normais (Tzeng et al., 2011).

Também foram observadas associações de ganho elevado (ARC menos eficaz) ou reduzida taxa de filtração glomerular, com maior gravidade de lesões de substancia branca a nível cerebral, o que já foi descrito previamente (Purkayastha et al., 2014, Yang et al., 2017). Este facto, apesar de não ser inovador, vem reforçar a hipótese de os pequenos vasos cerebrais com disfunção vasomotora estarem envolvidos. Não conseguimos, contudo, esclarecer se é a lesão microvascular que subjaz a disfunção de ARC ou o contrário.

Outro resultado importante foi o facto de encontrarmos um maior risco de transformação hemorrágica em doentes com ganho mais elevado e pior função renal. Um ganho mais elevado significa que os vasos de resistência cerebrais são menos capazes de amortecer as oscilações de PA, sendo que estas são transmitidas à rede capilar do parênquima cerebral. Esta disfunção vasomotora parece estar de acordo com a disrupção microvascular que contribui para a disfunção de BHE e risco de hemorragia e edema no enfarte em modelo animal (Simard et al., 2007). Esta tendência já tinha sido observada na Figura 1 do *"Capítulo 3: Transformação hemorrágica e edema cerebral no AVC isquémico agudo: conexão à autorregulação cerebral"*,

que, contudo, não atingiu o significado estatístico. Ao invés de utilizarmos os valores de ganho como variável contínua, aqui os valores foram categorizados em 3 classes ordinais. O baixo número de participantes (n=46) e a variabilidade de medição da AFT (Meel-van den Abeelen et al., 2014a) pode explicar a diferença de significância estatística entre estudos. Noutro contexto, em doentes com hemorragia intracerebral, os valores de ganho elevado também se associaram a hematomas de maior volume e risco de expansão do mesmo (Nakagawa et al., 2011, Reinhard et al., 2010, Ma et al., 2016), o que mostra que a disfunção da ARC participa na rutura microvascular cerebral.

O facto de o hemisfério sintomático não ter apresentado uma relação significativa entre risco de transformação hemorrágica e ganho parece ser inconsistente com a hipótese formulada. Isto pode ser observado nas Figuras 4 e 5 do Capítulo 4: Doença renal crónica e resultado funcional desfavorável no AVC isquémico agudo: será a autorregulação cerebral o elo de ligação perdido?. Contudo, vários fatores adicionais podem explicar este aparente paradoxo. Uma explicação possível é de cariz meramente estatístico, já que o número de casos do lado do hemisfério afetado é menor (com oclusão de M1, o que não permite a sua monitorização por DTC), reduzindo o poder estatístico. Do ponto de vista fisiopatológico, existe uma possibilidade de as oscilações de fluxo cerebral estarem artificialmente diminuídas por microtrombose (Balami et al., 2011, Wang & Lo, 2003), edema celular e intersticial (Simard et al., 2007), e fenómeno de não recirculação cerebral (Ames et al., 1968) na zona isquémica. Estes fatores poderão gerar um falso *"buffer"* das oscilações de PA e, por isso, um ganho reduzido, sem com isso querer dizer que a ARC seja mais eficiente.

Em conclusão, a disfunção renal mostrou uma associação paralela à ARC menos eficaz e ambos os fatores se associaram a uma maior gravidade de doença microvascular cerebral, uma transformação hemorrágica e um pior prognóstico. Seria interessante estudar com maior pormenor os doentes com biomarcadores de lesão renal como a cistatina C (Yang et al., 2017) e a proteína *Klotho* (Arking et al., 2005), os quais poderão ajudar a antever os doentes com menor capacidade de ARC e que poderão estar em risco de maior lesão neurológica e complicações hemorrágicas.

Doentes com insuficiência cardíaca e com estenose aórtica grave apresentam uma resposta autorreguladora cerebral superior no AVC isquémico agudo

No estudo exposto no *"Capítulo 5: Doentes com insuficiência cardíaca e com estenose aórtica grave apresentam uma resposta autorreguladora cerebral superior no AVC isquémico agudo"*,

descreveram-se pela primeira vez os efeitos da IC na ARC de doentes com AVC isquémico. Comparámos a resposta de ARC na fase aguda de AVC isquémico dentro de 6 horas de sintomas, às 24 horas e aos 3 meses entre dois grupos, com e sem IC. Tratando-se de uma análise *post-hoc*, não foi elaborada uma metodologia de amostragem robusta, tipo caso-controlo, pelo que nos limitámos a comparar oito casos de doentes com IC crónica identificados retrospetivamente a partir da coorte total (n=50) com o subgrupo sobrante, ou seja, sem IC. De modo não programado, selecionaram-se sobretudo doentes com valvulopatia aórtica grave como causa de IC (n=6/8). A isquemia cardíaca era prevalente e sobrepunha-se (n=6/8). Verificámos que o grupo de doentes com IC apresentava uma fase maior na banda de muito baixa frequência (ARC mais eficiente) do que os restantes doentes com AVC isquémico, durante a fase aguda até às primeiras 24 horas. Esta diferença desapareceu na fase crónica, aos 3 meses. Também houve uma correlação positiva, embora modesta, entre valores de fase e de troponina I na fase aguda, ou seja, uma melhor ARC associou-se a um aumento de marcadores de isquemia do miocárdio. Este estudo foi pioneiro pelo facto de descrever mais um mecanismo de como coração pode interagir com o cérebro no contexto do AVC isquémico agudo. Os resultados mostram uma resposta de ARC dinâmica aumentada (maior valor de fase na banda de muito baixa frequência) nestes doentes, apesar de não conseguirmos desvendar os mecanismos subjacentes com os dados disponíveis.

Uma apreciação intuitiva diria que as diferenças encontradas seriam justificadas por alterações hemodinâmicas sistémicas no contexto de IC. No entanto, tal não se verificou nesta coorte, já que PA, CO_2TE e FC eram comparáveis entre grupos. A gravidade da disfunção sistólica cardíaca (fração de ejeção) ou dos valores de peptídeo natriurético cerebral, este relacionado com a gravidade da IC, também não se correlacionaram com os parâmetros de ARC. Não podemos excluir que haja um efeito da própria estenose aórtica sobre a ARC, mas se tal fosse o caso, as alterações persistiriam aos 3 meses, já que nenhum doente foi submetido a cirurgia cardíaca, e não apenas presentes até às 24 horas.

Uma das hipóteses seria de a ARC estar a sofrer interferência pela hiperatividade simpática, que é característica nos doentes com IC (Haeusler et al., 2011) e também no AVC isquémico agudo (De Raedt et al., 2015). De facto, os doentes com IC apresentaram valores aumentados de Troponina Ie estes tiveram uma correlação positiva com a ARC. Uma atividade simpática exageradamente aumentada pode causar necrose dos miócitos que, no contexto da doença vascular cerebral aguda, costuma ser referido como miocardiopatia de stresse (De Raedt et al., 2015). Sabemos ainda que existe alguma evidência de que o simpático está envolvido no

controlo vascular cerebral (ser secção *"Neurogénicas"*). Contudo, a maior parte das alterações causadas pelo simpático referem-se à disfunção ou ablação do mesmo e não a um aumento da sua atividade (van Lieshout & Secher, 2008). Mais ainda, uma atividade simpática aumentada provocaria uma vasoconstrição cerebral nos doentes com IC, o que não é sugerido pela ausência de uma diferença significativa do iRVC entre os grupos com e sem IC. Infelizmente, uma prevalência elevada de AF no subgrupo de IC não permitiu a análise da variabilidade da FC, um instrumento útil para estudar o estado autonómico parassimpático ou simpático (Videira et al., 2016).

Outra possibilidade mais interessante é a de que o cérebro, sob hipoperfusão crónica pela IC, pudesse desenvolver efeitos diretos e/ou remotos de pré-condicionamento isquémico (Koch et al., 2014) e uma resposta autorreguladora cerebral mais eficaz pudesse ser uma das manifestações desse mesmo pré-condicionamento. Aliás, 6 dos 8 doentes com IC tinha história de isquemia miocárdica pré-existente, o que pode, adicionalmente, potenciar este mecanismo. Sabemos que o fator induzido pela hipoxia 1 (na nómina inglesa, *hypoxia-inducible factor-1*, HIF-1) está aumentado na IC, mesmo que apresente função ventricular esquerda preservada, e que os seus níveis se correlacionam com os da troponina I (Li et al., 2015). Esta via reage à hipóxia provocando o aumento do fator de crescimento endotelial vascular e as concentrações de eritropoietina (Sorond et al., 2015, Fernando et al., 2006). Também, em modelos animais, a quelação do ferro e ativação do HIF-1 mostrou ter algum efeito neuroprotetor na isquemia cerebral e hemorragia subaracnoideia (Prass et al., 2002, Bergeron et al., 2000, Hishikawa et al., 2008). Um estudo recente mostrou de forma clara que a desferroxamina promovia o aumento do HIF-1, assim como uma melhor ARC, particularmente um aumento de fase precisamente na banda de muito baixa frequência (0,03 – 0,07 Hz) (Sorond et al., 2015), o que se sobrepõem aos nossos resultados.

Este estudo mostra uma nova faceta da interação entre o cérebro e o coração, ao demonstrar que os doentes com IC podem despoletar uma resposta de ARC mais eficaz na fase aguda do AVC isquémico. Se compreendermos melhor os mecanismos moleculares que lhe estão subjacentes, nomeadamente no contexto de um pré-condicionamento isquémico, poderemos obter alvos interessantes que possam ser modulados em futuros ensaios terapêuticos e que possam beneficiar todos os doentes com AVC isquémico.

VII. CONCLUSÕES

Resumidamente, as principais conclusões inovadoras deste projeto de investigação foram:

- A idade e o sexo, por si só, não são fatores determinantes para o desempenho dos vários mecanismos de controlo vascular cerebral;
- Devemos ter precaução ao comparar os resultados de estudos que utilizaram diferentes métodos de avaliação da função vascular cerebral para investigar aspetos fisiológicos ou patológicos cerebrovasculares; pelo menos a ARC, a VR e o ANV não são correlacionáveis;
- Demonstrou-se pela primeira vez que a ARC dinâmica pode ser avaliada dentro de 6 horas de sintomas de AVC isquémico, janela de tempo durante a qual as decisões médicas são cruciais para o prognóstico;
- Uma disfunção da ARC parece estar envolvida na fisiopatologia do AVC isquémico agudo, do seguinte modo:
    - Uma ARC menos eficaz (fase reduzida) no AVC isquémico agudo coloca o tecido cerebral em risco de progressão para edema cerebral ou transformação hemorrágica;
    - Estas complicações estão associadas a uma resposta vasodilatadora inapropriada na fase aguda (< 6 horas de início de sintomas de AVC), o que também sugere disfunção vasomotora;
    - Uma ARC menos eficaz (fase reduzida) no AVC isquémico agudo (fase < 37°) associa-se a enfartes de maior volume às 24 horas, provavelmente por progressão isquémica na área de penumbra;
    - Os níveis de ARC modelam a relação da PA com volume de enfarte estabelecido às 24 horas. Assim, os doentes com uma ARC menos eficaz apresentam uma área de enfarte cerebral maior quanto menor a PA;
    - Deste modo, podemos afirmar que, em futuros ensaios clínicos, a ARC poderá ser um bom marcador de seleção dos doentes que mais beneficiam de terapêutica modificadora da PA na fase aguda;
- A ARC tem relevância para o prognóstico no AVC isquémico agudo;
    - Uma ARC mais eficaz (fase > 37°) associou-se de modo significativo a uma maior probabilidade de estar independente aos 3 meses;

- A disfunção renal avaliada em doentes com AVC isquémico agudo mostrou uma associação paralela a uma ARC menos eficaz, e ambos os fatores se associaram a uma maior gravidade de doença microvascular cerebral, uma transformação hemorrágica e um pior prognóstico;
- Os doentes com IC podem despoletar uma resposta de ARC mais eficaz na fase aguda do AVC isquémico, o que coloca a ARC como possível mecanismo de pré-condicionamento isquémico.

Em suma, a autorregulação cerebral dinâmica demonstrou ter um papel não desprezível no estudo e avaliação da isquemia cerebral aguda. Os resultados obtidos dão ânimo para se desenvolverem diferentes linhas de investigação com potencial interesse terapêutico, que poderão beneficiar o prognóstico dos doentes com AVC isquémico agudo.

VIII. PROPOSTAS E PROJETOS FUTUROS

Este projeto de investigação deixa várias questões em aberto às quais seria interessante responder no futuro com novas pesquisas para:

- Avaliar o comportamento de outros marcadores de ARC, como o cálculo do IARC espontâneo ou Mx, e outros modelos de pressão-velocidade, PRA+PCrE, de modo a poder determinar quais os parâmetros cerebrovasculares mais estáveis e sensíveis na determinação da desregulação vascular cerebral no AVC isquémico;
- Responder à questão: se a ARC pode estar alterada e não permitir fazer um *amortecimento* eficaz sobre as oscilações de PA, qual será o melhor intervalo de PA alvo para proteger a penumbra isquémica? Esta questão não pode ser respondida com um número tão reduzido de participantes. Um novo estudo prospetivo com maior recrutamento poderá ajudar na determinação desses valores, seguindo a mesma estratégia desenvolvida para a individualização da gestão hemodinâmica guiada pela "PPC ótima" no traumatismo crânio-encefálico (Dias et al., 2015);
- Estudar a hipótese de utilizar modelos não lineares ou multiparamétricos, dado que a relação entre a VFSC e a PA não é um fenómeno sempre linear (Mitsis et al., 2004);
- Responder à questão: pode a ARC ser modificável, i.e., farmacologicamente incrementada, de modo a conferir melhor proteção na zona de penumbra isquémica?

Um estudo mostrou como o cacau puro (Sorond et al., 2013) ou a desferroxamina (Sorond et al., 2015) podem melhorar a função vascular cerebral, o que seria interessante testar no AVC isquémico;

- Desenvolver novos estudos prospetivos que poderão beneficiar de monitorização da ARC, tais como na hemorragia cerebral primária ou na hemorragia subaracnoideia.

Estão também em curso projetos de linhas de investigação adicionais com ultrassonografia, em diferentes contextos de doença vascular, nomeadamente estudos de hemodinâmica e de risco vascular, como:

- Projeto de tese de mestrado sobre a ARC em doentes com esclerose múltipla. Existe um risco vascular desproporcional na esclerose múltipla, tanto de enfarte cerebral como de enfarte do miocárdio. Este estudo visa perceber se este risco poderá ser explicado por uma desregulação vasomotora subjacente;
- Projeto de tese de mestrado para determinar o modo como o sistema de controlo da PA periférico, ou seja, o BR arterial, interage com o controlo vascular cerebral avaliado pela ARC;
- Projeto de tese de doutoramento sobre as estenoses arteriais intracranianas significativas e a repercussão das alterações hemodinâmicas. Nomeadamente, este estudo pretende correlacionar o grau de estenose com a perturbação da perfusão e da regulação vasomotora distal.
- Projeto de tese de doutoramento sobre a lesão neurológica na cirurgia de substituição de válvula aórtica. Este projeto visa determinar marcadores passíveis de aplicação clínica, que permitam predizer a lesão neurológica (AVC, estado confusional agudo, declínio cognitivo) após cirurgia de substituição de válvula aórtica. Uma das vertentes é estudar a função vascular cerebral através da ARC e a VR ao CO_2. A hipótese do estudo é que uma desregulação vasomotora *a priori* poderá determinar uma menor capacidade de defesa perante o insulto hemodinâmico durante a cirurgia;
- Projeto de tese de doutoramento sobre biomarcadores de risco na doença microvascular cerebral (BioRiMiC). Este estudo acompanhará uma coorte de doentes hipertensos e visa compreender melhor o modo como os biomarcadores de doença macro e microvasculares influenciam a doença de pequenos vasos cerebrais. Entre outros parâmetros, será estudada a função vascular cerebral através da medição de ARC, VR ao CO_2 e ANV com prova visual. Assim, poderão ser desenvolvidos procedimentos não invasivos que permitam identificar precocemente os doentes com

maior risco de desenvolver esta doença e que possam ser integrados na prática clínica no futuro, nomeadamente, no desenvolvimento de estratégias para um controlo mais apertado dos fatores de risco vascular nestes doentes;

- Projeto de tese de doutoramento sobre a avaliação multiparamétrica da vascularização da coroide, retina e cerebral em doentes com coroidorretinopatia serosa central. Parte deste projeto tenta perceber se os doentes com esta patologia, que se acredita estar relacionada com a desregulação microvascular coroideia, poderá ter uma vasculopatia mais generalizada. Por esse motivo, será estudada a função vascular cerebral através da mediação de ARC, VR ao CO_2 e ANV com prova visual.

A monitorização da ARC acabou por se revelar útil no AVC isquémico agudo. No entanto, antes de partir para a sua aplicação na prática clínica é necessário mais trabalho de validação destas ferramentas. Nesta linha de pensamento, a equipa de investigação cerebrovascular da Unidade de Investigação e Desenvolvimento Cardiovascular da Faculdade de Medicina do Porto associou-se a um grupo multicêntrico de avaliação internacional que junta investigadores com interesse no estudo, validação e implementação da ARC – *Cerebral Autoregulation network* (CARnet). Criou-se recentemente um subgrupo do CARnet de colaboração subsidiária designado por *INiciative FOr Measurement of cerebral AuToregulation in Acute* Stroke (INFOMATAS) que, esperemos, no futuro possa contribuir para uma implementação com maior acuidade da medição da ARC no AVC isquémico agudo.

IX. BIBLIOGRAFIA

AASLID, R., LASH, S. R., BARDY, G. H., GILD, W. H. & NEWELL, D. W. 2003. Dynamic pressure--flow velocity relationships in the human cerebral circulation. *Stroke,* 34**,** 1645-9.

AASLID, R., LINDEGAARD, K. F., SORTEBERG, W. & NORNES, H. 1989. Cerebral autoregulation dynamics in humans. *Stroke,* 20**,** 45-52.

AASLID, R., MARKWALDER, T. M. & NORNES, H. 1982. Noninvasive transcranial Doppler ultrasound recording of flow velocity in basal cerebral arteries. *J Neurosurg,* 57**,** 769-74.

ABU-AMARAH, I., BIDANI, A. K., HACIOGLU, R., WILLIAMSON, G. A. & GRIFFIN, K. A. 2005. Differential effects of salt on renal hemodynamics and potential pressure transmission in stroke-prone and stroke-resistant spontaneously hypertensive rats. *Am J Physiol Renal Physiol,* 289**,** F305-13.

ADAMS, H. P., JR., BENDIXEN, B. H., KAPPELLE, L. J., BILLER, J., LOVE, B. B., GORDON, D. L. & MARSH, E. E., 3RD 1993. Classification of subtype of acute ischemic stroke. Definitions for use in a multicenter clinical trial. TOAST. Trial of Org 10172 in Acute Stroke Treatment. *Stroke,* 24**,** 35-41.

ADAMS, R. J., MCKIE, V. C., CARL, E. M., NICHOLS, F. T., PERRY, R., BROCK, K., MCKIE, K., FIGUEROA, R., LITAKER, M., WEINER, S. & BRAMBILLA, D. 1997. Long-term stroke risk in children with sickle cell disease screened with transcranial Doppler. *Ann Neurol,* 42**,** 699-704.

ADAMS, R. J., MCKIE, V. C., HSU, L., FILES, B., VICHINSKY, E., PEGELOW, C., ABBOUD, M., GALLAGHER, D., KUTLAR, A., NICHOLS, F. T., BONDS, D. R. & BRAMBILLA, D. 1998. Prevention of a first stroke by transfusions in children with sickle cell anemia and abnormal results on transcranial Doppler ultrasonography. *N Engl J Med,* 339**,** 5-11.

AGGARWAL, S., BROOKS, D. M., KANG, Y., LINDEN, P. K. & PATZER, J. F., 2ND 2008. Noninvasive monitoring of cerebral perfusion pressure in patients with acute liver failure using transcranial doppler ultrasonography. *Liver Transpl,* 14**,** 1048-57.

AHA 1997. American Heart Association. Heart and Stroke Facts Statistics: Dallas: American Heart Association.

AINSLIE, P. N. & DUFFIN, J. 2009. Integration of cerebrovascular CO2 reactivity and chemoreflex control of breathing: mechanisms of regulation, measurement, and interpretation. *Am J Physiol Regul Integr Comp Physiol,* 296**,** R1473-95.

AINSLIE, P. N. & OGOH, S. 2010. Regulation of cerebral blood flow in mammals during chronic hypoxia: a matter of balance. *Exp Physiol,* 95**,** 251-62.

ALEXANDROV, A. V. 2003. Ultrasound and angiography in the selection of patients for carotid endarterectomy. *Curr Cardiol Rep,* 5**,** 141-7.

ALEXANDROV, A. V., SLOAN, M. A., TEGELER, C. H., NEWELL, D. N., LUMSDEN, A., GARAMI, Z., LEVY, C. R., WONG, L. K., DOUVILLE, C., KAPS, M., TSIVGOULIS, G. & AMERICAN SOCIETY OF NEUROIMAGING PRACTICE GUIDELINES, C. 2012. Practice standards for transcranial Doppler (TCD) ultrasound. Part II. Clinical indications and expected outcomes. *J Neuroimaging,* 22**,** 215-24.

AMES, A., WRIGHT, R. L., KOWADA, M., THURSTON, J. M. & MAJNO, G. 1968. Cerebral ischemia. II. The no-reflow phenomenon. *Am J Pathol,* 52**,** 437-53.

AMIN, F. M., ASGHAR, M. S., HOUGAARD, A., HANSEN, A. E., LARSEN, V. A., DE KONING, P. J., LARSSON, H. B., OLESEN, J. & ASHINA, M. 2013. Magnetic resonance angiography of intracranial and extracranial arteries in patients with spontaneous migraine without aura: a cross-sectional study. *Lancet Neurol,* 12**,** 454-61.

ANDRESEN, J., SHAFI, N. I. & BRYAN, R. M., JR. 2006. Endothelial influences on cerebrovascular tone. *J Appl Physiol (1985),* 100**,** 318-27.

ARBAB, M. A., WIKLUND, L. & SVENDGAARD, N. A. 1986. Origin and distribution of cerebral vascular innervation from superior cervical, trigeminal and spinal ganglia investigated with retrograde and anterograde WGA-HRP tracing in the rat. *Neuroscience,* 19**,** 695-708.

ARIES, M. J., ELTING, J. W., DE KEYSER, J., KREMER, B. P. & VROOMEN, P. C. 2010. Cerebral autoregulation in stroke: a review of transcranial Doppler studies. *Stroke,* 41**,** 2697-704.

ARKING, D. E., ATZMON, G., ARKING, A., BARZILAI, N. & DIETZ, H. C. 2005. Association between a functional variant of the KLOTHO gene and high-density lipoprotein cholesterol, blood pressure, stroke, and longevity. *Circ Res,* 96**,** 412-8.

ARNOLDS, B. J. & VON REUTERN, G. M. 1986. Transcranial Doppler sonography. Examination technique and normal reference values. *Ultrasound Med Biol,* 12**,** 115-23.

AZEVEDO, E. & CASTRO, P. 2016. Cerebral autoregulation. *In:* CSIBA, L. & BARACCHINI, C. (eds.) *Manual of neurosonology.* Cambridge: Cambridge University Press.

AZEVEDO, E., CASTRO, P., SANTOS, R., FREITAS, J., COELHO, T., ROSENGARTEN, B. & PANERAI, R. 2011. Autonomic dysfunction affects cerebral neurovascular coupling. *Clin Auton Res,* 21**,** 395-403.

AZEVEDO, E., MENDES, A., SEIXAS, D., SANTOS, R., CASTRO, P., AYRES-BASTO, M., ROSENGARTEN, B. & OLIVEIRA, J. P. 2012. Functional transcranial Doppler: presymptomatic changes in Fabry disease. *Eur Neurol,* 67**,** 331-7.

AZEVEDO, E. & P., C. 2013. Novel Applications of Ultrasound Vascular Imaging. *In:* RAMALHO, J. N., CASTILLO, M. & SEMELKA, R. C. (eds.) *Vascular imaging of the central nervous system : physical principles, clinical applications and emerging techniques.* Hoboken, New Jersey: Wiley-Blackwell.

AZEVEDO, E., ROSENGARTEN, B., SANTOS, R., FREITAS, J. & KAPS, M. 2007. Interplay of cerebral autoregulation and neurovascular coupling evaluated by functional TCD in different orthostatic conditions. *J Neurol,* 254**,** 236-41.

AZEVEDO, E., TEIXEIRA, J., NEVES, J. C. & VAZ, R. 2000. Transcranial Doppler and brain death. *Transplant Proc,* 32**,** 2579-81.

BADCOCK, N. A., HOLT, G., HOLDEN, A. & BISHOP, D. V. 2012. dopOSCCI: a functional transcranial Doppler ultrasonography summary suite for the assessment of cerebral lateralization of cognitive function. *J Neurosci Methods,* 204**,** 383-8.

BAKKER, S. L., DE LEEUW, F. E., DE GROOT, J. C., HOFMAN, A., KOUDSTAAL, P. J. & BRETELER, M. M. 1999. Cerebral vasomotor reactivity and cerebral white matter lesions in the elderly. *Neurology,* 52**,** 578-83.

BAKKER, S. L., DE LEEUW, F. E., DEN HEIJER, T., KOUDSTAAL, P. J., HOFMAN, A. & BRETELER, M. M. 2004. Cerebral haemodynamics in the elderly: the rotterdam study. *Neuroepidemiology,* 23**,** 178-84.

BALAMI, J. S., CHEN, R. L., GRUNWALD, I. Q. & BUCHAN, A. M. 2011. Neurological complications of acute ischaemic stroke. *Lancet Neurol,* 10**,** 357-71.

BALESTRERI, M., CZOSNYKA, M., HUTCHINSON, P., STEINER, L. A., HILER, M., SMIELEWSKI, P. & PICKARD, J. D. 2006. Impact of intracranial pressure and cerebral perfusion pressure on severe disability and mortality after head injury. *Neurocrit Care,* 4**,** 8-13.

BAMFORD, J., SANDERCOCK, P., DENNIS, M., BURN, J. & WARLOW, C. 1991. Classification and natural history of clinically identifiable subtypes of cerebral infarction. *Lancet,* 337**,** 1521-6.

BANG, O. Y., BUCK, B. H., SAVER, J. L., ALGER, J. R., YOON, S. R., STARKMAN, S., OVBIAGELE, B., KIM, D., ALI, L. K., SANOSSIAN, N., JAHAN, R., DUCKWILER, G. R., VINUELA, F., SALAMON, N., VILLABLANCA, J. P. & LIEBESKIND, D. S. 2007. Prediction of hemorrhagic transformation after recanalization therapy using T2*-permeability magnetic resonance imaging. *Ann Neurol,* 62**,** 170-6.

BANG, O. Y., SAVER, J. L., ALGER, J. R., STARKMAN, S., OVBIAGELE, B. & LIEBESKIND, D. S. 2008. Determinants of the distribution and severity of hypoperfusion in patients with ischemic stroke. *Neurology,* 71**,** 1804-11.

BARBER, F. E., BAKER, D. W., NATION, A. W., STRANDNESS, D. E., JR. & REID, J. M. 1974. Ultrasonic duplex echo-Doppler scanner. *IEEE Trans Biomed Eng,* 21**,** 109-13.

BARNES, J. N., SCHMIDT, J. E., NICHOLSON, W. T. & JOYNER, M. J. 2012. Cyclooxygenase inhibition abolishes age-related differences in cerebral vasodilator responses to hypercapnia. *J Appl Physiol (1985),* 112**,** 1884-90.

BARTELS, E., FUCHS, H. H. & FLUGEL, K. A. 1995. Color Doppler imaging of basal cerebral arteries: normal reference values and clinical applications. *Angiology,* 46**,** 877-84.

BAUMGARTNER, R. W., ARNOLD, M., GONNER, F., STAIKOW, I., HERRMANN, C., RIVOIR, A. & MURI, R. M. 1997. Contrast-enhanced transcranial color-coded duplex sonography in ischemic cerebrovascular disease. *Stroke,* 28**,** 2473-8.

BAYLISS, W. M. 1902. On the local reactions of the arterial wall to changes of internal pressure. *J Physiol,* 28**,** 220-31.

BENARROCH, E. E. 1993. The central autonomic network: functional organization, dysfunction, and perspective. *Mayo Clin Proc,* 68**,** 988-1001.

BENY, J. L., NGUYEN, M. N., MARINO, M. & MATSUI, M. 2008. Muscarinic receptor knockout mice confirm involvement of M3 receptor in endothelium-dependent vasodilatation in mouse arteries. *J Cardiovasc Pharmacol,* 51**,** 505-12.

BERENGARUS, J. 1552. *Isagoge Breves Perlucide ac Uberime in Anatomicum Humani Corporis,* Bologna, B Hectoris.

BERGERON, M., GIDDAY, J. M., YU, A. Y., SEMENZA, G. L., FERRIERO, D. M. & SHARP, F. R. 2000. Role of hypoxia-inducible factor-1 in hypoxia-induced ischemic tolerance in neonatal rat brain. *Ann Neurol,* 48**,** 285-96.

BERKHEMER, O. A., FRANSEN, P. S., BEUMER, D., VAN DEN BERG, L. A., LINGSMA, H. F., YOO, A. J., SCHONEWILLE, W. J., VOS, J. A., NEDERKOORN, P. J., WERMER, M. J., VAN WALDERVEEN, M. A., STAALS, J., HOFMEIJER, J., VAN OOSTAYEN, J. A., LYCKLAMA A NIJEHOLT, G. J., BOITEN, J., BROUWER, P. A., EMMER, B. J., DE BRUIJN, S. F., VAN DIJK, L. C., KAPPELLE, L. J., LO, R. H., VAN DIJK, E. J., DE VRIES, J., DE KORT, P. L., VAN ROOIJ, W. J., VAN DEN BERG, J. S., VAN HASSELT, B. A., AERDEN, L. A., DALLINGA, R. J., VISSER, M. C., BOT, J. C., VROOMEN, P. C., ESHGHI, O., SCHREUDER, T. H., HEIJBOER, R. J., KEIZER, K., TIELBEEK, A. V., DEN HERTOG, H. M., GERRITS, D. G., VAN DEN BERG-VOS, R. M., KARAS, G. B., STEYERBERG, E. W., FLACH, H. Z., MARQUERING, H. A., SPRENGERS, M. E., JENNISKENS, S. F., BEENEN, L. F., VAN DEN BERG, R., KOUDSTAAL, P. J., VAN ZWAM, W. H., ROOS, Y. B., VAN DER LUGT, A., VAN OOSTENBRUGGE, R. J., MAJOIE, C. B. & DIPPEL, D. W. 2015. A randomized trial of intraarterial treatment for acute ischemic stroke. *N Engl J Med,* 372**,** 11-20.

BIDANI, A. K. & GRIFFIN, K. A. 2004. Pathophysiology of hypertensive renal damage: implications for therapy. *Hypertension,* 44**,** 595-601.

BIZEAU, A., GILBERT, G., BERNIER, M., HUYNH, M. T., BOCTI, C., DESCOTEAUX, M. & WHITTINGSTALL, K. 2017. Stimulus-evoked changes in cerebral vessel diameter: A study in healthy humans. *J Cereb Blood Flow Metab***,** 271678x17701948.

BOBAN, M., CRNAC, P., JUNAKOVIC, A., GARAMI, Z. & MALOJCIC, B. 2014. Blood flow velocity changes in anterior cerebral arteries during cognitive tasks performance. *Brain Cogn,* 84**,** 26-33.

BOYSEN, N. C., DRAGON, D. N. & TALMAN, W. T. 2009. Parasympathetic tonic dilatory influences on cerebral vessels. *Auton Neurosci,* 147**,** 101-4.

BRIER, A. 1897. Die Entstehung des Collateralkreislaufs. Thies I. Der arterielle Collateralkreislauf. . *Virchows Arch Pathol Anat Physiol Klin Med,* 147**,** 256-293.

BRUNDEGE, J. M. & DUNWIDDIE, T. V. 1997. Role of adenosine as a modulator of synaptic activity in the central nervous system. *Adv Pharmacol,* 39**,** 353-91.

BUDOHOSKI, K. P., CZOSNYKA, M., KIRKPATRICK, P. J., REINHARD, M., VARSOS, G. V., KASPROWICZ, M., ZABEK, M., PICKARD, J. D. & SMIELEWSKI, P. 2015. Bilateral failure of cerebral autoregulation is related to unfavorable outcome after subarachnoid hemorrhage. *Neurocrit Care,* 22**,** 65-73.

BUSIJA, D. W. & HEISTAD, D. D. 1984. Factors involved in the physiological regulation of the cerebral circulation. *Rev Physiol Biochem Pharmacol,* 101**,** 161-211.

BUTCHER, I., MAAS, A. I., LU, J., MARMAROU, A., MURRAY, G. D., MUSHKUDIANI, N. A., MCHUGH, G. S. & STEYERBERG, E. W. 2007. Prognostic value of admission blood pressure in traumatic brain injury: results from the IMPACT study. *J Neurotrauma,* 24**,** 294-302.

CAGNACCI, A., TARQUINI, R., PERFETTO, F., ARANGINO, S., ZANNI, A. L., CAGNACCI, P., FACCHINETTI, F. & VOLPE, A. 2003. Endothelin-1 and nitric oxide levels are related to cardiovascular risk factors but are not modified by estradiol replacement in healthy postmenopausal women. A cross-sectional and a randomized cross-over study. *Maturitas,* 44**,** 117-24.

CALDAS, J. R., PANERAI, R. B., HAUNTON, V. J., ALMEIDA, J. P., FERREIRA, G. S., CAMARA, L., NOGUEIRA, R. C., BOR-SENG-SHU, E., OLIVEIRA, M. L., GROEHS, R. R., FERREIRA-SANTOS, L., TEIXEIRA, M. J., GALAS, F. R., ROBINSON, T. G., JATENE, F. B. & HAJJAR, L. A. 2017. Cerebral blood flow autoregulation in ischemic heart failure. *Am J Physiol Regul Integr Comp Physiol,* 312**,** R108-R113.

CALVIERE, L., NASR, N., ARNAUD, C., CZOSNYKA, M., VIGUIER, A., TISSOT, B., SOL, J. C. & LARRUE, V. 2015. Prediction of Delayed Cerebral Ischemia After Subarachnoid Hemorrhage Using Cerebral Blood Flow Velocities and Cerebral Autoregulation Assessment. *Neurocrit Care,* 23**,** 253-8.

CAPLAN, L. R. 2006. *Stroke,* New York

Saint Paul, MN, Demos ;

AAN Press, American Academy of Neurology.

CAREY, B. J., EAMES, P. J., PANERAI, R. B. & POTTER, J. F. 2001. Carbon dioxide, critical closing pressure and cerebral haemodynamics prior to vasovagal syncope in humans. *Clin Sci (Lond),* 101**,** 351-8.

CAREY, B. J., PANERAI, R. B. & POTTER, J. F. 2003. Effect of aging on dynamic cerebral autoregulation during head-up tilt. *Stroke,* 34**,** 1871-5.

CARLSTROM, M., WILCOX, C. S. & ARENDSHORST, W. J. 2015. Renal autoregulation in health and disease. *Physiol Rev,* 95**,** 405-511.

CARVALHO, M. J., VAN DEN MEIRACKER, A. H., BOOMSMA, F., LIMA, M., FREITAS, J., VELD, A. J. & FALCAO DE FREITAS, A. 2000. Diurnal blood pressure variation in progressive autonomic failure. *Hypertension,* 35**,** 892-7.

CARVALHO, T. & CASTRO, P. 2013. Disfunções do Sistema Nervoso Autónomo. *In:* SÁ, M. J. (ed.) *Manual de Neurologia Clínica: Compreender as Doenças Neurológicas* 2nd ed. Porto: Edições Universidade Fernando Pessoa.

CASSAGLIA, P. A., GRIFFITHS, R. I. & WALKER, A. M. 2009. Cerebral sympathetic nerve activity has a major regulatory role in the cerebral circulation in REM sleep. *J Appl Physiol,* 106**,** 1050-6.

CASTRO, P., COSTA, A., ABREU, P., PENAS, S., FARIA, O. & AZEVEDO, E. 2016. Acute posterior multifocal placoid pigment epitheliopathy presenting with multiple brain and spinal cord infarctions. *Journal of the Neurological Sciences,* 361**,** 26-28.

CASTRO, P., SANTOS, R., FREITAS, J., ROSENGARTEN, B., PANERAI, R. & AZEVEDO, E. 2012. Adaptation of cerebral pressure-velocity hemodynamic changes of neurovascular coupling to orthostatic challenge. *Perspectives in Medicine,* 1**,** 290-296.

CASTRO, P. M., SANTOS, R., FREITAS, J., PANERAI, R. B. & AZEVEDO, E. 2014. Autonomic dysfunction affects dynamic cerebral autoregulation during Valsalva maneuver: comparison between healthy and autonomic dysfunction subjects. *J Appl Physiol (1985),* 117**,** 205-13.

CAULI, B., TONG, X. K., RANCILLAC, A., SERLUCA, N., LAMBOLEZ, B., ROSSIER, J. & HAMEL, E. 2004. Cortical GABA interneurons in neurovascular coupling: relays for subcortical vasoactive pathways. *J Neurosci,* 24**,** 8940-9.

CHURCHILL, P. C., CHURCHILL, M. C., GRIFFIN, K. A., PICKEN, M., WEBB, R. C., KURTZ, T. W. & BIDANI, A. K. 2002. Increased genetic susceptibility to renal damage in the stroke-prone spontaneously hypertensive rat. *Kidney Int,* 61**,** 1794-800.

CLAASSEN, J. A., LEVINE, B. D. & ZHANG, R. 2009. Dynamic cerebral autoregulation during repeated squat-stand maneuvers. *J Appl Physiol (1985),* 106**,** 153-60.

CLAASSEN, J. A., MEEL-VAN DEN ABEELEN, A. S., SIMPSON, D. M., PANERAI, R. B. & INTERNATIONAL CEREBRAL AUTOREGULATION RESEARCH, N. 2016. Transfer function analysis of dynamic cerebral autoregulation: A white paper from the International Cerebral Autoregulation Research Network. *J Cereb Blood Flow Metab*.

COHEN, Z., BONVENTO, G., LACOMBE, P. & HAMEL, E. 1996. Serotonin in the regulation of brain microcirculation. *Prog Neurobiol,* 50**,** 335-62.

COMAN, I. M. & POPESCU, B. A. 2015. Shigeo Satomura: 60 years of Doppler ultrasound in medicine. *Cardiovasc Ultrasound,* 13**,** 48.

CORNWELL, W. K., 3RD & LEVINE, B. D. 2015. Patients with heart failure with reduced ejection fraction have exaggerated reductions in cerebral blood flow during upright posture. *JACC Heart Fail,* 3**,** 176-9.

CORREIA, M., MAGALHAES, R., FELGUEIRAS, R., QUINTAS, C., GUIMARAES, L. & SILVA, M. C. 2017. Changes in stroke incidence, outcome, and associated factors in Porto between 1998 and 2011. *Int J Stroke,* 12**,** 169-179.

COSTA, A., FILIPE, J. P., SANTOS, R., FERREIRA, C., ABREU, P., AZEVEDO, E. & CASTRO, P. 2015. The role of transcranial Doppler ultrasonography inposterior reversible encephalopathy syndrome. *Cerebrovasc Dis,* 39**,** 28.

COVERDALE, N. S., BADROV, M. B. & KEVIN SHOEMAKER, J. 2016. Impact of age on cerebrovascular dilation versus reactivity to hypercapnia. *J Cereb Blood Flow Metab*.

CURIE, J. & CURIE, P. 1880. Développement, par pression, de l'électricité polaire dans les cristaux hémièdres à faces inclinées. *Comptes Rendus de l'Académie des Sciences,* 91**,** 294–295.

CURTZE, S., HAAPANIEMI, E., MELKAS, S., MUSTANOJA, S., PUTAALA, J., SAIRANEN, T., SIBOLT, G., TIAINEN, M., TATLISUMAK, T. & STRBIAN, D. 2015. White Matter Lesions Double the Risk of Post-Thrombolytic Intracerebral Hemorrhage. *Stroke*.

CZOSNYKA, M., BRADY, K., REINHARD, M., SMIELEWSKI, P. & STEINER, L. A. 2009. Monitoring of cerebrovascular autoregulation: facts, myths, and missing links. *Neurocrit Care,* 10**,** 373-86.

CZOSNYKA, M., SMIELEWSKI, P., KIRKPATRICK, P., LAING, R. J., MENON, D. & PICKARD, J. D. 1997. Continuous assessment of the cerebral vasomotor reactivity in head injury. *Neurosurgery,* 41**,** 11-7; discussion 17-9.

CZOSNYKA, M., SMIELEWSKI, P., KIRKPATRICK, P., MENON, D. K. & PICKARD, J. D. 1996. Monitoring of cerebral autoregulation in head-injured patients. *Stroke,* 27**,** 1829-34.

CZOSNYKA, M., SMIELEWSKI, P., PIECHNIK, S., AL-RAWI, P. G., KIRKPATRICK, P. J., MATTA, B. F. & PICKARD, J. D. 1999. Critical closing pressure in cerebrovascular circulation. *J Neurol Neurosurg Psychiatry,* 66**,** 606-11.

D'ESTERRE, C. D., ROVERSI, G., PADRONI, M., BERNARDONI, A., TAMBORINO, C., DE VITO, A., AZZINI, C., MARCELLO, O., SALETTI, A., CERUTI, S., LEE, T. Y. & FAINARDI, E. 2015. CT perfusion cerebral blood volume does not always predict infarct core in acute ischemic stroke. *Neurol Sci,* 36**,** 1777-83.

DAVIS, M. J. 2012. Perspective: physiological role(s) of the vascular myogenic response. *Microcirculation,* 19**,** 99-114.

DAWSON, S. L., BLAKE, M. J., PANERAI, R. B. & POTTER, J. F. 2000a. Dynamic but not static cerebral autoregulation is impaired in acute ischaemic stroke. *Cerebrovasc Dis,* 10**,** 126-32.

DAWSON, S. L., BLAKE, M. J., PANERAI, R. B. & POTTER, J. F. 2000b. Dynamic but not static cerebral autoregulation is impaired in acute ischaemic stroke. *Cerebrovasc Dis,* 10**,** 126-32.

DAWSON, S. L., PANERAI, R. B. & POTTER, J. F. 2003. Serial changes in static and dynamic cerebral autoregulation after acute ischaemic stroke. *Cerebrovasc Dis,* 16**,** 69-75.

DE RAEDT, S., DE VOS, A. & DE KEYSER, J. 2015. Autonomic dysfunction in acute ischemic stroke: an underexplored therapeutic area? *J Neurol Sci,* 348**,** 24-34.

DEPPE, M., KNECHT, S., LOHMANN, H. & RINGELSTEIN, E. B. 2004. A method for the automated assessment of temporal characteristics of functional hemispheric lateralization by transcranial Doppler sonography. *J Neuroimaging,* 14**,** 226-30.

DESNICK, R. J., BRADY, R., BARRANGER, J., COLLINS, A. J., GERMAIN, D. P., GOLDMAN, M., GRABOWSKI, G., PACKMAN, S. & WILCOX, W. R. 2003. Fabry disease, an under-recognized multisystemic disorder: expert recommendations for diagnosis, management, and enzyme replacement therapy. *Ann Intern Med,* 138**,** 338-46.

DEWITT, L. D. & WECHSLER, L. R. 1988. Transcranial Doppler. *Stroke,* 19**,** 915-21.

DGS 2015. *A saúde dos Portugueses. Perspetiva 2015 Lisboa, Portugal. Direção-Geral da Saúde, 2015*, Direção-Geral da Saúde.

DGS 2016. PORTUGAL Doenças Cérebro-Cardiovasculares em Números – 2015. Programa Nacional para as Doenças Cérebro-Cardiovasculares. Lisboa, Portugal. Direção-Geral da Saúde, 2015.

DI RIENZO, M., PARATI, G., CASTIGLIONI, P., TORDI, R., MANCIA, G. & PEDOTTI, A. 2001. Baroreflex effectiveness index: an additional measure of baroreflex control of heart rate in daily life. *Am J Physiol Regul Integr Comp Physiol,* 280**,** R744-51.

DIAS, C. 2014. Multimodal brain monitoring in neurocritical care practice. *IJCNMH,* Suppl1.

DIAS, C., SILVA, M. J., PEREIRA, E., MONTEIRO, E., MAIA, I., BARBOSA, S., SILVA, S., HONRADO, T., CEREJO, A., ARIES, M. J., SMIELEWSKI, P., PAIVA, J. A. & CZOSNYKA, M. 2015. Optimal Cerebral Perfusion Pressure Management at Bedside: A Single-Center Pilot Study. *Neurocrit Care,* 23**,** 92-102.

DIEHL, R. R. 2002. Cerebral autoregulation studies in clinical practice. *Eur J Ultrasound,* 16**,** 31-6.

DIEHL, R. R., LINDEN, D., LUCKE, D. & BERLIT, P. 1995. Phase relationship between cerebral blood flow velocity and blood pressure. A clinical test of autoregulation. *Stroke,* 26**,** 1801-4.

DIEHL, R. R., LINDEN, D., LUCKE, D. & BERLIT, P. 1998. Spontaneous blood pressure oscillations and cerebral autoregulation. *Clin Auton Res,* 8**,** 7-12.

DINEEN, N. E., BRODIE, F. G., ROBINSON, T. G. & PANERAI, R. B. 2010. Continuous estimates of dynamic cerebral autoregulation during transient hypocapnia and hypercapnia. *J Appl Physiol,* 108**,** 604-13.

DIRNAGL, U., IADECOLA, C. & MOSKOWITZ, M. A. 1999. Pathobiology of ischaemic stroke: an integrated view. *Trends Neurosci,* 22**,** 391-7.

DOHMEN, C., BOSCHE, B., GRAF, R., REITHMEIER, T., ERNESTUS, R. I., BRINKER, G., SOBESKY, J. & HEISS, W. D. 2007. Identification and clinical impact of impaired cerebrovascular autoregulation in patients with malignant middle cerebral artery infarction. *Stroke,* 38**,** 56-61.

DOPPLER, C. A. 1843. Über das farbige licht der Doppelsterne und einiger anderer Gestirne des Himmels. Abhandlungen der königl. böhm. *Gesellschaft der Wissenschaften,* 2.

DUVERNOY, H. M., DELON, S. & VANNSON, J. L. 1981. Cortical blood vessels of the human brain. *Brain Res Bull,* 7**,** 519-79.

EAMES, P. J., BLAKE, M. J., DAWSON, S. L., PANERAI, R. B. & POTTER, J. F. 2002. Dynamic cerebral autoregulation and beat to beat blood pressure control are impaired in acute ischaemic stroke. *J Neurol Neurosurg Psychiatry,* 72**,** 467-72.

EARLEY, S. & BRAYDEN, J. E. 2015. Transient receptor potential channels in the vasculature. *Physiol Rev,* 95**,** 645-90.

EBERT, T. J. 1990. Differential effects of nitrous oxide on baroreflex control of heart rate and peripheral sympathetic nerve activity in humans. *Anesthesiology,* 72**,** 16-22.

EDMONDS, H. L., JR., RODRIGUEZ, R. A., AUDENAERT, S. M., AUSTIN, E. H., 3RD, POLLOCK, S. B., JR. & GANZEL, B. L. 1996. The role of neuromonitoring in cardiovascular surgery. *J Cardiothorac Vasc Anesth,* 10**,** 15-23.

EDVINSSON, L. 1975. Neurogenic mechanisms in the cerebrovascular bed. Autonomic nerves, amine receptors and their effects on cerebral blood flow. *Acta Physiol Scand Suppl,* 427**,** 1-35.

EDVINSSON, L., FALCK, B. & OWMAN, C. 1977. Possibilities for a cholinergic action on smooth musculature and on sympathetic axons in brain vessels mediated by muscarinic and nicotinic receptors. *J Pharmacol Exp Ther,* 200**,** 117-26.

EDVINSSON, L., FREDHOLM, B. B., HAMEL, E., JANSEN, I. & VERRECCHIA, C. 1985. Perivascular peptides relax cerebral arteries concomitant with stimulation of cyclic adenosine monophosphate accumulation or release of an endothelium-derived relaxing factor in the cat. *Neurosci Lett,* 58**,** 213-7.

EDVINSSON, L., HARA, H. & UDDMAN, R. 1989. Retrograde tracing of nerve fibers to the rat middle cerebral artery with true blue: colocalization with different peptides. *J Cereb Blood Flow Metab,* 9**,** 212-8.

EDVINSSON, L. & KRAUSE, D., N. 2002. *Cerebral blood flow and metabolism,* Philadelphia, Lippincott, Williams &Wilkins.

EL KHOUDARY, S. R., SHIELDS, K. J., JANSSEN, I., HANLEY, C., BUDOFF, M. J., BARINAS-MITCHELL, E., EVERSON-ROSE, S. A., POWELL, L. H. & MATTHEWS, K. A. 2015. Cardiovascular Fat, Menopause, and Sex Hormones in Women: The SWAN Cardiovascular Fat Ancillary Study. *J Clin Endocrinol Metab,* 100**,** 3304-12.

ELHUSSEINY, A. & HAMEL, E. 2000. Muscarinic--but not nicotinic--acetylcholine receptors mediate a nitric oxide-dependent dilation in brain cortical arterioles: a possible role for the M5 receptor subtype. *J Cereb Blood Flow Metab,* 20**,** 298-305.

ENDOH, H., HONDA, T., KOMURA, N., SHIBUE, C., WATANABE, I. & SHIMOJI, K. 2000. The effects of nicardipine on dynamic cerebral autoregulation in patients anesthetized with propofol and fentanyl. *Anesth Analg,* 91**,** 642-6.

EUROPEAN STROKE ORGANISATION EXECUTIVE, C. & COMMITTEE, E. S. O. W. 2008. Guidelines for management of ischaemic stroke and transient ischaemic attack 2008. *Cerebrovasc Dis,* 25**,** 457-507.

EYDING, J., KROGIAS, C., SCHOLLHAMMER, M., EYDING, D., WILKENING, W., MEVES, S., SCHRODER, A., PRZUNTEK, H. & POSTERT, T. 2006. Contrast-enhanced ultrasonic parametric perfusion imaging detects dysfunctional tissue at risk in acute MCA stroke. *J Cereb Blood Flow Metab,* 26**,** 576-82.

FALLOPIUS, G. 1561. *Observationes Anatomicae,* Venice, MA Ulmus.

FARACI, F. M. & BRIAN, J. E., JR. 1994. Nitric oxide and the cerebral circulation. *Stroke,* 25**,** 692-703.

FARACI, F. M. & HEISTAD, D. D. 1990. Regulation of large cerebral arteries and cerebral microvascular pressure. *Circ Res,* 66**,** 8-17.

FAZEKAS, F., KLEINERT, R., OFFENBACHER, H., SCHMIDT, R., KLEINERT, G., PAYER, F., RADNER, H. & LECHNER, H. 1993. Pathologic correlates of incidental MRI white matter signal hyperintensities. *Neurology,* 43**,** 1683-9.

FEIGIN, V. L., ROTH, G. A., NAGHAVI, M., PARMAR, P., KRISHNAMURTHI, R., CHUGH, S., MENSAH, G. A., NORRVING, B., SHIUE, I., NG, M., ESTEP, K., CERCY, K., MURRAY, C. J., FOROUZANFAR, M. H., GLOBAL BURDEN OF DISEASES, I., RISK FACTORS, S. & STROKE EXPERTS WRITING, G. 2016. Global burden of stroke and risk factors in 188 countries, during 1990-2013: a systematic analysis for the Global Burden of Disease Study 2013. *Lancet Neurol,* 15**,** 913-24.

FELDMANN, E., WILTERDINK, J. L., KOSINSKI, A., LYNN, M., CHIMOWITZ, M. I., SARAFIN, J., SMITH, H. H., NICHOLS, F., ROGG, J., CLOFT, H. J., WECHSLER, L., SAVER, J., LEVINE, S. R., TEGELER, C., ADAMS, R. & SLOAN, M. 2007. The Stroke Outcomes and Neuroimaging of Intracranial Atherosclerosis (SONIA) trial. *Neurology,* 68**,** 2099-106.

FELLGIEBEL, A., MULLER, M. J., MAZANEK, M., BARON, K., BECK, M. & STOETER, P. 2005. White matter lesion severity in male and female patients with Fabry disease. *Neurology,* 65**,** 600-2.

FERNANDO, M. S., SIMPSON, J. E., MATTHEWS, F., BRAYNE, C., LEWIS, C. E., BARBER, R., KALARIA, R. N., FORSTER, G., ESTEVES, F., WHARTON, S. B., SHAW, P. J., O'BRIEN, J. T., INCE, P. G., FUNCTION, M. R. C. C. & AGEING NEUROPATHOLOGY STUDY, G. 2006. White matter lesions in an unselected cohort of the elderly: molecular pathology suggests origin from chronic hypoperfusion injury. *Stroke,* 37**,** 1391-8.

FLUCK, D., BEAUDIN, A. E., STEINBACK, C. D., KUMARPILLAI, G., SHOBHA, N., MCCREARY, C. R., PECA, S., SMITH, E. E. & POULIN, M. J. 2014. Effects of aging on the association between cerebrovascular responses to visual stimulation, hypercapnia and arterial stiffness. *Front Physiol,* 5**,** 49.

FOG, M. 1937. Cerebral circulation: The reaction of the pial arteries to a fall in blood pressure. *Archives of Neurology & Psychiatry,* 37**,** 351-364.

FOG, M. 1938. The Relationship between the Blood Pressure and the Tonic Regulation of the Pial Arteries. *J Neurol Psychiatry,* 1**,** 187-97.

FONTANA, J., WENZ, H., SCHMIEDER, K. & BARTH, M. 2015. Impairment of Dynamic Pressure Autoregulation Precedes Clinical Deterioration after Aneurysmal Subarachnoid Hemorrhage. *J Neuroimaging*.

FORBES, H. S. 1928. Cerebral circulation. I. Observation and measurement of pial vessels. . *Archives of Neurology & Psychiatry,* 19**,** 749-761.

FREITAS, J. 2010. *Sindromas de intolerância ortostática. Contribuição para o seu esclarecimento.* . Doctor, University of Porto.

FREITAS, J., ALMEIDA, J., AZEVEDO, E., CARVALHO, M. J., COSTA, O. & DE FREITAS, A. F. 1998. [Orthostatic intolerance. A review and clinical case]. *Rev Port Cardiol,* 17**,** 715-20.

FREITAS, J., AZEVEDO, E., SANTOS, R., MACIEL, M. J. & ROCHA-GONCALVES, F. 2015. Autonomic activity and biomarker behavior in supine position and after passive postural stress in different orthostatic intolerance syndromes. *Rev Port Cardiol,* 34**,** 543-9.

FREITAS, J., PEREIRA, S., LAGO, P., COSTA, O., CARVALHO, M. J. & FALCAO DE FREITAS, A. 1999. Impaired arterial baroreceptor sensitivity before tilt-induced syncope. *Europace,* 1**,** 258-65.

FREITAS, J., PUIG, J., CUNHA, D. L., COSTA, O. & DE FREITAS, A. F. 1994. [Syncope: how to deal with it?]. *Rev Port Cardiol,* 13**,** 133-40, 104.

FREITAS, J., SANTOS, R., AZEVEDO, E., CARVALHO, M., BOOMSMA, F., MEIRACKER, A., FALCAO DE FREITAS, A. & ABREU-LIMA, C. 2007. Hemodynamic, autonomic and neurohormonal behaviour of familial amyloidotic polyneuropathy and neurally mediated syncope patients during supine and orthostatic stress. *Int J Cardiol,* 116**,** 242-8.

FREITAS, J., SANTOS, R., AZEVEDO, E., COSTA, O., CARVALHO, M. & DE FREITAS, A. F. 2000. Clinical improvement in patients with orthostatic intolerance after treatment with bisoprolol and fludrocortisone. *Clin Auton Res,* 10**,** 293-9.

FURCHGOTT, R. F. & ZAWADZKI, J. V. 1980. The obligatory role of endothelial cells in the relaxation of arterial smooth muscle by acetylcholine. *Nature,* 288**,** 373-6.

GALEN, C. 1531. *De Anatomicis Administrationibus,* Paris, S. Colineus, Adrenarco JG.

GALVIN, S. D., CELI, L. A., THOMAS, K. N., CLENDON, T. R., GALVIN, I. F., BUNTON, R. W. & AINSLIE, P. N. 2010. Effects of age and coronary artery disease on cerebrovascular reactivity to carbon dioxide in humans. *Anaesth Intensive Care,* 38**,** 710-7.

GEEGANAGE, C. M. & BATH, P. M. 2009. Relationship between therapeutic changes in blood pressure and outcomes in acute stroke: a metaregression. *Hypertension,* 54**,** 775-81.

GEORGIADIS, D., SIEVERT, M., CENCETTI, S., UHLMANN, F., KRIVOKUCA, M., ZIERZ, S. & WERDAN, K. 2000. Cerebrovascular reactivity is impaired in patients with cardiac failure. *Eur Heart J,* 21**,** 407-13.

GIFFARD, C., YOUNG, A. R., KERROUCHE, N., DERLON, J. M. & BARON, J. C. 2004. Outcome of acutely ischemic brain tissue in prolonged middle cerebral artery occlusion: a serial positron emission tomography investigation in the baboon. *J Cereb Blood Flow Metab,* 24**,** 495-508.

GILLER, C. A. 1991. A Bedside Test for Cerebral Autoregulation Using Transcranial Doppler Ultrasound. *Acta Neurochirurgica,* 108**,** 7-14.

GIROUARD, H. & IADECOLA, C. 2006. Neurovascular coupling in the normal brain and in hypertension, stroke, and Alzheimer disease. *J Appl Physiol (1985),* 100**,** 328-35.

GONZALEZ, R. G., HAKIMELAHI, R., SCHAEFER, P. W., ROCCATAGLIATA, L., SORENSEN, A. G. & SINGHAL, A. B. 2010. Stability of large diffusion/perfusion mismatch in anterior circulation strokes for 4 or more hours. *BMC Neurol,* 10**,** 13.

GOYAL, M., MENON, B. K., VAN ZWAM, W. H., DIPPEL, D. W., MITCHELL, P. J., DEMCHUK, A. M., DAVALOS, A., MAJOIE, C. B., VAN DER LUGT, A., DE MIQUEL, M. A., DONNAN, G. A., ROOS, Y. B., BONAFE, A., JAHAN, R., DIENER, H. C., VAN DEN BERG, L. A., LEVY, E. I., BERKHEMER, O. A., PEREIRA, V. M., REMPEL, J., MILLAN, M., DAVIS, S. M., ROY, D., THORNTON, J., ROMAN, L. S., RIBO, M., BEUMER, D., STOUCH, B., BROWN, S., CAMPBELL, B. C., VAN OOSTENBRUGGE, R. J., SAVER, J. L., HILL, M. D. & JOVIN, T. G. 2016. Endovascular thrombectomy after large-vessel ischaemic stroke: a meta-analysis of individual patient data from five randomised trials. *Lancet,* 387**,** 1723-31.

HAEUSLER, K. G., LAUFS, U. & ENDRES, M. 2011. Chronic heart failure and ischemic stroke. *Stroke,* 42**,** 2977-82.

HALL, C. N., REYNELL, C., GESSLEIN, B., HAMILTON, N. B., MISHRA, A., SUTHERLAND, B. A., O'FARRELL, F. M., BUCHAN, A. M., LAURITZEN, M. & ATTWELL, D. 2014. Capillary pericytes regulate cerebral blood flow in health and disease. *Nature,* 508**,** 55-60.

HAMEL, E. 2006. Perivascular nerves and the regulation of cerebrovascular tone. *J Appl Physiol,* 100**,** 1059-64.

HAMNER, J. W. & TAN, C. O. 2014. Relative contributions of sympathetic, cholinergic, and myogenic mechanisms to cerebral autoregulation. *Stroke,* 45**,** 1771-7.

HARA, H., JANSEN, I., EKMAN, R., HAMEL, E., MACKENZIE, E. T., UDDMAN, R. & EDVINSSON, L. 1989. Acetylcholine and vasoactive intestinal peptide in cerebral blood vessels: effect of extirpation of the sphenopalatine ganglion. *J Cereb Blood Flow Metab,* 9**,** 204-11.

HARA, H., ZHANG, Q. J., KUROYANAGI, T. & KOBAYASHI, S. 1993. Parasympathetic cerebrovascular innervation: an anterograde tracing from the sphenopalatine ganglion in the rat. *Neurosurgery,* 32**,** 822-7; discussion 827.

HARDING, S. A. 2006. The role of vasodilators in the prevention and treatment of no-reflow following percutaneous coronary intervention. *Heart,* 92**,** 1191-3.
HARVEY, R. D. 2012. Muscarinic Receptor Agonists and Antagonists: Effects on Cardiovascular Function. *In:* FRYER, A. D., CHRISTOPOULOS, A. & NATHANSON, N. M. (eds.) *Muscarinic Receptors.* Berlin, Heidelberg: Springer Berlin Heidelberg.
HARVEY, W. 1628. *Exercitatio Anatomica de Motu Cordis et Sanguinis in Animalibus,* Francofurti, Fitzer.
HAUBRICH, C., KRUSKA, W., DIEHL, R. R., MOLLER-HARTMANN, W. & KLOTZSCH, C. 2003. Dynamic autoregulation testing in patients with middle cerebral artery stenosis. *Stroke,* 34**,** 1881-5.
HEISTAD, D. D., MARCUS, M. L. & ABBOUD, F. M. 1978. Role of large arteries in regulation of cerebral blood flow in dogs. *J Clin Invest,* 62**,** 761-8.
HENNERICI, M., RAUTENBERG, W., SITZER, G. & SCHWARTZ, A. 1987. Transcranial Doppler ultrasound for the assessment of intracranial arterial flow velocity--Part 1. Examination technique and normal values. *Surg Neurol,* 27**,** 439-48.
HETZEL, A., REINHARD, M., GUSCHLBAUER, B. & BRAUNE, S. 2003. Challenging cerebral autoregulation in patients with preganglionic autonomic failure. *Clin Auton Res,* 13**,** 27-35.
HILL, M. A., ZOU, H., POTOCNIK, S. J., MEININGER, G. A. & DAVIS, M. J. 2001. Invited review: arteriolar smooth muscle mechanotransduction: Ca(2+) signaling pathways underlying myogenic reactivity. *J Appl Physiol (1985),* 91**,** 973-83.
HILZ, M. J., KOLODNY, E. H., BRYS, M., STEMPER, B., HAENDL, T. & MARTHOL, H. 2004. Reduced cerebral blood flow velocity and impaired cerebral autoregulation in patients with Fabry disease. *J Neurol,* 251**,** 564-70.
HISHIKAWA, T., ONO, S., OGAWA, T., TOKUNAGA, K., SUGIU, K. & DATE, I. 2008. Effects of deferoxamine-activated hypoxia-inducible factor-1 on the brainstem after subarachnoid hemorrhage in rats. *Neurosurgery,* 62**,** 232-40; discussion 240-1.
HOSSMANN, K. A. 1994. Viability thresholds and the penumbra of focal ischemia. *Ann Neurol,* 36**,** 557-65.
HOSSMANN, K. A. 2006. Pathophysiology and therapy of experimental stroke. *Cell Mol Neurobiol,* 26**,** 1057-83.
HU, H. H., KUO, T. B., WONG, W. J., LUK, Y. O., CHERN, C. M., HSU, L. C. & SHENG, W. Y. 1999. Transfer function analysis of cerebral hemodynamics in patients with carotid stenosis. *J Cereb Blood Flow Metab,* 19**,** 460-5.
IADECOLA, C. 1993. Regulation of the cerebral microcirculation during neural activity: is nitric oxide the missing link? *Trends Neurosci,* 16**,** 206-14.
IADECOLA, C. 2004. Neurovascular regulation in the normal brain and in Alzheimer's disease. *Nat Rev Neurosci,* 5**,** 347-60.
IADECOLA, C. & NEDERGAARD, M. 2007. Glial regulation of the cerebral microvasculature. *Nat Neurosci,* 10**,** 1369-76.
IMHOLZ, B. P., WIELING, W., VAN MONTFRANS, G. A. & WESSELING, K. H. 1998. Fifteen years experience with finger arterial pressure monitoring: assessment of the technology. *Cardiovasc Res,* 38**,** 605-16.
IMMINK, R. V., VAN MONTFRANS, G. A., STAM, J., KAREMAKER, J. M., DIAMANT, M. & VAN LIESHOUT, J. J. 2005. Dynamic cerebral autoregulation in acute lacunar and middle cerebral artery territory ischemic stroke. *Stroke,* 36**,** 2595-600.
ITO, H. 2001. No reflow phenomenon in coronary heart disease. *J Cardiol,* 37 Suppl 1**,** 39-42.
IZZARD, A. S., GRAHAM, D., BURNHAM, M. P., HEERKENS, E. H., DOMINICZAK, A. F. & HEAGERTY, A. M. 2003. Myogenic and structural properties of cerebral arteries from the stroke-prone spontaneously hypertensive rat. *Am J Physiol Heart Circ Physiol,* 285**,** H1489-94.
JAUCH, E. C., SAVER, J. L., ADAMS, H. P., JR., BRUNO, A., CONNORS, J. J., DEMAERSCHALK, B. M., KHATRI, P., MCMULLAN, P. W., JR., QURESHI, A. I., ROSENFIELD, K., SCOTT, P. A., SUMMERS, D. R., WANG, D. Z., WINTERMARK, M. & YONAS, H. 2013a. Guidelines for the early management of patients with acute ischemic stroke: a guideline for healthcare professionals from the American Heart Association/American Stroke Association. *Stroke,* 44**,** 870-947.
JAUCH, E. C., SAVER, J. L., ADAMS, H. P., JR., BRUNO, A., CONNORS, J. J., DEMAERSCHALK, B. M., KHATRI, P., MCMULLAN, P. W., JR., QURESHI, A. I., ROSENFIELD, K., SCOTT, P. A., SUMMERS, D. R., WANG, D. Z., WINTERMARK, M., YONAS, H., AMERICAN HEART ASSOCIATION STROKE, C., COUNCIL ON CARDIOVASCULAR, N., COUNCIL ON PERIPHERAL VASCULAR, D. & COUNCIL ON CLINICAL, C. 2013b. Guidelines for the early management of patients with acute ischemic stroke: a guideline for healthcare professionals from the American Heart Association/American Stroke Association. *Stroke,* 44**,** 870-947.
JAUSS, M. & ZANETTE, E. 2000. Detection of right-to-left shunt with ultrasound contrast agent and transcranial Doppler sonography. *Cerebrovasc Dis,* 10**,** 490-6.
JENG, J. S., YIP, P. K., HUANG, S. J. & KAO, M. C. 1999. Changes in hemodynamics of the carotid and middle cerebral arteries before and after endoscopic sympathectomy in patients with palmar hyperhidrosis: preliminary results. *J Neurosurg,* 90**,** 463-7.
JOHNSON, P. C. 1981. Vascular Smooth Muscle. *Handbook of Physiology. The Cardiovascular System.* Bethesda: MD: American Physiological Society.
JOHNSON, P. C. 1986. Autoregulation of blood flow. *Circ Res,* 59**,** 483-95.
JORDAN, J., SHANNON, J. R., DIEDRICH, A., BLACK, B., COSTA, F., ROBERTSON, D. & BIAGGIONI, I. 2000. Interaction of carbon dioxide and sympathetic nervous system activity in the regulation of cerebral perfusion in humans. *Hypertension,* 36**,** 383-8.
KANEKO, Z. 1986. First steps in the development of the Doppler flowmeter. *Ultrasound Med Biol,* 12**,** 187-95.
KETY, S. S. & SCHMIDT, C. F. 1945. The determination of cerebral blood flow in man by the use of nitrous oxide in low concentrations. *Am J Physiol***,** 33–52.
KING, A. & MARKUS, H. S. 2009. Doppler embolic signals in cerebrovascular disease and prediction of stroke risk: a systematic review and meta-analysis. *Stroke,* 40**,** 3711-7.
KLABUNDE, R. 2011. Cardiovascular Physiology Concepts. Wolters Kluwer Health.
KLINGELHÖFER, J. 2016. Functional transcranial ultrasound. *In:* CSIBA, L. & BARACCHINI, C. (eds.) *Manual of neurosonology.* Cambridge: Cambridge University Press.
KNECHT, S., DEPPE, M., RINGELSTEIN, E. B., WIRTZ, M., LOHMANN, H., DRAGER, B., HUBER, T. & HENNINGSEN, H. 1998. Reproducibility of functional transcranial Doppler sonography in determining hemispheric language lateralization. *Stroke,* 29**,** 1155-9.
KNOT, H. J. & NELSON, M. T. 1998. Regulation of arterial diameter and wall [Ca2+] in cerebral arteries of rat by membrane potential and intravascular pressure. *J Physiol,* 508 (Pt 1)**,** 199-209.
KOCH, S., DELLA-MORTE, D., DAVE, K. R., SACCO, R. L. & PEREZ-PINZON, M. A. 2014. Biomarkers for ischemic preconditioning: finding the responders. *J Cereb Blood Flow Metab,* 34**,** 933-41.
KREJZA, J., MARIAK, Z., WALECKI, J., SZYDLIK, P., LEWKO, J. & USTYMOWICZ, A. 1999. Transcranial color Doppler sonography of basal cerebral arteries in 182 healthy subjects: age and sex variability and normal reference values for blood flow parameters. *AJR Am J Roentgenol,* 172**,** 213-8.

KUMAI, Y., KAMOUCHI, M., HATA, J., AGO, T., KITAYAMA, J., NAKANE, H., SUGIMORI, H., KITAZONO, T. & INVESTIGATORS, F. S. R. 2012. Proteinuria and clinical outcomes after ischemic stroke. *Neurology,* 78**,** 1909-15.

KUNZ, A. & IADECOLA, C. 2009. Cerebral vascular dysregulation in the ischemic brain. *Handb Clin Neurol,* 92**,** 283-305.

LAGI, A., CENCETTI, S., CORSONI, V., GEORGIADIS, D. & BACALLI, S. 2001. Cerebral vasoconstriction in vasovagal syncope: any link with symptoms? A transcranial Doppler study. *Circulation,* 104**,** 2694-8.

LANG, E. W., DIEHL, R. R. & MEHDORN, H. M. 2001. Cerebral autoregulation testing after aneurysmal subarachnoid hemorrhage: the phase relationship between arterial blood pressure and cerebral blood flow velocity. *Crit Care Med,* 29**,** 158-63.

LASSEN, N. A. 1959. Cerebral blood flow and oxygen consumption in man. *Physiol Rev,* 39**,** 183-238.

LAU, A. Y., ZHAO, Y., CHEN, C., LEUNG, T. W., FU, J., HUANG, Y., SUWANWELA, N. C., HAN, Z., TAN, K. S., RATANAKORN, D., MARKUS, H. S., WONG, K. S. & INVESTIGATORS, C. S. 2014. Dual antiplatelets reduce microembolic signals in patients with transient ischemic attack and minor stroke: subgroup analysis of CLAIR study. *Int J Stroke,* 9 Suppl A100**,** 127-32.

LEONARDI-BEE, J., BATH, P. M., PHILLIPS, S. J., SANDERCOCK, P. A. & GROUP, I. S. T. C. 2002. Blood pressure and clinical outcomes in the International Stroke Trial. *Stroke,* 33**,** 1315-20.

LI, G., LU, W. H., WU, X. W., CHENG, J., AI, R., ZHOU, Z. H. & TANG, Z. Z. 2015. Admission hypoxia-inducible factor 1alpha levels and in-hospital mortality in patients with acute decompensated heart failure. *BMC Cardiovasc Disord,* 15**,** 79.

LIEBESKIND, D. S. 2003. Collateral circulation. *Stroke,* 34**,** 2279-84.

LINDEGAARD, K. F., NORNES, H., BAKKE, S. J., SORTEBERG, W. & NAKSTAD, P. 1989. Cerebral vasospasm diagnosis by means of angiography and blood velocity measurements. *Acta Neurochir (Wien),* 100**,** 12-24.

LOUTZENHISER, R., GRIFFIN, K., WILLIAMSON, G. & BIDANI, A. 2006. Renal autoregulation: new perspectives regarding the protective and regulatory roles of the underlying mechanisms. *Am J Physiol Regul Integr Comp Physiol,* 290**,** R1153-67.

MA, H., GUO, Z. N., LIU, J., XING, Y., ZHAO, R. & YANG, Y. 2016. Temporal Course of Dynamic Cerebral Autoregulation in Patients With Intracerebral Hemorrhage. *Stroke,* 47**,** 674-81.

MADUREIRA, J., CASTRO, P. & AZEVEDO, E. 2017. Demographic and Systemic Hemodynamic Influences in Mechanisms of Cerebrovascular Regulation in Healthy Adults. *J Stroke Cerebrovasc Dis,* 26**,** 500-508.

MAGGIO, P., SALINET, A. S., PANERAI, R. B. & ROBINSON, T. G. 2013. Does hypercapnia-induced impairment of cerebral autoregulation affect neurovascular coupling? A functional TCD study. *J Appl Physiol (1985),* 115**,** 491-7.

MALOJCIC, B., GIANNAKOPOULOS, P., SOROND, F. A., AZEVEDO, E., DIOMEDI, M., OBLAK, J. P., CARRARO, N., BOBAN, M., OLAH, L., SCHREIBER, S. J., PAVLOVIC, A., GARAMI, Z., BORNSTEIN, N. M. & ROSENGARTEN, B. 2017. Ultrasound and dynamic functional imaging in vascular cognitive impairment and Alzheimer's disease. *BMC Med,* 15**,** 27.

MARKUS, H. S., DROSTE, D. W., KAPS, M., LARRUE, V., LEES, K. R., SIEBLER, M. & RINGELSTEIN, E. B. 2005. Dual antiplatelet therapy with clopidogrel and aspirin in symptomatic carotid stenosis evaluated using doppler embolic signal detection: the Clopidogrel and Aspirin for Reduction of Emboli in Symptomatic Carotid Stenosis (CARESS) trial. *Circulation,* 111**,** 2233-40.

MARKUS, H. S. & HARRISON, M. J. 1992. Estimation of cerebrovascular reactivity using transcranial Doppler, including the use of breath-holding as the vasodilatory stimulus. *Stroke,* 23**,** 668-73.

MARTINS, A. I., SARGENTO-FREITAS, J., SILVA, F., JESUS-RIBEIRO, J., CORREIA, I., GOMES, J. P., AGUIAR-GONCALVES, M., CARDOSO, L., MACHADO, C., RODRIGUES, B., SANTO, G. C. & CUNHA, L. 2016. Recanalization Modulates Association Between Blood Pressure and Functional Outcome in Acute Ischemic Stroke. *Stroke,* 47**,** 1571-6.

MATTEIS, M., TROISI, E., MONALDO, B. C., CALTAGIRONE, C. & SILVESTRINI, M. 1998. Age and sex differences in cerebral hemodynamics: a transcranial Doppler study. *Stroke,* 29**,** 963-7.

MCHEDLISHVILI, G. 1980. Physiological mechanisms controlling cerebral blood flow. *Stroke,* 11**,** 240-8.

MCHEDLISHVILI, G. I., MITAGVARIA, N. P. & ORMOTSADZE, L. G. 1973. Vascular mechanisms controlling a constant blood supply to the brain ("autoregulation"). *Stroke,* 4**,** 742-50.

MEEL-VAN DEN ABEELEN, A. S., SIMPSON, D. M., WANG, L. J., SLUMP, C. H., ZHANG, R., TARUMI, T., RICKARDS, C. A., PAYNE, S., MITSIS, G. D., KOSTOGLOU, K., MARMARELIS, V., SHIN, D., TZENG, Y. C., AINSLIE, P. N., GOMMER, E., MULLER, M., DORADO, A. C., SMIELEWSKI, P., YELICICH, B., PUPPO, C., LIU, X., CZOSNYKA, M., WANG, C. Y., NOVAK, V., PANERAI, R. B. & CLAASSEN, J. A. 2014a. Between-centre variability in transfer function analysis, a widely used method for linear quantification of the dynamic pressure-flow relation: the CARNet study. *Med Eng Phys,* 36**,** 620-7.

MEEL-VAN DEN ABEELEN, A. S., VAN BEEK, A. H., SLUMP, C. H., PANERAI, R. B. & CLAASSEN, J. A. 2014b. Transfer function analysis for the assessment of cerebral autoregulation using spontaneous oscillations in blood pressure and cerebral blood flow. *Med Eng Phys,* 36**,** 563-75.

MIJAJLOVIĆ, M. D., PAVLOVIĆ, A., BRAININ, M., HEISS, W. D., QUINN, T. J., IHLE-HANSEN, H. B., HERMANN, D. M., ASSAYAG, E. B., RICHARD, E., THIEL, A., KLIPER, E., SHIN, Y. I., KIM, Y. H., CHOI, S. H., JUNG, S., LEE, Y. B., SINANOVIĆ, O., LEVINE, D. A., SCHLESINGER, I., MEAD, G., MILOŠEVIĆ, V., LEYS, D., HAGBERG, G., URSIN, M. H., TEUSCHL, Y., PROKOPENKO, S., MOZHEYKO, E., BEZDENEZHNYKH, A., MATZ, K., ALEKSIĆ, V., MURESANU, D. F., KORCZYN, A. D. & BORNSTEIN, N. M. 2017. Post-stroke dementia – a comprehensive review. *BMC Med,* 15.

MITSIS, G. D., POULIN, M. J., ROBBINS, P. A. & MARMARELIS, V. Z. 2004. Nonlinear modeling of the dynamic effects of arterial pressure and CO2 variations on cerebral blood flow in healthy humans. *IEEE Trans Biomed Eng,* 51**,** 1932-43.

MOEHRING, M. A. & SPENCER, M. P. 2002. Power M-mode Doppler (PMD) for observing cerebral blood flow and tracking emboli. *Ultrasound Med Biol,* 28**,** 49-57.

MOLINA, C. A. & SAVER, J. L. 2005. Extending reperfusion therapy for acute ischemic stroke: emerging pharmacological, mechanical, and imaging strategies. *Stroke,* 36**,** 2311-20.

MOORE, D. F., ALTARESCU, G., LING, G. S., JEFFRIES, N., FREI, K. P., WEIBEL, T., CHARRIA-ORTIZ, G., FERRI, R., ARAI, A. E., BRADY, R. O. & SCHIFFMANN, R. 2002. Elevated cerebral blood flow velocities in Fabry disease with reversal after enzyme replacement. *Stroke,* 33**,** 525-31.

MOSSO, A. 1880. Sulla circolazione del sangue nel cervello dell'uomo. *R Accad Lincei,* 5**,** 237–358.

MULLIGAN, S. J. & MACVICAR, B. A. 2004. Calcium transients in astrocyte endfeet cause cerebrovascular constrictions. *Nature,* 431**,** 195-9.

MURRAY, C. J. & LOPEZ, A. D. 1997. Mortality by cause for eight regions of the world: Global Burden of Disease Study. *Lancet,* 349**,** 1269-76.

NABAVI, D. G., DROSTE, D. W., KEMENY, V., SCHULTE-ALTEDORNEBURG, G., WEBER, S. & RINGELSTEIN, E. B. 1998. Potential and limitations of echocontrast-enhanced ultrasonography in acute stroke patients: a pilot study. *Stroke,* 29**,** 949-54.

NAGANUMA, M., KOGA, M., SHIOKAWA, Y., NAKAGAWARA, J., FURUI, E., KIMURA, K., YAMAGAMI, H., OKADA, Y., HASEGAWA, Y., KARIO, K., OKUDA, S., NISHIYAMA, K., MINEMATSU, K. & TOYODA, K. 2011. Reduced estimated glomerular filtration rate is associated with stroke outcome after intravenous rt-PA: the Stroke Acute Management with Urgent Risk-Factor Assessment and Improvement (SAMURAI) rt-PA registry. *Cerebrovasc Dis,* 31**,** 123-9.

NAKAGAWA, K., SERRADOR, J. M., LAROSE, S. L. & SOROND, F. A. 2011. Dynamic cerebral autoregulation after intracerebral hemorrhage: A case-control study. *BMC Neurol,* 11**,** 108.

NAKAMURA, Y., ONO, H. & FROHLICH, E. D. 1999. Differential effects of T- and L-type calcium antagonists on glomerular dynamics in spontaneously hypertensive rats. *Hypertension,* 34**,** 273-8.

NELSON, E. & RENNELS, M. 1970. Innervation of intracranial arteries. *Brain,* 93**,** 475-90.

NEWELL, D. W. & AASLID, R. 1992. *Transcranial Doppler,* Nova Iorque, Raven Press.

NITAHARA, K. & DAN, K. 1998. Blood flow velocity changes in carotid and vertebral arteries with stellate ganglion block: measurement by magnetic resonance imaging using a direct bolus tracking method. *Reg Anesth Pain Med,* 23**,** 600-4.

NOLTE, J. & SUNDSTEN, J. W. 2009. The human brain : an introduction to its functional anatomy. *Blood supply of the brain.* 6th ed. Philadelphia, Pa.: Mosby Elsevier.

NOTH, U., KOTAJIMA, F., DEICHMANN, R., TURNER, R. & CORFIELD, D. R. 2008. Mapping of the cerebral vascular response to hypoxia and hypercapnia using quantitative perfusion MRI at 3 T. *NMR Biomed,* 21**,** 464-72.

NOUR, M., SCALZO, F. & LIEBESKIND, D. S. 2013. Ischemia-Reperfusion Injury in Stroke. *Interv Neurol,* 1**,** 185-99.

O'BRIEN, J. T., ERKINJUNTTI, T., REISBERG, B., ROMAN, G., SAWADA, T., PANTONI, L., BOWLER, J. V., BALLARD, C., DECARLI, C., GORELICK, P. B., ROCKWOOD, K., BURNS, A., GAUTHIER, S. & DEKOSKY, S. T. 2003. Vascular cognitive impairment. *Lancet Neurol,* 2**,** 89-98.

O'ROURKE, M. F. & SAFAR, M. E. 2005. Relationship between aortic stiffening and microvascular disease in brain and kidney: cause and logic of therapy. *Hypertension,* 46**,** 200-4.

OCON, A. J., KULESA, J., CLARKE, D., TANEJA, I., MEDOW, M. S. & STEWART, J. M. 2009. Increased phase synchronization and decreased cerebral autoregulation during fainting in the young. *Am J Physiol Heart Circ Physiol,* 297**,** H2084-95.

OGOH, S. 2008. Comments on Point:Counterpoint: Sympathetic activity does/does not influence cerebral blood flow. Autonomic nervous system influences dynamic cerebral blood flow. *J Appl Physiol (1985),* 105**,** 1370.

OGOH, S., DALSGAARD, M. K., SECHER, N. H. & RAVEN, P. B. 2007. Dynamic blood pressure control and middle cerebral artery mean blood velocity variability at rest and during exercise in humans. *Acta Physiol (Oxf),* 191**,** 3-14.

OLÁH, L. 2016. Ultrasound principles. *In:* CSIBA, L. & BARACCHINI, C. (eds.) *Manual of neurosonology.* Cambridge: Cambridge University Press.

OLESEN, S. P., CLAPHAM, D. E. & DAVIES, P. F. 1988. Haemodynamic shear stress activates a K+ current in vascular endothelial cells. *Nature,* 331**,** 168-70.

OLUIGBO, C. O., MAKONNEN, G., NAROUZE, S. & REZAI, A. R. 2011. Sphenopalatine ganglion interventions: technical aspects and application. *Prog Neurol Surg,* 24**,** 171-9.

OMBONI, S., PARATI, G., FRATTOLA, A., MUTTI, E., DI RIENZO, M., CASTIGLIONI, P. & MANCIA, G. 1993. Spectral and sequence analysis of finger blood pressure variability. Comparison with analysis of intra-arterial recordings. *Hypertension,* 22**,** 26-33.

OSOL, G., BREKKE, J. F., MCELROY-YAGGY, K. & GOKINA, N. I. 2002. Myogenic tone, reactivity, and forced dilatation: a three-phase model of in vitro arterial myogenic behavior. *Am J Physiol Heart Circ Physiol,* 283**,** H2260-7.

OSOL, G., LAHER, I. & CIPOLLA, M. 1991. Protein kinase C modulates basal myogenic tone in resistance arteries from the cerebral circulation. *Circ Res,* 68**,** 359-67.

OTITE, F., MINK, S., TAN, C. O., PURI, A., ZAMANI, A. A., MEHREGAN, A., CHOU, S., ORZELL, S., PURKAYASTHA, S., DU, R. & SOROND, F. A. 2014. Impaired cerebral autoregulation is associated with vasospasm and delayed cerebral ischemia in subarachnoid hemorrhage. *Stroke,* 45**,** 677-82.

OZKOR, M. A. & QUYYUMI, A. A. 2011. Endothelium-derived hyperpolarizing factor and vascular function. *Cardiol Res Pract,* 2011**,** 156146.

PANERAI, R. B. 1998. Assessment of cerebral pressure autoregulation in humans--a review of measurement methods. *Physiol Meas,* 19**,** 305-38.

PANERAI, R. B. 2003. The critical closing pressure of the cerebral circulation. *Med Eng Phys,* 25**,** 621-32.

PANERAI, R. B. 2009. Complexity of the human cerebral circulation. *Philos Transact A Math Phys Eng Sci,* 367**,** 1319-36.

PANERAI, R. B., EYRE, M. & POTTER, J. F. 2012. Multivariate modelling of cognitive-motor stimulation on neurovascular coupling: Transcranial Doppler used to characterize myogenic and metabolic influences. *Am J Physiol Regul Integr Comp Physiol*.

PANERAI, R. B., HAUNTON, V. J., HANBY, M. F., SALINET, A. S. & ROBINSON, T. G. 2016. Statistical criteria for estimation of the cerebral autoregulation index (ARI) at rest. *Physiol Meas,* 37**,** 661-72.

PANERAI, R. B., KELSALL, A. W., RENNIE, J. M. & EVANS, D. H. 1995. Estimation of critical closing pressure in the cerebral circulation of newborns. *Neuropediatrics,* 26**,** 168-73.

PANERAI, R. B., MOODY, M., EAMES, P. J. & POTTER, J. F. 2005. Cerebral blood flow velocity during mental activation: interpretation with different models of the passive pressure-velocity relationship. *J Appl Physiol,* 99**,** 2352-62.

PANERAI, R. B., RENNIE, J. M., KELSALL, A. W. & EVANS, D. H. 1998a. Frequency-domain analysis of cerebral autoregulation from spontaneous fluctuations in arterial blood pressure. *Med Biol Eng Comput,* 36**,** 315-22.

PANERAI, R. B., SAEED, N. P. & ROBINSON, T. G. 2015. Cerebrovascular effects of the thigh cuff maneuver. *Am J Physiol Heart Circ Physiol,* 308**,** H688-96.

PANERAI, R. B., SALINET, A. S., BRODIE, F. G. & ROBINSON, T. G. 2011. The influence of calculation method on estimates of cerebral critical closing pressure. *Physiol Meas,* 32**,** 467-82.

PANERAI, R. B., SAMMONS, E. L., SMITH, S. M., RATHBONE, W. E., BENTLEY, S., POTTER, J. F. & SAMANI, N. J. 2008. Continuous estimates of dynamic cerebral autoregulation: influence of non-invasive arterial blood pressure measurements. *Physiol Meas,* 29**,** 497-513.

PANERAI, R. B., WHITE, R. P., MARKUS, H. S. & EVANS, D. H. 1998b. Grading of cerebral dynamic autoregulation from spontaneous fluctuations in arterial blood pressure. *Stroke,* 29**,** 2341-6.

PAULSON, O. B., STRANDGAARD, S. & EDVINSSON, L. 1990. Cerebral autoregulation. *Cerebrovasc Brain Metab Rev,* 2**,** 161-92.

PIECHNIK, S. K., CHIARELLI, P. A. & JEZZARD, P. 2008. Modelling vascular reactivity to investigate the basis of the relationship between cerebral blood volume and flow under CO2 manipulation. *Neuroimage,* 39**,** 107-18.

POHL, U., HOLTZ, J., BUSSE, R. & BASSENGE, E. 1986. Crucial role of endothelium in the vasodilator response to increased flow in vivo. *Hypertension,* 8**,** 37-44.

POSTERT, T., FEDERLEIN, J., PRZUNTEK, H. & BUTTNER, T. 1997. Insufficient and absent acoustic temporal bone window: potential and limitations of transcranial contrast-enhanced color-coded sonography and contrast-enhanced power-based sonography. *Ultrasound Med Biol,* 23**,** 857-62.

POWERS, W. J., DERDEYN, C. P., BILLER, J., COFFEY, C. S., HOH, B. L., JAUCH, E. C., JOHNSTON, K. C., JOHNSTON, S. C., KHALESSI, A. A., KIDWELL, C. S., MESCHIA, J. F., OVBIAGELE, B. & YAVAGAL, D. R. 2015. 2015 AHA/ASA Focused Update of the 2013 Guidelines for the Early Management of Patients With Acute Ischemic Stroke Regarding Endovascular Treatment. *A Guideline for Healthcare Professionals From the American Heart Association/American Stroke Association*.

PRASS, K., RUSCHER, K., KARSCH, M., ISAEV, N., MEGOW, D., PRILLER, J., SCHARFF, A., DIRNAGL, U. & MEISEL, A. 2002. Desferrioxamine induces delayed tolerance against cerebral ischemia in vivo and in vitro. *J Cereb Blood Flow Metab,* 22**,** 520-5.

PURKAYASTHA, S., FADAR, O., MEHREGAN, A., SALAT, D. H., MOSCUFO, N., MEIER, D. S., GUTTMANN, C. R., FISHER, N. D., LIPSITZ, L. A. & SOROND, F. A. 2014. Impaired cerebrovascular hemodynamics are associated with cerebral white matter damage. *J Cereb Blood Flow Metab,* 34**,** 228-34.

PURKAYASTHA, S. & SOROND, F. A. 2014. Cerebral hemodynamics and the aging brain. *IJCNMH* S07.

RAEMER, D. B. & CALALANG, I. 1991. Accuracy of end-tidal carbon dioxide tension analyzers. *J Clin Monit,* 7**,** 195-208.

REINHARD, M., HETZEL, A., LAUK, M. & LUCKING, C. H. 2001. Dynamic cerebral autoregulation testing as a diagnostic tool in patients with carotid artery stenosis. *Neurol Res,* 23**,** 55-63.

REINHARD, M., NEUNHOEFFER, F., GERDS, T. A., NIESEN, W. D., BUTTLER, K. J., TIMMER, J., SCHMIDT, B., CZOSNYKA, M., WEILLER, C. & HETZEL, A. 2010. Secondary decline of cerebral autoregulation is associated with worse outcome after intracerebral hemorrhage. *Intensive Care Med,* 36**,** 264-71.

REINHARD, M., ROTH, M., GUSCHLBAUER, B., HARLOFF, A., TIMMER, J., CZOSNYKA, M. & HETZEL, A. 2005. Dynamic cerebral autoregulation in acute ischemic stroke assessed from spontaneous blood pressure fluctuations. *Stroke,* 36**,** 1684-9.

REINHARD, M., WIHLER, C., ROTH, M., HARLOFF, A., NIESEN, W. D., TIMMER, J., WEILLER, C. & HETZEL, A. 2008. Cerebral autoregulation dynamics in acute ischemic stroke after rtPA thrombolysis. *Cerebrovasc Dis,* 26**,** 147-55.

REUTERN, G. M., BUDINGEN, H. J., HENNERICI, M. & FREUND, H. J. 1976. [The diagnosis of stenoses and occlusions of the carotid arteries by means of directional Dopplersonography (author's transl)]. *Arch Psychiatr Nervenkr (1970),* 222**,** 191-207.

RINGELSTEIN, E. B., KAHLSCHEUER, B., NIGGEMEYER, E. & OTIS, S. M. 1990. Transcranial Doppler sonography: anatomical landmarks and normal velocity values. *Ultrasound Med Biol,* 16**,** 745-61.

RITTER, M. A., JURK, K., SCHRIEK, C., NABAVI, D. G., DROSTE, D. W., KEHREL, B. E. & BERND RINGELSTEIN, E. 2009. Microembolic signals on transcranial Doppler ultrasound are correlated with platelet activation markers, but not with platelet-leukocyte associates: a study in patients with acute stroke and in patients with asymptomatic carotid stenosis. *Neurol Res,* 31**,** 11-6.

ROBBINS, P. A., SWANSON, G. D., MICCO, A. J. & SCHUBERT, W. P. 1982. A fast gas-mixing system for breath-to-breath respiratory control studies. *J Appl Physiol Respir Environ Exerc Physiol,* 52**,** 1358-62.

ROCHA, H., CASTRO, P., SANTOS, R., AZEVEDO, E. & CARVALHO, M. 2014. Bilateral steno-occlusive disease of the middle cerebral artery: a case report with clinical-hemodynamic mismatch. *IJCNMH,* 1(Suppl. 1)**,** S26.

ROLFS, A., BOTTCHER, T., ZSCHIESCHE, M., MORRIS, P., WINCHESTER, B., BAUER, P., WALTER, U., MIX, E., LOHR, M., HARZER, K., STRAUSS, U., PAHNKE, J., GROSSMANN, A. & BENECKE, R. 2005. Prevalence of Fabry disease in patients with cryptogenic stroke: a prospective study. *Lancet,* 366**,** 1794-6.

ROSENGARTEN, B., DOST, A., KAUFMANN, A., GORTNER, L. & KAPS, M. 2002. Impaired cerebrovascular reactivity in type 1 diabetic children. *Diabetes Care,* 25**,** 408-10.

ROSENGARTEN, B., HUWENDIEK, O. & KAPS, M. 2001a. Neurovascular coupling and cerebral autoregulation can be described in terms of a control system. *Ultrasound Med Biol,* 27**,** 189-93.

ROSENGARTEN, B., HUWENDIEK, O. & KAPS, M. 2001b. Neurovascular coupling in terms of a control system: validation of a second-order linear system model. *Ultrasound Med Biol,* 27**,** 631-5.

ROTHWELL, P. M., COULL, A. J., SILVER, L. E., FAIRHEAD, J. F., GILES, M. F., LOVELOCK, C. E., REDGRAVE, J. N., BULL, L. M., WELCH, S. J., CUTHBERTSON, F. C., BINNEY, L. E., GUTNIKOV, S. A., ANSLOW, P., BANNING, A. P., MANT, D. & MEHTA, Z. 2005. Population-based study of event-rate, incidence, case fatality, and mortality for all acute vascular events in all arterial territories (Oxford Vascular Study). *Lancet,* 366**,** 1773-83.

ROULSTON, C. L., CALLAWAY, J. K., JARROTT, B., WOODMAN, O. L. & DUSTING, G. J. 2008. Using behaviour to predict stroke severity in conscious rats: post-stroke treatment with 3', 4'-dihydroxyflavonol improves recovery. *Eur J Pharmacol,* 584**,** 100-10.

ROY, C. S. & SHERRINGTON, C. S. 1890. On the Regulation of the Blood-supply of the Brain. *J Physiol,* 11**,** 85-158 17.

SAEED, A., DIBONA, G. F., GRIMBERG, E., NGUY, L., MIKKELSEN, M. L., MARCUSSEN, N. & GURON, G. 2014. High-NaCl diet impairs dynamic renal blood flow autoregulation in rats with adenine-induced chronic renal failure. *Am J Physiol Regul Integr Comp Physiol,* 306**,** R411-9.

SAEED, N. P., HORSFIELD, M. A., PANERAI, R. B., MISTRI, A. K. & ROBINSON, T. G. 2011. Measurement of cerebral blood flow responses to the thigh cuff maneuver: a comparison of TCD with a novel MRI method. *J Cereb Blood Flow Metab,* 31**,** 1302-10.

SAITO, K., MARKOWITZ, S. & MOSKOWITZ, M. A. 1988. Ergot alkaloids block neurogenic extravasation in dura mater: proposed action in vascular headaches. *Ann Neurol,* 24**,** 732-7.

SALINET, A. S., ROBINSON, T. G. & PANERAI, R. B. 2013. Active, passive, and motor imagery paradigms: component analysis to assess neurovascular coupling. *J Appl Physiol (1985),* 114**,** 1406-12.

SANTOS, G. A., PETERSEN, N., ZAMANI, A. A., DU, R., LAROSE, S., MONK, A., SOROND, F. A. & TAN, C. O. 2016. Pathophysiologic differences in cerebral autoregulation after subarachnoid hemorrhage. *Neurology,* 86**,** 1950-6.

SAQQUR, M., MOLINA, C. A., SALAM, A., SIDDIQUI, M., RIBO, M., UCHINO, K., CALLEJA, S., GARAMI, Z., KHAN, K., AKHTAR, N., O'ROURKE, F., SHUAIB, A., DEMCHUK, A. M., ALEXANDROV, A. V. & INVESTIGATORS, C. 2007. Clinical deterioration after

intravenous recombinant tissue plasminogen activator treatment: a multicenter transcranial Doppler study. *Stroke,* 38**,** 69-74.

SATOMURA, S. 1958. Study of the flow patterns in peripheral arteries by ultrasonics. *J Acoust Soc Jpn* 15**,** 151-158.

SCHONDORF, R., BENOIT, J. & STEIN, R. 2001. Cerebral autoregulation in orthostatic intolerance. *Ann N Y Acad Sci,* 940**,** 514-26.

SCHUBERT, R., LIDINGTON, D. & BOLZ, S. S. 2008. The emerging role of Ca2+ sensitivity regulation in promoting myogenic vasoconstriction. *Cardiovasc Res,* 77**,** 8-18.

SCHUBERT, R. & MULVANY, M. J. 1999. The myogenic response: established facts and attractive hypotheses. *Clin Sci (Lond),* 96**,** 313-26.

SEGAL, S. S. 2005. Regulation of blood flow in the microcirculation. *Microcirculation,* 12**,** 33-45.

SEGAL, S. S. 2008. Special Circulations. *In:* BOULPAEP, W. F. B. E. L. (ed.) *Medical Physiology.* W. B. Saunders Company.

SERCOMBE, R., AUBINEAU, P., EDVINSSON, L., MAMO, H., OWMAN, C. H., PINARD, E. & SEYLAZ, J. 1975. Neurogenic influence on local cerebral blood flow. Effect of catecholamines or sympathetic stimulation as correlated with the sympathetic innervation. *Neurology,* 25**,** 954-63.

SERRADOR, J. M., HUGHSON, R. L., KOWALCHUK, J. M., BONDAR, R. L. & GELB, A. W. 2006. Cerebral blood flow during orthostasis: role of arterial CO2. *Am J Physiol Regul Integr Comp Physiol,* 290**,** R1087-93.

SERRADOR, J. M., PICOT, P. A., RUTT, B. K., SHOEMAKER, J. K. & BONDAR, R. L. 2000. MRI measures of middle cerebral artery diameter in conscious humans during simulated orthostasis. *Stroke,* 31**,** 1672-8.

SERRADOR, J. M., SOROND, F. A., VYAS, M., GAGNON, M., ILOPUTAIFE, I. D. & LIPSITZ, L. A. 2005. Cerebral pressure-flow relations in hypertensive elderly humans: transfer gain in different frequency domains. *J Appl Physiol (1985),* 98**,** 151-9.

SHENKIN, H. A., CABIESES, F. & VAN DEN NOORDT, G. 1951. The effect of bilateral stellectomy upon the cerebral circulation of man. *J Clin Invest,* 30**,** 90-3.

SHIMIZU, T. 1994. Distribution and pathway of the cerebrovascular nerve fibers from the otic ganglion in the rat: anterograde tracing study. *J Auton Nerv Syst,* 49**,** 47-54.

SHOEMAKER, J. K., POZEG, Z. I. & HUGHSON, R. L. 1996. Forearm blood flow by Doppler ultrasound during test and exercise: tests of day-to-day repeatability. *Med Sci Sports Exerc,* 28**,** 1144-9.

SILVESTRINI, M., PAOLINO, I., VERNIERI, F., PEDONE, C., BARUFFALDI, R., GOBBI, B., CAGNETTI, C., PROVINCIALI, L. & BARTOLINI, M. 2009. Cerebral hemodynamics and cognitive performance in patients with asymptomatic carotid stenosis. *Neurology,* 72**,** 1062-8.

SILVESTRINI, M., TROISI, E., MATTEIS, M., CUPINI, L. M. & CALTAGIRONE, C. 1995. Involvement of the healthy hemisphere in recovery from aphasia and motor deficit in patients with cortical ischemic infarction: a transcranial Doppler study. *Neurology,* 45**,** 1815-20.

SILVESTRINI, M., VERNIERI, F., TROISI, E., PASSARELLI, F., MATTEIS, M., PASQUALETTI, P., ROSSINI, P. M. & CALTAGIRONE, C. 1999. Cerebrovascular reactivity in carotid artery occlusion: possible implications for surgical management of selected groups of patients. *Acta Neurol Scand,* 99**,** 187-91.

SIMARD, J. M., KENT, T. A., CHEN, M., TARASOV, K. V. & GERZANICH, V. 2007. Brain oedema in focal ischaemia: molecular pathophysiology and theoretical implications. *Lancet Neurol,* 6**,** 258-68.

SIMS, K., POLITEI, J., BANIKAZEMI, M. & LEE, P. 2009. Stroke in Fabry disease frequently occurs before diagnosis and in the absence of other clinical events: natural history data from the Fabry Registry. *Stroke,* 40**,** 788-94.

SLESSAREV, M., HAN, J., MARDIMAE, A., PRISMAN, E., PREISS, D., VOLGYESI, G., ANSEL, C., DUFFIN, J. & FISHER, J. A. 2007. Prospective targeting and control of end-tidal CO2 and O2 concentrations. *J Physiol,* 581**,** 1207-19.

SLOAN, M. A., ALEXANDROV, A. V., TEGELER, C. H., SPENCER, M. P., CAPLAN, L. R., FELDMANN, E., WECHSLER, L. R., NEWELL, D. W., GOMEZ, C. R., BABIKIAN, V. L., LEFKOWITZ, D., GOLDMAN, R. S., ARMON, C., HSU, C. Y., GOODIN, D. S., THERAPEUTICS & TECHNOLOGY ASSESSMENT SUBCOMMITTEE OF THE AMERICAN ACADEMY OF, N. 2004. Assessment: transcranial Doppler ultrasonography: report of the Therapeutics and Technology Assessment Subcommittee of the American Academy of Neurology. *Neurology,* 62**,** 1468-81.

SMEDA, J. S., VANVLIET, B. N. & KING, S. R. 1999. Stroke-prone spontaneously hypertensive rats lose their ability to auto-regulate cerebral blood flow prior to stroke. *J Hypertens,* 17**,** 1697-705.

SMIELEWSKI, P., CZOSNYKA, M., KIRKPATRICK, P., MCEROY, H., RUTKOWSKA, H. & PICKARD, J. D. 1996. Assessment of cerebral autoregulation using carotid artery compression. *Stroke,* 27**,** 2197-2203.

SMYTH, H. S., SLEIGHT, P. & PICKERIN.GW 1969. Reflex Regulation of Arterial Pressure during Sleep in Man - a Quantitative Method of Assessing Baroreflex Sensitivity. *Circulation Research,* 24**,** 109-&.

SOEHLE, M., CZOSNYKA, M., PICKARD, J. D. & KIRKPATRICK, P. J. 2004. Continuous assessment of cerebral autoregulation in subarachnoid hemorrhage. *Anesth Analg,* 98**,** 1133-9, table of contents.

SOINNE, L., HELENIUS, J., TATLISUMAK, T., SAIMANEN, E., SALONEN, O., LINDSBERG, P. J. & KASTE, M. 2003. Cerebral hemodynamics in asymptomatic and symptomatic patients with high-grade carotid stenosis undergoing carotid endarterectomy. *Stroke,* 34**,** 1655-61.

SOROND, F. A., GALICA, A., SERRADOR, J. M., KIELY, D. K., ILOPUTAIFE, I., CUPPLES, L. A. & LIPSITZ, L. A. 2010. Cerebrovascular hemodynamics, gait, and falls in an elderly population: MOBILIZE Boston Study. *Neurology,* 74**,** 1627-33.

SOROND, F. A., HURWITZ, S., SALAT, D. H., GREVE, D. N. & FISHER, N. D. 2013. Neurovascular coupling, cerebral white matter integrity, and response to cocoa in older people. *Neurology,* 81**,** 904-9.

SOROND, F. A., KIELY, D. K., GALICA, A., MOSCUFO, N., SERRADOR, J. M., ILOPUTAIFE, I., EGOROVA, S., DELL'OGLIO, E., MEIER, D. S., NEWTON, E., MILBERG, W. P., GUTTMANN, C. R. & LIPSITZ, L. A. 2011. Neurovascular coupling is impaired in slow walkers: the MOBILIZE Boston Study. *Ann Neurol,* 70**,** 213-20.

SOROND, F. A., TAN, C. O., LAROSE, S., MONK, A. D., FICHOROVA, R., RYAN, S. & LIPSITZ, L. A. 2015. Deferoxamine, Cerebrovascular Hemodynamics, and Vascular Aging: Potential Role for Hypoxia-Inducible Transcription Factor-1-Regulated Pathways. *Stroke,* 46**,** 2576-83.

SPENCER, M. P. 1977. Doppler ultrasonic imaging and non-invasive cerebrovascular evaluation. *Int J Neurol,* 11**,** 228-42.

SPENCER, M. P., REID, J. M., DAVIS, D. L. & PAULSON, P. S. 1974. Cervical carotid imaging with a continuous-wave Doppler flowmeter. *Stroke,* 5**,** 145-54.

STEINER, L. A., CZOSNYKA, M., PIECHNIK, S. K., SMIELEWSKI, P., CHATFIELD, D., MENON, D. K. & PICKARD, J. D. 2002. Continuous monitoring of cerebrovascular pressure reactivity allows determination of optimal cerebral perfusion pressure in patients with traumatic brain injury. *Crit Care Med,* 30**,** 733-8.

STRANDGAARD, S. & PAULSON, O. B. 1984. Cerebral autoregulation. *Stroke,* 15**,** 413-6.

STRBIAN, D., MERETOJA, A., PUTAALA, J., KASTE, M., TATLISUMAK, T. & HELSINKI STROKE THROMBOLYSIS REGISTRY, G. 2013. Cerebral edema in acute ischemic stroke patients treated with intravenous thrombolysis. *Int J Stroke,* 8**,** 529-34.

STRIDE, E., PORTER, C., PRIETO, A. G. & PANKHURST, Q. 2009. Enhancement of microbubble mediated gene delivery by simultaneous exposure to ultrasonic and magnetic fields. *Ultrasound Med Biol,* 35**,** 861-8.

STURZENEGGER, M., NEWELL, D. W. & AASLID, R. 1996. Visually evoked blood flow response assessed by simultaneous two-channel transcranial Doppler using flow velocity averaging. *Stroke,* 27**,** 2256-61.

SUN, D., HUANG, A., SMITH, C. J., STACKPOLE, C. J., CONNETTA, J. A., SHESELY, E. G., KOLLER, A. & KALEY, G. 1999. Enhanced release of prostaglandins contributes to flow-induced arteriolar dilation in eNOS knockout mice. *Circ Res,* 85**,** 288-93.

TAN, C. O., HAMNER, J. W. & TAYLOR, J. A. 2013. The role of myogenic mechanisms in human cerebrovascular regulation. *J Physiol,* 591**,** 5095-105.

TIECKS, F. P., DOUVILLE, C., BYRD, S., LAM, A. M. & NEWELL, D. W. 1996. Evaluation of impaired cerebral autoregulation by the Valsalva maneuver. *Stroke,* 27**,** 1177-82.

TIECKS, F. P., LAM, A. M., AASLID, R. & NEWELL, D. W. 1995a. Comparison of static and dynamic cerebral autoregulation measurements. *Stroke,* 26**,** 1014-9.

TIECKS, F. P., LAM, A. M., MATTA, B. F., STREBEL, S., DOUVILLE, C. & NEWELL, D. W. 1995b. Effects of the valsalva maneuver on cerebral circulation in healthy adults. A transcranial Doppler Study. *Stroke,* 26**,** 1386-92.

TIKHONOFF, V., ZHANG, H., RICHART, T. & STAESSEN, J. A. 2009. Blood pressure as a prognostic factor after acute stroke. *Lancet Neurol,* 8**,** 938-48.

TITIANOVA, E. & VASTAGH, I. 2016. Transcranial insonation. *In:* CSIBA, L. & BARACCHINI, C. (eds.) *Manual of neurosonology*. Cambridge: Cambridge University Press.

TOYODA, K. & NINOMIYA, T. 2014. Stroke and cerebrovascular diseases in patients with chronic kidney disease. *Lancet Neurol,* 13**,** 823-33.

TSIVGOULIS, G. & ALEXANDROV, A. V. 2009. Cerebral autoregulation impairment during wakefulness in obstructive sleep apnea syndrome is a potential mechanism increasing stroke risk. *Eur J Neurol,* 16**,** 283-4.

TZENG, Y. C., AINSLIE, P. N., COOKE, W. H., PEEBLES, K. C., WILLIE, C. K., MACRAE, B. A., SMIRL, J. D., HORSMAN, H. M. & RICKARDS, C. A. 2012. Assessment of cerebral autoregulation: the quandary of quantification. *Am J Physiol Heart Circ Physiol,* 303**,** H658-71.

TZENG, Y. C., CHAN, G. S., WILLIE, C. K. & AINSLIE, P. N. 2011. Determinants of human cerebral pressure-flow velocity relationships: new insights from vascular modelling and Ca(2)(+) channel blockade. *J Physiol,* 589**,** 3263-74.

TZENG, Y. C., LUCAS, S. J., ATKINSON, G., WILLIE, C. K. & AINSLIE, P. N. 2010. Fundamental relationships between arterial baroreflex sensitivity and dynamic cerebral autoregulation in humans. *J Appl Physiol (1985),* 108**,** 1162-8.

UMEYAMA, T., KUGIMIYA, T., OGAWA, T., KANDORI, Y., ISHIZUKA, A. & HANAOKA, K. 1995. Changes in cerebral blood flow estimated after stellate ganglion block by single photon emission computed tomography. *J Auton Nerv Syst,* 50**,** 339-46.

VAN LIESHOUT, J. J. & SECHER, N. H. 2008. Point:Counterpoint: Sympathetic activity does/does not influence cerebral blood flow. Point: Sympathetic activity does influence cerebral blood flow. *J Appl Physiol,* 105**,** 1364-6.

VAN LIESHOUT, J. J., WIELING, W., KAREMAKER, J. M. & SECHER, N. H. 2003. Syncope, cerebral perfusion, and oxygenation. *J Appl Physiol,* 94**,** 833-48.

VEMMOS, K. N., TSIVGOULIS, G., SPENGOS, K., ZAKOPOULOS, N., SYNETOS, A., MANIOS, E., KONSTANTOPOULOU, P. & MAVRIKAKIS, M. 2004. U-shaped relationship between mortality and admission blood pressure in patients with acute stroke. *J Intern Med,* 255**,** 257-65.

VERNIERI, F., PASQUALETTI, P., MATTEIS, M., PASSARELLI, F., TROISI, E., ROSSINI, P. M., CALTAGIRONE, C. & SILVESTRINI, M. 2001. Effect of collateral blood flow and cerebral vasomotor reactivity on the outcome of carotid artery occlusion. *Stroke,* 32**,** 1552-8.

VIDEIRA, G., CASTRO, P., VIEIRA, B., FILIPE, J. P., SANTOS, R., AZEVEDO, E., SA, M. J. & ABREU, P. 2016. Autonomic dysfunction in multiple sclerosis is better detected by heart rate variability and is not correlated with central autonomic network damage. *J Neurol Sci,* 367**,** 133-7.

VISOCCHI, M., CHIAPPINI, F., CIONI, B. & MEGLIO, M. 1996. Cerebral blood flow velocities and trigeminal ganglion stimulation. A transcranial Doppler study. *Stereotact Funct Neurosurg,* 66**,** 184-92.

VON REUTERN, G.-M., GOERTLER, M.-W., BORNSTEIN, N. M., SETTE, M. D., EVANS, D. H., GOERTLER, M.-W., HETZEL, A., KAPS, M., PERREN, F., RAZUMOVKY, A., SHIOGAI, T., TITIANOVA, E., TRAUBNER, P., VENKETASUBRAMANIAN, N., WONG, L. K. S. & YASAKA, M. 2012. Grading Carotid Stenosis Using Ultrasonic Methods. *Stroke,* 43**,** 916-921.

VORSTRUP, S., HENRIKSEN, L. & PAULSON, O. B. 1984. Effect of acetazolamide on cerebral blood flow and cerebral metabolic rate for oxygen. *J Clin Invest,* 74**,** 1634-9.

WAHLGREN, N., MOREIRA, T., MICHEL, P., STEINER, T., JANSEN, O., COGNARD, C., MATTLE, H. P., VAN ZWAM, W., HOLMIN, S., TATLISUMAK, T., PETERSSON, J., CASO, V., HACKE, W., MAZIGHI, M., ARNOLD, M., FISCHER, U., SZIKORA, I., PIEROT, L., FIEHLER, J., GRALLA, J., FAZEKAS, F. & LEES, K. R. 2016. Mechanical thrombectomy in acute ischemic stroke: Consensus statement by ESO-Karolinska Stroke Update 2014/2015, supported by ESO, ESMINT, ESNR and EAN. *Int J Stroke,* 11**,** 134-47.

WANG, X., LIN, W. H., ZHAO, Y. D., CHEN, X. Y., LEUNG, T. W., CHEN, C., FU, J., MARKUS, H., HAO, Q., WONG, K. S. & INVESTIGATORS, C. S. 2013. The effectiveness of dual antiplatelet treatment in acute ischemic stroke patients with intracranial arterial stenosis: a subgroup analysis of CLAIR study. *Int J Stroke,* 8**,** 663-8.

WANG, X. & LO, E. H. 2003. Triggers and mediators of hemorrhagic transformation in cerebral ischemia. *Mol Neurobiol,* 28**,** 229-44.

WARDLAW, J. M. 2010. Blood-brain barrier and cerebral small vessel disease. *J Neurol Sci,* 299**,** 66-71.

WARDLAW, J. M., DOUBAL, F., ARMITAGE, P., CHAPPELL, F., CARPENTER, T., MUNOZ MANIEGA, S., FARRALL, A., SUDLOW, C., DENNIS, M. & DHILLON, B. 2009. Lacunar stroke is associated with diffuse blood-brain barrier dysfunction. *Ann Neurol,* 65**,** 194-202.

WEPFER, J. J. 1658. *Observationes Anatomicae, Ex Cadaverius Eorum, Quo Sustulit Apoplexia, cum Exercitatione de Eius Loco Affecto,* Schaffhausen, JC Suterus.

WHITELEY, W. N., SLOT, K. B., FERNANDES, P., SANDERCOCK, P. & WARDLAW, J. 2012. Risk factors for intracranial hemorrhage in acute ischemic stroke patients treated with recombinant tissue plasminogen activator: a systematic review and meta-analysis of 55 studies. *Stroke,* 43**,** 2904-9.

WILLIAMS, L. R. & LEGGETT, R. W. 1989. Reference values for resting blood flow to organs of man. *Clin Phys Physiol Meas,* 10**,** 187-217.

WILLIE, C. K., COLINO, F. L., BAILEY, D. M., TZENG, Y. C., BINSTED, G., JONES, L. W., HAYKOWSKY, M. J., BELLAPART, J., OGOH, S., SMITH, K. J., SMIRL, J. D., DAY, T. A., LUCAS, S. J., ELLER, L. K. & AINSLIE, P. N. 2011. Utility of transcranial Doppler ultrasound for the integrative assessment of cerebrovascular function. *J Neurosci Methods,* 196**,** 221-37.

WILLIE, C. K., MACLEOD, D. B., SHAW, A. D., SMITH, K. J., TZENG, Y. C., EVES, N. D., IKEDA, K., GRAHAM, J., LEWIS, N. C., DAY, T. A. & AINSLIE, P. N. 2012. Regional brain blood flow in man during acute changes in arterial blood gases. *J Physiol,* 590**,** 3261-75.

WILLIE, C. K., TZENG, Y. C., FISHER, J. A. & AINSLIE, P. N. 2014. Integrative regulation of human brain blood flow. *J Physiol,* 592**,** 841-59.

WILLIS, T. 1664. *Cerebri Anatome: Cui Accessit Nervorum Descriptio et Usus,* London, J Flesher.

WONG, K. S., CHEN, C., FU, J., CHANG, H. M., SUWANWELA, N. C., HUANG, Y. N., HAN, Z., TAN, K. S., RATANAKORN, D., CHOLLATE, P., ZHAO, Y., KOH, A., HAO, Q., MARKUS, H. S. & INVESTIGATORS, C. S. 2010. Clopidogrel plus aspirin versus aspirin alone for reducing embolisation in patients with acute symptomatic cerebral or carotid artery stenosis (CLAIR study): a randomised, open-label, blinded-endpoint trial. *Lancet Neurol,* 9**,** 489-97.

YAMADA, M., LAMPING, K. G., DUTTAROY, A., ZHANG, W., CUI, Y., BYMASTER, F. P., MCKINZIE, D. L., FELDER, C. C., DENG, C. X., FARACI, F. M. & WESS, J. 2001. Cholinergic dilation of cerebral blood vessels is abolished in M(5) muscarinic acetylcholine receptor knockout mice. *Proc Natl Acad Sci U S A,* 98**,** 14096-101.

YAMAMOTO, M., MEYER, J. S., SAKAI, F. & YAMAGUCHI, F. 1980. Aging and cerebral vasodilator responses to hypercarbia: responses in normal aging and in persons with risk factors for stroke. *Arch Neurol,* 37**,** 489-96.

YANG, S., CAI, J., LU, R., WU, J., ZHANG, M. & ZHOU, X. 2017. Association Between Serum Cystatin C Level and Total Magnetic Resonance Imaging Burden of Cerebral Small Vessel Disease in Patients With Acute Lacunar Stroke. *J Stroke Cerebrovasc Dis,* 26**,** 186-191.

ZHANG, R., CRANDALL, C. G. & LEVINE, B. D. 2004a. Cerebral hemodynamics during the Valsalva maneuver: insights from ganglionic blockade. *Stroke,* 35**,** 843-7.

ZHANG, R. & LEVINE, B. D. 2007. Autonomic ganglionic blockade does not prevent reduction in cerebral blood flow velocity during orthostasis in humans. *Stroke,* 38**,** 1238-44.

ZHANG, R., WILSON, T. E., WITKOWSKI, S., CUI, J., CRANDALL, G. G. & LEVINE, B. D. 2004b. Inhibition of nitric oxide synthase does not alter dynamic cerebral autoregulation in humans. *Am J Physiol Heart Circ Physiol,* 286**,** H863-9.

ZHANG, R., ZUCKERMAN, J. H., GILLER, C. A. & LEVINE, B. D. 1998. Transfer function analysis of dynamic cerebral autoregulation in humans. *Am J Physiol,* 274**,** H233-41.

ZHANG, R., ZUCKERMAN, J. H., IWASAKI, K., WILSON, T. E., CRANDALL, C. G. & LEVINE, B. D. 2002. Autonomic neural control of dynamic cerebral autoregulation in humans. *Circulation,* 106**,** 1814-20.

ZIMMERMANN, C., WIMMER, M. & HABERL, R. L. 2004. L-Arginine-Mediated Vasoreactivity in Patients with a Risk of Stroke. *Cerebrovascular Diseases,* 17**,** 128-133.

ZIV, I., FLEMINGER, G., DJALDETTI, R., ACHIRON, A., MELAMED, E. & SOKOLOVSKY, M. 1992. Increased plasma endothelin-1 in acute ischemic stroke. *Stroke,* 23**,** 1014-6.

X. ANEXOS

Compilação dos artigos científicos iniciais sobre hemodinâmica que contribuíram para o desenvolvimento do projeto da dissertação

Adaptation of cerebral pressure-velocity hemodynamic changes of neurovascular coupling to orthostatic challenge

---

Castro, P., Santos, R., Freitas, J., Rosengarten, B., Panerai, R., & Azevedo, E. (2012). Adaptation of cerebral pressure-velocity hemodynamic changes of neurovascular coupling to orthostatic challenge. *Perspectives in Medicine, 1*(1–12), 290-296. doi: http://dx.doi.org/10.1016/j.permed.2012.02.052

Perspectives in Medicine (2012) 1, 290–296

ELSEVIER
URBAN & FISCHER

Bartels E, Bartels S, Poppert H (Editors):
New Trends in Neurosonology and Cerebral Hemodynamics — an Update.
Perspectives in Medicine (2012) 1, 290–296

journal homepage: www.elsevier.com/locate/permed

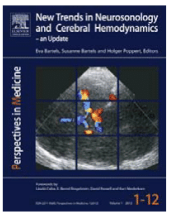

Adaptation of cerebral pressure-velocity hemodynamic changes of neurovascular coupling to orthostatic challenge

Pedro Castro[a,*], **Rosa Santos**[a], **João Freitas**[b], **Bernhard Rosengarten**[c], **Ronney Panerai**[d], **Elsa Azevedo**[a]

[a] *Dept. Neurology, Hospital São João, Faculty of Medicine of University of Porto, Portugal*
[b] *Autonomic Unit, Hospital São João, Faculty of Medicine of University of Porto, Portugal*
[c] *Dept. Neurology, University of Giessen, Germany*
[d] *Dept. Cardiovascular Sciences, University of Leicester, United Kingdom*

KEYWORDS
Transcranial Doppler;
Brain activation studies;
Cerebral hemodynamics;
Neurovascular coupling;
Cerebral autoregulation;
Critical closing pressure

Summary Neurovascular coupling (NVC), analysed by a control system approach, was shown to be unaffected by orthostatic challenge, but data is lacking regarding the mechanism of this interplay and the behaviour of other cerebrovascular reactivity parameters. We investigated the changes in different pressure—velocity models during functional transcranial Doppler (TCD), under different orthostatic conditions.

Thirteen healthy volunteers performed a reading test stimulation task in sitting, supine and head-up tilt (HUT) positions. CBF velocity was monitored with TCD in the posterior cerebral artery, and blood pressure was monitored with Finapres. Cerebrovascular resistance index (CVRi) was compared to a two-parameter model including resistance-area product (RAP) and critical closing pressure (CrCP), in the maximal and in the stable phases of flow response to visual stimulation.

All cerebrovascular resistance parameters decreased with visual stimulation but the magnitude of their variation in each orthostatic condition was not similar. From supine to HUT, CrCP variation decreased (both maximal and stable phase $p = 0.001$). CVRi variation increased from sitting to HUT positions (maximal $p = 0.039$; stable phase $p = 0.033$). RAP variation to visual stimulation did not change between the three positions (maximal $p = 0.077$; stable phase $p = 0.188$).

Abbreviations: NVC, neurovascular coupling; ABP, arterial blood pressure; TCD, transcranial Doppler; CBF, cerebral blood flow; BFV, blood flow velocity; MCA, middle cerebral artery; PCA, posterior cerebral artery; HR., heart rate; CVRi, cerebrovascular resistance index; CrCP, critical closing pressure; RAP, resistance-area product.

* Corresponding author at: Dept. Neurology, Hospital São João, Faculty of Medicine of University of Porto, Alameda Professor Hernani Monteiro, 4200-319 Porto, Portugal. Tel.: +351 931725181; fax: +351 220919086.
E-mail addresses: pedromacc@gmail.com (P. Castro), rosampsantos2@gmail.com (R. Santos), jppafreitas@sapo.pt (J. Freitas), Bernhard.Rosengarten@neuro.med.uni-giessen.de (B. Rosengarten), rp9@leicester.ac.uk (R. Panerai), elsaazevedo@netcabo.pt (E. Azevedo).

doi:10.1016/j.permed.2012.02.052

A 2-parameter model of vascular resistance provided better discrimination for the effects of posture on NVC as shown by the adaptive changes in CrCP with orthostatic challenge, in comparison with the classical use of CVRi. These findings suggest that although NVC seemed unaffected by orthostatic challenge, more complex vasoregulative mechanisms are activated in different orthostatic conditions that could potentially be of diagnostic or prognostic value.

Introduction

The brain has the capability of maintaining continuous vascular supply of oxygen and glucose to support active neuronal populations [1—3]. Neurovascular coupling (NVC) matches cerebral blood flow (CBF) to different cortical areas metabolic demand [1,2]. Another physiological mechanism, cerebral autoregulation, maintains CBF stable against changes in cerebral perfusion pressure and thus changes in arterial blood pressure (ABP) [4,5].

The NVC is studied with different techniques such as MRI, PET, SPECT and transcranial Doppler (TCD). Due to technical reasons the postural condition of the patients varies with these approaches. A recent focus on a disturbed NVC has been outlined in stroke [6], Alzheimer [7], and autonomic failure [8] diseases. For these reasons, a better understanding of NVC mechanism in different orthostatic conditions can have an impact both in scientific and clinical grounds.

There have been remarkable developments in the two last decades about our understanding of the underlying neurogenic, myogenic and metabolic components driving NVC [9,10]. Neurons, as well as astrocytes, seem to play an important role in focal CBF activation leading to upstream vasodilation from the microvasculature through pial arteries supplying focal activated area [11—13]. Probably, the same resistance vessels play an important role in the cerebral autoregulation [14], so that the vascular tonus of the cortical arterioles might be adjusted in accordance to the needs of both the cerebral autoregulation as well as the NVC. A previous study [15] has shown that activity-induced flow velocity responses under different orthostatic conditions can be compared with each other, but the mechanisms that keep NVC unaffected under orthostatic stress remained obscure. To further investigate this issue, we studied the behaviour of systemic and cerebral pressure—velocity parameters during functional TCD (fTCD) monitoring, under different orthostatic conditions, by extending the classical representation of cerebrovascular resistance to a more realistic 2-parameter model [21—23].

Materials and methods

Subjects

This study was performed in Hospital São João, a 1200-bed university hospital in Oporto. The local institutional ethical committee approved the study. After information and instruction each volunteer gave informed consent to participate in the study.

Thirteen young adult volunteers (8 male) with mean ± SD age 26.4 ± 8.7 years (range 18—48 years), were included. These subjects lacked classical cardiovascular risk factors and did not take any medication, except for birth control pills. They abstained from caffeine more than 12 h before the tests. Previously to the study, the volunteers performed a cervical and transcranial duplex scan, with a HDI 5000 device (Philips, USA). Normal findings and a good temporal acoustic bone window to ensure a good acquisition of velocity curves during the whole test were required as an inclusion criterion.

Measurements

The study was carried out in a quiet room with a constant temperature of approximately 22 °C. Systolic, mean and diastolic blood pressure and heart rate were monitored with a non-invasive finger cuff Finapres device (model 2300; Ohmeda, Englewood, CO, USA) holding the finger at heart level. A hand support was used to allow a constant position throughout the tests in the three different postural conditions [15,16].

For insonation through the temporal transcranial ultrasonic bone window, 2 MHz pulsed wave Doppler monitoring probes of a Multidop T2 Doppler device (DWL, Singen, Germany) were mounted on an individually fitted headband, to record flow velocity in the P2 segment of the left posterior cerebral artery (PCA), and the M1 segment of the right middle cerebral artery (MCA), as described elsewhere [15,17,18]. Beat-to-beat peak systolic, mean and end diastolic blood flow velocities (BFV), ABP, calculated heart rate (HR) and stimulus marker were digitally recorded in the Doppler device. Recordings were considered acceptable when the blood flow velocities could be detected bilaterally, with a clear envelope of the velocity spectrum during the entire cardiac cycle.

Visual-evoked paradigm

The visual-evoked paradigm consisted of 10 cycles, each with a resting phase of 20 s with closed eyes and a stimulating phase of 40 s of silent reading text columns. The text that the study subjects read was the same for all participants and free of strong emotional content. Changes between phases were signalled acoustically using a tone. The complete test cycle had a total duration of 10 min, and was repeated in each position — supine, sitting and 70° head-up tilt (HUT). The reading test and its reliability have been already validated against a checkerboard stimulation paradigm [19].

Data analysis

All signals were visually inspected to identify artifacts or noise, and narrow spikes were removed by linear interpolation. The heart—MCA distance was used to obtain estimates

of ABP in the MCA (ABP-MCA). Cerebrovascular resistance index (CVRi) was estimated by the ratio of mean ABP to mean BFV for each heartbeat. For both PCA and MCA, the instantaneous relationship between ABP and BFV was also used to estimate the critical closing pressure (CrCP) of the cerebral circulation, by extrapolation of the linear regression $BFV = a \times ABP + b$, as previously described [20—22]. The inverse of the linear regression slope was also obtained for each cardiac cycle, and it is referred to as ''resistance area product'' ($RAP = 1/a$) to differentiate it from CVRi [22,23]. The CrCP can be obtained from the value of ABP where $BFV = 0$, that is, $CrCP = -b/a$.

All beat-to-beat estimates were interpolated with a third-order polynomial and resampled at 0.2-s intervals to generate a time series with a uniform time base.

To become independent from the insonation angle, all parameters were normalized by the averaged value of the 5 s period prior to activation [8,15,17,19]. Ten cycles of 20 s rest (closed eyes) and 40 s stimulation (silent reading) were averaged for each volunteer at each position.

For each parameter, two different variables were calculated from the evoked CBF in response to visual task: (1) the maximal velocity variation during the 40 s of stimulation and (2) the averaged last 20 s corresponding to a stable phase of flow evoked response. The first one corresponds to the classical overshoot phase used in other fTCD investigations [24—29]; the second was included since it seems to be the most stable phase during activation, after the initial overshooting, and allows some comparison with the gain parameter of a second order analysis [14,15,19].

Statistics

Data were expressed as mean ± standard deviation (SD). Normal distribution of all variables was confirmed by Shapiro—Wilk test and homogeneity of the variances was assured by Levene's test.

Repeated-measures ANOVA with lower-bound adjustments for degrees of freedom were applied to compare absolute and relative data in the three positions — supine, sitting and HUT. Simple contrasts were applied to compare each two different positions in case of statistical significance, which was assumed for $p < 0.05$.

Results

Table 1 shows absolute resting values and relative maximal and stable phase (last 20 s) variations to visual stimulation of HR, mean ABP, mean BFV, CVRi, CrCP, and RAP, for PCA and MCA, in supine, sitting and HUT conditions.

Regarding only resting values, repeated-measures ANOVA showed a step increase in HR from supine to HUT positions ($p = 0.0001$), and of mean ABP from supine to sitting ($p = 0.0004$), then stabilizing. There was a step decrease in mean BFV of MCA from supine to HUT conditions ($p = 0.0004$) but for the PCA it seemed to remain constant ($p = 0.054$) in all positions. Concerning resting data of cerebrovascular resistance models, RAP did not change between different positions, while CVRi and CrCP resting values progressively increased from supine to HUT conditions, in both MCA ($p = 0.00001$ and $p = 0.0002$, respectively) and PCA ($p = 0.0002$ and $p = 0.00005$, respectively), although not reaching statistical significance between sitting and HUT in the case of CVRi of PCA ($p = 0.053$).

The variation of the parameters with visual stimulation can be visualized in Fig. 1A—F. Mean BFV in the PCA, had similar responses to visual stimulation in all positions (Fig. 1A, maximal $p = 0.076$; stable phase $p = 0.176$). All cerebrovascular resistance parameters decreased with visual stimulation in the three positions, but showed different patterns in response to orthostatic challenge: variation of CrCP diminished progressively between supine and HUT (maximal and stable phase $p = 0.001$); CVRi decreased slightly but significantly more from sitting to HUT positions (maximal $p = 0.036$; stable phase $p = 0.033$). RAP seemed to have decreased more in HUT conditions but there was no statistical significance (maximal $p = 0.077$; stable phase $p = 0.188$).

Although the MCA territory was used as a control, being theoretically a non-stimulated territory, it registered, similarly across all conditions, a small amplitude increment in mean BFV (5—10%), as well as a decrement of CVRi (6—9%), RAP (9—11%) and CrCP (11—17%) at maximal evoked flow phase, which then tended to decrease in the stable phase. For the MCA significant changes were only observed for BFV in maximal ($p = 0.035$) and CVRi in maximal ($p = 0.029$) and stable phases ($p = 0.043$).

Regarding systemic hemodynamic data, the changes of ABP and HR with stimulation ranged no more than 4%, with no significant differences between positions, except for maximal increment of ABP which was inferior during HUT compared to supine condition ($p = 0.045$).

Discussion

Main findings

We confirmed previous findings showing that the BFV response to a reading paradigm was not altered by different orthostatic challenges [15], but have also demonstrated that the sensitivity of NVC to orthostasis is in fact manifested by regulatory mechanisms influencing the instantaneous pressure—velocity relationship.

Specifically, variation of CrCP following visual stimulation was progressively reduced, more than a half, during orthostatic challenge. Opposed to this pattern, RAP and CVRi seemed to decrease slightly more during HUT. From the changes in CVRi, one would assume that despite rising baseline resting values with seating and HUT, the correspondingly larger decreases with orthostasis during NVC activation (Table 1) would simply reflect arteriolar vasodilation to match the increased demand for O_2. The problems with the single-parameter model of CVR are two-fold. First, it has been demonstrated that instantaneous pressure—velocity relationships of the cerebral circulation do not tend to intercept the pressure axis at the origin [20,22]. Second, CVRi cannot explain the complexities of the interplay between NVC and dynamic cerebral autoregulation [32]. This complexity can be appreciated by the changes in CrCP and RAP. Although the temporal response of RAP (Fig. 1) was not significantly different for the three body positions considered, overall it tends to reflect the myogenic response of dynamic

Table 1 Absolute resting values and relative maximal and stable phase (last 20 s) variations to visual stimulation of HR, mean ABP, mean BFV, CVRi, CrCP, and RAP, for PCA and MCA, in supine, sitting and HUT conditions.

	Supine	Sitting	Tilt	ANOVA p[¶]
HR				
Resting (bpm)	68.7 ± 9.4	76.3 ± 11.9[*]	86.3 ± 9.0[*,†]	0.0001
Maximal vel. phase (%)	4.4 ± 3.3	2.9 ± 3.2	2.8 ± 2.0	0.279
Resting (mmHg)	0.7 ± 2.6	0.2 ± 3.6	−1.4 ± 2.6	0.067
Mean ABP				
Stable phase (%)	73.2 ± 11.7	89.8 ± 9.3[*]	93.8 ± 9.7[*]	0.0004
Maximal vel. phase (%)	3.2 ± 2.0	2.1 ± 1.2	1.4 ± 1.2[*]	0.045
Stable phase (%)	−0.2 ± 1.6	−0.5 ± 1.6	−1.1 ± 2.0	0.223
MCA				
Mean BFV				
Resting (mmHg cm^{-1} s^{-2})	60.4 ± 12.4	56.0 ± 10.6[*]	52.1 ± 10.1[*,†]	0.0004
Maximal vel. phase (%)	5.5 ± 1.7	7.0 ± 2.5	9.5 ± 4.2[*]	0.035
Stable phase (%)	1.2 ± 3.1	2.1 ± 2.7	4.7 ± 3.8	0.011
CVRi				
Resting (mmHg cm^{-1} s^{-2})	1.3 ± 0.4	1.6 ± 0.2[*]	1.9 ± 0.3[*,†]	0.00002
Maximal vel. phase (%)	−6.2 ± 2.7	−6.0 ± 1.7	−9.3 ± 3.7[*,†]	0.029
Stable phase (%)	−1.9 ± 4.4	−3.0 ± 1.8	−6.0 ± 3.8[*,†]	0.043
RAP				
Resting (mmHg cm^{-1} s^{-2})	0.8 ± 0.2	0.9 ± 0.2	0.8 ± 0.1	0.338
Maximal vel. phase (%)	−11.2 ± 8.0	−8.8 ± 5.4	−11.0 ± 4.2	0.567
Stable phase (%)	−2.5 ± 5.4	−1.5 ± 3.5	−1.5 ± 3.3	0.773
CrCP				
Resting (mmHg)	26.5 ± 13.9	42.4 ± 9.0[*]	51.5 ± 9.1[*,†]	0.0004
Maximal vel. phase (%)	−17.3 ± 12.3	−11.2 ± 6.6	−11.0 ± 5.6	0.061
Stable phase (%)	0.5 ± 6.5	−1.7 ± 4.9	−4.7 ± 3.6	0.070
PCA				
Mean BFV				
Resting (mmHg cm^{-1} s^{-2})	36.7 ± 6.8	33.6 ± 6.7	33.0 ± 5.8	0.054
Maximal vel. phase (%)	−32.0 ± 6.4	−33.9 ± 9.5	−37.7 ± 8.1	0.076
Stable phase (%)	−23.4 ± 5.6	−24.2 ± 7.6	−26.4 ± 6.8	0.176
CVRi				
Resting (mmHg cm^{-1} s^{-2})	2.1 ± 0.6	2.8 ± 0.6[*]	2.9 ± 0.6[*]	0.00006
Maximal vel. phase (%)	−25.0 ± 4.5	−25.2 ± 4.9	−27.6 ± 3.7[*,†]	0.039
Stable phase (%)	−21.5 ± 5.1	−22.4 ± 4.8	−24.9 ± 4.4[*,†]	0.033
RAP				
Resting (mmHg cm^{-1} s^{-2})	1.2 ± 0.3	1.3 ± 0.3	1.2 ± 0.2	0.077
Maximal vel. phase (%)	−15.6 ± 5.6	−14.7 ± 4.9	−19.9 ± 6.1	0.077
Stable phase (%)	−9.4 ± 5.4	−6.4 ± 6.1	−11.4 ± 8.3	0.188
CrCP				
Resting (mmHg)	29.3 ± 9.9	46.6 ± 7.0[*]	56.5 ± 9.4[*,†]	0.00002
Maximal vel. phase (%)	−44.1 ± 19.9	−27.2 ± 12.8[*]	−18.9 ± 6.3[*,†]	0.001
Stable phase (%)	−27.2 ± 12.2	−17.9 ± 10.0[*]	−11.7 ± 5.1[*,†]	0.001

Heart rate (HR), arterial blood pressure (ABP), middle cerebral artery (MCA), posterior cerebral artery (PCA), cerebral blood flow velocity (BFV), cerebrovascular resistance index (CVRi), resistance area product (RAP), critical closing pressure (CrCP). Resting and activation values are presented in mean ± SD and normalized percentual variation, respectively.

[¶] Repeated-measures ANOVA p test comparing three positions.

[*] Repeated-measures ANOVA $p < 0.05$ for contrast to supine position.

[†] Repeated-measures ANOVA $p < 0.05$ for contrast between sitting and head-up tilt position.

autoregulation, mainly as a compensation for the drop in ABP following neural stimulation (Fig. 1E). It is likely that some of its change also contributed to the rise in CBV during the response (Fig. 1A). On the other hand, it can be speculated that the changes in CrCP are mainly reflecting the action of metabolic mechanisms [22,33]. If this is the case, then it is not possible to say that the NVC response to reading is entirely indifferent to orthostasis, since reading and HUT seem to require less metabolic-coupled changes than responses in the supine position.

Some studies have shown significant [30,35–37] or no statistically significant [38] increases in ABP and HR during mental activation. Moody et al. [30] analysed the hemodynamic changes of cerebral and systemic responses, putting

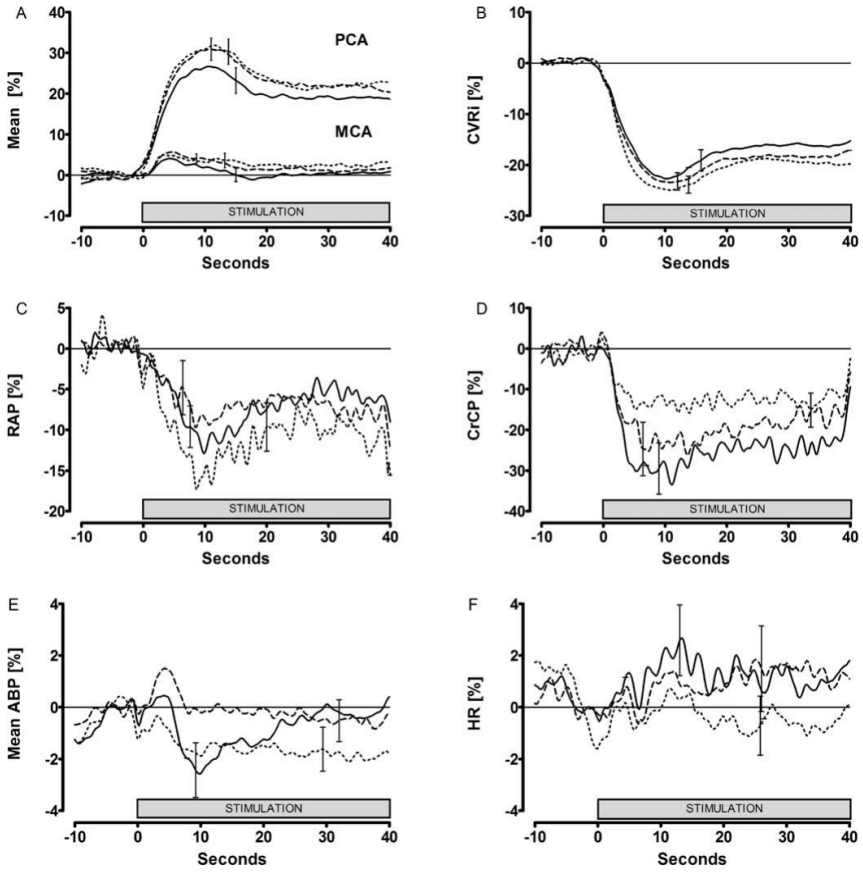

Figure 1 Group averaged normalized mean BFV (A), CVRi (B), RAP(C) and CrCP (D) of PCA [and mean BFV of MCA as a control (A)] and mean ABP (E) and HR (F) changes before and during 40 s of reading task (gray bar at bottom) in supine (*continuous line*), sitting (*dashed line*) and tilt (*dotted line*) positions. For clarity, only the largest ± SE is represented at the point of occurrence. (First 10 s of resting phase not shown only for graphical proposal.)

into evidence an initial ABP peak, ∼5 s after MCA cortical activation, that would drive an early-phase cerebral vasoconstriction reflected in increased CVRi and RAP, followed by metabolic vasodilatation. Our results showed non-significant changes in HR and ABP responses. A watchful eye through the curves of ABP in Fig. 1E might identify an initial ABP peak at ∼5 s only at sitting condition. Also, the previously described possible initial 'vasoconstriction response' [30] could not be demonstrated. With the same as ours activation paradigm, Rosengarten et al. [37] found no relevance of HR effects in regulative features of the activity—flow coupling during reading task. A possible explanation to discrepant findings between the studies can be a less demanding visual paradigm related to the PCA territory as compared to MCA-activation paradigm, rendering a less pronounced systemic/sympathetic response. On the other hand, even in a PCA evoked flow paradigm a small activation can sometimes be measured in the MCA territory, as in our study, which might reflect some activation of cortical areas, probably related to visual processing.

Limitations of the study

CO_2, a major determinant of cerebrovascular tone [31,33,34], was not evaluated, and could have influenced our results. However, we can speculate that relative hypocapnia in orthostasis [34], namely during HUT, and an assumed inverse relationship between CO_2 and CrCP [22], would cause absolute CrCP to increase from supine to HUT conditions and also would prevent a substantial decrease with cortical activation in HUT. Also, it is known that induced hypocapnia impairs NVC with a similar experimental protocol [29]. Given that these changes were not observed in our study, it is more likely that $PaCO_2$ remained relatively constant during the orthostatic challenges. The importance of CO_2 changes during mental activation was studied previously in a MCA-based protocol which analysed also CrCP—RAP variations [30] and found significant changes of CO_2 interacting with cerebral and systemic hemodynamic parameters. Nevertheless, the study by Moody et al. [35] adopted cognitive paradigms that can be much more stressful than plain reading and

hence might have caused significantly greater hyperventilation.

Conclusions

Taken together, we conclude that NVC has different pressure-autoregulatory adaptation mechanisms with orthostatic challenge, in spite of preserved cerebral evoked flow responses.

Analysis of the NVC response to reading based solely on the inspection of the BFV amplitude response gives the false impression of a lack of effect of orthostatic challenges. In reality, by looking separately at changes in RAP and CrCP, it is possible to appreciate the complex interplay of these responses at different levels of orthostatic challenge. Further work is needed to assess the response of these mechanisms in different cerebrovascular conditions and their potential diagnostic and prognostic value.

References

[1] Iadecola C. Neurovascular regulation in the normal brain and in Alzheimer's disease. Nat Rev 2004;5(5):347—60.

[2] Iadecola C. Regulation of the cerebral microcirculation during neural activity: is nitric oxide the missing link? Trends Neurosci 1993;16(6):206—14.

[3] Hossmann KA. Viability thresholds and the penumbra of focal ischemia. Ann Neurol 1994;36(4):557—65.

[4] Aaslid R, Lindegaard KF, Sorteberg W, Nornes H. Cerebral autoregulation dynamics in humans. Stroke: J Cereb Circ 1989;20(1):45—52.

[5] Paulson OB, Strandgaard S, Edvinsson L. Cerebral autoregulation. Cerebrovasc Brain Metab Rev 1990;2(2):161—92.

[6] Lin WH, Hao Q, Rosengarten B, Leung WH, Wong KS. Impaired neurovascular coupling in ischaemic stroke patients with large or small vessel disease. Eur J Neurol 2010;18(5):731—6.

[7] Rosengarten B, Paulsen S, Burr O, Kaps M. Neurovascular coupling in Alzheimer patients: effect of acetylcholine-esterase inhibitors. Neurobiol Aging 2009;30(12):1918—23.

[8] Azevedo E, Castro P, Santos R, Freitas J, Coelho T, Rosengarten B, et al. Autonomic dysfunction affects cerebral neurovascular coupling. Clin Auton Res 2011.

[9] Hamel E. Perivascular nerves and the regulation of cerebrovascular tone. J Appl Physiol 2006;100(3):1059—64.

[10] Iadecola C, Nedergaard M. Glial regulation of the cerebral microvasculature. Nat Neurosci 2007;10(11):1369—76.

[11] Cox SB, Woolsey TA, Rovainen CM. Localized dynamic changes in cortical blood flow with whisker stimulation corresponds to matched vascular and neuronal architecture of rat barrels. J Cereb Blood Flow Metab 1993;13(6):899—913.

[12] Ngai AC, Ko KR, Morii S, Winn HR. Effect of sciatic nerve stimulation on pial arterioles in rats. Am J Physiol 1988;254(1 (Pt 2)):H133—9.

[13] Silva AC, Lee SP, Iadecola C, Kim SG. Early temporal characteristics of cerebral blood flow and deoxyhemoglobin changes during somatosensory stimulation. J Cereb Blood Flow Metab 2000;20(1):201—6.

[14] Rosengarten B, Huwendiek O, Kaps M. Neurovascular coupling and cerebral autoregulation can be described in terms of a control system. Ultrasound Med Biol 2001;27(2):189—93.

[15] Azevedo E, Rosengarten B, Santos R, Freitas J, Kaps M. Interplay of cerebral autoregulation and neurovascular coupling evaluated by functional TCD in different orthostatic conditions. J Neurol 2007;254(2):236—41.

[16] Omboni S, Parati G, Frattola A, Mutti E, Di Rienzo M, Castiglioni P, et al. Spectral and sequence analysis of finger blood pressure variability. Comparison with analysis of intra-arterial recordings. Hypertension 1993;22(1):26—33.

[17] Azevedo E, Santos R, Freitas J, Rosas MJ, Gago M, Garrett C, et al. Deep brain stimulation does not change neurovascular coupling in non-motor visual cortex: an autonomic and visual evoked blood flow velocity response study. Parkinsonism Relat Disord 2010;16(9):600—3.

[18] Aaslid R, Markwalder TM, Nornes H. Noninvasive transcranial Doppler ultrasound recording of flow velocity in basal cerebral arteries. J Neurosurg 1982;57(6):769—74.

[19] Rosengarten B, Huwendiek O, Kaps M. Neurovascular coupling in terms of a control system: validation of a second-order linear system model. Ultrasound Med Biol 2001;27(5):631—5.

[20] Aaslid R, Lash SR, Bardy GH, Gild WH, Newell DW. Dynamic pressure—flow velocity relationships in the human cerebral circulation. Stroke: J Cereb Circ 2003;34(7):1645—9.

[21] Dawson SL, Panerai RB, Potter JF. Critical closing pressure explains cerebral hemodynamics during the Valsalva maneuver. J Appl Physiol 1999;86(2):675—80.

[22] Panerai RB. The critical closing pressure of the cerebral circulation. Med Eng Phys 2003;25(8):621—32.

[23] Evans DH, Levene MI, Shortland DB, Archer LN. Resistance index, blood flow velocity, and resistance-area product in the cerebral arteries of very low birth weight infants during the first week of life. Ultrasound Med Biol 1988;14(2):103—10.

[24] Aaslid R. Cerebral hemodynamics. New York: Raven Press; 1992.

[25] Conrad B, Klingelhofer J. Dynamics of regional cerebral blood flow for various visual stimuli. Exp Brain Res 1989;77(2):437—41.

[26] Gomez SM, Gomez CR, Hall IS. Transcranial Doppler ultrasonographic assessment of intermittent light stimulation at different frequencies. Stroke: J Cereb Circ 1990;21(12):1746—8.

[27] Wittich I, Klingelhöfer J, Sander D, Schwarze JJ. Visual evoked perfusion changes in the posterior cerebral artery during activity of various visual field sections. In: Klingelhöfer J, Bartels E, Ringelstein EB, Ebner TJ, editors. New trends in cerebral hemodynamics and neurosonology. Doetinchen: Elsevier; 1997. p. 548—56.

[28] Sturzenegger M, Newell DW, Aaslid R. Visually evoked blood flow response assessed by simultaneous two-channel transcranial Doppler using flow velocity averaging. Stroke: J Cereb Circ 1996;27(12):2256—61.

[29] Szabo K, Lako E, Juhasz T, Rosengarten B, Csiba L, Olah L. Hypocapnia induced vasoconstriction significantly inhibits the neurovascular coupling in humans. J Neurol Sci 2011;309(1—2):58—62.

[30] Moody M, Panerai RB, Eames PJ, Potter JF. Cerebral and systemic hemodynamic changes during cognitive and motor activation paradigms. Am J Physiol Regul Integr Comp Physiol 2005;288(6):R1581—8.

[31] Carey BJ, Eames PJ, Panerai RB, Potter JF. Carbon dioxide, critical closing pressure and cerebral haemodynamics prior to vasovagal syncope in humans. Clin Sci (Lond) 2001;101(4):351—8.

[32] Panerai RB, Moody M, Eames PJ, Potter JF. Cerebral blood flow velocity during mental activation: interpretation with different models of the passive pressure—velocity relationship. J Appl Physiol 2005;99(6):2352—62.

[33] Ainslie PN, Duffin J. Integration of cerebrovascular CO_2 reactivity and chemoreflex control of breathing: mechanisms of regulation, measurement, and interpretation. Am J Physiol Regul Integr Comp Physiol 2009;296(5):R1473—95.

[34] Serrador JM, Hughson RL, Kowalchuk JM, Bondar RL, Gelb AW. Cerebral blood flow during orthostasis: role of arterial CO_2. Am J Physiol Regul Integr Comp Physiol 2006;290(4): R1087—93.
[35] Sitzer M, Knorr U, Seitz RJ. Cerebral hemodynamics during sensorimotor activation in humans. J Appl Physiol 1994;77(6):2804—11.
[36] Tiecks FP, Haberl RL, Newell DW. Temporal patterns of evoked cerebral blood flow during reading. J Cereb Blood Flow Metab 1998;18(7):735—41.
[37] Rosengarten B, Budden C, Osthaus S, Kaps M. Effect of heart rate on regulative features of the cortical activity—flow coupling. Cerebrovasc Dis 2003;16(1): 47—52.
[38] Klingelhofer J, Matzander G, Sander D, Schwarze J, Boecker H, Bischoff C. Assessment of functional hemispheric asymmetry by bilateral simultaneous cerebral blood flow velocity monitoring. J Cereb Blood Flow Metab 1997;17(5): 577—85.

Autonomic dysfunction affects dynamic cerebral autoregulation during Valsalva maneuver: comparison between healthy and autonomic dysfunction subjects

---

Castro, P., Santos, R., Freitas, J., Panerai, R. B., & Azevedo, E. (2014). Autonomic dysfunction affects dynamic cerebral autoregulation during Valsalva maneuver: comparison between healthy and autonomic dysfunction subjects. *J Appl Physiol (1985), 117*(3), 205-213. doi: 10.1152/japplphysiol.00893.2013

J Appl Physiol 117: 205–213, 2014.
First published June 12, 2014; doi:10.1152/japplphysiol.00893.2013.

Autonomic dysfunction affects dynamic cerebral autoregulation during Valsalva maneuver: comparison between healthy and autonomic dysfunction subjects

Pedro M. Castro,[1] Rosa Santos,[1] João Freitas,[2] Ronney B. Panerai,[3] and Elsa Azevedo[1]

[1]*Department Neurology, São João Hospital Center, Faculty of Medicine of University of Porto, Porto, Portugal;* [2]*Autonomic Unit, São João Hospital Center, Faculty of Medicine of University of Porto, Porto, Portugal; and* [3]*Department of Cardiovascular Sciences and Biomedical Research Unit, University of Leicester, Leicester, United Kingdom*

Submitted 2 August 2013; accepted in final form 9 June 2014

Castro PM, Santos R, Freitas J, Panerai RB, Azevedo E. Autonomic dysfunction affects dynamic cerebral autoregulation during Valsalva maneuver: comparison between healthy and autonomic dysfunction subjects. *J Appl Physiol* 117: 205–213, 2014. First published June 12, 2014; doi:10.1152/japplphysiol.00893.2013.—The role of autonomic nervous system (ANS) in adapting cerebral blood flow (CBF) to arterial blood pressure (ABP) fluctuations [cerebral autoregulation (CA)] is still controversial. We aimed to study the repercussion of autonomic failure (AF) on dynamic CA during the Valsalva maneuver (VM). Eight AF subjects with familial amyloidotic polineuropahty (FAP) were compared with eight healthy controls. ABP and CBF velocity (CBFV) were measured continuously with Finapres and transcranial Doppler, respectively. Cerebrovascular response was evaluated by cerebrovascular resistance index (CVRi), critical closing pressure (CrCP), and resistance-area product (RAP) changes. Dynamic CA was derived from continuous estimates of autoregulatory index (ARI) [ARI(t)]. During phase II of VM, FAP subjects showed a more pronounced decrease in normalized CBFV (78 ± 19 and 111 ± 16%; $P = 0.002$), ABP (78 ± 19 and 124 ± 12%; $P = 0.0003$), and RAP (67 ± 17 and 89 ± 17%; $P = 0.019$) compared with controls. CrCP and CVRi increased similarly in both groups during strain. ARI(t) showed a biphasic variation in controls with initial increase followed by a decrease during phase II but in FAP this response was blunted (5.4 ± 3.0 and 2.0 ± 2.9; $P = 0.033$). Our data suggest that dynamic cerebral autoregulatory response is a time-varying phenomena during VM and that it is disturbed by autonomic dysfunction. This study also emphasizes the fact that RAP + CrCP model allowed additional insights into understanding of cerebral hemodynamics, showing a higher vasodilatory response expressed by RAP in AF and an equal CrCP response in both groups during the increased intracranial and intrathoracic pressure, while classical CVRi paradoxically suggests a cerebral vasoconstriction.

cerebral autoregulation; cerebral vasoreactivity; autonomic nervous system; Valsalva maneuver; transcranial Doppler

THE ROLE OF AUTONOMIC NERVOUS system (ANS) in the adaptation of the cerebral vasculature to arterial blood pressure (ABP) fluctuations, commonly referred to as dynamic cerebral autoregulation (CA), has been the subject of ongoing debate (5, 15, 22, 33, 50, 51, 53). Besides considerable physiological interest, it can have profound clinical impact since ANS dysfunction is related to cerebrovascular disease (10) and the cerebrovascular consequences of widely used parasympathatetic and sympathetic modulating drugs are largely ignored.

Address for reprint requests and other correspondence: P. Castro, Dept. Neurology, São João Hospital Center, Faculty of Medicine of Univ. of Porto, Alameda Professor Hernani Monteiro, 4200-319 Porto, Portugal (e-mail: pedromacc@gmail.com).

Contrary to earlier static methods of studying CA (41), dynamic CA reflects regulation of CBF in response to rapid changes of ABP (2, 16, 33, 48, 49, 57).

The Valsalva maneuver (VM) is particularly well suited for studying both dynamic CA (49, 55) and the involvement of ANS in the regulation of CBF because it challenges the cerebrovascular bed by inducing predictable changes in ABP and is extensively characterized in terms of autonomic contribution (19, 49). However, most indexes of dynamic CA assume steady-state physiological conditions (2, 15, 33, 48, 57), which are not strictly met during VM. Therefore, commonly used linear approaches, such as transfer function analysis (57), cannot be applied (17, 20, 25, 28, 32, 44, 55). Facing these problems, recent developments in modeling dynamic CA have led to nonstationary indexes of dynamic CA (17, 20, 25, 28, 32, 44). Particularly, continuous estimation of autoregulatory index (ARI) has been validated during transient changes induced by respiratory maneuvers (17, 35, 36, 40), but this approach has never been tested in VM. In addition to nonstationary indexes of CA, models of the instantaneous relationship between ABP and CBFV can also help to elucidate cerebral hemodynamics during the VM and the ANS influences thereupon. The CBFV response during VM was shown to be largely explained by changes in critical closing pressure (CrCP) (13), possibly reflecting the rise in central venous pressure and intracranial pressure previously reported (21, 42) while resistance-area product (RAP) seemed to reflect the vasodilation effort during the VM (13). The capability of this two-parameter model to separate metabolic and myogenic cerebrovascular mechanisms has been proposed during changes in posture and sensorimotor stimulation (5, 7, 27, 34, 37).

Our AF model consists of a population with familial amyloidotic polyneuropathy (FAP) type I (4). It is a hereditary autosomal dominant disease resulting from mutation of the transthyretin (TTR) gene, leading to deposition of abnormal protein in many organs, typically in the peripheral nerves (4). This causes early dysfunction of autonomic fibers being orthostatic hypotension the hallmark of the disease. The fact that central nervous system is usually spared (24) and the usual absence of classic vascular risk factors makes FAP a well-suited model to study the impact of AF on cerebrovascular regulation.

To understand the behavior of CA during VM and the role of ANS in cerebrovascular regulation, we aimed to compare dynamic CA changes between healthy and FAP patients during VM, testing two related hypotheses: *1*) dynamic CA does not

remain constant during VM in either controls or FAP subjects, and *2*) AF affects the dynamic CA response.

MATERIALS AND METHODS

This study was performed in São João Hospital Center, a university hospital in Porto, Portugal. The local institutional ethical committee approved the study. Each participant gave written and signed informed consent.

Population Studied

Eight FAP patients (7 male) with TTR Val30Met mutation and mean age of 31.4 ± 6.5 (range 23–43) yr were included in AF group. Only patients with severe (parasympathetic and sympathetic) AF were selected, as determined by a composite scoring system previously described (8) and detailed below. The control group consisted in eight healthy volunteers (5 male) from our hospital and faculty staff, with a mean age of 28.3 ± 5.9 yr (range 27–36). All participants performed a carotid and transcranial duplex scan, with a HDI 5000 device (Philips). Normal findings of extra- and intracranial vessels, and a good temporal acoustic bone window, were required as inclusion criteria. Classical risk factors including smoking, hypertension, diabetes mellitus, and dyslipidemia were exclusion criteria for all participants.

Experimental Protocol

Participants were asked to refrain from any medication, alcohol-, nicotine-, or caffeine-containing products for a minimum of 12 h. Evaluations were carried out in a quiet room with a constant temperature around 22°C. ABP and heart rate (HR) were continuously monitored in the left hand with a noninvasive finger cuff Finapres device (model 2300; Ohmeda, Englewood, CO) with its pressure height correction unit placed at heart level. CBFV was recorded in M1 segment of both middle cerebral arteries (MCA) at a depth of 50–55 mm with 2-MHz pulsed wave Doppler monitoring probes of a Multidop X4 Doppler device (DWL, Sipplingen, Germany) mounted on an individually fitted headband. Data were continuously stored in Doppler device for offline analysis.

VM was performed in supine position, after 5 min of resting, by instructing subjects to maintain an expiratory pressure of 40 mmHg for 20 s by blowing through a mouthpiece with the tube attached to a mercury manometer.

Autonomic Grading

To express the severity of AF of FAP, a previously described (8) composite grading system to score degree of autonomic dysfunction was applied. Four grades of autonomic failure were distinguished on the basis of HR difference to deep breathing, Valsalva HR ratio and overshoot in phase IV of VM, fall in systolic ABP during head-up tilt, and basal plasma norepinephrine. According to the autonomic evaluation, the included patients had grades III or IV corresponding to severe AF. The Valsalva ratio was calculated as maximal HR of phase IIb divided by minimal HR during phase IV (19).

Data Analysis

All signals were visually inspected to identify artifacts or noise, and narrow spikes were removed by linear interpolation. Since the patients were supine, the ABP at MCA was equivalent to that measured at the heart level. Mean beat-to-beat values were calculated for ABP and CBFV using the area between diastolic points. Two different pressure-velocity models were evaluated. Firstly, the classical CVRi was estimated by the ratio of mean ABP/mean CBFV for each heartbeat for both MCAs (2, 48). Secondly, the instantaneous relationship between ABP and CBFV was used to estimate the CrCP and RAP of the cerebral circulation for each cardiac cycle, using the first harmonic method (1, 34). Consequently, for each cardiac cycle, the fundamental frequency of ABP and CBFV was extracted from raw signals and aligned previously to calculation of the straight-line fit. Figure 1 gives examples of CBFV-ABP scatterplots and corresponding lines of best fit at resting and phase I of VM of one healthy subject.

All beat-to-beat estimates were interpolated with a third-order polynomial and resampled at 0.2-s intervals to generate a time series with a uniform time base. To correct for differences at baseline values and, in the case of CBFV, to become independent from the transcranial Doppler insonation angle, data were also normalized by their mean baseline values (period of 10 s before beginning of VM) and expressed in percentages.

Characteristic phases of VM were manually marked in individual ABP curves and were used to calculate the values of parameters in each phase. To assure that groups could be compared at similar time marks, the values for these phases in FAP subjects were obtained at points that represented the mean time of the fiducial marks from the control group. A recovery phase at 35 s from the beginning of phase I of VM was also added to analysis. To estimate representative group mean and SD of the temporal changes in parameters, the beginning of phase I was used to synchronize the calculations, since it is not affected by AF (19, 55). To further explore the cerebrovascular hemodynamic response to VM, we performed a subcomponent analysis of CBFV temporal changes and evaluated CA through calculation of continuous ARI, as explained below.

Components of CBFV during VM. To weight the separate contributions of ABP, CrCP, RAP, and CVRi to the CBFV responses

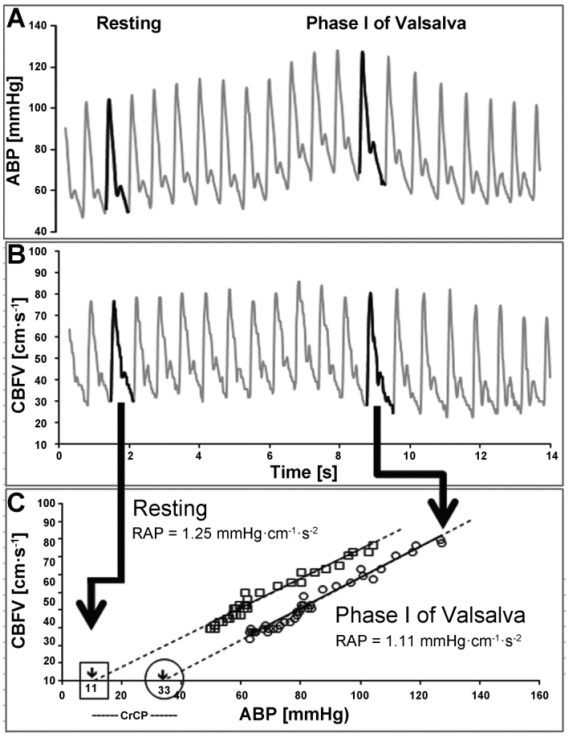

Fig. 1. Estimation of critical closing pressure (CrCP) and resistance-area product (RAP) from continuous recordings of arterial blood pressure (ABP; *A*) and cerebral blood flow velocity (CBFV; *B*) during the Valsalva maneuver (VM). One cycle at rest and one in phase I of the Valsalva were selected (solid line) for plotting CBFV against ABP (*C*). Note that CrCP shifts to higher values in phase I of the Valsalva while RAP is reduced.

induced by VM, we performed a subcomponent analysis as described previously (38). In summary, the two-parameter model, CBFV = (ABP − CrCP)/RAP, can be linearized given the small changes in RAP and further normalized (38) to represent any changes in CBFV as the sum of three subcomponents corresponding to the respective changes in ABP, CrCP, and RAP:

$$\Delta V = \Delta V_{ABP} + \Delta V_{CrCP} + \Delta V_{RAP}$$

With the use of a similar procedure for the single parameter model, CBFV = ABP/CVRi leads to:

$$\Delta V = \Delta V_{ABP} + \Delta V_{CVRi}$$

where the different terms represent the concomitant changes in ABP (Δv_{ABP}), CrCP (Δv_{CrCP}), RAP (Δv_{RAP}), and CVRi (Δv_{CVRi}), all in units of CBFV. The reference values were chosen as the mean value of the 10-s interval preceding VM and units are expressed in percentage after normalization. The main advantage of this approach is that at any given time changes in CBFV can be explained by corresponding changes in ABP and the model parameters. Of relevance, reductions in RAP, CVRi, or CrCP will all lead to increases in CBFV and for this reason the respective subcomponents will be represented by positive values. Previous work (38) suggested that Δv_{RAP} expresses predominantly the myogenic response to blood pressure changes, but this association has not been firmly established.

Continuous dynamic ARI. Time-varying estimates of dynamic autoregulation were based on the ARI (35) introduced by Tiecks et al. (48). In their original communication, a second-order differential equation model was used to generate template mean CBFV step responses to changes in mean ABP. Ten combinations of the gain, time constant, and damping coefficients of the differential equations define the ARI ranging from zero (absence of CA) to nine (best CA) (48). Noteworthy, classical calculation of a single ARI index for recordings lasting several minutes is not acceptable during maneuvers like VM that induce nonstationary time series. For this propose, a time-varying ARI [ARI(t)] was derived from autoregressive moving average (ARMA) models with time-varying parameters after implementation of Tiecks' model as an ARMA structure and use of the Walsh set of orthogonal basis functions to obtain ARMA models with time-varying parameters as previously described (35). Once those parameters are obtained, it is possible to calculate a corresponding CBFV step response for each instant of time, with each one leading to an estimate of ARI(t). A maximum of 19 orthogonal functions were adopted, and ARI(t) was calculated at 0.2-s intervals. Using this model, Panerai et al. (35) showed that ARI(t) presented characteristic time-varying patterns during respiratory maneuvers of apnea and hyperventilation, providing a physiological validation of this method.

Statistical Analysis

Normality of the variables was determined by Shapiro-Wilk test. Student's t-test was used to compare baseline resting values between groups and paired t-test to compare right and left MCA within each group. In the absence of statistically significant differences between parameters derived from the right and left MCA, these were averaged for all subsequent analyses. Two-way repeated measures ANOVA was used to find differences between groups and different phases of VM: within each group differences between phases were calculated using simple contrast with baseline resting values as reference; Bonferonni's post hoc test for multiple comparisons was used to detect differences between groups at each phase when interaction between group and phase factor was significant. Statistical significance was inferred at a $P < 0.05$ level.

RESULTS

All FAP subjects had severe grades (III and IV) of AF with the following group-averaged results: HR difference to deep breathing: 3.4 ± 2.7 beats/min; Valsalva HR ratio: 1.1 ± 0.1; 4 subjects with delayed and 4 with absent ABP overshoot in phase IV of VM; fall in systolic ABP during head-up tilt: 35.6 ± 27.2 mmHg; basal plasma norepinephrine: 78.6 ± 64.0 pg/ml; autonomic score: 7.6 ± 1.1. Baseline values for systemic and cerebral hemodynamic parameters were not different between FAP and controls (Table 1). In controls, VM showed ABP and CBFV patterns in agreement with previous studies (Fig. 2). Phase I, a purely mechanical hemodynamic challenge, showed similar responses in healthy and FAP groups, being characterized by a rapidly rising ABP, CVRi, and CrCP and almost unchanged CBFV, RAP, and HR (Fig. 2 and Table 2). There were marked differences between groups in all subsequent phases (Table 2). Systemic hemodynamic response of FAP group revealed known characteristics of AF: there was blunted HR response consistent with lower Valsalva ratio (1.1 ± 0.1 and 1.8 ± 0.4; $P = 0.0002$); ABP dropped significantly more in phase II ($P < 0.0001$). In addition to the changes in mean ABP, pulse pressure (systolic − diastolic) also showed marked differences between the two groups (Fig. 3), which reached significance in phases I, IIb, and IV (Table 2).

Mean CBFV dropped in both groups (Fig. 2) but deeper in FAP group and showed a blunted overshoot at phase IV compared with controls ($P = 0.001$). The two models of cerebrovascular resistance studied, CVRi and RAP + CrCP, were substantially different. At the beginning of phase II, there was a decrease in vascular resistance in both groups as expressed by RAP but this cerebral vasodilation response turned out to be more pronounced in FAP group and was still present at phase IV ($P = 0.001$). Nevertheless, this greater drop in RAP was not sufficient to restore CBFV to its baseline values in FAP compared with controls (Fig. 2*A*). CrCP increased similarly ($P = 0.235$) between phases I to III of VM in both groups (Fig. 2*D* and Table 2). At phase III, both groups showed rapid restoration of CrCP to baseline values immediately before CBFV overshoot, which was absent in FAP subjects (Fig. 2*A*). CVRi increased not differently ($P = 0.390$) between groups during phases I through III (Fig. 2*F* and Table 2).

Subcomponent Analysis

Further differences between FAP and controls and between the two different models of cerebrovascular resistance were

Table 1. *Baseline resting absolute values for systemic and cerebral hemodynamic parameters concerning right and left MCA for both controls and FAP patients*

Parameter	Control	FAP	P Value*
HR, beats/min	80.8 ± 8.3	82.9 ± 8.8	0.641
Mean ABP, mmHg	80.5 ± 10.9	90.6 ± 20.3	0.235
Pulse pressure, mmHg	54.3 ± 13.8	49.9 ± 13.1	0.523
Mean CBFV, cm/s	66.8 ± 12.2	67.3 ± 13.1	0.945
CrCP, mmHg	24.5 ± 14.9	30.0 ± 12.7	0.444
RAP, mmHg·cm^{-1}·s^{-2}	0.90 ± 0.26	0.90 ± 0.19	0.721
CVRi, mmHg·cm^{-1}·s^{-2}	1.00 ± 0.19	1.15 ± 0.34	0.165
ARI(t), AU	3.5 ± 3.2	4.7 ± 4.1	0.512

All values are given as means ± SD. MCA, middle cerebral arteries; FAP, familial amyloidotic polineuropahty; HR, heart rate; ABP, arterial blood pressure; CBFV, cerebral blood flow velocity; CVRi, cerebrovascular resistance index; RAP, resistance-area product; CrCP, critical closing pressure; ARI(t), continuous estimates of autoregulatory index; AU, arbitrary units. *P value for differences between FAP and control groups by Student's t-test.

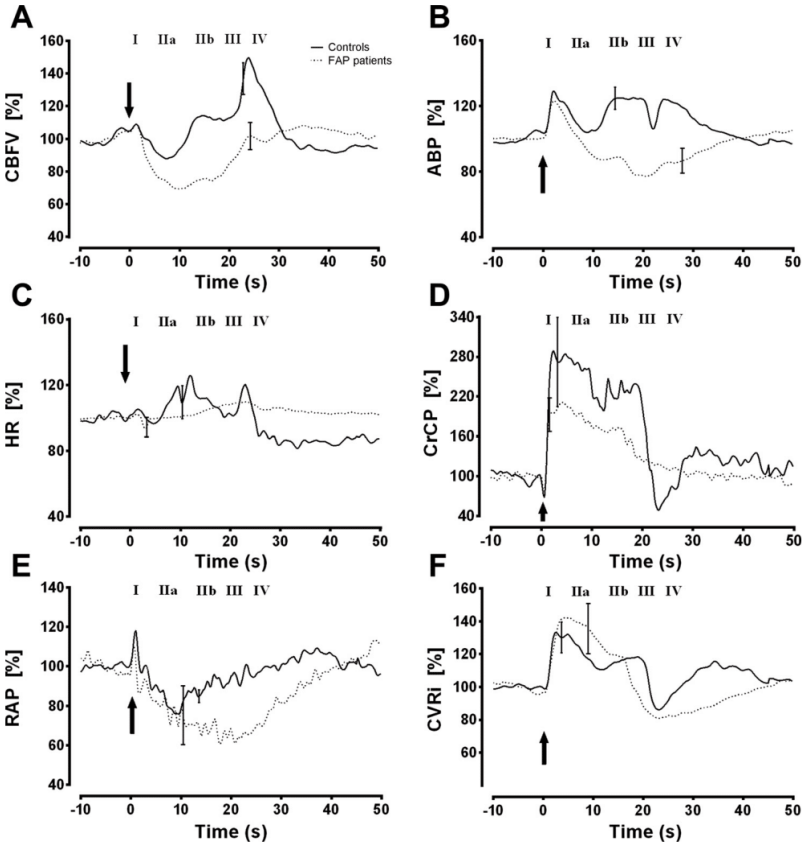

Fig. 2. Group-averaged normalized changes in mean CBFV (*A*), mean ABP (*B*), heart rate (HR; *C*), CrCP (*D*), resistance-area product (RAP; *E*), and cerebrovascular resistance index (CVRi; *F*) during the VM in controls (continuous line) and severe familial amyloidotic polineuropahty (FAP) patients (dashed line). Averaging was synchronized at ABP peak in phase I, and the beginning is marked by a vertical arrow. Characteristic phases of VM are shown in roman numerals. For clarity, only the largest ± SD bar is represented at the point of occurrence (wider horizontal top and bottom delimiters for FAP group).

revealed by subcomponent analysis (Fig. 4). Δv_{CVRi} showed a biphasic contribution to CBFV variation in both groups without significant differences (Table 3). On the other hand, Δv_{RAP} and Δv_{CrCP} had different temporal patterns with Δv_{RAP} showing marked differences ($P = 0.025$) for phases IIb, III, and IV while Δv_{CrCP} showed similar contribution ($P = 0.162$) to CBFV changes (Table 3).

Dynamic CA Response

Temporal changes of ARI(*t*) differed significantly between groups ($P = 0.020$; Fig. 5 and Table 3). A biphasic response was observed in controls, characterized by an initial increase in phases I-IIa, followed by a continuous drop until phase IV. In contrast, FAP response was practically unchanged despite a tendency to increase values towards the end of the maneuver. These mean temporal patterns were representative of individual ARI(*t*) curves with 8/8 and 5/8 individuals showing similar patterns to the mean of controls and FAP patients, respectively.

DISCUSSION

Main Findings

In this study we have shown that dynamic CA behaves as a time-varying phenomena during VM and that it is significantly affected by autonomic dysfunction. Our first hypothesis was substantiated by inspection of ARI(*t*) patterns in individual subjects, showing excellent agreement with the mean temporal patterns represented in Fig. 5, thus confirming their robustness. For the second hypothesis, the significant effect of autonomic dysfunction was confirmed by two very distinct approaches. In the first of these, the total variation in CBFV was broken down in its subcomponents thus reflecting the relative contribution of concomitant changes in ABP, CrCP, and RAP, showing marked differences between controls and FAP subjects. In particular, despite the larger drop in RAP in FAP, Fig. 2*A* indicates that these were not enough to restore CBFV to its baseline values as observed for controls. The second approach, involving the use of ARMA modeling to obtain estimates of ARI(*t*), again showed marked differences between the two groups as discussed below.

Finally, we also confirmed previous studies (7, 13, 38) showing that a two-parameter model (RAP + CrCP) provides clearer discrimination of changes in cerebral hemodynamics than the classical, single CVRi parameter.

Dynamic CA control during VM

In healthy subjects, dynamic CA as assessed by continuous estimates of ARI(*t*) showed a biphasic response to VM, with an initial increase followed by a continuous drop until strain was released. To our knowledge, this is first time that continuous

Table 2. *Normalized values of variation of cerebral and systemic hemodynamic parameters during each phase of the Valsalva maneuver for controls and FAP patients*

Parameter	Phase I	Phase IIa	Phase IIb	Phase III	Phase IV	Recovery	ANOVA *P*‡
HR, %							
Control	105 ± 9	116 ± 12*	101 ± 14	109 ± 17	113 ± 20	83 ± 7*	0.023
FAP	101 ± 2	100 ± 2†	108 ± 9	109 ± 8*	109 ± 8	103 ± 5†	
Mean ABP, %							
Control	128 ± 13*	105 ± 4	124 ± 12*	106 ± 14	123 ± 12*	99 ± 8	<0.0001
FAP	122 ± 11*	90 ± 14*†	78 ± 19*†	78 ± 15*†	84 ± 16*†	101 ± 19	
Pulse Pressure, %							
Control	114 ± 15*	90 ± 14	124 ± 28*	94 ± 26	137 ± 37*	120 ± 21*	0.001
FAP	102 ± 3†	83 ± 19*	72 ± 12*†	78 ± 10*	83 ± 15*†	105 ± 26	
Mean CBFV, %							
Control	107 ± 8	93 ± 10*	111 ± 16	118 ± 15*	150 ± 24*	92 ± 16	0.001
FAP	107 ± 10	69 ± 11*†	78 ± 19*†	91 ± 19*†	101 ± 23†	105 ± 17*	
CrCP, %							
Control	268 ± 178*	244 ± 132*	212 ± 142*	109 ± 54	57 ± 58	121 ± 49	0.235
FAP	196 ± 61*	177 ± 44*	130 ± 67*	121 ± 37	116 ± 27	93 ± 13	
RAP, %							
Control	98 ± 15	77 ± 8*	89 ± 17	90 ± 14	96 ± 10	105 ± 14	0.001
FAP	87 ± 13	76 ± 29*	67 ± 17*†	64 ± 13*†	66 ± 14*†	100 ± 17	
CVRi, %							
Control	127 ± 22*	115 ± 11*	118 ± 17*	92 ± 13	87 ± 14	111 ± 19	0.390
FAP	120 ± 16*	113 ± 41	97 ± 35	83 ± 20	81 ± 17*	97 ± 17	

All values are given in percentage (normalized). *$P < 0.05$, level of significance for differences between baseline values and each of the Valsalva maneuver phases obtained by repeated-measures ANOVA. †$P < 0.05$, level of significance for differences between familial amyloidotic polineuropahty (FAP) and control groups obtained by repeated-measures ANOVA. ‡*P* value for interaction between phase and group by two-way repeated-measures ANOVA.

estimates of dynamic CA changes were described in VM. The initial increase of ARI(*t*) could represent the cerebrovascular autoregulatory effort to bring CBFV levels back to baseline in response to sudden increase of CrCP and effective reduction of perfusion pressure (ABP − CrCP), taking into account that the autoregulatory response normally takes from 2–5 s to be manifested (Fig. 4). However, FAP patients showed no changes in ARI(*t*) at the same phases despite similar variations of ABP and CrCP. Thus cerebral perfusion pressure changes probably do not explain dynamic CA augmentation at this point. Interestingly, pulse pressure seemed to be the only factor (Table 1 and Figs. 2 and 3), with striking differences between the two groups at this phase, showing an increase in healthy subjects and decreasing immediately in FAP patients, despite equivalent challenges from changes in ABP and CBFV. Pulse pressure is regarded as proportional to cardiac output and inversely related to cardiovascular compliance (12). In a beat-by-beat analysis, especially in young subjects, stroke volume changes seem to be the principal factor affecting pulse pressure variation (3). Therefore, sudden increase of cardiac output could trigger augmented ARI(*t*) in normal subjects, which is not observed in FAP patients as expected from their AF (19). Cardiac output seems to play a role in CA (52), perhaps mediated through endothelial factors (56), but some caution is warranted since there are recent data providing evidence to the contrary (14). However, FAP patients are not healthy subjects and infiltration of abnormal protein TTR in the vessel wall can affect aortic compliance, thus affecting pulse pressure changes.

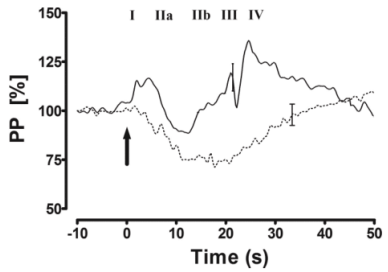

Fig. 3. Group-averaged normalized arterial pulse pressure (PP; systolic − diastolic) for controls (solid line) and FAP patients (dashed line). Averaging was synchronized at ABP rise in phase I indicated by the vertical arrow. For clarity, only the largest ± SD bar is represented at the point of occurrence.

At phase II other factors emerge and their complex interplay can contribute to the steady fall of dynamic CA until strain release. Firstly, sympathetic activation is known to be an important factor in increasing ABP, HR, and cardiac output at this stage (19). ARI(*t*) decline seems to parallel sympathetic activation (19), but the contribution of the sympathetic nervous system to CBF control is still under dispute (26, 43, 51). Moreover, during autonomic blockade, lower body negative pressure induces a decrease in CBFV, even if blood pressure is maintained by infusion of a pressor drug. This observation confirms that CBF can be influenced by peripheral changes without the participation of the sympathetic nervous system (56). However, long-standing data suggest that ANS cerebrovascular control is more effective under dynamic than steady-state conditions (6, 46). Indeed, there are data demonstrating depression of dynamic CA during orthostatic stress (29), ganglionic blockade (58), and even physiological phenomena like rapid eye movement sleep (9) and neurovascular coupling (5, 37, 39). The fact that the FAP group demonstrated a different response with a less pronounced decrease in CA may corroborate this hypothesis. Secondly, hypercapnia induced by the maneuver (21) may account for dynamic CA variations (2, 17, 18). However, cerebrovascular and autonomic responses during VM were described as unrelated to P_{CO_2} changes (13, 54, 55). Finally, intracranial pressure elevation is associated with deterioration of dynamic CA as measured by Mx in traumatic

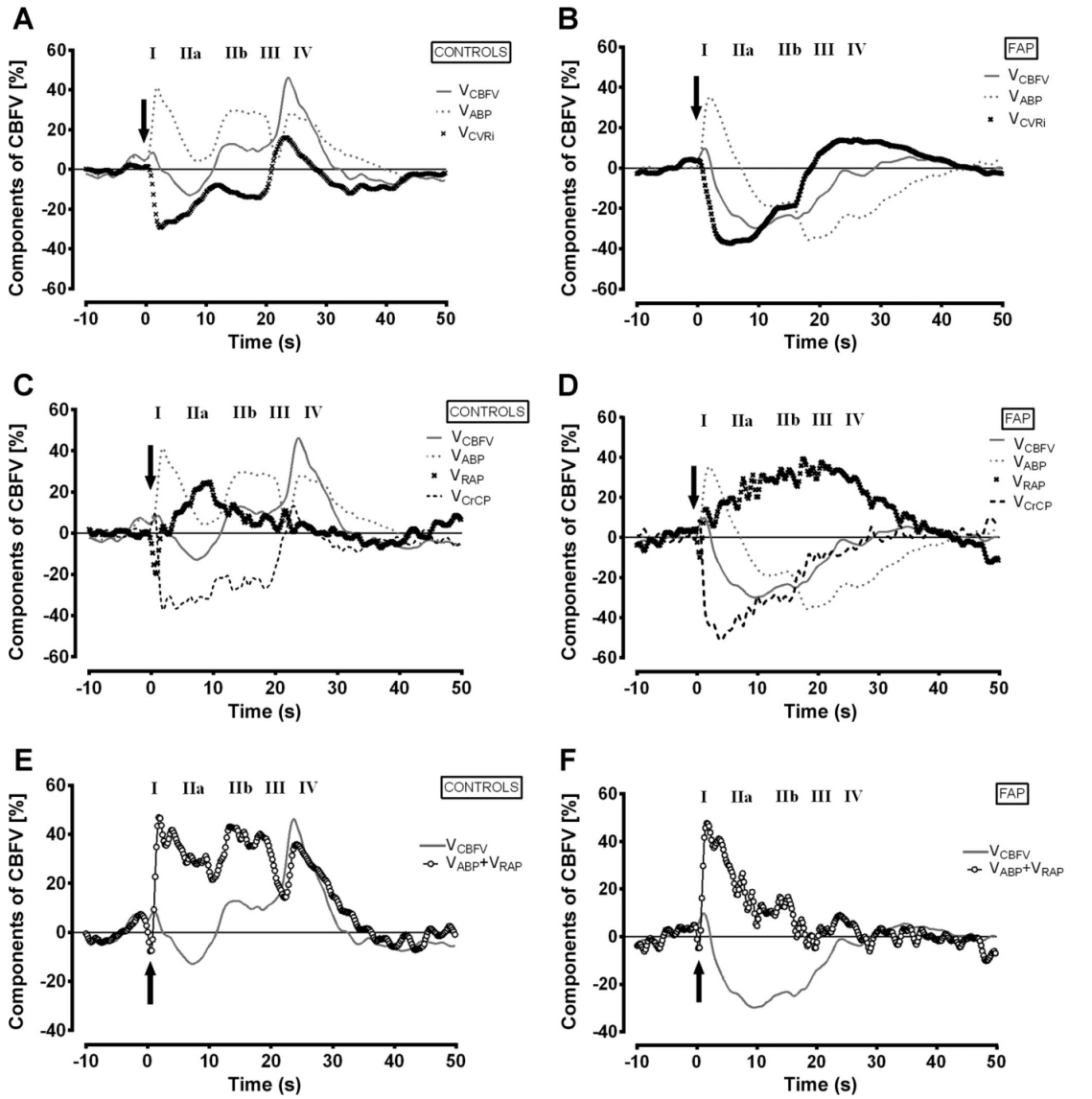

Fig. 4. Group-averaged normalized mean CBFV changes (grey continuous line) and its subcomponents of CVRi and RAP + CrCP models for control (*A* and *C*, respectively) and FAP (*B* and *D*, respectively) groups. Δv_{ABP}, ABP subcomponent, grey dotted line; Δv_{CrCP}, CrCP subcomponent, dashed dark line; Δv_{CVRi}, CVRi subcomponent, and Δv_{RAP}, RAP subcomponent are marked with "x". The sum of ABP and CVR subcomponents are presented with line width white circle marks. Averaging was synchronized at ABP rise in phase I indicated by the vertical arrow.

brain injury (11). However, during VM, intracranial pressure increases a maximum of 23.5 mmHg (21), and at this range Mx remained normal (11).

The short-term modulation of CA during VM raises important questions for further studies of CA (and other physiological control systems): at some stages enhanced CA is observed, while at other times CA seems to be absent, even in healthy controls. For example, at phase III, where CBFV is high and the drop in ABP helps to restore CBFV to baseline. Active autoregulation at this stage might keep CBFV artificially high, undoing the effect of the restoration of ABP in returning the flow to baseline.

Effect of Autonomic Dysfunction on Normal Cerebrovascular Control

In FAP patients, ARI(t) was practically unchanged during strain but increased towards the end of the maneuver, which confers a completely different pattern from control group. Overall, the clear-cut distinct pattern of ARI(t) during VM,

Table 3. *Normalized CBFV changes and its components (ABP, CrCP, and RAP, and CVRi) and ARI(t) absolute values changes during all phases of the Valsalva maneuver for controls and FAP patients*

Parameter	Phase I	Phase IIa	Phase IIb	Phase III	Phase IV	Recovery	ANOVA P‡
Δv, %							
Control	5 ± 9	−12 ± 8*	13 ± 17	20 ± 15*	49 ± 23*	−6 ± 14	0.00002
FAP	5 ± 11	−28 ± 10*†	−23 ± 18*†	−8 ± 19†	2 ± 23†	8 ± 18	
Δv_{ABP}, %							
Control	42 ± 19*	8 ± 12	34 ± 17*	6 ± 20	34 ± 17*	7 ± 14	0.0002
FAP	35 ± 19*	−4 ± 24	−33 ± 27*†	−31 ± 18*†	−22 ± 23*†	−4 ± 33	
Δv_{CVRi}, %							
Control	−24 ± 20*	−23 ± 13*	−12 ± 15*	−11 ± 12*	16 ± 12*	−13 ± 21	0.139
FAP	−18 ± 14*	−32 ± 14*	−6 ± 29	12 ± 19	15 ± 16*	9 ± 17	
Δv_{CrCP} , %							
Control	−40 ± 27*	−37 ± 10*	−32 ± 19*	7 ± 25	7 ± 19	−7 ± 8*	0.162
FAP	−44 ± 25*	−44 ± 20*	−19 ± 24	−10 ± 19	−9 ± 14	3 ± 11	
Δv_{RAP}, %							
Control	3 ± 12	22 ± 12*	9 ± 17	9 ± 15	5 ± 11	−8 ± 18	0.025
FAP	12 ± 13*	28 ± 18*	39 ± 14*†	36 ± 12*†	34 ± 15*†	8 ± 24	
$\Delta v_{RAP} + \Delta v_{ABP}$, %							
Control	44 ± 21*	26 ± 9*	37 ± 8*	14 ± 17*	30 ± 8*	1 ± 14	0.024
FAP	44 ± 28*	22 ± 11*	3 ± 16†	3 ± 15	−5 ± 19†	3 ± 10	
ARI(t), AU							
Control	7.8 ± 0.9*	5.4 ± 2.2	3.7 ± 3.7	1.2 ± 3.2*	0.6 ± 0.9*	5.5 ± 3.0	0.020
FAP	3.3 ± 3.5†	2.2 ± 3.0†	5.4 ± 3.2	4.0 ± 3.5	5.8 ± 3.5†	7.2 ± 3.2	

All values are given in percentage (normalized) except for ARI(t), which are means ± SD. Δv, changes in CBFV. *$P < 0.05$, level of significance for differences between baseline values and each of the Valsalva maneuver phases obtained by repeated-measures ANOVA. †$P < 0.05$, level of significance for differences between FAP and control groups obtained by repeated-measures ANOVA. ‡P value for interaction between phase and group by two-way repeated-measures ANOVA.

compared with controls, strongly suggests a major role for ANS involvement in dynamic CA, as proposed by other groups (9, 29, 58). The suggestion of an increase in ARI(t) during late phase II and III might represent the attempt of cerebrovascular control to restore CBF in the face of a higher drop of ABP (34, 38). This response pattern may not simply imply impaired CA, as patients can achieve very high ARI and values during baseline (Table 1) and recovery seem similar (Fig. 5). They are also able to modulate ARI and RAP, but they do so differently than controls. This altered response could be explained solely by the different ABP patterns. However, in phase I the initial increase ABP was similar between groups (Fig. 2 and Table 1) but increased ARI(t) was shown only by controls. Future studies are needed to address these additional questions generated from our results.

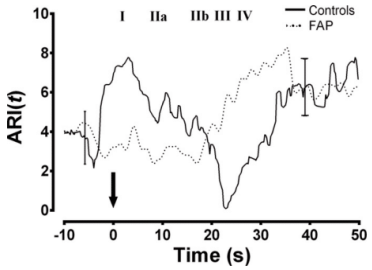

Fig. 5. Group-averaged normalized autoregulatory index changes [ARI(t)] during the VM for controls (continuous line) and FAP (dotted line) groups. Averaging was synchronized at ABP rise in phase I and the beginning is marked by a vertical arrow. For clarity, only the largest ± SD bar is represented at the point of occurrence (wider horizontal top and bottom delimiters for FAP group).

Mechanisms of Cerebrovascular Control During VM and Physiological Correlates

Previous studies (21, 42) have characterized changes in cerebral hemodynamics during VM using invasive measurements (electromagnetic flowmeter), confirming that between phases I to III there is an increase in cerebrospinal fluid pressure (CSFP) of 7.5 mmHg and a decrease in internal carotid blood flow by 21%. Cerebrovascular resistance, calculated as (mean ABP − CSFP)/blood flow, decreased during strain, meaning cerebral vasodilation, and increased during phase IV. Dawson et al. (13), using transcranial Doppler, showed the same temporal profile by using the RAP + CrCP model. Particularly, RAP seemed to change in accordance with the cerebrovascular effort of vasodilation during VM, and CrCP very closely accompanied the changes in intrathoracic and intracranial pressures (13). Our results not only match those of Dawson et al. (13) in the healthy group but also reinforce the value of the CrCP + RAP model over CVRi by showing that the same physiological correlates could be interpreted in a different response caused by autonomic dysfunction. During the normal response to VM, RAP varies as expected, reflecting the cerebral vasodilation effort during phase II (21). AF caused a larger CBFV reduction during phase II compared with controls, consistent with previous studies with ganglionic blockade (55). This is accompanied by a substantial drop in ABP, which is related to adrenergic dysfunction (19). This cerebral vasodilation seems to be better explained by the longer and deeper RAP reduction, while CVRi suggests a paradoxical cerebral vasoconstriction (21, 49). We speculate that RAP is more sensitive to ABP variations and, therefore, behaves as a myogenic component of cerebrovascular regulation. Previous studies support this as-

sumption (6, 34, 37, 38). We have previously reported (5) blunted ABP response in FAP patients when changing from supine to the sitting position with only RAP reflecting cerebrovascular differences. This suggests the presence of cerebral vasodilation in adaptation to ABP challenge, which was already documented earlier (23, 31). Also, RAP and not CrCP seems to follow ABP, possibly a myogenic response (37), explaining different CBFV responses during neurovascular coupling paradigms (45). Contrary to CrCP, RAP seem not to be disturbed by metabolic components during complex neurovascular activation (37, 45) and CO_2 changes (27, 37).

On the other hand, CrCP increased during strain in both groups, despite the presence of AF, giving credit to the hypothesis that it represents intracranial pressure changes during phase II (13). At the end of the VM, we did not observe an increased CBFV that would suggest a "hyperemic response" due to autonomic dysfunction as it was reported by Zhang et al. (55) with ganglionic blockade. However, these authors used, as a model of AF, an otherwise healthy population that was artificially and acutely deprived of their autonomic function. Long-standing autonomic dysfunction might have induced adaptive changes of cerebral vasculature dynamics (22, 23, 53) in chronically denervated FAP subjects.

Study Limitations

An important methodological point concerns to the use of transcranial Doppler for measurements of cerebral blood flow. Changes in CBFV reflect changes in cerebral blood flow only if the diameter of the insonated artery remains constant. However, several studies suggested that the diameter of the middle cerebral artery remains relatively stable during rapid alterations in arterial pressure (30) and during simulated orthostasis (47).

Noninvasive measurements of BP in the finger could also be suspected as a source of spurious influence due to random fluctuations in the blood flow circulation of the hand and could be regarded as a source of spurious noise during CrCP and RAP calculations. However, a previous investigation has shown that estimates of ARI(t) obtained with the moving-window ARMA technique were very similar to those derived from direct catheter-tip BP measurements in the ascending aorta (40). Spontaneous BP fluctuations have been often adopted to measure dynamic CA but cannot be assumed to be physiologically equivalent to those induced by the thigh-cuff maneuver (2). Some caution over the results obtained are also inherent to the methods to assess autoregulation, as ARI, RAP, or CrCP are only estimates of some abstraction of different aspects of vascular control. This includes the interpretation of changes in RAP as caused by myogenic regulation. Although there is some evidence for this association, based on previous studies (7, 37, 38), its generalization is premature and further studies are needed. Another limitation of the present investigation maybe the lack of CO_2 measurement. Previous studies have not found significant changes in CO_2 during the procedure (13, 54, 55), but we cannot rule out the possibility that small changes in $PaCO_2$ might have influenced our results, although similar changes in $PaCO_2$ would be expected for both groups. Finally, our study enrolled a relatively small number of patients. FAP is a rare disease, and nowadays patients are treated earlier, namely with pacemaker and liver transplantation, which were exclusion criteria for the study. Nevertheless, this population is very homogeneous in its disease process and lacks vascular risks factors, like diabetes, that would make it difficult to discern the effects of autonomic dysfunction among other vascular aggressors.

Conclusions

In summary, by applying a recently designed continuous estimation of ARI, we could measure, for the first time, the dynamic CA performance during VM. Our data suggest that dynamic CA undergoes temporal changes during the VM and that it is significantly altered in subjects with severe autonomic failure. Moreover, a two-parameter model, including CrCP and RAP, allowed a clearer insight into cerebral hemodynamics than the CVRi alone. Further physiological studies are needed to describe the multiple interactions between ABP changes and cerebrovascular parameters in response to different maneuvers in patient populations with ANS dysfunction.

DISCLOSURES

No conflicts of interest, financial or otherwise, are declared by the author(s).

AUTHOR CONTRIBUTIONS

Author contributions: P.M.C., R.S., J.F., R.B.P., and E.A. conception and design of research; P.M.C. and R.B.P. analyzed data; P.M.C., R.B.P., and E.A. interpreted results of experiments; P.M.C. prepared figures; P.M.C. drafted manuscript; P.M.C., J.F., R.B.P., and E.A. edited and revised manuscript; P.M.C., R.S., J.F., R.B.P., and E.A. approved final version of manuscript; R.S. performed experiments.

REFERENCES

1. **Aaslid R, Lash SR, Bardy GH, Gild WH, Newell DW.** Dynamic pressure–flow velocity relationships in the human cerebral circulation. *Stroke* 34: 1645–1649, 2003.
2. **Aaslid R, Lindegaard KF, Sorteberg W, Nornes H.** Cerebral autoregulation dynamics in humans. *Stroke* 20: 45–52, 1989.
3. **Alfie J, Waisman GD, Galarza CR, Camera MI.** Contribution of stroke volume to the change in pulse pressure pattern with age. *Hypertension* 34: 808–812, 1999.
4. **Andrade C.** A peculiar form of peripheral neuropathy; familiar atypical generalized amyloidosis with special involvement of the peripheral nerves. *Brain* 75: 408–427, 1952.
5. **Azevedo E, Castro P, Santos R, Freitas J, Coelho T, Rosengarten B, Panerai R.** Autonomic dysfunction affects cerebral neurovascular coupling. *Clin Auton Res* 21: 395–403, 2011.
6. **Baumbach GL, Heistad DD.** Effects of sympathetic stimulation and changes in arterial pressure on segmental resistance of cerebral vessels in rabbits and cats. *Circ Res* 52: 527–533, 1983.
7. **Carey BJ, Eames PJ, Panerai RB, Potter JF.** Carbon dioxide, critical closing pressure and cerebral haemodynamics prior to vasovagal syncope in humans. *Clin Sci (Lond)* 101: 351–358, 2001.
8. **Carvalho MJ, van Den Meiracker AH, Boomsma F, Lima M, Freitas J, Veld AJ, Falcao De Freitas A.** Diurnal blood pressure variation in progressive autonomic failure. *Hypertension* 35: 892–897, 2000.
9. **Cassaglia PA, Griffiths RI, Walker AM.** Cerebral sympathetic nerve activity has a major regulatory role in the cerebral circulation in REM sleep. *J Appl Physiol* 106: 1050–1056, 2009.
10. **Cohen JA, Estacio RO, Lundgren RA, Esler AL, Schrier RW.** Diabetic autonomic neuropathy is associated with an increased incidence of strokes. *Auton Neurosci* 108: 73–78, 2003.
11. **Czosnyka M, Smielewski P, Kirkpatrick P, Menon DK, Pickard JD.** Monitoring of cerebral autoregulation in head-injured patients. *Stroke* 27: 1829–1834, 1996.
12. **Dart AM, Kingwell BA.** Pulse pressure–a review of mechanisms and clinical relevance. *J Am Coll Cardiol* 37: 975–984, 2001.
13. **Dawson SL, Panerai RB, Potter JF.** Critical closing pressure explains cerebral hemodynamics during the Valsalva maneuver. *J Appl Physiol* 86: 675–680, 1999.

14. **Deegan BM, Devine ER, Geraghty MC, Jones E, Olaighin G, Serrador JM.** The relationship between cardiac output and dynamic cerebral autoregulation in humans. *J Appl Physiol* 109: 1424–1431, 2010.
15. **Diehl RR.** Cerebral autoregulation studies in clinical practice. *Eur J Ultrasound* 16: 31–36, 2002.
16. **Diehl RR, Linden D, Lucke D, Berlit P.** Phase relationship between cerebral blood flow velocity and blood pressure. A clinical test of autoregulation. *Stroke* 26: 1801–1804, 1995.
17. **Dineen NE, Brodie FG, Robinson TG, Panerai RB.** Continuous estimates of dynamic cerebral autoregulation during transient hypocapnia and hypercapnia. *J Appl Physiol* 108: 604–613, 2010.
18. **Edwards MR, Devitt DL, Hughson RL.** Two-breath CO_2 test detects altered dynamic cerebrovascular autoregulation and CO_2 responsiveness with changes in arterial P_{CO_2}. *Am J Physiol Regul Integr Comp Physiol* 287: R627–R632, 2004.
19. **Freeman R.** Assessment of cardiovascular autonomic function. *Clin Neurophysiol* 117: 716–730, 2006.
20. **Giller CA, Mueller M.** Linearity and nonlinearity in cerebral hemodynamics. *Med Eng Phys* 25: 633–646, 2003.
21. **Greenfield JC Jr, Rembert JC, Tindall GT** Transient changes in cerebral vascular resistance during the Valsalva maneuver in man. *Stroke* 15: 76–79, 1984.
22. **Hilz MJ, Axelrod FB, Steingrueber M, Stemper B.** Valsalva maneuver suggests increased rigidity of cerebral resistance vessels in familial dysautonomia. *Clin Auton Res* 12: 385–392, 2002.
23. **Horowitz DR, Kaufmann H.** Autoregulatory cerebral vasodilation occurs during orthostatic hypotension in patients with primary autonomic failure. *Clin Auton Res* 11: 363–367, 2001.
24. **Hou X, Aguilar MI, Small DH.** Transthyretin and familial amyloidotic polyneuropathy. Recent progress in understanding the molecular mechanism of neurodegeneration. *FEBS J* 274: 1637–1650, 2007.
25. **Latka M, Turalska M, Glaubic-Latka M, Kolodziej W, Latka D, West BJ.** Phase dynamics in cerebral autoregulation. *Am J Physiol Heart Circ Physiol* 289: H2272–H2279, 2005.
26. **LeMarbre G, Stauber S, Khayat RN, Puleo DS, Skatrud JB, Morgan BJ.** Baroreflex-induced sympathetic activation does not alter cerebrovascular CO_2 responsiveness in humans. *J Physiol* 551: 609–616, 2003.
27. **Maggio P, Salinet AS, Panerai RB, Robinson TG.** Does hypercapnia-induced impairment of cerebral autoregulation affect neurovascular coupling? A functional TCD study. *J Appl Physiol* 115: 491–497, 2013.
28. **Mitsis GD, Poulin MJ, Robbins PA, Marmarelis VZ.** Nonlinear modeling of the dynamic effects of arterial pressure and CO_2 variations on cerebral blood flow in healthy humans. *IEEE Trans Biomed Eng* 51: 1932–1943, 2004.
29. **Mitsis GD, Zhang R, Levine BD, Marmarelis VZ.** Cerebral hemodynamics during orthostatic stress assessed by nonlinear modeling. *J Appl Physiol* 101: 354–366, 2006.
30. **Newell DW, Aaslid R, Lam A, Mayberg TS, Winn HR.** Comparison of flow and velocity during dynamic autoregulation testing in humans. *Stroke* 25: 793–797, 1994.
31. **Novak V, Novak P, Spies JM, Low PA.** Autoregulation of cerebral blood flow in orthostatic hypotension. *Stroke* 29: 104–111, 1998.
32. **Novak V, Yang AC, Lepicovsky L, Goldberger AL, Lipsitz LA, Peng CK.** Multimodal pressure-flow method to assess dynamics of cerebral autoregulation in stroke and hypertension. *Biomed Eng Online* 3: 39, 2004.
33. **Panerai RB.** Assessment of cerebral pressure autoregulation in humans–a review of measurement methods. *Physiol Meas* 19: 305–338, 1998.
34. **Panerai RB.** The critical closing pressure of the cerebral circulation. *Med Eng Phys* 25: 621–632, 2003.
35. **Panerai RB, Dineen NE, Brodie FG, Robinson TG.** Spontaneous fluctuations in cerebral blood flow regulation: contribution of $PaCO_2$. *J Appl Physiol* 109: 1860–1868, 2010.
36. **Panerai RB, Eames PJ, Potter JF.** Variability of time-domain indices of dynamic cerebral autoregulation. *Physiol Meas* 24: 367–381, 2003.
37. **Panerai RB, Eyre M, Potter JF.** Multivariate modelling of cognitive-motor stimulation on neurovascular coupling: transcranial Doppler used to characterize myogenic and metabolic influences. *Am J Physiol Regul Integr Comp Physiol* 303: R395–R407, 2012.
38. **Panerai RB, Moody M, Eames PJ, Potter JF.** Cerebral blood flow velocity during mental activation: interpretation with different models of the passive pressure-velocity relationship. *J Appl Physiol* 99: 2352–2362, 2005.
39. **Panerai RB, Moody M, Eames PJ, Potter JF.** Dynamic cerebral autoregulation during brain activation paradigms. *Am J Physiol Heart Circ Physiol* 289: H1202–H1208, 2005.
40. **Panerai RB, Sammons EL, Smith SM, Rathbone WE, Bentley S, Potter JF, Samani NJ.** Continuous estimates of dynamic cerebral autoregulation: influence of non-invasive arterial blood pressure measurements. *Physiol Meas* 29: 497–513, 2008.
41. **Paulson OB, Strandgaard S, Edvinsson L.** Cerebral autoregulation. *Cerebrovasc Brain Metab Rev* 2: 161–192, 1990.
42. **Pott F, van Lieshout JJ, Ide K, Madsen P, Secher NH.** Middle cerebral artery blood velocity during a Valsalva maneuver in the standing position. *J Appl Physiol* 88: 1545–1550, 2000.
43. **Przybylowski T, Bangash MF, Reichmuth K, Morgan BJ, Skatrud JB, Dempsey JA.** Mechanisms of the cerebrovascular response to apnoea in humans. *J Physiol* 548: 323–332, 2003.
44. **Rowley AB, Payne SJ, Tachtsidis I, Ebden MJ, Whiteley JP, Gavaghan DJ, Tarassenko L, Smith M, Elwell CE, Delpy DT.** Synchronization between arterial blood pressure and cerebral oxyhaemoglobin concentration investigated by wavelet cross-correlation. *Physiol Meas* 28: 161–173, 2007.
45. **Salinet AS, Robinson TG, Panerai RB.** Active, passive, and motor imagery paradigms: component analysis to assess neurovascular coupling. *J Appl Physiol* 114: 1406–1412, 2013.
46. **Sercombe R, Lacombe P, Aubineau P, Mamo H, Pinard E, Reynier-Rebuffel AM, Seylaz J.** Is there an active mechanism limiting the influence of the sympathetic system on the cerebral vascular bed? Evidence for vasomotor escape from sympathetic stimulation in the rabbit. *Brain Res* 164: 81–102, 1979.
47. **Serrador JM, Picot PA, Rutt BK, Shoemaker JK, Bondar RL.** MRI measures of middle cerebral artery diameter in conscious humans during simulated orthostasis. *Stroke* 31: 1672–1678, 2000.
48. **Tiecks FP, Lam AM, Aaslid R, Newell DW.** Comparison of static and dynamic cerebral autoregulation measurements. *Stroke* 26: 1014–1019, 1995.
49. **Tiecks FP, Lam AM, Matta BF, Strebel S, Douville C, Newell DW.** Effects of the Valsalva maneuver on cerebral circulation in healthy adults. A transcranial Doppler study. *Stroke* 26: 1386–1392, 1995.
50. **van Lieshout JJ, Secher NH.** Last Word on Point:Counterpoint: Sympathetic activity does/does not influence cerebral blood flow. *J Appl Physiol* 105: 1374, 2008.
51. **van Lieshout JJ, Secher NH.** Point:Counterpoint: Sympathetic activity does/does not influence cerebral blood flow. *J Appl Physiol* 105: 1364–1366, 2008.
52. **Van Lieshout JJ, Wieling W, Karemaker JM, Secher NH.** Syncope NH, cerebral perfusion, oxygenation. *J Appl Physiol* 94: 833–848, 2003.
53. **Vokatch N, Grotzsch H, Mermillod B, Burkhard PR, Sztajzel R.** Is cerebral autoregulation impaired in Parkinson's disease? A transcranial Doppler study. *J Neurol Sci* 254: 49–53, 2007.
54. **Wallasch TM, Kropp P.** Cerebrovascular response to Valsalva maneuver: methodology, normal values, and retest reliability. *J Clin Ultrasound* 40: 540–546, 2012.
55. **Zhang R, Crandall CG, Levine BD.** Cerebral hemodynamics during the Valsalva maneuver: insights from ganglionic blockade. *Stroke* 35: 843–847, 2004.
56. **Zhang R, Levine BD.** Autonomic ganglionic blockade does not prevent reduction in cerebral blood flow velocity during orthostasis in humans. *Stroke* 38: 1238–1244, 2007.
57. **Zhang R, Zuckerman JH, Giller CA, Levine BD.** Transfer function analysis of dynamic cerebral autoregulation in humans. *Am J Physiol Heart Circ Physiol* 274: H233–H241, 1998.
58. **Zhang R, Zuckerman JH, Iwasaki K, Wilson TE, Crandall CG, Levine BD.** Autonomic neural control of dynamic cerebral autoregulation in humans. *Circulation* 106: 1814–1820, 2002.

Indexes of cerebral autoregulation do not reflect impairment in syncope: insights from head-up tilt test of vasovagal and autonomic failure

---

Castro, P. M., Freitas, J., Santos, R., Panerai, R. B., & Azevedo, E. (2017). Indexes of cerebral autoregulation do not reflect impairment in syncope: insights from head-up tilt test of vasovagal and autonomic failure subjects*. Eur J Appl Physiol, 117(9)*, 1817-1831. doi: 10.1007/s00421-017-3674-1

Eur J Appl Physiol (2017) 117:1817–1831
DOI 10.1007/s00421-017-3674-1

ORIGINAL ARTICLE

Indexes of cerebral autoregulation do not reflect impairment in syncope: insights from head-up tilt test of vasovagal and autonomic failure subjects

Pedro Castro[1] · João Freitas[2] · Rosa Santos[1] · Ronney Panerai[3] · Elsa Azevedo[1]

Received: 27 March 2017 / Accepted: 26 June 2017 / Published online: 5 July 2017

Abstract

Purpose The study of dynamic cerebral autoregulation (CA), which adapts cerebral blood flow to arterial blood pressure (ABP) fluctuations, has been limited in orthostatic intolerance syndromes, mainly due to its stationary prerequisites hardly to meet during maneuvers to provoke syncope itself. New techniques of continuous estimates of CA could overcome this pitfall. We aimed to evaluate CA during head-up tilt test in common conditions causing syncope.

Methods We compared three groups: eight controls; eight patients with autonomic failure due to familial amyloidotic polyneuropathy; eight patients with vasovagal syncope (VVS). ABP and cerebral blood flow velocity (CBFV) were measured with Finometer® and transcranial Doppler. We calculated cerebrovascular resistance index (CVRi), critical closing pressure (CrCP) and resistance area product (RAP), and derived CA continuously from autoregulation index [ARI(t)].

Results With HUTT, AF subjects showed a pronounced decrease in CBFV (-36 ± 17 versus $-7 \pm 6\%$, $p < 0.0001$), ABP (-29 ± 27 versus $7 \pm 12\%$, $p < 0.0001$) and RAP (-17 ± 23 versus $3 \pm 18\%$, $p < 0.0001$) but not CVRi ($p = 0.110$). VVS subjects showed progressive cerebral vasoconstriction prior to syncope, (reduced CBFV 19 ± 15 versus 1 ± 6, $p < 0.000$; increased RAP 12 ± 18 versus $2 \pm 3\%$, $p = 0.024$ and CVRi 12 ± 18 versus $2 \pm 3\%$, $p = 0.005$). ARI(t) increased significantly in AF patients (5.7 ± 1.2 versus 6.9 ± 1.2, $p = 0.040$) and VVS (5.8 ± 1.2 versus 7.3 ± 1.2, $p = 0.015$) in response to ABP fall during syncope.

Conclusions Our data suggest that dynamic cerebral autoregulatory response to orthostatic challenge is neither affected by autonomic dysfunction nor in neutrally mediated syncope. This study also emphasizes that RAP + CrCP model is more informative than CVRi, mainly during cerebral vasodilatory response to orthostatic hypotension.

Keywords Cerebral blood flow · Cerebral vasoreactivity · Autonomic nervous system · Head-up tilt · Transcranial Doppler · Syncope · Orthostatic intolerance

Abbreviations

CA	Cerebral autoregulation
CBFV	Cerebral blood flow velocity
MCA	Middle cerebral artery
CrCP	Critical closing pressure
RAP	Resistance area product
CVRi	Cerebrovascular resistance index
ARI	Autoregulation index

Communicated by Massimo Pagani.

✉ Pedro Castro
pedromacc@gmail.com

João Freitas
jppafreitas@sapo.pt

Rosa Santos
rosampsantos2@gmail.com

Ronney Panerai
rp9@leicester.ac.uk

Elsa Azevedo
eazevedo@med.up.pt

[1] Department of Neurology, São João Hospital Center, Faculty of Medicine of University of Porto, Alameda Professor Hernani Monteiro, 4200-319 Porto, Portugal

[2] Autonomic Unit, São João Hospital Center, Faculty of Medicine of University of Porto, Porto, Portugal

[3] Department of Cardiovascular Sciences and NIH Biomedical Research Centre, University of Leicester, Leicester, UK

ARI(t)	Time-varying autoregulation index
AF	Autonomic failure
VVS	Vasovagal syncope
ARMA	Autoregressive moving-average
ANOVA	Analysis of variance
HUTT	Head-up tilt test
VLF	Very low frequency
LF	Low frequency
HF	High frequency
ABP	Arterial blood pressure
HR	Heart rate
CO_2	Carbon dioxide

Introduction

Orthostatic posture ignites complex and critical hemodynamic changes to assure that blood flow is preserved in critical organs like the brain (Castro et al. 2012; Van Lieshout et al. 2003). Systemic neutrally mediated and hormonal mechanisms have been widely studied (Van Lieshout et al. 2003; Freitas et al. 2007; Goldstein et al. 2003; Carey et al. 2001a, b) but organ-specific vascular regulatory mechanisms may also play their role (Castro et al. 2012; Van Lieshout et al. 2003). In what concerns to the brain, it is well documented that cerebral vasculature is able to adapt arterial blood pressure (ABP) fluctuations, commonly referred to as cerebral autoregulation (CA) (Zhang et al. 1998).

The study of the role of CA in syncope has been characterized by mixed results. This could be explained in part by the heterogeneous medical conditions but also by technical aspects used to calculate CA. Most indices of dynamic CA assume steady state physiological conditions (Zhang et al. 2002; Claassen et al. 2016; Mitsis et al. 2006; Tiecks et al. 1995) which are not strictly met during orthostatic stress, particularly with head-up tilt test (HUTT). Therefore, commonly used linear approaches, such as transfer function analysis (Zhang et al. 1998), may not be applied (Dineen et al. 2010; Latka et al. 2005; Rowley et al. 2007; Mitsis et al. 2004). As a consequence, the ability to obtain estimates of CA in orthostatic intolerance syndromes has been limited by the non-stationarity of physiological mechanisms that preclude the use of more established techniques such as transfer function analysis (TFA) (Dineen et al. 2010; Latka et al. 2005; Castro et al. 2014; Rowley et al. 2007; Mitsis et al. 2004).

Techniques of continuous CA estimation could overcome this pitfall (Dineen et al. 2010; Castro et al. 2014; Panerai et al. 2015). Recent developments in modeling dynamic CA have led to nonstationary indices of dynamic CA (Dineen et al. 2010; Giller and Mueller 2003; Latka et al. 2005; Mitsis et al. 2004; Novak et al. 2004; Rowley et al. 2007; Panerai et al. 2016). One relevant recent development is the possibility of obtaining continuous estimates of ARI with temporal resolution of a few seconds. The feasibility of this approach has been demonstrated in recordings obtained at rest (Panerai et al. 2008, 2005), during respiratory maneuvers such as breath holding or hyperventilation (Dineen et al. 2010; Panerai et al. 2010), during Valsalva maneuver (Castro et al. 2014) and tight cuff release (Panerai et al. 2015).

Time-varying changes in dynamic CA parameters have not been described during HUTT in healthy subjects as well as in patients with orthostatic intolerance. HUTT is also particularly well suited for the involvement of autonomic nervous system by inducing predictable changes in ABP in different conditions like vasovagal syncope (Ocon et al. 2009; Goldstein et al. 2003; Carey et al. 2001a, b; Schondorf et al. 2001a, b; Lagi et al. 2001) and autonomic failure (Blaber et al. 1997; Horowitz and Kaufmann 2001; Novak et al. 1998; Bondar et al. 1997). Therefore, continuous assessment of CA during HUTT may not only give further hints into the pathophysiology of syncope but also derive new data concerning the role of autonomic nervous system in regulation of cerebral blood flow.

In addition to nonstationary indices of CA, we can also use models of instantaneous relationship between ABP and CBFV that can also help to elucidate cerebral hemodynamics during the Valsalva and the autonomic influences thereupon (Castro et al. 2014). The CBFV response during Valsalva maneuver was shown to be largely explained by changes in critical closing pressure (CrCP) (Dawson et al. 1999), possibly reflecting the rise in central venous pressure and intracranial pressure previously reported (Greenfield et al. 1984; Pott et al. 2000), while resistance area product (RAP) seemed to reflect the vasodilation effort (Dawson et al. 1999; Castro et al. 2014). The capability of this 2-parameter model to separate metabolic and myogenic cerebrovascular mechanisms has been proposed during changes in posture and sensorimotor stimulation (Maggio et al. 2013; Azevedo et al. 2011; Carey et al. 2001a; Panerai 2003; Panerai et al. 2012).

Taken together, the overall approach can provide further insights into cerebral hemodynamics in the context of orthostatic stress as well and provide future clinical benefits in diagnosis and treatment.

To understand the behavior of CA during orthostatic challenge and the role of autonomic nervous system in cerebrovascular regulation, we aimed to compare dynamic CA changes between healthy subjects, VVS and AF patients during HUTT. We tested whether dynamic CA remains constant during orthostatic stress and autonomic dysfunction or if hyperadrenergic status conditions (Freitas et al. 2007; Goldstein et al. 2003) of VVS could affect that response.

Materials and methods

This study was performed in São João Hospital Center, a University Hospital in Porto, Portugal. The local institutional ethical committee approved the study. Each participant gave written informed consent.

Population studied

We compared three groups of subjects: healthy controls, patients with AF due to familial amyloidotic polyneuropathy and patients with VVS. Our AF model consists of eight patients (6 males), age of 31.4 ± 6.5 (range 23–43) years, with familial amyloidotic polyneuropathy type I (4) caused by transthyretin gene Val-30Met mutation. It is a hereditary autosomal dominant disease leading to deposition of abnormal transthyretin in many organs, typically in the peripheral nerves (4). This causes early dysfunction of autonomic fibers being orthostatic hypotension a hallmark of the disease. Autonomic characteristics of this group were detailed in previous work (Castro et al. 2014). In summary, we selected only patients with severe AF (Carvalho et al. 2000) and all had orthostatic hypotension (fall in systolic/diastolic ABP during HUTT of at least 20/10 mmHg) with incapacitating symptoms. The facts that central nervous system is usually spared (26) and the usual absence of classic vascular risk factors, makes this disease a well-suited model to study the impact of AF on cerebrovascular regulation. VVS group consisted of 8 patients (4 male) aged 30.2 ± 8.7 (range 23–42) years old, who had frequent repetitive clinical vasovagal syncope episodes (more than six episodes in the last 2 years) and a positive passive 70° HUTT with reproduction of symptoms without pharmacological provocation. These patients re-experienced syncope in the study during HUTT with a mean lag time of 26 ± 6 min (range 13–41). The VVS group was characterized before as having increased adrenergic activity, particularly increased adrenaline production and higher frequency systolic ABP variability in response to HUTT, that was analyzed in previous work (Freitas et al. 2007). The control group consisted of 8 healthy volunteers (5 male) from our hospital and faculty staff, with a mean age of 28.3 ± 5.9 years old (range 27–36). All participants performed a carotid and transcranial duplex scan, with a HDI 5000 device (Philips, USA). Normal findings of extra- and intracranial vessels, and a good temporal acoustic bone window, were required as inclusion criteria. Classical risk factors including smoking, hypertension, diabetes mellitus and dyslipidemia were exclusion criteria for all participants.

Experimental protocol

Participants were asked to refrain from any medication, alcohol-, nicotine-, or caffeine-containing products for a minimum of 12 h. Evaluations were carried out in a quiet room with a constant temperature around 22 °C. ABP and heart rate (HR) were continuously monitored in the left hand with a non-invasive finger cuff Finapres® device (model 2300; Ohmeda, Englewood, CO, USA) with its pressure height correction unit placed at heart level. CBFV was recorded in M1 segment of both middle cerebral arteries (MCA) at depth of 50–55 mm with 2 MHz pulsed wave Doppler monitoring probes of a Multidop® X4 Doppler device (DWL, Sipplingen, Germany) mounted on an individually fitted headband. Data were continuously stored for offline analysis.

Data recording began after 30 min of bed rest, during 10 min in supine position, and then during tilting at 70° HUTT for a maximum of 45 min or until syncope occurred.

Data analysis

All signals were visually inspected to identify artifacts or noise, and narrow spikes were removed by linear interpolation. In supine condition, ABP at MCA was equivalent to that measured at heart level but during HUTT ABP was adjusted to heart–brain distance. Mean beat-to-beat values were calculated for ABP and CBFV using the area between diastolic points. Two different pressure–velocity models were evaluated. Firstly, the classical cerebrovascular resistance index (CVRi) was estimated by the ratio of mean ABP/mean CBFV for each heartbeat, for both MCAs (Aaslid et al. 1989; Tiecks et al. 1995). Secondly, the instantaneous relationship between ABP and CBFV was used to estimate the CrCP and RAP of the cerebral circulation for each cardiac cycle, using the first harmonic method (Aaslid et al. 2003; Panerai 2003). Consequently, for each cardiac cycle, the fundamental frequency of ABP and CBFV was extracted from raw signals and aligned previously to calculation of the straight-line fit (further details in "Appendix"). CVRi calculation assumes that there is a linear relationship between ABP and CBFV, i.e., flow ceases only when ABP is zero. However, at various vascular beds, including the brain, flow stops at higher values of ABP (Panerai 2003). This parameter has been shown to be important to cerebrovascular tone control mainly reflecting changes due to metabolic stimulus to cerebral blood flow, like cognitive (Salinet et al. 2013), CO_2 (Panerai 2003) and intracranial pressure (Castro et al. 2014). Taking this into account, the CrCP + RAP model provides a more accurate representation of the relationship between ABP and CBFV.

Some evidence suggests that RAP follows physiologically changes presumed to be predominantly myogenic (Castro et al. 2014; Panerai et al. 2005).

All beat-to-beat estimates were interpolated with a third-order polynomial and resampled at 0.2-s intervals to generate a time series with a uniform time-base. To correct for differences at baseline values and, in the case of CBFV, to become independent from the TCD insonation angle, data were also normalized by their mean baseline values.

We compared the three groups during the first 3 min of HUTT and data were normalized to the beginning of HUTT. Additionally, we compared VVS and controls in the last 5 min before and 1 min after the time of occurrence of syncope. For this purpose, data were normalized with reference to syncope. To assure that controls could be compared at similar time marks, we normalized the data in this group at 26 min (mean time of syncope in VVS group during HUTT). To further explore the cerebrovascular hemodynamic response to HUTT, we evaluated CA by two methods, by transfer function analysis and through calculation of continuous ARI, as explained below.

Transfer function analysis

Dynamic CA was assessed by Transfer Function Analysis (TFA) by calculating coherence, gain and phase parameters from beat-to-beat spontaneous oscillations in CBFV and ABP (Claassen et al. 2016). TFA parameter settings were in compliance with standard recommendations (Claassen et al. 2016): 10 min of data interpolated at 10 Hz with a third-order polynomial spline; window length of 102 s; Hanning anti-leakage window; 50% superposition window, triangular smooth filtering. Values were reported in three spectral bands: very low frequency (VLF: 0.02–0.07 Hz), low frequency (LF: 0.07–0.20 Hz) and high frequency (HF: 0.20–0.50 Hz). CA is believed to operate at slower VLF and LF bands as a high-pass filter (Meel-van den Abeelen et al. 2014). Lower coherence (correlation coefficient), lower gain (damping of ABP oscillations) and higher phase (speed of the autoregulatory response) between oscillations of ABP and CBFV tend to indicate more effective CA.

Baseline and continuous dynamic autoregulation index

Using the inverse fast Fourier transform of the transfer function, the CBFV response to a step change in ABP was also derived (Panerai 2008; Zhang et al. 1998). The CBFV step response was compared with 10 template curves proposed by Tiecks et al. (1995) and the best fit curve corresponded to the ARI (Panerai 2008). An interpolation procedure was adopted to obtain real values of ARI (as opposed to only integer values) by fitting a second-order polynomial to the integer values of ARI neighboring the region of minimum error (Panerai 2008). Values of ARI = 0 indicate the absence of CA, while ARI = 9 corresponds to the most efficient CA that can be observed (Tiecks et al. 1995). A new procedure was adopted using the normalized mean square error for fitting the model to the CBFV step response and a minimum threshold for the LF coherence function to accept or reject estimates of ARI (Panerai et al. 2016).

Noteworthy, classical calculation of a single ARI index for recordings lasting several minutes is not acceptable during maneuvers like Valsalva maneuver that induce non-stationary time-series. For this propose, a time-varying ARI [ARI(t)] was derived from a autoregressive–moving-average (ARMA) structure after implementation of Tiecks' model and use of the Walsh set of orthogonal basis functions to obtain ARMA models with time-varying parameters as previously described (Panerai et al. 2010). Once those parameters are obtained, it is possible to calculate a corresponding CBFV step response for each instant of time, each one leading to an estimate of ARI(t). A maximum of 19 orthogonal functions were adopted and ARI(t) was calculated at 0.2-s intervals. Using this model, Panerai et al. (2010) showed that ARI(t) presented characteristic time-varying patterns during respiratory maneuvers of apnoea and hyperventilation, providing a physiological validation of this method. We also showed significant changes during Valsalva maneuver due to AF (Castro et al. 2014).

Statistical analysis

Normality of the variables was determined by Shapiro–Wilk test. ANOVA and Student's t test was used to compare baseline resting values between groups and paired t test to compare right and left MCA within each group. In the absence of statistically significant differences between parameters derived from the right and left MCA, these were averaged for all subsequent analyses. Two-way repeated-measures ANOVA was used to find differences between groups and different phases of HUTT: within each group differences between phases were calculated using simple contrast with reference to baseline resting values for the first part of HUTT and to the time period of syncope in VVS or equivalent in controls; Bonferoni's post hoc test for multiple comparisons was used to detect differences between groups at each stage when interaction between group and phase factor was significant. Statistical significance was inferred at a $p < 0.05$ level.

Results

Baseline values for systemic and cerebral hemodynamic parameters were not different between AF, VVS and controls (Table 1) except for significantly reduced ABP and

Table 1 Baseline resting absolute values for systemic and cerebral hemodynamic parameters concerning right and left MCA for controls, vasovagal syncope (VVS) and autonomic failure (AF) patients

Parameter	Control	VVS	AF	*p* value*
HR, bpm	81 ± 8	71 ± 8.4	82.9 ± 8.8	0.641
CV, %	5.0 ± 1.3	5.6 ± 2.6	1.9 ± 1.9†,∫	<0.001
Mean ABP, mmHg	81 ± 11	78 ± 9	91 ± 20	0.235
CV, %	4.4 ± 0.9	3.9 ± 1.1	2.3 ± 0.7†∫	<0.001
PP, mmHg	50 ± 13	48 ± 12	50 ± 9.3	0.914
Mean CBFV, cm/s				
Right MCA	66 ± 15	68 ± 11	64 ± 12	0.737
Left MCA	68 ± 11	69 ± 12	72 ± 14	0.428
CV, %				
Right MCA	5.2 ± 1.3	6.1 ± 1.1	5.5 ± 1.4	0.559
Left MCA	5.1 ± 1.5	6.0 ± 1.2	5.3 ± 1.9	0.754
CrCP, mmHg				
Right MCA	24 ± 15	28 ± 15	32 ± 15	0.301
Left MCA	24 ± 15	26 ± 18	26 ± 11	0.444
RAP, mmHg/cm/s^2				
Right MCA	0.89 ± 0.30	0.77 ± 0.13	0.88 ± 0.18	0.722
Left MCA	0.90 ± 0.27	0.76 ± 0.17	0.85 ± 0.21	0.732
CVRi, mmHg/cm/s^2				
Right MCA	1.00 ± 0.19	1.17 ± 0.19	1.18 ± 0.34	0.166
Left MCA	1.00 ± 0.19	1.15 ± 0.24	1.01 ± 0.36	0.634

All values are given as mean ± SD

HR heart rate, *CV* coefficient of variation, *ABP* arterial blood pressure, *PP* pulse pressure, *CBFV* cerebral blood flow velocity, *CVRi* cerebrovascular resistance index, *RAP* resistance area product, *CrCP* critical closing pressure

* ANOVA *p* value for differences between AF, VVS and control groups

†,∫Student's *t* test *p* value of for differences between AF and control or VVS groups, respectively

Table 2 Baseline resting absolute values for systemic and cerebral hemodynamic parameters concerning right and left MCA for both controls, Vasovagal syncope (VVS) and autonomic failure (AF) patients

Parameter	Control	VVS	AF	*p* value*
Mean CBFV power, cm^2/s^2	14.0 ± 7.0	14.5 ± 7.0	13.1 ± 10	0.859
Mean ABP power, mmHg^2	11.1 ± 4.7	12.1 ± 8.4	4.1 ± 3.0†,∫	0.003
Coherence, a.u.				
VLF (0.02–0.07 Hz)	0.44 ± 0.08	0.47 ± 0.11	0.18 ± 0.09	<0.001
LF (0.07–0.15 Hz)	0.63 ± 0.15	0.56 ± 0.18	0.32 ± 0.24	<0.001
HF (0.15–0.5 Hz)	0.55 ± 0.22	0.55 ± 0.16	0.52 ± 0.22	0.737
Gain, %/mmHg				
VLF	1.10 ± 0.27	1.31 ± 0.92	1.34 ± 0.54	0.169
LF	1.81 ± 0.31	1.70 ± 0.44	1.51 ± 0.38	0.377
HF	2.01 ± 0.30	1.69 ± 0.41	1.72 ± 0.43	0.498
Phase, radians				
VLF	1.18 ± 0.28	0.82 ± 0.47	1.67 ± 0.96	0.160
LF	0.87 ± 0.16	0.68 ± 0.34	0.80 ± 0.36	0.378
HF	0.30 ± 0.36	0.03 ± 0.38	0.37 ± 0.23	0.611
ARI(*t*), (a.u)	7.1 ± 1.2	6.3 ± 1.4	6.9 ± 1.2	0.346

All values are given as mean ± SD

ABP arterial blood pressure, *CBFV* cerebral blood flow velocity, *VLF* very low, *LF* low and *HF* high frequency bands of transfer function from ABP to CBFV, *ARI* continuous estimates of Cerebral Autoregulation Index

* ANOVA *p* value for differences between AF, VVS and control groups

†,∫Student's *t* test *p* value of for differences between AF and control or VVS groups, respectively

HR variability in AF group (either coefficient of variation of mean ABP and HR ($p < 0.001$) and as mean ABP power spectral density power ($p < 0.001$; Table 2). Despite that, CBFV variability was similar in AF as compared to VVS or controls (coefficient of variation, Table 1 and spectral density power, Table 2). Table 2 and Fig. 1 show the results for TFA and classic ARI calculations. ARI, gain and phase were similar among groups. Despite that, AF patients showed lower coherence at VLF and LF bands ($p < 0.001$).

Hemodynamic response to HUTT

The initial response results to HUTT are detailed in Table 2. With the exception of HR and CrCP, all other parameters presented significant longitudinal differences on a repeated-measures ANOVA ($p < 0.01$). After 30 s of HUTT, AF group, as expected, showed marked decrease in mean ABP (around 30%, $p < 0.0001$) as well as in ABP pulse pressure (around 40%, $p < 0.0001$). This group also showed a similar decrease in mean CBFV (around 30%, $p < 0.0001$). RAP and CVRi, indexes representing cerebral vascular tonus, behave differently during HUTT in AF vs controls. CVRi did not detect significant changes ($p = 0.110$). However, RAP showed significant decrease (around 20%, $p < 0.0001$), meaning cerebral vasodilation induced by HUTT. CrCP did not change significantly during HUTT ($p = 0.126$) although it showed some tendency to decrease around 2.5–3 min of initial HUTT in AF subjects. This may represent mixed effects of returning the tilt table to 0° in some patients due to orthostatic pre-syncopal symptoms before the stipulated 3 min by protocol ($n = 3$).

VVS and controls showed no significant differences during initial HUTT, without changes in CVRi ($p = 0.110$), as observed in Fig. 2f. The hemodynamic changes during the last 5 min preceding syncope in VVS and corresponding

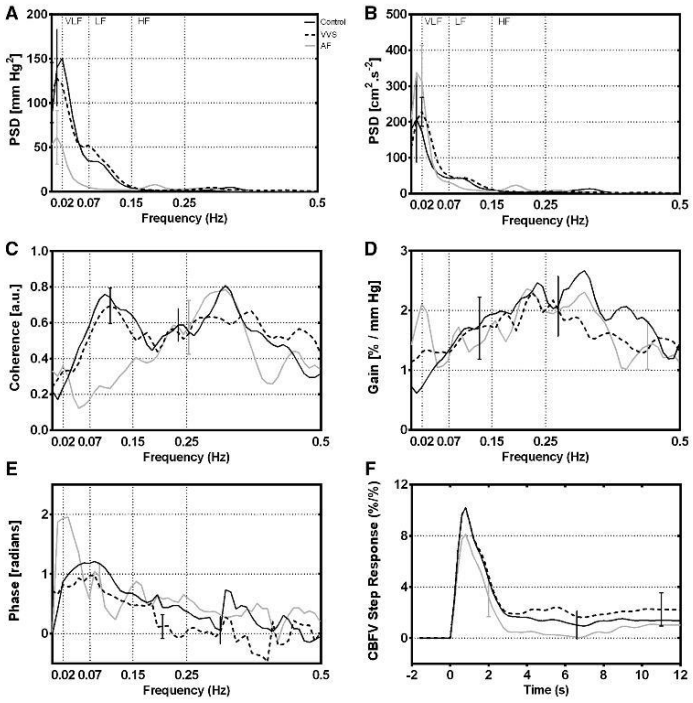

Fig. 1 Comparison of group-averaged parameters of dynamic cerebral autoregulation between control (*black continuous line*), Vasovagal Syncope (VVS; *black dashed line*) and Autonomic failure (AF; *gray line*) groups at supine resting position. **a**–**e** Transfer Function analysis results, along 0–0.5 Hz frequency range, of mean arterial blood pressure (ABP) and mean cerebral blood flow velocity (CBFV) spectra **a** power spectra of mean ABP and **b** mean CBFV and transfer function **c** coherence, **d** normalized gain and **e** phase. Very low (VLF), low (LF) and high (HF) frequency bands of transfer function from ABP to CBFV. CBFV step response **f** is used to calculate classical autoregulation index (ARI). For clarity, only the largest ± SE *bar* is represented at the point of occurrence (control group does not have *whiskers* on *top*)

time in controls are presented in Fig. 3, and the respective statistical analysis in Table 4. Whereas controls maintained relatively stable values of hemodynamic parameters during late HUTT, VVS patients showed already significant changes 5 min before and during syncope. Prior to syncope, VVS subjects showed progressive cerebral vasoconstriction (reduced CBFV 19 ± 15 versus 1 ± 6%, $p < 0.0001$; increased RAP 12 ± 18 versus 2 ± 3%, $p = 0.024$ and CVRi 12 ± 18 versus 2 ± 3%, $p = 0.005$). During syncope and compared to controls, there was significant decrease in mean ABP and Pulse Pressure (both ~40%, $p = 0.001$). CBFV also decreased around 25% ($p = 0.003$). RAP and CVRi decreased around 30% ($p = 0001$ and $p = 0.030$, respectively) meaning a cerebral vasodilation response to ABP fall. CrCP remained unchanged ($p = 0.862$).

Dynamic CA response during HUTT

The changes in dynamic CA throughout the orthostatic test were compared in all the three groups at initial HUTT (Fig. 4a; Table 3) and between VVS and controls in the 300 s preceding and the 60 s following syncope (Fig. 4b; Table 4). In healthy subjects, ARI(t) did not change significantly during HUTT. However, VVS and AF patients showed a time-varying behavior of dynamic CA in response to ABP fall at initial orthostatic challenge. At initial HUTT, AF patients tended to achieve higher values of ARI(t) around 120–180 s compared to baseline values (Fig. 4a, $p < 0.001$), which was delayed from the time ABP drop reached its nadir at ~60 s (Fig. 2a, gray line). Considering VVS group, ARI(t) trends during HUTT were similar to controls ($p > 0.05$, Fig. 4a) but at late HUTT ARI(t) increased significantly ($p < 0.01$) in response to ABP fall with syncope (marked at 0 s in Figs. 3a, 4b), reaching its highest value within around ~20–30 s (Fig. 4b).

Discussion

Main findings

Continuous assessment of dynamic CA status during HUTT has not been described previously. In this study,

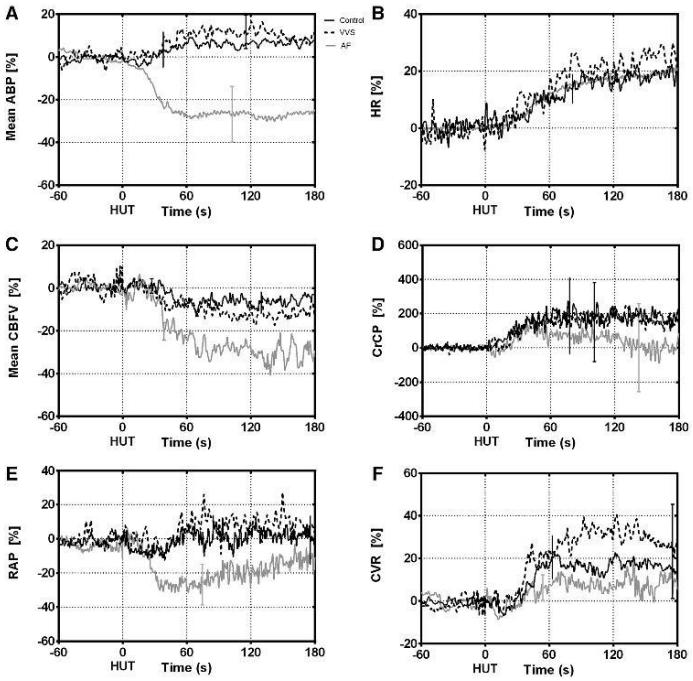

Fig. 2 Group-averaged normalized changes in mean cerebral blood flow (CBFV; **a**), mean arterial blood pressure (ABP; **b**), heart rate (HR; **c**), critical closing pressure (CrCP; **d**), resistance area product (RAP; **e**) and cerebrovascular resistance index (CVRi; **f**) during the first 3 min of 70° Head-up Tilt Test (HUTT). Comparison between control (*black continuous line*), Vasovagal Syncope (VVS; *black dashed line*) and autonomic failure (AF; *gray line*) groups. Averaging was synchronized at beginning of HUTT. For clarity, only the largest ± SE *bar* is represented at the point of occurrence (control group does not have *whiskers* on *top*)

we have shown that CA, obtained by ARMA modeling to obtain estimates of ARI(*t*), is a time-varying phenomena during orthostatic stress and shows an increased performance in response to ABP fall due to autonomic dysfunction or neutrally mediated syncope.

Most of the previous studies of dynamic CA based on HUTT have estimated temporal changes in cardiovascular resistance by the ratio mean ABP/CBFV (i.e., CVRi). However, CVRi does not provide a realistic representation of instantaneous pressure-flow curves of the cerebral circulation (7, 28). A considerable number of studies have shown that as ABP is reduced, cerebral blood flow (or velocity) tends to reach zero for ABP values that are significantly greater than zero. This value of ABP has been called the CrCP of the cerebral circulation (1, 7, 9, 28). Conversely, the slope of instantaneous pressure–velocity relationships has been termed RAP to take into account the dimensional units of the ratio ΔABP/ΔCBFV (11). To our knowledge, time-varying changes in RAP and CrCP during orthostatic hypotension have not been reported before. Following the drop in mean BP, RAP is significantly reduced, with minimal changes in CrCP (Fig. 2e, f). We also confirmed previous studies (Carey et al. 2001a; Dawson et al. 1999; Panerai et al. 2005; Castro et al. 2012, 2014) showing that a 2-parameter model (RAP + CrCP), can provide clearer discrimination of changes in cerebral hemodynamics than the classical single CVRi parameter, in subjects with autonomic failure (Castro et al. 2014).

Effects of autonomic dysfunction in the control of CA at rest

CA was assessed by two distinct methods at rest. The first one was by transfer function analysis, one of the most commonly used methods in the literature (Claassen et al. 2016). In this method, CA is regarded as a high-pass filter between ABP input to CFBV output, provided that a linear relationship is assured by critical values of coherence function. CA was also compared accordingly to ARI values derived from CBFV step response.

Patients with AF or recurrent VVS did not have significant differences compared to healthy subjects. However, AF patients showed low coherence values at low frequency bands, particularly at 0.07–0.15 Hz, where CA is believed to be active. This is certainly a consequence of very low ABP variability (Table 2), which reduces signal-to-noise

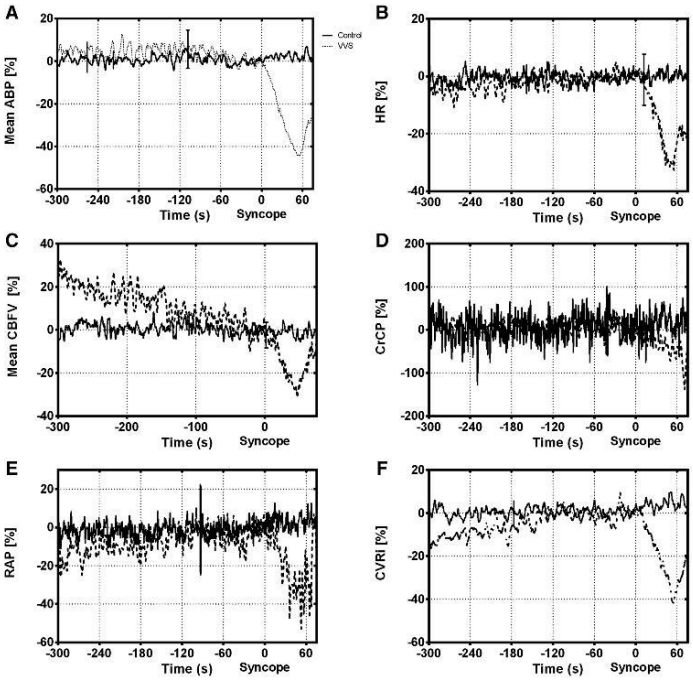

Fig. 3 Group-averaged normalized changes in mean CBFV (**a**), mean ABP (**b**), HR (**c**), CrCP (**d**), RAP (**e**) and CVRi (**f**) during the last 5 min of 70° Head-up Tilt Test (HUTT) before syncope in VVS and corresponding time in controls (26 min of HUTT). Comparison between control (*black continuous line*) and Vasovagal Syncope (VVS; *black dashed line*). Averaging was synchronized at time of syncope during of HUTT in VVS group. All cases of control group was synchronized at the median time of syncope occurrence in VVS group (27 min). For clarity, only the largest ± SE *bar* is represented at the point of occurrence (control group does not have *whiskers* on *top*)

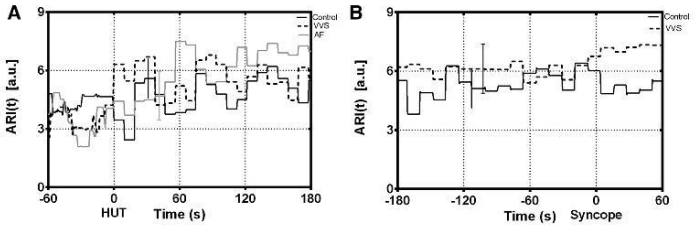

Fig. 4 Group-averaged normalized changes in Cerebral Autoregulation Index [ARI(*t*)] during the (70° Head-up Tilt Test (HUTT). In **a**, the first 3 min of HUTT are compared between controls (*black continuous line*), Vasovagal Syncope (VVS; *black dashed line*) and autonomic failure (AF; *gray line*) patients and data is synchronized at beginning of HUTT. In **b**, data from VVS patients was synchronized at time of syncope. For comparison, the data of control was synchronized at 27 min of HUTT which was the median time of syncope of VVS group. For clarity, only the largest ± SE *bar* is represented at the point of occurrence (control group does not have *whiskers* on *top*)

ratio with CBFV, undermining the validity of the TFA in AF. With such low coherence values, gain and phase data cannot be reliability calculated within these frequency bands (Claassen et al. 2016).

Curiously, Zhang et al. (1998) reported similar low coherence between ABP and CBFV when otherwise healthy subjects were subjected to autonomic ganglion blockade. However, when slow blood pressure oscillations were introduced by negative lower-body pressure, gain and phase remained altered, and concluded that autonomic dysfunction impaired CA intrinsically. In contrast, our results show no differences in gain and phase. One explanation

Table 3 Response of cerebral and systemic hemodynamic parameters during first 3 min of HUT, for controls, Vasovagal syncope (VVS) and autonomic failure (AF) patients

Parameter	Hemodynamic response to 70° HUT				ANOVA $p^{\ddagger}$
	30 s	60 s	120 s	180 s	
Mean ABP, %					
Control	−2 ± 5	4 ± 8	6 ± 10*	7 ± 12*	<0.0001
VVS	1 ± 3	7 ± 6*	12 ± 3*	10 ± 4*	
AF	−7 ± 8	−24 ± 17*†	−27 ± 23*†	−29 ± 27*†	
PP, %					
Control	−4 ± 12	−5 ± 11	−10 ± 9*	10 ± 10*	<0.0001
VVS	3 ± 8	−12 ± 12*	−12 ± 10*	−12 ± 14*	
AF	−3 ± 13*	−31 ± 18*†	−39 ± 22*†	−38 ± 26*†	
HR, %					
Control	−2 ± 6	3 ± 9	9 ± 12*	12 ± 13*	0.470
VVS	2 ± 4	11 ± 7*	20 ± 10*	24 ± 11*	
AF	0 ± 5	6 ± 9*	16 ± 13*	18 ± 14*	
Mean CBFV, %					
Control	1 ± 6	−3 ± 6	−6 ± 5*	−7 ± 6*	<0.0001
VVS	1 ± 4	−7 ± 10	−11 ± 7*	−12 ± 9*	
AF	−5 ± 8	−26 ± 11*†	−33 ± 14*†	−36 ± 17*†	
CrCP, %					
Control	31 ± 140	146 ± 295*	174 ± 320*	168 ± 230*	0.126
VVS	51 ± 122	149 ± 150*	188 ± 140*	181 ± 158*	
AF	5 ± 194	99 ± 121*	63 ± 203	9 ± 176	
RAP, %					
Control	−6 ± 9*	−3 ± 14	1 ± 16	3 ± 18	<0.0001
VVS	0 ± 11	−1 ± 13	9 ± 18	10 ± 19	
AF	−7 ± 10*	−26 ± 14*†	−22 ± 20*†	−17 ± 23*†	
CVRi, %					
Control	−2 ± 6	11 ± 13*	17 ± 18*	19 ± 19*	0.110
VVS	0 ± 4	17 ± 14*	30 ± 12*	30 ± 19*	
AF	−3 ± 5	2 ± 21	2 ± 26	3 ± 30	
ARI(*t*), a.u					
Control	3.6 ± 1.4	4.8 ± 1.3	4.7 ± 1.4	5.8 ± 1.3	0.040
VVS	5.2 ± 1.3	4.6 ± 1.2	5.4 ± 1.3	5.7 ± 1.2	
AF	4.2 ± 1.1	4.2 ± 1.0	6.2 ± 1.2*	6.9 ± 1.2*†	

All values are given in percentage (normalized), except for continuous estimates of Autoregulation Index [ARI(*t*)]

HUT head-up tilt, *HR* heart rate, *ABP* arterial blood pressure, *PP* pulse pressure, *CBFV* cerebral blood flow velocity, *CVRi* cerebrovascular resistance index, *RAP* resistance area product, *CrCP* critical closing pressure

* Significance for differences from baseline ($p < 0.05$)

† Significance for differences compared to controls ($p < 0.05$)

‡ p value of two-way repeated-measures ANOVA

may be related to the models of AF used. Those authors induced at transitory AF status in an otherwise healthy population but our AF group, of chronically denervated familial autonomic polyneuropathy patients, has long standing autonomic dysfunction which might have induced adaptive changes of cerebral vasculature dynamics (Horowitz and Kaufmann 2001; Hilz et al. 2002; Vokatch et al. 2007). Our previous work with Valsalva maneuver (Castro et al. 2014) with the same AF group, also suggested some chronic vascular adaptation as these patients did not show an increased CBFV post Valsalva that would suggest a "hyperemic response" due to autonomic dysfunction as it was reported by Zhang et al. (2004), again using ganglionic blockade. Other possible explanation is the non-ABP influences on CBFV, as arterial CO_2. Marmarelis et al. (2012) obtained models demonstrating the existence of nonlinearities in the

Table 4 Variation of cerebral and systemic hemodynamic parameters during last 5 min of HUT before syncope for VVS patients compared to controls

Parameter	Last 5 min of 70° HUT before syncope						ANOVA $p^{\ddagger}$
	−300 s	−180 s	−60 s	Sync. $t = 0$	+30 s	+60 s	
Mean ABP, %							
Control	1 ± 3	1 ± 4	2 ± 5	0 ± 1	2 ± 4	2 ± 5	<0.0001
VVS	5 ± 9	6 ± 5	5 ± 4	1 ± 4	−12 ± 7*†	−38 ± 18*†	
PP, %							
Control	1 ± 6	1 ± 8	3 ± 9	−1 ± 3	3 ± 7	−4 ± 11	<0.0001
VVS	19 ± 22*†	−12 ± 11*†	10 ± 11*	−1 ± 5	−8 ± 5*†	−22 ± 28†	
HR, %							
Control	−1 ± 3	−1 ± 4	−1 ± 4	0 ± 3	0 ± 3	1 ± 4	0.002
VVS	−4 ± 11	−2 ± 8	−1 ± 5	0 ± 4	−5 ± 10	−25 ± 19*†	
Mean CBFV, %							
Control	1 ± 3	1 ± 5	1 ± 4	−1 ± 2	−1 ± 3	−2 ± 5	<0.0001
VVS	19 ± 15*†	12 ± 9*†	7 ± 7*	2 ± 5	−9 ± 11*†	−23 ± 11*†	
CrCP, %							
Control	0 ± 35	3 ± 27	6 ± 28	0 ± 47	−4 ± 33	1 ± 19	0.546
VVS	2 ± 25	5 ± 32	−1 ± 54	1 ± 26	−22 ± 65	−75 ± 73	
RAP, %							
Control	2 ± 3	−2 ± 7	−1 ± 6	3 ± 8	3 ± 8	2 ± 8	0.024
VVS	−12 ± 18*†	−7 ± 12	−3 ± 10	−3 ± 6	−9 ± 13†	−30 ± 15*†	
CVRi, %							
Control	2 ± 4	1 ± 6	1 ± 6	0 ± 2	3 ± 5	4 ± 4	0.005
VVS	−10 ± 15*†	−3 ± 9	0 ± 8	−1 ± 4	−6 ± 7†	−30 ± 25*†	
ARI(t), a.u							
Control	4.7 ± 1.2	4.9 ± 1.8	5.0 ± 1.7	5.3 ± 1.1	5.3 ± 1.0	4.9 ± 1.7	0.015
VVS	5.2 ± 1.1	5.2 ± 1.0	5.4 ± 2.1	5.1 ± 1.1	7.1 ± 1.1*†	7.3 ± 1.2*†	

All values are given in percentage (normalized) except for continuous estimates of Autoregulation Index [ARI(t)]

HUT head-up tilt, *HR* heart rate, *ABP* arterial blood pressure, *PP* pulse pressure, *CBFV* cerebral blood flow velocity, *CVRi* cerebrovascular resistance index, *RAP* resistance area product, *CrCP* critical closing pressure, *Sync.* time of occurrence of syncope

* Significance for differences from baseline ($p < 0.05$)

† Significance for differences between controls and Vasovagal syncope (VVS) patients ($p < 0.05$)

‡ p value of two-way repeated-measures ANOVA

CA process within the dynamic range of the analyzed data, especially in the frequency range below 0.08 Hz. They have further shown that the CO_2 effects on cerebral blood flow are more nonlinear than the pressure effects and that they are manifested mostly in the low frequency range from 0.02 to 0.08 Hz. Unfortunately, we did not have CO_2 monitoring in this study, to allow a comparison.

Nevertheless, continuous estimates of ARI(t) could overcome non-stationeries of the ABP-CBFV relationship and this parameter, in fact, was not significantly different between AF and healthy controls. In previous study, we also noticed that before and after Valsalva maneuver, ARI(t) was similar between AF and healthy subjects (Castro et al. 2014), which is in accordance with the results of the present study. Noteworthy, the way RAP adapted to the changes in mean ABP across the different stages of tilting (Table 3), demonstrates an active CA and supports the hypothesis that RAP changes mainly reflect myogenic control of cerebral blood flow (Carey et al. 2001a; Castro et al. 2014; Maggio et al. 2013; Panerai et al. 2005, 2012).

Effects of increased sympathetic (adrenergic) activity in the control of CA at rest

VVS patients did not have significant differences of ARI(t) or TFA parameters compared with healthy or AF subjects. VVS is considered to have increased sympathetic outflow (Goldstein et al. 2003), with disproportionate increase in adrenaline production. This was also demonstrated in this same VVS group, even at rest (Freitas et al. 2007). This sympathetic imbalance aggravates during orthostatic stress (Goldstein et al. 2003; Freitas et al. 2007), which is one of

the mechanisms believed to contribute to the predisposition for syncope by increasing systolic ABP variability and decreasing baroreflex gain (Freitas et al. 2007). We can conclude that increased adrenergic activity does not seem to affect CA, at least in these types of patients.

Dynamic CA response to orthostatic stress in healthy subjects and autonomic modulation

In healthy subjects, dynamic CA, as assessed by continuous estimates of ARI(*t*), showed a tendency to be stable in response to HUTT. To our knowledge, this is the first time that continuous estimates of dynamic CA changes were described in HUTT. Overall, the more or less superimposed patterns of ARI(*t*) during HUTT, both in AF and VVS subjects in comparison with controls, strongly suggests that there is no major autonomic involvement in dynamic CA response to HUTT, as proposed by other groups (Mitsis et al. 2006; Cassaglia et al. 2009; Zhang et al. 2002). The suggestion of an increase in ARI(*t*) during ABP fall of VVS syncope or orthostatic hypotension of AF might represent the attempt of cerebrovascular control to restore CBFV in the face of a higher drop of ABP (Panerai 2003; Panerai et al. 2005). In contrast to our results, Mitsis et al. (2006), using a two-input, nonlinear model of cerebral hemodynamics, suggested that dynamic CA was reduced under orthostatic stress. However, this reduced regulatory capability was mainly detected at VLF range, while ARI(*t*) instead refers to LF range. Also, the different results could be due to distinct used methods, as they applied lower-body negative pressure and we used HUTT. Nevertheless, the authors show significant contribution of CO_2 to CA measurement and therefore we must be careful in our conclusions. It might be the case that hyperventilation and associated hypocapnia at the end of HUTT in VVS group could be the responsible for increased ARI*t* values (Dineen et al. 2010). Future work should try to find if CO_2 is responsible for these differences.

Mechanisms of cerebrovascular control during orthostatic stress

The mild increase in mean ABP and decrease in mean CBFV in healthy and VVS subjects are well documented before (Carey et al. 2001a, b; Dan et al. 2002; Diehl et al. 1999; Schondorf et al. 1997; Van Lieshout et al. 2003; Claydon and Hainsworth 2003; Zhang and Levine 2007). This causes an increase in CVRi which is mainly driven by an increase in CrCP while RAP remains stable (Van Lieshout et al. 2003; Panerai 2003). On the other hand, the changes in hemodynamic resistance parameters due to AF were not reported yet in literature. In AF group, during HUTT, RAP varies as expected, reflecting the cerebral vasodilation effort. AF group showed a larger reduction in CBFV during HUTT compared to controls, consistent with previous studies with ganglionic blockade (Zhang et al. 2004; Brooks et al. 1989). This is accompanied by a substantial drop in ABP which is related to adrenergic dysfunction (Freeman 2006). This cerebral vasodilation seems to be better explained, however, by the longer and deeper RAP reduction, while CVRi suggests no active change during this period. The same awkward response in CVRi in comparison to physiological decrease in RAP was noticed previously during Valsalva maneuver in healthy (Azevedo et al. 2011; Dawson et al. 1999) and patients with autonomic dysfunction (Castro et al. 2014). We speculate that RAP is more sensitive to ABP changes and, therefore, could behave as a myogenic component of cerebrovascular regulation. Previous studies support this assumption (6, 34, 37, 38). We have previously reported (Azevedo et al. 2011) blunted ABP response in AF patients when changing from supine to the sitting position with only RAP parameter reflecting cerebrovascular differences. This suggests the presence of cerebral vasodilation in adaptation to ABP challenge which was already documented previously (Novak et al. 1998; Horowitz and Kaufmann 2001). Also, RAP and not CrCP seems to follow ABP, possibly by a myogenic response (Panerai et al. 2012), explaining different CBFV responses during neurovascular coupling paradigms (Salinet et al. 2013). Contrary to CrCP, RAP seem not to be disturbed by metabolic components during complex neurovascular activation (Panerai et al. 2012; Salinet et al. 2013) or CO_2 changes (Maggio et al. 2013; Panerai et al. 2012).

We confirmed the results from previous studies that have demonstrated preservation of indices of dynamic CA in healthy subjects throughout orthostasis (Carey et al. 2001b). We also confirm that CA is intact in VVS subjects at initial HUTT but failed to show that there was a CA decline before or after syncope occurrence (7). This might imply that VVS subjects may not be a homogenous group and there could be different pathophysiological conditions leading to neurally mediated reflex syncope. In VVS group, the decrease in CBFV and increase in RAP and CVRi before syncope suggest that cerebral vasoconstriction probably is caused by hyperventilation and hypocapnia, as already reported by Carey el al, which showed that a decline in CO_2 in the last 3 min before syncope could be the responsible factor for this finding (6).

Study limitations

An important methodological concern could be the use of transcranial Doppler for measurements of cerebral blood flow. Changes in CBFV reflect changes in cerebral blood flow only if the diameter of the insonated artery remains

constant. However, several studies suggested that the diameter of the middle cerebral artery remains relatively stable during rapid alterations in arterial pressure (Newell et al. 1994) and during simulated orthostasis (Serrador et al. 2000). Despite this, some authors argue that this may not be the case under higher variations of CO_2 (Willie et al. 2012) which cannot be excluded in orthostatic challenge. Nitrous oxide, which is a vasodilatation agent, does not seem change CBFV or CA at MCA level (Harrison et al. 2002) but recent work comparing with other cerebral flow methods indirectly suggests that MCA caliber may indeed increase during nitroprusside infusion (Stewart et al. 2013). Previous work also showed that hypoxia (Willie et al. 2012) as glycerol trinitrate (Hansen et al. 2007) causes vasodilatation of MCA. Also, importantly, blood pressure response can be affected by the bioavailability of nitrous oxide (Michishita et al. 2016), especially in older female which could be important in cerebral autoregulation results, despite the fact that our individuals were young.

Continuous non-invasive measurements of ABP at peripheral have some limitations. Firstly, orthostatic challenge causes changes in wave reflection from the periphery and modify the relationship between central and peripheral blood pressure (Tabara et al. 2005), the former usually being underestimated. In second hand, it could also be suspected as a source of spurious influence due to random fluctuations in the blood flow circulation of the hand and could be regarded as a source of spurious noise during CrCP and RAP calculations. However, a previous investigation has shown that estimates of ARI(t) obtained with the moving-window ARMA technique were very similar to those derived from direct catheter-tip BP measurements in the ascending aorta (Panerai et al. 2008). Spontaneous BP fluctuations have been often adopted to measure dynamic CA but cannot be assumed to be physiologically equivalent to those induced by the thigh cuff maneuver (Aaslid et al. 1989). Some caution over the results obtained is also inherent to the methods to assess autoregulation, as ARI(t), RAP or CrCP are only estimates of some abstraction of different aspects of vascular control. This includes the interpretation of changes in RAP as caused by myogenic regulation. Although there is some evidence for this association, based on previous studies (Carey et al. 2001a; Panerai et al. 2005, 2012), its generalization is premature and further studies are needed. Another limitation of the present investigation may be the lack of CO_2 measurement. Although some studies have not found significant changes in CO_2 during this procedure (Dawson et al. 1999; Zhang et al. 2004; Wallasch and Kropp 2012) other authors reported CO_2 influences in cerebrovascular resistance and autoregulation parameters (Carey et al. 2001a; Zuj et al. 2012). Therefore, we cannot rule out the possibility that small changes in arterial CO_2 might have influenced our results, although similar changes in arterial CO_2 would be expected for all the groups. This issue might be relevant in orthostatic intolerance since hyperventilation induced by orthostatic hypotension and/or intolerance can produce CO_2 changes and also affect CA (Mitsis et al. 2004). Finally, our study enrolled a relatively small number of patients. Familial amyloid polyneuropathy is a rare disease, and nowadays patients are treated earlier, namely with pacemaker implantation and liver transplantation, that were exclusion criteria for the study. Nevertheless, this population is very homogeneous in its disease process and has absence of vascular risks factors, like diabetes, that would make it difficult to discern the effects of autonomic dysfunction among other vascular modulators and aggressors.

Conclusions

In summary, by applying a recently designed continuous estimation of ARI(t), we could measure, for the first time, the dynamic CA performance during HUTT in response to orthostatic hypotension and to reflex syncope. Our data suggest that dynamic cerebral autoregulatory response to orthostatic challenge is not affected by autonomic dysfunction or hyperadrenergic conditions observed in neurally mediated syncope. This study also emphasizes that RAP + CrCP model can be more informative than CVRi, namely during cerebral vasodilatory response to orthostatic hypotension.

Author contributions PC: (1) Analyzed data; (2) Interpreted results of experiments; (3) Prepared figures; (4) Drafted manuscript; (5) Edited and revised manuscript; (6) Approved final version of manuscript. JF: (1) Conception and design of research; (2) Performed experiments (3) Edited and revised manuscript; (3) Approved final version of manuscript. RS: (1) Performed experiments; (2) Approved final version of manuscript. RP: (1) Designed software; (2) Analyzed data; (3) Interpreted results of experiments; (4) revised manuscript; (5) Approved final version of manuscript. EA: (1) Conception and design of research; (2) Interpreted results of experiments; (3) Edited and revised manuscript; (4) Approved final version of manuscript

Compliance with ethical standards

Conflict of interest The authors report no disclosures.

Appendix

Critical closing pressure and resistance area product calculations

After the first harmonic is derived from ABP (P1) and CBFV (V1) for each cardiac cycle, the resistance area product (RAP) can be calculated as:

$$\mathrm{RAP} = \frac{\mathrm{P1}}{\mathrm{V1}}. \quad (1)$$

And the critical closing pressure (CrCP) can then be obtained as:

$$\mathrm{CrCP} = \mathrm{MAP} - V_{\mathrm{mean}} \cdot \mathrm{RAP}, \quad (2)$$

where MAP is the mean ABP for the cardiac cycle and V_{mean} the corresponding mean CBFV.

Transfer function analysis

From beat-to-beat values of mean CBFV and mean ABP, we can obtain the corresponding auto-spectra, S_{xx} and S_{yy}, with the fast Fourier transform, as well as the cross-spectra, S_{xy}, with the Welch method (Claassen et al. 2016). We deduce the oscillatory influence of ABP over CBFV at a given frequency f by the transfer function H:

$$H(f) = \frac{S_{xy}(f)}{S_{xx}(f)}. \quad (3)$$

From its real H_{R} and imaginary parts H_{I} we can then derive:

$$\text{gain,} \quad |H(f)| = \sqrt{(|H_{\mathrm{R}}(f)|^2 + |H_{\mathrm{I}}(f)|^2)}, \quad (4)$$

$$\text{phase,} \quad \varphi = \tan^{-1}\left(\frac{H_{\mathrm{I}}(f)}{H_{\mathrm{R}}(f)}\right). \quad (5)$$

T To assess how much of the output (CBFV) power is explained by the corresponding input (ABP) power at each frequency, we calculate the coherence between spectra ($\gamma^2(f)$) by the formula:

$$\gamma^2 = \frac{\left|S_{xy}(f)\right|^2}{\left|S_{xx}(f) \cdot S_{yy}(f)\right|}. \quad (6)$$

ARMA implementation of Tiecks' model

The model proposed by Tiecks et al. (1995) uses a second-order differential equation to predict the velocity signal $V(t)$ corresponding to a relative pressure change given by $\mathrm{d}P(t)$ by the formula:

$$V(t) = 1 + \mathrm{d}P(t) - K \times x_2(t), \quad (7)$$

where K represents a gain parameter in the second-order differential equation, an $x_2(t)$ is a state variable obtained from the following state equation system representing a second-order linear differential equation modeled by gain (K), time constant (T) and dampening factor (D). So, for a gives sampling frequency f and each sample discrete value n:

$$x2n = x2n - 1 - \frac{x1 - 2D \cdot x2n - 1}{f \cdot T}, \quad (8)$$

$$x1n = x1n - 1 + \frac{\mathrm{d}Pn - x2n - 1}{f \cdot T}. \quad (9)$$

In the original proposal of Tiecks et al. (1995), only 10 combinations of the parameters K, D, and T were considered, according to the values given in their Table 3, which also shows the corresponding value of ARI for each combination of these parameters.

The building of an ARMA model based on Tiecks' model is extensively detailed in previous work (Dineen et al. 2010). For the sake of simplicity, we resume main formulas of the method here. Firstly we express the transfer function as Z-transforms, and then applying an inverse Z transform to derive:

$$v(n) = a \times p(n) + b\left[p(n-1) - v(n-1)\right] + c[p(n-2)v(n-2)], \quad (10)$$

where $p(n)$ and $v(n)$ are discrete samples of $V(t)$ and $P(t)$, respectively.

Once the ARMA parameters have been estimated, the CBFV step response can be obtained from Eq. (10), and the ARI parameter can then be extracted by least squares fitting of the corresponding Tiecks et al. (1995) model responses using the first N_{fit} samples of the ARMA step response.

References

Aaslid R, Lindegaard KF, Sorteberg W, Nornes H (1989) Cerebral autoregulation dynamics in humans. Stroke 20(1):45–52

Aaslid R, Lash SR, Bardy GH, Gild WH, Newell DW (2003) Dynamic pressure–flow velocity relationships in the human cerebral circulation. Stroke 34(7):1645–1649. doi:10.1161/01.STR.0000077927.63758.B6

Azevedo E, Castro P, Santos R, Freitas J, Coelho T, Rosengarten B, Panerai R (2011) Autonomic dysfunction affects cerebral neurovascular coupling. Clin Auton Res 21(6):395–403. doi:10.1007/s10286-011-0129-3

Blaber AP, Bondar RL, Stein F, Dunphy PT, Moradshahi P, Kassam MS, Freeman R (1997) Transfer function analysis of cerebral autoregulation dynamics in autonomic failure patients. Stroke 28(9):1686–1692

Bondar RL, Dunphy PT, Moradshahi P, Kassam MS, Blaber AP, Stein F, Freeman R (1997) Cerebrovascular and cardiovascular responses to graded tilt in patients with autonomic failure. Stroke 28(9):1677–1685

Brooks DJ, Redmond S, Mathias CJ, Bannister R, Symon L (1989) The effect of orthostatic hypotension on cerebral blood flow and middle cerebral artery velocity in autonomic failure, with observations on the action of ephedrine. J Neurol Neurosurg Psychiatry 52(8):962–966

Carey BJ, Eames PJ, Panerai RB, Potter JF (2001a) Carbon dioxide, critical closing pressure and cerebral haemodynamics prior to vasovagal syncope in humans. Clin Sci (Lond) 101(4):351–358

Carey BJ, Manktelow BN, Panerai RB, Potter JF (2001b) Cerebral autoregulatory responses to head-up tilt in normal subjects

and patients with recurrent vasovagal syncope. Circulation 104(8):898–902

Carvalho MJ, van Den Meiracker AH, Boomsma F, Lima M, Freitas J, Veld AJ, Falcao De Freitas A (2000) Diurnal blood pressure variation in progressive autonomic failure. Hypertension 35(4):892–897

Cassaglia PA, Griffiths RI, Walker AM (2009) Cerebral sympathetic nerve activity has a major regulatory role in the cerebral circulation in REM sleep. J Appl Physiol 106(4):1050–1056. doi:10.1152/japplphysiol.91349.2008

Castro P, Santos R, Freitas J, Rosengarten B, Panerai R, Azevedo E (2012) Adaptation of cerebral pressure-velocity hemodynamic changes of neurovascular coupling to orthostatic challenge. Perspect Med. doi:10.1016/j.permed.2012.1002.1052 **(Available online 1028 March 2012)**

Castro PM, Santos R, Freitas J, Panerai RB, Azevedo E (2014) Autonomic dysfunction affects dynamic cerebral autoregulation during Valsalva maneuver: comparison between healthy and autonomic dysfunction subjects. J Appl Physiol 117(3):205–213. doi:10.1152/japplphysiol.00893.2013

Claassen JA, Meel-van den Abeelen AS, Simpson DM, Panerai RB, International Cerebral Autoregulation Research N (2016) Transfer function analysis of dynamic cerebral autoregulation: a white paper from the International Cerebral Autoregulation Research Network. J Cereb Blood Flow Metab. doi:10.1177/0271678X15626425

Claydon VE, Hainsworth R (2003) Cerebral autoregulation during orthostatic stress in healthy controls and in patients with posturally related syncope. Clin Auton Res 13(5):321–329. doi:10.1007/s10286-003-0120-8

Dan D, Hoag JB, Ellenbogen KA, Wood MA, Eckberg DL, Gilligan DM (2002) Cerebral blood flow velocity declines before arterial pressure in patients with orthostatic vasovagal presyncope. J Am Coll Cardiol 39(6):1039–1045

Dawson SL, Panerai RB, Potter JF (1999) Critical closing pressure explains cerebral hemodynamics during the Valsalva maneuver. J Appl Physiol 86(2):675–680

Diehl RR, Linden D, Chalkiadaki A, Diehl A (1999) Cerebrovascular mechanisms in neurocardiogenic syncope with and without postural tachycardia syndrome. J Auton Nerv Syst 76(2–3):159–166

Dineen NE, Brodie FG, Robinson TG, Panerai RB (2010) Continuous estimates of dynamic cerebral autoregulation during transient hypocapnia and hypercapnia. J Appl Physiol 108(3):604–613. doi:10.1152/japplphysiol.01157.2009

Freeman R (2006) Assessment of cardiovascular autonomic function. Clin Neurophysiol 117(4):716–730. doi:10.1016/j.clinph.2005.09.027

Freitas J, Santos R, Azevedo E, Carvalho M, Boomsma F, Meiracker A, Falcao de Freitas A, Abreu-Lima C (2007) Hemodynamic, autonomic and neurohormonal behaviour of familial amyloidotic polyneuropathy and neurally mediated syncope patients during supine and orthostatic stress. Int J Cardiol 116(2):242–248. doi:10.1016/j.ijcard.2006.03.052

Giller CA, Mueller M (2003) Linearity and non-linearity in cerebral hemodynamics. Med Eng Phys 25(8):633–646

Goldstein DS, Holmes C, Frank SM, Naqibuddin M, Dendi R, Snader S, Calkins H (2003) Sympathoadrenal imbalance before neurocardiogenic syncope. Am J Cardiol 91(1):53–58

Greenfield JC Jr, Rembert JC, Tindall GT (1984) Transient changes in cerebral vascular resistance during the Valsalva maneuver in man. Stroke 15(1):76–79

Hansen JM, Pedersen D, Larsen VA, Sanchez-del-Rio M, Alvarez Linera JR, Olesen J, Ashina M (2007) Magnetic resonance angiography shows dilatation of the middle cerebral artery after infusion of glyceryl trinitrate in healthy volunteers. Cephalalgia Int J Headache 27(2):118–127. doi:10.1111/j.1468-2982.2006.01257.x

Harrison JM, Girling KJ, Mahajan RP (2002) Effects of propofol and nitrous oxide on middle cerebral artery flow velocity and cerebral autoregulation. Anaesthesia 57(1):27–32

Hilz MJ, Axelrod FB, Steingrueber M, Stemper B (2002) Valsalva maneuver suggests increased rigidity of cerebral resistance vessels in familial dysautonomia. Clin Auton Res 12(5):385–392. doi:10.1007/s10286-002-0027-9

Horowitz DR, Kaufmann H (2001) Autoregulatory cerebral vasodilation occurs during orthostatic hypotension in patients with primary autonomic failure. Clin Auton Res 11(6):363–367

Lagi A, Cencetti S, Corsoni V, Georgiadis D, Bacalli S (2001) Cerebral vasoconstriction in vasovagal syncope: any link with symptoms? A transcranial Doppler study. Circulation 104(22):2694–2698

Latka M, Turalska M, Glaubic-Latka M, Kolodziej W, Latka D, West BJ (2005) Phase dynamics in cerebral autoregulation. Am J Physiol Heart Circ Physiol 289(5):H2272–H2279. doi:10.1152/ajpheart.01307.2004

Maggio P, Salinet AS, Panerai RB, Robinson TG (2013) Does hypercapnia-induced impairment of cerebral autoregulation affect neurovascular coupling? A functional TCD study. J Appl Physiol 115(4):491–497. doi:10.1152/japplphysiol.00327.2013

Marmarelis V, Shin D, Zhang R (2012) Linear and nonlinear modeling of cerebral flow autoregulation using principal dynamic modes. Open Biomed Eng J 6:42–55. doi:10.2174/1874230001206010042

Meel-van den Abeelen AS, van Beek AH, Slump CH, Panerai RB, Claassen JA (2014) Transfer function analysis for the assessment of cerebral autoregulation using spontaneous oscillations in blood pressure and cerebral blood flow. Med Eng Phys 36(5):563–575. doi:10.1016/j.medengphy.2014.02.001

Michishita R, Ohta M, Ikeda M, Jiang Y, Yamato H (2016) An exaggerated blood pressure response to exercise is associated with nitric oxide bioavailability and inflammatory markers in normotensive females. Hypertens Res Off J Jpn Soc Hypertens 39(11):792–798. doi:10.1038/hr.2016.75

Mitsis GD, Poulin MJ, Robbins PA, Marmarelis VZ (2004) Nonlinear modeling of the dynamic effects of arterial pressure and CO_2 variations on cerebral blood flow in healthy humans. IEEE Trans Biomed Eng 51(11):1932–1943. doi:10.1109/TBME.2004.834272

Mitsis GD, Zhang R, Levine BD, Marmarelis VZ (2006) Cerebral hemodynamics during orthostatic stress assessed by nonlinear modeling. J Appl Physiol 101(1):354–366. doi:10.1152/japplphysiol.00548.2005

Newell DW, Aaslid R, Lam A, Mayberg TS, Winn HR (1994) Comparison of flow and velocity during dynamic autoregulation testing in humans. Stroke 25(4):793–797

Novak V, Novak P, Spies JM, Low PA (1998) Autoregulation of cerebral blood flow in orthostatic hypotension. Stroke 29(1):104–111

Novak V, Yang AC, Lepicovsky L, Goldberger AL, Lipsitz LA, Peng CK (2004) Multimodal pressure-flow method to assess dynamics of cerebral autoregulation in stroke and hypertension. Biomed Eng Online 3(1):39. doi:10.1186/1475-925X-3-39

Ocon AJ, Kulesa J, Clarke D, Taneja I, Medow MS, Stewart JM (2009) Increased phase synchronization and decreased cerebral autoregulation during fainting in the young. Am J Physiol Heart Circ Physiol 297(6):H2084–H2095. doi:10.1152/ajpheart.00705.2009

Panerai RB (2003) The critical closing pressure of the cerebral circulation. Med Eng Phys 25(8):621–632

Panerai RB (2008) Cerebral autoregulation: from models to clinical applications. Cardiovasc Eng 8(1):42–59. doi:10.1007/s10558-007-9044-6

Panerai RB, Moody M, Eames PJ, Potter JF (2005) Cerebral blood flow velocity during mental activation: interpretation with different models of the passive pressure–velocity relationship. J Appl Physiol 99(6):2352–2362. doi:10.1152/japplphysiol.00631.2005

Panerai RB, Sammons EL, Smith SM, Rathbone WE, Bentley S, Potter JF, Samani NJ (2008) Continuous estimates of dynamic cerebral autoregulation: influence of non-invasive arterial blood pressure measurements. Physiol Meas 29(4):497–513. doi:10.1088/0967-3334/29/4/006

Panerai RB, Dineen NE, Brodie FG, Robinson TG (2010) Spontaneous fluctuations in cerebral blood flow regulation: contribution of $PaCO_2$. J Appl Physiol 109(6):1860–1868. doi:10.1152/japplphysiol.00857.2010

Panerai RB, Eyre M, Potter JF (2012) Multivariate modelling of cognitive-motor stimulation on neurovascular coupling: transcranial Doppler used to characterize myogenic and metabolic influences. Am J Physiol Regul Integr Comp Physiol. doi:10.1152/ajpregu.00161.2012

Panerai RB, Saeed NP, Robinson TG (2015) Cerebrovascular effects of the thigh cuff maneuver. Am J Physiol Heart Circ Physiol 308(7):H688–H696. doi:10.1152/ajpheart.00887.2014

Panerai RB, Haunton VJ, Hanby MF, Salinet AS, Robinson TG (2016) Statistical criteria for estimation of the cerebral autoregulation index (ARI) at rest. Physiol Meas 37(5):661–672. doi:10.1088/0967-3334/37/5/661

Pott F, van Lieshout JJ, Ide K, Madsen P, Secher NH (2000) Middle cerebral artery blood velocity during a valsalva maneuver in the standing position. J Appl Physiol 88(5):1545–1550

Rowley AB, Payne SJ, Tachtsidis I, Ebden MJ, Whiteley JP, Gavaghan DJ, Tarassenko L, Smith M, Elwell CE, Delpy DT (2007) Synchronization between arterial blood pressure and cerebral oxyhaemoglobin concentration investigated by wavelet cross-correlation. Physiol Meas 28(2):161–173. doi:10.1088/0967-3334/28/2/005

Salinet AS, Robinson TG, Panerai RB (2013) Active, passive, and motor imagery paradigms: component analysis to assess neurovascular coupling. J Appl Physiol 114(10):1406–1412. doi:10.1152/japplphysiol.01448.2012

Schondorf R, Benoit J, Wein T (1997) Cerebrovascular and cardiovascular measurements during neurally mediated syncope induced by head-up tilt. Stroke 28(8):1564–1568

Schondorf R, Benoit J, Stein R (2001a) Cerebral autoregulation in orthostatic intolerance. Ann N Y Acad Sci 940:514–526

Schondorf R, Stein R, Roberts R, Benoit J, Cupples W (2001b) Dynamic cerebral autoregulation is preserved in neurally mediated syncope. J Appl Physiol 91(6):2493–2502

Serrador JM, Picot PA, Rutt BK, Shoemaker JK, Bondar RL (2000) MRI measures of middle cerebral artery diameter in conscious humans during simulated orthostasis. Stroke 31(7):1672–1678

Stewart JM, Medow MS, DelPozzi A, Messer ZR, Terilli C, Schwartz CE (2013) Middle cerebral O_2 delivery during the modified Oxford maneuver increases with sodium nitroprusside and decreases during phenylephrine. Am J Physiol Heart Circ Physiol 304(11):H1576–H1583. doi:10.1152/ajpheart.00114.2013

Tabara Y, Nakura J, Kondo I, Miki T, Kohara K (2005) Orthostatic systolic hypotension and the reflection pressure wave. Hypertens Res Off J Jpn Soc Hypertens 28(6):537–543. doi:10.1291/hypres.28.537

Tiecks FP, Lam AM, Aaslid R, Newell DW (1995) Comparison of static and dynamic cerebral autoregulation measurements. Stroke 26(6):1014–1019

Van Lieshout JJ, Wieling W, Karemaker JM, Secher NH (2003) Syncope, cerebral perfusion, and oxygenation. J Appl Physiol 94(3):833–848. doi:10.1152/japplphysiol.00260.2002

Vokatch N, Grotzsch H, Mermillod B, Burkhard PR, Sztajzel R (2007) Is cerebral autoregulation impaired in Parkinson's disease? A transcranial Doppler study. J Neurol Sci 254(1–2):49–53. doi:10.1016/j.jns.2006.12.017

Wallasch TM, Kropp P (2012) Cerebrovascular response to valsalva maneuver: methodology, normal values, and retest reliability. J Clin Ultrasound JCU 40(9):540–546. doi:10.1002/jcu.21936

Willie CK, Macleod DB, Shaw AD, Smith KJ, Tzeng YC, Eves ND, Ikeda K, Graham J, Lewis NC, Day TA, Ainslie PN (2012) Regional brain blood flow in man during acute changes in arterial blood gases. J Physiol 590(14):3261–3275. doi:10.1113/jphysiol.2012.228551

Zhang R, Levine BD (2007) Autonomic ganglionic blockade does not prevent reduction in cerebral blood flow velocity during orthostasis in humans. Stroke 38(4):1238–1244. doi:10.1161/01.STR.0000260095.94175.d0

Zhang R, Zuckerman JH, Giller CA, Levine BD (1998) Transfer function analysis of dynamic cerebral autoregulation in humans. Am J Physiol 274(1 Pt 2):H233–H241

Zhang R, Zuckerman JH, Iwasaki K, Wilson TE, Crandall CG, Levine BD (2002) Autonomic neural control of dynamic cerebral autoregulation in humans. Circulation 106(14):1814–1820

Zhang R, Crandall CG, Levine BD (2004) Cerebral hemodynamics during the Valsalva maneuver: insights from ganglionic blockade. Stroke 35(4):843–847. doi:10.1161/01.STR.0000120309.84666.AE

Zuj KA, Arbeille P, Shoemaker JK, Blaber AP, Greaves DK, Xu D, Hughson RL (2012) Impaired cerebrovascular autoregulation and reduced CO(2) reactivity after long duration spaceflight. Am J Physiol Heart Circ Physiol 302(12):H2592–H2598. doi:10.1152/ajpheart.00029.2012

Autonomic dysfunction affects cerebral neurovascular coupling

---

Azevedo, E., Castro, P., Santos, R., Freitas, J., Coelho, T., Rosengarten, B., & Panerai, R. (2011). Autonomic dysfunction affects cerebral neurovascular coupling. *Clin Auton Res, 21*(6), 395-403. doi: 10.1007/s10286-011-0129-3

Clin Auton Res
DOI 10.1007/s10286-011-0129-3

RESEARCH ARTICLE

Autonomic dysfunction affects cerebral neurovascular coupling

Elsa Azevedo · Pedro Castro · Rosa Santos · João Freitas · Teresa Coelho · Bernhard Rosengarten · Ronney Panerai

Received: 12 February 2011 / Accepted: 17 May 2011

Abstract
Objective Autonomic failure (AF) affects the peripheral vascular system, but little is known about its influence on cerebrovascular regulation. Patients with familial amyloidotic polyneuropathy (FAP) were studied as a model for AF.
Methods Ten mild (FAPm), 10 severe (FAPs) autonomic dysfunction FAP patients, and 15 healthy controls were monitored in supine and sitting positions for arterial blood pressure (ABP) and heart rate (HR) with arterial volume clamping, and for blood flow velocity (BFV) in posterior (PCA) and contralateral middle cerebral arteries (MCA) with transcranial Doppler. Analysis included resting BFV, cerebrovascular resistance parameters (cerebrovascular resistance index, CVRi; resistance area product, RAP; and critical closing pressure, CrCP), and neurovascular coupling through visually evoked BFV responses in PCA (gain, rate time, attenuation, and natural frequency).
Results In non-stimulation conditions, in each position, there were no significant differences between the groups, regarding HR, BP, resting BFV, and vascular resistance parameters. Sitting ABP was higher than in supine in the three groups, although only significantly in controls. Mean BFV was lower in sitting in all the groups, lacking statistical significance only in FAPs PCA. CVRi and CrCP increased with sitting in all the groups, while RAP increased in controls but decreased in FAPm and FAPs. In visual stimulation conditions, FAPs comparing to controls had a significant decrease of natural frequency, in supine and sitting, and of rate time and gain in sitting position.
Interpretation These results demonstrate that cerebrovascular regulation is affected in FAP subjects with AF, and that it worsens with orthostasis.

Keywords Autonomic nervous system · Neurovascular coupling · Vascular resistance · Transcranial Doppler ultrasonography

E. Azevedo (✉) · P. Castro · R. Santos
Department of Neurology, Hospital São João,
Faculty of Medicine of University of Porto,
Alameda Professor Hernani Monteiro, 4200-319 Porto, Portugal
e-mail: elsaazevedo@netcabo.pt

J. Freitas
Autonomic Unit, Hospital São João,
Faculty of Medicine of University of Porto, Porto, Portugal

T. Coelho
FAP Clinical Unit, Hospital Santo António, Porto, Portugal

B. Rosengarten
Department of Neurology, University of Giessen,
Giessen, Germany

R. Panerai
Department of Cardiovascular Sciences,
University of Leicester, Leicester, UK

Introduction

As the brain is highly vulnerable to insufficient oxygen and substrate supply, it depends on two effective and fast acting regulative mechanisms to assure adequate cerebral perfusion [17, 21]. The neurovascular coupling (NC) adapts cerebral blood flow (CBF) in accordance with the cortical activity, whereas the cerebral autoregulation (CA) maintains constant CBF despite fluctuations in perfusion pressure. Whereas the definitive physiological structures still remain to be resolved, both mechanisms act simultaneously governing adequate CBF [3, 21].

Published online: 28 July 2011

It is well known that patients with autonomic failure (AF) have a dysregulation of the peripheral vasculature [7, 11]. In contrast, it was reported that the capability of the cerebral autoregulation still remains preserved [5, 6, 29]. However, in clinical practice, subjects with AF frequently experience neurological symptoms under orthostatic challenge, even without orthostatic hypotension, which might reflect inappropriate perfusion of the brain.

The familial amyloidotic polyneuropathy (FAP) type I, also known as Portuguese type of FAP, is a hereditary autosomal dominant disease. It leads to amyloid deposition in many organs and tissues, typically the peripheral nerves [2]. A mutation was described in the transthyretin (TTR) gene [26], and the abnormal variant, usually TTR Val30-Met, is the major component of the deposited amyloid [26]. Unlike the oculoleptomeningeal form of FAP, in TTR Val30Met, cerebral vessels and the brain are nearly spared [16]. Symptom onset is usually in the third decade, with autonomic and sensorimotor polyneuropathy. An early failure of autonomic nervous system (ANS) is usually observed, with incapacitating orthostatic hypotension being its clinical hallmark [8]. These characteristics make FAP a well-suited model to study the role of the AF in the regulation of CBF. A further advantage is the usual absence of classic vascular risk factors in FAP that could interfere with the results.

Our aim was to investigate the cerebral hemodynamics in subjects with mild and severe AF, with an emphasis on NC, under different orthostatic conditions.

Materials and methods

This study was performed in Hospital São João, a university hospital in Porto, Portugal. The local institutional ethical committee approved the study that was performed in accordance with the ethical standards laid down in the 1964 Declaration of Helsinki. Each patient gave an informed consent prior to the inclusion in the study.

According to autonomic evaluation described below, 10 female patients with a mean age of 34.9 ± 8.2 (24–50) years, were diagnosed as mild AF (FAPm), and 10 patients (3 females and 7 males), with a mean age of 34.3 ± 6.8 (27–48) years, as severe AF (FAPs). All these patients had the same mutation, TTR Val30Met, and no classic vascular risk factors.

The control group consisted of 15 healthy volunteers (7 females) from hospital or faculty staff, with a mean age of 27.4 ± 8.7 years (age range 19–48), without classic vascular risk factors or medication, except for birth control pills. Although the age does not exactly fit the patients group, it seems to be adequate, since it was shown that NC parameters remain unaffected with aging [22]. Patients and controls underwent a cervical and transcranial duplex scan (HDI 5000 device, Philips, USA). Normal findings of extra- and intracranial vessels and a good temporal acoustic bone window were required as an inclusion criterion.

The evaluations were carried out in a quiet room with a temperature of approximately 22°C. Arterial blood pressure (ABP) and heart rate (HR) were continuously monitored in the left hand with a non-invasive finger cuff Finapres device (model 2300; Ohmeda, Englewood, CO, USA) holding the finger at heart level.

Autonomic evaluation

A composite grading system to score degree of autonomic dysfunction was applied, as previously described [7]. On the basis of ABP and HR responses to the Valsalva maneuver, 60° head-up tilting and deep-breathing, and of plasma norepinephrine levels, four grades of AF were distinguished [7]. Because of the limited number of patients, groups I and II were assumed to have mild (FAPm) and groups III and IV to have severe autonomic dysfunction (FAPs). Although the tests that led to the present score did not disclose changes in group I, it has been shown a mild autonomic impairment with HR variability spectral analysis even in this subset [7], justifying its inclusion with group II as mild FAP. Autonomic results of both groups are summarized in Table 1.

Cerebral blood flow evaluation

For insonation through the temporal transcranial ultrasonic bone window, 2 MHz pulsed wave Doppler monitoring probes of a Multidop T2 Doppler device (DWL, Sipplingen, Germany) were mounted on an individually fitted headband, to record flow velocity in the P2 segment of the left posterior cerebral artery (PCA), and the M1 segment of the right middle cerebral artery (MCA), as described elsewhere in detail [4]. Beat-to-beat peak systolic, mean and end diastolic blood flow velocities (BFV), ABP and stimulus marker were digitally recorded in the Doppler device.

The visual-evoked paradigm consisted of 10 cycles, each with a resting phase of 20 s with closed eyes and a stimulating phase of 40 s of silent reading text columns. The text that the study subjects read was the same for all participants and free of strong emotional content. Changes between phases were signaled acoustically using a tone. One test set had a total duration of 10 min, and was repeated in each position—supine and sitting. The reading test and its reliability were already validated against a checkerboard stimulation paradigm [24].

Table 1 Indices of autonomic evaluation, in mild (FAPm) and severe (FAPs) FAP patients, according to the score degree of autonomic damage [7]

Autonomic index	FAPm	FAPs
HR difference to deep breathing (bpm)	18.1 ± 5.5	7.4 ± 2.8
Valsalva HR ratio	1.6 ± 0.2	1.1 ± 0.1
BP overshoot in phase IV of valsalva (%)	70% P, 30% D	60% D, 40% A
Fall in systolic BP in HUT (mmHg)	<5	29.7 ± 26.2
Basal plasma norepinephrine (pg/mL)	152 ± 75.6	68 ± 60.6
Total score	1.1 ± 1.1	6.6 ± 1.4

HR heart rate, *BP* blood pressure, *HUT* head-up tilt, *P* present, *D* delayed, *A* absent

All values are given in mean ± SD except for BP overshoot in phase IV of Valsalva which is in mean %

Data analysis

All signals were visually inspected to identify artifacts or noise, and narrow spikes were removed by linear interpolation [20]. The heart-MCA distance [20] was used to obtain estimates of ABP in the MCA (ABP-MCA). For MCA and PCA, an index of cerebrovascular resistance (CVRi) was estimated by the ratio of mean ABP to mean BFV for each heartbeat. The instantaneous relationship between ABP and BFV was also used to estimate the critical closing pressure (CrCP) of the cerebral circulation, by extrapolation of the linear regression $\mathrm{BFV} = a \times \mathrm{ABP} + b$, as previously described [1, 9, 19]. The inverse of the linear regression slope was also obtained for each cardiac cycle, and it is referred to as "resistance area product" ($\mathrm{RAP} = 1/a$) to differentiate it from CVRi [10, 19]. The CrCP can then be obtained from the value of ABP where $\mathrm{BFV} = 0$, that is, $\mathrm{CrCP} = -b/a$. All beat-to-beat estimates were interpolated with a third-order polynomial and resampled at 0.2-s intervals to generate a time series with a uniform time base.

For evaluating the NC, ten cycles of 20 s rest (closed eyes) and 40 s stimulation (silent reading) were averaged for each subject at each position, for both MCA and PCA. Mean absolute resting values were recorded during the phase of eye closure, 5 s before visual stimulation. The visually evoked absolute flow velocity data was then normalized to this interval, into relative data, to get independence from the insonation angle, and because it was shown that flow velocity changes are closely correlated to flow changes [27].

For functional Doppler data analysis, peak systolic flow velocities were used because they are less prone to artifacts [25]. The evoked flow velocity responses over the 40 s stimulation period were averaged and analyzed using a software tool for identifying and specifying control systems (Vascochecker, DWL, Sipplingen, Germany). The typical hemodynamic flow velocity responses were expressed in parameters of a second-order linear system with the following equation G(s) were specified:

$$G(\mathrm{s}) = [K(1 + Tv\,s)]/[s^2/\omega^2 + 2\xi * s/\omega + 1]$$

where K represents the gain, Tv the rate time, ω the undamped natural angular frequency (natural frequency), and ξ the attenuation parameter of the system [18]. These parameters describe the main aspects of the hemodynamic cerebral blood flow velocity adaptation. Rate time indicates the initial steepness of the flow velocity increase. Natural frequency is assumed to represent the oscillating properties of the system, whereas the attenuation describes dampening features of the system such as the elastic properties of the wall vessel [23]. The parameter gain describes the relative flow velocity difference between stable flow conditions of rest and stimulation.

Because of the severity of autonomic impairment in the major affected patient group, and for avoiding symptoms such as dizziness, blurred vision or near syncope to interfere with the functional Doppler-test, we only compared data between the supine and sitting positions, abstaining from the standing position [14].

Statistics

Non-parametric tests were used because of the reduced number of elements in each group. Kruskal–Wallis test was used to compare hemodynamic and control system parameters data between groups in each position. In case of significance, Mann–Whitney test was used to discriminate between groups. Wilcoxon rank test was performed to compare changes between the supine and sitting conditions. Statistical significance was inferred at a $p < 0.05$ level.

Results

All selected patients and controls were able to perform the complete hemodynamic functional transcranial Doppler tests in both orthostatic conditions—supine and

sitting—without the typical neurological complaints of orthostatic hypotension. Nevertheless, due to data artifacts, only 6 FAPm and 7 FAPs could have all the parameters analyzed in both positions.

The indices of autonomic evaluation are shown in Table 1, together with the group-averaged results of mild and severe FAP patients, according to the score degree of autonomic damage [7].

Table 2 shows the data for HR, mean ABP, resting BFV, CVRi, CrCP, and RAP, for PCA and MCA, in supine and sitting resting conditions. In each position, there were no significant differences between the groups control, FAPm and FAPs, regarding any of the mentioned variables, in either the PCA or the MCA.

Comparing supine and sitting conditions in each group, there was a significant increase in heart rate in controls and FAPs. In sitting the BP was higher than in supine in all the groups, although only significantly in controls. Mean BFV was lower in sitting in all groups, in both PCA and MCA, lacking statistical significance only in FAPs PCA. The parameters of vascular resistance CVRi and CrCP increased with sitting in all the groups, while RAP increased in controls but decreased significantly in FAPm and FAPs, in both PCA and MCA.

The results for functional TCD and for the vasoreactivity parameters changes with stimulation in PCA are presented in Table 3. Comparing groups with Kruskal–Wallis, a significant difference occurred for the natural frequency. The Mann–Whitney test revealed that the severe dysautonomic patients had significantly smaller values for the natural frequency as compared to controls and to mildly affected patients. The difference remained similar after orthostatic challenge. Regarding the rate time, the severe affected patients had a lower value as compared to controls in the sitting position, and concerning gain the severe affected patients had a lower value as compared to controls and to mildly affected patients, in the sitting position. Table 3 also shows the changes in RAP and CrCP following mental activation with the reading test. No significant differences between FAP groups and controls were observed in the supine position. During the sitting position though, the differential changes in RAP and CrCP help to explain and complement the results of the evoked BFV differences observed due to changes in posture. For controls, most of the change in BFV is dominated by a change in CrCP. However, for FAPm there is competing change in RAP which is not observed in FAPs.

Figure 1 shows, for the three groups, in supine and sitting positions, the evoked blood flow velocity responses, with the typical time course of an initial steep increase, followed by an overshoot, before curves stabilize on a plateau. In the figure it is evident the decrease in rate time and gain in FAPs sitting position, indicating possibly inappropriate blood supply of metabolic active neurons in a moderate orthostatic challenge.

Table 4 presents the arterial blood pressure, heart rate and right MCA hemodynamic variations during reading task, in supine and sitting positions. We found no significant differences in the variation with visual stimulation of these parameters between the three groups.

Discussion

This study shows, for the first time, an impaired NC in individuals with AF, worsening under a moderate orthostatic challenge without hypotension. The NC evaluated by a control system approach was complemented by the analysis of variation of vasoreactivity parameters.

Patients with severe AF had a significantly reduced BFV response (gain parameter) to functional activation, and a decreased rate time. Since the difference was not present in the supine position, a primary neurovascular dysfunction cannot explain the present findings. This could suggest that major changes in NC only occur in severely affected sympathetic nervous system, when submitted to orthostatic challenge, although an increase in parasympathetic dysfunction could also explain an impaired cerebral vasodilatation [13].

Interestingly, mean ABP, resting BFV and vascular resistance indices (CVRi, CrCP and RAP) in PCA and MCA, in each position, were not different between groups, which excludes either orthostatic hypotension or decreased BFV as responsible factors for these alterations. However, the reduced gain parameter indicates inadequate perfusion of the brain under functional activation. Reduced cerebral oxygenation during orthostatic challenge with hypotension has been previously reported in patients with AF [14]. Our data show that patients with AF can have an inadequate functional cortical hyperemia, even without hypotension.

The NC parameter natural frequency was significantly lower only in the severe affected patients, in both positions. This might raise the hypothesis that it could be an inherent feature of cerebral neurovascular uncoupling in severe autonomic dysfunction, eventually resulting from dysfunction of sympathetic innervation of posterior circulation precapillaries. Although in FAP vessel infiltration with amyloid could also explain this effect, by affecting myogenic autoregulatory response, relevant brain changes have been described mainly in other FAP type of mutations than TTR Val30Met [12]. Therefore, direct measurement of microcirculatory hemodynamic response of the visual cortex (e.g. with arterial spin labeling MRI) would be very intriguing. One could speculate whether conducting similar study in patients with cerebral amyloid angiopathy and without autonomic dysfunction, would yield similar results.

Table 2 Hemodynamic data in both PCA and MCA, between supine and sitting positions, for controls, mild (FAPm) and severe (FAPs) FAP patients

	Controls $N = 15$	$p^{\dagger}$	FAPm $N = 6$	$p^{\dagger}$	FAPs $N = 7$	$p^{\dagger}$	$p^{\ddagger}$
HR (bmp)							
Supine	70.23 ± 9.24	0.001	75.33 ± 6.24	n.s.	77.07 ± 11.41	0.028	n.s.
Sitting	76.51 ± 11.12		80.66 ± 10.55		85.38 ± 14.37		n.s.
Mean ABP (mmHg)							
Supine	74.63 ± 12.21	0.002	82.15 ± 10.75	n.s.	83.28 ± 11.75	n.s.	n.s.
Sitting	90.38 ± 8.12		87.61 ± 7.48		86.9 ± 16.67		n.s.
PCA BFV							
Systolic (cm s^{-1})							
Supine	60.69 ± 13.06	0.036	60.23 ± 6.46	n.s.	57.14 ± 10.29	n.s.	n.s.
Sitting	58.46 ± 12.44		58.06 ± 5.06		60.6 ± 7.35		n.s.
Mean (cm s^{-1})							
Supine	37.96 ± 9.02	0.009	40.55 ± 3.93	0.028	37.05 ± 8.48	n.s.	n.s.
Sitting	35.09 ± 8.14		37.57 ± 3.71		33.69 ± 5.59		n.s.
Diastolic (cm s^{-1})							
Supine	20.98 ± 7.43	n.s.	24.91 ± 2.41	n.s.	23.06 ± 6.21	n.s.	n.s.
Sitting	19.12 ± 5.1		23.57 ± 3.36		19.11 ± 5.63		n.s.
PCA vascular resistance							
CVRi (mmHg cm^{-1} s^{-2})							
Supine	2.34 ± 0.67	0.001	1.96 ± 0.26	0.028	2.05 ± 0.6	n.s.	n.s.
Sitting	2.69 ± 0.63		2.34 ± 0.27		2.62 ± 0.64		n.s.
RAP (mmHg cm^{-1} s^{-2})							
Supine	1.26 ± 0.29	n.s.	1.30 ± 0.20	0.028	1.38 ± 0.27	0.028	n.s.
Sitting	1.34 ± 0.32		1.10 ± 0.31		1.05 ± 0.31		n.s.
CrCP (mmHg)							
Supine	28.03 ± 9.02	0.002	27.00 ± 6.22	0.028	32.26 ± 20.25	0.018	n.s.
Sitting	45.09 ± 10.39		46.09 ± 11.41		50.5 ± 20.76		n.s.
MCA BFV							
Systolic (cm s^{-1})							
Supine	103.82 ± 18.84	n.s.	98.78 ± 11.74	n.s.	96.1 ± 16.51	n.s.	n.s.
Sitting	99.85 ± 20.62		97.18 ± 10.97		100.28 ± 17.96		n.s.
Mean (cm s^{-1})							
Supine	65.17 ± 14.77	0.015	65.4 ± 8.45	0.028	62.75 ± 10.61	0.028	n.s.
Sitting	61.01 ± 12.95		61.42 ± 5.7		58.35 ± 9.41		n.s.
Diastolic (cm s^{-1})							
Supine	40.8 ± 10.57	n.s.	42.4 ± 8.11	n.s.	41.61 ± 6.83	0.043	n.s.
Sitting	38.25 ± 8.13		40.29 ± 6.02		36.75 ± 6.1		n.s.
MCA vascular resistance							
CVRi (mmHg cm^{-1} s^{-2})							
Supine	1.2 ± 0.32	0.001	1.23 ± 0.16	0.028	1.38 ± 0.46	n.s.	n.s.
Sitting	1.54 ± 0.28		1.43 ± 0.13		1.58 ± 0.65		n.s.
RAP (mmHg cm^{-1} s^{-2})							
Supine	0.78 ± 0.21	n.s.	0.83 ± 0.21	0.028	0.85 ± 0.1	0.028	n.s.
Sitting	0.85 ± 0.21		0.69 ± 0.29		0.68 ± 0.18		n.s.

Table 2 continued

	Controls $N = 15$	$p^{\dagger}$	FAPm $N = 6$	$p^{\dagger}$	FAPs $N = 7$	$p^{\dagger}$	$p^{\ddagger}$
CrCP (mmHg)							
Supine	25.08 ± 12.96	0.012	25.97 ± 7.87	0.028	29.3 ± 16.78	0.018	n.s.
Sitting	40.15 ± 12.58		45.66 ± 13.18		47.84 ± 19.07		n.s.

HR heart rate, *ABP* arterial blood pressure, *PCA* posterior cerebral artery, *MCA* middle cerebral artery, *BFV* blood flow velocity, *CVRi* cerebrovascular resistance index, *RAP* resistance area product, *CrCP* critical closing pressure

All values are given in mean ± SD

† Wilcox paired test p value for differences between supine and sitting positions

‡ Kruskal–Wallis and Mann–Whitney test p values for differences between groups

Table 3 Functional TCD and cerebrovascular resistance parameters changes in PCA during reading task, in supine and sitting positions, for controls, mild (FAPm) and severe (FAPs) FAP patients

	Controls $N = 15$	$p^{\dagger}$	FAPm $N = 6$	$p^{\dagger}$	FAPs $N = 7$	$p^{\dagger}$	$p^{\ddagger}$
Functional TCD							
Gain (cm s^{-1})							
Supine	15.85 ± 6.14	n.s.	21.96 ± 4.18	n.s.	17.82 ± 8.28	n.s.	n.s
Sitting	16.77 ± 6.18		19.75 ± 3.25		11.24 ± 5.02		S–C: 0.045
							S-M: 0.007
Nat. Freq. (Hz)							
Supine	0.23 ± 0.04	n.s.	0.22 ± 0.06	n.s.	0.16 ± 0.05	n.s.	S–C: 0.010
Sitting	0.24 ± 0.05		0.2 ± 0.03		0.17 ± 0.08		S–C: 0.018
Attenuation							
Supine	0.54 ± 0.21	n.s.	0.76 ± 0.28	n.s.	0.61 ± 0.29	n.s.	n.s
Sitting	0.53 ± 0.18		0.51 ± 0.16		0.5 ± 0.18		n.s.
Rate time (s)							
Supine	4.89 ± 3.05	n.s.	5.7 ± 4.57	n.s.	3.51 ± 1.3	n.s.	n.s.
Sitting	4.93 ± 2.6		3.64 ± 1.19		2.04 ± 1.67		S–C: 0.005
Vascular resistance							
ΔCVRi (%)							
Supine	−20.17 ± 5.21	n.s.	−22.37 ± 1.95	n.s.	−22.92 ± 6.13	n.s.	n.s.
Sitting	−21.9 ± 4.89		−22.68 ± 3.51		−18.83 ± 5.05		n.s.
ΔRAP (%)							
Supine	−8.88 ± 4.93	n.s.	−11.24 ± 2.88	n.s.	−12.15 ± 5.08	n.s.	n.s.
Sitting	−5.71 ± 5.96		−13.13 ± 5.13		−7.17 ± 5.5		n.s.
ΔCrCP (%)							
Supine	−28.96 ± 12.22	n.s.	−33.45 ± 14.24	0.028	−30.20 ± 31.16	n.s.	n.s.
Sitting	−22.51 ± 10.86		−13.02 ± 7.81		−12.61 ± 7.4		n.s.

All values are given in mean ± SD

Nat. Freq. natural frequency; ΔCVRi, variation of cerebrovascular resistance index, *ΔRAP* resistance area product, *ΔCrCP* critical closing pressure, during visual-evoked paradigm stimulation

† Wilcoxon paired test p value for differences between supine and sitting positions

‡ Kruskal–Wallis and Mann–Whitney test p values for differences between groups

Nevertheless, the conclusions would be difficult to interpret as, contrary to our FAP population, patients with amyloid angiopathy are much older, with expected higher prevalence of vascular risk factors, and usually the diagnosis is made after an intracerebral hemorrhage that could interfere with the results of neurovascular coupling.

The variations of the parameters of vascular resistance CrCP and RAP between supine and sitting positions were

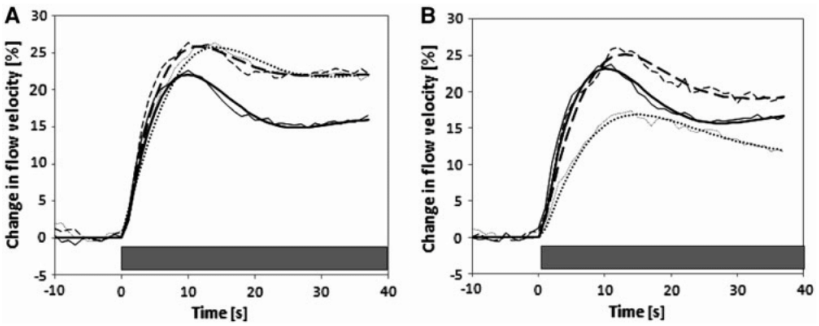

Fig. 1 Group averaged peak systolic evoked flow velocity responses during 40 s of reading task (*gray bar* at bottom), in supine (**a**) and sitting (**b**) positions, for the different groups. Controls are represented in *continuous lines*, FAP mild group with *dashed lines* and FAP severe group with *dotted lines*. *Thin lines* represent measured response and *thick lines* are modeled blood flow data of the second-order linear system obtained with Vascochecker 1.0

Table 4 Arterial blood pressure, heart rate and right MCA hemodynamic variation during reading task, in supine and sitting positions, for controls, mild (FAPm) and severe (FAPs) FAP patients

	Controls $N = 15$	$p^{\dagger}$	FAPm $N = 6$	$p^{\dagger}$	FAPs $N = 7$	$p^{\dagger}$	$p^{\ddagger}$
ΔABP (%)							
Supine	−1.33 ± 2.14	n.s	−0.29 ± 2.20	n.s	−0.42 ± 0.95	n.s	n.s
Sitting	−0.02 ± 1.45		0.36 ± 0.83		0.24 ± 1.51		n.s
ΔHR (%)							
Supine	1.71 ± 2.22	n.s	1.20 ± 2.33	n.s	0.01 ± 0.52	n.s	n.s
Sitting	0.52 ± 2.44		2.25 ± 1.55		0.61 ± 0.92		n.s
MCA							
Gain (%)							
Supine	0.94 ± 2.30	n.s	3.69 ± 3.22	n.s	2.18 ± 13.19	n.s	n.s.
Sitting	1.54 ± 1.82		6.21 ± 7.87		1.99 ± 2.26		n.s.
ΔCVRi (%)							
Supine	1.75 ± 4.28	n.s	−4.83 ± .2.45	n.s	−4.85 ± 2.99	n.s	n.s
Sitting	−2.56 ± 1.97		−5.95 ± 2.42		−4.78 ± 2.99		n.s.
ΔRAP (%)							
Supine	−3.06 ± 5.95	n.s	−2.95 ± 5.20	n.s	−5.65 ± 4.03	n.s	n.s.
Sitting	0.50 ± 3.99		−5.25 ± 4.88		2.63 ± 4.15		n.s.
ΔCrCP (%)							
Supine	0.80 ± 8.20	n.s	−6.68 ± 8.17	n.s	0.70 ± 6.84	n.s	n.s.
Sitting	−4.12 ± 5.24		−0.32 ± 3.32		−2.15 ± 1.79		n.s

MCA, right middle cerebral artery; ΔABP, ΔHR, ΔCVRi, ΔRAP and ΔCrCP, percentual variation of mean arterial blood pressure, heart rate, Cerebrovascular Resistance Index, Resistance Area Product, and Critical Closing Pressure, respectively, during visual-evoked paradigm stimulation

† Wilcoxon paired test p value for differences between supine and sitting positions

‡ Kruskal–Wallis and Mann–Whitney test *p* values for differences between groups

also not previously described. While CVRi and CrCP increased with sitting in all the groups, RAP increased in controls but decreased in FAPm and FAPs, in both PCA and MCA, which might suggest predominantly myogenic cerebral vasodilation [19, 20] in adaptation to orthostatic challenge in FAP patients.

Changes in RAP and CrCP in PCA following visual activation are also described for the first time. These changes confirm the additional discrimination provided by these parameters in comparison with the more conventional CVRi [19]. No significant differences between FAP groups and controls were observed in the supine position.

Nevertheless, during the sitting position the differential changes in RAP and CrCP help to explain and complement the results of the evoked BFV differences observed due to changes in posture. For controls, most of the change in BFV is dominated by a change in CrCP, while for FAPm there is competing change in RAP which is not observed in FAPs. These differences between FAP and controls and between the two FAP groups, suggest a complex interplay between the consequences of AF and BFV regulatory mechanisms in the sitting position, as compared to supine. At this stage any attempts of interpretation are highly speculative. In the presence of AF, removing the sympathetic contribution might result in greater involvement of local myogenic and metabolic regulatory mechanisms, which have been correlated with changes in RAP and CrCP respectively [20]. In summary, we hypothesize that with reduced sympathetic control in the upright position, FAPm retains a greater level of local control of BFV than FAPs. Inducing changes in BP in the sitting position in patients with FAP, for example with the use of thigh cuff maneuvers, might provide useful information to clarify this proposition.

These results raise again the question about the role of ANS in the control of cerebral vasoreactivity, which is said to be relatively weak [30]. At an intracerebral level, where NC occurs, there are no autonomic nerves surrounding blood vessels [13]. Nevertheless, perhaps ANS has a role in the relative distribution of cerebral blood flow to areas with different degrees of activity at any given moment.

Although the Doppler measures velocity rather than flow, caliber effects of the insonated basal cerebral vessels between the different conditions are not likely, as was shown by Serrador [27].

One limitation of the present investigation is the lack of CO_2 measurement during BFV monitoring. Since it has been shown to be an important parameter in cerebral hemodynamics [15, 28], we cannot exclude a possible role in the given results. Nevertheless, all the subjects were evaluated in the same conditions, allowing a comparison of the groups.

Another limitation of this study might be the small number of studied patients. It is a rare disease, and nowadays patients are treated earlier, namely with pacemaker and liver transplantation, that were exclusion criteria for the study. Nevertheless, this population is very homogeneous in its disease process, although differing in the degree of dysautonomy with time course, allowing our data to bring insights into a possible role of AF on neurovascular coupling. It would be interesting to investigate this subject in other disease processes that also course with AF.

In conclusion, AF seems to affect NC independently of posture. Additionally, despite similar vasodilatory response in both positions, change from supine to sitting positions in dysautonomic patients interfered with evoked blood flow responses, suggesting inappropriate functional cerebral perfusion in orthostatic conditions in FAP patients with AF.

Conflict of interest The authors declare that they have no conflict of interest.

References

1. Aaslid R, Lash SR, Bardy GH, Gild WH, Newell DW (2003) Dynamic pressure-flow velocity relationships in the human cerebral circulation. Stroke 34:1645–1649
2. Andrade C (1952) A peculiar form of peripheral neuropathy; familiar atypical generalized amyloidosis with special involvement of the peripheral nerves. Brain 75:408–427
3. Azevedo E, Rosengarten B, Santos R, Freitas J, Kaps M (2007) Interplay of cerebral autoregulation and neurovascular coupling evaluated by functional TCD in different orthostatic conditions. J Neurol 254:236–241
4. Azevedo E, Santos R, Freitas J, Rosas MJ, Gago M, Garrett C, Rosengarten B (2010) Deep brain stimulation does not change neurovascular coupling in non-motor visual cortex: an autonomic and visual evoked blood flow velocity response study. Parkinsonism Relat Disord 16:600–603
5. Bondar RL, Dunphy PT, Moradshahi P, Kassam MS, Blaber AP, Stein F, Freeman R (1997) Cerebrovascular and cardiovascular responses to graded tilt in patients with autonomic failure. Stroke 28:1677–1685
6. Brooks DJ, Redmond S, Mathias CJ, Bannister R, Symon L (1989) The effect of orthostatic hypotension on cerebral blood flow and middle cerebral artery velocity in autonomic failure, with observations on the action of ephedrine. J Neurol Neurosurg Psychiatry 52:962–966
7. Carvalho MJ, van Den Meiracker AH, Boomsma F, Lima M, Freitas J, Veld AJ, Falcao De Freitas A (2000) Diurnal blood pressure variation in progressive autonomic failure. Hypertension 35:892–897
8. Carvalho MJ, van den Meiracker AH, Boomsma F, Man in 't Veld AJ, Freitas J, Costa O, de Freitas AF (1997) Improved orthostatic tolerance in familial amyloidotic polyneuropathy with unnatural noradrenaline precursor L-threo-3,4-dihydroxyphenylserine. J Auton Nerv Syst 62:63–71
9. Dawson SL, Panerai RB, Potter JF (1999) Critical closing pressure explains cerebral hemodynamics during the Valsalva maneuver. J Appl Physiol 86:675–680
10. Evans DH, Levene MI, Shortland DB, Archer LN (1988) Resistance index, blood flow velocity, and resistance-area product in the cerebral arteries of very low birth weight infants during the first week of life. Ultrasound Med Biol 14:103–110
11. Freitas J, Santos R, Azevedo E, Carvalho M, Boomsma F, Meiracker A, Falcao de Freitas A, Abreu-Lima C (2007) Hemodynamic, autonomic and neurohormonal behaviour of familial amyloidotic polyneuropathy and neurally mediated syncope patients during supine and orthostatic stress. Int J Cardiol 116:242–248
12. Goren H, Steinberg MC, Farboody GH (1980) Familial oculoleptomeningeal amyloidosis. Brain 103:473–495
13. Hamel E (2006) Perivascular nerves and the regulation of cerebrovascular tone. J Appl Physiol 100:1059–1064
14. Harms MP, Colier WN, Wieling W, Lenders JW, Secher NH, van Lieshout JJ (2000) Orthostatic tolerance, cerebral oxygenation,

and blood velocity in humans with sympathetic failure. Stroke 31:1608–1614
15. Harper AM, Glass HI (1965) Effect of alterations in the arterial carbon dioxide tension on the blood flow through the cerebral cortex at normal and low arterial blood pressures. J Neurol Neurosurg Psychiatry 28:449–452
16. Hou X, Aguilar MI, Small DH (2007) Transthyretin and familial amyloidotic polyneuropathy. Recent progress in understanding the molecular mechanism of neurodegeneration. FEBS J 274: 1637–1650
17. Iadecola C (2004) Neurovascular regulation in the normal brain and in Alzheimer's disease. Nat Rev 5:347–360
18. Melsa JL, Shultz DG, Rohrs CE (1990) Linear control systems, 2nd edn. Englewood Cliffs, Prentice-Hall, NJ
19. Panerai RB (2003) The critical closing pressure of the cerebral circulation. Med Eng Phys 25:621–632
20. Panerai RB, Moody M, Eames PJ, Potter JF (2005) Cerebral blood flow velocity during mental activation: interpretation with different models of the passive pressure-velocity relationship. J Appl Physiol 99:2352–2362
21. Paulson OB, Strandgaard S, Edvinsson L (1990) Cerebral autoregulation. Cerebrovasc Brain Metab Rev 2:161–192
22. Rosengarten B, Aldinger C, Spiller A, Kaps M (2003) Neurovascular coupling remains unaffected during normal aging. J Neuroimaging 13:43–47
23. Rosengarten B, Budden C, Osthaus S, Kaps M (2003) Effect of heart rate on regulative features of the cortical activity-flow coupling. Cerebrovasc Dis 16:47–52
24. Rosengarten B, Huwendiek O, Kaps M (2001) Neurovascular coupling in terms of a control system: validation of a second-order linear system model. Ultrasound Med Biol 27:631–635
25. Rosengarten B, Kaps M (2002) Peak systolic velocity Doppler index reflects most appropriately the dynamic time course of intact cerebral autoregulation. Cerebrovasc Dis 13:230–234
26. Saraiva MJ, Birken S, Costa PP, Goodman DS (1984) Family studies of the genetic abnormality in transthyretin (prealbumin) in Portuguese patients with familial amyloidotic polyneuropathy. Ann NY Acad Sci 435:86–100
27. Serrador JM, Picot PA, Rutt BK, Shoemaker JK, Bondar RL (2000) MRI measures of middle cerebral artery diameter in conscious humans during simulated orthostasis. Stroke 31:1672–1678
28. Shapiro W, Wasserman AJ, Baker JP, Patterson JL Jr (1970) Cerebrovascular response to acute hypocapnic and eucapnic hypoxia in normal man. J Clin Invest 49:2362–2368
29. Thomas DJ, Bannister R (1980) Preservation of autoregulation of cerebral blood flow in autonomic failure. J Neurol Sci 44:205–212
30. van Lieshout JJ, Secher NH (2008) Last Word on Point:Counterpoint: sympathetic activity does/does not influence cerebral blood flow. J Appl Physiol 105:1374

Functional transcranial Doppler: presymptomatic changes in Fabry disease

---

Azevedo, E., Mendes, A., Seixas, D., Santos, R., Castro, P., Ayres-Basto, M.,... Oliveira, J. P. (2012). Functional transcranial Doppler: presymptomatic changes in Fabry disease. *Eur Neurol, 67*(6), 331-337. doi: 10.1159/000337906

Original Paper

European Neurology

Eur Neurol 2012;67:331–337
DOI: 10.1159/000337906

Received: October 3, 2011
Accepted: February 27, 2012
Published online: May 4, 2012

Functional Transcranial Doppler: Presymptomatic Changes in Fabry Disease

Elsa Azevedo[a] Amélia Mendes[a] Daniela Seixas[c] Rosa Santos[a] Pedro Castro[a] Margarida Ayres-Basto[d] Bernhard Rosengarten[e] João Paulo Oliveira[b]

Departments of [a]Neurology and [b]Medical Genetics, Hospital São João, Faculty of Medicine of University of Porto, [c]Department of Imaging, Hospital Vila Nova de Gaia/Espinho, Vila Nova de Gaia, and Faculty of Medicine of University of Porto, and [d]Department of Neuroradiology, Hospital São João, Porto, Portugal; [e]Department of Neurology, University of Giessen, Giessen, Germany

Key Words
Fabry disease · Neurovascular coupling · Cerebral blood flow · Cerebrovascular disease · Cerebrovascular ultrasound · Magnetic resonance angiography · Magnetic resonance imaging · Transcranial Doppler

Abstract
Background and Aim: Cerebrovascular disease may progress asymptomatically in the early stages of Fabry disease (FD). Our aim was to test whether functional transcranial Doppler (fTCD) could provide useful data in the evaluation of these presymptomatic FD patients. ***Methods:*** A cohort of 12 adult FD patients from families with the classical phenotype of the disease was evaluated with fTCD in the posterior cerebral artery. ***Results:*** Compared to healthy controls, resting blood velocities were significantly lower in the FD cohort ($p = 0.032$ for systolic, $p = 0.021$ for diastolic). FTCD suggested a disturbed neurovascular coupling in the visual cortex of FD patients, with lower gain ($p = 0.007$) and rate time ($p = 0.019$). Men had a significantly higher attenuation ($p = 0.013$) and lower natural frequency ($p = 0.046$) than the heterozygous women. ***Conclusion:*** These data are the first to suggest that patients with FD may develop cortical vascular dysfunction in the territory of the posterior circulation, early in the natural history of the disease. If the present findings are confirmed in larger, prospective studies, fTCD will be useful for assessing stroke risk in as yet asymptomatic FD patients, improving preventive therapeutic management.

Introduction

Fabry disease (FD) is a rare X-linked disorder caused by deficiency of the lysosomal enzyme α-galactosidase. The catabolic defect leads to systemic accumulation of neutral glycosphingolipids, mostly globotriaosylceramide (Gb3). Vascular endothelial and smooth muscle cells are major sites of Gb3 deposition, correlating with the development of a complex vasculopathy [1]. Stroke and transient ischemic attacks (TIA) are frequent complications, and in some affected women cerebrovascular disease (CVD) may be as severe as in hemizygous males [2, 3]. Stroke can occur in the absence of any other major signs of FD, preceding its diagnosis in a significant number of patients [2]. FD may present as ischemic cryptogenic stroke in young adults [4], predominating the small-vessel type [2].

E.A. and A.M. contributed equally to the article and share first authorship.

KARGER

Fax +41 61 306 12 34
E-Mail karger@karger.ch
www.karger.com

0014–3022/12/0676–0331$38.00/0

Accessible online at:
www.karger.com/ene

Prof. Dr. Elsa Azevedo
Department of Neurology, Hospital São João and
Faculty of Medicine of University of Porto
Alameda Prof. Hernâni Monteiro, PT–4200-319 Porto (Portugal)
Tel. +351 917 783 527, E-Mail elsaazevedo@netcabo.pt

There is evidence of increased intima-media thickness (IMT) of the common carotid artery (CCA) in males as well as in females with FD [5]. Elevated cerebral blood flow velocities (BFV) were reported in males [6], but other investigators could not replicate those findings [7]. Typical features of brain involvement include large- and small-vessel strokes, vascular dolichoectasia, white matter lesions (WML), pulvinar hyperintensity in magnetic resonance imaging (MRI) T_1-weighted images ('pulvinar sign'), as well as various cerebral blood flow and diffusion brain changes [3, 8–10]. MRI has been proposed for protocol baseline and follow-up assessments of FD patients [11].

Although enzyme replacement therapy (ERT) has a therapeutic effect on some of the major complications of FD, at most the clinical impact on CVD appears to be small [12]. Identification of reliable neuroimaging and hemodynamic non-invasive surrogate markers of preclinical central nervous system disease, and of the efficacy of ERT upon CVD, would be a major advance for the clinical follow-up of FD patients.

Since the posterior circulation seems especially vulnerable in FD [3], we postulated that functional abnormalities in this territory might be evident even in asymptomatic patients, and precede visible structural changes. Therefore, the main purpose of this study was to test whether functional transcranial Doppler (fTCD) of the posterior circulation could provide useful data in the evaluation of FD patients with no prior history of stroke or TIA, and correlate the fTCD results with brain structural and angiographic MRI data.

Patients and Methods

All adult patients carrying an α-galactosidase gene *(GLA)* mutation associated with the classical phenotype of FD, followed at a single university hospital, were invited to undergo cervical and transcranial vascular ultrasound studies and brain MRI and magnetic resonance angiography (MRA), as well as a comprehensive neurologic examination, if they had no history of symptomatic CVD. Depending on patient gender [13], diagnostic criteria for FD were absent or significantly low α-galactosidase enzyme activity in plasma or leukocyte assays and/or identification of a pathogenic *GLA* mutation on molecular genetics testing. Past clinical and laboratory data were retrieved from the patients' medical records. The study protocol was approved by the Hospital Ethics Committee and written informed consent was required for enrolment.

Ultrasound and Magnetic Resonance Imaging Evaluation

Cervical and transcranial vascular ultrasound scans were performed with a Philips HDI 5000 ultrasound imaging platform (Philips Healthcare, Andover, Mass., USA). Morphologic and hemodynamic parameters of the cervical arterial segments and hemodynamic parameters of the basal cerebral arteries were evaluated. IMT was measured along the far wall of distal CCA [14], and the average of the values of maximal IMT of right and left sides was calculated.

Brain MRI and MRA studies were performed in a Siemens Magnetom Symphony™ 1.5 Tesla scanner (Siemens Healthcare, Erlangen Germany). The imaging protocol included T_1-weighted spin echo, proton density/T_2-weighted turbo spin echo, T_2-weighted fluid attenuation inversion recovery (FLAIR), and T_2-weighted gradient echo sequences, as well as 3D time-of-flight arterial MRA. The presence of any brain or arterial lesions, as well as their type and location, was recorded for each patient. Hyperintensity of the pulvinar was specifically sought on T_1-weighted imaging. Diameters of the basilar artery (BA) were measured in the time-of-flight sequence [10], using the OsiriX imaging processing software, version 3.7.1 (Open Source™, Antoine Rosset©, 2003–2010) [15]. The BA diameter was defined as the average of caudal, intermediate, and rostral arterial diameters, measured manually on the sagittal plane. Brain tissue volumes, normalized for subject head size, were estimated with brain-imaging analysis software SIENAX [16, 17], available as part of the FMRIB Software Library (FSL; University of Oxford, 2002). SIENAX allows the calculation of the total volume of brain tissue, including independent estimates of grey matter (GM) and white matter (WM) volumes. Brain GM and WM volumes reported for healthy adults using fully-automated MR image analysis were used for comparison [18]. All the MRI and MRA data were analyzed by a single investigator (D.S.) who was blinded as to the results of clinical and ultrasound evaluations.

Functional Transcranial Doppler

FTCD was carried out with a Multi-Dop T_2 transcranial Doppler system (DWL, Sipplingen, Germany), in a sitting position, in conditions described elsewhere in detail [19]. A 2-MHz pulsed-wave Doppler monitoring probe, mounted on an individually fitted headband, was positioned to record BFV in the posterior cerebral artery (PCA) P2 segment. Continuous beat-to-beat recordings of peak systolic and end-diastolic BFV were stored on the Doppler device for offline analysis. All the fTCD studies were performed by the same investigator (R.S.) who was blinded as to the clinical and brain-imaging data.

The visual-evoked paradigm performed to assess the neurovascular coupling consisted of 10 cycles, each with a resting phase of 20 s with eyes closed and a stimulating phase of 40 s of silent text reading. Changes between phases were acoustically signaled. The reading test and its reliability were validated against a checkerboard stimulation paradigm [20].

Doppler data were analyzed using a control system model, allowing description of the main hemodynamic features of the evoked BFV adaptation [20]. Data were transformed to relative values, to become independent of the insonation angle. Peak systolic data were evaluated because they are less prone to Doppler artifacts [21]. Data were expressed in terms of a second-order linear system with the equation $G(s) = [K (1 + T_v s)]/[s_2/\omega_2 + 2 \xi \cdot s/\omega + 1]$, where 'K' stands for 'gain', 'T_v' for 'rate time', 'ω' for 'undampened natural angular frequency' ('natural frequency'), and 'ξ' for 'attenuation' [20]. These parameters describe the main aspects of the hemodynamic cerebral BFV adaptation. Rate time

indicates the initial steepness of the BFV increase. Natural frequency is assumed to represent oscillatory properties of the system, like tonus and speed, whereas attenuation describes dampening features, such as the elastic properties of the wall vessel [22]. Gain describes the relative BFV difference between stable flow conditions of rest and stimulation. Calculations were done with a professional software tool for evaluating blood flow data (Vascochecker 1.0, Hamm, Germany). The resting BFV during the closed eyes phase were calculated from a time span of 5 s before the stimulation started.

These fTCD patient data were compared to those obtained under the same testing conditions, in 20 healthy subjects (28.4 ± 9.2 years) without vascular risk factors, recruited among the hospital and university staff.

Statistical Analysis

Continuous data are expressed as the mean ± SD and categorical variables as frequency distributions. The Shapiro-Wilk test was used to check the normality of distribution of continuous variables. The independent Student's t test or the Mann-Whitney test were used as appropriate for comparisons between patients and controls and patients' gender subgroups. Correlations were determined with the Pearson, Spearman or the point-biserial correlation coefficients. Statistical calculations were performed with SPSS Statistics 17.0 software (SPSS Inc., Chicago, Ill., USA). A p value <0.05 was considered statistically significant.

Results

Clinical and Imaging Characteristics

Twelve patients (5 males) of four different families fulfilled the enrolment criteria and were evaluated. Their demographic, genetic and clinical features are summarized in table 1. The neurological examination was unremarkable in all. Mean age was 35.8 ± 12.8 years, higher in the female subcohort (41.7 ± 10.6 vs. 27.4 ± 11.5 years, p = 0.042). Eight patients (5 males) had been on ERT for a mean of 2.8 ± 1.3 years.

None of the patients showed atherosclerotic plaques or hemodynamic changes on the cervical ultrasound study, nor hemodynamic signs on TCD suggestive of stenosis of the basal cerebral arteries. Mean left-right CCA-IMT was 0.66 ± 0.18 mm in males and 0.86 ± 0.23 mm in females. All 4 patients (3 females) aged >45 years showed multiple small WML on proton density-weighted and T_2-weighted sequences, mainly located in periventricular and frontotemporoparietal WM regions. According to the Fazekas classification system of MRI signal abnormalities [23], the eldest man and the eldest woman scored Fazekas III, and the other 2 women scored Fazekas II and Fazekas I. The pulvinar sign was not observed in any patient. On MRA, abnormally elongated or tortuous arteries were identified in 3 men (60%; mean age 31 ± 14.7 years) and 5 women (71%; mean age 47.2 ± 5.9 years), predominantly the internal carotid, middle cerebral and basilar arteries. This feature correlated positively with age (p = 0.032). The mean BA diameter was 3.66 ± 0.72 mm, with no significant gender difference, but significantly larger in the older patients (p = 0.041). For males and females, we have found respectively a WM volume of 0.33 ± 0.03 and 0.36 ± 0.04 liters, a GM volume of 1.07 ± 0.12 and 1.07 ± 0.12 liters, and a total brain volume of 1.398 ± 0.095 and 1.462 ± 0.087 liters. For comparison, the mean GM and WM volumes reported in the literature for normal subjects were, respectively, 0.829 and 0.454 liters for males and 0.747 and 0.395 liters for females (22).

Functional Transcranial Doppler

Table 2 summarizes the fTCD results. Compared to healthy controls, FD patients had lower resting peak systolic and end-diastolic BFV in PCA (p = 0.032 and p = 0.021, respectively), lower gain (p = 0.007) and lower rate time (p = 0.019). Among the FD cohort, men had lower natural frequency (p = 0.046) and higher attenuation (p = 0.013) than heterozygous women. Figure 1 shows the time course dynamic evoked BFV response in PCA during the reading task.

Discussion

The results of this study suggest, for the first time, that FD patients with no prior history of stroke or TIA may have disturbed blood flow regulation of the neurovascular coupling mechanism. The finding of decreased PCA resting blood flow in our patients agrees with the results of Hilz et al. [7], who observed reduced cerebral BFV and impaired autoregulation in a study of 22 affected males at mild stages of FD. In contrast, Moore et al. [6] reported significantly higher baseline cerebral BFV in 26 males with FD enrolled in a controlled trial of ERT. Since the patients' mean PCA peak systolic BFV reported in that study did not differ significantly from our own findings, the disparate conclusions are due to the different ranges of the corresponding values in the control subjects. The reasons for this discrepancy are not clear but may not be explained by the age difference between the two cohorts [24].

None of our patients had clinical or imaging evidence of neurodegeneration of the visual cortex, which could explain the decreased resting BFV in the PCA. Our fTCD findings are therefore indicative of a disturbed neurovascular coupling in the visual cortex of FD patients. The

Eur Neurol 2012;67:331–337

Table 1. Demographic, genetic and clinical features of the patients

Gender	M	M	M	M	M	F	F	F	F	F	F	F
Age at examination/ age at diagnosis, years	48/17	23/21	23/20	22/19	21/18	54/37	51/48	48/46	44/44	39/31	30/14	26/24
Age at start of ERT, years	43	20	22	21	20	–	50	47	–	34	–	–
GLA mutation	p.C94S	p.R220X	p.Δ239I	dupEx2_4	dupEx2_4	p.C94S	p.Δ239I	p.R220X	dupEx2_4	p.R220X	p.C94S	p.R220X
Leukocyte α-gal activity	0	1.2	0.38	0.6	0.1	47	20	18	18	20	20	–
Vascular risk factors	HT	T	–	–	L	HT, DM, L	HT, L	T	–	HT, L, T	L	–
Angiokeratomas	+	++	++	+	+	+	–	+	–	+	–	–
Cornea verticillata	✓	✓	✓	✓	✓	✓	✓	✓	✓	✓	✓	✓
Cataracts	–	✓	–	–	–	–	–	–	–	–	–	–
Retinal vascular tortuosity	✓	✓	✓	✓	✓	✓	–	–	–	–	–	–
Echo/ECG abnormalities	LVH, SB, PH	–	SB	SB	SB	LVH, RBBB	LVH, PH	LVH	SB, AVB1	–	–	–
Arrhythmias	AF	–	–	–	–	–	–	–	–	–	–	–
Chronic kidney disease	ESRD/HD	CKD2	CKD1	CKD1	CKD1	CKD1	CKD2	CKD2	CKD1	CKD3	CKD1	CKD1
Proteinuria	+++	+	+	++	++	+	+	++	+	+++	–	–
Headaches	✓	–	✓	–	–	–	–	✓	✓	✓	✓	–
Psychiatric disease[1]	–	–	–	–	–	D, P	–	–	–	–	D, B	–
Hearing loss	✓	–	–	–	–	–	–	–	–	–	–	–
Acroparesthesias	✓	–	✓	✓	✓	✓	✓	✓	–	–	–	–
Hypohidrosis	✓	–	–	–	–	–	–	–	✓	–	–	–
Abdominal pain[1]	✓	–	–	–	–	–	–	–	–	–	✓	–
Exercise intolerance	✓	–	✓	✓	✓	–	–	–	–	–	–	–

α-gal = α-Galactosidase; HT = hypertension; DM = diabetes mellitus, type 2; L = dyslipidemia; T = tobacco smoking; LVH = left ventricular hypertrophy; AF = atrial fibrillation; SB = sinus bradycardia; PH = pulmonary hypertension; RBBB = complete right bundle branch block; AVB1 = first-degree atrioventricular block; ESRD/HD = end-stage renal disease, on chronic hemodialysis; CKD = chronic kidney disease, stages according to estimated glomerular filtration rate (eGFR), based on serum creatinine levels, race, gender and age; CKD1 = eGFR ≥90 ml/min/1.73 m^2; CKD2 = eGFR 89–60 ml/min/1.73 m^2; CKD3 = eGFR 59–30 ml/min/1.73 m^2; D = depression; P = psychotic episode(s); B = bulimia.

✓ = Symptom or phenotypic manifestation present; – = symptom or phenotypic manifestation not present; +, ++, +++ = phenotypic manifestation graded as to severity, from mild (or scarce) to severe (or numerous). For proteinuria: + = 150–300 mg/day; ++ = 300–3,500 mg/day; +++ = >3,500 mg/day.

[1] Disease or symptom requiring medical treatment.

Normal range for leukocyte α-gal activity: 30–84 nmol/h/mg.

Table 2. TCD data: resting BFV and functional TCD parameters in posterior cerebral artery

	Fabry group		Control group	
	males (n = 5)	females (n = 7)	male (n = 8)	female (n = 12)
PCA SFV, cm/s	47.37 ± 10.63	49.65 ± 10.21	52.89 ± 8.76	63.82 ± 14.36
Total	48.70 ± 9.97 *(p = 0.032)		58.35 ± 12.80	
PCA DFV, cm/s	10.33 ± 5.56	14.80 ± 6.27	16.20 ± 4.14	19.89 ± 7.00
Total	12.94 ± 6.17 *(p = 0.021)		18.41 ± 6.18	
Gain, %	11.47 ± 3.36	13.35 ± 11.34 *(p = 0.042)	17.36 ± 7.57	19.18 ± 7.45
Total	12.57 ± 8.67 *(p = 0.007)		18.45 ± 7.35	
Natural frequency, 1/s	0.18 ± 0.04 †(p = 0.046)	0.24 ± 0.05 †(p = 0.046)	0.23 ± 0.05	0.22 ± 0.07
Total	0.22 ± 0.05		0.23 ± 0.06	
Attenuation	0.64 ± 0.17 †(p = 0.013)	0.34 ± 0.17 *(p = 0.034) †(p = 0.013)	0.48 ± 0.15	0.56 ± 0.18
Total	0.47 ± 0.22		0.53 ± 0.17	
Rate time, s	2.98 ± 2.32	2.60 ± 1.23 *(p = 0.021)	3.84 ± 1.92	5.20 ± 2.51
Total	2.76 ± 1.68 *(p = 0.019)		4.65 ± 2.34	

TCD = Transcranial Doppler; PCA = posterior cerebral artery; SFV = systolic blood flow velocity; DFV = diastolic blood flow velocity.

p* = Statistical difference between Fabry and control groups; p† = statistical difference between genders within groups; n.s. = p > 0.05. Values expressed in means ± SD.

decreased rate time and gain reflect a lower hemodynamic response to visual activation tasks [25, 26]. As data from animal experiments suggest that this response might be related to a deficit in the nitric oxide system [27], our results fit into the hypothesis of an impaired functioning of the endothelial nitric oxide system in FD [28]. Attenuation and natural frequency were, respectively, significantly higher and significantly lower in males as compared to the females, suggesting that the FD males may have dysfunction of resistance brain arteries since the early stages of disease. Of note, these same fTCD parameters are known to be disturbed in patients with vascular dementia, diabetes mellitus and migraine attacks [29–31]. Although it is plausible that these fTCD results are related to endothelial dysfunction, we cannot exclude an autonomic nervous system involvement in the cerebrovascular regulation, as shown in other diseases associated with autonomic failure [32].

The results of the additional imaging studies were important to characterize in more detail our patient cohort. As in earlier studies of FD patients [5], the increased CCA-IMT was not related to the presence of focal atherosclerotic plaques. It is possible that increased IMT reflects not only early atherosclerosis, but also non-atherosclerotic vessel wall hypertrophy as a result of smooth muscle cell hyperplasia and fibrocellular hypertrophy [14], which are typical features of the vascular pathology of FD [12]. The WML are typically found in association with FD even in young adults, and its prevalence increases with age [2, 33], as observed in our cohort. They are most probably caused by small-vessel ischemic damage in the territories of the perforating arteries [33]. The lack of any atherosclerotic plaques in our patients is in agreement with this interpretation. Although it has been suggested that pulvinar hyperintensity on MRI T_1-weighted images is a common and distinctive brain-imaging feature of FD [8], this sign was not identified in any of our patients. A plausible explanation is the small size and young age of our male cohort, since the pulvinar sign has been described predominantly in men and is rarely seen before the age of 30 years [8, 34]. Elongated and/or tortuous vessels in both the anterior and the posterior brain arterial territories were a frequent MRA finding in our patients, with predilection to internal carotid, middle cerebral and basilar arteries, which agrees with the literature [35]. The mean BA diameter in our patients was higher than the reported by Fellgiebel et al. (3.66 ± 0.72 vs. 3.3 ± 0.59 mm), increased slightly with age and showed no significant gender difference. Although the overall mean ages of the two patient cohorts were similar, the different age distribution of the male and female cohorts in our series is a plausible explanation for the discordant results.

Although the volume of brain tissue measured in our patients were within the normal range, the WM/GM vol-

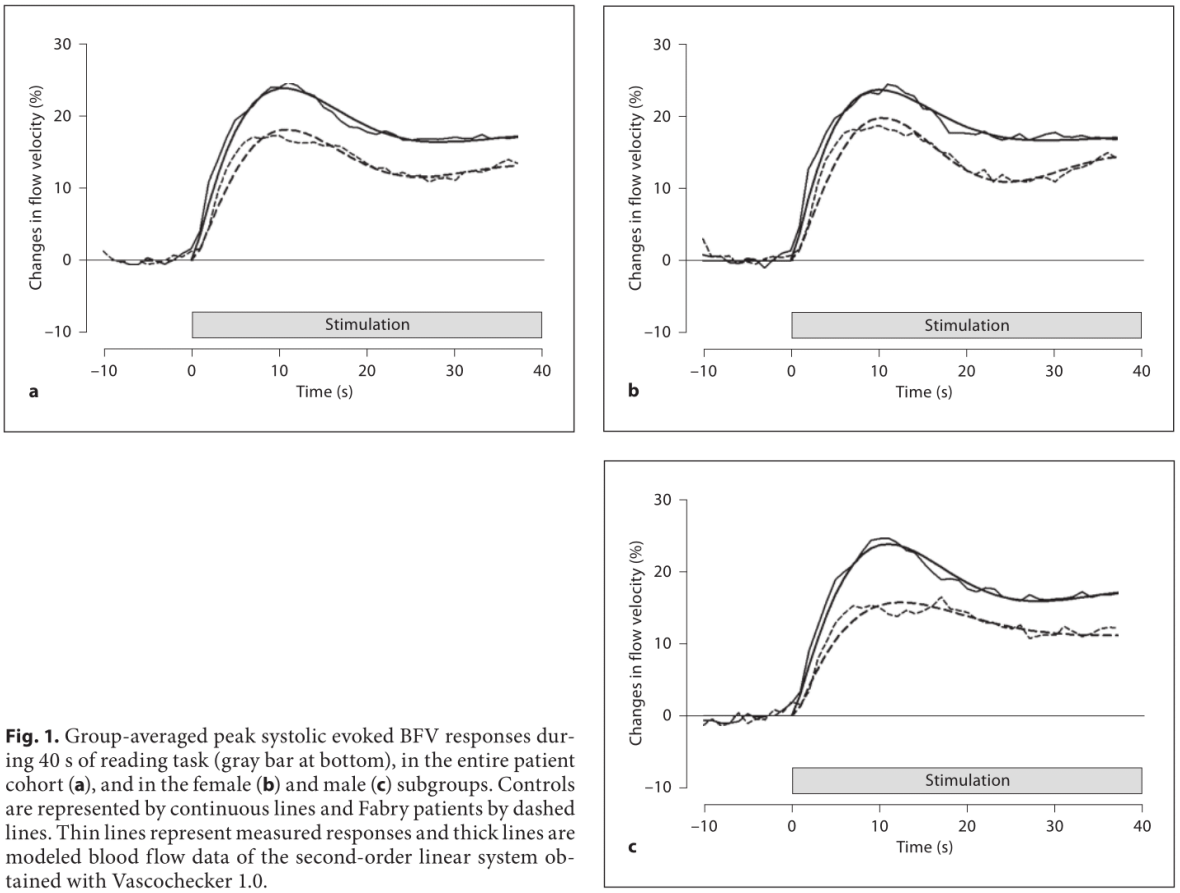

Fig. 1. Group-averaged peak systolic evoked BFV responses during 40 s of reading task (gray bar at bottom), in the entire patient cohort (**a**), and in the female (**b**) and male (**c**) subgroups. Controls are represented by continuous lines and Fabry patients by dashed lines. Thin lines represent measured responses and thick lines are modeled blood flow data of the second-order linear system obtained with Vascochecker 1.0.

ume ratios were significantly lower than previously reported for healthy adults [18]. The lack of published estimates of GM and WM volume in FD patients, and the uncontrolled design of our study, makes more difficult the interpretation of these findings. Since in healthy individuals there is no significant decline in WM volume with age, in contrast to GM volume [18], our findings are worth testing in a larger, appropriately controlled patient cohort, as an additional MRI feature of early brain involvement in FD.

In conclusion, FD patients of both genders, without prior history of stroke or TIA, may have disturbed neurovascular coupling in the visual cortex, as well as decreased resting PCA BFV, and decreased WM/GM volume ratio. These findings support the role of fTCD, along with duplex ultrasound and MR techniques, in the evaluation of FD patients, since early stages of disease. The evidence of disturbed neurovascular coupling in the visual cortex and the abnormal WM/GM volume ratio are new findings that need to be confirmed in future studies.

Disclosure Statement

J.P.O. is a member of the European Advisory Board of the Fabry Registry, sponsored by Genzyme Corp., and has received speaker fees, travel grants and research support from Genzyme Corp. All other authors have no conflicts of interest to disclose.

References

1 Rombach SM, Twickler TB, Aerts JM, Linthorst GE, Wijburg FA, Hollak CE: Vasculopathy in patients with Fabry disease: current controversies and research directions. Mol Gen Metab 2010;99:99–108.
2 Sims K, Politei J, Banikazemi M, Lee P: Stroke in Fabry disease frequently occurs before diagnosis and in the absence of other clinical events: natural history data from the Fabry registry. Stroke 2009;40:788–794.
3 Fellgiebel A, Muller MJ, Ginsberg L: CNS manifestations of Fabry's disease. Lancet Neurol 2006;5:791–795.
4 Rolfs A, Bottcher T, Zschiesche M, Morris P, Winchester B, Bauer P, Walter U, Mix E, Lohr M, Harzer K, Strauss U, Pahnke J, Grossmann A, Benecke R: Prevalence of Fabry disease in patients with cryptogenic stroke: a prospective study. Lancet 2005;366:1794–1796.
5 Barbey F, Brakch N, Linhart A, Jeanrenaud X, Palecek T, Bultas J, Burnier M, Hayoz D: Increased carotid intima-media thickness in the absence of atherosclerotic plaques in an adult population with Fabry disease. Acta Paediatr Suppl 2006;95:63–68.
6 Moore DF, Altarescu G, Ling GS, Jeffries N, Frei KP, Weibel T, Charria-Ortiz G, Ferri R, Arai AE, Brady RO, Schiffmann R: Elevated cerebral blood flow velocities in Fabry disease with reversal after enzyme replacement. Stroke 2002;33:525–531.
7 Hilz MJ, Kolodny EH, Brys M, Stemper B, Haendl T, Marthol H: Reduced cerebral blood flow velocity and impaired cerebral autoregulation in patients with Fabry disease. J Neurol 2004;251:564–570.
8 Burlina AP, Manara R, Caillaud C, Laissy JP, Severino M, Klein I, Burlina A, Lidove O: The pulvinar sign: frequency and clinical correlations in Fabry disease. J Neurol 2008;255:738–744.
9 Albrecht J, Dellani PR, Muller MJ, Schermuly I, Beck M, Stoeter P, Gerhard A, Fellgiebel A: Voxel-based analyses of diffusion tensor imaging in Fabry disease. J Neurol Neurosurg Psychiatry 2007;78:964–969.
10 Fellgiebel A, Keller I, Marin D, Muller MJ, Schermuly I, Yakushev I, Albrecht J, Bellhauser H, Kinateder M, Beck M, Stoeter P: Diagnostic utility of different MRI and MR angiography measures in Fabry disease. Neurology 2009;72:63–68.
11 Eng CM, Germain DP, Banikazemi M, Warnock DG, Wanner C, Hopkin RJ, Bultas J, Lee P, Sims K, Brodie SE, Pastores GM, Strotmann JM, Wilcox WR: Fabry disease: guidelines for the evaluation and management of multi-organ system involvement. Genet Med 2006;8:539–548.
12 Schiffmann R: Fabry disease. Pharmacol Ther 2009;122:65–77.
13 Desnick RJ, Brady R, Barranger J, Collins AJ, Germain DP, Goldman M, Grabowski G, Packman S, Wilcox WR: Fabry disease, an under-recognized multisystemic disorder: expert recommendations for diagnosis, management, and enzyme replacement therapy. Ann Intern Med 2003;138:338–346.
14 Touboul PJ, Hennerici MG, Meairs S, Adams H, Amarenco P, Bornstein N, Csiba L, Desvarieux M, Ebrahim S, Fatar M, Hernandez Hernandez R, Jaff M, Kownator S, Prati P, Rundek T, Sitzer M, Schminke U, Tardif JC, Taylor A, Vicaut E, Woo KS, Zannad F, Zureik M: Mannheim Carotid Intima-Media Thickness Consensus (2004–2006). An update on behalf of the Advisory Board of the 3rd and 4th Watching the Risk Symposium, 13th and 15th European Stroke Conferences, Mannheim 2004 and Brussels 2006. Cerebrovasc Dis 2007;23:75–80.
15 Rosset A, Spadola L, Ratib O: Osiri X: an open-source software for navigating in multidimensional DICOM images. J Digit Imaging 2004;17:205–216.
16 Smith SM, De Stefano N, Jenkinson M, Matthews PM: Normalized accurate measurement of longitudinal brain change. J Comp Assist Tomogr 2001;25:466–475.
17 Smith SM, Zhang Y, Jenkinson M, Chen J, Matthews PM, Federico A, De Stefano N: Accurate, robust, and automated longitudinal and cross-sectional brain change analysis. Neuroimage 2002;17:479–489.
18 Good CD, Johnsrude IS, Ashburner J, Henson RN, Friston KJ, Frackowiak RS: A voxel-based morphometric study of ageing in 465 normal adult human brains. Neuroimage 2001;14:21–36.
19 Azevedo E, Santos R, Freitas J, Rosas MJ, Gago M, Garrett C, Rosengarten B: Deep brain stimulation does not change neurovascular coupling in non-motor visual cortex: an autonomic and visual evoked blood flow velocity response study. Parkinsonism Relat Disord 2010;16:600–603.
20 Rosengarten B, Huwendiek O, Kaps M: Neurovascular coupling in terms of a control system: validation of a second-order linear system model. Ultrasound Med Biol 2001;27:631–635.
21 Rosengarten B, Aldinger C, Kaufmann A, Kaps M: Comparison of visually evoked peak systolic and end diastolic blood flow velocity using a control system approach. Ultrasound Med Biol 2001;27:1499–1503.
22 Rosengarten B, Budden C, Osthaus S, Kaps M: Effect of heart rate on regulative features of the cortical activity-flow coupling. Cerebrovasc Dis 2003;16:47–52.
23 Fazekas F, Chawluk JB, Alavi A, Hurtig HI, Zimmerman RA: MR signal abnormalities at 1.5 T in Alzheimer's dementia and normal aging. AJR Am J Roentgenol 1987;149:351–356.
24 Rosengarten B, Aldinger C, Spiller A, Kaps M: Neurovascular coupling remains unaffected during normal aging. J Neuroimaging 2003;13:43–47.
25 Hao Q, Wong LK, Lin WH, Leung TW, Kaps M, Rosengarten B: Ethnic influences on neurovascular coupling: a pilot study in Whites and Asians. Stroke 2010;41:383–384.
26 Rosengarten B, Grebe M, Muller A, Voss RK, Kaps M: Severity of coronary artery disease but not degree of coronary stenosis is correlated to cerebrovascular reactivity. Cerebrovasc Dis 2009;28:290–297.
27 Buerk DG, Ances BM, Greenberg JH, Detre JA: Temporal dynamics of brain tissue nitric oxide during functional forepaw stimulation in rats. Neuroimage 2003;18:1–9.
28 Moore DF, Scott LT, Gladwin MT, Altarescu G, Kaneski C, Suzuki K, Pease-Fye M, Ferri R, Brady RO, Herscovitch P, Schiffmann R: Regional cerebral hyperperfusion and nitric oxide pathway dysregulation in Fabry disease: reversal by enzyme replacement therapy. Circulation 2001;104:1506–1512.
29 Rosengarten B, Dost A, Kaufmann A, Gortner L, Kaps M: Impaired cerebrovascular reactivity in type 1 diabetic children. Diabetes Care 2002;25:408–410.
30 Rosengarten B, Sperner J, Gorgen-Pauly U, Kaps M: Cerebrovascular reactivity in adolescents with migraine and tension-type headache during headache-free interval and attack. Headache 2003;43:458–463.
31 Rosengarten B, Paulsen S, Molnar S, Kaschel R, Gallhofer B, Kaps M: Activation-flow coupling differentiates between vascular and Alzheimer type of dementia. J Neurol Sci 2007;257:149–154.
32 Azevedo E, Castro P, Santos R, Freitas J, Coelho T, Rosengarten B, Panerai R: Autonomic dysfunction affects cerebral neurovascular coupling. Clin Auton Res 2011;21:395–403.
33 Crutchfield KE, Patronas NJ, Dambrosia JM, Frei KP, Banerjee TK, Barton NW, Schiffmann R: Quantitative analysis of cerebral vasculopathy in patients with Fabry disease. Neurology 1998;50:1746–1749.
34 Moore DF, Ye F, Schiffmann R, Butman JA: Increased signal intensity in the pulvinar on T_1-weighted images: a pathognomonic MR imaging sign of Fabry disease. AJNR Am J Neuroradiol 2003;24:1096–1101.
35 Fellgiebel A, Keller I, Martus P, Ropele S, Yakushev I, Bottcher T, Fazekas F, Rolfs A: Basilar artery diameter is a potential screening tool for Fabry disease in young stroke patients. Cerebrovasc Dis 2011;31:294–299.

Autonomic dysfunction in multiple sclerosis is better detected by heart rate of variability and is not correlated with central autonomic network damage

---

Videira, G., Castro, P., Vieira, B., Filipe, J. P., Santos, R., Azevedo, E., Sá, M.J., Abreu, P. (2016). Autonomic dysfunction in multiple sclerosis is better detected by heart rate variability and is not correlated with central autonomic network damage. *J Neurol Sci, 367*, 133-137. doi: 10.1016/j.jns.2016.05.049

Journal of the Neurological Sciences 367 (2016) 133–137

Contents lists available at ScienceDirect

Journal of the Neurological Sciences

journal homepage: www.elsevier.com/locate/jns

Autonomic dysfunction in multiple sclerosis is better detected by heart rate variability and is not correlated with central autonomic network damage

Gonçalo Videira [a,*], Pedro Castro [a], Bítia Vieira [a], João Pedro Filipe [b], Rosa Santos [a], Elsa Azevedo [a], Maria José Sá [a,c], Pedro Abreu [a]

[a] Dept. Neurology, Centro Hospitalar de São João, Faculty of Medicine of University of Porto, Al. Prof. Hernâni Monteiro, 4200-319 Porto, Portugal
[b] Dept. Neuroradiology, Centro Hospitalar de São João, Al. Prof. Hernâni Monteiro, 4200-319 Porto, Portugal
[c] Faculty of Health Sciences, University Fernando Pessoa, Praça 9 de Abril 349, 4249-004 Porto, Portugal

ARTICLE INFO

Article history:
Received 17 April 2016
Received in revised form 19 May 2016
Accepted 24 May 2016
Available online 25 May 2016

Keywords:
Autonomic nervous system
Central autonomic network
Heart rate variability
Magnetic resonance imaging
Multiple sclerosis

ABSTRACT

Background: MS-associated autonomic dysfunction (AD) in multiple sclerosis (MS) is poorly understood and the best method for its detection unestablished. We compared classical Ewing battery and newer methods as heart rate variability (HRV) and spontaneous baroreflex sensibility (BRS) to detect AD in MS and related them to central autonomic network (CAN) lesions.
Methods: We enrolled 20 relapsing-remitting MS patients, median age of 36 (interquartile range 32–46) years, disease duration of 5.5 (2.2–6.8) years, Expanded Disability Status Scale (EDSS) score of 1.0 (1.0–1.5) and 20 age- and gender-matched healthy controls. We assessed Ewing battery and spontaneous HRV and BRS. CAN involvement was evaluated by magnetic resonance imaging.
Results: HRV showed both parasympathetic and sympathetic significant impairment in MS ($p < 0.05$). From Ewing battery only isometric test was significantly decreased in MS ($p = 0.006$). Disease duration and severity, lesion burden and CAN involvement were not correlated with laboratorial parameters.
Conclusions: Our MS cohort had both sympathetic and parasympathetic dysfunction independently from disease duration, neurological deficits and lesion burden or CAN involvement. HRV analysis maybe more useful than classical Ewing battery to screen AD.

1. Introduction

Along the course of multiple sclerosis (MS) the autonomic nervous system (ANS) seems to be increasingly affected [1]. Indeed, it is estimated that as much as 18 to 42% of patients present autonomic dysfunction (AD) symptoms, yet, these quality of life disturbing symptoms are frequently overlooked by the clinicians [2–6]. Some reasons may contribute: firstly, the occurrence of MS symptoms with greater clinical impact, such as motor, sensory or visual changes, may somewhat hide AD; secondly, the best method to detect AD in MS remains unestablished, despite the recognized usefulness of some laboratory tests [2,3,7–10] and of standardized questionnaires [1,11] to diagnose AD in MS patients; and finally, the pathophysiology of AD in MS is poorly understood [11]. ANS control centres within central nervous system, called the central autonomic network (CAN), have not yet been properly studied, although some specific spinal and brain locations have been proposed [12].

The main objective of our study is to compare the performance of the classical standardized Ewing battery of cardiovascular tests [13] with newer methods based on heart rate variability (HRV) and spontaneous baroreflex function (BRS) to detect AD in MS patients. Additionally, we aim to test the hypothesis that the presence of AD in MS may be related to CAN involvement which would contribute to better understating of AD pathophysiology.

2. Materials and methods

2.1. Studied population

In this matched case-control study, 20 relapsing-remitting MS patients from Centro Hospitalar São João were randomly proposed to

* Corresponding author at: Dept. Neurology, Centro Hospitalar de São João, Faculty of Medicine of University of Porto, Portugal.
E-mail addresses: pgoncalomv@gmail.com (G. Videira), pedromacc@gmail.com (P. Castro), vieira.bitia@gmail.com (B. Vieira), mail.jpfilipe@gmail.com (J.P. Filipe), rosampsantos2@gmail.com (R. Santos), eazevedo@med.up.pt (E. Azevedo), mjsa@med.up.pt (M.J. Sá), pmabreu@netcado.pt (P. Abreu).

http://dx.doi.org/10.1016/j.jns.2016.05.049
0022-510X/

participate. Inclusion criteria for involvement were definitive diagnosis of MS (according to the 2010 McDonald criteria) and age above 18 years old. Those with active disease or treatment with corticosteroids within 8 weeks of enrolment were excluded. Control group consisted of 20 age- and sex-matched healthy subjects, recruited from the hospital and university staff. Exclusion study criteria was the presence of any disorder that could interfere with the autonomic function. The *Ethics Committee of Centro Hospitalar São João* approved this work and all the participants gave written informed consent.

2.2. Clinical assessment

A MS specialist evaluated the patients less than 1 month before enrolment. Age, gender, detailed neurological examination, time of disease, annualized relapse rate [14] and Expanded Disability Status Scale (EDSS) [15] score were recorded. Every relapse and respective location (optic nerve, brain hemispheres, brainstem or spinal cord) were registered, based on clinical and imaging findings [16].

2.3. Autonomic tests

Participants were asked to stop alcohol, coffee, smoking and any medication that could alter autonomic function 24 h before testing. Evaluations were carried out in a quiet room with a constant temperature around 22 °C. Blood pressure was continuously monitored in the non-dominant hand with a Finometer device (FMS, Amsterdam, Netherlands) with its pressure height correction unit placed at heart level. Heart rate (HR) and R-R intervals (RRi) were assessed from a 3-lead ECG. All data were digitally recorded at 400 Hz in commercial analogue-digital converter for offline analysis with dedicated software based on MATLAB (Natick, USA).

After autonomic tests have been explained [10] and maximum contraction strength in dominant hand (or non-paretic hand if dominant was affected) was measured with a dynamometer, the subject was positioned supine and rested for 30 min. Next, Ewing battery was applied as described previously [17]. Shortly, we calculated [10]: expiratory–to–inspiratory amplitude ratio of HR (E:I ratio) during synchronized deep breathing at 6 cycles/min; the Valsalva ratio (VR), i.e., averaged HR ratio between II and IV phases of three Valsalva manoeuvres [9]; the quotient of RRi around 30th beat by that at the 15th after standing; the difference between the systolic blood pressure (SBP) at rest and after standing during 5 min to assess orthostatic hypotension; and diastolic blood pressure (DBP) response to handgrip isometric work at 30% of his maximum strength for 5 min. Each test was scored as normal (zero), borderline (one) and abnormal (two) and the sum resulted in Ewing score [13].

2.4. Heart rate variability and spontaneous baroreflex sensitivity

The last 10 min of resting recording were used to analyse short-term HRV and BRS in both time and frequency domains [10]. HRV was assessed in time domain using standard deviation (SDNN), root mean squared difference (rMSSD) and proportion of successive intervals greater than 50 ms (pNN50%) of normal RRi (NN). On frequency domain, HRV was characterized by total power (TP) spectrum of RRi [18], at low frequency (LF; 0.04–0.15 Hz) for sympathetic ANS and at high frequency for parasympathetic (HF; 0.15–0.40 Hz), the LF/HF ratio, and normalized LF (LFnu) and HF (HFnu) [19]. For BRS in time domain, we used sequence method based on the identification of all spontaneous sequences of ≥3 consecutive beats of increase or decrease of SBP (≥1 mmHg), the baroreflex response of lengthening or shortening of RRi (≥3 ms) [20,21]. The slope of regression line between SBP/RRi is the BRS [21]. In frequency domain, BRS was achieved by spectral method using the cross-correlation gain between the power spectral densities of SBP on that of RRi at LF and HF bands [22]. Lower HRV [20] and BRS [22] correlates with worse AD.

2.5. MRI

Brain MRI was obtained within less than a year before enrolment. Spinal MRI analysed was the last performed. None of the subjects experienced relapse after imaging. Presence of T2-weighted lesions in the white matter adjacent to the following CAN structures was assessed: insula, anterior cingulate cortex, hypothalamus, amygdala, periaqueductal grey matter (PAG), parabrachial nucleus, nucleus of the solitary tract, ventrolateral reticular formation of the medulla and medullary raphe. A CAN score was calculated adding 1 point for each CAN structure affected (maximum of 9 points). The number of all T2-weighted lesions was then counted in supratentorial areas, brainstem, cerebellum, spinal cord and total number of lesions. The presence of lesions on T1-weighted images, enhancing or non-enhancing, was also assessed. MRI protocols included studies performed on 1.5 T (Siemens MAGNETOM SymphonyTim syngo) and 3 T (Siemens MAGNETOM TrioTim syngo) scanners with, at least, coronal and axial T1-weighted images (511–750 ms/8.6–8.7 ms [TR/TE]), spin-echo or fast spin-echo axial proton density (3770–4000 ms/11-22 ms [TR/TE]) and T2-weighted images (3770–4000 ms/88–106 ms [TR/TE]), and axial and sagittal fluid-attenuated inversion-recovery (FLAIR) images (8000–9000 ms/91–93 ms [TR/TE]), all with 5 mm section thickness. Contrast-enhanced T1-weighted images were obtained with 0.1 mmol/kg gadolinium using typical T1-weighted parameters as described above.

2.6. Statistical analyses

Shapiro-Wilk test was used to inspect normality of continuous variables. Student *t*-test or Mann-Whitney were used to compare the distribution across two groups. Pearson or Spearman rho coefficients were used to determine the correlation between two variables. Statistical significance was inferred at $p < 0.05$ level. All statistics were performed using IBM Statistical Package for Social Sciences (SPSS) Statistics v21™.

3. Results

MS patients (12 women) had median age of 36 [interquartile range (IQR) 32–46] years, disease duration of 5.5 (2.2–6.8) years, EDSS of 1.0 (1.0–1.5) and annualized relapse rate was 0.33 (0–0.48) relapses/year. Detailed clinical data is presented in Table 1.

3.1. Autonomic assessment: comparing MS and control groups

Hemodynamic data and autonomic tests results of MS and healthy controls are compared in Table 2. Baseline blood pressure and HR were similar ($p < 0.05$). Ewing battery showed no significant differences except for isometric handgrip subtest, which was weaker in MS ($p = 0.006$). This test was abnormal in 14 MS patients (70%) as well as in 5 controls (25%). E:I ratio tended to be lower in the MS ($p = 0.063$). BRS was similar between groups ($p < 0.05$). As for HRV, MS patients had lower SDNN ($p = 0.007$), rMSSD ($p = 0.028$), pNN50% ($p = 0.011$), power at LF ($p = 0.024$) and HF ($p = 0.021$) bands, but similar LF/HF ratio ($p = 0.689$).

3.2. MS group: relationship between clinical features and laboratory tests

There was no correlation between autonomic laboratorial results and age, gender, EDSS and annualized relapse rate ($p > 0.05$). A previous brainstem syndrome relapse was associated with a higher Ewing score ($p = 0.010$).

One patient didn't have MRI results available for analysis. The presence of any spinal, brainstem or CAN lesion was not associated with autonomic laboratorial results except for spinal involvement and a higher SDNN ($p = 0.042$) and a tendency for higher rMSSD ($p = 0.053$) and pNN50% ($p = 0.066$). There was no significant association between

Table 1
Individual clinical data of MS patients.

ID	Gender	Age	Disease duration	EDSS	Medication	ARR	Brainstem relapse	Spinal relapse
1	F	33	4	1.0	Interferon-β1a	0.25	Yes	No
2	F	27	1	1.0	Interferon-β1a	0.00	No	No
3	F	23	2	0.0	Interferon-β1a	0.00	No	No
4	F	45	25	2.0	Interferon-β1a	0.33	Yes	Yes
5	M	32	5	1.0	Interferon-β1a	0.00	No	No
6	M	48	2	2.5	Glatiramer acetate	0.00	No	No
7	M	35	5	1.0	Natalizumab	0.20	Yes	Yes
8	F	46	6	1.5	Natalizumab	0.50	Yes	No
9	M	32	10	0.0	Natalizumab	0.00	No	No
10	M	48	19	2.5	Glatiramer	0.00	Yes	Yes
11	M	27	6	1.0	Natalizumab	0.50	Yes	Yes
12	F	48	3	1.5	Glatiramer acetate	0.43	No	Yes
13	F	47	7	1.5	Interferon-β1a	0.42	Yes	No
14	F	44	6	1.0	Interferon-β1a	0.33	Yes	Yes
15	M	35	7	1.0	Fingolimod	0.42	Yes	Yes
16	F	40	6	1.0	Dimethyl fumarate	0.66	No	No
17	F	32	6	1.5	Interferon-β1a	0.66	Yes	Yes
18	M	35	0	1.0	Interferon-β1a	0.00	No	No
19	F	40	0	1.0	Glatiramer acetate	0.00	No	No
20	F	32	5	1.5	Natalizumab	0.40	Yes	No

F: female; M: male; EDSS: Expanded Disability Status Scale; ARR: annualised relapse rate.

Table 3
MRI data of MS patients focusing in central autonomic network.

Frequency of affected areas [absolute (%)]		
Brainstem		10 (56%)
Spinal		14 (78%)
CAN	Insula	5 (28%)
	Anterior cingulate	13 (72%)
	Hypothalamus	2 (11%)
	Amygdala	1 (6%)
	Periaqueductal grey	4 (22%)
	Parabrachial nucleus	1 (6%)
	Nucleus of the solitary tract	1 (6%)
	VLRM	1 (6%)
	Medullary raphe	2 (11%)
	Score [median (IQR)]	2 (1–3)
T2 lesions count [median (IQR)]		
	Total	22 (12–39)
	Supratentorial	16 (8–33)
	Brainstem	1 (0–4)
	Cerebellum	0 (0–1)
	Spinal	2 (1–5)
Any gadolinium enhanced lesion [absolute (%)]		4 (22)
Any T1 black holes [absolute (%)]		15 (83)

VLRM: ventrolateral reticular formation of the medulla lesion; raphe: medullary raphe lesion; Total: total number of lesions; T2: T2-weighted; T1 black holes: T1-weighted gadolinium enhanced lesions. Results are in absolute (percentage) or median and interquartile range IQR (P25–P75), as appropriate.

the either number of total or regional CAN lesions and autonomic evaluation (Ewing total and each subtest, BRS and HRV results). The exception was insular involvement, which was significantly associated with a higher LF/HF [1.1 (0.6–2.1) vs 0.9 (0.4–1.3), $p = 0.035$]. See Table 3 for detailed imaging analysis.

4. Discussion

We are unware of similar MS studies with combination of clinical, classical and newer autonomic tests, as well as imaging findings. Our study found evidence of sympathetic and parasympathetic AD in MS patients as compared to healthy subjects.

Table 2
Comparison of autonomic test and symptoms scores between MS and control group.

Parameters	MS group	Control group	*p* Value
Baseline hemodynamic data			
SBP	120 (112–139)	125 (117–139)	0.416
DBP	56 (46–67)	56 (51–62)	0.990
HR	70.5 (64–73)	64.5 (59–75.25)	0.525
Ewing battery tests			
E:I ratio (bpm) [score]	18 (14–26) [1 (0–1)]	26 (18–34) [0 (0–0)]	0.063 [0.108]
Valsalva ratio [score]	1.8 (1.6–2.1) [0 (0–0)]	1.8 (1.7–2.4) [0 (0–0)]	0.765 [0.989]
30:15 ratio [score]	1.3 (1.2–1.6) [0 (0–0)]	1.5 (1.2–1.7) [0 (0–0)]	0.313 [0.799]
Standing (mm Hg) [score]	7 (0−12) [0 (0–1)]	−1 (−6–10) [0 (0–0)]	0.347 [0.429]
Isometric test (mm Hg) [score]	7 (4–11) [2 (1–2)]	16 (10−22) [0 (0–2)]	0.002 [0.006]
Total score	3 (2–3)	1 (0–2)	<0.001
Spontaneous baroreflex sensitivity (BRS)			
BRS up (ms/mmHg)	11.8 (8.7–15.2)	17.4 (10.5–27.0)	0.192
BRS down (ms/mmHg)	14.6 (9.6–25.7)	18.6 (14.6–28.4)	0.238
BRS (ms/mmHg)	13.2 (9.7–18.6)	18.8 (13.3–23.7)	0.365
LF gain (ms/mmHg)	7.6 (5.0–11-1)	11.6 (5.4–18.8)	0.640
HF gain (ms/mmHg)	6.2 (4.2–9.5)	7.1 (6.0–10.0)	0.277
Heart rate variability (HRV)			
SDNN (ms)	32.6 (27.8–43.2)	50.2 (40.0–72.2)	0.007
rMSSD (ms)	30.0 (20.8–37.8)	52.2 (30.5–62.5)	0.028
pNN50% (ms)	6.0 (0.6–13.1)	20.6 (7.4–37.2)	0.011
LF: 0.04–0.15 Hz (ms^2)	205.8 (179.1–328.6)	605.9 (254.9–1768.9)	0.024
HF: 0.14–0.40 Hz (ms^2)	256.3 (130.1–521.7)	1027.4 (295.2–1497.0)	0.021
Total power	931.6 (644.4–1268.1)	2222.3 (895.4–4441.1)	0.052
LFnu	0.5 (0.3–0.6)	0.5 (0.4–0.6)	0.758
HFnu	0.5 (0.3–0.6)	0.5 (0.4–0.6)	0.765
LF/HF ratio	1.2 (0.5–2.2)	1.0 (0.6–1.8)	0.689

Bpm: beats per minute; mmHg: millimeters of mercury; ms: milliseconds; SBP: systolic blood pressure; DBP: diastolic blood pressure; E:I: expiratory to inspiratory, LF: low frequency; HF: high frequency; nu: normalized; BRS: spontaneous baroreflex sensitivity.

Short-term HRV analysis was the most robust AD test, since it was fairly consistent across multiple parameters. MS patients showed reduced autonomic activity in both time and frequency domains. While time domain concerns parasympathetic ANS, frequency domain tries to discriminate sympathetic (LF band) from parasympathetic (HF band) dysfunction. A preserved LF/HF ratio suggests that both systems are equally affected, which agrees with other studies [23–25]. Short-term HRV attractiveness relies in the fact that it takes just 5 to 10 min of resting ECG recording, contrary to the relatively cumbersome and Ewing battery. Unlike HRV, BRS did not differ between MS and healthy subjects. HRV predominantly measures tonic vagal activity, while BRS assesses reflex vagal activity [26] and so, our MS patients may have a lower tonic parasympathetic activity while maintaining a well-preserved baroreflex function. BRS dysfunction has been implied in fatal arrhythmia in the elderly and after myocardial infarctions [22]; in fact, cardiovascular disorders are clinical features rarely seen in MS [27].

Ewing battery did not reveal significant dysfunction in MS patients. Only the handgrip test revealed blunt blood pressure response to isometric contraction in a significant amount of MS subjects (75%), which indicates sympathetic dysfunction, but also in 25% of controls. Other studies obtained similar results with this manoeuvre [1,2,12]. Handgrip test is highly dependent on voluntary effort and its results could be related to fatigue and worst physical condition of MS patients, instead of sympathetic dysfunction [28].

Compared to other studies our MS sample was smaller, had a globally low EDSS [3,4,12] and low disease duration [1,12], which might explain the absence of overt sympathetic failure with orthostatic hypotension, as previously reported [2,29]. Yet, in line with the literature, we found no correlation of autonomic tests results with disease severity (EDSS) [1,4,27] or duration [24,27].

We have not found any association between CAN affection and autonomic test results, except for insula. Interestingly, insular lesions associated with higher LF/HF ratio. This shifting to a predominance of sympathetic tonus was already described following right insular cortex ischemic infarction [30]. To our knowledge, this has not been described in MS before.

A possible limitation of our method is the fact that we retrospectively analysed white matter lesions near these structures and not locus itself. More sensible MRI sequences could be more clarifying on this regard.

Also, we didn't assess sudomotor function, as other authors do when studying AD in MS [1,2,4,11]. Evaluation of sudomotor dysfunction in MS faces major challenges. Most quantitative studies rely on postganglionic sympathetic cholinergic evaluation, which is not presumed to be affected by MS. Sympathetic skin response (SSR) has been well characterized before in MS, being abnormal in 29–45% of MS patients [2,11] and associating with brainstem involvement [31]. However, since it relies on supraspinal reflex pathways, caution must be taken when considering its autonomic testing specificity. Thermoregulatory sweat test, which incorporates central autonomic control assessment, is limited to highly specialized centres and not clinically available. Nevertheless, it was recently found that sweat glands have decreased function in moderate to severe MS patients, presumably due to central chronic deregulation [32]. This warrants further investigation in future studies and quantitative sudomotor function should also be addressed instead of cardiovascular autonomic testing.

5. Conclusions

In our MS patients, autonomic dysfunction was not associated with disease duration, its severity and lesion burden. In our cohort, simple autonomic tests like short-term heart rate variability analysis can reveal autonomic impairment more appropriately than classical cardiovascular assessment. Despite the mentioned limitations, our study emphasizes that clinicians should be aware of autonomic dysfunction early in the course of the disease.

Disclosure of conflicts of interest

Nothing to disclose.

Acknowledgments

None.

References

[1] D.I. Gunal, N. Afsar, T. Tanridag, S. Aktan, Autonomic dysfunction in multiple sclerosis: correlation with disease-related parameters, Eur. Neurol. 48 (1) (2002) 1–5.
[2] A.J. McDougall, J.G. McLeod, Autonomic nervous system function in multiple sclerosis, J. Neurol. Sci. 215 (1–2) (2003) 79–85.
[3] A.R. Acevedo, C. Nava, N. Arriada, A. Violante, T. Corona, Cardiovascular dysfunction in multiple sclerosis, Acta Neurol. Scand. 101 (2) (2000) 85–88.
[4] A. Kodounis, E. Stamboulis, T.S. Constantinidis, A. Liolios, Measurement of autonomic dysregulation in multiple sclerosis, Acta Neurol. Scand. 112 (6) (2005) 403–408.
[5] E. Lensch, W.H. Jost, Autonomic disorders in multiple sclerosis, Autoimmune Dis. 2011 (2011) 803841.
[6] C.A. Haensch, J. Jorg, Autonomic dysfunction in multiple sclerosis, J. Neurol. 253 (Suppl. 1) (2006) I3–I9.
[7] L.A. Hale, H. Nukada, L.J. Du Plessis, K.C. Peebles, Clinical screening of autonomic dysfunction in multiple sclerosis, Physiother. Res. Int. 14 (1) (2009) 42–55.
[8] E. Azevedo, P. Castro, R. Santos, J. Freitas, T. Coelho, B. Rosengarten, et al., Autonomic dysfunction affects cerebral neurovascular coupling, Clin. Auton. Res. 21 (6) (2011) 395–403.
[9] P.M. Castro, R. Santos, J. Freitas, R.B. Panerai, E. Azevedo, Autonomic dysfunction affects dynamic cerebral autoregulation during Valsalva maneuver: comparison between healthy and autonomic dysfunction subjects, J. Appl. Physiol. 117 (3) (2014) 205–213.
[10] J. Freitas, R. Santos, E. Azevedo, M. Carvalho, F. Boomsma, A. Meiracker, et al., Hemodynamic, autonomic and neurohormonal behaviour of familial amyloidotic polyneuropathy and neurally mediated syncope patients during supine and orthostatic stress, Int. J. Cardiol. 116 (2) (2007) 242–248.
[11] N. Kale, S. Magana, J. Agaoglu, O. Tanik, Assessment of autonomic nervous system dysfunction in multiple sclerosis and association with clinical disability, Neurol. Int. 1 (1) (2009) e5.
[12] A. Saari, U. Tolonen, E. Paakko, K. Suominen, J. Pyhtinen, K. Sotaniemi, et al., Cardiovascular autonomic dysfunction correlates with brain MRI lesion load in MS, Clin. Neurophysiol. 115 (6) (2004) 1473–1478.
[13] D.J. Ewing, B.F. Clarke, Diagnosis and management of diabetic autonomic neuropathy, Br. Med. J. (Clin. Res. Ed.) 285 (6346) (1982) 916–918.
[14] T. Saida, K. Tashiro, Y. Itoyama, T. Sato, Y. Ohashi, Z. Zhao, et al., Interferon beta-1b is effective in Japanese RRMS patients: a randomized, multicenter study, Neurology 64 (4) (2005) 621–630.
[15] J.F. Kurtzke, Rating neurologic impairment in multiple sclerosis: an expanded disability status scale (EDSS), Neurology 33 (11) (1983) 1444–1452.
[16] C.H. Polman, S.C. Reingold, B. Banwell, M. Clanet, J.A. Cohen, M. Filippi, et al., Diagnostic criteria for multiple sclerosis: 2010 revisions to the McDonald criteria, Ann. Neurol. 69 (2) (2011) 292–302.
[17] D.J. Ewing, C.N. Martyn, R.J. Young, B.F. Clarke, The value of cardiovascular autonomic function tests: 10 years experience in diabetes, Diabetes Care 8 (5) (1985) 491–498.
[18] L.A. Campos, V.L. Pereira Jr., A. Muralikrishna, S. Albarwani, S. Bras, S. Gouveia, Mathematical biomarkers for the autonomic regulation of cardiovascular system, Front. Physiol. 4 (2013) 279.
[19] M. Bettoni, M. Zimmermann, Autonomic tone variations before the onset of paroxysmal atrial fibrillation, Circulation 105 (23) (2002) 2753–2759.
[20] R. Freeman, Assessment of cardiovascular autonomic function, Clin. Neurophysiol. 117 (4) (2006) 716–730.
[21] G. Parati, M. Di Rienzo, G. Mancia, How to measure baroreflex sensitivity: from the cardiovascular laboratory to daily life, J. Hypertens. 18 (1) (2000) 7–19.
[22] M.T. La Rovere, G.D. Pinna, G. Raczak, Baroreflex sensitivity: measurement and clinical implications, Ann. Noninvasive Electrocardiol. 13 (2) (2008) 191–207.
[23] Heart rate variability. Standards of measurement, physiological interpretation, and clinical use. Task Force of the European Society of Cardiology and the North American Society of Pacing and Electrophysiology, Eur. Heart J. 17 (3) (1996) 354–381.
[24] D. Mahovic, N. Lakusic, Progressive impairment of autonomic control of heart rate in patients with multiple sclerosis, Arch. Med. Res. 38 (3) (2007) 322–325.
[25] J.A. Monge-Argiles, F. Palacios-Ortega, J.A. Vila-Sobrino, J. Matias-Guiu, Heart rate variability in multiple sclerosis during a stable phase, Acta Neurol. Scand. 97 (2) (1998) 86–92.
[26] S.H. Hohnloser, T. Klingenheben, A. van de Loo, E. Hablawetz, H. Just, P.J. Schwartz, Reflex versus tonic vagal activity as a prognostic parameter in patients with sustained ventricular tachycardia or ventricular fibrillation, Circulation 89 (3) (1994) 1068–1073.
[27] T. Tombul, O. Anlar, M. Tuncer, N. Huseyinoglu, B. Eryonucu, Impaired heart rate variability as a marker of cardiovascular autonomic dysfunction in multiple sclerosis, Acta Neurol. Belg. 111 (2) (2011) 116–120.
[28] S. Merkelbach, U. Dillmann, C. Kolmel, I. Holz, M. Muller, Cardiovascular autonomic dysregulation and fatigue in multiple sclerosis, Mult. Scler. 7 (5) (2001) 320–326.

[29] P. Flachenecker, K. Reiners, M. Krauser, A. Wolf, K.V. Toyka, Autonomic dysfunction in multiple sclerosis is related to disease activity and progression of disability, Mult. Scler. 7 (5) (2001) 327–334.
[30] S. Meyer, M. Strittmatter, C. Fischer, T. Georg, B. Schmitz, Lateralization in autonomic dysfunction in ischemic stroke involving the insular cortex, Neuroreport 15 (2) (2004) 357–361.
[31] A. Saari, U. Tolonen, E. Paakko, K. Suominen, J. Pyhtinen, K.A. Sotaniemi, et al., Sympathetic skin responses in multiple sclerosis, Acta Neurol. Scand. 118 (4) (2008) 226–231.
[32] S.L. Davis, T.E. Wilson, J.M. Vener, C.G. Crandall, J.H. Petajan, A.T. White, Pilocarpine-induced sweat gland function in individuals with multiple sclerosis, J. Appl. Physiol. 98 (5) (2005) 1740–1744.